Wei Ren
Yongcan Cao

Distributed Coordination of Multi-agent Networks

Emergent Problems, Models, and Issues

Springer

Communications and Control Engineering

Wei Ren • Yongcan Cao

Distributed Coordination of Multi-agent Networks

Emergent Problems, Models, and Issues

Springer

Wei Ren
Dept. Electrical & Computer Engineering
Utah State University
Old Main Hill 4120
84322-4120 Logan Utah
USA
wei.ren@usu.edu

Yongcan Cao
Dept. Electrical & Computer Engineering
Utah State University
Old Main Hill 4120
84322-4120 Logan Utah
USA

Cover design: eStudio Calamar S.L.

Printed on acid-free paper

This work is dedicated to

My parents, Hongyi Ren and Liying Wang, and
My son, Kaden
– Wei Ren

My wife, Yuman Wei, and
My parents, Guangyao Cao and Yanpin Xie
– Yongcan Cao

Preface

In the past two decades, scientists across diverse fields have been trying to identify the underlying mechanisms of networked systems. Biologists use networks to study the working and wiring of transcriptional regulatory circuits. Sociologists use networks to predict the behavior of techno-social systems. Physicists use networks to model and predict the emergence of behavior norms, and use quantitative methods to analyze the resulting networked systems. Across different fields, network scientists are making a dramatic progress and pushing network analysis to its limits. In engineering, researchers study how to assemble and coordinate individual physical devices into a coherent whole to perform a common task. This gives rise to a very active and exciting research field—multi-agent systems. With numerous civilian, homeland security, and military applications, multi-agent systems place high demands on features such as low cost, high adaptivity and scalability, increased flexibility, great robustness, and easy maintenance. To meet these demands, the current trend is to design distributed algorithms that rely on only local interaction to achieve global group behavior.

This book introduces emergent problems, models, and issues in distributed coordination of multi-agent networks. These problems, models, and issues represent some emergent research directions in the field of multi-agent systems. Emergent problems include collective periodic motion coordination, collective tracking with a dynamic leader, and containment control with multiple leaders. These problems extend the existing application domains of multi-agent networks. In particular, collective periodic motion coordination is appropriate for applications involving agent networks with repetitive movements, collective tracking guarantees tracking of a dynamic leader by multiple followers in the presence of reduced interaction and partial measurements, and containment control enables maneuvering of multiple followers by multiple leaders. Emergent models include networked Lagrangian systems and networked fractional-order systems. These models result from physical constraints or complex environments in which multi-agent systems operate. In particular, Lagrangian models represent a class of mechanical systems including autonomous vehicles, robotic manipulators, and walking robots, and fractional-order models are more realistic representations of systems operating in complex environments than

integer-order models. Emergent issues include the sampled-data setting, optimality aspect, and time delay. These issues are realistic and important in real-world applications. In particular, the sampled-data setting is relevant when agents interact with their neighbors intermittently rather than continuously, the optimality aspect plays an important role in designing energy-efficient algorithms, and the time delay effect is inevitable in networked systems.

This book is divided into four parts. The first part introduces preliminaries (Chap. 1) and overviews recent research in distributed multi-agent coordination (Chap. 2). The second part introduces emergent problems in distributed multi-agent coordination, namely, collective periodic motion coordination (Chap. 3), collective tracking with a dynamic leader (Chap. 4), and containment control with multiple leaders (Chap. 5). The third part introduces emergent models in distributed multi-agent coordination, namely, networked Lagrangian systems (Chap. 6) and networked fractional-order systems (Chap. 7). The fourth part introduces emergent issues in distributed multi-agent coordination, namely, sampled-data setting (Chap. 8), optimality aspect (Chap. 9), and time delay (Chap. 10). We maintain a website http://www.neng.usu.edu/ece/faculty/wren/book/coordination at which can be found sample simulation and experimental videos and other useful materials associated with the book.

Utah State University, Logan, Utah   Wei Ren
                                                                                                          Yongcan Cao

Acknowledgements

Contents

Part I
Preliminaries and Literature Review

Chapter 1
Preliminaries

This chapter introduces notations used in the book, algebraic graph theory background, algebra and matrix theory background, linear and nonlinear system theory background, nonsmooth analysis background, and time-delay system theory background.

1.1 Notations

$\equiv$	identically equal
$\triangleq$	defined as
$\forall$	for all
$\exists$	if there exists
$\implies$	implies
$\in$	belongs to
$\notin$	does not belong to
$\subset$	a strict subset of
$\subseteq$	a subset of
$\mapsto$	maps to
$\bigcup$	union
$\bigcap$	intersection
$\backslash$	excludes
$\varnothing$	empty set
$\rightarrow$	tends to
$\sum$	summation
$\prod$	left product
$\otimes$	Kronecker product
max	maximum
min	minimum
sup	supremum, the least upper bound
inf	infimum, the greatest lower bound

∞	infinity
$\mathbb{R}$	set of real numbers
$\mathbb{R}^p$	set of $p \times 1$ real vectors
$\mathbb{R}^{m \times n}$	set of $m \times n$ real matrices
$\mathbb{C}$	set of complex numbers
$\mathbb{C}^+$	set of complex numbers with positive real parts
$\mathbb{C}^p$	set of $p \times 1$ complex vectors
$B(x, \epsilon)$	open ball centered at x with radius ϵ
$\mathscr{B}(S)$	set whose elements are all of the possible subsets of $S \subseteq \mathbb{R}^d$
$|z|$	amplitude of number z
$\bar{z}$	complex conjugate of number z
$\arg(z)$	phase of number z
$\mathrm{Re}(z)$	real part of number z
$\mathrm{Im}(z)$	imaginary part of number z
x^T	transpose of a real vector x
$\|x\|$	2-norm of a real vector x
$\|x\|_p$	p-norm of a real vector x
$\|A\|$	induced 2-norm of a real matrix A
$\|A\|_p$	induced p-norm of a real matrix A
$A > 0$	a positive matrix A
$A \geq 0$	a nonnegative matrix A
e^x	exponential of a real number x
e^A	exponential of a real matrix A
$\rho(A)$	spectral radius of matrix A
$\lambda_i(A)$	the ith eigenvalue of matrix A
$\lambda_{\max}(A)$	the maximum eigenvalue of a real symmetric matrix A
$\lambda_{\min}(A)$	the minimum eigenvalue of a real symmetric matrix A
$\det(A)$	determinant of matrix A
$\mathrm{rank}(A)$	rank of matrix A
$\mathrm{diag}(a_1, \ldots, a_p)$	a diagonal matrix with diagonal entries a_1 to a_p
$\mathrm{diag}(A_1, \ldots, A_p)$	a block diagonal matrix with diagonal blocks A_1 to A_p
$\sin$	sine function
$\cos$	cosine function
sgn	signum function
$\tanh$	tangent hyperbolic function
$\Gamma(\cdot)$	Gamma function
$\mathrm{Co}(\cdot)$	convex hull
$d(x, M)$	distance from a point x to a set M, $\inf_{y \in M} \|x - y\|$
$K[\cdot]$	differential inclusion
$D^+ f$	upper right-hand derivative of a function $f(t)$
$\mathfrak{L}\{\cdot\}$	Laplace transform
$\mathbf{1}_p$	$p \times 1$ column vector of all ones
$\mathbf{0}_p$	$p \times 1$ column vector of all zeros
ι	imaginary unit
I_m	$m \times m$ identity matrix

$0_{m \times n}$	$m \times n$ zero matrix
$\mathscr{G}$	graph
$\mathscr{V}$	node set of a graph
$\mathscr{E}$	edge set of a graph
$\mathscr{A}$	adjacency matrix
$\mathscr{L}$	nonsymmetric Laplacian matrix
$\mathscr{N}_i$	neighbor set of agent i

1.2 Algebraic Graph Theory Background

Suppose that a team of agents *interacts* with each other through a *communication* or *sensing network* or a combination of both. It is natural to model the interaction among agents by directed or undirected graphs. Suppose that a team consists of p agents. A *directed graph* of order p is a pair $(\mathscr{V}, \mathscr{E})$, where $\mathscr{V} \triangleq \{1, \ldots, p\}$ is a finite nonempty *node* set and $\mathscr{E} \subseteq \mathscr{V} \times \mathscr{V}$ is an *edge* set of ordered pairs of nodes, called *edges*. We define $\mathscr{G} \triangleq (\mathscr{V}, \mathscr{E})$. The edge (i, j) in the edge set of a directed graph denotes that agent j can obtain information from agent i, but not necessarily *vice versa*. Self-edges (i, i) are not allowed unless otherwise indicated. For the edge (i, j), i is the *parent node* and j is the *child node*. If an edge $(i, j) \in \mathscr{E}$, then node i is a *neighbor* of node j. The set of neighbors of node i is denoted as $\mathscr{N}_i$. In contrast to a directed graph, the pairs of nodes in an *undirected graph* are unordered, where the edge (i, j) denotes that agents i and j can obtain information from each other. Note that an undirected graph can be viewed as a special case of a directed graph, where an edge (i, j) in the undirected graph corresponds to the edges (i, j) and (j, i) in the directed graph. A *weighted graph* associates a weight with every edge in the graph. In this book, all graphs are weighted. The *union* of a collection of graphs is a graph whose node and edge sets are the unions of the node and edge sets of the graphs in the collection.

A *directed path* is a sequence of edges in a directed graph of the form (i_1, i_2), $(i_2, i_3), \ldots$. An *undirected path* in an undirected graph is defined analogously. In a directed graph, a *cycle* is a directed path that starts and ends at the same node. A directed graph is *strongly connected* if there is a directed path from every node to every other node. An undirected graph is *connected* if there is an undirected path between every pair of distinct nodes. An undirected graph is *fully connected* if there is an edge between every pair of distinct nodes. A directed graph is *complete* if there is an edge from every node to every other node. A *directed tree* is a directed graph in which every node has exactly one parent except for one node, called the *root*, which has no parent and which has directed paths to all other nodes. Note that a directed tree has no cycle because every edge is oriented away from the root. In undirected graphs, a *tree* is a graph in which every pair of nodes is connected by exactly one undirected path.
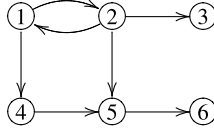
Fig. 1.1 Directed graph among six agents. An *arrow* from node i to node j indicates that agent j can obtain information from agent i. This directed graph contains two directed spanning trees with root nodes 1 and 2 but is not strongly connected because nodes 3, 4, 5, and 6 do not have directed paths to all other nodes

A *subgraph* $(\mathcal{V}^s, \mathcal{E}^s)$ of $(\mathcal{V}, \mathcal{E})$ is a graph such that $\mathcal{V}^s \subseteq \mathcal{V}$ and $\mathcal{E}^s \subseteq \mathcal{E} \cap (\mathcal{V}^s \times \mathcal{V}^s)$. A *directed spanning tree* $(\mathcal{V}^s, \mathcal{E}^s)$ of the directed graph $(\mathcal{V}, \mathcal{E})$ is a subgraph of $(\mathcal{V}, \mathcal{E})$ such that $(\mathcal{V}^s, \mathcal{E}^s)$ is a directed tree and $\mathcal{V}^s = \mathcal{V}$. An *undirected spanning tree* of an undirected graph is defined analogously. The directed graph $(\mathcal{V}, \mathcal{E})$ *has* or *contains* a directed spanning tree if a directed spanning tree is a subgraph of $(\mathcal{V}, \mathcal{E})$. Note that the directed graph $(\mathcal{V}, \mathcal{E})$ has a directed spanning tree if and only if $(\mathcal{V}, \mathcal{E})$ has at least one node with directed paths to all other nodes. In undirected graphs, the existence of an undirected spanning tree is equivalent to being connected. However, in directed graphs, the existence of a directed spanning tree is a weaker condition than being strongly connected. Figure 1.1 shows a directed graph that contains more than one directed spanning tree but is not strongly connected. Nodes 1 and 2 are both roots of directed spanning trees because both have directed paths to all other nodes. However, the directed graph is not strongly connected because nodes 3, 4, 5, and 6 do not have directed paths to all other nodes.

The *adjacency* matrix $\mathcal{A} \triangleq [a_{ij}] \in \mathbb{R}^{p \times p}$ of a directed graph $(\mathcal{V}, \mathcal{E})$ is defined such that a_{ij} is a positive weight if $(j, i) \in \mathcal{E}$, and $a_{ij} = 0$ if $(j, i) \notin \mathcal{E}$. Self-edges are not allowed (i.e., $a_{ii} = 0$) unless otherwise indicated. The adjacency matrix of an undirected graph is defined analogously except that $a_{ij} = a_{ji}$ for all $i \neq j$ because $(j, i) \in \mathcal{E}$ implies $(i, j) \in \mathcal{E}$. Note that a_{ij} denotes the weight for the edge $(j, i) \in \mathcal{E}$. If the weight is not relevant, then a_{ij} is set equal to 1 if $(j, i) \in \mathcal{E}$. The *in-degree* and *out-degree* of node i are defined as, respectively, $\sum_{j=1}^{p} a_{ij}$ and $\sum_{j=1}^{p} a_{ji}$. A node i is *balanced* if $\sum_{j=1}^{p} a_{ij} = \sum_{j=1}^{p} a_{ji}$. A graph is *balanced* if $\sum_{j=1}^{p} a_{ij} = \sum_{j=1}^{p} a_{ji}$, for all i. For an undirected graph, $\mathcal{A}$ is symmetric, and thus every undirected graph is balanced.

Define the matrix $\mathcal{L} \triangleq [\ell_{ij}] \in \mathbb{R}^{p \times p}$ as

$$\ell_{ii} = \sum_{j=1, j \neq i}^{p} a_{ij}, \qquad \ell_{ij} = -a_{ij}, \ i \neq j. \tag{1.1}$$

Note that if $(j, i) \notin \mathcal{E}$ then $\ell_{ij} = -a_{ij} = 0$. The matrix $\mathcal{L}$ satisfies

$$\ell_{ij} \leq 0, \ i \neq j, \quad \sum_{j=1}^{p} \ell_{ij} = 0, \ i = 1, \dots, p. \tag{1.2}$$

For an undirected graph, $\mathscr{L}$ is symmetric and is called the *Laplacian matrix*. However, for a directed graph, $\mathscr{L}$ is not necessarily symmetric and is sometimes called the *nonsymmetric Laplacian matrix* [2] or *directed Laplacian matrix* [160].

Remark 1.1. Note that $\mathscr{L}$ in (1.1) can be equivalently defined as $\mathscr{L} \triangleq D - \mathscr{A}$, where $D \triangleq [d_{ij}] \in \mathbb{R}^{p \times p}$ is the *in-degree matrix* given as $d_{ij} = 0$, $i \neq j$, and $d_{ii} = \sum_{j=1}^{p} a_{ij}$, $i = 1, \ldots, p$. Also note that for directed graphs, the definition of the nonsymmetric Laplacian matrix given by (1.1) is different from the common definition of a Laplacian matrix for a directed graph in the graph theory literature (e.g., [109]). However, we adopt the definition given by (1.1) for directed graphs due to its relevance to coordination algorithms.

In both the undirected and directed cases, because $\mathscr{L}$ has zero row sums, 0 is an eigenvalue of $\mathscr{L}$ with an associated eigenvector $\mathbf{1}_p$. Note that $\mathscr{L}$ is diagonally dominant and has nonnegative diagonal entries. According to Gershgorin's disc theorem (see Lemma 1.18), for an undirected graph, all nonzero eigenvalues of $\mathscr{L}$ are positive ($\mathscr{L}$ is symmetric positive semidefinite), whereas, for a directed graph, all nonzero eigenvalues of $\mathscr{L}$ have positive real parts.

Lemma 1.1 ([1, 248]). *Let $\mathscr{L}$ be the nonsymmetric Laplacian matrix (respectively, Laplacian matrix) associated with the directed graph $\mathscr{G}$ (respectively, the undirected graph $\mathscr{G}$) of order p. Then for the directed graph $\mathscr{G}$ (respectively, the undirected graph $\mathscr{G}$), $\mathscr{L}$ has at least one zero eigenvalue and all its nonzero eigenvalues have positive real parts (respectively, are positive). Furthermore, $\mathscr{L}$ has a simple zero eigenvalue and all other eigenvalues have positive real parts (respectively, are positive) if and only if $\mathscr{G}$ has a directed spanning tree (respectively, is connected). In addition, $\mathscr{L} \mathbf{1}_p = \mathbf{0}_p$ and there exists a nonnegative vector (see Sect. 1.3 for a definition) $\mathbf{p} \in \mathbb{R}^p$ satisfying $\mathbf{p}^T \mathscr{L} = 0_{1 \times p}$ and $\mathbf{p}^T \mathbf{1}_p = 1$.[1]*

Remark 1.1 Note that $\mathscr{L}x$, where $x \triangleq [x_1, \ldots, x_p]^T \in \mathbb{R}^p$, is a column stack vector of $\sum_{j=1}^{p} a_{ij}(x_i - x_j)$, $i = 1, \ldots, p$. If $\mathscr{G}$ is undirected (and hence $\mathscr{L}$ is symmetric), then $x^T \mathscr{L} x = \frac{1}{2} \sum_{i=1}^{p} \sum_{j=1}^{p} a_{ij}(x_i - x_j)^2$. If $\mathscr{G}$ is undirected connected, then Lemma 1.1 implies that $\mathscr{L}x = \mathbf{0}_p$ or $x^T \mathscr{L} x = 0$ if and only if $x_i = x_j$, for all $i, j = 1, \ldots, p$.

For an undirected graph, let $\lambda_i(\mathscr{L})$ be the ith eigenvalue of $\mathscr{L}$ with $\lambda_1(\mathscr{L}) \leq \lambda_2(\mathscr{L}) \leq \cdots \leq \lambda_p(\mathscr{L})$, so that $\lambda_1(\mathscr{L}) = 0$. For an undirected graph, $\lambda_2(\mathscr{L})$ is the *algebraic connectivity*, which is positive if and only if the undirected graph is connected according to Lemma 1.1. The algebraic connectivity quantifies the convergence rate of consensus algorithms [148].

Lemma 1.2 ([214]). *Let $\mathscr{L}$ be the nonsymmetric Laplacian matrix associated with the directed graph $\mathscr{G}$. If $\mathscr{G}$ is balanced, then $x^T \mathscr{L} x \geq 0$, where $x \triangleq [x_1, \ldots, x_p]^T \in \mathbb{R}^p$. If $\mathscr{G}$ is strongly connected and balanced, then $x^T \mathscr{L} x = 0$ if and only $x_i = x_j$, for all $i, j = 1, \ldots, p$.*

---

[1] Here, $\mathbf{1}_p$ and $\mathbf{p}$ are, respectively, right and left eigenvectors of $\mathscr{L}$ associated with the zero eigenvalue. If $\mathscr{G}$ has a directed spanning tree (respectively, is connected), then $\mathbf{p}$ is unique.

Lemma 1.3 ([248, Lemma 2.10]). *Suppose that* $z \triangleq [z_1^T, \ldots, z_p^T]^T$ *with* $z_i \in \mathbb{R}^m$. *Let* $\mathscr{A} \in \mathbb{R}^{p \times p}$ *and* $\mathscr{L} \in \mathbb{R}^{p \times p}$ *be, respectively, the adjacency matrix and the nonsymmetric Laplacian matrix associated with the directed graph* $\mathscr{G}$. *Then the following five conditions are equivalent.*

(i) $\mathscr{L}$ *has a simple zero eigenvalue with an associated eigenvector* $\mathbf{1}_p$ *and all other eigenvalues have positive real parts;*
(ii) $(\mathscr{L} \otimes I_m)z = 0$ *if and only if* $z_1 = \cdots = z_p$;
(iii) *Consensus is reached for the closed-loop system* $\dot{z} = -(\mathscr{L} \otimes I_m)z$ *or equivalently* $\dot{z}_i = -\sum_{j=1}^n a_{ij}(z_i - z_j)$, *where* a_{ij} *is the* (i,j)*th entry of* $\mathscr{A}$. *That is, for all* $z_i(0)$ *and all* $i, j = 1, \ldots, p$, $\|z_i(t) - z_j(t)\| \to 0$ *as* $t \to \infty$;
(iv) *The directed graph* $\mathscr{G}$ *has a directed spanning tree;*
(v) *The rank of* $\mathscr{L}$ *is* $p - 1$.

Lemma 1.4 ([248, Lemma 2.11]). *Suppose that* z, $\mathscr{A}$, *and* $\mathscr{L}$ *are defined in Lemma* 1.3. *Then the following four conditions are equivalent.*

(i) *The directed graph* $\mathscr{G}$ *has a directed spanning tree and node* k *has no neighbor;*[2]
(ii) *The directed graph* $\mathscr{G}$ *has a directed spanning tree and every entry of the* k*th row of* $\mathscr{L}$ *is zero;*
(iii) *Consensus is reached for the closed-loop system* $\dot{z} = -(\mathscr{L} \otimes I_m)z$ *or equivalently* $\dot{z}_i = -\sum_{j=1}^n a_{ij}(z_i - z_j)$. *In particular, for all* $z_i(0)$ *and all* $i = 1, \ldots, p$, $z_i(t) \to z_k(0)$ *as* $t \to \infty$;
(iv) *Node* k *is the only node that has directed paths to all other nodes in* $\mathscr{G}$.

Lemma 1.5 ([248, Theorem 2.33]). *Let* $\mathscr{A}(t) \in \mathbb{R}^{p \times p}$ *and* $\mathscr{L}(t) \in \mathbb{R}^{p \times p}$ *be, respectively, the adjacency matrix and the nonsymmetric Laplacian matrix associated with the directed graph* $\mathscr{G}(t) \triangleq [\mathscr{V}(t), \mathscr{E}(t)]$. *Suppose that* $\mathscr{A}(t)$ *is piecewise continuous and its nonzero and hence positive entries are both uniformly lower and upper bounded (i.e.,* $a_{ij}(t) \in [\underline{a}, \overline{a}]$, *where* $0 < \underline{a} < \overline{a}$, *if* $(j,i) \in \mathscr{E}(t)$ *and* $a_{ij}(t) = 0$ *otherwise). Let* $t_0, t_1, \ldots$ *be the time sequence corresponding to the times at which* $\mathscr{A}(t)$ *switches, where it is assumed that* $t_i - t_{i-1} \geq t_L$, $\forall i = 1, 2, \ldots$ *with* t_L *a positive constant. Consensus is reached for the closed-loop system* $\dot{z} = -[\mathscr{L}(t) \otimes I_m]z$ *or equivalently* $\dot{z}_i = -\sum_{j=1}^n a_{ij}(t)(z_i - z_j)$ *if there exists an infinite sequence of contiguous, nonempty, uniformly bounded time-intervals* $[t_{i_j}, t_{i_{j+1}})$, $j = 1, 2, \ldots$, *starting at* $t_{i_1} = t_0$, *with the property that the union of* $\mathscr{G}(t)$ *across each such interval has a directed spanning tree.*

Lemma 1.6. *Let* $\mathscr{G}$ *be the directed graph (respectively, undirected graph) for* p *followers, labeled as agents or followers* 1 *to* p. *Let* $\mathscr{A} \triangleq [a_{ij}] \in \mathbb{R}^{p \times p}$ *and* $\mathscr{L} \in \mathbb{R}^{p \times p}$ *be, respectively, the adjacency matrix and the nonsymmetric Laplacian matrix (respectively, Laplacian matrix) associated with* $\mathscr{G}$. *Suppose that in addition to the* p *followers, there exists a leader, labeled as agent* 0. *Let* $\overline{\mathscr{G}}$ *be the corresponding directed graph for agents* 0 *to* p *(i.e., the leader and all followers). Let*

---

[2] At most one such node can exist when the directed graph has a directed spanning tree.

$\overline{\mathscr{A}} \in \mathbb{R}^{(p+1)\times(p+1)}$ *and* $\overline{\mathscr{L}} \in \mathbb{R}^{(p+1)\times(p+1)}$ *be the corresponding adjacency and nonsymmetric Laplacian matrix associated with* $\overline{\mathscr{G}}$. *Here* $\overline{\mathscr{A}} \triangleq \left[\begin{smallmatrix} 0 & 0_{1\times p} \\ a & \mathscr{A} \end{smallmatrix}\right]$, *where* $\overline{a} \triangleq [a_{10}, \dots, a_{p0}]^T$ *and* $a_{i0} > 0$, $i = 1, \dots, p$, *if agent* 0 *is a neighbor of agent* i *and* $a_{i0} = 0$ *otherwise, and* $\overline{\mathscr{L}} \triangleq \left[\begin{smallmatrix} 0 & 0_{1\times p} \\ -\overline{a} & H \end{smallmatrix}\right]$, *where* $H \triangleq \mathscr{L} + \mathrm{diag}\,(a_{10}, \dots, a_{p0})$.[3] *When* $\mathscr{G}$ *is directed* (*respectively, undirected*), *all eigenvalues of* H *have positive real parts* (*respectively,* H *is symmetric positive definite*) *if and only if in the directed graph* $\overline{\mathscr{G}}$ *the leader has directed paths to all followers.*

Proof: Note that in the directed graph $\overline{\mathscr{G}}$, the leader has no neighbor. Therefore, it follows from Lemma 1.4 that the condition that in $\overline{\mathscr{G}}$ the leader has directed paths to all followers is equivalent to the condition that $\overline{\mathscr{G}}$ has a directed spanning tree and the leader has no neighbor. It follows from Lemma 1.3 that rank$(\overline{\mathscr{L}}) = p$ if and only if $\overline{\mathscr{G}}$ has a directed spanning tree. Note that rank$(\overline{\mathscr{L}}) = $ rank$([-\overline{a}|H])$. Because each row sum of $\overline{\mathscr{L}}$ is zero, it follows that $-\overline{a} + H\mathbf{1}_p = \mathbf{0}_p$, which implies that for the p by $p + 1$ matrix $[-\overline{a}|H]$ its first column is dependent on its last p columns. It thus follows that rank$([-\overline{a}|H]) = $ rank(H). Therefore, it follows that rank$(H) = p$ or equivalently H has full rank and hence has no zero eigenvalue if and only if in $\overline{\mathscr{G}}$ the leader has directed paths to all followers. Note that H is diagonally dominant and has nonnegative diagonal entries. It follows from Gershgorin's disc theorem (see Lemma 1.18) that all nonzero eigenvalues of H have positive real parts. Combining the above arguments shows that when $\mathscr{G}$ is directed, all eigenvalues of H have positive real parts if and only if in $\overline{\mathscr{G}}$ the leader has directed paths to all followers. When $\mathscr{G}$ is undirected, H is symmetric. It thus follows that H is symmetric positive definite if and only if in $\overline{\mathscr{G}}$ the leader has directed paths to all followers. ∎

Remark 1.2 Suppose that $\mathscr{G}$ is undirected. A special case of Lemma 1.6 is that if $\mathscr{G}$ is connected and at least one $a_{i0} > 0$, then H is symmetric positive definite. Another special case is that if all $a_{i0} > 0$, then H is symmetric positive definite.

Given a matrix $S \triangleq [s_{ij}] \in \mathbb{R}^{p\times p}$, the *directed graph of* S, denoted by $\mathbb{D}(S)$, is the directed graph with node set $\mathscr{V} \triangleq \{1, \dots, p\}$ such that there is an edge in $\mathbb{D}(S)$ from j to i if and only if $s_{ij} \neq 0$ (cf. [122, p. 357]). In other words, the entries of the adjacency matrix satisfy $a_{ij} > 0$ if $s_{ij} \neq 0$ and $a_{ij} = 0$ if $s_{ij} = 0$.

1.3 Algebra and Matrix Theory Background

We need the following definitions and lemmas from algebra and matrix theory.

A vector x or a matrix A is *nonnegative* (respectively, *positive*), denoted as $x \geq 0$ (respectively, $x > 0$) or $A \geq 0$ (respectively, $A > 0$), if all of its components

---

[3] Note that here for convenience we label the agents from 0 to p rather than from 1 to $p + 1$ and hence the entries of $\overline{\mathscr{A}}$ and $\overline{\mathscr{L}}$ are labeled accordingly. Also note that according to $\overline{\mathscr{A}}$, the leader has no neighbor.

or entries are nonnegative (respectively, positive). Given two nonnegative matrices $A, B \in \mathbb{R}^{p \times q}$, $A \geq B$ (respectively, $A > B$) denotes that $A - B$ is nonnegative (respectively, positive). Given two nonnegative square matrices A and B, if $A \geq \gamma B$, where γ is a positive scalar, the directed graph of B is a subgraph of the directed graph of A.

A square nonnegative matrix is *row stochastic* if all of its row sums are 1 [122, p. 526]. Every $n \times n$ row-stochastic matrix has 1 as an eigenvalue with an associated eigenvector $\mathbf{1}_n$. The spectral radius of a row-stochastic matrix is 1 because 1 is an eigenvalue and Gershgorin's disc theorem (see Lemma 1.18) implies that all of the eigenvalues are contained in a closed unit disc. It is straightforward to verify that the product of two row-stochastic matrices is still a row-stochastic matrix. A row-stochastic matrix $P \in \mathbb{R}^{n \times n}$ is called *indecomposable and aperiodic* (SIA) if $\lim_{k \to \infty} P^k = \mathbf{1}_n y^T$, where y is some $n \times 1$ column vector [304].

Lemma 1.7 ([122, Lemma 8.2.7 part(i), p. 498]). *Let $A \in \mathbb{R}^{n \times n}$ be given, let $\lambda \in \mathbb{C}$ be given, and suppose that x and y are vectors such that* (i) $Ax = \lambda x$, (ii) $A^T y = \lambda y$, *and* (iii) $x^T y = 1$. *If $|\lambda| = \rho(A) > 0$, where λ is the only eigenvalue of A with modulus $\rho(A)$, then $\lim_{m \to \infty} (\lambda^{-1} A)^m = x y^T$.*

Lemma 1.8 ([132]). *Let $m \geq 2$ be a positive integer and let $P_1, P_2, \ldots, P_m$ be nonnegative $n \times n$ matrices with positive diagonal entries, then $P_1 P_2 \cdots P_m \geq \gamma(P_1 + P_2 + \cdots + P_m)$, where γ is a positive scalar and can be specified from the matrices P_i, $i = 1, \ldots, m$.*

Lemma 1.9 ([248, Corollary 2.18, Lemma 2.19]). *Suppose that $A \in \mathbb{R}^{n \times n}$ is a row-stochastic matrix with positive diagonal entries. If the directed graph of A has a directed spanning tree, then A is SIA.*

Lemma 1.10 ([248, Lemma 2.16]). *Suppose that a nonnegative matrix $A \in \mathbb{R}^{n \times n}$ has the same row sums given by μ. Then μ is an eigenvalue of A with an associated eigenvector $\mathbf{1}_n$ and $\rho(A) = \mu$. The matrix A has a simple eigenvalue equal to μ if and only if the directed graph of A has a directed spanning tree.*

Lemma 1.11 ([248, Theorem 2.20]). *Suppose that $z \triangleq [z_1^T, \ldots, z_p^T]^T$ with $z_i \in \mathbb{R}^m$. Let $\mathscr{G} \triangleq (\mathscr{V}, \mathscr{E})$ be the directed graph associated with p agents. Given the system $z[k+1] = (D \otimes I_m) z[k]$, where k is the discrete-time index, and $D \triangleq [d_{ij}] \in \mathbb{R}^{p \times p}$ is a row-stochastic matrix with positive diagonal entries satisfying that $d_{ij} > 0$, $\forall i \neq j$, if $(j, i) \in \mathscr{E}$ and $d_{ij} = 0$ otherwise. Then consensus is reached, that is, for all $z_i[0]$ and all $i, j = 1, \ldots, p$, $\|z_i[k] - z_j[k]\| \to 0$ as $t \to \infty$, if and only if $\mathscr{G}$ has a directed spanning tree.*

Lemma 1.12 ([304]). *Let $S_1, S_2, \ldots, S_k \in \mathbb{R}^{n \times n}$ be a finite set of SIA matrices with the property that for each sequence $S_{i_1}, S_{i_2}, \ldots, S_{i_j}$ of positive length, the matrix product $S_{i_j} S_{i_{j-1}} \cdots S_{i_1}$ is SIA. Then, for each infinite sequence $S_{i_1}, S_{i_2}, \ldots$, there exists a column vector y such that*

$$\lim_{j \to \infty} S_{i_j} S_{i_{j-1}} \cdots S_{i_1} = \mathbf{1}_n y^T.$$

Definition 1.1 ([4]). A matrix $D \in \mathbb{R}^{n \times n}$ is called *semiconvergent* if $\lim_{k \to \infty} D^k$ exists.

Lemma 1.13 ([4]). *Let there be a nonnegative matrix $P \triangleq [p_{ij}] \in \mathbb{R}^{n \times n}$, where $\rho(P) \leq 1$ and $p_{ii} > 0$. Let $\alpha \geq 1$. Then the following three statements hold*:

(a) *There exists a nonnegative matrix $B \in \mathbb{R}^{n \times n}$, where $\rho(B) \leq \alpha$ and $I_n - P = (\alpha I_n - B)^2$, if and only if the iteration method*

$$X_{i+1} = \frac{1}{2\alpha}\big[P + (\alpha^2 - 1)I_n + X_i^2\big], \quad X_0 = 0_{n \times n}, \tag{1.3}$$

is convergent. In this case, $B \geq X^\star = \lim_{i \to \infty} X_i$, $X^\star \geq 0$, $\rho(X^\star) \leq \alpha$, $\operatorname{diag}_i(X^\star) > 0$, where $\operatorname{diag}_i(\cdot)$ denotes the ith diagonal entry of a square matrix, $i = 1, \ldots, n$, and $(\alpha I_n - X^\star)^2 = I_n - P$.

(b) *If (1.3) is convergent, it follows that P and $\frac{X^\star}{\alpha}$ are semiconvergent.*

(c) *If P is semiconvergent, then (1.3) is convergent for all $\alpha \geq 1$. Denote in this case the limit of the iteration method*

$$Y_{i+1} = \frac{1}{2}\big(P + Y_i^2\big), \quad Y_0 = 0_{n \times n},$$

by $Y^\star$. The equation $\alpha I_n - X^\star = I_n - Y^\star$ holds.

Definition 1.2 ([4]). Let $\alpha \in \mathbb{R}$ and $C \in \mathbb{R}^{n \times n}$. A matrix $B \triangleq [b_{ij}] \in \mathbb{R}^{n \times n}$ is called an *M-matrix* if it can be written as

$$B = \alpha I_n - C,$$

where $\alpha > 0, C \geq 0$, and $\rho(C) \leq \alpha$. The matrix B is called a *nonsingular M-matrix* if $\rho(C) < \alpha$.

Lemma 1.14 ([4]). *An M-matrix $B \in \mathbb{R}^{n \times n}$ has exactly one M-matrix as its square root if the characteristic polynomial of B has at most one simple zero root.*

Lemma 1.15. *An $n \times n$ M-matrix that has a zero eigenvalue with a corresponding eigenvector $\mathbf{1}_n$ is a nonsymmetric Laplacian matrix.*

Proof: The proof follows from Definition 1.2 and the definition of a nonsymmetric Laplacian matrix. ∎

Lemma 1.16 ([4]). *Let $Z^{n \times n} \triangleq \{B = [b_{ij}] \in \mathbb{R}^{n \times n} | b_{ij} \leq 0, i \neq j\}$. A matrix $B \in Z^{n \times n}$ is a nonsingular M-matrix if and only if B has a square root that is a nonsingular M-matrix.*

Lemma 1.17 ([4]). *A matrix $B \in Z^{n \times n}$, where $Z^{n \times n}$ is defined in Lemma 1.16, is a nonsingular M-matrix if and only if B^{-1} exists and B^{-1} is nonnegative.*

Lemma 1.18 ([122, Theorem 6.1.1 (Gershgorin's disc theorem), p. 344]). *Let* $A \triangleq [a_{ij}] \in \mathbb{R}^{n \times n}$*, and let*

$$R_i'(A) \triangleq \sum_{j=1, j \neq i}^{n} |a_{ij}|, \quad i = 1, \ldots, n,$$

denote the deleted absolute row sums of A. Then all eigenvalues of A are located in the union of n discs

$$\bigcup_{i=1}^{n} \{ z \in \mathbb{C} : |z - a_{ii}| \leq R_i'(A) \}.$$

Furthermore, if a union of k of these n discs forms a connected region that is disjoint from all of the remaining $n - k$ discs, then there are precisely k eigenvalues of A in this region.

Lemma 1.19 (Hölder inequality). *Let* $1 \leq p, q \leq \infty$ *with* $\frac{1}{p} + \frac{1}{q} = 1$*. Then, for all vectors* $f \in \mathbb{R}^k$ *and* $g \in \mathbb{R}^k$,

$$\left| f^T g \right| \leq \|f\|_p \|g\|_q.$$

Lemma 1.20 (See e.g., [125]). *Given a rotation matrix* $R \in \mathbb{R}^{3 \times 3}$*, let* $\mathbf{a} \triangleq [a_1, a_2, a_3]^T$ *and* θ *denote, respectively, the Euler axis (i.e., the unit vector in the direction of rotation) and the Euler angle (i.e., the rotation angle). The eigenvalues of R are 1, $e^{\iota\theta}$, and $e^{-\iota\theta}$ with associated right eigenvectors given by, respectively,* $\varsigma_1 = \mathbf{a}$, $\varsigma_2 = [(a_2^2 + a_3^2) \sin^2(\frac{\theta}{2}), -a_1 a_2 \sin^2(\frac{\theta}{2}) + \iota a_3 \sin(\frac{\theta}{2}) |\sin(\frac{\theta}{2})|,$ $-a_1 a_3 \sin^2(\frac{\theta}{2}) - \iota a_2 \sin(\frac{\theta}{2}) |\sin(\frac{\theta}{2})|]^T$*, and* $\varsigma_3 = \overline{\varsigma}_2$ *and associated left eigenvectors given by, respectively,* $\varpi_1 = \varsigma_1$, $\varpi_2 = \overline{\varsigma}_2$*, and* $\varpi_3 = \overline{\varsigma}_3$.

Lemma 1.21 ([111, 163]). *Suppose that* $U \in \mathbb{R}^{p \times p}$*,* $V \in \mathbb{R}^{q \times q}$*,* $X \in \mathbb{R}^{p \times p}$*, and* $Y \in \mathbb{R}^{q \times q}$*. The following statements are true.*

(i) $(U + X) \otimes V = U \otimes V + X \otimes V$.
(ii) $(U \otimes V)(X \otimes Y) = UX \otimes VY$.
(iii) $(U \otimes V)^T = U^T \otimes V^T$.
(iv) *Suppose that U and V are invertible. Then* $(U \otimes V)^{-1} = U^{-1} \otimes V^{-1}$.
(v) *If U and V are symmetric, so is $U \otimes V$.*
(vi) *If U and V are symmetric positive definite (respectively, positive semidefinite), so is $U \otimes V$.*
(vii) *Suppose that U has the eigenvalues β_i with associated eigenvectors $f_i \in \mathbb{C}^p$, $i = 1, \ldots, p$, and V has the eigenvalues ρ_j with associated eigenvectors $g_j \in \mathbb{C}^q$, $j = 1, \ldots, q$. Then the pq eigenvalues of $U \otimes V$ are $\beta_i \rho_j$ with associated eigenvectors $f_i \otimes g_j$, $i = 1, \ldots, p$, $j = 1, \ldots, q$.*

Lemma 1.22 ([155, Schur's formula]). *Let* $A_{11}, A_{12}, A_{21}, A_{22} \in \mathbb{R}^{n \times n}$ *and* $M = \begin{bmatrix} A_{11} & A_{12} \\ A_{21} & A_{22} \end{bmatrix}$*. Then* $\det(M) = \det(A_{11} A_{22} - A_{12} A_{21})$ *if* A_{11}*,* A_{12}*,* A_{21}*, and* A_{22} *commute pairwise.*

Lemma 1.23 ([228]). *For any $a, b \in \mathbb{R}^n$ and any symmetric positive-definite matrix $\Phi \in \mathbb{R}^{n \times n}$, $2a^T b \leq a^T \Phi^{-1} a + b^T \Phi b$.*

Lemma 1.24 ([122, Theorem 4.2.2 (Rayleigh-Ritz theorem), p. 176]). *Let $A \in \mathbb{R}^{n \times n}$ be symmetric. Then $\lambda_{\min}(A) x^T x \leq x^T A x \leq \lambda_{\max}(A) x^T x$ for all $x \in \mathbb{R}^n$, $\lambda_{\min}(A) = \min_{x \neq \mathbf{0}_n} \frac{x^T A x}{x^T x} = \min_{x^T x = 1} \frac{x^T A x}{x^T x}$, and $\lambda_{\max}(A) = \max_{x \neq \mathbf{0}_n} \frac{x^T A x}{x^T x} = \max_{x^T x = 1} \frac{x^T A x}{x^T x}$.*

Lemma 1.25 ([122, Theorem 5.6.9]). *Let $A \in \mathbb{R}^{n \times n}$. If $\| \cdot \|$ is any matrix norm, then $\rho(A) \leq \|A\|$.*

Lemma 1.26 ([122, Lemma 5.6.10]). *Let $A \in \mathbb{R}^{n \times n}$ and $\varepsilon > 0$. There is a matrix norm $\| \cdot \|$ such that $\rho(A) \leq \|A\| \leq \rho(A) + \varepsilon$.*

Lemma 1.27 ([122, Theorem 5.6.12]). *Let $A \in \mathbb{R}^{n \times n}$. Then $\lim_{k \to \infty} A^k = 0_{n \times n}$ if and only if $\rho(A) < 1$.*

Lemma 1.28 ([122, Corollary 5.6.16]). *Let $A \in \mathbb{R}^{n \times n}$. If $\| \cdot \|$ is a matrix norm and $\|A\| < 1$. Then $I_n - A$ is invertible and $(I_n - A)^{-1} = \sum_{i=0}^{\infty} A^i$.*

1.4 Linear and Nonlinear System Theory Background

We need the following definitions and lemmas from linear and nonlinear system theory.

Consider a linear time-invariant system given by

$$\dot{x} = Ax + Bu, \tag{1.4}$$

where $x \in \mathbb{R}^n$ is the state vector, $u \in \mathbb{R}^m$ is the control input, $A \in \mathbb{R}^{n \times n}$, and $B \in \mathbb{R}^{n \times m}$. The solution to (1.4) is given by

$$x(t) = e^{A(t-t_0)} x(t_0) + \int_{t_0}^t e^{A(t-\tau)} Bu(\tau) \, d\tau.$$

Letting $t_0 = kT$ and $t = (k+1)T$, where k is the discrete-time index and T is the sampling period, we can obtain the exact discrete-time model as

$$x(kT + T) = e^{AT} x(kT) + \int_{kT}^{kT+T} e^{A(kT+T-\tau)} Bu(\tau) \, d\tau.$$

With zero-order hold, the control input becomes $u(t) = u(kT)$, $kT \leq t < (k+1)T$. It then follows that

$$x[k + 1] = e^{AT} x[k] + \left(\int_0^T e^{A\sigma} \, d\sigma \right) Bu[k],$$

where $x[k] \stackrel{\triangle}{=} x(kT)$ and $u[k] \stackrel{\triangle}{=} u(kT)$.

Definition 1.3 ([66]). A function $f : \mathbb{R}^d \mapsto \mathbb{R}^m$ is *locally Lipschitz* at $x \in \mathbb{R}^d$ if there exist $L_x, \epsilon \in (0, \infty)$ such that

$$\left\| f(y) - f(y') \right\| \leq L_x \| y - y' \|,$$

for all $y, y' \in B(x, \epsilon)$.

Definition 1.4 ([272, Chap. 3]). Consider the autonomous system

$$\dot{x} = f(x), \tag{1.5}$$

where $f : D \mapsto \mathbb{R}^n$ is a locally Lipschitz map from a domain $D \subseteq \mathbb{R}^n$ into $\mathbb{R}^n$. Let $x = \mathbf{0}_n$ be an equilibrium point for (1.5). Then an equilibrium point $x = \mathbf{0}_n$ is said to be *stable* if, for any $\epsilon_1 > 0$, there exists $\epsilon_2 > 0$, such that if $\| x(0) \| < \epsilon_2$, then $\| x(t) \| < \epsilon_1$ for every $t \geq 0$. The equilibrium point $x = \mathbf{0}_n$ is *asymptotically stable* if it is stable, and if in addition there exists some $\epsilon_3 > 0$ such that $\| x(0) \| < \epsilon_3$ implies that $x(t) \to \mathbf{0}_n$ as $t \to \infty$. The equilibrium point $x = \mathbf{0}_n$ is *exponentially stable* if there exist two strictly positive numbers ϵ_4 and ϵ_5 such that

$$\forall t \geq 0, \quad \left\| x(t) \right\| \leq \epsilon_4 \left\| x(0) \right\| e^{-\epsilon_5 t}$$

in some ball around the origin. If the stability of the equilibrium point $x = \mathbf{0}_n$ holds for all initial states, $x = \mathbf{0}_n$ is said to be *globally stable*. The equilibrium point $x = \mathbf{0}_n$ is *globally asymptotically stable* (respectively, *globally exponentially stable*) when $x = \mathbf{0}_n$ is asymptotically stable (respectively, exponentially stable) for all initial states.

Lemma 1.29 ([147, Theorem 4.2]). *Let* $x = \mathbf{0}_n$ *be an equilibrium point for* (1.5). *Let* $V : \mathbb{R}^n \mapsto \mathbb{R}$ *be a continuously differentiable function such that*

- $V(\mathbf{0}_n) = 0$ *and* $V(x) > 0$, $\forall x \neq \mathbf{0}_n$,
- $\| x \| \to \infty \implies V(x) \to \infty$,[4]
- $\dot{V}(x) < 0$, $\forall x \neq \mathbf{0}_n$.

Then $x = \mathbf{0}_n$ *is globally asymptotically stable.*

Definition 1.5 ([147, p. 127]). A set M is said to be an *invariant set* with respect to (1.5) if $x(0) \in M$ implies $x(t) \in M$, $\forall t \in \mathbb{R}$. A set M is said to be a *positively invariant set* if $x(0) \in M$ implies $x(t) \in M$, $\forall t \geq 0$.

Lemma 1.30 ([272, Theorem 3.4 (Local Invariance Set Theorem)]). *Consider the autonomous system* (1.5). *Let* $V : \mathbb{R}^n \mapsto \mathbb{R}$ *be a continuously differentiable function. Assume that*

- *For some* $c > 0$, *the region* Ω_c *defined by* $V(x) < c$ *is bounded*;
- $\dot{V}(x) \leq 0$, $\forall x \in \Omega_c$.

---

[4] A function satisfying this condition is said to be *radially unbounded.*

Let E be the set of all points in Ω_c where $\dot{V}(x) = 0$, and let M be the largest invariant set in E. Then every solution $x(t)$ starting in Ω_c approaches M, as $t \to \infty$.

Lemma 1.31 ([272, Theorem 3.5 (Global Invariance Set Theorem)]). *Consider the autonomous system* (1.5). *Let $V : \mathbb{R}^n \mapsto \mathbb{R}$ be a continuously differentiable function. Assume that*

- $\dot{V}(x) \leq 0$, $\forall x \in \mathbb{R}^n$;
- $V(x) \to \infty$ as $\|x\| \to \infty$.

Let E be the set of all points where $\dot{V}(x) = 0$, and let M be the largest invariant set in E. Then all solutions globally asymptotically converge to M, as $t \to \infty$.

Definition 1.6 ([147, Chap. 4]). Consider the nonautonomous system

$$\dot{x} = f(t, x), \tag{1.6}$$

where $f : [0, \infty) \times D \mapsto \mathbb{R}^n$ is piecewise continuous in t and locally Lipschitz in x on $[0, \infty) \times D$, and $D \subset \mathbb{R}^n$ is a domain that contains the origin $x = \mathbf{0}_n$. Let $x = \mathbf{0}_n$ be an equilibrium point for (1.6) at $t = t_0 \geq 0$, i.e., $f(t, t_0) = \mathbf{0}_n, \forall t \geq t_0$. Then the equilibrium point $x = \mathbf{0}_n$ is said to be *stable* if, for any $\epsilon_1 > 0$, there exists $\epsilon_2 = \epsilon_2(\epsilon_1, t_0) > 0$, such that if $\|x(t_0)\| < \epsilon_2$, then $\|x(t)\| < \epsilon_1$ for every $t \geq t_0$. The equilibrium point $x = \mathbf{0}_n$ is *uniformly stable* if it is stable and $\epsilon_2 = \epsilon_2(\epsilon_1) > 0$ is independent of t_0. The equilibrium point $x = \mathbf{0}_n$ is *asymptotically stable* if it is stable, and if in addition there exists some $\epsilon_3 = \epsilon_3(t_0) > 0$ such that $\|x(t_0)\| < \epsilon_3$ implies that $x(t) \to \mathbf{0}_n$ as $t \to \infty$. The equilibrium point $x = \mathbf{0}_n$ is *uniformly asymptotically stable* if it is asymptotically stable and $\epsilon_3 > 0$ is independent of t_0. The equilibrium point $x = \mathbf{0}_n$ is *exponentially stable* if there exist three strictly positive numbers $\epsilon_4 = \epsilon_4(t_0)$, $\epsilon_5 = \epsilon_5(t_0)$, and $\epsilon_6 = \epsilon_6(t_0)$ such that for $t \geq t_0$

$$\|x(t)\| \leq \epsilon_4 \|x(t_0)\| e^{-\epsilon_5(t-t_0)}, \quad \forall \|x(t_0)\| < \epsilon_6.$$

The equilibrium point $x = \mathbf{0}_n$ is *uniformly exponentially stable* if it is exponentially stable, and $\epsilon_4 > 0$, $\epsilon_5 > 0$, and $\epsilon_6 > 0$ are independent of t_0. If the (uniform) stability of the equilibrium point $x = \mathbf{0}_n$ holds for all initial states $x(t_0)$, $x = \mathbf{0}_n$ is said to be *globally (uniformly) stable*. The equilibrium point $x = \mathbf{0}_n$ is *globally (uniformly) asymptotically stable* [respectively, *globally (uniformly) exponentially stable*] when $x = \mathbf{0}_n$ is (uniformly) asymptotically stable [respectively, (uniformly) exponentially stable] for all initial states $x(t_0)$.

Lemma 1.32 ([147, Theorems 4.8 and 4.9]). *Let $x = \mathbf{0}_n$ be an equilibrium point for* (1.6) *and $D \subset \mathbb{R}^n$ be a domain that contains $x = \mathbf{0}_n$. Let $V : [0, \infty) \times D \mapsto \mathbb{R}$ be a continuously differentiable function such that*

$$W_1(x) \leq V(t, x) \leq W_2(x),$$

$$\frac{\partial V}{\partial t} + \frac{\partial V}{\partial x} f(t, x) \leq 0 \tag{1.7}$$

for any $t \geq 0$ and $x \in D$, where $W_1(x)$ and $W_2(x)$ are continuous positive-definite functions on D. Then $x = \mathbf{0}_n$ is uniformly stable. Suppose that $V : [0, \infty) \times D \mapsto \mathbb{R}$ is a continuously differentiable function satisfying (1.7) *and*

$$\frac{\partial V}{\partial t} + \frac{\partial V}{\partial x} f(t, x) \leq -W_3(x)$$

for any $t \geq 0$ and $x \in D$, where $W_3(x)$ is a continuous positive-definite function on D. Then $x = \mathbf{0}_n$ is uniformly asymptotically stable. Moreover, if $D \in \mathbb{R}^n$ and $W_1(x)$ is radially unbounded, then $x = \mathbf{0}_n$ is globally uniformly asymptotically stable.

Definition 1.7 ([272, p. 123]). A function g is said to be *uniformly continuous* on $[0, \infty)$ if

$$\forall R > 0, \ \exists \eta(R) > 0, \ \forall t_1 > 0, \ t > 0, \ |t - t_1| < \eta \implies |g(t) - g(t_1)| < R.$$

Lemma 1.33 ([272, Lemma 4.2 (Barbalat)]). *If the differentiable function $f(t)$ has a finite limit, as $t \to \infty$, and if $\dot{f}(t)$ is uniformly continuous,[5] then $\dot{f}(t) \to 0$, as $t \to \infty$.*

Lemma 1.34 ([272, Lemma 4.3 (Lyapunov-like Lemma)]). *If a scalar function $V(t, x)$ satisfies the following conditions*:

- $V(t, x)$ *is lower bounded*;
- $\dot{V}(t, x)$ *is negative semidefinite*;
- $\dot{V}(t, x)$ *is uniformly continuous in t*;

then $\dot{V}(t, x) \to 0$, as $t \to \infty$.[6]

Definition 1.8 ([147, Definition 4.2, p. 144]). A continuous function $\alpha : [0, a) \mapsto [0, \infty)$ is said to belong to *class $\mathscr{K}$* if it is strictly increasing and $\alpha(0) = 0$. It is said to belong to *class $\mathscr{K}_\infty$* if $a = \infty$ and $\alpha(r) \to \infty$, as $r \to \infty$.

Lemma 1.35 ([146, Lemma 3.5]). *Let $V(x) : D \mapsto \mathbb{R}$ be a continuous positive-definite function defined on a domain $D \subset \mathbb{R}^n$ that contains the origin $x = \mathbf{0}_n$. Let $B(\mathbf{0}_n, r) \subset D$ for some $r > 0$. Then, there exist class $\mathscr{K}$ functions α_1 and α_2, defined on $[0, r]$, such that*

$$\alpha_1(\|x\|) \leq V(x) \leq \alpha_2(\|x\|)$$

for all $x \in B(\mathbf{0}_n, r)$. Moreover, if $D = \mathbb{R}^n$ and $V(x)$ is radially unbounded, then α_1 and α_2 can be chosen to belong to class $\mathscr{K}_\infty$ and the foregoing inequality holds for all $x \in \mathbb{R}^n$.

---

[5] A sufficient condition for a differentiable function to be uniformly continuous is that its derivative is bounded.

[6] Lemma 1.34 follows from Lemma 1.33.

Lemma 1.36 (Matrosov's theorem restated in [158, 220]). *Given the nonautonomous system* (1.6), *where* $f(t, \mathbf{0}_n) \equiv \mathbf{0}_n$ *and* f *is such that solutions exist and are unique. Let* $V(t, x)$ *and* $W(t, x)$ *be continuous functions on domain* $[0, \infty) \times D$ *and satisfy the following four conditions*:

1. $V(t, x)$ *is positive definite and decrescent.*[7]
2. $\dot{V}(t, x) \leq U(x) \leq 0$, *where* $U(x)$ *is continuous.*
3. $|W(t, x)|$ *is bounded.*
4. $\max[d(x, M), |\dot{W}(t, x)|] \geq \gamma(\|x\|)$, *where* $M \triangleq \{x | U(x) = 0\}$, $d(x, M)$ *denotes the distance from* x *to the set* M, *and* $\gamma(\cdot)$ *is a class* $\mathcal{K}$ *function.*

Then the equilibrium of (1.6), $x = \mathbf{0}_n$, *is uniformly asymptotically stable on* D.

Lemma 1.37 ([220]). *Condition 4 in Lemma* 1.36 *is satisfied if the following two conditions are satisfied:*

1. *The function* $\dot{W}(t, x)$ *is continuous in both arguments and* $\dot{W}(t, x) = g[\beta(t), x]$, *where* g *is continuous in both arguments and* $\beta(t)$ *is continuous and bounded.*
2. *There exists a class* $\mathcal{K}$ *function,* α, *such that* $|\dot{W}(t, x)| \geq \alpha(\|x\|)$ *for all* $x \in M$, *where* M *is the set defined in Lemma* 1.36.

1.5 Nonsmooth Analysis Background

We need the following definitions and lemmas from nonsmooth analysis.

Definition 1.9 ([92]). Consider a differential equation

$$\dot{x} = f(t, x) \tag{1.8}$$

with a piecewise continuous vector-valued function $f(t, x)$. Let $F(t, x)$ be the smallest convex closed set containing all the limit values of the vector-valued function $f(t, x^\star)$ for $x^\star \to x$ and a constant t. A vector function $x(t)$ is called a *Filippov solution* of (1.8) if $x(t)$ is absolutely continuous and

$$\dot{x} \in F(t, x) \tag{1.9}$$

almost everywhere. Here $x(t)$ is called a solution of the *differential inclusion* (1.9). For simplicity, we often use 'a.e.' to replace 'almost everywhere'. Also $K[f](t, x)$ is often used to denote $F(t, x)$ [221].

Lemma 1.38 ([92]). *Given* (1.8), *let* $f(t, x)$ *be measurable and locally essentially bounded, that is, bounded on a bounded neighborhood of every point excluding sets of measure zero. Then, for all* $x_0 \in \mathbb{R}^n$, *there exists a Filippov solution of* (1.8) *with the initial condition* $x(0) = x_0$.

---

[7] Here $V(t, x)$ is said to be *positive-definite* if $V(t, x) \geq W_1(x)$ for some positive-definite function $W_1(x)$. $V(t, x)$ is said to be *decrescent* if $V(t, x) \leq W_2(x)$ for some positive-definite function $W_2(x)$.

Definition 1.10 ([266]). For a locally Lipschitz function $V : \mathbb{R} \times \mathbb{R}^n \mapsto \mathbb{R}$, define the *generalized gradient* of V at (t, x) by $\partial V(t,x) \triangleq \text{Co}\{\lim_{i\to\infty}[[\frac{\partial V(t,x)}{\partial x}]^T,$ $\frac{\partial V(t,x)}{\partial t}]^T | (t_i, x_i) \to (t, x), (t_i, x_i) \notin \Omega_V\}$, where Ω_V is the set of measure zero where the gradient of V with respect to x or t is not defined. The *set-valued Lie derivative* of $V(t, x)$ with respect to t is defined as $\widetilde{L}_F V(t, x) \triangleq$ $\bigcap_{\xi \in \partial V(t,x)} \xi^T \begin{bmatrix} K[f](t,x) \\ 1 \end{bmatrix}$. In particular, if the function $V(t, x)$ has no explicit dependence on t, the generalized gradient of $V(x)$ at x becomes $\partial V(x) \triangleq$ $\text{Co}\{\lim_{i\to\infty} \frac{\partial V(x)}{\partial x} | x_i \to x, x_i \notin \Omega_V\}$ and the set-valued Lie derivative of $V(x)$ with respect to t becomes $\widetilde{L}_F V(x) \triangleq \bigcap_{\xi \in \partial V(x)} \xi^T K[f](t, x)$.

Definition 1.11 ([66]). Given $f : \mathbb{R}^d \mapsto \mathbb{R}$, the *right directional derivative* of f at x in the direction $v \in \mathbb{R}^d$ is defined as

$$f'(x; v) = \lim_{h\to 0^+} \frac{f(x + hv) - f(x)}{h}$$

when this limit exists. On the other hand, the *generalized directional derivative* of f at x in the direction $v \in \mathbb{R}^d$ is defined as

$$f^\circ(x; v) = \limsup_{y\to x, h\to 0^+} \frac{f(y + hv) - f(y)}{h}.$$

When they are equal, the function is *regular*.

Definition 1.12 ([147]). Let $f : [0, \infty) \mapsto \mathbb{R}^n$ be a continuous function. The *upper right-hand derivative* of $f(t)$ is given by $D^+ f(t) = \limsup_{h\to 0^+} \frac{1}{h}[f(t+h) - f(t)]$.

Lemma 1.39 ([266, Theorem 3.1]). *Given* (1.8)*, let* $f(t, x)$ *be locally essentially bounded and* $0 \in K[f](t, 0)$ *in a region* $Q \supset \{t | t_0 \leq t < \infty\} \times \{x \in \mathbb{R}^n | \|x\| < r\}$*, where* $r > 0$*. Also, let* $V : \mathbb{R} \times \mathbb{R}^n \mapsto \mathbb{R}$ *be a regular function satisfying*

$$V(t, \mathbf{0}_n) = 0,$$

and

$$0 < V_1(\|x\|) \leq V(t, x) \leq V_2(\|x\|), \quad \forall x \neq \mathbf{0}_n$$

in Q for some class $\mathscr{K}$ *functions* V_1 *and* V_2*. Then*

1. $\max \widetilde{L}_F V(t, x) \leq 0$ *in Q implies that* $x(t) = \mathbf{0}_n$ *is* uniformly stable.
2. *If in addition, there is a class* $\mathscr{K}$ *function* $\omega(\cdot)$ *in Q such that the set-valued Lie derivative of* $V(t, x)$ *satisfies*

$$\max \widetilde{L}_F V(t, x) \leq -\omega(x) < 0, \quad \forall x \neq \mathbf{0}_n,$$

then $x = \mathbf{0}_n$ *is* uniformly asymptotically stable.

Lemma 1.40 ([266, Theorem 3.2 (Invariance Principle for Differential Inclusions)]). *Let* Ω *be a compact set such that every Filippov solution to the autonomous*

system $\dot{x} = f(x)$, $x(0) = x(t_0)$, *starting in Ω is unique and remains in Ω for all* $t \geq t_0$. *Let $V : \Omega \mapsto \mathbb{R}$ be a time independent regular function such that $v \leq 0$ for all $v \in \widetilde{L}_F V(x)$ (If $\widetilde{L}_F V(x)$ is the empty set, then this is trivially satisfied). Define* $S \triangleq \{x \in \Omega | 0 \in \widetilde{L}_F V(x)\}$. *Then every trajectory in Ω converges to the largest invariant set in the closure of S.*

1.6 Time-delay System Theory Background

We need the following definitions and lemmas from time-delay system theory.

For a given differentiable $x(t)$, according to Leibniz–Newton formula [114], we have that

$$x(t - \tau) = x(t) - \int_{-\tau}^{0} \dot{x}(t + s) \, ds. \tag{1.10}$$

Suppose that $f : \mathbb{R} \times \mathbb{C}_{n,\tau} \mapsto \mathbb{R}^n$ is continuous, where $\mathbb{C}_{n,\tau}$ denotes the Banach space of continuous vector functions mapping the interval $[-\tau, 0]$ into $\mathbb{R}^n$ with the topology of uniform convergence. Consider the *retarded functional differential equation* (RFDE)

$$\dot{x}(t) = f(t, x_t). \tag{1.11}$$

Let $\phi \triangleq x_t$ be defined as $x_t(\theta) = x(t + \theta)$, $\theta \in [-\tau, 0]$. Suppose that appropriate initial conditions are defined on the delay interval $[t_0 - \tau, t_0]$: $x_{t_0}(\theta) = \phi(\theta)$, $\forall \theta \in [-\tau, 0]$, where $t_0 \in \mathbb{R}$. Specifically, we assume that the initial condition satisfies $x(\theta) = 0$, $\forall \theta \in [t_0 - \tau, t_0]$, in this book. Suppose that the solution $x(t_0, \phi)(t)$ through (t_0, ϕ) is continuous in (t_0, ϕ, t) in the domain of definition of the function [209].

Definition 1.13 ([114]). The solution $x(t_0, \phi)$ of the RFDE (1.11) is *uniformly ultimately bounded* if there is a $\beta > 0$ such that for any $\alpha > 0$, there is a constant $T_0(\alpha) > 0$ such that $\|x(t_0, \phi)(t)\| \leq \beta$ for $t \geq t_0 + T_0(\alpha)$ for all $t_0 \in \mathbb{R}$, $\phi \in \mathbb{C}_{n,\tau}$, and $\|\phi\|_c \leq \alpha$, where $\|\phi\|_c \triangleq \sup_{-\tau \leq t \leq 0} \|\phi(t)\|$ stands for the norm of a function ϕ.

Suppose that $\mathscr{D} : \mathbb{R} \times \mathbb{C}_{n,\tau} \mapsto \mathbb{R}^n$ is a linear operator on the second variable such that $\mathscr{D}(t, \phi) = A(t)\phi(0) - G(t, \phi)$, $A(t)$ is a continuous nonsingular matrix, and $G(t, \phi) = \int_{-h}^{0}[d\mu(t, \theta)]\phi(\theta)$ satisfies $\|\int_{-s+}^{0}[d\mu(t, \theta)]\phi(\theta)\| \leq \gamma(s, t)\|\phi\|$ for $0 \leq s \leq h$, where μ is an $n \times n$ matrix function of bounded variation on θ, γ is continuous, and $\gamma(0, t) = 0$ for $t \geq 0$. If $g : \mathbb{R} \times \mathbb{C}_{n,\tau} \mapsto \mathbb{R}^n$ is a continuous function, then the relation

$$\frac{d}{dt}\mathscr{D}(t, x_t) = g(t, x_t) \tag{1.12}$$

is a *neutral functional differential equation* (NFDE) [182].

Definition 1.14 ([182]). Consider the NFDE (1.12). Suppose that the operator $\mathscr{D}$ is stable. It defines a *uniform ultimately bounded* process if there is a $\beta > 0$ such that for any $\alpha > 0$, there is a constant $T_0(\alpha) > 0$ such that $\|x(t_0, \phi)(t)\| \leq \beta$ for $t \geq t_0 + T_0(\alpha)$ for all $t_0 \in \mathbb{R}$, $\phi \in \mathbb{C}_{n,\tau}$, and $\|\phi\|_c \leq \alpha$.

Lemma 1.41 ([154, 209, Degenerate Lyapunov–Krasovskii Stability Theorem]). *Consider the NFDE (1.12). Suppose that the operator $\mathscr{D}$ is stable, $g : \mathbb{R} \times \mathbb{C}_{n,\tau} \mapsto \mathbb{R}^n$ takes $\mathbb{R} \times$ (bounded sets of $\mathbb{C}_{n,\tau}$) into bounded sets of $\mathbb{R}^n$, and $u(s)$, $v(s)$ and $w(s)$ are continuous, nonnegative, and non-decreasing functions with $u(s), v(s) > 0$ for $s \neq 0$ and $u(0) = v(0) = 0$. If there exists a continuous functional $V : \mathbb{R} \times \mathbb{C}_{n,\tau} \times \mathbb{C}_{n,\tau} \mapsto \mathbb{R}^n$, such that*

(i) $u(\|\mathscr{D}(t, \phi)\|) \leq V[t, \mathscr{D}(t, \phi), \phi] \leq v(\|\phi\|_c)$,
(ii) $\dot{V}[t, \mathscr{D}(t, \phi), \phi] \leq -w[\|\mathscr{D}(t, \phi)\|]$,

then the solution of (1.12) is uniformly asymptotically stable.

Lemma 1.42 ([114, Lyapunov–Razumikhin Uniformly Ultimately Bounded Theorem]). *Consider the RFDE (1.11). Suppose that $f : \mathbb{R} \times \mathbb{C}_{n,\tau} \mapsto \mathbb{R}^n$ takes $\mathbb{R} \times$ (bounded sets of $\mathbb{C}_{n,\tau}$) into bounded sets of $\mathbb{R}^n$ and $u, v, w : [0, \infty) \mapsto [0, \infty)$ are continuous, non-decreasing functions with $u(s) \to \infty$ as $s \to \infty$. If there are a continuous functional $V : \mathbb{R} \times \mathbb{R}^n \mapsto \mathbb{R}$, a continuous non-decreasing function $p : [0, \infty) \mapsto [0, \infty)$, where $p(s) > s$ for $s > 0$, and a constant scalar $H \geq 0$ such that $u(\|x\|) \leq V(t, x) \leq v(\|x\|)$, $\forall t \in \mathbb{R}$, $\forall x \in \mathbb{R}^n$, and $\dot{V}[t, x(t)] \leq -w[\|x(t)\|]$ if $\|x(t)\| \geq H$ and $V[t + \theta, x(t + \theta)] < p\{V[t, x(t)]\}$, $\forall \theta \in [-\tau, 0]$, then the solution of (1.11) is* uniformly ultimately bounded.

Lemma 1.43 ([114, 182, Lyapunov–Razumikhin Uniformly Ultimately Bounded Theorem For Neutral Type Systems]). *Consider the NFDE (1.12). Suppose that the operator $\mathscr{D}$ is stable. Also suppose that $g : \mathbb{R} \times \mathbb{C}_{n,\tau} \mapsto \mathbb{R}^n$ take $\mathbb{R} \times$ (bounded sets of $\mathbb{C}_{n,\tau}$) into bounded sets of $\mathbb{R}^n$, and $u, v, w : [0, \infty) \mapsto [0, \infty)$ are continuous, non-decreasing functions with $u(s) \to \infty$ as $s \to \infty$. If there is a continuous functional $V : \mathbb{R} \times \mathbb{R}^n \mapsto \mathbb{R}$ and a continuous non-decreasing function $p : [0, \infty) \mapsto [0, \infty)$, where $p(s) > s$ for $s > 0$, and a constant $H \geq 0$ such that $u(\|x\|) \leq V(t, x) \leq v(\|x\|)$, $\forall t \in \mathbb{R}$, $\forall x \in \mathbb{R}^n$, and $\dot{V}[t, \mathscr{D}(t, \phi)] \leq -w[\|\mathscr{D}(t, \phi)\|]$ if $\|\mathscr{D}(t, \phi)\| \geq H$ and $V[t + \theta, x(t + \theta)] < p\{V[t, \mathscr{D}(t, \phi)]\}$, $\forall \theta \in [-\tau, 0]$, then the solution of the (1.12) is* uniformly ultimately bounded.

Lemma 1.44 ([209]). *Given the original system*

$$\dot{x}(t) = Ax(t - \tau_1) + Bx(t - \tau_2) \tag{1.13}$$

and the system after model transformation

$$\frac{d}{dt}\left[x(t) + A\int_{-\tau_1}^{0} x(t + \theta)d\theta + B\int_{-\tau_2}^{0} x(t + \theta)d\theta\right] = (A + B)x(t), \tag{1.14}$$

the stability of (1.14) *implies the stability of* (1.13) *if*

$$1 + \lambda_i(A)\frac{1 - e^{-s\tau_1}}{s} + \lambda_i(B)\frac{1 - e^{-s\tau_2}}{s} \neq 0,$$

for all $s \in \mathbb{C}^+$.

1.7 Notes

Section 1.2 is based mainly on [248]. Section 1.3 is based mainly on [4, 111, 122, 132, 163, 228, 304]. Section 1.4 is based mainly on [66, 147, 158, 220, 272]. Section 1.5 is based mainly on [66, 92, 147, 221, 266]. Section 1.6 is based mainly on [114, 154, 182, 209].

Chapter 2
Overview of Recent Research in Distributed Multi-agent Coordination

This chapter overviews recent research results in distributed multi-agent coordination. Distributed coordination of multiple autonomous agents, including unmanned aerial vehicles (UAVs), unmanned ground vehicles (UGVs), and unmanned underwater vehicles (UUVs), has been a very active research topic in the systems and controls society. The recent research results in distributed multi-agent coordination are roughly categorized as consensus, distributed formation control, distributed optimization, distributed task assignment, distributed estimation and control, and intelligent coordination. A short discussion is given to propose several future research directions and problems that deserve further investigation.

2.1 Introduction

Control theory can be dated back to the beginning of last century when the Wright brothers made their first flight in 1903. Since then, control theory has received more and more attention, especially during the World War II when control theory has been developed and applied to fire-control systems, missile navigation and control, and various electronic devices. Over the past several decades, modern control theory has been developed due to the booming of spacecraft technology and large-scale systems.

During the development of the control theory, control of a single system has relatively matured and many control methodologies have been developed, such as proportional-integral-derivative (PID) control, adaptive control, intelligent control, and robust control. In the past two decades, the control of multiple interconnected systems has drawn more and more attention because many benefits can be obtained when replacing a solo complicated system with several simple systems. Two approaches are commonly used for the control of multiple interconnected systems: a centralized approach and a distributed approach. The centralized approach is based on the assumption that a powerful central station is available to control a group of systems. Essentially, the centralized approach is a direct extension of the traditional

single-system based control methodology. Instead, the distributed approach does not require the existence of a central station with a tradeoff that this approach is far more complex than the centralized one. However, the distributed approach is more promising due to inevitable physical constraints, such as limited communication/sensing range, low bandwidth, and large number of systems involved.

Recently, the control of a group of autonomous agents including UAVs, UGVs, and UUVs, has been investigated intensively from different perspectives. The main control objective is to have the agents work together in a cooperative fashion. Here *cooperative* refers to the close relationship among all agents in the team with *information sharing* playing an important role. Distributed coordination of multiple autonomous agents has become an active research topic because many advantages can be achieved accordingly, such as robustness, adaptivity, flexibility, and scalability.

The study of distributed control of multiple autonomous agents was motivated by the work in distributed computing [183], management science [70, 302], and physics [295]. In controls society, the pioneer work was given in [292, 293] where an asynchronous agreement problem was studied for distributed decision making problems. In what follows, [90, 132, 200, 214, 247] studied consensus algorithms under various information flow constraints. Several recent special issues on distributed coordination from 2004 to 2009 include IEEE Transactions on Automatic Control (Vol. 49, No. 9, 2004), IEEE Transactions on Control Systems Technology (Vol. 15, No. 4, 2007), Proceedings of the IEEE (Vol. 94, No. 4, 2007), ASME Journal of Dynamic Systems, Measurement, and Control (Vol. 129, No. 5, 2007), International Journal of Robust and Nonlinear Control (Vol. 17, No. 10–11, 2007), International Journal of Adaptive Control and Signal Processing (Vol. 21, No. 2–3, 2007), IET Control Theory and Applications (Vol. 1, No. 2, 2007), and SIAM Journal on Control and Optimization (Vol. 48, No. 1, 2009).

In this chapter, we overview recent research results in distributed multi-agent coordination from 2006 to 2009.[1] For research results before 2006, the readers are referred to [169, 207, 215, 250]. We roughly categorize the recent research results based on the following directions:[2]

1. Consensus/agreement/synchronization/rendezvous. In this direction, various problems have been investigated towards driving a group of agents to some common state. In many cases, the four words can be used without discrimination.
2. Distributed formation control.[3] Distributed *formation control* refers to the behavior that the agents form a certain geometrical configuration through local interaction with/without a group reference.

---

[1] Here we primarily focus on the results that appeared in major control/robotics journals although many results might have appeared in other fields or in conferences.

[2] Note that the classification is by no means complete, and the overview will by no means cover all recent research results.

[3] In fact, consensus can be considered a special case of formation control. We have explicitly overviewed consensus because consensus, a fairly basic problem in distributed multi-agent coordination, has received significant research attention, and therefore deserves special attention in the overview.

3. Distributed optimization. As is known to us, optimization always plays an important role in both theoretical study and practical applications. Significant effort has been put into this research topic upon the birth of control theory. Optimization in distributed multi-agent coordination has been studied under both individual and global objectives.

4. Distributed estimation and control. In order to tackle distributed coordination problems, it is, sometimes, assumed that some global information is available to each individual agent. This assumption disobeys the virtue of distributed multi-agent coordination. As an alternative, distributed estimation and control methodologies have been proposed in which some unknown global information can be estimated locally.

5. Distributed task assignment. An interesting problem involved in sensor/robotic networks is to achieve task assignment in a distributed fashion. Examples include task/resource allocation, coverage control, and scheduling.

6. Intelligent coordination. The term *intelligent coordination* refers to the coordinated behavior of a group of agents with intelligence. In this problem, research has been conducted towards introducing intelligent mechanisms into traditional coordination problems or investigating the behavior of a group of intelligent agents from the perspective of coordination.

2.2 Consensus

Consider a group of n agents with single-integrator dynamics given by

$$\dot{r}_i(t) = u_i(t), \quad i = 1, \ldots, n \tag{2.1}$$

where $r_i(t) \in \mathbb{R}$ and $u_i(t) \in \mathbb{R}$ are, respectively, the state and the control input associated with the ith agent. Here for simplicity of presentation we have assumed that all agents are in a one-dimensional space. However, all results hereafter are still valid for the high-dimensional space by introduction of the Kronecker product. A common consensus algorithm for (2.1) is given by

$$u_i(t) = \sum_{j=1}^{n} a_{ij} \big[r_j(t) - r_i(t) \big], \tag{2.2}$$

where a_{ij} is the (i, j)th entry of the adjacency matrix $\mathcal{A}$ associated with the graph $\mathcal{G}$ characterizing the interaction among the n agents. The objective of (2.2) is to *reach* or *achieve* consensus, i.e., for all $r_i(0)$ and all $i, j = 1, \ldots, n$, $|r_i(t) - r_j(t)| \rightarrow 0$ as $t \rightarrow \infty$. The main idea behind (2.2) is that each agent's state is driven towards the states of its neighbors (see Lemmas 1.3–1.5 for some convergence results on consensus). In the following, we will overview the recent research results in consensus according to different research problems.

2.2.1 Delay Effect

It can be observed that the consensus algorithm (2.2) assumes that each agent can obtain the states of its neighbors without time delay. This assumption poses an obvious limitation because time delay appears in every practical system and, therefore, deserves consideration in the consensus problem. In particular, two types of time delays, i.e., *communication delay* and *input delay*, have been considered in the existing literature. When there exists communication delay, (2.2) becomes

$$u_i(t) = \sum_{j=1}^n a_{ij} \big[r_j(t - T_{ij}) - r_i(t) \big], \tag{2.3}$$

where T_{ij} represents the communication delay from the jth agent to the ith agent. When there exists input delay, (2.2) becomes

$$u_i(t) = \sum_{j=1}^n a_{ij} \big[r_j(t - T_p) - r_i(t - T_p) \big], \tag{2.4}$$

where T_p represents the input delay. It is worth mentioning that the communication and input delays might be time-varying and there might exist both communication and input delays. In addition to time delay, it is also important to consider packet dropouts when the agents exchange information. Fortunately, consensus with packet dropouts can be considered a special case of consensus with time delay because old information needs to be used in the presence of packet dropouts. The main problem involved in consensus with time delay is to study the effect of time delay in terms of whether consensus can be reached ultimately, also called *consensusability* [186].

In order to study the delay effect on consensus, the authors in [214] present conditions on the maximum allowed time delay without damaging consensus in a continuous-time setting. In particular, it is shown that the maximum allowed time delay is bounded by a threshold determined by the out-degree of the interaction graph. The authors in [309] study the discrete-time case and present necessary and/or sufficient conditions under both fixed and switching interaction graphs. Further studies are given in [310], which shows that bounded communication delay will not affect the consensusability. Different from the analysis in [214, 309, 310] where matrix theory and the properties of row-stochastic matrices are frequently used, the authors in [290] study the effect of both the communication delay and the input delay on the consensusability based on the frequency-domain analysis. It is shown that the communication delay does not affect the consensusability while the input delay does. In a similar manner, consensus with time delay is studied for systems with different dynamics, i.e., (2.1) replaced with other complex system dynamics, under different scenarios [23, 41, 57, 61, 173, 178, 195, 285, 291, 298, 300, 318], including average consensus where a group of agents reaches the average of their initial states [23, 285], consensus over complex networks [41, 173, 300], and robust

consensus [178, 291]. The main tools in the stability analysis include Lyapunov functions [41, 173], passivity [318], and contraction [298].

2.2.2 Convergence Speed

Convergence speed is another interesting topic in the study of the consensus problem. Convergence speed is used to characterize how fast consensus is reached. Using (2.2) for (2.1), if the graph $\mathcal{G}$ is undirected, the worst-case convergence speed is determined by [214] as

$$\min_{r \neq \mathbf{0}_n \ \& \ \mathbf{1}_n^T r = 0} \frac{r^T \mathcal{L} r}{\|r\|^2} = \lambda_2(\mathcal{L}), \tag{2.5}$$

where $r \triangleq [r_1, \ldots, r_n]^T$, $\mathcal{L}$ is the Laplacian matrix, and $\lambda_2(\mathcal{L})$ represents the second smallest eigenvalue of $\mathcal{L}$. In order to increase the convergence speed, the authors in [148] propose an iterative algorithm to maximize the second smallest eigenvalue of a state-dependent Laplacian matrix by employing a semidefinite programming solver. In addition to the second smallest eigenvalue of the Laplacian matrix, a commonly used definition of the convergence speed is given by [216, 308]

$$\rho \triangleq \lim_{t \to \infty \ \& \ r(t) \neq r^\star} \left[\frac{\|r(t) - r^\star\|}{\|r(0) - r^\star\|} \right]^{\frac{1}{t}}, \tag{2.6}$$

where $r^\star \in \mathbb{R}^n$ represents the final consensus equilibrium, which is given by $\sigma \mathbf{1}_n$, where σ is a constant real number. To achieve the fastest convergence speed, the corresponding optimization problem becomes $\max_{u_i(t)} \rho$. In [308], the authors cast the problem of finding the fastest convergence speed into a semidefinite programming problem. In [150], the authors study the problem of reaching the fast average consensus, i.e., $r^\star = \frac{r^T(0) \mathbf{1}_n}{n} \mathbf{1}_n$ in (2.6). In particular, the authors proposed two numerical solutions: the qth-order spectral norm minimization and gradient sampling. The convergence speed defined in (2.6) is studied in both the deterministic and stochastic settings. In the deterministic setting, [5, 6, 216] study the convergence speed and present the estimate or the lower bound of the convergence speed. On the other hand, [3, 115, 331] study the convergence speed in a stochastic setting. In particular, the authors in [331] study the per-step convergence factor, which can be considered the measurement of the convergence speed.

2.2.3 Stochastic Setting

Existing research on the consensus problem is mainly conducted under the assumption that the interaction graph is deterministic. However, due to the existence of

communication failures, packet dropouts, and unstable communication channels, it is of great importance to study the consensus problem in a stochastic setting where the interaction graph evolves according to some random distributions, for example, binomial distribution.

In the deterministic setting, consensus is reached if all agents ultimately reach an agreement on some common state. In the stochastic setting, consensus is reached almost surely (respectively, in the mean square sense or with probability one) if all agents reach an agreement on some common state almost surely (respectively, in the mean square sense or with probability one). Consensus over a stochastic network is first studied in [115]. Sufficient conditions on the interaction graph is given to guarantee consensus with probability one and the rate of convergence is also studied. The authors in [3, 128, 185, 232, 286, 305, 328] continue the study of the consensus problem over a stochastic network in different settings. In particular, more general results on consensus in the stochastic setting are given in [3, 232, 286, 305]. The authors in [286] present necessary and sufficient conditions to guarantee consensus almost surely. Note that the condition in [286] is analogous to that in [200, 247] with the exception that the conditions and results are in the stochastic setting. Note that the properties of the row-stochastic matrices play a crucial role in the convergence analysis.

2.2.4 Complex Systems

In addition to the study of the consensus problem for systems with simple dynamics, for example, single-integrator dynamics, double-integrator dynamics, or general linear systems [172, 294], consensus for complex systems is also an interesting topic and has received significant research attention. Here we use the term *consensus for complex systems* to refer to the study of the consensus problem when the system dynamics are nonlinear [15, 55, 60, 64, 66, 71, 76, 77, 123, 177, 208, 258, 267, 277, 320, 321, 329, 330, 333] or the consensus algorithm itself is nonlinear [67, 129, 130]. The main system dynamics studied in the consensus problem include oscillators [60], complex networks [321, 329], nonholonomic mobile robots [76], passive systems [333], and rigid bodies [15, 64, 208, 239, 258]. Similar to the consensus algorithms proposed for systems with simple dynamics, the consensus algorithms proposed in these papers are also based on the state differences with an exception that some additional terms are required to ensure consensus. Note that although the objective is also to guarantee the agreement on the final states, the problem is more complicated due to the nonlinearity of the closed-loop systems. In addition, the properties of row-stochastic matrices might not be applied to the convergence analysis. The main control techniques and approaches used in the stability analysis include adaptive control [329], pinning control [55], dissipativity theory [277], nonsmooth analysis [66, 76, 129], and Lyapunov functions [15, 60, 64, 76, 208, 258].

2.2.5 Quantization

Consensus under quantization has been studied recently with the motivation from digital signal processing. Here *quantized consensus* refers to consensus when the measurements are digital rather than analog. Therefore, the information received by each agent is digital. In [143], a quantized gossip algorithm is proposed and the convergence analysis is studied. In particular, the bound of the convergence time for a fully connected undirected graph is shown to be polynomial in the number of agents. In [48], the authors introduce coding/decoding strategies in quantized consensus and show that the convergence rate depends on the accuracy of the quantization but not the coding/decoding strategies. In [165, 166], quantized consensus is studied via gossip algorithms under an undirected connected interaction graph. In addition, both the lower and upper bounds of the convergence time are investigated.

2.2.6 Sampled-data Setting

Consensus in a sampled-data setting, here called *sampled-data consensus*, has been investigated recently with the motivation from the fact that the system dynamics are normally continuous while the measurements and control inputs might only be made in a discrete-time setting. Sampled-data consensus is mainly investigated in [33, 36, 99, 101, 116, 312, 313]. Consensus for single-integrator dynamics is studied in a sampled-data setting under both fixed and switching interaction graphs in [312, 313] where necessary and/or sufficient conditions are presented to guarantee consensus. Consensus for double-integrator dynamics is studied in a sampled-data setting under both fixed and switching interaction graphs in [33, 36, 99, 101, 116]. Various approaches, including Lyapunov theory [116], matrix theory [33], infinite product of row-stochastic matrices [36], and linear matrix inequalities [99, 101], have been used to determine necessary and/or sufficient conditions to guarantee consensus.

2.2.7 Finite-time Convergence

Reaching consensus in a finite time, here called *finite-time consensus*, has been studied recently. For a group of n agents with dynamics given in (2.1), the objective is to design $u_i(t)$ such that $r_i(t) = r_j(t)$ for $t \geq \overline{T}$, where $\overline{T}$ is a constant. Here $\overline{T}$ is also called the consensus time. Finite-time consensus for single-integrator dynamics in a continuous-time setting is solved in [66, 130, 138, 311]. Finite-time consensus for double-integrator dynamics in a continuous-time setting is studied in [297]. It is well known that linear consensus algorithms normally guarantee exponential or asymptotical convergence but not finite-time convergence. Hence, an important characteristic in the proposed finite-time consensus algorithms is the introduction of the signum function.

2.2.8 Asynchronous Effect

In most existing research of the consensus problem, it is assumed that all agents update their states synchronously. Note that the synchronized update requires a synchronized clock for a group of agents. However, the synchronized clock might not exist in real applications. This motivates the study of consensus algorithms with asynchronous updates. That is, each agent updates its state disregard of the update times of the other agents. In [310], consensus for single-integrator dynamics is studied with asynchronous updates and time delays by using the properties of row-stochastic matrices. The authors in [43] solve asynchronous consensus for single-integrator dynamics using matrix theory and graph theory. On the other hand, paracontracting theory is employed in [89] to solve asynchronous consensus for single-integrator dynamics.

2.3 Distributed Formation Control

Formation control has been a very interesting research topic in the controls society where a certain geometric pattern is formed with/without a group reference. The group reference, sometimes also called a leader or a virtual leader, represents the objective of interest for the whole group. Formation control without a group reference, here called *formation producing*, refers to the behavior that a group of agents achieves some geometric pattern in the absence of any group reference. Formation control with a group reference, here called *formation tracking*, refers to the behavior that a group of agents achieves a desired geometric formation and follows the group reference. In the following, we will overview recent research results in formation control, including formation producing, formation tracking, connectivity maintenance, and controllability, in the context of distributed multi-agent coordination with local interaction.

2.3.1 Formation Producing

We overview the existing literature based on different approaches used in the stability analysis.

2.3.1.1 Matrix Theory Approach

Due to the nature of multi-agent systems, matrix theory has been used frequently in the stability analysis of formation producing. In [226], the authors propose a cyclic-pursuit-based strategy and show that different behaviors for a group of agents, i.e., converging to a single point, a circle, or a logarithmic spiral pattern, can be

achieved by changing a common offset angle. The stability analysis relies on characterizing the eigenvalues of a circulant matrix in the closed-loop system. Motivated by [226], Cartesian coordinate coupling is introduced to consensus algorithms in [244] to achieve three different collective motions: rendezvous, move on circular orbits, or follow logarithmic spiral curves. In [187], the collective motion for nonholonomic robots is studied for a cyclic pursuit model. In [153], the authors use complex polynomials to represent the space of permutation-invariant multi-robot formations, where the roots of the complex polynomials correspond to the configurations of the robots in the formation. In [273], cooperative multi-agent formation is studied based on parallel estimation-based decentralized control. In addition, necessary conditions on the interaction graph are presented to guarantee the stability of simultaneous parallel estimation and control.

2.3.1.2 Lyapunov-based Approach

Another important approach used in formation producing is the Lyapunov-based approach, where the system stability can be proved by finding a proper Lyapunov function. In [77], the formation feasibility and velocity alignment problem is investigated. In [78], the inverse agreement problem is studied, where the team members are forced to disperse in the workspace. In particular, the minimum distance between every pair of agents is larger than a specific lower bound. In [223], the circular collective motion on a sphere is studied under both fixed and switching interaction graphs. In [69, 170, 202, 289], *flocking* of a group of agents is investigated in different cases under fixed and switching interaction graphs, where a group of agents moves cohesively and the inter-agent collision is avoided. In [97], the Queue-formation structure is investigated in the formation producing problem, where the communication load can be reduced by dividing the information flow into two subgroups: the fast time scale and the slow time scale. In [82], the author studies formation producing with bounded control. In [327], the authors propose control laws to steer particles to an invariant pattern corresponding to a constant orbit value characterizing the curve of the trajectory and constant separations.

2.3.1.3 Graph Rigidity Approach

Graph rigidity has been an important approach in formation producing. For a given number of agents, the edges in the interaction graph are closely related to the shape of the formation. Therefore, distributed controllers can be designed to guarantee desired edge distances. In [213], graph rigidity is used to achieve formation producing for a group of agents under an undirected interaction graph. In [117], the authors study the construction and transformation of two-dimensional persistent graphs, where persistence is a generalization of rigidity in directed graphs. Through primitive operations, the minimally persistent formation can be obtained

from any other one while minimal persistence is preserved throughout the reorganization process. Further study on formation producing using graph rigidity and persistence can be found in [157, 319] where a nonlinear control law [319] and a gradient-based control law [157] are designed such that a rigid formation can be obtained.

2.3.1.4 Receding Horizon Approach

Receding horizon control (RHC), also called *model predictive control* (MPC), has been introduced in the formation producing problem. RHC is essentially a finite-horizon optimization problem. In [86, 87], the authors investigate distributed formation producing via distributed RHC. In [96], a distributed RHC approach is used to solve formation producing in the presence of time delay.

2.3.2 Formation Tracking

Although formation control without a group reference is interesting, it is sometimes more meaningful to study formation control in the presence of a group reference that represents the objective of interest for the whole group. We also overview the existing literature based on the approaches used in the stability analysis.

2.3.2.1 Matrix Theory Approach

In [45, 240], a special case of formation tracking for single-integrator dynamics in the presence of a time-varying group reference is studied in both continuous-time and discrete-time settings. In [233], formation tracking is solved through a two-level consensus approach where agents reach an agreement on the virtual leader's state at one level and are guaranteed to converge to the desired formation about the virtual leader at the other level. In [149], target-capturing formation control based on a cyclic pursuit strategy is proposed and studied for nonholonomic mobile robots. In particular, collision avoidance is shown to be achieved as well. In [236], a general framework is presented to design cooperative control strategies for a group of dynamical systems by studying the properties of the augmentation of reducible and irreducible nonnegative matrices. In addition, the approach can be applied to multiple heterogeneous systems. In [255], formation control with a constant final velocity is studied through ring coupling. In [307], the authors study synchronization of a group of agents on some desired signal that has the same dynamics as the agents and is available to only a portion of the agents.

2.3.2.2 Potential Function Approach

Potential functions have been used frequently in the formation tracking problem, where a controller is designed based on the gradient of the corresponding potential function. By properly choosing the potential function, the desired group behavior can be guaranteed. Motivated by the results in [212], the authors in [280] extend the flocking study in [212] to the case when there exists a group reference. That is, a group of agents moves cohesively with the group reference and inter-agent collision is avoided. In particular, the state information of the group reference is assumed to be available to all agents. In [268], flocking is studied under the assumption that the group reference's acceleration is known to each agent. In [83], formation control of a group of nonholonomic mobile robots is solved by using a bump function and a potential function. In addition, collision avoidance mechanism is introduced without requiring switching control even if the robots have limited sensing ranges.

2.3.2.3 Lyapunov-based Approach

In [299], the authors study conditions for distributed tracking in dynamic networks in the presence of different types of leaders, which has potential applications in biology, e.g., in evolutionary processes and disease propagation. In [84, 85], formation control of multiple nonholonomic mobile robots is solved by model transformation with/without uncertainties. In [104], coordinated path following of a group of agents is studied in the presence of communication losses and time delays. In particular, the authors derive conditions such that the path following errors are driven to a small neighborhood of zero. In [218], three nonlinear leader–follower formation control algorithms based on, respectively, full state feedback, robust state feedback, and output feedback, are proposed to solve the formation control problem for a group of nonholonomic mobile robots. In [180], synchronization of a group of spacecraft on elliptical orbits is solved by using a nonlinear adaptive controller. In [51], a distributed control law is designed for nonhonolomic mobile robots to achieve a circular motion around a stationary or moving beacon. In [224], a distributed coordination algorithm is proposed to guarantee convergence of agents to a set of trajectories that moves along closed curves.

2.3.2.4 Other Approaches

In addition to the aforementioned approaches, there are also some other approaches used to achieve formation tracking. Formation producing and formation tracking are studied in [91] via partial differential equations. In [113], leader-following formation control is solved without the measurement of the leader's velocity. In particular, an observer is designed to estimate the leader's velocity. In [75], formation tracking of nonholonomic mobile robots is solved by using neural networks. The control law is designed by using a backstepping technique and is based on the integration of

the signum function. Collision avoidance is considered as well. In [14], formation tracking is solved when the constant velocity of the leader is available to a portion of the followers by using an adaptive control design.

2.3.3 Connectivity Maintenance

In both consensus and formation control problems, it is often assumed that the interaction graph satisfies certain conditions. For example, the interaction graph is connected or has a directed spanning tree. Note that a communication model is often distance-based. That is, two agents can communicate with each other only if their distance is smaller than a certain threshold. In order to guarantee that consensus or formation control can be achieved ultimately, connectivity maintenance mechanism has also been studied recently. The connectivity maintenance mechanism is mainly studied in [98, 133, 269, 279, 282, 324, 325]. The main approach used is to define artificial potentials in a proper way such that if two agents are neighbors at a certain time instant, they will always be neighbors afterwards. In [133], consensus with connectivity maintenance is solved when the weights for the edges of the interaction graph are defined properly. In [98], rendezvous of a group of agents with connectivity maintenance is solved based on a perimeter minimizing algorithm. In [282], a controller based on a properly designed potential function is proposed to solve rendezvous of a group of nonholonomic robots with connectivity maintenance. In [279, 324, 326], connectivity maintenance for flocking of a group of agents is studied based on properly designed potential functions.

2.3.4 Controllability

Controllability in distributed multi-agent coordination has been an interesting research topic recently. A multi-agent system is *controllable* if each agent in the system can be steered to a certain position by controlling one agent in the system, which is also called the *leader*. In [288], the author studies the controllability of multi-agent systems in the present of a leader. Necessary and sufficient conditions are presented based on the eigenvalues of a submatrix of the Laplacian matrix. Interestingly, it is further shown that increasing the algebraic connectivity does not necessarily increase the controllability. Further results on controllability of multi-agent systems are presented from a graph-theoretical perspective. In [134, 135], necessary conditions on the controllability are presented. In particular, equitable partitions are introduced in [134] to improve the controllability results presented in [135]. In [237], the authors investigate the relationship between the network symmetry structure and the controllability. Note that [134, 135, 237, 288] focus on the fixed interaction graph case. Different from [134, 135, 237], the authors in [137, 181] study the controllability of multi-agent systems under a switching interaction

graph. In particular, the authors in [137] take time delays into account and derive sufficient conditions for controllability.

2.4 Distributed Optimization

Optimization is an important issue in the systems and controls society. The main objective of optimization is to find the optimal strategy under some given cost function. Optimization in distributed multi-agent coordination has been studied recently in two directions, namely, convergence speed and cost functions. One important problem studied in consensus is the convergence speed, which characterizes how fast consensus can be achieved. We refer the readers to Sect. 2.2.2 for the problem. In addition to the fastest convergence speed that is studied as the objective to optimize, various cost functions including both individual cost functions and global cost functions are also studied as the objectives to optimize.

2.4.1 Individual Cost Functions

In this case, the cost function for one agent is defined based on its own and its neighbors' states. In [260, 261], a semi-distributed optimal control problem is studied in the presence of finite-horizon individual cost functions in both leaderless and leader-following cases. In [140], finite-time optimal consensus with input and linear state constraints is solved by using a primal decomposition and subgradient method. In [19], a nonlinear consensus protocol is proposed such that a group of agents can reach an agreement on certain functions of all agents' initial states. Meanwhile, it is shown that the proposed consensus protocol is optimal with respect to certain individual cost functions. In [105], the authors study the coordination problem of a group of robots working under a collision avoidance constraint, where each individual robot strives to optimize its own objective—the elapsed time. The problem is solved based on the notion of *Pareto optimality*.

2.4.2 Global Cost Functions

In this case, the cost function depends on information of the whole group. In [124], the authors study an optimal control problem with free final time and partially constrained final states, which mimics some behaviors in foraging trail optimization. In [188], the authors study optimal sensor placement and motion coordination. The main problem is to maximize a particular class of global cost functions. In [107], mission planning of a group of unhabited underwater vehicles is solved via a receding horizon mixed-integer constrained quadratic optimal control problem, which

is then partitioned into smaller subproblems and solved in a parallel and distributed manner using a distributed Nash-based game approach. In [257], the authors study consensus in terms of the extrema of some global cost function. In particular, consensus and anticonsensus (balance) can be achieved via, respectively, maximizing and minimizing the cost function. In [127], the authors study the optimal coordination problem with formation pattern and collision avoidance constraints by minimizing a global cost function. Through a case study, it is shown that the solution is optimal for sufficiently close starting and final positions. In [26], an optimal distributed control problem is studied via the study of an infinite-horizon *linear-quadratic regulator* (LQR) problem. Then a distributed controller is constructed by analyzing the properties of the local LQR problem. In addition, the relationship among stability, robustness, and the spectrum of a certain matrix is presented as well. In [203], the authors also study an infinite-horizon LQR problem. Different from [26], a special class of operators, called *spatially decaying* operators, is introduced. In [35], the authors study an optimal linear consensus problem from an infinite-horizon LQR perspective. Different from [26, 203], the authors in [35] show that the optimal interaction graph corresponds to a complete directed graph. Different from [26, 35, 203] where an infinite-horizon cost function is used, the authors in [95] propose cooperative control algorithms to minimize a finite-horizon global cost function that includes both the regulation and cooperation objectives. In [142], the authors study a formation controller design so that some desired properties can be optimized. In particular, through the use of a dynamic protocol, formations of real robots are shown to move significantly faster and with greater precision. In [74], minimization of the total travel distance or the minimax distance that the agents must travel is solved using convex optimization.

2.5 Distributed Task Assignment

Distributed task assignment refers to the study of task assignment of a group of agents in a distributed manner, which can be roughly categorized as coverage control, scheduling, and surveillance.

2.5.1 Coverage Control

Recently, *coverage control* has been an active research direction in mobile sensor networks. The main objective is to properly assign the mobile sensors' motion in order to maximize the detection probability. Let Q be a convex space with ϕ representing the distribution density function, which denotes the probability that some event takes place over Q [68]. Let there exist a group of n mobile sensors whose

locations are given by $P \triangleq [p_1, \ldots, p_n]$, where p_i denotes the location of sensor i. Note that the sensor performance at a point q degrades with respect to the distance $\|q - p_i\|$. Then use a nondecreasing differentiable function f can be used to describe the sensor performance. The coverage control problem is essentially to find a local controller for each mobile sensor such that the cost function

$$J \triangleq \sum_{i=1}^{n} \int f\big(\|q - p_i\|\big) \phi(q)\,\mathrm{d}q$$

is minimized.[4] A complete distributed, scalable coverage control strategy is derived in [68]. In addition, the closed-loop system is adaptive and asynchronous. Several further results about coverage control have also been presented recently. In [131], precise coverage control with collision avoidance is studied under fully and partially connected interaction graphs. In [100], the connection between coverage control and consensus under a cyclic interaction graph is studied. Both the coverage control problem and the average consensus problem can be considered a special class of the distributed optimization problems. In [167], the coverage control of a network of robotic agents with limited-range communication and anisotropic sensing capabilities is studied. By approximating the expected-value objective function, a gradient-based distributed coverage control algorithm is developed. Different from [68, 100, 131, 167], the authors in [204] study the optimal sensor placement problem via minimizing the trace of a weighted covariance matrix. In particular, the optimization problem can be converted to a convex optimization problem.

2.5.2 Scheduling

Distributed scheduling refers to the scheduling of a group of agents in a distributed manner. In [139], the authors study the optimal scheduling sequence to fuel a group of UAVs *via* dynamic programming. In [94], a coordination strategy based on task-load balancing is proposed under a fixed interaction graph. In [197], the distributed adaptive scheduling is solved by choosing the task timings as the consensus variable. In [22], the authors solve task assignment for flocking by using a metric routing algorithm. In [9], the authors study the efficient routing problem when a group of autonomous vehicles must visit multiple targets generated by a random process. Control strategies are presented to minimize the expected time between the time when a target appears and the time when an agent visits the target. Further results are also presented to understand the effect of the inter-agent communication and the knowledge of the stochastic process.

---

[4] Note that coverage control can be treated as an optimization problem.

2.5.3 Surveillance

Distributed surveillance means the monitoring of a certain area by using a group of agents coordinated in a distributed fashion. In [151], a perimeter surveillance problem is studied and experimental results on multiple UAVs are presented to show the effectiveness. In [198], the authors propose a distributed cooperative control algorithm to drive a group of autonomous vehicles to patrol some area that exceeds the communication and sensing capabilities of the vehicles. In addition, a proper distribution of the vehicles is achieved within a finite time. In [106], a cooperative surveillance problem for a group of UAVs is studied in the presence of unstable communications, time delays, uncertainty in target locations, and imperfect vehicle search sensors. Different from the problems studied in [106, 151, 198], the authors in [227] study a scenario where a group of robots moves towards their individual targets without collision. In [314], the authors study a cooperative search problem where a group of UAVs are used to find the targets in an unknown environment. In particular, an opportunistic-cooperative-learning based distributed strategy is proposed to solve the problem and the bounds of the search time are presented. In [93], the authors study the distribution of a group of heterogeneous vehicles over a certain space that includes several areas in the presence of uncertainty. Scalable allocation strategies are developed to guarantee a desired vehicle distribution in these areas. In [226], different behaviors for a group of vehicles, namely, converging to a single point, a circle, or a logarithmic spiral pattern, are shown to be achieved for a cyclic pursuit model by changing a common offset angle. In addition, by changing the common offset angle based on the locally available information, the paths of the vehicles can be guaranteed to cover a certain area. In [287], the authors study a cooperative sensor placement problem in which a group of mobile sensors is deployed to monitor multiple stationary targets. The cost function used in [287] is nonlinear and nonsmooth.

2.6 Distributed Estimation and Control

Due to the absence of global information that can be used to achieve group coordination, distributed estimation and control has received significant attention recently. Under the distributed estimation and control framework, the first problem is to design distributed local estimators such that some global information can be estimated in finite/infinite time. The second problem is to design distributed local controllers based on the local estimator such that the closed-loop system is stable. It is worthwhile to emphasize that the closed-loop system with both distributed estimators and controllers is much more complicated than that with only distributed controllers.

In [315], the authors present a unified framework of distributed estimation and control to solve a distributed coordination problem. Both proportional-like and proportional-and-integral-like distributed estimation algorithms are proposed and analyzed. In [184], the unified distributed estimation and control framework in [315]

is applied to environmental modeling and experimental results are presented as a proof of concept. In [184, 315], it is assumed that no noisy signal exists in the measurements. In [278], the authors study overlapping distributed estimation by using a consensus-like approach in the presence of white noise. The proposed approach is based on a synergy between local *Kalman filters* and a dynamic consensus strategy for the agents. In [28], the authors consider the distributed estimation problem, where each sensor has some noisy linear measurement of some unknown parameter. By using a consensus-like diffusion scheme, the local estimate of each node will finally converge to the true parameter. In [205], the authors study the accuracy of position estimation for groups of mobile robots performing cooperative localization in the presence of white noise. In [332], the authors study cooperative tracking of a type of nonlinear robots. In particular, cooperative sensors are used to estimate the relative posture. In [234], radar position estimation and configuration optimization are studied via the minimization of position errors. In addition to the state estimation in the aforementioned papers, the authors in [73] investigate the estimation of a spatially distributed process via the minimization of expected state estimation errors.

2.7 Intelligent Coordination

In traditional coordination problems, it is often assumed that each agent responds to local information. This assumption is simple and, therefore, the complexity of the closed-loop system is low. Recently, distributed coordination in the presence of intelligence, referred to as *intelligent coordination*, has been studied from different perspectives, especially from economy, social science, and management science. The main feature in intelligent coordination is that each agent is intelligent, and therefore chooses the best possible response based on its own objective. We overview existing results in two aspects: pursuer-invader problem and game theory.

2.7.1 Pursuer–invader Problem

In the *pursuer–invader problem*, there exist a group of pursuers and one invader. The objective of the pursuers is to find and track the invader while the objective of the invader is to escape the pursuers. In [40], the authors study the pursuer–invader problem and presented a five-phase controller to solve this problem. In [25], the authors study the pursuer-invader problem for Dubins-like vehicles when the velocity of the invader is bounded. Similar to [40], the authors propose a five-phase controller to solve the problem. The discrete-time case of the pursuit-evasion problem in [25] is studied in [24].

2.7.2 Game Theory

Recently, *game theory* is also introduced to distributed multi-agent coordination. In [112], formation control is studied via a *linear-quadratic (LQ) Nash differential game* and a RHC-based approach is used. In [296], the authors study the problem of *learning Markov games* using learning automata. In [88], the authors propose and study multi-agent systems with symbiotic learning and evolution (Masbiole) based on symbiosis in the ecosystem. It is further shown that Masbiole can escape from the *Nash equilibria*. In [301], the authors study the role of cooperation in a coupling game. By adding cooperation, it is shown that benefits can be increased. In [21], the authors study consensus with unknown but bounded disturbances. Due to the existence of unknown but bounded disturbances, the local controller under a traditional consensus protocol is bounded. The authors propose a lazy rule, where each agent chooses the minimal control input based on the traditional consensus algorithm. In [20], a consensus-like protocol is derived in noncooperative games. Under the proposed protocol, it is shown that the players converge to the unique *Pareto optimal Nash equilibrium*.

2.8 Discussion

We have reviewed the recent research in distributed multi-agent coordination. The main objective of this overview is to briefly summarize the state-of-the-art in distributed multi-agent coordination. In addition to the aforementioned theoretical results, many experiments are also conducted to validate the theoretical results, for example, [7, 16, 118, 159, 211, 251]. Although the theoretical study and experimental validation have solved many problems in distributed multi-agent coordination, there are still a number of research problems that deserve further investigation. We summarize these problems as follows:

- Quantization effect in distributed coordination problems. Most existing research focuses on the study of distributed coordination problems by assuming that both control inputs and measurements are continuous analog values. However, the use of digital signal processing technique requires digital inputs and measurements. Therefore, it is important and meaningful to investigate the quantization effect in distributed coordination problems. Note that although the quantization effect has been studied in some coordination problems, the quantization effect still deserves further consideration in many other distributed coordination problems.
- Optimization with both individual and global cost functions. The optimization problem in distributed multi-agent coordination has been studied in the presence of either an individual or a global cost function. In real systems, each individual agent has both local and global objectives with corresponding individual and global cost functions. Therefore, optimization of the combined objectives is more realistic and meaningful. Another interesting problem is to investigate the rela-

tionship between the individual cost function and the global cost function. One interesting problem is how to balance the individual cost function and the global cost function.

- Intelligent coordination. Intelligent coordination has potential applications in not only engineering but also in economics, social science, etc. Although several research problems have been studied recently, there are still many open questions, especially the understanding of group behavior in the presence of intelligence. One interesting problem is how we can interpret complex networks and stabilize the complex networks in the presence of intelligence.

- Competition and cooperation. Right now, most research is conducted based on local cooperation but not competition. This poses an obvious limitation because competition also plays an important role in group coordination in reality. For example, due to the lack of competition, the final consensus equilibrium using the traditional consensus algorithms is limited to a weighted average of the initial states. One interesting question is how to introduce competition to distributed coordination to represent more realistic scenarios.

- Centralization and decentralization. Note that decentralization shows obvious benefits over centralization, such as scalability and robustness. However, decentralization also has its own drawbacks. One drawback is that each agent cannot effectively predict the group behavior based on only local information. Accordingly, the group behavior cannot be controlled in some sense. As an interesting example of this drawback, economic crisis can be used to illustrate the disadvantages of decentralization. One interesting question is how we can balance decentralization and centralization to improve the system performance.

2.9 Notes

For further literature review on distributed multi-agent coordination and related problems, see [8, 17, 27, 49, 53, 58, 63, 84, 102, 132, 169, 193, 207, 215, 222, 235, 248, 250, 265, 270, 274, 306, 315] and references therein.

Part II
Emergent Problems in Distributed Multi-agent Coordination

Chapter 3
Collective Periodic Motion Coordination

This chapter introduces a collective periodic motion coordination problem. Coordinated periodic motions play an important role in applications involving multi-agent networks with repetitive movements such as cooperative patrol, mapping, sampling, or surveillance. We introduce two types of algorithms. For the first type, we introduce Cartesian coordinate coupling to existing distributed consensus algorithms for respectively, single-integrator dynamics and double-integrator dynamics, to generate collective motions, namely, rendezvous, circular patterns, and logarithmic spiral patterns in the three-dimensional space. It is shown that the interaction graph and the value of the Euler angle in the case of single-integrator dynamics and the interaction graph, the damping gain, and the value of the Euler angle in the case of double-integrator dynamics affect the resulting collective motions. We show that when the nonsymmetric Laplacian matrix has certain properties, the damping gain is above a certain bound in the case of double-integrator dynamics, and the Euler angle is below, equal, or above a critical value, the agents will eventually rendezvous, move on circular orbits, or follow logarithmic spiral curves lying on a plane normal to the Euler axis. For the second type, we introduce coupled second-order linear harmonic oscillators with local interaction to generate synchronized oscillatory motions. We analyze convergence conditions under, respectively, directed fixed and switching interaction graphs. It is shown that the coupled harmonic oscillators can be synchronized under mild network connectivity conditions. The theoretical result is also applied to synchronized motion coordination in multi-agent systems as a proof of concept.

3.1 Cartesian Coordinate Coupling

In this section, we introduce Cartesian coordinate coupling to existing distributed consensus algorithms for respectively, single-integrator dynamics and double-integrator dynamics, through a rotation matrix in the three-dimensional space, analyze the convergence properties, and quantitatively characterize the resulting collective

motions, namely, convergence to a point, circular patterns with concentric orbits, and logarithmic spiral curves lying on a plane normal to the Euler axis, under a general interaction graph. The resulting collective motions are expected to have applications in rendezvous, persistent surveillance, and coverage control with teams of heterogeneous agents. It is shown that the interaction graph and the value of the Euler angle in the case of single-integrator dynamics and the interaction graph, the damping gain, and the value of the Euler angle in the case of double-integrator dynamics affect the resulting collective motions. The analysis relies on algebraic graph theory, matrix theory, and properties of the Kronecker product.

3.1.1 Single-integrator Dynamics

Consider n agents with single-integrator dynamics given by

$$\dot{r}_i = u_i, \quad i = 1, \ldots, n, \tag{3.1}$$

where $r_i \in \mathbb{R}^m$ is the position and $u_i \in \mathbb{R}^m$ is the control input associated with the ith agent. We introduce a distributed algorithm with Cartesian coordinate coupling for (3.1) as

$$u_i = -\sum_{j=1}^{n} a_{ij} C(r_i - r_j), \quad i = 1, \ldots, n, \tag{3.2}$$

where a_{ij} is the (i, j)th entry of the adjacency matrix $\mathcal{A} \in \mathbb{R}^{n \times n}$ associated with the directed graph $\mathcal{G} \triangleq (\mathcal{V}, \mathcal{E})$ characterizing the interaction among the n agents, and $C \in \mathbb{R}^{m \times m}$ denotes a Cartesian coordinate coupling matrix. In this book, it is assumed that all agents share a common inertial coordinate frame. This assumption will not be explicitly mentioned in later chapters unless it is necessary for facilitating analysis. In this section, we focus on the case where C is a rotation matrix while a similar analysis can be extended to the case where C is a general matrix.

Remark 3.1 Note that the existing consensus algorithm for (3.1) (see e.g., [248, Chap. 2]) corresponds to the case where $C = I_m$. That is, using the existing consensus algorithm for (3.1), the components of r_i (i.e., the Cartesian coordinates of agent i) are decoupled while using (3.2) the components of r_i are coupled.

Using (3.2), (3.1) can be written in a vector form as

$$\dot{r} = -(\mathcal{L} \otimes C)r, \tag{3.3}$$

where $r \triangleq [r_1^T, \ldots, r_n^T]^T$ and $\mathcal{L} \in \mathbb{R}^{n \times n}$ is the nonsymmetric Laplacian matrix associated with $\mathcal{A}$ and hence $\mathcal{G}$. Before moving on, we need the following definition:

Definition 3.1. Let μ_i, $i = 1, \ldots, n$, be the ith eigenvalue of $-\mathcal{L}$ with an associated right eigenvector w_i and an associated left eigenvector ν_i. Also let $\arg(\mu_i) = 0$ for

$\mu_i = 0$ and $\arg(\mu_i) \in (\frac{\pi}{2}, \frac{3\pi}{2})$ for all $\mu_i \neq 0$.[1] Without loss of generality, suppose that μ_i is labeled such that $\arg(\mu_1) \leq \arg(\mu_2) \leq \cdots \leq \arg(\mu_n)$.[2]

Theorem 3.2. *Suppose that the directed graph $\mathcal{G}$ has a directed spanning tree. Let the control algorithm for (3.1) be given by (3.2), where $r_i \triangleq [x_i, y_i, z_i]^T$ and C is the 3×3 rotation matrix R defined in Lemma 1.20. Let μ_i, w_i, ν_i, and $\arg(\mu_i)$ be defined in Definition 3.1, $\mathbf{p} \in \mathbb{R}^n$ be defined in Lemma 1.1, and $\mathbf{a} \triangleq [a_1, a_2, a_3]^T$, ς_k, and ϖ_k be defined in Lemma 1.20.*

1. *If $|\theta| < \theta_s^c$, where $\theta_s^c \triangleq \frac{3\pi}{2} - \arg(\mu_n)$, the agents will eventually rendezvous at the position $[\mathbf{p}^T x(0), \mathbf{p}^T y(0), \mathbf{p}^T z(0)]$, where x, y, and z are, respectively, the column stack vectors of x_i, y_i, and z_i.*
2. *If $|\theta| = \theta_s^c$ and $\arg(\mu_n)$ is the unique maximum phase of μ_i, all agents will eventually move on circular orbits with the center $[\mathbf{p}^T x(0), \mathbf{p}^T y(0), \mathbf{p}^T z(0)]$ and the period $\frac{2\pi}{|\mu_n|}$. The radius of the orbit for agent i is given by $2|w_{n(i)}(\frac{\nu_n^T}{\nu_n^T w_n} \otimes \frac{\varpi_2^T}{\varpi_2^T \varsigma_2})r(0)|\sqrt{a_2^2 + a_3^2}\sin^2(\frac{\theta}{2})$, where $w_{n(i)}$ is the ith component of w_n. The relative radius of the orbits is equal to the relative magnitude of $w_{n(i)}$. The relative phase of the agents on their orbits is equal to the relative phase of $w_{n(i)}$. The circular orbits are on a plane normal to the Euler axis $\mathbf{a}$.*
3. *If $\arg(\mu_n)$ is the unique maximum phase of μ_i and $\theta_s^c < |\theta| < \frac{3\pi}{2} - \arg(\mu_{n-1})$, all agents will eventually move along logarithmic spiral curves with the center $[\mathbf{p}^T x(0), \mathbf{p}^T y(0), \mathbf{p}^T z(0)]$, the growing rate $|\mu_n| \cos(\arg(\mu_n) + |\theta|)$, and the period $\frac{2\pi}{|\mu_n \sin(\arg(\mu_n) + |\theta|)|}$. The radius of the logarithmic spiral curve for agent i is given by*

$$2\left|w_{n(i)}\left(\frac{\nu_n^T}{\nu_n^T w_n} \otimes \frac{\varpi_2^T}{\varpi_2^T \varsigma_2}\right)r(0)\right|e^{[|\mu_n|\cos(\arg(\mu_n) + |\theta|)]t}\sqrt{a_2^2 + a_3^2}\sin^2\left(\frac{\theta}{2}\right).$$

The relative radius of the logarithmic spiral curves is equal to the relative magnitude of $w_{n(i)}$. The relative phase of the agents on their curves is equal to the relative phase of $w_{n(i)}$. The logarithmic spiral curves are on a plane normal to the Euler axis $\mathbf{a}$.

Proof: It follows from Lemmas 1.20 and 1.21 and Definition 3.1 that the eigenvalues of $-(\mathcal{L} \otimes R)$ are μ_i, $\mu_i e^{\iota\theta}$, and $\mu_i e^{-\iota\theta}$ with the associated right eigenvectors $w_i \otimes \varsigma_1$, $w_i \otimes \varsigma_2$, and $w_i \otimes \varsigma_3$, respectively, and the associated left eigenvectors $\nu_i \otimes \varpi_1$, $\nu_i \otimes \varpi_2$, and $\nu_i \otimes \varpi_3$, respectively. That is, the eigenvalues of $-(\mathcal{L} \otimes R)$ correspond to the eigenvalues of $-\mathcal{L}$ rotated by angles 0, θ, and $-\theta$, respectively. Let λ_ℓ, $\ell = 1, \ldots, 3n$, denote the ℓth eigenvalue of $-(\mathcal{L} \otimes R)$. Without loss of generality, let $\lambda_{3i-2} = \mu_i$, $\lambda_{3i-1} = \mu_i e^{\iota\theta}$, and $\lambda_{3i} = \mu_i e^{-\iota\theta}$, $i = 1, \ldots, n$. Because the directed graph $\mathcal{G}$ has a directed spanning tree, it follows from Lemma 1.1 that $-\mathcal{L}$ has a

---

[1] Note that according to Lemma 1.1, $-\mathcal{L}$ has at least one zero eigenvalue and all its nonzero eigenvalues have negative real parts.

[2] It follows from Lemma 1.1 that $\mu_1 = 0$. Without loss of generality, let $w_1 = \mathbf{1}_n$ and $\nu_1 = \mathbf{p}$, where $\mathbf{p} \in \mathbb{R}^n$ is defined in Lemma 1.1.

simple zero eigenvalue and all other eigenvalues have negative real parts. According to Definition 3.1, we let $\mu_1 = 0$ and $\mathrm{Re}(\mu_i) < 0$, $i = 2, \ldots, n$. According to Lemma 1.1, we let $w_1 = \mathbf{1}_n$ and $\nu_1 = \mathbf{p}$ without loss of generality. Because $\mu_1 = 0$ and $\mu_i \neq 0, i = 2, \ldots, n$, it follows that $-(\mathcal{L} \otimes R)$ has exactly three zero eigenvalues (i.e., $\lambda_1 = \lambda_2 = \lambda_3 = 0$).

Note that $-(\mathcal{L} \otimes R)$ can be written in the Jordan canonical form as MJM^{-1}, where the columns of M, denoted by m_k, $k = 1, \ldots, 3n$, can be chosen to be the right eigenvectors or generalized right eigenvectors of $-(\mathcal{L} \otimes R)$ associated with the eigenvalue λ_k, the rows of M^{-1}, denoted by p_k^T, $k = 1, \ldots, 3n$, can be chosen to be the left eigenvectors or generalized left eigenvectors of $-(\mathcal{L} \otimes R)$ associated with the eigenvalue λ_k such that $p_k^T m_k = 1$ and $p_k^T m_\ell = 0$, $k \neq \ell$, and J is the Jordan block diagonal matrix with λ_k being the diagonal entries. Noting that $\lambda_k = 0$, $k = 1, 2, 3$, we can choose $m_k = \mathbf{1}_n \otimes \varsigma_k$ and $p_k = \mathbf{p} \otimes \frac{\varpi_k}{\varpi_k^T \varsigma_k}$, $k = 1, 2, 3$. Note that $e^{-(\mathcal{L} \otimes R)t} = M e^{Jt} M^{-1}$. Also note that $\lim_{t \to \infty} e^{J_\ell t} = 0_{q \times q}$ when $J_\ell \in \mathbb{R}^{q \times q}$ is a Jordan block corresponding to an eigenvalue with a negative real part.

For the first statement of the theorem, note that $\mu_1 = 0$ and $\mathrm{Re}(\mu_i) < 0$, $i = 2, \ldots, n$. Also note from Definition 3.1 that $\arg(\mu_i) \in [\arg(\mu_2), \arg(\mu_n)] \subset (\frac{\pi}{2}, \frac{3\pi}{2})$, $i = 2, \ldots, n$. Noting that all complex eigenvalues of $-\mathcal{L}$ are in conjugate pairs, it follows that $\arg(\mu_2) = 2\pi - \arg(\mu_n)$. If $|\theta| < \theta_s^c$, then all $\arg(\mu_i)$, $\arg(\mu_i e^{\iota\theta})$, and $\arg(\mu_i e^{-\iota\theta})$ are within $(\frac{\pi}{2}, \frac{3\pi}{2})$, $i = 2, \ldots, n$, which implies that $\mathrm{Re}(\lambda_\ell) < 0$, $\ell = 4, \ldots, 3n$. Noting that $\lambda_k = 0$, $k = 1, 2, 3$, it follows that $\lim_{t \to \infty} r(t) = \lim_{t \to \infty} e^{-(\mathcal{L} \otimes R)t} r(0) = (\sum_{k=1}^{3} m_k p_k^T) r(0) = (\mathbf{1}_n \mathbf{p}^T \otimes I_3) r(0)$. It thus follows that $x_i(t) \to \mathbf{p}^T x(0)$, $y_i(t) \to \mathbf{p}^T y(0)$, and $z_i(t) \to \mathbf{p}^T z(0)$ as $t \to \infty$. That is, all agents will eventually rendezvous at $[\mathbf{p}^T x(0), \mathbf{p}^T y(0), \mathbf{p}^T z(0)]$.

For the second statement of the theorem, if $\theta = \theta_s^c$ (respectively, $\theta = -\theta_s^c$), then μ_n rotated by an angle θ (respectively, $-\theta$) will locate on the imaginary axis, that is, $\lambda_{3n-1} = \mu_n e^{\iota\theta} = -|\mu_n|\iota$ (respectively, $\lambda_{3n} = \mu_n e^{-\iota\theta} = -|\mu_n|\iota$), while $\mu_2 = \overline{\mu_n}$ rotated by an angle $-\theta$ (respectively, θ) will also locate on the imaginary axis, that is, $\lambda_6 = \mu_2 e^{-\iota\theta} = |\mu_n|\iota$ (respectively, $\lambda_5 = \mu_2 e^{\iota\theta} = |\mu_n|\iota$). Because $\arg(\mu_n)$ is the unique maximum phase of μ_i, λ_{3n-1} (respectively, λ_{3n}) and λ_6 (respectively, λ_5) are the only two nonzero eigenvalues of $-(\mathcal{L} \otimes R)$ on the imaginary axis and all other nonzero eigenvalues have negative real parts. In the following, we focus on $\theta = \theta_s^c$ since the analysis for $\theta = -\theta_s^c$ is similar except that the agents will move in reverse directions. Note that $\lambda_k = 0$, $k = 1, 2, 3$, and $\mathrm{Re}(\lambda_\ell) < 0$ for all $\ell \neq 1, 2, 3, 3n-1, 6$. Noting that $\lambda_{3n-1} = -|\mu_n|\iota$ and $\lambda_6 = |\mu_n|\iota$, we can choose $m_{3n-1} = w_n \otimes \varsigma_2$, $p_{3n-1} = \frac{\nu_n}{\nu_n^T w_n} \otimes \frac{\varpi_2}{\varpi_2^T \varsigma_2}$, $m_6 = \overline{m_{3n-1}}$, and $p_6 = \overline{p_{3n-1}}$. Note that $r(t) = e^{-(\mathcal{L} \otimes R)t} r(0)$. It follows that $\|r(t) - (\sum_{k=1}^{3} m_k p_k^T + e^{-\iota|\mu_n|t} m_{3n-1} p_{3n-1}^T + e^{\iota|\mu_n|t} m_6 p_6^T) r(0)\| \to 0$ as $t \to \infty$. Define $c(t) \triangleq (e^{-\iota|\mu_n|t} m_{3n-1} p_{3n-1}^T + e^{\iota|\mu_n|t} m_6 p_6^T) r(0)$. Let $c_k(t)$ be the kth component of $c(t)$, $k = 1, \ldots, 3n$. It follows that $c_{3(i-1)+\ell}(t) = 2\mathrm{Re}(e^{-\iota|\mu_n|t} w_{n(i)} \varsigma_{2(\ell)} p_{3n-1}^T r(0))$, where $i = 1, \ldots, n$, $\ell = 1, 2, 3$, and $\varsigma_{2(\ell)}$ denotes the ℓth component of ς_2. After some manipulation, it follows that $c_{3(i-1)+\ell}(t) = 2|\varsigma_{2(\ell)} w_{n(i)} p_{3n-1}^T r(0)| \times \cos\{|\mu_n|t - \arg[w_{n(i)} p_{3n-1}^T r(0)] - \arg[\varsigma_{2(\ell)}]\}$, $i = 1, \ldots, n$, $\ell = 1, 2, 3$. Therefore, it follows that $\|x_i(t) - [\mathbf{p}^T x(0) + c_{3i-2}(t)]\| \to 0$, $\|y_i(t) - [\mathbf{p}^T y(0) + $

$c_{3i-1}(t)]\| \to 0$, and $\|z_i(t) - [\mathbf{p}^T z(0) + c_{3i}(t)]\| \to 0$ as $t \to \infty$. After some manipulation, it can be verified that $\|[c_{3i-2}(t), c_{3i-1}(t), c_{3i}(t)]^T\| = 2|w_{n(i)}p_{3n-1}^T \times r(0)|\sqrt{a_2^2 + a_3^2}\sin^2(\frac{\theta}{2})$, which is a constant. It thus follows that all agents will eventually move on circular orbits with the center $[\mathbf{p}^T x(0), \mathbf{p}^T y(0), \mathbf{p}^T z(0)]$ and the period $\frac{2\pi}{|\mu_n|}$. The radius of the orbit for agent i is given by $2|w_{n(i)}p_{3n-1}^T r(0)| \times \sqrt{a_2^2 + a_3^2}\sin^2(\frac{\theta}{2})$. Note that the relative radius of the orbits is equal to the relative magnitude of $w_{n(i)}$. In addition, it is straightforward to see that the relative phase of the agents on their orbits is equal to the relative phase of $w_{n(i)}p_{3n-1}^T r(0)$, which is equivalent to the relative phase of $w_{n(i)}$. Note from Lemma 1.20 that the Euler axis $\mathbf{a}$ is orthogonal to both $\mathrm{Re}(\varsigma_2)$ and $\mathrm{Im}(\varsigma_2)$, where $\mathrm{Re}(\cdot)$ and $\mathrm{Im}(\cdot)$ are applied componentwise. It can thus be verified that $\mathbf{a}$ is orthogonal to $[c_{3i-2}(t), c_{3i-1}(t), c_{3i}(t)]^T$, which implies that the circular orbits are on a plane normal to $\mathbf{a}$.

For the third statement of the theorem, if $\arg(\mu_n)$ is the unique maximum phase of μ_i and $\theta_s^c < \theta < \frac{3\pi}{2} - \arg(\mu_{n-1})$ (respectively, $\arg(\mu_{n-1}) - \frac{3\pi}{2} < \theta < -\theta_s^c$), then μ_n rotated by an angle θ (respectively, $-\theta$) will have a positive real part, that is, $\lambda_{3n-1} = \mu_n e^{\iota\theta} = |\mu_n|e^{\iota(\arg(\mu_n)+\theta)}$ (respectively, $\lambda_{3n} = \mu_n e^{-\iota\theta} = |\mu_n|e^{\iota[\arg(\mu_n)-\theta]}$), while $\mu_2 = \overline{\mu_n}$ rotated by an angle $-\theta$ (respectively, θ) will also have a positive real part, that is, $\lambda_6 = \mu_2 e^{-\iota\theta} = |\mu_n|e^{-\iota(\arg(\mu_n)+\theta)}$ (respectively, $\lambda_5 = \mu_2 e^{\iota\theta} = |\mu_n|e^{-\iota[\arg(\mu_n)-\theta]}$). In addition, λ_{3n-1} (respectively, λ_{3n}) and λ_6 (respectively, λ_5) are the only two eigenvalues of $-(\mathcal{L} \otimes R)$ with positive real parts and all other nonzero eigenvalues have negative real parts. In the following, we focus on $\theta_s^c < \theta < \frac{3\pi}{2} - \arg(\mu_{n-1})$ since the analysis for $\arg(\mu_{n-1}) - \frac{3\pi}{2} < \theta < -\theta_s^c$ is similar except that all agents will move in reverse directions. Note that $\lambda_k = 0$, $k = 1, 2, 3$, $\mathrm{Re}(\lambda_{3n-1}) > 0$, $\mathrm{Re}(\lambda_6) > 0$, and $\mathrm{Re}(\lambda_k) < 0$ otherwise. Similar to the proof of the second statement, define $c(t) \triangleq \{e^{|\mu_n|e^{\iota(\arg(\mu_n)+\theta)}t}m_{3n-1}p_{3n-1}^T + e^{|\mu_n|e^{-\iota[\arg(\mu_n)+\theta]}t}m_6 p_6^T\}r(0)$. Let $c_k(t)$, $k = 1, \ldots, 3n$, be the kth component of $c(t)$. Also let $\varrho_i = |w_{n(i)}p_{3n-1}^T r(0)|$ and $\varphi_i = \arg[w_{n(i)}p_{3n-1}^T r(0)]$. It follows that $\|x_i(t) - [\mathbf{p}^T x(0) + c_{3i-2}(t)]\| \to 0$, $\|y_i(t) - [\mathbf{p}^T y(0) + c_{3i-1}(t)]\| \to 0$, and $\|z_i(t) - [\mathbf{p}^T z(0) + c_{3i}(t)]\| \to 0$ as $t \to \infty$, where

$$c_{3(i-1)+\ell}(t) = 2|\varsigma_{2(\ell)}|\varrho_i e^{\{|\mu_n|\cos[\arg(\mu_n)+\theta]\}t}$$
$$\times \cos(\{|\mu_n|\sin[\arg(\mu_n)+\theta]\}t + \varphi_i + \arg[\varsigma_{2(\ell)}]),$$

$i = 1, \ldots, n, \ell = 1, 2, 3$. Similar to the argument for the second statement, it can be verified that

$$\left\|[c_{3i-2}(t), c_{3i-1}(t), c_{3i}(t)]^T\right\| = 2\varrho_i e^{\{|\mu_n|\cos[\arg(\mu_n)+\theta]\}t}\sqrt{a_2^2 + a_3^2}\sin^2\left(\frac{\theta}{2}\right),$$

which is growing with time. It thus follows that all agents will eventually move along logarithmic spiral curves. The statement then follows directly. ∎

Corollary 3.1. *Suppose that the directed graph $\mathcal{G}$ has a directed spanning tree. Let the control algorithm for (3.1) be given by (3.2), where $r_i \triangleq [x_i, y_i]^T$ and C is the 2×2 rotation matrix given by $R(\theta) \triangleq \begin{bmatrix} \cos(\theta) & \sin(\theta) \\ -\sin(\theta) & \cos(\theta) \end{bmatrix}$.*

1. If $|\theta| < \theta_s^c$, where $\theta_s^c \triangleq \frac{3\pi}{2} - \arg(\mu_n)$, the agents will eventually rendezvous at the position $[\mathbf{p}^T x(0), \mathbf{p}^T y(0)]$, where x and y are, respectively, the column stack vectors of x_i and y_i, and $\mathbf{p} \in \mathbb{R}^n$ is defined in Lemma 1.1.

2. If $|\theta| = \theta_s^c$ and $\arg(\mu_n)$ is the unique maximum phase of μ_i, all agents will eventually move on circular orbits with the center $[\mathbf{p}^T x(0), \mathbf{p}^T y(0)]$ and the period $\frac{2\pi}{|\mu_n|}$. The radius of the orbit for agent i is given by $2|w_{n(i)}(\frac{\nu_n^T}{\nu_n^T w_n} \otimes [\frac{1}{2}, -\frac{1}{2}\iota])r(0)|$. The relative radius of the orbits is equal to the relative magnitude of $w_{n(i)}$. The relative phase of the agents on their orbits is equal to the relative phase of $w_{n(i)}$.

3. If $\arg(\mu_n)$ is the unique maximum phase of μ_i and $\theta_s^c < |\theta| < \frac{3\pi}{2} - \arg(\mu_{n-1})$, all agents will eventually move along logarithmic spiral curves with the center $[\mathbf{p}^T x, \mathbf{p}^T y]$, the growing rate $|\mu_n| \cos[\arg(\mu_n) + |\theta|]$, and the period $\frac{2\pi}{|\mu_n \sin[\arg(\mu_n)+|\theta|]|}$. The radius of the logarithmic spiral curve for agent i is given by

$$2\left|w_{n(i)}\left(\frac{\nu_n^T}{\nu_n^T w_n} \otimes \left[\frac{1}{2}, -\frac{1}{2}\iota\right]\right)r(0)\right|e^{\{|\mu_n|\cos[\arg(\mu_n)+|\theta|]\}t}.$$

The relative radius of the logarithmic spiral curves is equal to the relative magnitude of $w_{n(i)}$. The relative phase of the agents on their curves is equal to the relative phase of $w_{n(i)}$.

Proof: The eigenvalues of $R(\theta)$ are given by $e^{\iota\theta}$ and $e^{-\iota\theta}$, with the associated right eigenvectors $[1, \iota]^T$ and $[1, -\iota]^T$ and left eigenvectors $[1, -\iota]^T$ and $[1, \iota]^T$, respectively. The rest of the proof follows from that of Theorem 3.2. ∎

Corollary 3.2. *Suppose that the directed graph $\mathcal{G}$ is a unidirectional ring (i.e., a cyclic pursuit graph). Also suppose that $a_{ij} = 1$ if $(j, i) \in \mathcal{E}$ and $a_{ij} = 0$ otherwise. Let the control algorithm for (3.1) be given by (3.2), where r_i and C are given as in Corollary 3.1.*

1. If $|\theta| < \frac{\pi}{n}$, the agents will eventually rendezvous at the position $[\mathbf{p}^T x(0), \mathbf{p}^T y(0)]$, where x, y, and $\mathbf{p}$ are defined in Corollary 3.1.

2. If $|\theta| = \frac{\pi}{n}$, all agents will eventually move on the same circular orbit with the center $[\mathbf{p}^T x(0), \mathbf{p}^T y(0)]$, the period $\frac{\pi}{\sin(\frac{\pi}{n})}$, and the radius $2|w_{n(i)}(\frac{\nu_n^T}{\nu_n^T w_n} \otimes [\frac{1}{2}, -\frac{1}{2}\iota])r(0)|$.[3] In addition, all agents will eventually be evenly distributed on the orbit.

3. If $\frac{\pi}{n} < |\theta| < \frac{2\pi}{n}$, all agents will eventually move along logarithmic spiral curves with the center $[\mathbf{p}^T x(0), \mathbf{p}^T y(0)]$, the growing rate $2\sin(\frac{\pi}{n})\sin(|\theta| - \frac{\pi}{n})$, the period $\frac{\pi}{\sin(\pi/n)\cos(|\theta|-\pi/n)}$, and the radius $2|w_{n(i)}(\frac{\nu_n^T}{\nu_n^T w_n} \otimes [\frac{1}{2}, -\frac{1}{2}\iota])r(0)| \times e^{2[\sin(\frac{\pi}{n})\sin(|\theta|-\frac{\pi}{n})]t}$. In addition, the phases of all agents will eventually be evenly distributed.

Proof: Note that if $\mathcal{G}$ is a unidirectional ring and $a_{ij} = 1$ if $(j, i) \in \mathcal{E}$ and $a_{ij} = 0$ otherwise, then $\mathcal{L}$ is a circulant matrix. Also note that a circulant matrix can be

---

[3] In this case, all $w_{n(i)}$, $i = 1, \ldots, n$, have the same magnitude.
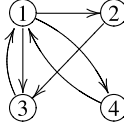
Fig. 3.1 Interaction graph for four agents. An *arrow* from j to i denotes that agent j is a neighbor of agent i

diagonalized by a Fourier matrix. The proof then follows Corollary 3.1 directly by use of the properties of the eigenvalues of a circulant matrix and the properties of the Fourier matrix. ∎

Remark 3.3 Note that when $\mathcal{G}$ is a unidirectional ring (i.e., a cyclic pursuit graph) but different positive weights are chosen for a_{ij}, where $(j, i) \in \mathcal{E}$, all agents will move on orbits with different radii and their phases will not be evenly distributed.

Example 3.1. To illustrate, consider four agents with the directed graph $\mathcal{G}$ shown by Fig. 3.1. Let $\mathcal{L}$ associated with $\mathcal{G}$ be given by

$$
\begin{bmatrix}
1.5 & 0 & -1.1 & -0.4 \\
-1.2 & 1.2 & 0 & 0 \\
-0.1 & -0.5 & 0.6 & 0 \\
-1 & 0 & 0 & 1
\end{bmatrix}.
\tag{3.4}
$$

It can be computed that $\theta_s^c = \frac{3\pi}{2} - \arg(\mu_4) = 1.2975$ rad, where $\mu_4 = -1.6737 - 0.4691\iota$ and $\arg(\mu_4) \in (\pi, \frac{3\pi}{2})$. Let R be the rotation matrix corresponding to the Euler axis $\mathbf{a} = \frac{1}{14}[1, 2, 3]^T$ and the Euler angle $\theta = \theta_s^c$. Figures 3.2, 3.3, and 3.4 show, respectively, the eigenvalues of $-\mathcal{L}$ and $-(\mathcal{L} \otimes R)$ when $\theta = \theta_s^c - 0.1$, $\theta = \theta_s^c$, and $\theta = \theta_s^c + 0.1$. Note that the eigenvalues of $-(\mathcal{L} \otimes R)$ correspond to the eigenvalues of $-\mathcal{L}$ rotated by angles 0, θ, and $-\theta$. Note that in Fig. 3.2, all nonzero eigenvalues of $-(\mathcal{L} \otimes R)$ are in the open left half plane. In Fig. 3.3, the eigenvalues of $-(\mathcal{L} \otimes R)$ corresponding to μ_4 rotated by an angle θ and $\mu_2 = \overline{\mu_4}$ rotated by an angle $-\theta$ are located on the imaginary axis while all other nonzero eigenvalues are located in the open left half plane. In Fig. 3.4, the eigenvalues of $-(\mathcal{L} \otimes R)$ corresponding to μ_4 rotated by an angle θ and $\mu_2 = \overline{\mu_4}$ rotated by an angle $-\theta$ are located in the open right half plane while all other nonzero eigenvalues are located in the open left half plane.

3.1.2 Double-integrator Dynamics

Consider n agents with double-integrator dynamics given by

$$
\dot{r}_i = v_i, \qquad \dot{v}_i = u_i, \quad i = 1, \ldots, n,
\tag{3.5}
$$
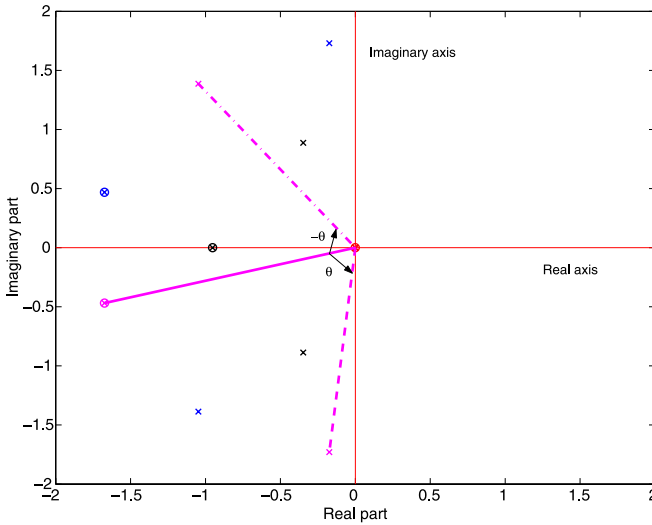
Fig. 3.2 Eigenvalues of $-\mathcal{L}$ and $-(\mathcal{L} \otimes R)$ with $\theta = \theta_s^c - 0.1$. *Circles* denote the eigenvalues of $-\mathcal{L}$ while x-marks denote the eigenvalues of $-(\mathcal{L} \otimes R)$. The eigenvalues of $-(\mathcal{L} \otimes R)$ correspond to the eigenvalues of $-\mathcal{L}$ rotated by angles 0, θ, and $-\theta$, respectively. In particular, the eigenvalues obtained by rotating μ_4 by angles 0, θ, and $-\theta$ are shown by, respectively, the *solid line*, the *dashed line*, and the *dashdot line*. Because $\theta < \theta_s^c$, all nonzero eigenvalues of $-(\mathcal{L} \otimes R)$ are in the *open left half plane*
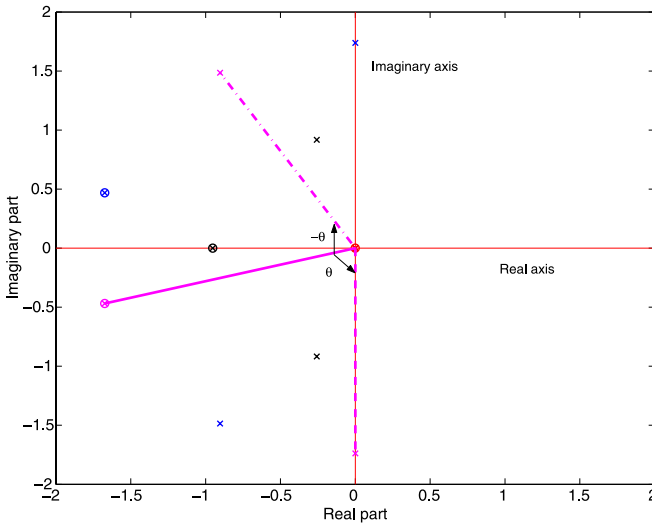
Fig. 3.3 Eigenvalues of $-\mathcal{L}$ and $-(\mathcal{L} \otimes R)$ with $\theta = \theta_s^c$. *Circles* denote the eigenvalues of $-\mathcal{L}$ while x-marks denote the eigenvalues of $-(\mathcal{L} \otimes R)$. The eigenvalues of $-(\mathcal{L} \otimes R)$ correspond to the eigenvalues of $-\mathcal{L}$ rotated by angles 0, θ, and $-\theta$, respectively. In particular, the eigenvalues obtained by rotating μ_4 by angles 0, θ, and $-\theta$ are shown by, respectively, the *solid line*, the *dashed line*, and the *dashdot line*. Because $\theta = \theta_s^c$, two nonzero eigenvalues of $-(\mathcal{L} \otimes R)$ are on the *imaginary axis*

Fig. 3.4 Eigenvalues of $-\mathcal{L}$ and $-(\mathcal{L} \otimes R)$ with $\theta = \theta_s^c + 0.1$. *Circles* denote the eigenvalues of $-\mathcal{L}$ while x-marks denote the eigenvalues of $-(\mathcal{L} \otimes R)$. The eigenvalues of $-(\mathcal{L} \otimes R)$ correspond to the eigenvalues of $-\mathcal{L}$ rotated by angles 0, θ, and $-\theta$, respectively. In particular, the eigenvalues obtained by rotating μ_4 by angles 0, θ, and $-\theta$ are shown by, respectively, the *solid line*, the *dashed line*, and the *dashdot line*. Because $\theta > \theta_s^c$, two nonzero eigenvalues of $-(\mathcal{L} \otimes R)$ are in the *open right half plane*

where $r_i \in \mathbb{R}^m$ and $v_i \in \mathbb{R}^m$ are, respectively, the position and velocity of the ith agent, and $u_i \in \mathbb{R}^m$ is the control input. We introduce a distributed algorithm with Cartesian coordinate coupling for (3.5) as

$$u_i = -\sum_{j=1}^{n} a_{ij} C(r_i - r_j) - \alpha v_i, \quad i = 1, \ldots, n, \tag{3.6}$$

where a_{ij} is defined as in (3.2), $C \in \mathbb{R}^{m \times m}$ denotes a Cartesian coordinate coupling matrix, and α is a positive constant. In this section, we focus on the case where C is a rotation matrix while a similar analysis can be extended to the case where C is a general matrix.

Remark 3.4 Note that the existing consensus algorithm for (3.5) (see, e.g., [248, Chap. 4]) corresponds to the case where $C = I_m$. That is, using the existing consensus algorithm for (3.5), the components of r_i (i.e., the Cartesian coordinates of agent i) are decoupled while using (3.6) the components of r_i are coupled.

Before moving on, we need the following lemma.

Lemma 3.1. *Let ξ_i be the ith eigenvalue of $A \in \mathbb{R}^{n \times n}$ with, respectively, an associated right eigenvector q_i and an associated left eigenvector s_i. Also let $B \triangleq \begin{bmatrix} 0_{n \times n} & I_n \\ A & -\alpha I_n \end{bmatrix}$, where α is a positive scalar. Then the eigenvalues of B are*

given by $\zeta_{2i-1} = \frac{-\alpha+\sqrt{\alpha^2+4\xi_i}}{2}$ with, respectively, the associated right and left eigenvectors $\begin{bmatrix} q_i \\ \zeta_{2i-1}q_i \end{bmatrix}$ and $\begin{bmatrix} (\zeta_{2i-1}+\alpha)s_i \\ s_i \end{bmatrix}$ and $\zeta_{2i} = \frac{-\alpha-\sqrt{\alpha^2+4\xi_i}}{2}$, with, respectively, the associated right and left eigenvectors given by $\begin{bmatrix} q_i \\ \zeta_{2i}q_i \end{bmatrix}$ and $\begin{bmatrix} (\zeta_{2i}+\alpha)s_i \\ s_i \end{bmatrix}$. When $\mathrm{Re}(\xi_i) < 0$, $\mathrm{Re}(\zeta_{2i-1}) < 0$ and $\mathrm{Re}(\zeta_{2i}) < 0$ if and only if $\alpha > \frac{|\mathrm{Im}(\xi_i)|}{\sqrt{\mathrm{Re}(-\xi_i)}}$.

Proof: For the first statement, suppose that ζ is an eigenvalue of B with an associated right eigenvector $\begin{bmatrix} f \\ g \end{bmatrix}$, where $f, g \in \mathbb{C}^n$. It follows that $\begin{bmatrix} 0_{n\times n} & I_n \\ A & -\alpha I_n \end{bmatrix}\begin{bmatrix} f \\ g \end{bmatrix} = \zeta\begin{bmatrix} f \\ g \end{bmatrix}$, which implies $g = \zeta f$ and $Af - \alpha g = \zeta g$. It thus follows that $Af = (\zeta^2 + \alpha\zeta)f$. Noting that $Aq_i = \xi_i q_i$, we let $f = q_i$ and $\zeta^2 + \alpha\zeta = \xi_i$. That is, each eigenvalue of A, ξ_i, corresponds to two eigenvalues of B, denoted by $\zeta_{2i-1,2i} = \frac{-\alpha\pm\sqrt{\alpha^2+4\xi_i}}{2}$. Because $g = \zeta f$, it follows that the right eigenvectors associated with ζ_{2i-1} and ζ_{2i} are, respectively, $\begin{bmatrix} q_i \\ \zeta_{2i-1}q_i \end{bmatrix}$ and $\begin{bmatrix} q_i \\ \zeta_{2i}q_i \end{bmatrix}$. A similar analysis can be used to find the left eigenvectors of B associated with ζ_{2i-1} and ζ_{2i}.

For the second statement, note that $\sqrt{\alpha^2 + 4\xi_i}$ has a nonnegative real part. Because $\zeta_{2i} = \frac{-\alpha-\sqrt{\alpha^2+4\xi_i}}{2}$, it follows that $\mathrm{Re}(\zeta_{2i}) < 0$ if $\alpha > 0$. It is left to show the conditions under which $\mathrm{Re}(\zeta_{2i-1}) < 0$. Suppose that α_i^* is the critical value for α such that ζ_{2i-1} is on the imaginary axis. Let $\zeta_{2i-1} = \eta_i \iota$, where $\eta_i \in \mathbb{R}$. After some manipulation, it follows that $\alpha_i^* = \frac{|\mathrm{Im}(\xi_i)|}{\sqrt{\mathrm{Re}(-\xi_i)}}$. Note that $\mathrm{Re}(\xi_i) < 0$. It is straightforward to verify that if $\alpha > \alpha_i^*$ (respectively, $\alpha < \alpha_i^*$), then ζ_{2i-1} has a negative (respectively, positive) real part. Therefore, when $\mathrm{Re}(\xi_i) < 0$, $\mathrm{Re}(\zeta_{2i-1}) < 0$ and $\mathrm{Re}(\zeta_{2i}) < 0$ if and only if $\alpha > \frac{|\mathrm{Im}(\xi_i)|}{\sqrt{\mathrm{Re}(-\xi_i)}}$. ∎

Theorem 3.5. *Suppose that the directed graph $\mathcal{G}$ has a directed spanning tree. Let the control algorithm for (3.5) be given by (3.6), where $r_i \triangleq [x_i, y_i, z_i]^T$ and $v_i \triangleq [v_{xi}, v_{yi}, v_{zi}]^T$. Let μ_i, w_i, ν_i, and $\arg(\mu_i)$ be defined in Definition 3.1, $\mathbf{p} \in \mathbb{R}^n$ be defined in Lemma 1.1, and $\mathbf{a} \triangleq [a_1, a_2, a_3]^T$, ς_k, and ϖ_k be defined in Lemma 1.20.*

1. *Suppose that $C = I_3$. Then all agents will eventually rendezvous if and only if $\alpha > \alpha^c$, where $\alpha^c \triangleq \max_{\mu_i\neq 0} \frac{|\mathrm{Im}(\mu_i)|}{\sqrt{\mathrm{Re}(-\mu_i)}}$. The rendezvous position is given by*

$$\left\{ \mathbf{p}^T\left[x(0) + \frac{v_x(0)}{\alpha}\right], \mathbf{p}^T\left[y(0) + \frac{v_y(0)}{\alpha}\right], \mathbf{p}^T\left[z(0) + \frac{v_z(0)}{\alpha}\right] \right\}, \qquad (3.7)$$

   where x, y, z, v_x, v_y, and v_z are, respectively, column stack vectors of x_i, y_i, z_i, v_{xi}, v_{yi}, and v_{zi}.

2. *Suppose that $C = R$, where R is the 3×3 rotation matrix defined in Lemma 1.20, and $\alpha > \alpha^c$. Given $|\mu_i|$, $i = 2, \ldots, n$, let $\psi_i^l \in (\frac{\pi}{2}, \pi)$ (respectively, $\psi_i^u \in (\pi, \frac{3\pi}{2})$) be the solution to $|\mu_i|\sin^2(\psi_i) + \alpha^2\cos(\psi_i) = 0$ if $\arg(\mu_i) \in (\frac{\pi}{2}, \pi]$ (respectively, $\arg(\mu_i) \in [\pi, \frac{3\pi}{2})$). If $|\theta| < \theta_d^c$, where $\theta_d^c \triangleq \min_{\arg(\mu_i)\in[\pi,\frac{3\pi}{2}]}[\psi_i^u - \arg(\mu_i)]$, then all agents will eventually rendezvous at the position given by (3.7).*

3. *Under the assumption of part 2, if $|\theta| = \theta_d^c$ and there exists a unique $\arg(\mu_\kappa) \in [\pi, \frac{3\pi}{2})$ such that $\psi_\kappa^u - \arg(\mu_\kappa) = \theta_d^c$, then all agents will eventually move on circular orbits with the center given by (3.7) and the period $\frac{\pi\alpha}{|\mu_\kappa \sin(\psi_\kappa^u)|}$. The radius of the orbit for agent i is given by $2|w_{\kappa(i)} p_c^T [r(0)^T, v(0)^T]^T| \sqrt{a_2^2 + a_3^2} \sin^2(\frac{\theta}{2})$, where $w_{\kappa(i)}$ is the ith component of w_κ and*

$$p_c \triangleq \frac{1}{(2\sigma_c + \alpha)\nu_\kappa^T w_\kappa \varpi_2^T \varsigma_2} \begin{bmatrix} (\sigma_c + \alpha)(\nu_\kappa \otimes \varpi_2) \\ \nu_\kappa \otimes \varpi_2 \end{bmatrix},$$

where $\sigma_c \triangleq \iota \frac{2|\mu_\kappa|\sin(\psi_\kappa^u)}{\alpha}$. The relative radius of the orbits is equal to the relative magnitude of $w_{\kappa(i)}$. The relative phase of the agents on their orbits is equal to the relative phase of $w_{\kappa(i)}$. The circular orbits are on a plane normal to the Euler axis $\mathbf{a}$.

4. *Under the assumption of part 2, if there exists a unique $\arg(\mu_\kappa) \in [\pi, \frac{3\pi}{2})$ such that $\psi_\kappa^u - \arg(\mu_\kappa) = \theta_d^c$ and $\theta_d^c < |\theta| < \min_{\arg(\mu_i) \in [\pi, \frac{3\pi}{2}),\, i \neq \kappa}[\psi_i^u - \arg(\mu_i)]$, then all agents will eventually move along logarithmic spiral curves with the center given by (3.7), the growing rate $\mathrm{Re}(\sigma_s)$, where $\sigma_s \triangleq \frac{-\alpha + \sqrt{\alpha^2 + 4\lambda_s}}{2}$ with $\lambda_s \triangleq \mu_\kappa e^{\iota|\theta|}$, and the period $\frac{2\pi}{|\mathrm{Im}(\sigma_s)|}$. The radius of the logarithmic spiral curve for agent i is*

$$2|w_{\kappa(i)} p_s^T [r(0)^T, v(0)^T]^T e^{\mathrm{Re}(\sigma_s)t} \sqrt{a_2^2 + a_3^2} \sin^2\left(\frac{\theta}{2}\right),$$

where $p_s \triangleq \frac{1}{(2\sigma_s + \alpha)\nu_\kappa^T w_\kappa \varpi_2^T \varsigma_2} \begin{bmatrix} (\sigma_s + \alpha)(\nu_\kappa \otimes \varpi_2) \\ \nu_\kappa \otimes \varpi_2 \end{bmatrix}$. The relative radius of the logarithmic spiral curves is equal to the relative magnitude of $w_{\kappa(i)}$. The relative phase of the agents on their curves is equal to the relative phase of $w_{\kappa(i)}$. The curves are on a plane normal to the Euler axis $\mathbf{a}$.

Proof: For the first statement, if $C = I_3$, then (3.5) using (3.6) can be written in a vector form as

$$\begin{bmatrix} \dot{r} \\ \dot{v} \end{bmatrix} = \left(\underbrace{\begin{bmatrix} 0_{n \times n} & I_n \\ -\mathcal{L} & -\alpha I_n \end{bmatrix}}_{\Psi} \otimes I_3 \right) \begin{bmatrix} r \\ v \end{bmatrix}, \tag{3.8}$$

where $r \triangleq [r_1^T, \ldots, r_n^T]^T$ and $v \triangleq [v_1^T, \ldots, v_n^T]^T$. Note from Lemma 3.1 that each eigenvalue μ_i of $-\mathcal{L}$ corresponds to two eigenvalues of Ψ given by $\zeta_{2i-1} = \frac{-\alpha + \sqrt{\alpha^2 + 4\mu_i}}{2}$ with the associated right and left eigenvectors given by, respectively, $\begin{bmatrix} w_i \\ \zeta_{2i-1} w_i \end{bmatrix}$ and $\begin{bmatrix} (\zeta_{2i-1} + \alpha)\nu_i \\ \nu_i \end{bmatrix}$ and $\zeta_{2i} = \frac{-\alpha - \sqrt{\alpha^2 + 4\mu_i}}{2}$, with the associated right and left eigenvectors given by, respectively, $\begin{bmatrix} w_i \\ \zeta_{2i} w_i \end{bmatrix}$ and $\begin{bmatrix} (\zeta_{2i} + \alpha)\nu_i \\ \nu_i \end{bmatrix}$ where $i = 1, \ldots, n$. Because the directed graph $\mathcal{G}$ has a directed spanning tree, it follows from Lemma 1.1 that $-\mathcal{L}$ has a simple zero eigenvalue and all other eigenvalues have negative real parts. According to Definition 3.1, we let $\mu_1 = 0$ and $\mathrm{Re}(\mu_i) < 0$, $i = 2, \ldots, n$. According to Lemma 1.1, we let $w_1 = \mathbf{1}_n$ and $\nu_1 = \mathbf{p}$ without loss of

generality. It thus follows that $\zeta_1 = 0$[4] with the associated right and left eigenvectors given by, respectively, $\begin{bmatrix} \mathbf{1}_n \\ \mathbf{0}_n \end{bmatrix}$ and $\begin{bmatrix} \alpha\mathbf{P} \\ \mathbf{P} \end{bmatrix}$ and $\zeta_2 = -\alpha$.

We first show that the agents will eventually rendezvous at the position given by (3.7) if and only if Ψ defined in (3.8) has a simple zero eigenvalue and all other eigenvalues have negative real parts. For the sufficiency part, similar to the proof of Theorem 3.2, we write Ψ in the Jordan canonical form as $\Psi = MJM^{-1}$, where the columns of M, denoted by $m_k, k = 1, \ldots, 2n$, can be chosen to be the right eigenvectors or generalized right eigenvectors of Ψ associated with the eigenvalue ζ_k, the rows of M^{-1}, denoted by $p_k^T, k = 1, \ldots, 2n$, can be chosen to be the left eigenvectors or the generalized left eigenvectors of Ψ associated with eigenvalue ζ_k such that $p_k^T m_k = 1$ and $p_k^T m_\ell = 0$, $k \neq \ell$, and J is the Jordan block diagonal matrix with ζ_k being the diagonal entries. Noting that $\zeta_1 = 0$, we choose $m_1 = \begin{bmatrix} \mathbf{1}_n \\ \mathbf{0}_n \end{bmatrix}$ and $p_1 = \begin{bmatrix} \mathbf{P} \\ \frac{1}{\alpha}\mathbf{P} \end{bmatrix}$. Note that $e^{\Psi t} = Me^{Jt}M^{-1}$. Also note that $\lim_{t\to\infty} e^{J_\ell t} = 0_{q_\ell \times q_\ell}$ when $J_\ell \in \mathbb{R}^{q_\ell \times q_\ell}$ is a Jordan block corresponding to an eigenvalue with a negative real part. If Ψ has a simple zero eigenvalue and all other eigenvalues have negative real parts, then $\lim_{t\to\infty} e^{\Psi t} = M(\lim_{t\to\infty} e^{Jt})M^{-1} = \begin{bmatrix} \mathbf{1}_n \\ \mathbf{0}_n \end{bmatrix} \begin{bmatrix} \mathbf{p}^T & \frac{1}{\alpha}\mathbf{p}^T \end{bmatrix}$. It thus follows that

$$\lim_{t\to\infty} \begin{bmatrix} r(t) \\ v(t) \end{bmatrix} = \lim_{t\to\infty} (e^{\Psi t} \otimes I_3) \begin{bmatrix} r(0) \\ v(0) \end{bmatrix} = \left[\left(\begin{bmatrix} \mathbf{1}_n \\ \mathbf{0}_n \end{bmatrix} \begin{bmatrix} \mathbf{p}^T & \frac{1}{\alpha}\mathbf{p}^T \end{bmatrix} \right) \otimes I_3 \right] \begin{bmatrix} r(0) \\ v(0) \end{bmatrix},$$

which implies that $x_i(t) \to \mathbf{p}^T x(0) + \frac{1}{\alpha}\mathbf{p}^T v_x(0)$, $y_i(t) \to \mathbf{p}^T y(0) + \frac{1}{\alpha}\mathbf{p}^T v_y(0)$, $z_i(t) \to \mathbf{p}^T z(0) + \frac{1}{\alpha}\mathbf{p}^T v_z(0)$, $v_{xi}(t) \to 0$, $v_{yi}(t) \to 0$, and $v_{zi}(t) \to 0$ as $t \to \infty$. Equivalently, it follows that all agents will eventually rendezvous at the position given by (3.7). For the necessity part, if the agents eventually rendezvous at the position given by (3.7), we know that $\lim_{t\to\infty} e^{\Psi t} = M(\lim_{t\to\infty} e^{Jt})M^{-1}$ has a rank one, which implies that $\lim_{t\to\infty} e^{Jt}$ has a rank one. Therefore, if the sufficient condition does not hold, it is easy to see that $\lim_{t\to\infty} e^{Jt}$ has a rank larger than one, which results in a contradiction.

We next show that Ψ has a simple zero eigenvalue and all other eigenvalues have negative real parts if and only if $\alpha > \alpha^c$. Note that $\zeta_2 < 0$ if $\alpha > 0$ because $\zeta_2 = -\alpha$. Because $\mathrm{Re}(\mu_i) < 0$, $i = 2, \ldots, n$, it follows from Lemma 3.1 that ζ_{2i-1} and ζ_{2i}, $i = 2, \ldots, n$, have negative real parts if and only if $\alpha > \frac{|\mathrm{Im}(\mu_i)|}{\sqrt{\mathrm{Re}(-\mu_i)}}$, $i = 2, \ldots, n$. Combining the above arguments shows that Ψ has a simple zero eigenvalue and all other eigenvalues have negative real parts if and only if $\alpha > \alpha^c$.

For the second statement, using (3.6), (3.5) can be written in a vector form as

$$\begin{bmatrix} \dot{r} \\ \dot{v} \end{bmatrix} = \underbrace{\begin{bmatrix} 0_{3n \times 3n} & I_{3n} \\ -(\mathcal{L} \otimes R) & -\alpha I_{3n} \end{bmatrix}}_{\Sigma} \begin{bmatrix} r \\ v \end{bmatrix}. \tag{3.9}$$

---

[4] Therefore, Ψ has at least one zero eigenvalue.

As in the proof of Theorem 3.2, let $\lambda_{3i-2} = \mu_i$, $\lambda_{3i-1} = \mu_i e^{\iota\theta}$, and $\lambda_{3i} = \mu_i e^{-\iota\theta}$, $i = 1, \ldots, n$, be the eigenvalues of $-(\mathcal{L} \otimes R)$. Note from Lemma 3.1 that each λ_k corresponds to two eigenvalues of Σ, defined in (3.9), given by $\sigma_{2k-1,2k} = \frac{-\alpha \pm \sqrt{\alpha^2 + 4\lambda_k}}{2}$, $k = 1, \ldots, 3n$. Because $\mu_1 = 0$, it follows that $\lambda_1 = \lambda_2 = \lambda_3 = 0$, which in turn implies that $\sigma_1 = \sigma_3 = \sigma_5 = 0$ and $\sigma_2 = \sigma_4 = \sigma_6 = -\alpha$. Because all $\sqrt{\alpha^2 + 4\lambda_k}$ have nonnegative real parts, it follows that all σ_{2k}, $k = 1, \ldots, 3n$, have negative real parts if $\alpha > 0$. Given $\alpha > 0$ and $\chi_i = |\mu_i| e^{\iota \arg(\chi_i)}$, $i = 2, \ldots, n$, ψ_i^l and ψ_i^u are the critical values for $\arg(\chi_i) \in [0, 2\pi)$ such that $\frac{-\alpha + \sqrt{\alpha^2 + 4\chi_i}}{2}$ is on the imaginary axis. In particular, if $\arg(\chi_i) = \psi_i^l$ (respectively, ψ_i^u), then $\frac{-\alpha + \sqrt{\alpha^2 + 4\chi_i}}{2} = \iota \frac{2|\mu_i| \sin(\arg(\psi_i^l))}{\alpha}$ (respectively, $\iota \frac{2|\mu_i| \sin(\arg(\psi_i^u))}{\alpha}$), $i = 2, \ldots, n$. If $\arg(\chi_i) \in (\psi_i^l, \psi_i^u)$ (respectively, $\arg(\chi_i) \in [0, \psi_i^l) \cup (\psi_i^u, 2\pi)$), then $\frac{-\alpha + \sqrt{\alpha^2 + 4\chi_i}}{2}$ has negative (respectively, positive) real parts. Because $\alpha > \alpha^c$, the first statement implies that all $\frac{-\alpha + \sqrt{\alpha^2 + 4\mu_i}}{2}$, $i = 2, \ldots, n$, have negative real parts, which in turn implies that $\arg(\mu_i) \in (\psi_i^l, \psi_i^u)$, $i = 2, \ldots, n$. If $|\theta| < \theta_d^c$, then $\arg(\lambda_{3i-2})$, $\arg(\lambda_{3i-1})$, and $\arg(\lambda_{3i})$ are all within (ψ_i^l, ψ_i^u), which implies that σ_{6i-5}, σ_{6i-3}, and σ_{6i-1}, $i = 2, \ldots, n$, all have negative real parts. Therefore, if $|\theta| < \theta_d^c$, then Σ has exactly three zero eigenvalues and all other eigenvalues have negative real parts.

Similar to the proof of Theorem 3.2, we write Σ in the Jordan canonical form as MJM^{-1}, where the columns of M, denoted by m_k, $k = 1, \ldots, 6n$, can be chosen to be the right eigenvectors or generalized right eigenvectors of Σ associated with the eigenvalue σ_k, the rows of M^{-1}, denoted by p_k^T, $k = 1, \ldots, 6n$, can be chosen to be the left eigenvectors or generalized left eigenvectors of Σ associated with the eigenvalue σ_k such that $p_k^T m_k = 1$ and $p_k^T m_\ell = 0$, $k \neq \ell$, and J is the Jordan block diagonal matrix with σ_k being the diagonal entries. As in the proof of Theorem 3.2, the right and left eigenvectors of $-(\mathcal{L} \otimes R)$ associated with the eigenvalue $\lambda_\ell = 0$ are, respectively, $\mathbf{1}_n \otimes \varsigma_\ell$ and $\mathbf{p} \otimes \varpi_\ell$, where $\ell = 1, 2, 3$. It in turn follows from Lemma 3.1 that the right and left eigenvectors of Σ associated with $\sigma_{2\ell-1} = 0$ are, respectively, $\begin{bmatrix} \mathbf{1}_n \otimes \varsigma_\ell \\ \mathbf{0}_{3n} \end{bmatrix}$ and $\begin{bmatrix} \alpha \mathbf{p} \otimes \varpi_\ell \\ \mathbf{p} \otimes \varpi_\ell \end{bmatrix}$, where $\ell = 1, 2, 3$. We can choose $m_{2\ell-1} = \begin{bmatrix} \mathbf{1}_n \otimes \varsigma_\ell \\ \mathbf{0}_{3n} \end{bmatrix}$ and $p_{2\ell-1} = \begin{bmatrix} \mathbf{p} \otimes \frac{\varpi_\ell}{\varpi_\ell^T \varsigma_\ell} \\ \mathbf{p} \otimes \frac{\varpi_\ell}{\alpha \varpi_\ell^T \varsigma_\ell} \end{bmatrix}$, where $\ell = 1, 2, 3$. Note that $p_{2\ell-1}^T m_{2\ell-1} = 1$ and $p_{2\ell-1}^T m_{2k-1} = 0$, where $k, \ell = 1, 2, 3$ and $k \neq \ell$. Noting that $\sigma_{2\ell-1} = 0$, $\ell = 1, 2, 3$, it follows that $\lim_{t \to \infty} \begin{bmatrix} r(t) \\ v(t) \end{bmatrix} = (\lim_{t \to \infty} M e^{Jt} M^{-1}) \begin{bmatrix} r(0) \\ v(0) \end{bmatrix} = (\sum_{\ell=1}^3 m_{2\ell-1} p_{2\ell-1}^T) \begin{bmatrix} r(0) \\ v(0) \end{bmatrix}$, which implies that $x_i(t) \to \mathbf{p}^T x(0) + \frac{1}{\alpha} \mathbf{p}^T v_x(0)$, $y_i(t) \to \mathbf{p}^T y(0) + \frac{1}{\alpha} \mathbf{p}^T v_y(0)$, $z_i(t) \to \mathbf{p}^T z(0) + \frac{1}{\alpha} \mathbf{p}^T v_z(0)$, $v_{xi}(t) \to 0$, $v_{yi}(t) \to 0$, and $v_{zi}(t) \to 0$ as $t \to \infty$. Equivalently, it follows that all agents will eventually rendezvous at the position given by (3.7).

For the third statement, if $\theta = \theta_d^c$ (respectively, $\theta = -\theta_d^c$) and there exists a unique $\arg(\mu_\kappa) \in [\pi, \frac{3\pi}{2})$ such that $\psi_\kappa^u - \arg(\mu_\kappa) = \theta_d^c$, then $\lambda_{3\kappa-1} = \mu_\kappa e^{\iota\theta} = |\mu_\kappa| e^{\iota\psi_\kappa^u}$ (respectively, $\lambda_{3\kappa} = \mu_\kappa e^{-\iota\theta} = |\mu_\kappa| e^{\iota\psi_\kappa^u}$), which implies that $\sigma_{6\kappa-3} = \frac{-\alpha + \sqrt{\alpha^2 + 4\lambda_{3\kappa-1}}}{2} = \iota \frac{2|\mu_\kappa| \sin(\psi_\kappa^u)}{\alpha}$ (respectively, $\sigma_{6\kappa-1} = \frac{-\alpha + \sqrt{\alpha^2 + 4\lambda_{3\kappa}}}{2} = $

$\iota \frac{2|\mu_\kappa| \sin(\psi_\kappa^u)}{\alpha}$). Noting that the complex eigenvalues of Σ are in conjugate pairs, it follows that Σ has an eigenvalue equal to $\overline{\sigma_{6\kappa-3}} = -\iota \frac{2|\mu_\kappa| \sin(\psi_\kappa^u)}{\alpha}$ (respectively, $\overline{\sigma_{6\kappa-1}} = -\iota \frac{2|\mu_\kappa| \sin(\psi_\kappa^u)}{\alpha}$), denoted by σ_* for simplicity. In this case, Σ has exactly three zero eigenvalues, two nonzero eigenvalues are on the imaginary axis, and all other eigenvalues have negative real parts. In the following, we focus on $\theta = \theta_d^c$ because the analysis for $\theta = -\theta_d^c$ is similar except that all agents will move in reverse directions. Note from Lemma 3.1 that the right and left eigenvectors associated with $\sigma_{6\kappa-3}$ are, respectively, $\left[\begin{smallmatrix} w_\kappa \otimes \varsigma_2 \\ \sigma_{6\kappa-3}(w_\kappa \otimes \varsigma_2) \end{smallmatrix} \right]$ and $\left[\begin{smallmatrix} (\sigma_{6\kappa-3}+\alpha)(\nu_\kappa \otimes \varpi_2) \\ \nu_\kappa \otimes \varpi_2 \end{smallmatrix} \right]$. We can choose $m_{6\kappa-3} = \left[\begin{smallmatrix} w_\kappa \otimes \varsigma_2 \\ \sigma_{6\kappa-3}(w_\kappa \otimes \varsigma_2) \end{smallmatrix} \right]$ and $p_{6\kappa-3} = \frac{1}{(2\sigma_{6\kappa-3}+\alpha)\nu_\kappa^T w_\kappa \varpi_2^T \varsigma_2} \left[\begin{smallmatrix} (\sigma_{6\kappa-3}+\alpha)(\nu_\kappa \otimes \varpi_2) \\ \nu_\kappa \otimes \varpi_2 \end{smallmatrix} \right]$. Note that $p_{6\kappa-3}^T m_{6\kappa-3} = 1$. Similarly, it follows that m_* and p_* correspond to σ_* are given by $m_* = \overline{m_{6\kappa-3}}$ and $p_* = \overline{p_{6\kappa-3}}$. Therefore, by following a similar proof to that of the second statement of Theorem 3.2, we can show that all agents will eventually move on circular orbits with the center given by (3.7) and the period $\frac{\pi \alpha}{|\mu_\kappa \sin(\psi_\kappa^u)|}$. The radius of the orbit for agent i is given by $2|w_{\kappa(i)} p_{6\kappa-3}^T \times [r^T(0), v^T(0)]^T| \sqrt{a_2^2 + a_3^2} \sin^2(\frac{\theta}{2})$. The relative radius of the orbits is equal to the relative magnitude of $w_{\kappa(i)}$. In addition, the relative phase of the agents is equal to the relative phase of $w_{\kappa(i)}$. By following a similar proof to that of the second statement of Theorem 3.2, it follows that the circular orbits are on a plane normal to the Euler axis $\mathbf{a}$.

For the fourth statement, if there exists a unique $\arg(\mu_\kappa) \in [\pi, \frac{3\pi}{2})$ such that $\psi_\kappa^u - \arg(\mu_\kappa) = \theta_d^c$ and $\theta_d^c < \theta < \min_{\arg(\mu_i) \in [\pi, \frac{3\pi}{2}), i \neq \kappa} [\psi_i^u - \arg(\mu_i)]$ (respectively, $-\min_{\arg(\mu_i) \in [\pi, \frac{3\pi}{2}), i \neq \kappa} [\psi_i^u - \arg(\mu_i)] < \theta < -\theta_d^c$), then $\lambda_{3\kappa-1} = \mu_\kappa e^{\iota \theta} = |\mu_\kappa| e^{\iota [\arg(\mu_\kappa) + \theta]}$ (respectively, $\lambda_{3\kappa} = \mu_\kappa e^{-\iota \theta} = |\mu_\kappa| e^{\iota [\arg(\mu_\kappa) - \theta]}$), where $\arg(\mu_\kappa) + \theta > \psi_\kappa^u$ (respectively, $\arg(\mu_\kappa) - \theta > \psi_\kappa^u$), which implies that $\sigma_{6\kappa-3} = \frac{-\alpha + \sqrt{\alpha^2 + 4\lambda_{3\kappa-1}}}{2}$ (respectively, $\sigma_{6\kappa-1} = \frac{-\alpha + \sqrt{\alpha^2 + 4\lambda_{3\kappa}}}{2}$) has a positive real part. A similar argument as above shows that Σ has exactly three zero eigenvalues and two eigenvalues with positive real parts and all other eigenvalues have negative real parts. By following a similar procedure to the proof of the third statement of Theorem 3.2, we can show that all agents will eventually move along logarithmic spiral curves with the center given by (3.7), the growing rate $\text{Re}(\sigma_{6\kappa-3})$, and the period $\frac{2\pi}{|\text{Im}(\sigma_{6\kappa-3})|}$. ∎

Remark 3.6 Unlike the single-integrator case, the critical value θ_d^c for double-integrator dynamics depends on both α and $\mathcal{L}$. Note that $\theta_d^c < \theta_s^c$. When α increases to infinity, θ_d^c approaches θ_s^c. Note that besides the interaction graph and the Euler angle, α plays an important role in (3.6).

Example 3.2. To illustrate, we consider the same $\mathcal{G}$ and $\mathcal{L}$ as in Example 3.1. It can be computed that $\theta_d^c = 0.3557$ rad. Note that θ_d^c is smaller than θ_s^c in Example 3.1. Let R be the rotation matrix corresponding to the Euler axis $\mathbf{a} = \frac{1}{14}[1, 2, 3]^T$ and the Euler angle $\theta = \theta_d^c$. Figure 3.5 shows the eigenvalues of $-\mathcal{L}$ and $-(\mathcal{L} \otimes R)$. Note that the eigenvalues of $-(\mathcal{L} \otimes R)$ correspond to the eigenvalues of $-\mathcal{L}$ rotated by angles 0, θ, and $-\theta$. Figure 3.6 shows the eigenvalues of Σ. Note that each eigenvalue of $-(\mathcal{L} \otimes R)$, λ_k, correspond to two eigenvalues of Σ, $\sigma_{2k-1,2k}$, where $\sigma_{2k-1,2k} =$
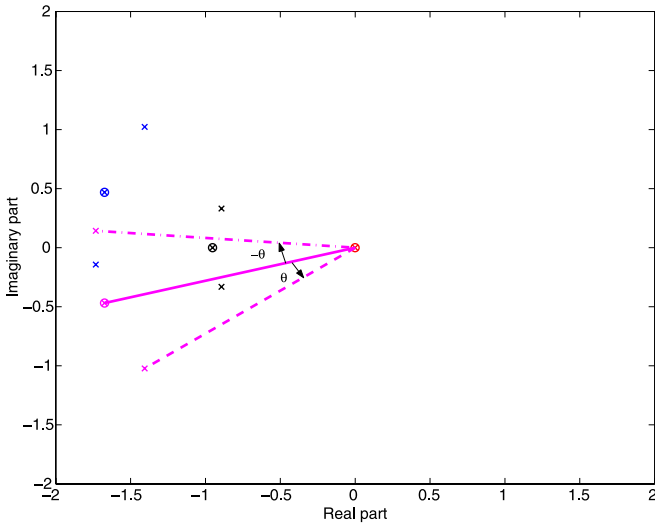
Fig. 3.5 Eigenvalues of $-\mathcal{L}$ and $-(\mathcal{L} \otimes R)$ with $\theta = \theta_d^c$. *Circles* denote the eigenvalues of $-\mathcal{L}$ while x-marks denote the eigenvalues of $-(\mathcal{L} \otimes R)$. The eigenvalues of $-(\mathcal{L} \otimes R)$ correspond to the eigenvalues of $-\mathcal{L}$ rotated by angles 0, θ, and $-\theta$, respectively. In particular, the eigenvalues obtained by rotating μ_4 by angles 0, θ, and $-\theta$ are shown by, respectively, the *solid line*, the *dashed line*, and the *dashdot line*
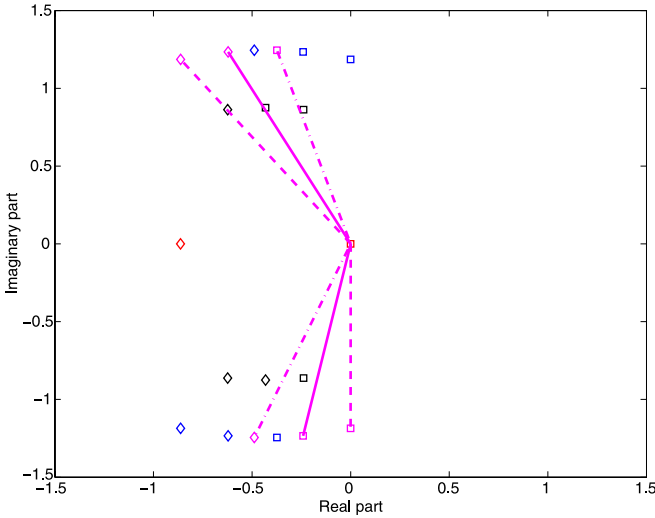
Fig. 3.6 Eigenvalues of Σ. *Squares* denote the eigenvalues computed by $\sigma_{2k-1} = \frac{-\alpha + \sqrt{\alpha^2 + 4\lambda_k}}{2}$ while *diamonds* denote the eigenvalues computed by $\sigma_{2k} = \frac{-\alpha - \sqrt{\alpha^2 + 4\lambda_k}}{2}$, $k = 1, \ldots, 12$. In particular, the eigenvalues of Σ correspond to $\lambda_{10} = \mu_4$, $\lambda_{11} = \mu_4 e^{\iota\theta}$, and $\lambda_{12} = \mu_4 e^{-\iota\theta}$ are shown by, respectively, the *solid line*, the *dashed line*, and the *dashdot line*. Because $\theta = \theta_d^c$, two nonzero eigenvalues of Σ are on the *imaginary axis*

$\frac{-\alpha \pm \sqrt{\alpha^2 + 4\lambda_k}}{2}$, $k = 1, \ldots, 12$. Because $\theta = \theta_d^c$, two nonzero eigenvalues of Σ are located on the imaginary axis as shown in Fig. 3.6.

3.1.3 Simulation

In this subsection, we study collective motions of four agents using, respectively, (3.2) and (3.6). Suppose that the interaction graph is given by Fig. 3.1 and $\mathcal{L}$ is given by (3.4). Let θ_s^c, θ_d^c, and **a** be given in Examples 3.1 and 3.2. Using (3.6), it can be computed that $\alpha^c = 0.3626$. We let $\alpha = 0.8626$. Note that there exists a unique $\arg(\mu_4) \in [\pi, \frac{3\pi}{2})$ such that $\psi_4^u - \arg(\mu_4) = \theta_d^c$ (i.e., $\kappa = 4$ in Theorem 3.5). Note that a right eigenvector of $-\mathcal{L}$ associated with the eigenvalue μ_4 is $w_4 = [-0.2847 - 0.2820\iota, 0.7213, -0.2501 + 0.1355\iota, 0.4809 + 0.0837\iota]^T$. Also note that $\mathbf{p} = [0.2502, 0.1911, 0.4587, 0.1001]^T$.

Figures 3.7, 3.8, and 3.9 show, respectively, the trajectories of the four agents using (3.2) with $\theta = \frac{\theta_s^c}{2}$, $\theta = \theta_s^c$, and $\theta_s^c + 0.1$. Note that all agents eventually rendezvous when $\theta = \frac{\theta_s^c}{2}$, move on circular orbits when $\theta = \theta_s^c$, and move along logarithmic spiral curves when $\theta = \theta_s^c + 0.1$. Also note that when $\theta = \theta_s^c$, the relative radius of the circular orbits (respectively, the relative phase of the agents) is equal to the relative magnitude (respectively, phase) of the components of w_4. In addition, the trajectories of all agents are normal to the Euler axis **a** in all cases.

Figures 3.10, 3.11, 3.12, and 3.13 show, respectively, the trajectories of the four agents using (3.6) with $R = I_3$, $\theta = \theta_d^c - 0.2$, $\theta = \theta_d^c$, and $\theta = \theta_d^c + 0.2$. Note that all agents eventually rendezvous at the position given by (3.7) when $R = I_3$ or
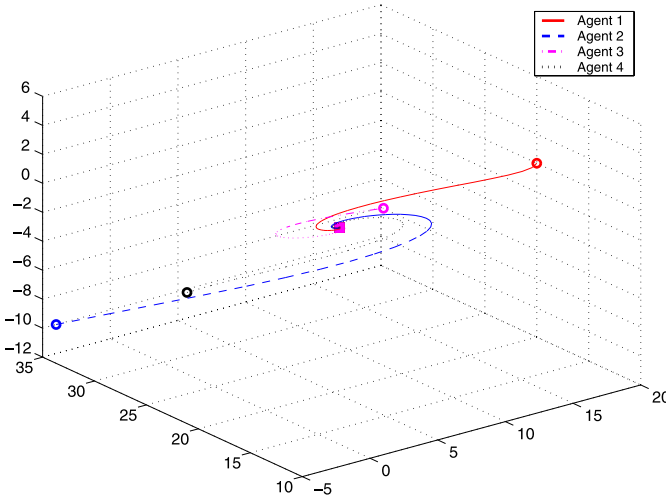
Fig. 3.7 Trajectories of the four agents using (3.2) with $\theta = \frac{\theta_s^c}{2}$. *Circles* denote the starting positions of the agents while the *squares* denote the snapshots of the agents at 10 s
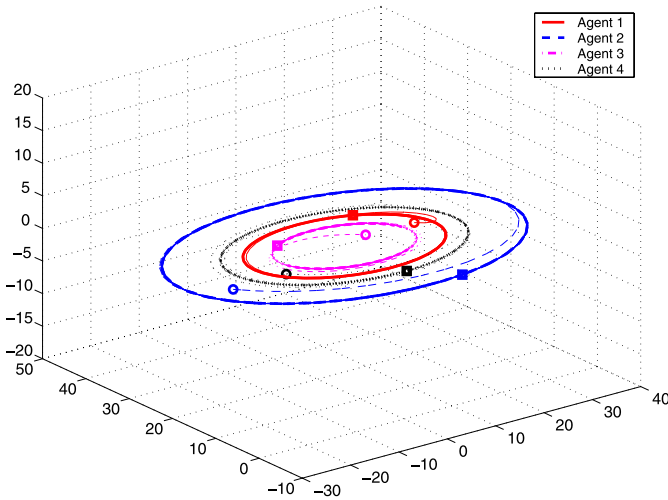
Fig. 3.8 Trajectories of the four agents using (3.2) with $\theta = \theta_s^c$. *Circles* denote the starting positions of the agents while the *squares* denote the snapshots of the agents at 30 s
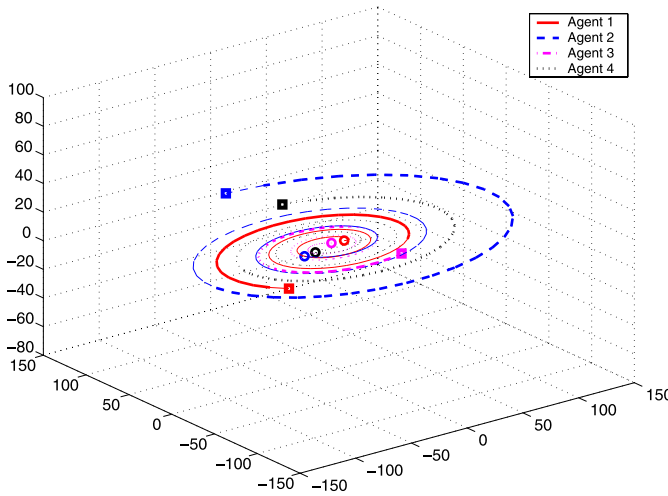
Fig. 3.9 Trajectories of the four agents using (3.2) with $\theta = \theta_s^c + 0.1$. *Circles* denote the starting positions of the agents while the *squares* denote the snapshots of the agents at 10 s

$\theta = \theta_d^c - 0.2$, move on circular orbits when $\theta = \theta_d^c$, and move along logarithmic spiral curves when $\theta = \theta_d^c + 0.2$. While similar motions to those using (3.2) are observed, the critical value for the Euler angle, the period of the circular motion, and the period and the growing rate of the logarithmic spiral motion using (3.6) are different from those using (3.2) even if the interaction graph and $\mathcal{L}$ are chosen to be the same.
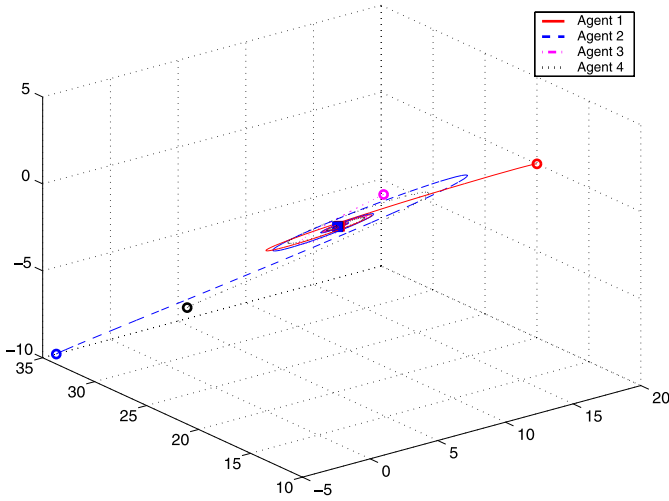
Fig. 3.10 Trajectories of the four agents using (3.6) with $R = I_3$. *Circles* denote the starting positions of the agents while the *squares* denote the snapshots of the agents at 20 s
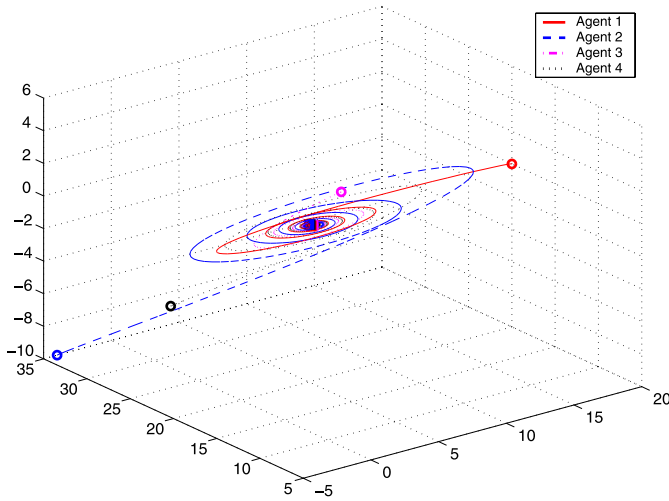
Fig. 3.11 Trajectories of the four agents using (3.6) with $\theta = \theta_d^c - 0.2$. *Circles* denote the starting positions of the agents while the *squares* denote the snapshots of the agents at 30 s

3.2 Coupled Harmonic Oscillators

In this section, we study coupled second-order linear harmonic oscillators with local interaction to achieve synchronized oscillatory motions. We will analyze convergence conditions under, respectively, directed fixed and switching interaction graphs.
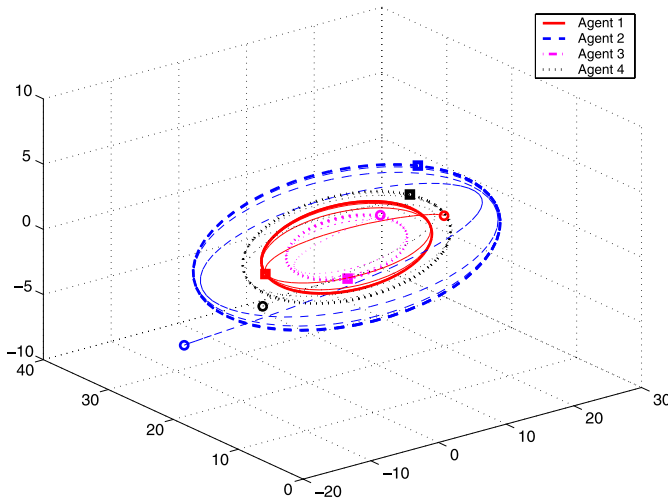
Fig. 3.12 Trajectories of the four agents using (3.6) with $\theta = \theta_d^c$. *Circles* denote the starting positions of the agents while the *squares* denote the snapshots of the agents at 30 s
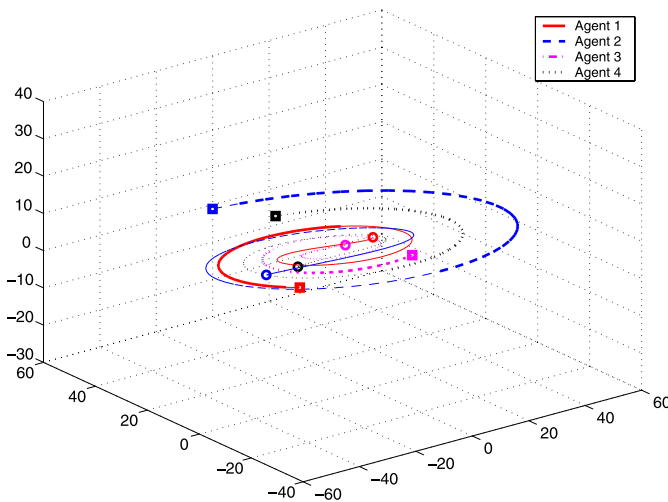
Fig. 3.13 Trajectories of the four agents using (3.6) with $\theta = \theta_d^c + 0.2$. *Circles* denote the starting positions of the agents while the *squares* denote the snapshots of the agents at 10 s

3.2.1 Problem Statement

When two objects of mass m are connected by a damper with the coefficient b and are each attached to fixed supports by identical springs with the spring constant k,

they can be represented by

$$m\ddot{x}_1 + kx_1 + b(\dot{x}_1 - \dot{x}_2) = 0, \qquad (3.10a)$$
$$m\ddot{x}_2 + kx_2 + b(\dot{x}_2 - \dot{x}_1) = 0, \qquad (3.10b)$$

where $x_i \in \mathbb{R}$ denotes the position of the ith object. Motivated by (3.10), we study n coupled harmonic oscillators with local interaction of the form

$$\ddot{x}_i + \alpha(t)x_i + \sum_{j=1}^{n} a_{ij}(t)(\dot{x}_i - \dot{x}_j) = 0, \quad i = 1, \ldots, n, \qquad (3.11)$$

where $x_i \in \mathbb{R}$ is the position of the ith oscillator, $\alpha(t)$ is a positive gain at time t, and $a_{ij}(t)$ is the (i,j)th entry of the adjacency matrix $\mathcal{A}(t)$ associated with the directed graph $\mathcal{G}(t) \triangleq [\mathcal{V}, \mathcal{E}(t)]$ characterizing the interaction among the n oscillators at time t (i.e., $a_{ij}(t) > 0$ if oscillator i can obtain the velocity of oscillator j at time t and $a_{ij}(t) = 0$ otherwise). While (3.11) conceptually represents a system where n virtual masses are connected by virtual dampers, the purpose of this section is to adopt (3.11) as a distributed algorithm for synchronization of the positions and velocities of n networked point-mass agents.

Let $r_i \triangleq x_i$ and $v_i \triangleq \dot{x}_i$. Equation (3.11) can be written as

$$\dot{r}_i = v_i,$$
$$\dot{v}_i = -\alpha(t)r_i - \sum_{j=1}^{n} a_{ij}(t)(v_i - v_j), \quad i = 1, \ldots, n. \qquad (3.12)$$

Let $r \triangleq [r_1, \ldots, r_n]^T$ and $v \triangleq [v_1, \ldots, v_n]^T$. Equation (3.12) can be written in a vector form as

$$\begin{bmatrix} \dot{r} \\ \dot{v} \end{bmatrix} = \underbrace{\begin{bmatrix} 0_{n \times n} & I_n \\ -\alpha(t)I_n & -\mathcal{L}(t) \end{bmatrix}}_{\mathcal{Q}} \begin{bmatrix} r \\ v \end{bmatrix}, \qquad (3.13)$$

where $\mathcal{L}(t) \in \mathbb{R}^{n \times n}$ is the nonsymmetric Laplacian matrix associated with $\mathcal{A}(t)$ and hence $\mathcal{G}(t)$ at time t. In the following, we focus on the one-dimensional space for simplicity of presentation. However, all results hereafter are still valid for any high-dimensional space by use of the properties of the Kronecker product.

3.2.2 Convergence Under Directed Fixed Interaction

In this subsection, we consider convergence of (3.12) under a directed fixed interaction graph. Here we assume that both α and $\mathcal{L}$ in (3.13) are constant. Both leaderless and leader-following cases will be addressed. We need the following lemmas for our main result.

Lemma 3.2. *Let μ_i be the ith eigenvalue of $-\mathcal{L}$. Also let $\chi_{ri} \in \mathbb{C}^n$ and $\chi_{\ell i} \in \mathbb{C}^n$ be, respectively, the right and left eigenvectors of $-\mathcal{L}$ associated with μ_i. Then the eigenvalues of $\mathcal{Q}$, defined in (3.13), are given by $\lambda_{i\pm} = \frac{\mu_i \pm \sqrt{\mu_i^2 - 4\alpha}}{2}$ with the associated right eigenvectors $\varphi_{ri\pm} = [\chi_i^T, \lambda_{i\pm}\chi_i^T]^T$ and left eigenvectors $\varphi_{\ell i\pm} = [\chi_{\ell i}^T, -\frac{\lambda_{i\pm}}{\alpha}\chi_{\ell i}^T]^T$.*

Proof: Let λ be an eigenvalue of $\mathcal{Q}$ and $\varphi_r = [x_r^T, y_r^T]^T \in \mathbb{C}^{2n}$ be an associated right eigenvector. Then we get that

$$\begin{bmatrix} 0_{n\times n} & I_n \\ -\alpha I_n & -\mathcal{L} \end{bmatrix} \begin{bmatrix} x_r \\ y_r \end{bmatrix} = \lambda \begin{bmatrix} x_r \\ y_r \end{bmatrix}. \tag{3.14}$$

It follows from (3.14) that

$$y_r = \lambda x_r, \tag{3.15a}$$

$$-\alpha x_r - \mathcal{L}y_r = \lambda y_r. \tag{3.15b}$$

Combining (3.15a) and (3.15b) gives $-\mathcal{L}x_r = \frac{\lambda^2 + \alpha}{\lambda}x_r$. Suppose that μ is an eigenvalue of $-\mathcal{L}$ with an associated right eigenvector χ_r. It follows that $\frac{\lambda^2 + \alpha}{\lambda} = \mu$ and $x_r = \chi_r$. Therefore, it follows that λ satisfies

$$\lambda^2 - \mu\lambda + \alpha = 0 \tag{3.16}$$

and $\varphi_r = [\chi_r^T, \lambda\chi_r^T]^T$ according to (3.15a). Noting that μ_i is the ith eigenvalue of $-\mathcal{L}$ with an associated right eigenvector χ_{ri}, it follows from (3.16) that the eigenvalues of $\mathcal{Q}$ are given by $\lambda_{i\pm} = \frac{\mu_i \pm \sqrt{\mu_i^2 - 4\alpha}}{2}$ with the associated right eigenvectors $\varphi_{ri\pm} = [\chi_{ri}^T, \lambda_{i\pm}\chi_{ri}^T]^T$.

Similarly, let $\varphi_\ell = [x_\ell^T, y_\ell^T]^T \in \mathbb{C}^{2n}$ be a left eigenvector of $\mathcal{Q}$ associated with the eigenvalue λ. Then we get that

$$[x_\ell^T, y_\ell^T] \begin{bmatrix} 0_{n\times n} & I_n \\ -\alpha I_n & -\mathcal{L} \end{bmatrix} = \lambda[x_\ell^T, y_\ell^T]. \tag{3.17}$$

It follows from (3.17) that

$$y_\ell^T = -\frac{\lambda}{\alpha}x_\ell^T, \tag{3.18a}$$

$$x_\ell^T - y_\ell^T\mathcal{L} = \lambda y_\ell^T. \tag{3.18b}$$

Combining (3.18a) and (3.18b) gives that $-x_\ell^T\mathcal{L} = \frac{\lambda^2 + \alpha}{\lambda}x_\ell^T$. A similar argument to that of the right eigenvectors shows that the left eigenvectors of $\mathcal{Q}$ associated with $\lambda_{i\pm}$ are $\varphi_{\ell i\pm} = [\chi_{\ell i}^T, -\frac{\lambda_{i\pm}}{\alpha}\chi_{\ell i}^T]^T$. ∎

In the leaderless case, we have the following theorem.

Theorem 3.7. *Let $\mathbf{p} \in \mathbb{R}^n$ be defined in Lemma 1.1. Let μ_i, $\lambda_{i\pm}$, $\varphi_{ri\pm}$, and $\varphi_{\ell i\pm}$ be defined in Lemma 3.2. Suppose that the directed graph $\mathcal{G}$ has a directed spanning*

tree. Using (3.12), $|r_i(t) - [\cos(\sqrt{\alpha}t)\mathbf{p}^T r(0) + \frac{1}{\sqrt{\alpha}}\sin(\sqrt{\alpha}t)\mathbf{p}^T v(0)]| \to 0$ *and*
$|v_i(t) - [-\sqrt{\alpha}\sin(\sqrt{\alpha}t)\mathbf{p}^T r(0) + \cos(\sqrt{\alpha}t)\mathbf{p}^T v(0)]| \to 0$ *as* $t \to \infty$.

Proof: Note that the directed graph $\mathcal{G}$ has a directed spanning tree. It follows from Lemma 1.1 that $-\mathcal{L}$ has a simple zero eigenvalue with an associated right eigenvector $\mathbf{1}_n$ and left eigenvector $\mathbf{p}$ that satisfies $\mathbf{p} \geq 0$, $\mathbf{p}^T\mathcal{L} = 0$, and $\mathbf{p}^T\mathbf{1}_n = 1$. In addition, all other eigenvalues of $-\mathcal{L}$ have negative real parts. Without loss of generality, let $\mu_1 = 0$ and then we get that $\text{Re}(\mu_i) < 0$, $i = 2, \ldots, n$. Accordingly, it follows from Lemma 3.2 that $\lambda_{1\pm} = \pm\sqrt{\alpha}\iota$ with the associated right and left eigenvectors given by

$$\varphi_{r1\pm} = \left[\mathbf{1}_n^T, \pm\sqrt{\alpha}\iota\mathbf{1}_n^T\right]^T, \qquad \varphi_{\ell1\pm} = \left[\mathbf{p}^T, \pm\frac{1}{\sqrt{\alpha}\iota}\mathbf{p}^T\right]^T. \qquad (3.19)$$

Because $\text{Re}(\mu_i) < 0$, $i = 2, \ldots, n$, it follows that $\text{Re}(\lambda_{i-}) = \text{Re}(\frac{\mu_i - \sqrt{\mu_i^2 - 4\alpha}}{2}) < 0$, $i = 2, \ldots, n$. Noting that $\lambda_{i+}\lambda_{i-} = \alpha$, $i = 2, \ldots, n$, it follows that $\arg(\lambda_{i+}) = -\arg(\lambda_{i-})$. Therefore, it follows that $\text{Re}(\lambda_{i+}) < 0$, $i = 2, \ldots, n$.

Note that $\mathcal{Q}$ can be written in the Jordan canonical form as

$$\mathcal{Q} = \underbrace{[w_1, \ldots, w_{2n}]}_{P} \begin{bmatrix} \sqrt{\alpha}\iota & 0 & 0_{1\times(2n-2)} \\ 0 & -\sqrt{\alpha}\iota & 0_{1\times(2n-2)} \\ 0_{(2n-2)\times1} & 0_{(2n-2)\times1} & \overline{J} \end{bmatrix} \underbrace{\begin{bmatrix} \nu_1^T \\ \vdots \\ \nu_{2n}^T \end{bmatrix}}_{P^{-1}}, \qquad (3.20)$$

where $w_i \in \mathbb{R}^{2n}$, $i = 1, \ldots, 2n$, can be chosen to be the right eigenvectors or generalized eigenvectors of $\mathcal{Q}$, $\nu_i \in \mathbb{R}^{2n}$, $i = 1, \ldots, 2n$, can be chosen to be the left eigenvectors or generalized eigenvectors of $\mathcal{Q}$, and $\overline{J}$ is the Jordan upper diagonal block matrix corresponding to the eigenvalues λ_{i+} and λ_{i-}, $i = 2, \ldots, n$. Because $P^{-1}P = I_{2n}$, w_i and ν_i must satisfy that $\nu_i^T w_i = 1$ and $\nu_i^T w_k = 0$, where $i \neq k$. Accordingly, we let $w_1 = \varphi_{r1+}$, $w_2 = \varphi_{r1-}$, $\nu_1 = \frac{1}{2}\varphi_{\ell1+}$, and $\nu_2 = \frac{1}{2}\varphi_{\ell1-}$, where $\varphi_{r1\pm}$ and $\varphi_{\ell\pm}$ are defined in (3.19).

Let

$$\Phi(t) \triangleq e^{\sqrt{\alpha}\iota t} \begin{bmatrix} \mathbf{1}_n \\ \sqrt{\alpha}\iota\mathbf{1}_n \end{bmatrix} \begin{bmatrix} \frac{1}{2}\mathbf{p}^T, & \frac{1}{2\sqrt{\alpha}\iota}\mathbf{p}^T \end{bmatrix}$$

$$+ e^{-\sqrt{\alpha}\iota t} \begin{bmatrix} \mathbf{1}_n \\ -\sqrt{\alpha}\iota\mathbf{1}_n \end{bmatrix} \begin{bmatrix} \frac{1}{2}\mathbf{p}^T, & -\frac{1}{2\sqrt{\alpha}\iota}\mathbf{p}^T \end{bmatrix}$$

$$= \begin{bmatrix} \cos(\sqrt{\alpha}t)\mathbf{1}_n\mathbf{p}^T & \frac{1}{\sqrt{\alpha}}\sin(\sqrt{\alpha}t)\mathbf{1}_n\mathbf{p}^T \\ -\sqrt{\alpha}\sin(\sqrt{\alpha}t)\mathbf{1}_n\mathbf{p}^T & \cos(\sqrt{\alpha}t)\mathbf{1}_n\mathbf{p}^T \end{bmatrix}.$$

Because $e^{\mathcal{Q}t} = Pe^{Jt}P^{-1}$ and $\lim_{t\to\infty} e^{\overline{J}t} = 0_{(2n-2)\times(2n-2)}$, it follows that $\lim_{t\to\infty} \|e^{\mathcal{Q}t} - \Phi(t)\| = 0$. The solution to (3.13) is given by $\begin{bmatrix} r(t) \\ v(t) \end{bmatrix} = e^{\mathcal{Q}t}\begin{bmatrix} r(0) \\ v(0) \end{bmatrix}$.
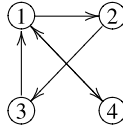
Fig. 3.14 Directed fixed graph $\mathcal{G}$. An *arrow* from j to i denotes that agent j is a neighbor of agent i
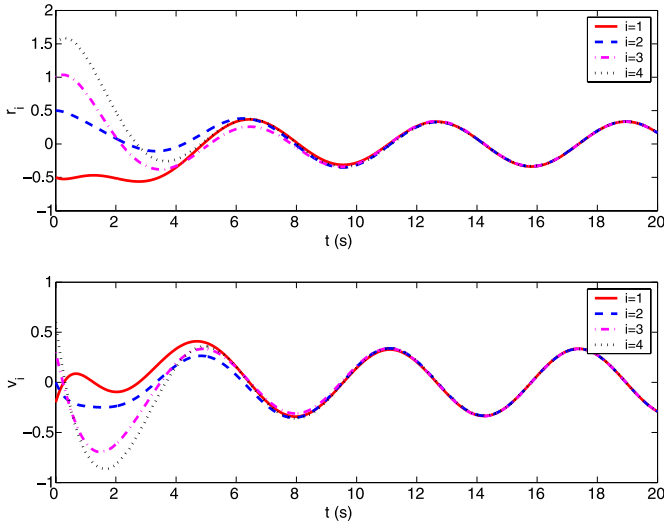
Fig. 3.15 Evolution of the oscillator states using (3.12) with $\alpha = 1$ and $\mathcal{G}$ shown in Fig. 3.14

Therefore, it follows that

$$\left| r_i(t) - \left[\cos(\sqrt{\alpha}t)\mathbf{p}^T r(0) + \frac{1}{\sqrt{\alpha}}\sin(\sqrt{\alpha}t)\mathbf{p}^T v(0) \right] \right| \to 0$$

and

$$\left| v_i(t) - \left[-\sqrt{\alpha}\sin(\sqrt{\alpha}t)\mathbf{p}^T r(0) + \cos(\sqrt{\alpha}t)\mathbf{p}^T v(0) \right] \right| \to 0$$

as $t \to \infty$. ∎

Example 3.3. To illustrate, we show simulation results involving four coupled harmonic oscillators using (3.12) under the directed fixed graph $\mathcal{G}$ as shown in Fig. 3.14. Note that $\mathcal{G}$ in this case has a directed spanning tree, implying that the condition of Theorem 3.7 is satisfied. We assume that $a_{ij} = 1$ if $(j,i) \in \mathcal{E}$ and $a_{ij} = 0$ otherwise. Figures 3.15 and 3.16 show, respectively, the evolution of the oscillator states with $\alpha = 1$ and $\alpha = 4$. Note that the oscillator states are synchronized for both $\alpha = 1$ and $\alpha = 4$. However, the value of α has an effect on the amplitude and frequency of the synchronized states.

Under the condition of Theorem 3.7, all r_i converge to a common oscillatory trajectory, so do all v_i. That is, the n coupled harmonic oscillators are synchronized.
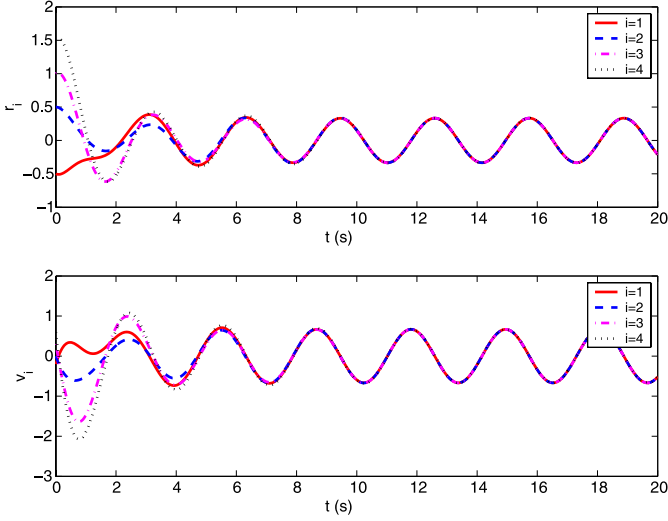
Fig. 3.16 Evolution of the oscillator states using (3.12) with $\alpha = 4$ and $\mathcal{G}$ shown in Fig. 3.14

We next consider the case where there exist n followers, labeled as oscillators or followers 1 to n, and a leader, labeled as oscillator 0 with states r_0 and v_0. Here the leader can be virtual or physical. Let $\mathcal{G} \triangleq (\mathcal{V}, \mathcal{E})$ be the directed graph characterizing the interaction among the n followers. Let $\overline{\mathcal{G}} \triangleq (\overline{\mathcal{V}}, \overline{\mathcal{E}})$ be the directed graph characterizing the interaction among the leader and the followers corresponding to $\mathcal{G}$.

Suppose that r_0 and v_0 satisfy

$$\dot{r}_0 = v_0, \qquad \dot{v}_0 = -\alpha r_0, \tag{3.21}$$

where α is a positive gain. In this case, we study the system

$$\begin{aligned} \dot{r}_i &= v_i, \\ \dot{v}_i &= -\alpha r_i - \sum_{j=0}^{n} a_{ij}(v_i - v_j), \quad i = 1, \ldots, n, \end{aligned} \tag{3.22}$$

where $a_{ij}, i, j = 1, \ldots, n$ is the (i,j)th entry of the adjacency matrix $\mathcal{A}$ associated with $\mathcal{G}$, and a_{i0} is a positive constant if the leader is a neighbor of oscillator i and $a_{i0} = 0$ otherwise.

Corollary 3.3. *Suppose that in $\overline{\mathcal{G}}$ the leader has directed paths to all followers 1 to n. Using (3.22), $|r_i(t) - r_0(t)| \to 0$ and $|v_i(t) - v_0(t)| \to 0$ as $t \to \infty$, where*

$$\begin{aligned} r_0(t) &= \cos(\sqrt{\alpha}t)r_0(0) + \frac{1}{\alpha}\sin(\sqrt{\alpha}t)v_0(0), \\ v_0(t) &= -\sqrt{\alpha}\sin(\sqrt{\alpha}t)r_0(0) + \cos(\sqrt{\alpha}t)v_0(0). \end{aligned} \tag{3.23}$$

Proof: It is straightforward to show that the solution to (3.21) is given by (3.23). Consider a team consisting of $n + 1$ oscillators (oscillators 0 to n). The proof is a direct application of that of Theorem 3.7. ∎

We also consider the case where there exist deviations between oscillator states. In this case, we study the system

$$\dot{r}_i = v_i,$$
$$\dot{v}_i = -\alpha(r_i - \delta_i) - \sum_{j=0}^{n} a_{ij}(v_i - v_j), \quad i = 1, \ldots, n, \tag{3.24}$$

where δ_i is a constant, and α and $a_{ij}, i = 1, \ldots, n, j = 0, \ldots, n$ are defined as in (3.22).

Corollary 3.4. *Suppose that in $\overline{\mathcal{G}}$ the leader has directed paths to all followers 1 to n. Using (3.24), $|r_i(t) - [r_0(t) + \delta_i]| \to 0$ and $|v_i(t) - v_0(t)| \to 0$ as $t \to \infty$, where $r_0(t)$ and $v_0(t)$ are defined in Corollary 3.3.*

Proof: Let $\tilde{r}_i \triangleq r_i - \delta_i$. Noting that $\dot{\tilde{r}}_i = v_i$, it follows from Corollary 3.3 that $|\tilde{r}_i(t) - r_0(t)| \to 0$ and $|v_i(t) - v_0(t)| \to 0$ as $t \to \infty$ with $\tilde{r}_i$ playing the role of r_i in (3.22). ∎

3.2.3 Convergence Under Directed Switching Interaction

In this subsection, we consider convergence of (3.12) under a directed switching interaction graph. We consider two cases, namely, (i) the directed graph $\mathcal{G}(t)$ is strongly connected and balanced at each time instant; and (ii) the directed graph $\mathcal{G}(t)$ has a directed spanning tree at each time instant.

Let $\mathcal{P}$ denote a set indexing the class of all possible directed graphs $\mathcal{G}_p$, where $p \in \mathcal{P}$, defined on n nodes. The adjacency matrix and the nonsymmetric Laplacian matrix associated with $\mathcal{G}_p$ are denoted by, respectively, $\mathcal{A}_p$ and $\mathcal{L}_p$. Note that $\mathcal{P}$ is a finite set by definition. Suppose that (3.12) can be written as

$$\begin{bmatrix} \dot{r} \\ \dot{v} \end{bmatrix} = \underbrace{\begin{bmatrix} 0_{n \times n} & I_n \\ -\alpha_{\sigma(t)} I_n & -\mathcal{L}_{\sigma(t)} \end{bmatrix}}_{\mathcal{Q}_{\sigma(t)}} \begin{bmatrix} r \\ v \end{bmatrix}, \tag{3.25}$$

where $\sigma : [0, \infty) \mapsto \mathcal{P}$ is a piecewise constant switching signal with switching times $t_0, t_1, \ldots, \alpha_{\sigma(t)}$ is a positive gain associated with the directed graph $\mathcal{G}_{\sigma(t)}$, and $\mathcal{L}_{\sigma(t)}$ is the nonsymmetric Laplacian matrix associated with $\mathcal{A}_{\sigma(t)}$ and hence $\mathcal{G}_{\sigma(t)}$.

Theorem 3.8. *Suppose that $\sigma(t) \in \mathcal{P}_{sb}$, where $\mathcal{P}_{sb} \subset \mathcal{P}$ denotes the set indexing the class of all possible directed graphs defined on n nodes that are strongly connected and balanced. Also suppose that $\alpha_{\sigma(t)} \equiv \alpha_{sb}$, where α_{sb} is a positive scalar. Using (3.12), $|r_i(t) - r_j(t)| \to 0$ and $|v_i(t) - v_j(t)| \to 0$ as $t \to \infty$.*

Proof: [5] Consider the Lyapunov function candidate

$$V = \frac{1}{2}\alpha_{sb}r^T r + \frac{1}{2}v^T v. \tag{3.26}$$

Noting that $\dot{v}$ is discontinuous due to switches of interaction graphs, we have $\dot{v} \in^{a.e.} K[-\mathcal{L}_{\sigma(t)}v] - \alpha_{sb}r$, where $K[\cdot]$ is a differential inclusion and *a.e.* stands for "almost everywhere". The set-valued Lie derivative of V is given by $\widetilde{L}_F V = \alpha_{sb}v^T r + v^T[-\alpha_{sb}r + \phi_v] = v^T\phi_v$, where ϕ_v is an arbitrary element of $K[-\mathcal{L}_{\sigma(t)}v]$. Note that the directed graph $\mathcal{G}_{\sigma(t)}$ is strongly connected and balanced. It follows from Lemma 1.2 that $-v^T\mathcal{L}_{\sigma(t)}v \le 0$, which implies that $\max_{\phi_v \in K[-\mathcal{L}_{\sigma(t)}v]}(v^T\phi_v) = \max(K[-v^T\mathcal{L}_{\sigma(t)}v]) = 0$. In particular, $\max(K[-v^T\mathcal{L}_{\sigma(t)}v]) = 0$ if and only if $v_i = v_j$, which in turn implies that $\dot{v}_i = \dot{v}_j$. Noting that $\alpha_{\sigma(t)} \equiv \alpha_{sb}$, it follows from (3.25) (see also (3.12)) that $r_i = r_j$ when $v_i = v_j$ and $\dot{v}_i = \dot{v}_j$. It thus follows from Lemma 1.40 that $|r_i(t) - r_j(t)| \to 0$ and $|v_i(t) - v_j(t)| \to 0$ as $t \to \infty$. ∎

Let $r_{ij} \triangleq r_i - r_j$ and $v_{ij} \triangleq v_i - v_j$. Also let $\tilde{r} \triangleq [r_{12}, r_{23}, \ldots, r_{(n-1)n}]^T$ and $\tilde{v} \triangleq [v_{12}, v_{23}, \ldots, v_{(n-1)n}]^T$. Equation (3.25) can be rewritten as

$$\begin{bmatrix} \dot{\tilde{r}} \\ \dot{\tilde{v}} \end{bmatrix} = \underbrace{\begin{bmatrix} 0_{n-1} & I_{n-1} \\ -\alpha_{\sigma(t)}I_{n-1} & -\mathcal{D}_{\sigma(t)} \end{bmatrix}}_{\mathcal{R}_{\sigma(t)}} \begin{bmatrix} \tilde{r} \\ \tilde{v} \end{bmatrix}, \tag{3.27}$$

where $\mathcal{D}_{\sigma(t)} \in \mathbb{R}^{(n-1)\times(n-1)}$ can be derived from $\mathcal{L}_{\sigma(t)}$. Before moving on, we need the following lemma.

Lemma 3.3 ([201, Lemma 2]). *Let $\{A_p : p \in \mathcal{P}\}$ be a closed bounded set of real $n \times n$ matrices. Suppose that for each $p \in \mathcal{P}$, A_p is stable, and let a_p and χ_p be any finite nonnegative and positive numbers, respectively, for which $\|e^{A_p t}\| \le e^{a_p - \chi_p t}$, $t \ge 0$. Suppose that τ_0 is a number satisfying $\tau_0 > \sup_{p \in \mathcal{P}}\{\frac{a_p}{\chi_p}\}$. For any admissible switching signal $\sigma : [0, \infty) \to \mathcal{P}$ with dwell time no smaller than τ_0, the transition matrix of A_σ satisfies that $\|\Phi(t, \mu)\| \le e^{a - \chi(t-\mu)}$, $\forall t \ge \mu \ge 0$, where $a \triangleq \sup_{p \in \mathcal{P}}\{a_p\}$ and $\chi \triangleq \inf_{p \in \mathcal{P}}\{\chi_p - \frac{a_p}{\tau_0}\}$.*

Theorem 3.9. *Let $\mathcal{P}_{st} \subset \mathcal{P}$ denote the set indexing the class of all possible directed graphs defined on n nodes that have a directed spanning tree. The following two statements hold:*

1. *The matrix $\mathcal{R}_p$ defined in (3.27) is stable for each $p \in \mathcal{P}_{st}$.*
2. *Let $a_p \ge 0$ and $\chi_p > 0$, for which $\|e^{\mathcal{R}_p t}\| \le e^{a_p - \chi_p t}$, $t \ge 0$. Suppose that $\sigma(t) \in \mathcal{P}_{st}$. If $t_{k+1} - t_k > \sup_{p \in \mathcal{P}_{st}}\{\frac{a_p}{\chi_p}\}$, $\forall k = 0, 1, \ldots$, then using (3.12), $|r_i(t) - r_j(t)| \to 0$ and $|v_i(t) - v_j(t)| \to 0$ as $t \to \infty$.*

---

[5] The proof is motivated by that of Theorem 1 in [289], which relies on differential inclusions and nonsmooth analysis. We only sketch the main steps of the proof.

Proof: For the first statement, note that Theorem 3.7 implies that for each $p \in \mathcal{P}_{st}$ and all $i, j = 1, \ldots, n$, $|r_i(t) - r_j(t)| \to 0$ and $|v_i(t) - v_j(t)| \to 0$ as $t \to \infty$, which implies that $\|\tilde{r}(t)\| \to 0$ and $\|\tilde{v}(t)\| \to 0$ as $t \to \infty$. It thus follows from (3.27) that $\mathcal{R}_p$ is stable for each $p \in \mathcal{P}_{st}$.

For the second statement, under the condition of the theorem, because $\mathcal{R}_p$ is stable for each $p \in \mathcal{P}_{st}$, it follows from Lemma 3.3 that the switched system (3.27) is globally exponentially stable if $t_{k+1} - t_k > \sup_{p \in \mathcal{P}_{st}} \{\frac{a_p}{\chi_p}\}$, $\forall k = 0, 1, \ldots$. Equivalently, it follows that under the same condition $|r_i(t) - r_j(t)| \to 0$ and $|v_i(t) - v_j(t)| \to 0$ as $t \to \infty$. ∎

Remark 3.10 Note that Theorem 3.9 imposes a bound on how fast the interaction graph can switch while Theorem 3.8 does not. Also note that the convergence condition in Theorem 3.9 is only a sufficient condition. When there exists a leader, the analysis can follow a similar line to that of Theorems 3.8 and 3.9.

Example 3.4. To illustrate, we show simulation results involving four coupled harmonic oscillators using (3.12) under a directed switching interaction graph. We first let $\alpha_{\sigma(t)} \equiv 1$ and $\mathcal{G}(t)$ switches randomly from $\{\mathcal{G}_{(1)}, \mathcal{G}_{(2)}, \mathcal{G}_{(3)}\}$ as shown in Fig. 3.17. We assume that $a_{ij} = 1$ if $(j, i) \in \mathcal{E}$ and $a_{ij} = 0$ otherwise. Here we let $t_0 = 0$ s and choose t_k randomly from $(2k - 2, 2k)$ s, $k = 1, 2, \ldots$. Note that $\mathcal{G}_{(1)}$–$\mathcal{G}_{(3)}$ shown in Fig. 3.17 are all strongly connected and balanced, implying that the condition of Theorem 3.8 is satisfied. Figure 3.18 shows the evolution of the oscillator states in this case. Note that all oscillator states are synchronized. We then let $\alpha_{\sigma(t)}$ switch randomly from $\{\alpha_{(1)}, \alpha_{(2)}, \alpha_{(3)}\}$, where

$$\alpha_{(1)} = 1, \qquad \alpha_{(2)} = 4, \qquad \alpha_{(3)} = 9 \qquad (3.28)$$

and $\mathcal{G}(t)$ switches randomly from $\{\mathcal{G}_{(1)}, \mathcal{G}_{(2)}, \mathcal{G}_{(3)}\}$ as shown in Fig. 3.19. Here we again let $t_0 = 0$ s and choose t_k randomly from $(2k - 2, 2k)$ s, $k = 1, 2, \ldots$. Note that $\mathcal{G}_{(1)}$–$\mathcal{G}_{(3)}$ shown in Fig. 3.19 all have a directed spanning tree, implying that the condition of Theorem 3.9 is satisfied. Figure 3.20 shows the evolution of the oscillator states in this case. In contrast to the previous case, the oscillator states do not approach a uniform amplitude and frequency due to switching of α values. However, all oscillator states are still synchronized.

(a) $\mathcal{G}_{(1)}$ (b) $\mathcal{G}_{(2)}$ (c) $\mathcal{G}_{(3)}$
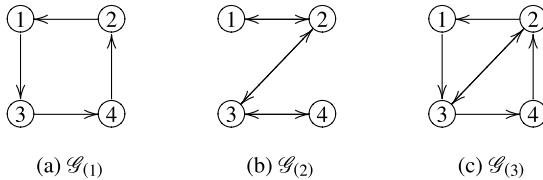
Fig. 3.17 Directed graphs $\mathcal{G}_{(1)}$–$\mathcal{G}_{(3)}$. All $\mathcal{G}_{(1)}$–$\mathcal{G}_{(3)}$ are strongly connected and balanced. An *arrow* from j to i denotes that agent j is a neighbor of agent i
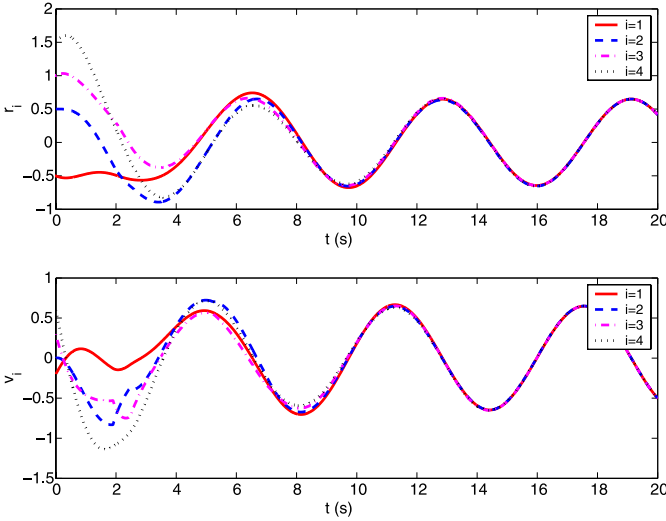
Fig. 3.18 Evolution of the oscillator states using (3.12) when $\alpha_{\sigma(t)} \equiv 1$ and $\mathcal{G}(t)$ switches from $\{\mathcal{G}_{(1)}, \mathcal{G}_{(2)}, \mathcal{G}_{(3)}\}$ as shown in Fig. 3.17

(a) $\mathscr{G}_{(1)}$ (b) $\mathscr{G}_{(2)}$ (c) $\mathscr{G}_{(3)}$
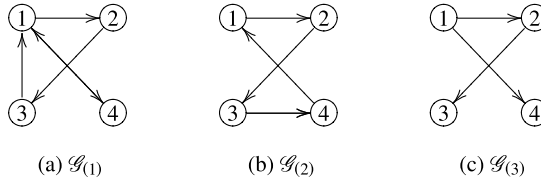
Fig. 3.19 Directed graphs $\mathcal{G}_{(1)}$–$\mathcal{G}_{(3)}$. All of them have a directed spanning tree. An *arrow* from j to i denotes that agent j is a neighbor of agent i

3.2.4 Application to Motion Coordination in Multi-agent Systems

In this subsection, we apply (3.24) to motion coordination in multi-agent systems. Suppose that there are four point-mass agents in the team with dynamics give by $\dot{p}_i = q_i$ and $\dot{q}_i = w_i$, $i = 1, \ldots, 4$, where $p_i \triangleq [x_i, y_i]^T$ is the position, $q_i \triangleq [v_{xi}, v_{yi}]^T$ is the velocity, and $w_i \triangleq [w_{xi}, w_{yi}]^T$ is the acceleration input. Also suppose that there exists a virtual leader, labeled as agent 0, with the position $p_0 \triangleq [x_0, y_0]^T$ and the velocity $q_0 \triangleq [v_{x0}, v_{y0}]^T$, and p_0 and q_0 satisfy

$$\dot{p}_0 = q_0, \qquad \dot{q}_0 = -\alpha p_0, \tag{3.29}$$

where α is a positive constant. We apply (3.24) to design w_{xi} and w_{yi}, respectively, as
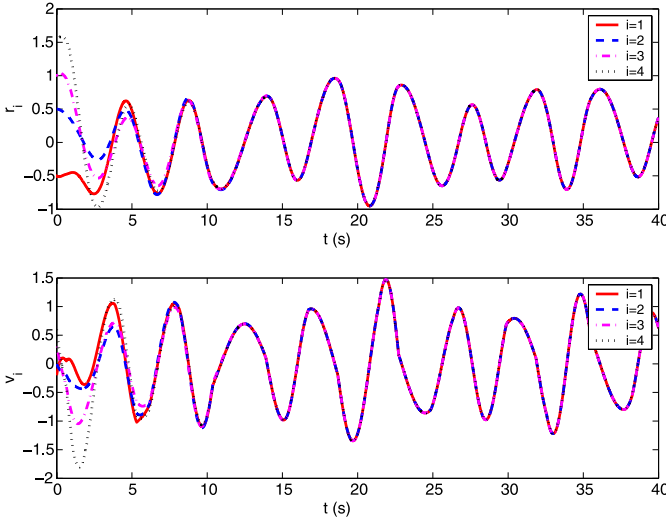
Fig. 3.20 Evolution of the oscillator states using (3.12) when $\alpha_{\sigma(t)}$ switches from (3.28) and $\mathcal{G}(t)$ switches from $\{\mathcal{G}_{(1)}, \mathcal{G}_{(2)}, \mathcal{G}_{(3)}\}$ as shown in Fig. 3.19

Table 3.1 Parameters and initial conditions used in the simulation

$\alpha = 1$
$\delta_{x1} = 0, \delta_{x2} = 4, \delta_{x3} = 0, \delta_{x4} = 4$
$\delta_{y1} = 0, \delta_{y2} = 0, \delta_{y3} = -4, \delta_{y4} = -4$
$x_0(0) = 1, x_1(0) = 1.2, x_2(0) = 0.8, x_3(0) = 1.4, x_4(0) = 0.5$
$y_0(0) = -1, y_1(0) = -1.2, y_2(0) = -0.8, y_3(0) = -0.7, y_4(0) = 1.5$
$v_{x0}(0) = 1, v_{x1}(0) = 0.2, v_{x2}(0) = 0.3, v_{x3}(0) = 0.4, v_{x4}(0) = 0.5$
$v_{y0}(0) = 1, v_{y1}(0) = 0.4, v_{y2}(0) = 0.6, v_{y3}(0) = 0.8, v_{y4}(0) = 1$

$$w_{xi} = -\alpha(x_i - \delta_{xi}) - \sum_{j=0}^{n} a_{ij}(v_{xi} - v_{xj}),$$

$$w_{yi} = -\alpha(y_i - \delta_{yi}) - \sum_{j=0}^{n} a_{ij}(v_{yi} - v_{yj}),$$

where δ_{xi} and δ_{yi} are constant.

Parameters and initial conditions used in the simulation are shown in Table 3.1. By solving (3.29), it is straightforward to show that the trajectory of the virtual leader follows an elliptic orbit.

Figure 3.21 shows the interaction graph for agents 1 to 4 and the virtual leader (i.e., agent 0). We let $a_{ij} = 1$, $i, j = 0, \ldots, 4$, if $(j, i) \in \overline{\mathcal{E}}$ and $a_{ij} = 0$ otherwise. Figure 3.22 shows the complete trajectories and snapshots of the four agents.
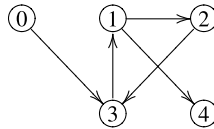
Fig. 3.21 Interaction graph for the four agents and the virtual leader. An *arrow* from j to i denotes that agent j is a neighbor of agent i
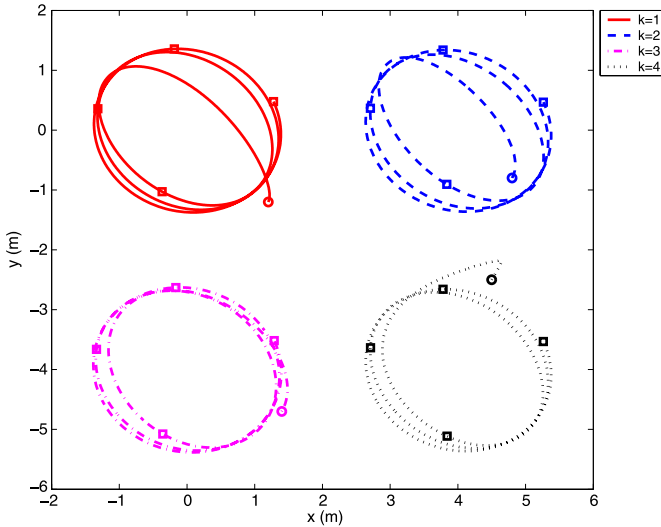
Fig. 3.22 Complete trajectories of the four agents. *Circles* show the snapshot at $t = 0$ s while *squares* show the snapshots at $t = 5, 10, 15, 20$ s

Note that the four agents are able to synchronize their motions and move on elliptic orbits.

3.3 Notes

The results in this chapter are based mainly on [241–244]. For further results on collective periodic motion coordination, see [141, 175, 176, 187, 226, 238, 262, 263, 271, 281]. In particular, a cyclic pursuit strategy, where each agent pursues only one other agent with the interaction graph forming a unidirectional ring, is studied for agents with single-integrator dynamics in [176, 271] while for mobile agents subject to nonholonomic constraints in [187]. The cyclic pursuit strategy is generalized in [226] by letting each agent pursue one other agent along the line of sight rotated by a common offset angle. It is shown that depending on the common offset angle, the agents can achieve different symmetric formations, namely, convergence to a single point, a circle, or a logarithmic spiral pattern in the two-dimensional space.

The result is further extended in [238] to deal with single- and double-integrator models in the three-dimensional space. In particular, it is shown that more robust, locally stable motions on circular orbits can be achieved by making the rotation angle a function of the relative positions of the agents. Symmetric formations are also studied by adopting models based on the Frenet–Serret equations of motion [141] or by exploring the connections between phase models of coupled oscillators and kinematic models of steered particle groups [262, 263]. In addition, a collective rotating formation control problem, where all agents surround a common point with a desired formation structure, is investigated in [175] for double-integrator agents in the two-dimensional space. In [281], synchronization of coupled second-order linear harmonic oscillators is revisited under a dynamic proximity graph. It is shown that the coupled second-order linear harmonic oscillators can always be synchronized without imposing any graph connectivity assumption.

Chapter 4
Collective Tracking with a Dynamic Leader

This chapter introduces a collective tracking problem in the presence of a dynamic leader. The problem has applications in formation flying, body guard, and target tracking. We solve the distributed collective tracking problem via a variable structure approach when there exists a dynamic leader who is a neighbor of only a subset of a group of followers, all followers have only local interaction, and only partial measurements of the states of the leader and the followers are available. In the context of collective tracking, we focus on both coordinated tracking and swarm tracking algorithms. The objective of coordinated tracking is that a group of followers intercepts a dynamic leader with local interaction. The objective of swarm tracking is that a group of followers moves cohesively with a dynamic leader while avoiding inter-agent collision with local interaction. Both single-integrator dynamics and double-integrator dynamics are considered. Several simulation examples are presented as a proof of concept.

4.1 Problem Statement

Although *leaderless coordination* is useful in applications such as cooperative rendezvous of a group of agents, there are many applications that require a dynamic leader. Here the leader can be virtual or physical. Examples include formation flying, body guard, and target tracking applications. The objective of *coordinated tracking* is that a group of followers intercepts a dynamic leader with local interaction. The objective of *swarm tracking* is that a group of followers moves cohesively with a dynamic leader while avoiding inter-agent collision with local interaction. In the context of this chapter, we use the term *collective tracking* to refer to both coordinated tracking and swarm tracking. We focus on solving a distributed collective tracking problem via a variable structure approach when there exists a dynamic leader under the following three assumptions: (i) The dynamic leader is a neighbor of only a subset of a group of followers; (ii) There exists only local interaction among all followers; (iii) The velocity measurements of the dynamic leader and all

followers in the case of single-integrator dynamics or the acceleration measurements of the dynamic leader and all followers in the case of double-integrator dynamics are not required. In contrast to the assumptions that appeared in the literature, the three assumptions are more general and practical.

The contributions of this chapter are twofold. In the case of single-integrator dynamics, we propose a distributed coordinated tracking algorithm without velocity measurements under both fixed and switching interaction graphs. In particular, we show that distributed coordinated tracking can be achieved in finite time. We then extend the result to achieve distributed swarm tracking without velocity measurements. In the case of double-integrator dynamics, we first propose two distributed coordinated tracking algorithms without acceleration measurements when the velocity of the dynamic leader is varying under, respectively, a fixed and switching interaction graph. In particular, we show that the proposed algorithms guarantee at least global exponential tracking. We then propose a distributed coordinated tracking algorithm and a distributed swarm tracking algorithm when the velocity of the dynamic leader is constant. When the velocity of the dynamic leader is varying, distributed swarm tracking is solved by introducing a distributed estimator. For distributed coordinated tracking, a mild connectivity requirement is proposed by adopting an adaptive connectivity maintenance mechanism in which the control weights are adjusted in a proper way. Similarly, a mild connectivity requirement is proposed for distributed swarm tracking by adopting a connectivity maintenance mechanism in which the potential function is defined in a proper way.

Suppose that in addition to n followers, labeled as agents or followers 1 to n, there exists a dynamic leader, labeled as agent 0. Let $\mathcal{G} \triangleq (\mathcal{V}, \mathcal{E})$ be the undirected graph characterizing the interaction among the n followers. Let $\overline{\mathcal{G}} \triangleq (\overline{\mathcal{V}}, \overline{\mathcal{E}})$ be the directed graph characterizing the interaction among the leader and the followers corresponding to $\mathcal{G}$. In the following, we assume that all agents are in a one-dimensional space for the simplicity of presentation. However, all results hereafter are still valid for the m-dimensional ($m > 1$) space by the introduction of the Kronecker product.

4.2 Collective Tracking for Single-integrator Dynamics

In this section, we study distributed collective tracking for single-integrator dynamics. Suppose that the leader has a (time-varying) position r_0 and velocity $\dot{r}_0$. We assume that $|\dot{r}_0| \leq \gamma_\ell$, where γ_ℓ is a positive constant.

4.2.1 Coordinated Tracking Under Fixed and Switching Interaction

In this subsection, we design u_i for (3.1) such that all followers intercept the dynamic leader with local interaction in the absence of velocity measurements. We

propose the distributed coordinated tracking algorithm for (3.1) as

$$u_i = -\alpha \sum_{j=0}^{n} a_{ij}(r_i - r_j) - \beta \operatorname{sgn}\left[\sum_{j=0}^{n} a_{ij}(r_i - r_j)\right], \qquad (4.1)$$

where a_{ij}, $i, j = 1, \ldots, n$, is the (i, j)th entry of the adjacency matrix $\mathcal{A} \in \mathbb{R}^{n \times n}$ associated with the undirected graph $\mathcal{G}$, a_{i0}, $i = 1, \ldots, n$, is a positive constant if the leader is a neighbor of follower i and $a_{i0} = 0$ otherwise, α is a nonnegative constant, and β is a positive constant. We first consider the case of a fixed interaction graph.

Remark 4.1 Due to the introduction of the signum function, the proposed algorithms in this chapter are discontinuous. Therefore, we study the Filippov solutions of the closed-loop systems using the proposed discontinuous algorithms via the nonsmooth analysis in Sect. 1.5. It follows from Lemma 1.38 that the Filippov solutions of the closed-loop systems exist because the signum function is measurable and locally essentially bounded.

Theorem 4.2. *Suppose that the fixed undirected graph $\mathcal{G}$ is connected and at least one a_{i0} is nonzero (and hence positive). Using (4.1) for (3.1), if $\beta > \gamma_\ell$, then $|r_i(t) - r_0(t)| \to 0$ in finite time. In particular, $r_i(t) = r_0(t)$ for any $t \geq \bar{t}$, where*

$$\bar{t} = \frac{\sqrt{\tilde{r}^T(0) M \tilde{r}(0)} \sqrt{\lambda_{\max}(M)}}{(\beta - \gamma_\ell) \lambda_{\min}(M)}, \qquad (4.2)$$

where $\tilde{r}$ is the column stack vector of $\tilde{r}_i$, $i = 1, \ldots, n$, with $\tilde{r}_i \triangleq r_i - r_0$, and $M \triangleq \mathcal{L} + \operatorname{diag}(a_{10}, \ldots, a_{n0})$ with $\mathcal{L}$ being the Laplacian matrix associated with $\mathcal{A}$ and hence $\mathcal{G}$.

Proof: Noting that $\tilde{r}_i = r_i - r_0$, we can rewrite the closed-loop system of (3.1) using (4.1) as

$$\dot{\tilde{r}}_i = -\alpha \sum_{j=0}^{n} a_{ij}(\tilde{r}_i - \tilde{r}_j) - \beta \operatorname{sgn}\left[\sum_{j=0}^{n} a_{ij}(\tilde{r}_i - \tilde{r}_j)\right] - \dot{r}_0. \qquad (4.3)$$

Equation (4.3) can be written in a vector form as

$$\dot{\tilde{r}} = -\alpha M \tilde{r} - \beta \operatorname{sgn}(M \tilde{r}) - \mathbf{1}_n \dot{r}_0,$$

where $\tilde{r}$ and M are defined in (4.2), and $\operatorname{sgn}(\cdot)$ is defined componentwise. Because the fixed undirected graph $\mathcal{G}$ is connected and at least one a_{i0} is nonzero (and hence positive), it follows from Lemma 1.6 that M is symmetric positive definite.

Consider the Lyapunov function candidate $V = \frac{1}{2} \tilde{r}^T M \tilde{r}$. According to Definition 1.10, the set-valued Lie derivative of V is given by

$$\widetilde{L}_F V = \bigcap_{\xi \in \partial V(\tilde{r})} \xi^T K \big[-\alpha M \tilde{r} - \beta \operatorname{sgn}(M\tilde{r}) - \mathbf{1}_n \dot{r}_0 \big],$$

where $\partial V(\tilde{r})$ is the generalized gradient of V at $\tilde{r}$. Because V is continuously differentiable with respect to $\tilde{r}$, $\partial V(\tilde{r}) = \{M\tilde{r}\}$, which is a singleton. Therefore, it follows that

$$\begin{aligned}
\widetilde{L}_F V &= \tilde{r}^T M K \big[-\alpha M \tilde{r} - \beta \operatorname{sgn}(M\tilde{r}) - \mathbf{1}_n \dot{r}_0 \big] \\
&= K \big[-\alpha \tilde{r}^T M^2 \tilde{r} - \beta \left\| M\tilde{r} \right\|_1 - \dot{r}_0 \tilde{r}^T M \mathbf{1}_n \big] \\
&= \big\{ -\alpha \tilde{r}^T M^2 \tilde{r} - \beta \left\| M\tilde{r} \right\|_1 - \dot{r}_0 \tilde{r}^T M \mathbf{1}_n \big\},
\end{aligned} \tag{4.4}$$

where we have used the fact that $\tilde{r}^T M K[-\beta \operatorname{sgn}(M\tilde{r})] = K[-\beta \tilde{r}^T M \operatorname{sgn}(M\tilde{r})] = \{-\beta \left\| M\tilde{r} \right\|_1\}$. It follows that $\widetilde{L}_F V$ is a singleton, whose only element is actually $\dot{V}$. Therefore, it follows that

$$\begin{aligned}
\max \widetilde{L}_F V = \dot{V} &\leq -\alpha \tilde{r}^T M^2 \tilde{r} - \beta \left\| M\tilde{r} \right\|_1 - \dot{r}_0 \left\| M\tilde{r} \right\|_1 \\
&\leq -\alpha \tilde{r}^T M^2 \tilde{r} - (\beta - \gamma_\ell) \left\| M\tilde{r} \right\|_1,
\end{aligned} \tag{4.5}$$

where we have used Lemma 1.19 to obtain the first inequality and $|\dot{r}_0| \leq \gamma_\ell$ to obtain the second inequality. Note that M^2 is symmetric positive definite, α is nonnegative, and $\beta > \gamma_\ell$. Therefore, it follows that $\max \widetilde{L}_F V$ is negative definite. It then follows from Lemma 1.39 that $\tilde{r}(t) \to \mathbf{0}_n$ as $t \to \infty$.

We next show that V will decrease to zero in finite time (i.e., $\|\tilde{r}(t)\| \to 0$ in finite time). Note that $V \leq \frac{1}{2} \lambda_{\max}(M) \|\tilde{r}\|_2^2$. It then follows from (4.5) that the derivative of V satisfies

$$\begin{aligned}
\dot{V} &\leq -(\beta - \gamma_\ell) \left\| M\tilde{r} \right\|_2 = -(\beta - \gamma_\ell) \sqrt{\tilde{r}^T M^2 \tilde{r}} \\
&\leq -(\beta - \gamma_\ell) \sqrt{\lambda_{\min}^2(M) \|\tilde{r}\|_2^2} = -(\beta - \gamma_\ell) \lambda_{\min}(M) \|\tilde{r}\|_2 \\
&\leq -(\beta - \gamma_\ell) \frac{\sqrt{2} \lambda_{\min}(M)}{\sqrt{\lambda_{\max}(M)}} \sqrt{V}.
\end{aligned}$$

After some manipulation, we can get that

$$2\sqrt{V(t)} \leq 2\sqrt{V(0)} - (\beta - \gamma_\ell) \frac{\sqrt{2} \lambda_{\min}(M)}{\sqrt{\lambda_{\max}(M)}} t.$$

Therefore, we have $V(t) = 0$ when $t \geq \bar{t}$, where $\bar{t}$ is given by (4.2). This completes the proof. ∎

Remark 4.3 Letting $x(t) \in \mathbb{R}^p$ be a continuous function with respect to t, it can be computed that $x^T(t) K[\operatorname{sgn}[x(t)]] = K[x^T(t)\operatorname{sgn}[x(t)]]$. Because $x^T(t) \operatorname{sgn}[x(t)]$ is continuous, we have $x^T(t) K[\operatorname{sgn}[x(t)]] = x^T(t) \operatorname{sgn}[x(t)]$. In the following, we will repeatedly use this property in our proofs. For simplicity of presentation, we will not explicitly mention this property in the following proofs. The Lyapunov

theorem for nonsmooth systems stated in Lemma 1.39 and the invariance principle for differential inclusions stated in Lemma 1.40 will be used for stability analysis.

Let $\overline{\mathcal{N}}_i \subseteq \{0, 1, \ldots, n\}$ denote the neighbor set of follower i in the team consisting of the n followers and the leader. We next consider the case of a switching interaction graph by assuming that $j \in \overline{\mathcal{N}}_i(t), i = 1, \ldots, n, j = 0, \ldots, n$, if $|r_i - r_j| < r_s$ at time t and $j \notin \overline{\mathcal{N}}_i(t)$ otherwise, where r_s denotes the communication/sensing radius of the agents. In this case, we consider the distributed coordinated tracking algorithm for (3.1) as

$$u_i = -\alpha \sum_{j \in \overline{\mathcal{N}}_i(t)} b_{ij}(r_i - r_j) - \beta \operatorname{sgn}\left[\sum_{j \in \overline{\mathcal{N}}_i(t)} b_{ij}(r_i - r_j) \right], \qquad (4.6)$$

where α is a nonnegative constant, β is a positive constant, and b_{ij}, $i = 1, \ldots, n$, $j = 0, \ldots, n$, are positive constants.

Theorem 4.4. *Suppose that the undirected graph $\mathcal{G}(t)$ is connected and the leader is a neighbor of at least one follower (i.e., $0 \in \overline{\mathcal{N}}_i(t)$ for some i) at each time instant. Using (4.6) for (3.1), if $\beta > \gamma_\ell$, then $|r_i(t) - r_0(t)| \to 0$ as $t \to \infty$.*

Proof: Let $V_{ij} = \frac{1}{2} b_{ij}(r_i - r_j)^2$, $i, j = 1, \ldots, n$, when $|r_i - r_j| < r_s$ and $V_{ij} = \frac{1}{2} b_{ij} r_s^2$ when $|r_i - r_j| \geq r_s$. Also let $V_{i0} = \frac{1}{2} b_{i0}(r_i - r_0)^2$, $i = 1, \ldots, n$, when $|r_i - r_0| < r_s$ and $V_{i0} = \frac{1}{2} b_{i0} r_s^2$ when $|r_i - r_0| \geq r_s$. Consider the Lyapunov function candidate $V = \frac{1}{2} \sum_{i=1}^{n} \sum_{j=1}^{n} V_{ij} + \sum_{i=1}^{n} V_{i0}$. Note that V is not smooth but is regular.

Define $r \overset{\triangle}{=} [r_0, \ldots, r_n]^T$ and $u \overset{\triangle}{=} [u_0, \ldots, u_n]^T$, where $u_0 \overset{\triangle}{=} \dot{r}_0$ and u_i, $i = 1, \ldots, n$, is defined in (4.6). The set-valued Lie derivative of V is given by

$$\widetilde{L}_F V = \bigcap_{\xi \in \partial V(r)} \xi^T K[u]$$

$$= \frac{1}{2} \sum_{i=1}^{n} \sum_{j=1}^{n} \left(\bigcap_{\xi_{ij}^i \in \partial V_{ij}(r_i)} K\left[\xi_{ij}^i \left\{ -\alpha \sum_{j \in \overline{\mathcal{N}}_i(t)} b_{ij}(r_i - r_j) \right. \right. \right.$$

$$\left. \left. - \beta \operatorname{sgn}\left[\sum_{j \in \overline{\mathcal{N}}_i(t)} b_{ij}(r_i - r_j) \right] \right\} \right]$$

$$+ \bigcap_{\xi_{ij}^j \in \partial V_{ij}(r_j)} K\left[\xi_{ij}^j \left\{ -\alpha \sum_{i \in \overline{\mathcal{N}}_j(t)} b_{ji}(r_j - r_i) \right. \right.$$

$$\left. \left. \left. - \beta \operatorname{sgn}\left[\sum_{i \in \overline{\mathcal{N}}_j(t)} b_{ji}(r_j - r_i) \right] \right\} \right] \right)$$

$$+ \sum_{i=1}^{n} \left(\bigcap_{\xi_{i0}^i \in \partial V_{i0}(r_i)} K\left[\xi_{i0}^i \left\{ -\alpha \sum_{0 \in \overline{\mathcal{N}}_i(t)} b_{ij}(r_i - r_0) \right. \right. \right.$$

$$-\beta \operatorname{sgn}\left[\sum_{0\in\mathcal{N}_i(t)} b_{ij}(r_i - r_0)\right]\right\}\right] + \bigcap_{\xi_{i0}^0 \in \partial V_{i0}(r_0)} K\left[\xi_{i0}^0 \dot{r}_0\right]\right),$$

where $\partial V(r)$ is the generalized gradient of V at r, $\partial V_{ij}(r_i)$ is the generalized gradient of V_{ij} at r_i, and we have used the fact that $K[x(t)f(t)] = x(t)K[f(t)]$ for any continuous function $x(t) \in \mathbb{R}$ to derive the second equality. Define $\Upsilon \triangleq -K[\alpha \sum_{j\in\mathcal{N}_i(t)} b_{ij}(r_i - r_j) + \beta \operatorname{sgn}[\sum_{j\in\mathcal{N}_i(t)} b_{ij}(r_i - r_j)]]$. Let $a \in \widetilde{L}_F V$. It follows from Definition 1.10 that for all $\xi_{ij}^i \in \partial V_{ij}(r_i)$, there exists $\phi_r^i \in \Upsilon$ such that $a = \frac{1}{2}\sum_{i=1}^n \sum_{j=1}^n [\xi_{ij}^i \phi_r^i + \xi_{ij}^j \phi_r^j] + \sum_{i=1}^n [\xi_{i0}^i \phi_r^i + \xi_{i0}^0 \dot{r}_0]$. Choose $\phi_r^i = -\alpha \sum_{j=0}^n \xi_{ij}^i - \beta \operatorname{sgn}(\sum_{j=0}^n \xi_{ij}^i) \in \Upsilon$. Note that $\xi_{ij}^i = -\xi_{ij}^j$. It then follows that

$$
\begin{aligned}
a =& \frac{1}{2}\sum_{i=1}^n \sum_{j=1}^n \left\{ \xi_{ij}^i\left[-\alpha\sum_{j=1}^n \xi_{ij}^i - \beta\operatorname{sgn}\left(\sum_{j=1}^n \xi_{ij}^i\right)\right]\right. \\
&\left. + \xi_{ij}^j\left[-\alpha\sum_{j=1}^n \xi_{ij}^i - \beta\operatorname{sgn}\left(\sum_{j=1}^n \xi_{ij}^j\right)\right]\right\} \\
&+ \sum_{i=1}^n \left\{ \xi_{i0}^i\left[-\alpha\sum_{j=1}^n \xi_{ij}^i - \beta\operatorname{sgn}\left(\sum_{j=1}^n \xi_{ij}^i\right)\right] + \xi_{i0}^0 \dot{r}_0 \right\} \\
=& -\alpha\sum_{i=1}^n \left[\sum_{j=0}^n \xi_{ij}^i\right]^2 - \beta\sum_{i=1}^n \left|\sum_{j=0}^n \xi_{ij}^i\right| + \sum_{i=1}^n \xi_{0i}^i \dot{r}_0. \\
=& -\alpha\sum_{i=1}^n \left[\sum_{j=0}^n \xi_{ij}^i\right]^2 - \beta\sum_{i=1}^n \left|\sum_{j=0}^n \xi_{ij}^i\right| + \dot{r}_0\sum_{i=1}^n \xi_{0i}^i + \dot{r}_0\sum_{i=1}^n\sum_{j=1}^n \xi_{ij}^i \quad (4.7) \\
=& -\alpha\sum_{i=1}^n \left[\sum_{j=0}^n \xi_{ij}^i\right]^2 - \beta\sum_{i=1}^n \left|\sum_{j=0}^n \xi_{ij}^i\right| + \dot{r}_0\sum_{i=1}^n\sum_{j=0}^n \xi_{ij}^i \\
\leq& -\alpha\sum_{i=1}^n \left[\sum_{j=0}^n \xi_{ij}^i\right]^2 - \beta\sum_{i=1}^n \left|\sum_{j=0}^n \xi_{ij}^i\right| + \dot{r}_0\sum_{i=1}^n \left|\sum_{j=0}^n \xi_{ij}^i\right| \\
\leq& -\alpha\sum_{i=1}^n \left[\sum_{j=0}^n \xi_{ij}^i\right]^2 - (\beta - \gamma_\ell)\sum_{i=1}^n \left|\sum_{j=0}^n \xi_{ij}^i\right|, \quad (4.8)
\end{aligned}
$$

where we have used the fact that $\sum_{i=1}^n \sum_{j=1}^n \xi_{ij}^i = 0$ to derive (4.7) and $|\dot{r}_0| \leq \gamma_\ell$ to derive (4.8). Based on the definition of V_{ij}, it follows that $\partial V_{ij}(r_i) = \{0\}$, $\partial V_{ij}(r_i) = \{b_{ij}(r_i - r_j)\}$, or $\partial V_{ij}(r_i) = \operatorname{Co}[0, b_{ij}(r_i - r_j)]$. After some manipulation, we have

$$a \leq \max\left(K\left[-\alpha\tilde{r}^T\left[\widehat{M}(t)\right]^2\tilde{r} - (\beta - \gamma_\ell)\left\|\widehat{M}(t)\tilde{r}\right\|_1\right]\right),$$

where $\tilde{r}$ is the column stack vector of $\tilde{r}_i$, $i = 1, \ldots, n$, with $\tilde{r}_i \triangleq r_i - r_0$, and $\widehat{M}(t) \triangleq [\hat{m}_{ij}(t)] \in \mathbb{R}^{n \times n}$ is defined as

$$
\hat{m}_{ij}(t) \triangleq \begin{cases} -b_{ij}, & j \in \overline{\mathcal{N}}_i(t), \ j \neq i, \\ 0, & j \notin \overline{\mathcal{N}}_i(t), \ j \neq i, \\ \sum_{k \in \overline{\mathcal{N}}_i(t)} b_{ik}, & j = i. \end{cases} \tag{4.9}
$$

When the undirected graph $\mathcal{G}(t)$ is connected and the leader is a neighbor of at least one follower (i.e., $0 \in \overline{\mathcal{N}}_i(t)$ for some i) at each time instant, it follows from Lemma 1.6 that $\widehat{M}(t)$ is symmetric positive definite at each time instant. Because $\beta > \gamma_\ell$, it then follows that the maximum element of the set-valued Lie derivative of V is negative definite under the condition of the theorem. It then follows from Lemma 1.39 that $\|\tilde{r}(t)\| \to 0$ as $t \to \infty$. Therefore, we can get that $|r_i(t) - r_0(t)| \to 0$ as $t \to \infty$. ∎

Remark 4.5 Under the condition of Theorem 4.4, distributed coordinated tracking can be achieved in finite time under a switching interaction graph. However, in contrast to the result in Theorem 4.2, it is not easy to explicitly compute the bound of the time (i.e., $\bar{t}$ in Theorem 4.2) because the switching pattern of the interaction graph also plays an important role in determining the bound of the time.

4.2.2 Swarm Tracking Under Switching Interaction

In this subsection, we extend the distributed coordinated tracking algorithm in Sect. 4.2.1 to achieve distributed swarm tracking. The objective here is to design u_i for (3.1) such that all followers move cohesively with the dynamic leader while avoiding inter-agent collision with local interaction in the absence of velocity measurements. Before moving on, we need to define potential functions which will be used in the distributed swarm tracking algorithms.

Definition 4.1. The potential function V_{ij} is a differentiable, nonnegative function of $\|r_i - r_j\|$[1] satisfying the following conditions:

1. V_{ij} achieves its unique minimum when $\|r_i - r_j\|$ is equal to its desired value d_{ij}.
2. $V_{ij} \to \infty$ if $\|r_i - r_j\| \to 0$.
3. $\frac{\partial V_{ij}}{\partial(\|r_i - r_j\|)} = 0$ if $\|r_i - r_j\| \geq r_s$, where $r_s > \max_{i,j} d_{ij}$ is a positive constant denoting the communication/sensing radius of the agents.
4. $V_{ii} = c$, $i = 1, \ldots, n$, where c is a positive constant.

---

[1] In this definition, r_i can be m-dimensional.

Lemma 4.1. *Let V_{ij} be defined in Definition* 4.1. *The following equality holds*

$$\frac{1}{2} \sum_{i=1}^{n} \sum_{j=1}^{n} \left(\frac{\partial V_{ij}}{\partial r_i} \dot{r}_i + \frac{\partial V_{ij}}{\partial r_j} \dot{r}_j \right) = \sum_{i=1}^{n} \sum_{j=1}^{n} \frac{\partial V_{ij}}{\partial r_i} \dot{r}_i.$$

Proof: Note that

$$
\begin{aligned}
\frac{1}{2} \sum_{i=1}^{n} \sum_{j=1}^{n} \left(\frac{\partial V_{ij}}{\partial r_i} \dot{r}_i + \frac{\partial V_{ij}}{\partial r_j} \dot{r}_j \right) &= \frac{1}{2} \sum_{i=1}^{n} \sum_{j=1}^{n} \frac{\partial V_{ij}}{\partial r_i} \dot{r}_i - \frac{1}{2} \sum_{i=1}^{n} \sum_{j=1}^{n} \frac{\partial V_{ij}}{\partial r_i} \dot{r}_j \\
&= \frac{1}{2} \sum_{i=1}^{n} \sum_{j=1}^{n} \frac{\partial V_{ij}}{\partial r_i} \dot{r}_i - \frac{1}{2} \sum_{j=1}^{n} \sum_{i=1}^{n} \frac{\partial V_{ji}}{\partial r_j} \dot{r}_i \\
&= \frac{1}{2} \sum_{i=1}^{n} \sum_{j=1}^{n} \frac{\partial V_{ij}}{\partial r_i} \dot{r}_i + \frac{1}{2} \sum_{j=1}^{n} \sum_{i=1}^{n} \frac{\partial V_{ij}}{\partial r_i} \dot{r}_i \\
&= \sum_{i=1}^{n} \sum_{j=1}^{n} \frac{\partial V_{ij}}{\partial r_i} \dot{r}_i,
\end{aligned}
$$

where we have used the fact that $\frac{\partial V_{ij}}{\partial r_i} = -\frac{\partial V_{ij}}{\partial r_j}$ from Definition 4.1. Therefore, the lemma holds. ∎

We propose the distributed swarm tracking algorithm for (3.1) as

$$u_i = -\alpha \sum_{j \in \overline{\mathcal{N}}_i(t)} \frac{\partial V_{ij}}{\partial r_i} - \beta \operatorname{sgn}\left[\sum_{j \in \overline{\mathcal{N}}_i(t)} \frac{\partial V_{ij}}{\partial r_i} \right], \tag{4.10}$$

where α is a nonnegative constant, β is a positive constant, and $\overline{\mathcal{N}}_i(t)$ is defined in Sect. 4.2.1, and V_{ij} is defined in Definition 4.1.

Theorem 4.6. *Suppose that the undirected graph $\mathcal{G}(t)$ is connected and the leader is a neighbor of at least one follower (i.e., $0 \in \overline{\mathcal{N}}_i(t)$ for some i) at each time instant. Using* (4.10) *for* (3.1), *if $\beta > \gamma_\ell$, the followers will ultimately stay close to the leader and the inter-agent collision is avoided.*

Proof: Consider the Lyapunov function candidate

$$V = \frac{1}{2} \sum_{i=1}^{n} \sum_{j=1}^{n} V_{ij} + \sum_{i=1}^{n} V_{i0}.$$

Note that V is continuously differentiable with respect to r_i and r_j. It follows that

$$
\begin{aligned}
\max \widetilde{L}_F V = \dot{V} &= \frac{1}{2} \sum_{i=1}^{n} \sum_{j=1}^{n} \left(\frac{\partial V_{ij}}{\partial r_i} \dot{r}_i + \frac{\partial V_{ij}}{\partial r_j} \dot{r}_j \right) + \sum_{i=1}^{n} \left(\frac{\partial V_{i0}}{\partial r_i} \dot{r}_i + \frac{\partial V_{i0}}{\partial r_0} \dot{r}_0 \right) \\
&= \sum_{i=1}^{n} \sum_{j=1}^{n} \frac{\partial V_{ij}}{\partial r_i} \dot{r}_i + \sum_{i=1}^{n} \left(\frac{\partial V_{i0}}{\partial r_i} \dot{r}_i + \frac{\partial V_{i0}}{\partial r_0} \dot{r}_0 \right) \tag{4.11}
\end{aligned}
$$

$$= \sum_{i=1}^{n}\sum_{j=1}^{n}\frac{\partial V_{ij}}{\partial r_i}\left[-\alpha\sum_{j=0}^{n}\frac{\partial V_{ij}}{\partial r_i} - \beta\,\mathrm{sgn}\left(\sum_{j=0}^{n}\frac{\partial V_{ij}}{\partial r_i}\right)\right]$$

$$+ \sum_{i=1}^{n}\frac{\partial V_{i0}}{\partial r_i}\left[-\alpha\sum_{j=0}^{n}\frac{\partial V_{ij}}{\partial r_i} - \beta\,\mathrm{sgn}\left(\sum_{j=0}^{n}\frac{\partial V_{ij}}{\partial r_i}\right)\right] + \sum_{i=1}^{n}\frac{\partial V_{i0}}{\partial r_0}\dot{r}_0$$

$$= -\alpha\sum_{i=1}^{n}\left(\sum_{j=0}^{n}\frac{\partial V_{ij}}{\partial r_i}\right)^2 - \beta\sum_{i=1}^{n}\left|\sum_{j=0}^{n}\frac{\partial V_{ij}}{\partial r_i}\right| + \sum_{i=1}^{n}\frac{\partial V_{i0}}{\partial r_0}\dot{r}_0$$

$$= -\alpha\sum_{i=1}^{n}\left(\sum_{j=0}^{n}\frac{\partial V_{ij}}{\partial r_i}\right)^2 - \beta\sum_{i=1}^{n}\left|\sum_{j=0}^{n}\frac{\partial V_{ij}}{\partial r_i}\right| + \sum_{i=1}^{n}\frac{\partial V_{i0}}{\partial r_0}\dot{r}_0$$

$$+ \sum_{i=1}^{n}\sum_{j=1}^{n}\frac{\partial V_{ij}}{\partial r_i}\dot{r}_0 \tag{4.12}$$

$$\leq -\alpha\sum_{i=1}^{n}\left(\sum_{j=0}^{n}\frac{\partial V_{ij}}{\partial r_i}\right)^2 - \beta\sum_{i=1}^{n}\left|\sum_{j=0}^{n}\frac{\partial V_{ij}}{\partial r_i}\right| + |\dot{r}_0|\sum_{i=1}^{n}\left|\sum_{j=0}^{n}\frac{\partial V_{ij}}{\partial r_i}\right|,$$

where we have used Lemma 4.1 to derive (4.11) and the fact that $\sum_{i=1}^{n}\sum_{j=1}^{n}\frac{\partial V_{ij}}{\partial r_i} = 0$ to derive (4.12). Because $\beta > \gamma_\ell$, we get $\max \widetilde{L}_F V \leq 0$, which in turn proves the theorem by applying Lemma 1.39. ∎

4.3 Collective Tracking for Double-integrator Dynamics

In this section, we study distributed collective tracking for double-integrator dynamics. Suppose that the leader has a (time-varying) position r_0 and velocity v_0.

4.3.1 Coordinated Tracking when the Leader's Velocity is Varying

In this subsection, we assume that the leader has a varying velocity (i.e., v_0 is time-varying). We assume that $|\dot{v}_0| \leq \varphi_\ell$, where φ_ℓ is a positive constant. The objective here is to design u_i for (3.5) such that all followers intercepts the dynamic leader with local interaction in the absence of acceleration measurements. We propose the distributed coordinated tracking algorithm for (3.5) as

$$u_i = -\sum_{j=0}^{n} a_{ij}\big[(r_i - r_j) + \alpha(v_i - v_j)\big]$$

$$- \beta\,\mathrm{sgn}\left\{\sum_{j=0}^{n} a_{ij}\big[\gamma(r_i - r_j) + (v_i - v_j)\big]\right\}, \tag{4.13}$$

where a_{ij}, $i = 1, \ldots, n$, $j = 0, 1, \ldots, n$, is defined as in (4.1), and α, β, and γ are positive constants. We first consider the case of a fixed interaction graph. Before moving on, we need the following lemma.

Lemma 4.2. *Suppose that the fixed undirected graph* $\mathcal{G}$ *is connected and at least one* a_{i0} *is nonzero* (*and hence positive*). *Let* $P \overset{\triangle}{=} \begin{bmatrix} \frac{1}{2}M^2 & \frac{\gamma}{2}M \\ \frac{\gamma}{2}M & \frac{1}{2}M \end{bmatrix}$ *and* $Q \overset{\triangle}{=} \begin{bmatrix} \gamma M^2 & \frac{\alpha\gamma}{2}M^2 \\ \frac{\alpha\gamma}{2}M^2 & \alpha M^2 - \gamma M \end{bmatrix}$, *where* γ *and* α *are positive constants and* $M \overset{\triangle}{=} \mathcal{L} + \mathrm{diag}(a_{10}, \ldots, a_{n0})$. *If* γ *satisfies*

$$0 < \gamma < \min\left\{ \sqrt{\lambda_{\min}(M)}, \frac{4\alpha\lambda_{\min}(M)}{4 + \alpha^2\lambda_{\min}(M)} \right\}, \tag{4.14}$$

then both P *and* Q *are symmetric positive definite.*

Proof: When the fixed undirected graph $\mathcal{G}$ is connected and at least one a_{i0} is nonzero (and hence positive), it follows from Lemma 1.6 that M is symmetric positive definite. Therefore, M can be diagonalized as $M = \Psi^{-1}\Lambda\Psi$, where $\Lambda = \mathrm{diag}(\lambda_1, \ldots, \lambda_n)$ with λ_i being the ith eigenvalue of M. It then follows that P can be written as

$$P = \begin{bmatrix} \Psi^{-1} & 0_{n \times n} \\ 0_{n \times n} & \Psi^{-1} \end{bmatrix} \underbrace{\begin{bmatrix} \frac{1}{2}\Lambda^2 & \frac{\gamma}{2}\Lambda \\ \frac{\gamma}{2}\Lambda & \frac{1}{2}\Lambda \end{bmatrix}}_{F} \begin{bmatrix} \Psi & 0_{n \times n} \\ 0_{n \times n} & \Psi \end{bmatrix}. \tag{4.15}$$

Let μ be an eigenvalue of F. Because Λ is a diagonal matrix, it follows from (4.15) that μ satisfies $(\mu - \frac{1}{2}\lambda_i^2)(\mu - \frac{1}{2}\lambda_i) - \frac{\gamma^2}{4}\lambda_i^2 = 0$, which can be simplified as

$$\mu^2 - \frac{1}{2}(\lambda_i^2 + \lambda_i)\mu + \frac{1}{4}(\lambda_i^3 - \gamma^2\lambda_i^2) = 0. \tag{4.16}$$

Because F is symmetric, the roots of (4.16) are real. Therefore, all roots of (4.16) are positive if and only if $\frac{1}{2}(\lambda_i^2 + \lambda_i) > 0$ and $\frac{1}{4}(\lambda_i^3 - \gamma^2\lambda_i^2) > 0$. Because $\lambda_i > 0$, it follows that $\frac{1}{2}(\lambda_i^2 + \lambda_i) > 0$. When $\gamma^2 < \lambda_i$, it follows that $\frac{1}{4}(\lambda_i^3 - \gamma^2\lambda_i^2) > 0$. It thus follows that when $\gamma^2 < \lambda_i$, the roots of (4.16) are positive. Noting that P has the same eigenvalues as F, we can get that P is positive definite if $0 < \gamma < \sqrt{\lambda_{\min}(M)}$.

By following a similar analysis, we can get that Q is positive definite if $0 < \gamma < \frac{4\alpha\lambda_{\min}(M)}{4 + \alpha^2\lambda_{\min}(M)}$. Combining the above arguments proves the lemma. ∎

Theorem 4.7. *Suppose that the fixed undirected graph* $\mathcal{G}$ *is connected and at least one* a_{i0} *is nonzero* (*and hence positive*). *Using* (4.13) *for* (3.5), *if* $\beta > \varphi_\ell$ *and* γ *satisfies* (4.14), *then* $|r_i(t) - r_0(t)| \to 0$ *and* $|v_i(t) - v_0(t)| \to 0$ *globally exponentially as* $t \to \infty$. *In particular, it follows that*

$$\left\| \begin{bmatrix} \tilde{r}^T(t), & \tilde{v}^T(t) \end{bmatrix}^T \right\| \leq \kappa_1 e^{-\kappa_2 t}, \tag{4.17}$$

where $\tilde{r}$ and $\tilde{v}$ are, respectively, the column stack vectors of $\tilde{r}_i$ and $\tilde{v}_i$, $i = 1, \ldots, n$, with $\tilde{r}_i \triangleq r_i - r_0$ and $\tilde{v}_i \triangleq v_i - v_0$, P and Q are defined in Lemma 4.2, $\kappa_1 \triangleq \sqrt{\frac{[\tilde{r}^T(0),\, \tilde{v}^T(0)]P[\tilde{r}^T(0),\, \tilde{v}^T(0)]^T}{\lambda_{\min}(P)}}$, and $\kappa_2 \triangleq \frac{\lambda_{\min}(Q)}{2\lambda_{\max}(P)}$.

Proof: Noting that $\tilde{r}_i = r_i - r_0$ and $\tilde{v}_i = v_i - v_0$, we rewrite the closed-loop system of (3.5) using (4.13) as

$$\dot{\tilde{r}}_i = \tilde{v}_i,$$

$$\dot{\tilde{v}}_i = -\sum_{j=0}^{n} a_{ij}\big[(\tilde{r}_i - \tilde{r}_j) + \alpha(\tilde{v}_i - \tilde{v}_j)\big] \tag{4.18}$$
$$\quad - \beta \operatorname{sgn}\left\{\sum_{j=0}^{n} a_{ij}\big[\gamma(\tilde{r}_i - \tilde{r}_j) + (\tilde{v}_i - \tilde{v}_j)\big]\right\} - \dot{v}_0.$$

Equation (4.18) can be written in a vector form as

$$\dot{\tilde{r}} = \tilde{v},$$
$$\dot{\tilde{v}} = -M\tilde{r} - \alpha M\tilde{v} - \beta \operatorname{sgn}[M(\gamma\tilde{r} + \tilde{v})] - \mathbf{1}_n \dot{v}_0,$$

where $\tilde{r}$ and $\tilde{v}$ are defined in (4.17) and $M \triangleq \mathcal{L} + \operatorname{diag}(a_{10}, \ldots, a_{n0})$.

Consider the Lyapunov function candidate

$$V = \big[\,\tilde{r}^T,\, \tilde{v}^T\,\big] P \begin{bmatrix} \tilde{r} \\ \tilde{v} \end{bmatrix} = \frac{1}{2}\tilde{r}^T M^2 \tilde{r} + \frac{1}{2}\tilde{v}^T M\tilde{v} + \gamma\tilde{r}^T M\tilde{v}. \tag{4.19}$$

Note that according to Lemma 4.2, P is symmetric positive definite when γ satisfies (4.14). It follows that

$$\max \widetilde{L}_F V = \dot{V} = \tilde{r}^T M^2 \tilde{v} + \tilde{v}^T M\dot{\tilde{v}} + \gamma\tilde{v}^T M\tilde{v} + \gamma\tilde{r}^T M\dot{\tilde{v}}$$

$$= -\big[\,\tilde{r}^T,\, \tilde{v}^T\,\big] Q \begin{bmatrix} \tilde{r} \\ \tilde{v} \end{bmatrix} - \big(\gamma\tilde{r}^T + \tilde{v}^T\big) M\big\{\beta\operatorname{sgn}\big[M(\gamma\tilde{r} + \tilde{v})\big] + \mathbf{1}_n\dot{v}_0\big\}$$

$$\leq -\big[\,\tilde{r}^T,\, \tilde{v}^T\,\big] Q \begin{bmatrix} \tilde{r} \\ \tilde{v} \end{bmatrix} - (\beta - \varphi_\ell)\big\|M(\gamma\tilde{r} + \tilde{v})\big\|_1, \tag{4.20}$$

where the last inequality follows from the fact that $|\dot{v}_0| \leq \varphi_\ell$. Note that according to Lemma 4.2, Q is symmetric positive definite when γ satisfies (4.14). Also note that $\beta > \varphi_\ell$. It follows that $\max \widetilde{L}_F V$ is negative definite. Therefore, it follows from Lemma 1.39 that $\|\tilde{r}(t)\| \to 0$ and $\|\tilde{v}(t)\| \to 0$ as $t \to \infty$. Equivalently, it follows that $|r_i(t) - r_0(t)| \to 0$ and $|v_i(t) - v_0(t)| \to 0$ as $t \to \infty$.

We next show that distributed coordinated tracking is achieved at least globally exponentially. Note that $V \leq \lambda_{\max}(P)\|[\tilde{r}^T,\ \tilde{v}^T]^T\|^2$. It then follows from (4.20) that

$$\dot{V} \leq -\left[\,\tilde{r}^T, \tilde{v}^T\,\right] Q \begin{bmatrix} \tilde{r} \\ \tilde{v} \end{bmatrix} \leq -\lambda_{\min}(Q)\left\|\begin{bmatrix} \tilde{r} \\ \tilde{v} \end{bmatrix}^T\right\|^2 \leq -\frac{\lambda_{\min}(Q)}{\lambda_{\max}(P)}V.$$

Therefore, we can get $V(t) \leq V(0)e^{-\frac{\lambda_{\min}(Q)}{\lambda_{\max}(P)}t}$. Note also that $V \geq \lambda_{\min}(P) \times \|[\tilde{r}^T,\ \tilde{v}^T]^T\|^2$. After some manipulation, we can get (4.17). ∎

Remark 4.8 In the proof of Theorem 4.7, the Lyapunov function is chosen as (4.19). Here P can also be chosen as $P \triangleq \begin{bmatrix} \frac{1}{2}M & \frac{\gamma}{2}M \\ \frac{\gamma}{2}M & \frac{1}{2}M \end{bmatrix}$ and the derivative of V also satisfies (4.20) with $Q \triangleq \begin{bmatrix} \gamma M^2 & \frac{\alpha\gamma}{2}M^2 + \frac{M^2 - \gamma M}{2} \\ \frac{\alpha\gamma}{2}M^2 + \frac{M^2 - \gamma M}{2} & \alpha M^2 - \gamma M \end{bmatrix}$. By following a similar analysis to that of Lemma 4.2, we can show that there always exist positive α and γ such that both P and Q are symmetric positive definite and derive proper conditions for α and γ. In particular, one special choice for α and γ is $\alpha\gamma = 1$ and $\gamma < \frac{4\lambda_{\min}(M)}{4\lambda_{\min}(M)+1}$.

We next consider the case of a switching interaction graph. We propose the distributed coordinated tracking algorithm for (3.5) as

$$\begin{aligned} u_i = &-\sum_{j\in\mathcal{N}_i(t)} b_{ij}\big[(r_i - r_j) + \alpha(v_i - v_j)\big] \\ &-\beta\sum_{j\in\overline{\mathcal{N}}_i(t)} b_{ij}\bigg(\mathrm{sgn}\Big\{\sum_{k\in\mathcal{N}_i(t)} b_{ik}\big[\gamma(r_i - r_k) + (v_i - v_k)\big]\Big\} \\ &-\mathrm{sgn}\Big\{\sum_{k\in\mathcal{N}_j(t)} b_{jk}\big[\gamma(r_j - r_k) + (v_j - v_k)\big]\Big\}\bigg), \end{aligned} \qquad (4.21)$$

where $\overline{\mathcal{N}}_i(t)$ is defined in Sect. 4.2.1, b_{ij}, $i = 1,\ldots,n, j = 0,\ldots,n$, are positive constants, and α, β, and γ are positive constants.[2] Before moving on, we need the following lemma.

Lemma 4.3. *Suppose that the undirected graph $\mathcal{G}(t)$ is connected and the leader is a neighbor of at least one follower (i.e., $0 \in \mathcal{N}_i(t)$ for some i) at each time instant. Let $\widehat{M}(t)$ be defined as in (4.9). Let $\widehat{P}(t) \triangleq \begin{bmatrix} \frac{1}{2}\widehat{M}(t) & \frac{\gamma}{2}I_n \\ \frac{\gamma}{2}I_n & \frac{1}{2}I_n \end{bmatrix}$ and $\widehat{Q}(t) \triangleq \begin{bmatrix} \gamma\widehat{M}(t) & \frac{\alpha\gamma}{2}\widehat{M}(t) \\ \frac{\alpha\gamma}{2}\widehat{M}(t) & \alpha\widehat{M}(t)-\gamma I_n \end{bmatrix}$, where α and γ are positive constants. If γ satisfies*

$$0 < \gamma < \min_t\bigg\{ \sqrt{\lambda_{\min}\big(\widehat{M}(t)\big)},\ \frac{4\alpha\lambda_{\min}(\widehat{M}(t))}{4 + \alpha^2\lambda_{\min}(\widehat{M}(t))} \bigg\}, \qquad (4.22)$$

then both $\widehat{P}(t)$ and $\widehat{Q}(t)$ are symmetric positive definite at each time instant.

Proof: The proof is similar to that of Lemma 4.2 and is hence omitted here. ∎

---

[2] Because the leader has no neighbor, we let $\mathrm{sgn}\{\sum_{k\in\mathcal{N}_0(t)} b_{0k}[\gamma(r_0 - r_k) + (v_0 - v_k)]\} = 0$.

Theorem 4.9. *Suppose that the undirected graph $\mathcal{G}(t)$ is connected and the leader is a neighbor of at least one follower (i.e., $0 \in \overline{\mathcal{N}}_i(t)$ for some i) at each time instant. Using (4.21) for (3.5), if $\beta > \varphi_\ell$ and (4.22) is satisfied, then $|r_i(t) - r_0(t)| \to 0$ and $|v_i(t) - v_0(t)| \to 0$ as $t \to \infty$.*

Proof: Let V_{ij} and V_{i0} be defined as in the proof of Theorem 4.4. Consider the Lyapunov function candidate $V = \frac{1}{2} \sum_{i=1}^{n} \sum_{j=1}^{n} V_{ij} + \sum_{i=1}^{n} V_{i0} + \frac{1}{2}\tilde{v}^T \tilde{v} + \gamma \tilde{r}^T \tilde{v}$, where $\tilde{r}$ and $\tilde{v}$ are, respectively, the column stack vectors of $\tilde{r}_i$ and $\tilde{v}_i$, $i = 1, \ldots, n$, with $\tilde{r}_i \triangleq r_i - r_0$ and $\tilde{v}_i \triangleq v_i - v_0$. Note that V can be written as

$$V = \left[\, \tilde{r}^T,\, \tilde{v}^T \,\right] \widehat{P}(t) \begin{bmatrix} \tilde{r} \\ \tilde{v} \end{bmatrix} + \frac{1}{4} \sum_{i=1}^{n} \sum_{j \notin \mathcal{N}_i(t), j \neq 0} b_{ij} r_s^2 + \frac{1}{2} \sum_{0 \in \overline{\mathcal{N}}_i(t)} b_{i0} r_s^2, \quad (4.23)$$

where $\widehat{P}(t)$ is defined in Lemma 4.3. Note also that according to Lemma 4.3, $\widehat{P}(t)$ is symmetric positive definite when (4.22) is satisfied. By following a similar line to the proof of Theorem 4.7 and using nonsmooth analysis, we can obtain that the maximum element of the set-valued Lie derivative of V is negative definite under the condition of the theorem. Therefore, it follows from Lemma 1.39 that $|r_i(t) - r_0(t)| \to 0$ and $|v_i(t) - v_0(t)| \to 0$ as $t \to \infty$. ∎

Remark 4.10 It can be noted that (4.21) requires the availability of the information from both the neighbors (i.e., one-hop neighbors) and the neighbors' neighbors (i.e., two-hop neighbors). However, *accurate* measurements of the two-hop neighbors' information are not necessary because only the signs (i.e., '+' or '−') are required in (4.21). In fact, (4.21) can be easily implemented in real systems in the sense that follower i, $i = 1, \ldots, n$, shares both its own state (i.e., position and velocity) and the sign of $\sum_{j \in \overline{\mathcal{N}}_i(t)} b_{ij}[\gamma(r_i - r_j) + (v_i - v_j)]$ with its neighbors. Note that follower i also has to compute $\sum_{j \in \overline{\mathcal{N}}_i(t)} b_{ij}(r_i - r_j)$ and $\sum_{j \in \overline{\mathcal{N}}_i(t)} b_{ij}(v_i - v_j)$ in (4.21) [correspondingly, $\sum_{j=0}^{n} a_{ij}(r_i - r_j)$ and $\sum_{j=0}^{n} a_{ij}(v_i - v_j)$ in (4.13)] in order to derive the corresponding control input for itself.

Remark 4.11 Under the condition of Theorem 4.9, the distributed coordinated tracking algorithm (4.21) guarantees at least global exponential tracking under a switching interaction graph. However, in contrast to the result in Theorem 4.7, it might not be easy to explicitly compute the decay rate (i.e., κ_2 in Theorem 4.9) because the switching pattern of the interaction graph will play an important role in determining the decay rate.

Remark 4.12 Similar to the analysis in Remark 4.8, in the Lyapunov function (4.23), we can choose $\widehat{P} \triangleq \begin{bmatrix} \frac{1}{2}I_n & \frac{\gamma}{2}I_n \\ \frac{\gamma}{2}I_n & \frac{1}{2}I_n \end{bmatrix}$. It then follows that $\widehat{Q}(t) \triangleq \begin{bmatrix} \gamma \widehat{M}(t) & \frac{\alpha\gamma}{2}\widehat{M}(t) + \frac{\widehat{M}(t) - \gamma I_n}{2} \\ \frac{\alpha\gamma}{2}\widehat{M}(t) + \frac{\widehat{M}(t) - \gamma I_n}{2} & \alpha\widehat{M}(t) - \gamma I_n \end{bmatrix}$. We can show that there always exist positive α and γ such that both $\widehat{P}$ and $\widehat{Q}(t)$ are symmetric positive definite and derive proper conditions for α and γ. In particular, one special choice for α and γ is $\alpha\gamma = 1$ and $\gamma < \min_t \frac{4\lambda_{\min}[\widehat{M}(t)]}{4\lambda_{\min}[\widehat{M}(t)] + 1}$.

Remark 4.13 In Theorems 4.4 and 4.9, it is assumed that the undirected graph $\mathcal{G}(t)$ is connected and the leader is a neighbor of at least one follower at each time instant. However, this poses an obvious constraint in real applications because the connectivity requirement is not necessarily always satisfied. Next, we propose an adaptive connectivity maintenance mechanism in which the control weights b_{ij}, $i = 1, \ldots, n, j = 0, \ldots, n$, in (4.6) and (4.21) is redefined as follows:

1. b_{ij} is a function of $\|r_i - r_j\|$.
2. When $\|r_i(0) - r_j(0)\| \geq r_s$, $b_{ij}(t) = 1$ if $\|r_i(t) - r_j(t)\| < r_s$ and $b_{ij}(t) = 0$ otherwise.
3. When $\|r_i(0) - r_j(0)\| < r_s$, $b_{ij}(t)$ is defined such that:

   (i) $b_{ij}(0) > 0$;
   (ii) $b_{ij}(t)$ is nondecreasing;
   (iii) $b_{ij}(t)$ is differentiable (or differentiable almost everywhere);
   (iv) $b_{ij}(t)$ goes to infinity if $\|r_i(t) - r_j(t)\|$ goes to r_s.

The motivation here is to maintain the initially existing connectivity patterns. That is, if two followers are neighbors of each other (respectively, the leader is a neighbor of a follower) at $t = 0$,[3] the two followers are guaranteed to be neighbors of each other (respectively, the leader is guaranteed to be a neighbor of this follower) at $t > 0$. However, if two followers are not neighbors of each other (respectively, the leader is not a neighbor of a follower) at $t = 0$, the two followers are not necessarily guaranteed to be neighbors of each other (respectively, the leader is not necessarily guaranteed to be a neighbor of this follower) at $t > 0$.

Using the proposed adaptive connectivity maintenance mechanism, the coordinated tracking algorithm for (3.1) can be chosen as

$$
u_i = -\alpha \sum_{j \in \overline{\mathcal{N}}_i(t)} b_{ij}(t)(r_i - r_j) - \beta \sum_{j \in \overline{\mathcal{N}}_i(t)} b_{ij}(t)
$$
$$
\times \left\{ \mathrm{sgn}\left[\sum_{k \in \mathcal{N}_i(t)} b_{ik}(t)(r_i - r_k) \right] - \mathrm{sgn}\left[\sum_{k \in \mathcal{N}_j(t)} b_{jk}(t)(r_j - r_k) \right] \right\} \quad (4.24)
$$

with the Lyapunov function chosen as $V = \frac{1}{2}\tilde{r}^T \tilde{r}$ while the coordinated tracking algorithm for (3.5) can be chosen as (4.21) with the Lyapunov function chosen as $V = [\tilde{r}^T, \tilde{v}^T]\widehat{P}\left[\begin{smallmatrix} \tilde{r} \\ \tilde{v} \end{smallmatrix}\right]$ with $\widehat{P}$ chosen as in Remark 4.12. According to the definition of $\widehat{M}(t)$ in (4.9), for $0 \leq t_1 < t_2$, $x^T[\widehat{M}(t_1) - \widehat{M}(t_2)]x \leq 0$ for all vectors $x \in \mathbb{R}^n$ under the connectivity maintenance mechanism. Let $y \in \mathbb{R}^n$ be a right eigenvector of $\widehat{M}(t_2)$ associated with the eigenvalue $\lambda_{\min}[\widehat{M}(t_2)]$, i.e., $\widehat{M}(t_2)y = \lambda_{\min}[\widehat{M}(t_2)]y$. It follows that $y^T\lambda_{\min}[\widehat{M}(t_2)]y = y^T\widehat{M}(t_2)y \geq y^T\widehat{M}(t_1)y \geq y^T\lambda_{\min}[\widehat{M}(t_1)]y$, where we have used Lemma 1.24. Because $y^Ty \neq 0$, it follows that $\lambda_{\min}[\widehat{M}(t_2)] \geq \lambda_{\min}[\widehat{M}(t_1)]$. This implies that $\lambda_{\min}[\widehat{M}(t)]$ is non-decreasing

---

[3] Equivalently, a pair of followers are within the communication/sensing range of each other (respectively, the leader is within the communication/sensing range of a follower).

with respect to time. Therefore, there always exist α and γ satisfying the conditions in Remark 4.12. When the control gains are chosen properly (i.e., $\alpha \geq 0$ and $\beta > \gamma_\ell$ for single-integrator dynamics and α and γ satisfies Remark 4.12 and $\beta > \varphi_\ell$ for double-integrator dynamics), it can be shown that distributed coordinated tracking can be guaranteed for both single-integrator dynamics and double-integrator dynamics if the undirected graph $\mathcal{G}(t)$ is initially connected and the leader is initially a neighbor of at least one follower (i.e., at $t = 0$). The proof follows a similar analysis to that of the corresponding algorithm in the absence of the connectivity maintenance mechanism except that the initially existing connectivity patterns can be maintained because otherwise $\max \widetilde{L}_F V = \dot{V} \to -\infty$ as $|r_i(t) - r_j(t)| \to r_s$ by noting that $b_{ij}(t)|r_i(t) - r_j(t)| \to \infty$ as $|r_i(t) - r_j(t)| \to r_s$, $\max \widetilde{L}_F V = \dot{V} \leq -\alpha \tilde{r}^T \widehat{M}(t)\tilde{r} - (\beta - \gamma_\ell)\|\widehat{M}(t)\tilde{r}\|_1$ for single-integrator dynamics, and $\max \widetilde{L}_F V = \dot{V} \leq -[\tilde{r}^T, \; \tilde{v}^T]\widehat{Q}(t)\left[\begin{smallmatrix}\tilde{r}\\\tilde{v}\end{smallmatrix}\right]$ for double-integrator dynamics, where $\widehat{Q}(t)$ is defined in Remark 4.12.

4.3.2 Coordinated Tracking when the Leader's Velocity is Constant

In this subsection, we assume that the leader has a constant velocity (i.e., v_0 is constant). We propose the distributed coordinated tracking algorithm for (3.5) as

$$u_i = -\sum_{j=0}^{n} a_{ij}(r_i - r_j) - \beta \operatorname{sgn}\left[\sum_{j=0}^{n} a_{ij}(v_i - v_j)\right], \qquad (4.25)$$

where a_{ij} is defined as in (4.1) and β is a positive constant. We first consider a fixed interaction graph.

Theorem 4.14. *Suppose that the fixed undirected graph $\mathcal{G}$ is connected and at least one a_{i0} is nonzero (and hence positive). Using (4.25) for (3.5), $|r_i(t) - r_0(t)| \to 0$ and $v_i(t) \to v_0$ as $t \to \infty$.*

Proof: Letting $\tilde{r}_i \overset{\triangle}{=} r_i - r_0$ and $\tilde{v}_i \overset{\triangle}{=} v_i - v_0$, we can rewrite the closed-loop system of (3.5) using (4.25) as

$$\begin{aligned} \dot{\tilde{r}}_i &= \tilde{v}_i, \\ \dot{\tilde{v}}_i &= -\sum_{j=0}^{n} a_{ij}(\tilde{r}_i - \tilde{r}_j) - \beta \operatorname{sgn}\left[\sum_{j=0}^{n} a_{ij}(\tilde{v}_i - \tilde{v}_j)\right]. \end{aligned} \qquad (4.26)$$

Equation (4.26) can be written in a vector form as

$$\dot{\tilde{r}} = \tilde{v}, \quad \dot{\tilde{v}} = -M\tilde{r} - \beta \operatorname{sgn}(M\tilde{v}), \qquad (4.27)$$

where $\tilde{r}$ and $\tilde{v}$ are, respectively, the column stack vectors of $\tilde{r}_i$ and $\tilde{v}_i$, $i = 1, \ldots, n$, and $M \overset{\triangle}{=} \mathcal{L} + \operatorname{diag}(a_{10}, \ldots, a_{n0})$.

Consider the Lyapunov function candidate $V = \frac{1}{2}\tilde{r}^T M^2 \tilde{r} + \frac{1}{2}\tilde{v}^T M \tilde{v}$. It follows that

$$\max \widetilde{L}_F V = \dot{V} = \tilde{r}^T M^2 \tilde{v} + \tilde{v}^T M \dot{\tilde{v}}$$
$$= \tilde{r}^T M^2 \tilde{v} + \tilde{v}^T M \big[-M\tilde{r} - \beta \operatorname{sgn}(M\tilde{v}) \big] = -\beta \, \|M\tilde{v}\|_1 .$$

Because M is symmetric positive definite under the condition of the theorem, it follows that $\dot{V}$ is negative semidefinite. Note that $\dot{V} \equiv 0$ implies that $\tilde{v} \equiv \mathbf{0}_n$ and hence $\dot{\tilde{v}} = \mathbf{0}_n$, which in turn implies that $\tilde{r} \equiv \mathbf{0}_n$ from (4.27). By using Lemma 1.40, it follows that $\tilde{r}(t) \to \mathbf{0}_n$ and $\tilde{v}(t) \to \mathbf{0}_n$ as $t \to \infty$. Equivalently, it follows that $|r_i(t) - r_0(t)| \to 0$ and $v_i(t) \to v_0$ as $t \to \infty$. ∎

Remark 4.15 In contrast to (4.13) and (4.21), which require both accurate position and velocity measurements, (4.25) does not necessarily require *accurate* velocity measurements because the velocity measurements are only used to calculate the sign (i.e., '+' or '-'). Therefore, (4.25) is more robust to measurement inaccuracy.

4.3.3 Swarm Tracking when the Leader's Velocity is Constant

In this subsection, we study distributed swarm tracking under a switching interaction graph when the leader's velocity, v_0, is constant. We propose the distributed swarm tracking algorithm for (3.5) as

$$u_i = -\sum_{j \in \mathcal{N}_i(t)} \frac{\partial V_{ij}}{\partial r_i} - \beta \sum_{j \in \overline{\mathcal{N}}_i(t)} b_{ij}$$
$$\times \left\{ \operatorname{sgn}\left[\sum_{k \in \overline{\mathcal{N}}_i(t)} b_{ik}(v_i - v_k) \right] - \operatorname{sgn}\left[\sum_{k \in \overline{\mathcal{N}}_j(t)} b_{jk}(v_j - v_k) \right] \right\}, \quad (4.28)$$

where V_{ij} is the potential function defined in Definition 4.1, $\overline{\mathcal{N}}_i(t)$ is defined as in Sect. 4.2.1, β is a positive constant, and b_{ij}, $i = 1, \ldots, n$, $j = 0, \ldots, n$, are positive constants. Note that (4.28) requires both the one-hop and two-hop neighbors' information.

Theorem 4.16. *Suppose that the undirected graph $\mathcal{G}(t)$ is connected and the leader is a neighbor of at least one follower (i.e., $0 \in \overline{\mathcal{N}}_i(t)$ for some i) at each time instant. Using (4.28) for (3.5), the velocity differences of all followers and the leader will ultimately converge to zero (i.e., the inter-agent distance will be maintained ultimately), $\lim_{t \to \infty} \sum_{j \in \mathcal{N}_i(t)} \frac{\partial V_{ij}}{\partial r_i} = 0, i = 1, \ldots, n$, and the inter-agent collision is avoided.*

Proof: Letting $\tilde{r}_i \triangleq r_i - r_0$ and $\tilde{v}_i \triangleq v_i - v_0$, we can rewrite the closed-loop system of (3.5) using (4.28) as

$$\dot{\tilde{r}}_i = \tilde{v}_i,$$

$$\dot{\tilde{v}}_i = -\sum_{j \in \mathcal{N}_i(t)} \frac{\partial V_{ij}}{\partial \tilde{r}_i} - \beta \sum_{j \in \mathcal{N}_i(t)} b_{ij}$$

$$\times \left\{ \mathrm{sgn}\left[\sum_{k \in \mathcal{N}_i(t)} b_{ik}(\tilde{v}_i - \tilde{v}_k) \right] - \mathrm{sgn}\left[\sum_{k \in \mathcal{N}_j(t)} b_{jk}(\tilde{v}_j - \tilde{v}_k) \right] \right\}.$$

Consider the Lyapunov function candidate

$$V = \frac{1}{2}\sum_{i=1}^{n}\sum_{j=1}^{n} V_{ij} + \sum_{i=1}^{n} V_{i0} + \frac{1}{2}\tilde{v}^T \tilde{v}, \qquad (4.29)$$

where $\tilde{v}$ is a column stack vector of $\tilde{v}_i$. It follows that

$$\max \widetilde{L}_F V = \dot{V}$$

$$= \frac{1}{2}\sum_{i=1}^{n}\sum_{j=1}^{n}\left(\frac{\partial V_{ij}}{\partial \tilde{r}_i}\dot{\tilde{r}}_i + \frac{\partial V_{ij}}{\partial \tilde{r}_j}\dot{\tilde{r}}_j \right) + \sum_{i=1}^{n}\left(\frac{\partial V_{i0}}{\partial \tilde{r}_i}\dot{\tilde{r}}_i + \frac{\partial V_{i0}}{\partial \tilde{r}_0}\dot{\tilde{r}}_0 \right) + \tilde{v}^T \dot{\tilde{v}}$$

$$= \sum_{i=1}^{n}\sum_{j=1}^{n}\frac{\partial V_{ij}}{\partial \tilde{r}_i}\dot{\tilde{r}}_i + \sum_{i=1}^{n}\frac{\partial V_{i0}}{\partial \tilde{r}_i}\dot{\tilde{r}}_i - \sum_{i=1}^{n}\tilde{v}_i \sum_{j=0}^{n}\frac{\partial V_{ij}}{\partial \tilde{r}_i}$$

$$- \beta \tilde{v}^T \widehat{M}(t)\, \mathrm{sgn}\big[\widehat{M}(t)\tilde{v}\big] \qquad (4.30)$$

$$= -\beta \big\|\widehat{M}(t)\tilde{v}\big\|_1, \qquad (4.31)$$

where $\widehat{M}(t)$ is defined in (4.9), (4.30) is derived by using Lemma 4.1 and the fact that $\dot{\tilde{r}}_0 = 0$, and (4.31) is derived by using the fact that $\widehat{M}(t)$ is symmetric. By following a similar analysis to that in the proof of Theorem 4.14, it follows from Lemma 1.40 that $v_i(t) \to v_0$ and $\sum_{j \in \mathcal{N}_i(t)} \frac{\partial V_{ij}}{\partial r_i} \to 0$ as $t \to \infty$, which in turn proves the theorem. ∎

4.3.4 Swarm Tracking when the Leader's Velocity is Varying

In this subsection, we assume that the leader's velocity, v_0, is varying (i.e., the leader's acceleration is, in general, nonzero.). We assume that $|\dot{v}_0| \leq \varphi_\ell$, where φ_ℓ is a positive constant. We propose the following distributed swarm tracking algorithm with a distributed estimator for (3.5) as

$$u_i = -\gamma\, \mathrm{sgn}\left[\sum_{j \in \mathcal{N}_i(t)} b_{ij}(\hat{v}_{i0} - \hat{v}_{j0}) \right] - \sum_{j \in \mathcal{N}_i(t)} \frac{\partial V_{ij}}{\partial r_i} - \beta \sum_{j \in \mathcal{N}_i(t)} b_{ij}$$

$$\times \left\{ \mathrm{sgn}\left[\sum_{k \in \mathcal{N}_i(t)} b_{ik}(v_i - v_k) \right] - \mathrm{sgn}\left[\sum_{k \in \mathcal{N}_j(t)} b_{jk}(v_j - v_k) \right] \right\}, \qquad (4.32)$$

where γ and β are positive constants, $b_{ij}, i = 1, \ldots, n, j = 0, \ldots, n$, are positive constants, V_{ij} is the potential function defined in Definition 4.1, $\overline{\mathcal{N}}_i(t)$ is defined in Sect. 4.2.1, and

$$\dot{\hat{v}}_{i0} = -\gamma \operatorname{sgn}\left[\sum_{j \in \mathcal{N}_i(t)} b_{ij}(\hat{v}_{i0} - \hat{v}_{j0})\right], \quad i = 1, \ldots, n, \qquad (4.33)$$

with $\hat{v}_{i0}$ being the ith agent's estimate of the leader's velocity and $\hat{v}_{00} \triangleq v_0$. Here (4.33) is a distributed estimator motivated by the results in Sect. 4.2.1.

Theorem 4.17. *Suppose that the undirected graph $\mathcal{G}(t)$ is connected and the leader is a neighbor of at least one follower (i.e., $0 \in \overline{\mathcal{N}}_i(t)$ for some i) at each time instant. Using (4.32) for (3.5), if $\gamma > \varphi_\ell$, the velocity differences of all followers and the leader will ultimately converge to zero (i.e., the inter-agent distance will be maintained ultimately), $\lim_{t \to \infty} \sum_{j \in \overline{\mathcal{N}}_i(t)} \frac{\partial V_{ij}}{\partial r_i} = 0, i = 1, \ldots, n$, and the inter-agent collision is avoided.*

Proof: Letting $\tilde{r}_i \triangleq r_i - r_0$ and $\tilde{v}_i \triangleq v_i - v_0$, we can rewrite the closed-loop system of (3.5) using (4.32) as

$$\begin{aligned}
\dot{\tilde{r}}_i &= \tilde{v}_i, \\
\dot{\tilde{v}}_i &= -\gamma \operatorname{sgn}\left[\sum_{j \in \mathcal{N}_i(t)} b_{ij}(\hat{v}_{i0} - \hat{v}_{j0})\right] - \sum_{j \in \overline{\mathcal{N}}_i(t)} \frac{\partial V_{ij}}{\partial \tilde{r}_i} - \beta \sum_{j \in \mathcal{N}_i(t)} b_{ij} \\
&\quad \times \left\{\operatorname{sgn}\left[\sum_{k \in \overline{\mathcal{N}}_i(t)} b_{ik}(\tilde{v}_i - \tilde{v}_k)\right] - \operatorname{sgn}\left[\sum_{k \in \overline{\mathcal{N}}_j(t)} b_{jk}(\tilde{v}_j - \tilde{v}_k)\right]\right\} - \dot{v}_0.
\end{aligned}$$
$$(4.34)$$

For (4.33), it follows from Theorem 4.4 that there exists positive $\bar{t}$ such that $\hat{v}_{i0}(t) \equiv v_0(t)$ for any $t \geq \bar{t}$. Note that $\dot{\hat{v}}_{i0}$ in (4.33) is a switching signal, which is different from $\dot{v}_0(t)$ at each time instant. However, for $\bar{t} \leq t_1 \leq t_2$, we have that $\int_{t_1}^{t_2} \dot{\hat{v}}_{i0}(t)\, dt = \int_{t_1}^{t_2} \dot{v}_0(t)\, dt$ by noting that $\hat{v}_{i0}(t) \equiv v_0(t)$ for any $t \geq \bar{t}$. Therefore, r_i and v_i will remain unchanged when $-\gamma \operatorname{sgn}[\sum_{j \in \mathcal{N}_i(t)} b_{ij}(\hat{v}_{i0} - \hat{v}_{j0})]$ (equivalently, $\dot{\hat{v}}_{i0}$) in (4.34) is replaced with $\dot{v}_0$ for $t \geq \bar{t}$. For $0 \leq t \leq \bar{t}$, by choosing the Lyapunov function candidate as (4.29), we can get

$$\max \widetilde{L}_F V = \dot{V} \leq -\beta\|\widehat{M}(t)\tilde{v}\|_1 + (\gamma + \varphi_\ell)\|\tilde{v}\|_1$$
$$\leq (\gamma + \varphi_\ell)\sqrt{n}\,\|\tilde{v}\|_2 \leq (\gamma + \varphi_\ell)\sqrt{n}\sqrt{2V},$$

which implies that $V(t) \leq (\sqrt{V(0)} + \frac{(\gamma+\varphi_\ell)\sqrt{n}}{\sqrt{2}}\bar{t})^2$ for $0 \leq t \leq \bar{t}$. That is, $V(t)$ is bounded for $0 \leq t \leq \bar{t}$. For $t > \bar{t}$, by replacing $-\gamma \operatorname{sgn}[\sum_{j \in \mathcal{N}_i(t)} b_{ij}(\hat{v}_{i0} - \hat{v}_{j0})]$ (equivalently, $\dot{\hat{v}}_{i0}$) in (4.34) with $\dot{v}_0$ and choosing the Lyapunov function candidate as (4.29), we can get $\max \widetilde{L}_F V = \dot{V} \leq -\beta\|\widehat{M}(t)\tilde{v}\|_1$. It follows from

a similar analysis to that in the proof of Theorem 4.16 and Lemma 1.40 that $|v_i(t) - v_0(t)| \to 0$ and $\sum_{j \in \overline{\mathcal{N}}_i(t)} \frac{\partial V_{ij}}{\partial r_i} \to 0$ as $t \to \infty$. This completes the proof. ■

Remark 4.18 Note that (4.28) and (4.32) require the availability of both the one-hop and two-hop neighbors' information. The availability of the leader's information (i.e., the position, velocity, and acceleration) to all followers is not required in (4.28) due to the fact that v_0 is constant and in (4.32) due to the introduction of the distributed estimator. In addition, (4.28) does not require *accurate* velocity measurements of the leader and the followers while (4.32) does not require *accurate* velocity measurements of the followers because the velocity measurements are only used to calculate the signs (i.e., '+' or '−'). Therefore, (4.28) and (4.32) are robust to velocity measurement inaccuracy.

Remark 4.19 In Theorems 4.6, 4.16, and 4.17, it is assumed that the undirected graph $\mathcal{G}(t)$ is connected and the leader is a neighbor of at least one follower at each time instant. However, this poses an obvious constraint in real applications because the connectivity requirement is not necessarily always satisfied. In the following, a mild connectivity requirement is proposed for distributed swarm tracking by adopting a connectivity maintenance mechanism in which the potential function in Definition 4.1 is redefined as follows:

1. When $\|r_i(0) - r_j(0)\| \geq r_s$, V_{ij} is defined as in Definition 4.1.
2. When $\|r_i(0) - r_j(0)\| < r_s$, V_{ij} is defined such that Conditions 1, 2, and 4 in Definition 4.1 are satisfied and Condition 3 in Definition 4.1 is replaced with the condition that $V_{ij} \to \infty$ as $\|r_i - r_j\| \to r_s$. The motivation here is also to maintain the initially existing connectivity patterns as in Remark 4.13.

Using the potential function defined above, distributed swarm tracking can be guaranteed for both single-integrator dynamics (cf. Theorem 4.6) and double-integrator dynamics (cf. Theorems 4.16 and 4.17) if the undirected graph $\mathcal{G}(t)$ is initially connected (i.e., $t = 0$), the leader is initially a neighbor of at least one follower, and the other conditions for the control gains are satisfied. The proof follows directly from those of Theorems 4.6, 4.16, and 4.17 except that a pair of followers who are neighbors of each other initially will always be the neighbors of each other (correspondingly, if the leader is initially a neighbor of a follower, the leader will always be a neighbor of this follower) because otherwise the potential function will go to infinity. This contradicts the fact that $\dot{V} \leq 0$ as shown in the proofs of Theorems 4.6 and 4.16 and the facts that $V(t)$ is bounded for $0 \leq t < \bar{t}$ and $\dot{V} \leq 0$ for $t \geq \bar{t}$ as shown in the proof of Theorem 4.17.

To illustrate the connectivity maintenance mechanism as proposed in Remark 4.19, we compare two different potential functions V_{ij}^1 and V_{ij}^2 whose derivatives satisfy, respectively,

(a) Potential function V_{ij}^1. (b) Potential function V_{ij}^2.
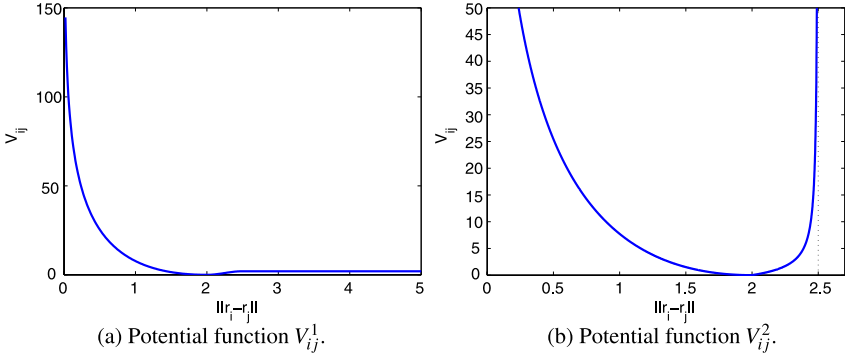
Fig. 4.1 Potential functions V_{ij}^1 and V_{ij}^2 with $r_s = 2.5$ and $d_{ij} = 2$

$$\frac{\partial V_{ij}^1}{\partial r_i} = \begin{cases} 0, & \|r_i - r_j\| > r_s, \\ \frac{2\pi(r_i-r_j)\sin[2\pi(\|r_i-r_j\|-d_{ij})]}{\|r_i-r_j\|}, & d_{ij} < \|r_i - r_j\| \le r_s, \\ \frac{20(r_i-r_j)}{\|r_i-r_j\|}\frac{\|r_i-r_j\|-d_{ij}}{\|r_i-r_j\|}, & \|r_i - r_j\| \le d_{ij}, \end{cases} \tag{4.35}$$

and

$$\frac{\partial V_{ij}^2}{\partial r_i} = \begin{cases} \frac{r_i-r_j}{\|r_i-r_j\|}\frac{\|r_i-r_j\|-d_{ij}}{(\|r_i-r_j\|-r_s)^2}, & d_{ij} < \|r_i - r_j\| < r_s, \\ 20\frac{r_i-r_j}{\|r_i-r_j\|}\frac{\|r_i-r_j\|-d_{ij}}{\|r_i-r_j\|}, & \|r_i - r_j\| \le d_{ij}, \end{cases} \tag{4.36}$$

where $r_s = 2.5$ and $d_{ij} = 2$. Figure 4.1 shows the plot of the potential functions V_{ij}^1 and V_{ij}^2.[4] It can be seen from Fig. 4.1(b) that V_{ij}^2 approaches infinity as the distance $\|r_i - r_j\|$ approaches r_s. However, V_{ij}^1 does not have the property (cf. Fig. 4.1(a)). In particular, V_{ij}^1 satisfies Condition 3 in Definition 4.1 as shown in Fig. 4.1(a). In addition, both V_{ij}^1 and V_{ij}^2 satisfy Conditions 1, 2, and 4 in Definition 4.1. According to Remark 4.19, we can choose the potential function as V_{ij}^2 when $\|r_i(0)-r_j(0)\| < r_s$ and V_{ij}^1 otherwise.

Remark 4.20 From the proofs of all theorems, it can be seen that the condition that $\mathcal{G}$ is undirected connected and the leader is a neighbor of at least one follower in each theorem can be relaxed to be that $\mathcal{G}$ is undirected and in $\overline{\mathcal{G}}$ the leader has directed paths to all followers (see Lemma 1.6).

4.4 Simulation

In this section, we present several simulation examples to validate some theoretical results in the previous sections. We consider a team consisting of six followers and

---

[4] Note that neither V_{ij}^1 nor V_{ij}^2 is unique because for any positive constant c, $V_{ij}^1 + c$ and $V_{ij}^2 + c$ are also potential functions satisfying, respectively, (4.35) and (4.36). We only plot one possible choice for them.

(a) Graph 1   (b) Graph 2
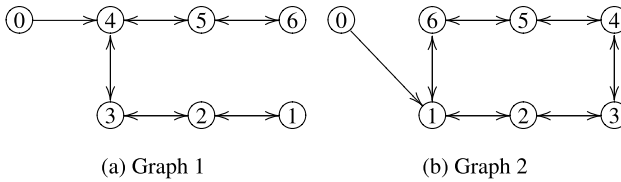
Fig. 4.2 Interaction graphs for the six followers and the leader. An *edge* between node i and node j means that followers i and j are neighbors of each other while an *arrow* from node 0 to node i means that the leader is a neighbor of follower i
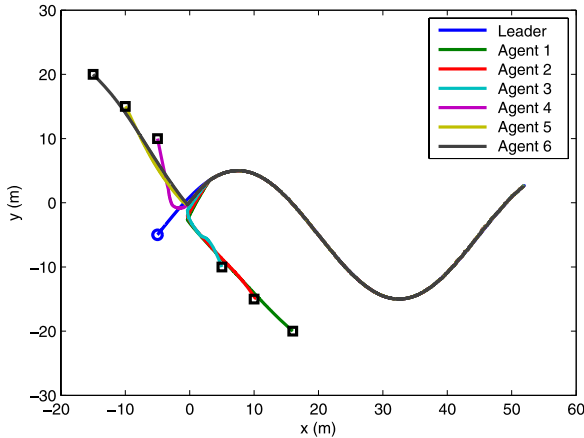
Fig. 4.3 Trajectories of the followers and the leader using (4.1). The *circle* denotes the starting position of the leader while the *squares* denote the starting positions of the followers

a leader in the two-dimensional space. We let $r_i \triangleq [r_{ix}, r_{iy}]^T$ and $v_i \triangleq [v_{ix}, v_{iy}]^T$, where r_{ix} and r_{iy} denote, respectively, the x and y positions of agent i while v_{ix} and v_{iy} denote, respectively, the x and y velocities of agent i. We also let $a_{ij} = 1$ if $(j, i) \in \overline{\mathcal{E}}$ and $a_{ij} = 0$ otherwise.

In the case of single-integrator dynamics, the interaction graph is chosen as in Fig. 4.2(a). It can be noted that the undirected graph $\mathcal{G}$ for all followers 1 to 6 is connected and the leader is a neighbor of follower 4. Using (4.1), we choose $r_0(t) = [t - 5, -5 + 10\sin(\frac{\pi t}{25})]^T$, $\alpha = 1$, and $\beta = 1.5$. The trajectories of the followers and the leader are shown in Fig. 4.3. The tracking errors of the x and y positions are shown in, respectively, Figs. 4.4(a) and 4.4(b). It can be seen from Fig. 4.4 that the tracking errors converge to zero in finite time. That is, all followers intercept the dynamic leader accurately after a finite period of time as also shown in Fig. 4.3.

For distributed swarm tracking in the case of single-integrator dynamics, we choose $r_s = 2.5$, $d_{ij} = 2$, $\alpha = 1$, and $\beta = 3$. The partial derivative of the potential function is chosen as in (4.35). Using (4.10) for (3.1), Fig. 4.5 shows the consecutive snapshots of distributed swarm tracking with 48 followers and a leader. The initial

(a) *x* position.   (b) *y* position.
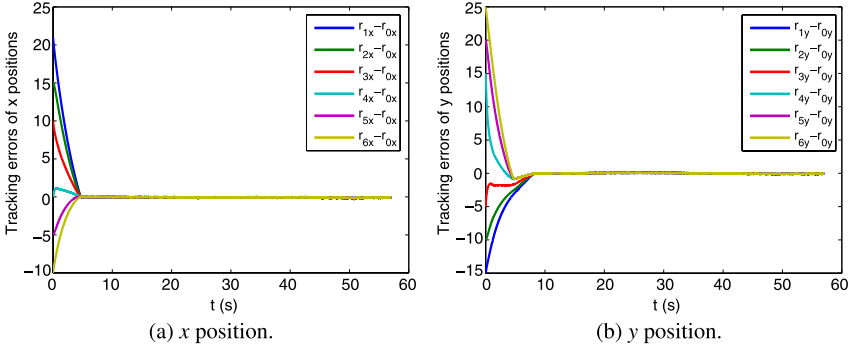
Fig. 4.4 Position tracking errors using (4.1)

states of the followers are randomly chosen from the square box $[-5, 15]^2$ and $r_0(t)$ is chosen as $[t, 5 + 10\sin(\frac{\pi t}{25})]^T$. It can be seen that the followers ultimately stay close to the leader and the inter-agent collision is avoided.

In the case of double-integrator dynamics, the interaction graph is chosen as in Fig. 4.2(b). It can be noted that the undirected graph $\mathcal{G}$ for all followers 1 to 6 is connected as well and the leader is a neighbor of follower 1. Using (4.13), we choose $r_0(t) = [t, t + \sin(t)]^T$, $\alpha = 1$, $\beta = 5$, and $\gamma = 0.1$. The trajectories of the followers and the leader are shown in Fig. 4.6. The tracking errors of the x and y positions are shown in Figs. 4.7(a) and 4.7(b). The tracking errors of the x and y velocities are shown in Figs. 4.7(c) and 4.7(d). It can be seen from Fig. 4.7 that the tracking errors ultimately converge to zero. That is, all followers ultimately intercept the dynamic leader as also shown in Fig. 4.6.

For distributed swarm tracking in the case of double-integrator dynamics, we choose $r_s = 2.5$, $d_{ij} = 2$, $\beta = 5$, and $b_{ij} = 1$ if $(j, i) \in \overline{\mathcal{N}}_i$ and $b_{ij} = 0$ otherwise. The partial derivative of the potential function is chosen as in (4.35). When the leader's velocity is constant, the initial states of the followers are randomly chosen from the square box $[-5, 10]^2$ and $r_0(t)$ is chosen as $[t, 2t + 5]^T$. Using (4.28) for (3.5), Fig. 4.8 shows the consecutive snapshots of distributed swarm tracking with 49 followers and a leader. When the leader's velocity is varying, the initial states of the followers are randomly chosen from the square box $[-5, 15]^2$ and $r_0(t)$ is chosen as $[t, 5 + t + 2\sin(t)]^T$. We choose $\gamma = 3$. Using (4.32) for (3.5), Fig. 4.9 shows the consecutive snapshots of distributed swarm tracking with 50 followers and a leader. Due to the random choice of the initial states, the agents form separated subgroups initially. As a result, fragmentation appears in this case. However, for each subgroup, the relative distances of the followers and the leader if the leader is in the subgroup remain unchanged ultimately.

For distributed coordinated tracking with the connectivity maintenance mechanism in Remark 4.13, we choose $r_s = 3$ and $b_{ij}(t)$ according to Remark 4.13 with $\frac{d}{dt}b_{ij}(t) = \frac{100\|r_i(t) - r_j(t)\|}{r_s^2 - \|r_i(t) - r_j(t)\|^2}$ and $b_{ij}(0) = 1$. Using (4.24) for (3.1) with the connectivity maintenance mechanism in Remark 4.13, we choose $\alpha = 1$ and $\beta = 3$.

(a) t=0 s

(b) t=5 s

(c) t=10 s

(d) t=40 s
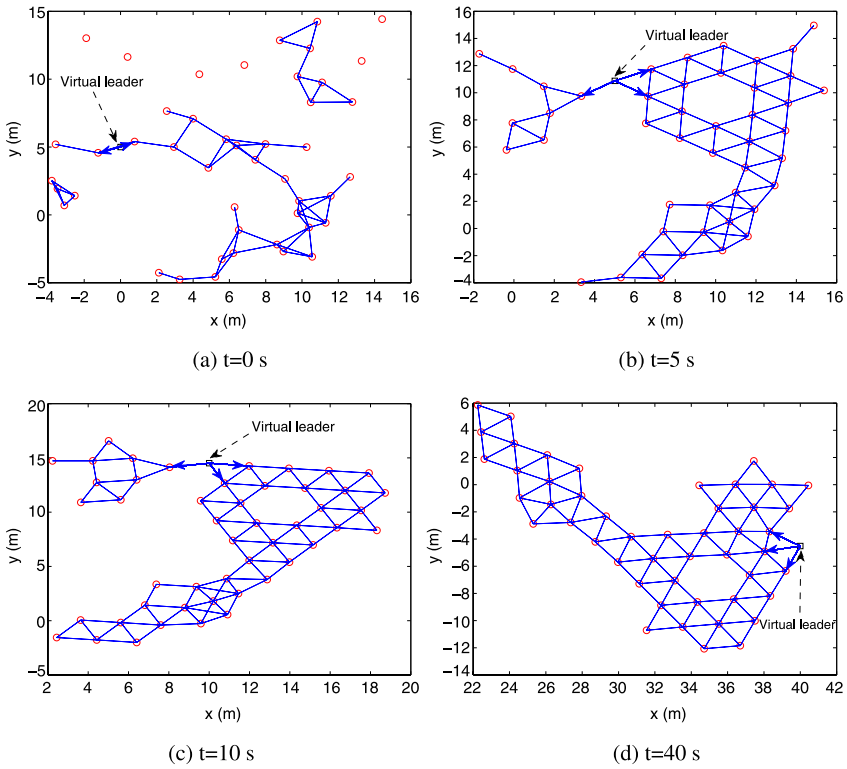
Fig. 4.5 Distributed swarm tracking with 48 followers and a leader using (4.10). The *circles* denote the positions of the followers while the *square* denotes the position of the leader. An edge connecting two followers means that the two followers are neighbors of each other while an *arrow* from the leader to a follower means that the leader is a neighbor of the follower
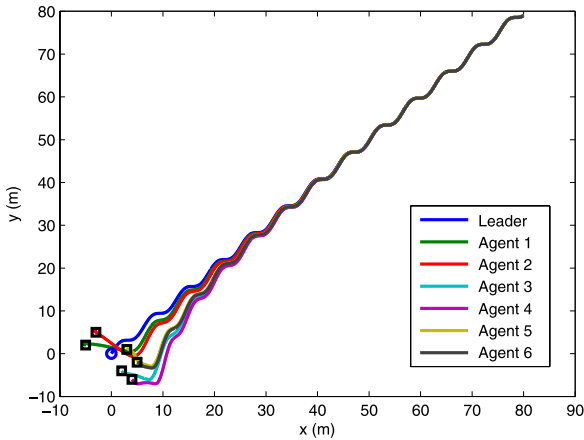
Fig. 4.6 Trajectories of the followers and the leader using (4.13). The *circle* denotes the starting position of the leader while the *squares* denote the starting positions of the followers

(a) *x* position

(b) *y* position

(c) *x* velocity
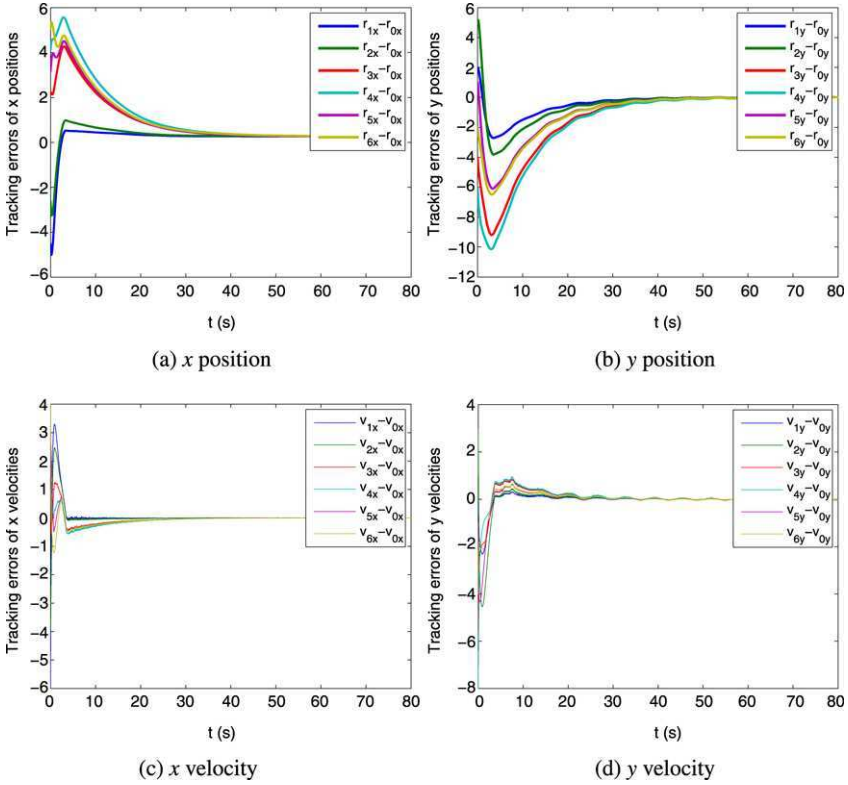
(d) *y* velocity

Fig. 4.7 Position and velocity tracking errors using (4.13)

Figure 4.10 shows the trajectories of the followers and the leader. The initial positions of the followers are randomly chosen from the square box $[-2, 2]^2$ and $r_0(t)$ is chosen as $[t, 3\sin(\frac{\pi t}{10})]^T$. The tracking errors of the x and y positions are shown in Figs. 4.11(a) and 4.11(b). It can be seen that the tracking errors ultimately converge to zero. That is, all followers ultimately intercept the dynamic leader as also shown in Fig. 4.10. Using (4.21) for (3.5) with the connectivity maintenance mechanism in Remark 4.13, we choose $\alpha = 1$, $\beta = 3$, and $\gamma = 0.1$. Figure 4.12 shows the trajectories of the followers and the leader. The initial positions of the followers are randomly chosen from the square box $[-2, 2]^2$ and $r_0(t)$ is chosen as $[t, t+\sin(t)]^T$. The tracking errors of the x and y positions are shown in Figs. 4.13(a) and 4.13(b). It can be seen from Fig. 4.13 that the tracking errors ultimately converge to zero. That is, all followers ultimately intercept the dynamic leader as also shown in Fig. 4.12.

For distributed swarm tracking with the connectivity maintenance mechanism as in Remark 4.19, all parameters are chosen the same as those for distributed swarm tracking without connectivity maintenance. When two followers are initially neighbors of each other or the leader is initially a neighbor of some follower(s), the partial derivative of the corresponding potential function is chosen as (4.36). Otherwise, the

(a) t=0 s

(b) t=2.5 s

(c) t=5 s

(d) t=10 s
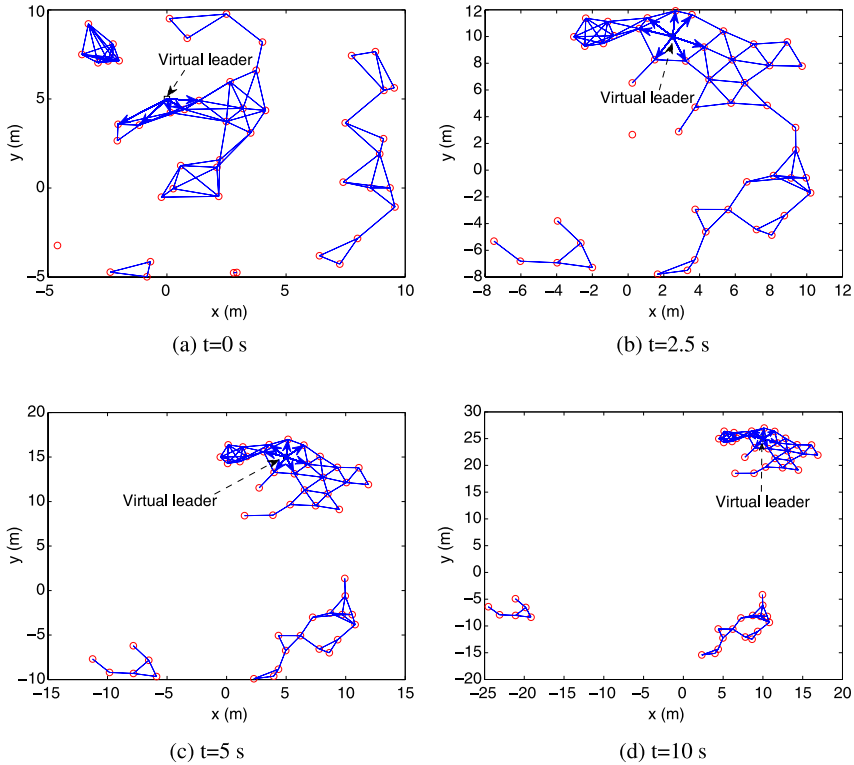
Fig. 4.8 Distributed swarm tracking with 49 followers and a leader using (4.28). The *circles* denote the positions of the followers while the *square* denotes the position of the leader. An *edge* connecting two followers means that the two followers are neighbors of each other while an *arrow* from the leader to a follower means that the leader is a neighbor of the follower

partial derivative of the potential function is chosen as (4.35). The initial positions of the followers are randomly chosen from the square box $[-6, 4]^2$ and $r_0(t)$ is chosen as $[t, 5 + 10\sin(\frac{\pi t}{25})]^T$. In the case of single-integrator dynamics, Fig. 4.14 shows the consecutive snapshots of distributed swarm tracking with 50 followers and a leader with the connectivity maintenance mechanism in Remark 4.19. In the case of double-integrator dynamics when the leader's velocity is constant, Fig. 4.15 shows the consecutive snapshots of distributed swarm tracking with 50 followers and a leader with the connectivity maintenance mechanism in Remark 4.19. In the case of double-integrator dynamics when the leader's velocity is varying, Fig. 4.16 shows the consecutive snapshots of distributed swarm tracking with 50 followers and a leader with the connectivity maintenance mechanism in Remark 4.19. It can be seen that at each snapshot the interaction graph for the 50 followers is connected and the leader is a neighbor of at least one follower because of the initial connectivity and the existence of the connectivity maintenance mechanism. Meanwhile, the relative distances of the followers and the leader remain unchanged ultimately. In contrast

(a) t=0 s   (b) t=2.5 s

(c) t=5 s   (d) t=10 s
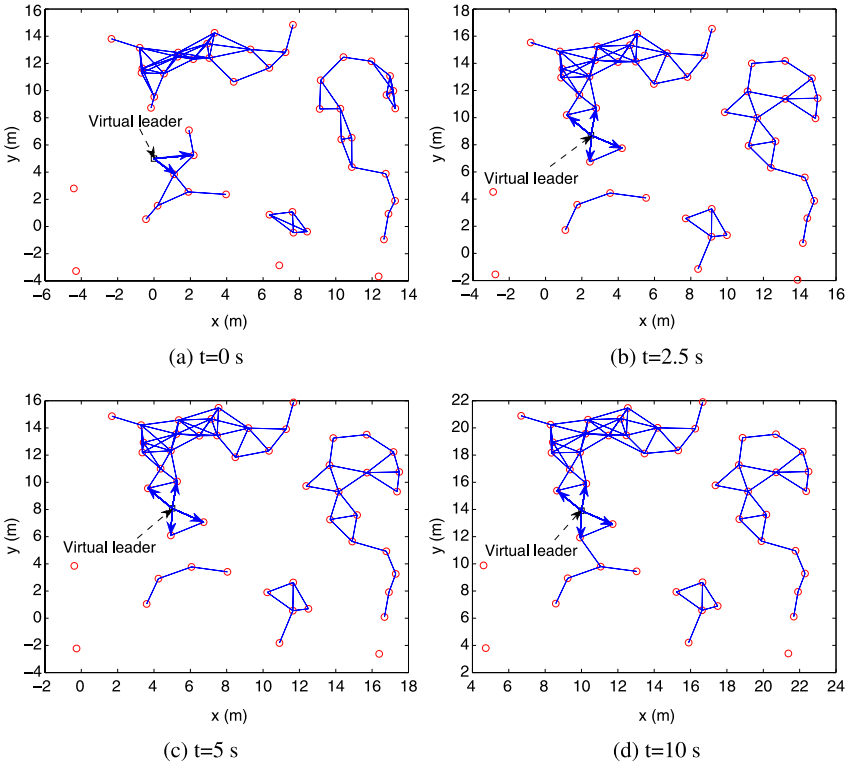
Fig. 4.9 Distributed swarm tracking with 50 followers and a leader using (4.32). The *circles* denote the positions of the followers while the *square* denotes the position of the leader. An *edge* connecting two followers means that the two followers are neighbors of each other while *arrow* from the leader to a follower means that the leader is a neighbor of the follower
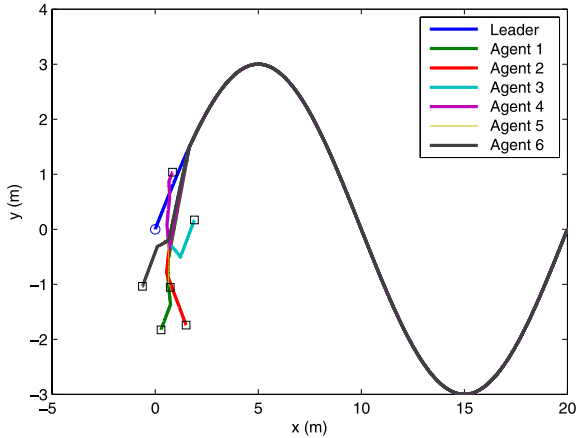
Fig. 4.10 Trajectories of the followers and the leader using (4.24) in the presence of the connectivity maintenance mechanism in Remark 4.13. The *circle* denotes the starting position of the leader while the *squares* denote the starting positions of the followers
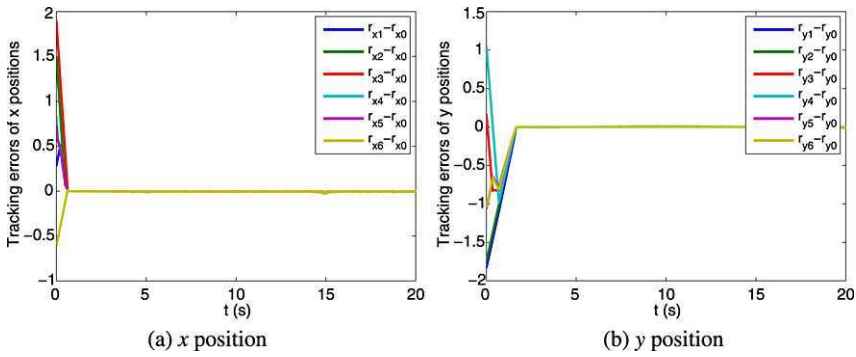
Fig. 4.11 Position tracking errors using (4.24) in the presence of the connectivity maintenance mechanism in Remark 4.13
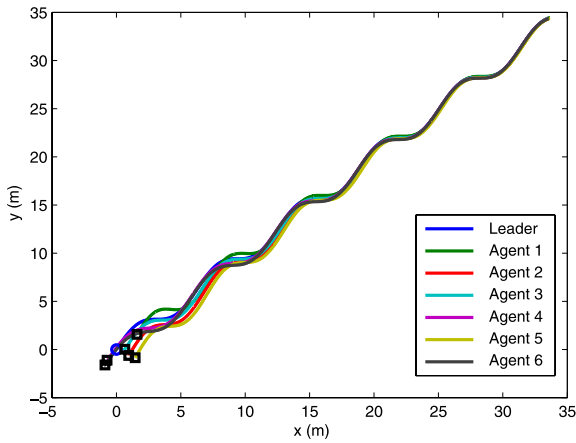
Fig. 4.12 Trajectories of the followers and the leader using (4.21) in the presence of the connectivity maintenance mechanism in Remark 4.13. The *circle* denotes the starting position of the leader while the *squares* denote the starting positions of the followers
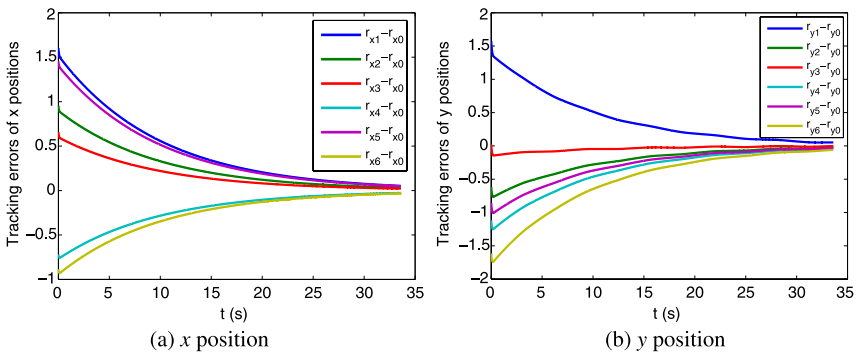
Fig. 4.13 Position tracking errors using (4.21) in the presence of the connectivity maintenance mechanism in Remark 4.13

(a) t=0 s   (b) t=2.5 s

(c) t=5 s   (d) t=10 s
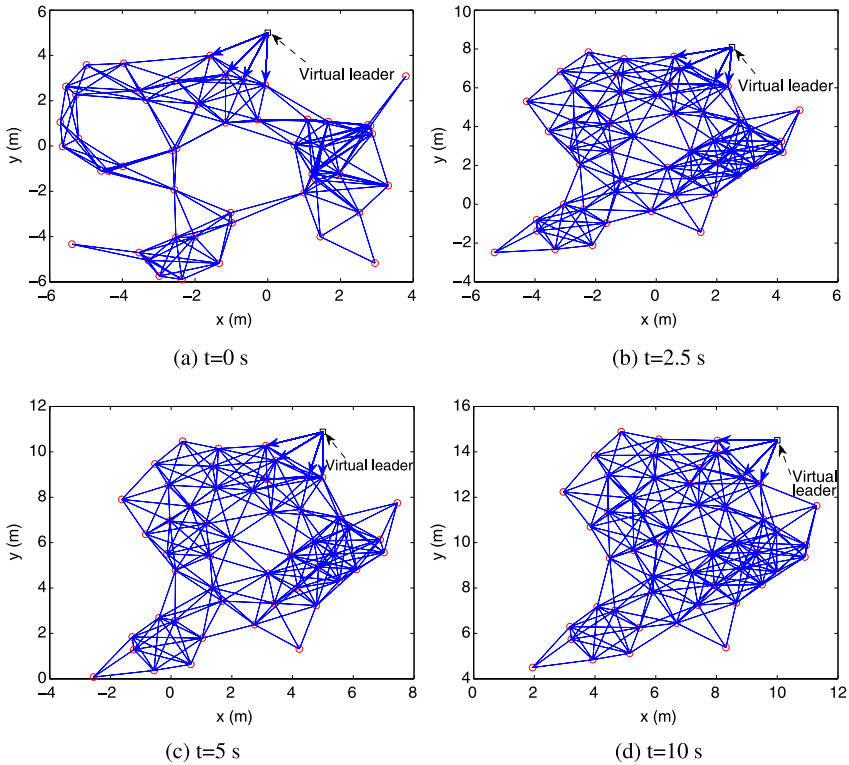
Fig. 4.14 Distributed swarm tracking with 50 followers and a leader using (4.10) in the presence of the connectivity maintenance mechanism in Remark 4.19. The *circles* denote the positions of the followers while the *square* denotes the position of the leader. An *edge* connecting two followers means that the two followers are neighbors of each other while an *arrow* from the leader to a follower means that the leader is a neighbor of the follower

to Figs. 4.5, 4.8, and 4.9 where the initially existing connectivity patterns might not always exist, the initially existing connectivity patterns in Figs. 4.14, 4.15, and 4.16 always exist due to the existence of the connectivity maintenance mechanism.

4.5 Notes

The results in this chapter are based mainly on [37–39]. For other results related to coordinated tracking, see [120, 121, 228, 246]. In particular, [120, 121] propose and analyze a coordinated tracking algorithm under an undirected switching interaction graph. However, [120, 121] require the availability of the leader's acceleration input to all followers and/or the design of distributed observers. Reference [246] proposes a proportional-and-derivative-like coordinated tracking algorithm under a directed
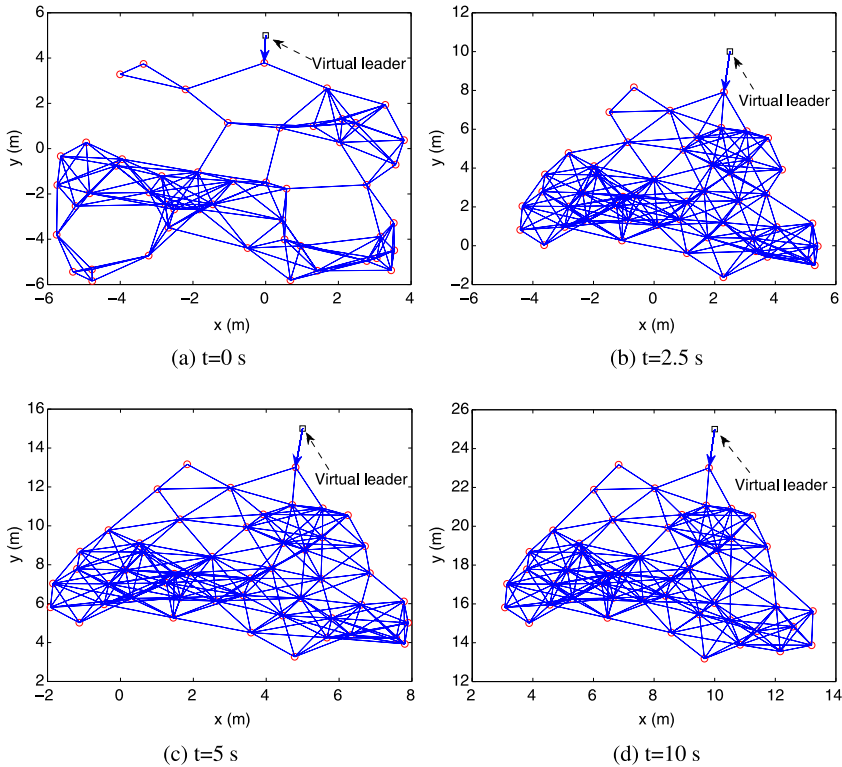
Fig. 4.15 Distributed swarm tracking with 50 followers and a leader using (4.28) in the presence of the connectivity maintenance mechanism in Remark 4.19. The *circles* denote the positions of the followers while the *square* denotes the position of the leader. An *edge* connecting two followers means that the two followers are neighbors of each other while an *arrow* from the leader to a follower means that the leader is a neighbor of the follower

interaction graph. However, [246] requires the estimates of the leader's velocity and the followers' velocities. Reference [228] studies a coordinated tracking algorithm with time-varying delays. However, [228] requires the velocity measurements of the followers and an estimator to estimate the leader's velocity. For other results related to swarm tracking, see [212, 268, 280, 317]. In particular, [212] studies a flocking algorithm in the presence of a leader under the assumption that the leader's velocity is constant and is available to all followers. Reference [280] extends the results in [212] in two aspects. When the leader has a constant velocity, [280] requires accurate position and velocity measurements of the leader. When the leader has a varying velocity, [280] requires that the leader's position, velocity, and acceleration be available to all followers. In [268], flocking of a group of autonomous agents with a dynamic leader is solved by using a set of switching control laws. However, [268] requires the availability of the acceleration of the leader to all followers. Reference [317] studies a swarm tracking algorithm via a variable structure approach

(a) t=0 s

(b) t=2.5 s

(c) t=5 s

(d) t=10 s
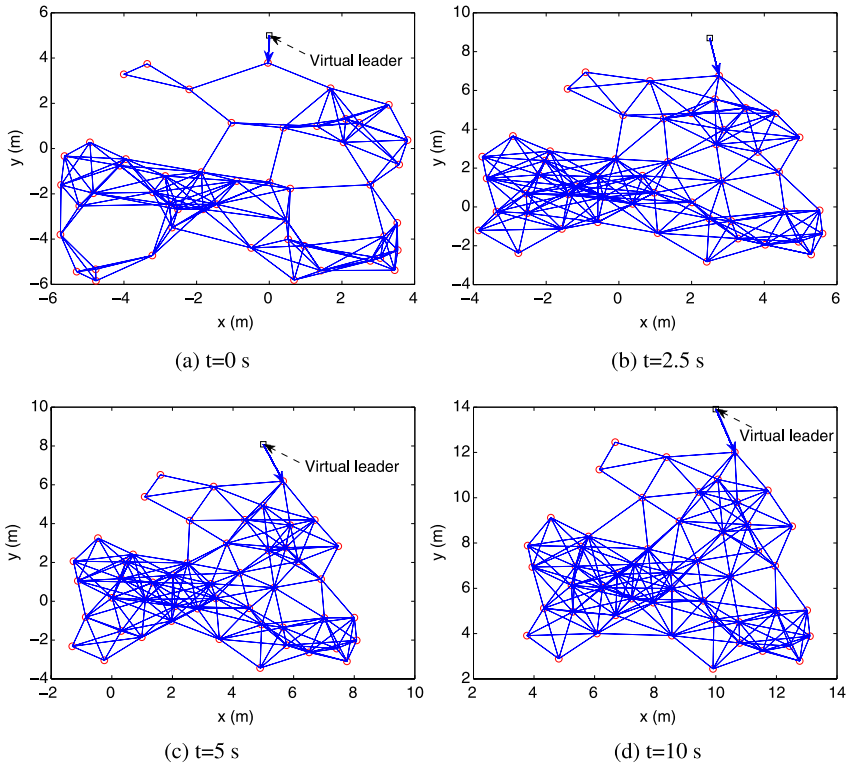
Fig. 4.16 Distributed swarm tracking with 50 followers and a leader using (4.32) in the presence of the connectivity maintenance mechanism in Remark 4.19. The *circles* denote the positions of the followers while the *square* denotes the position of the leader. An *edge* connecting two followers means that the two followers are neighbors of each other while an *arrow* from the leader to a follower means that the leader is a neighbor of the follower

using artificial potentials and the sliding mode control technique. However, [317] requires the availability of the leader's position to all followers and all-to-all inter-action among all followers. For other results related to connectivity maintenance, see [98, 133, 282, 326]. In [98], rendezvous of a group of agents with connectivity maintenance is solved by using a perimeter minimizing algorithm. In [133], con-sensus in the presence of connectivity maintenance is solved by properly defining the weights for the edges of the interaction graph. In [282], a controller based on a properly designed potential function is proposed to solve rendezvous of a group of nonholonomic robots with connectivity maintenance. In [326], connectivity mainte-nance for flocking of a group of agents is studied, where proper potential functions are proposed. However, the connectivity maintenance strategy in [326] requires that the number of edges in the interaction graph be always nondecreasing. That is, if a pair of followers are neighbors of each other (respectively, the leader is a neighbor

of a follower) at some time instant T,[5] then the pair of followers are always neighbors of each other (respectively, the leader is always a neighbor of this follower) at any time $t > T$. This requirement might not be applicable in reality, especially in large-scale systems where the number of the agents is large, because the size of the team of agents will become very compact with the increasing number of edges. Meanwhile, the computation burden will increase significantly as well. In contrast, the connectivity maintenance mechanism with the corresponding potential function proposed in Remark 4.19 takes into consideration these practical issues. In addition, *hysteresis* is introduced to the connectivity maintenance strategy in [326] to avoid the singularity of the Lyapunov function. However, the hysteresis is not required in the potential function proposed in Remark 4.19.

---

[5] Equivalently, a pair of followers are within the communication/sensing range of each other (respectively, the leader is within the communication/sensing range of a follower).

Chapter 5
Containment Control with Multiple Leaders

This chapter introduces a containment control problem, where a group of followers is driven by a group of leaders to be in the convex hull spanned by the leaders. The problem has applications in hazardous material handling, search and rescue, and cooperative transport. We consider three cases, namely, containment control with multiple stationary leaders, containment control with multiple dynamic leaders, and containment control with swarming behavior. Simulation results are presented to illustrate the theoretical results.

5.1 Problem Statement

In a *containment control* problem, there exist multiple leaders and multiple followers and the objective is to drive the followers to be in the *convex hull* spanned by the leaders. The study of containment control is motivated by numerous potential applications. For example, a team of heterogeneous agents moves from one location to another when only a portion of the agents is equipped with necessary sensors to detect the hazardous obstacles. Those agents equipped with the necessary sensors are normally designated as *leaders* while the other agents are designated as *followers*. By detecting the locations of the hazardous obstacles, the leaders can form a moving safety area. Then the team can arrive at the destination safely given that the followers always stay within the moving safety area spanned by the leaders.

This chapter studies distributed containment control in three aspects, namely, containment control with multiple *stationary leaders*, containment control with multiple *dynamic leaders*, containment control with *swarming behavior*. In the case of multiple stationary leaders, necessary and sufficient conditions on the directed fixed or switching interaction graph are derived such that all followers will ultimately be driven to be in the stationary convex hull spanned by the stationary leaders for arbitrary initial conditions in any dimensional space. When the directed interaction graph is fixed, we partition the nonsymmetric Laplacian matrix and explore its properties to derive the convergence result. When the directed interaction graph

is switching, the commonly adopted decoupling technique based on the Kronecker product in a high-dimensional space can no longer be applied and we hence present a *coordinate transformation technique* to derive the convergence result. In the case of multiple dynamic leaders, we propose a distributed tracking control algorithm without velocity measurements. When the directed interaction graph is fixed, we derive conditions on the interaction graph and the control gain to guarantee that all followers will ultimately be driven to be in the dynamic convex hull spanned by the dynamic leaders for arbitrary initial conditions in any dimensional space. When the directed interaction graph is switching, we derive conditions on the interaction graph and the control gain such that all followers will ultimately be driven to be in the *minimal hyperrectangle* that contains the dynamic leaders and each of its hyperplanes is normal to one axis of the inertial coordinate frame in any dimensional space. We also show via some examples that it might be very difficult to find distributed containment control algorithms without velocity measurements to guarantee that all followers will ultimately be driven to be in the dynamic convex hull spanned by the dynamic leaders under a mild connectivity condition on switching interaction graphs in a high-dimensional space. In the case of swarming behavior, we propose distributed algorithms by introducing potential functions to define the interaction forces between neighboring agents. The algorithms guarantee that all followers are driven toward the convex hull spanned by the leaders with bounded containment control error while achieving group cohesion (and hence connectivity maintenance) and group dispersion (and hence collision avoidance) among the leaders and the followers.

Definition 5.1. A point $x(t) \in D \subseteq \mathbb{R}^m$ is said to *converge* to a set $S(t) \subseteq D \subseteq \mathbb{R}^m$ if $\lim_{t \to \infty} d[x(t), S(t)] = 0$. A follower is said to *converge* to a set formed by the leaders if the position of the follower converges to the set formed by the positions of the leaders.

Definition 5.2. For the n-agent system, according to the role assignment mechanism, the agents are divided into two subgroups, namely, the leaders and the followers. Unless otherwise mentioned, it is assumed that the leaders have no neighbors while the followers have. Suppose that there are n_ℓ leaders and n_f followers, where $n_\ell + n_f = n$. We use $\mathcal{V}_L$ and $\mathcal{V}_F$ to denote, respectively, the leader set and the follower set. The directed graph $\mathcal{G}$ has a *united directed spanning tree* if for each of the n_f followers, there exists at least one leader that has a directed path to the follower.

Definition 5.3. Let C be a set in a real vector space $D \subseteq \mathbb{R}^m$. The set C is *convex* if, for any x and y in C, the point $(1 - z)x + zy$ is in C for any $z \in [0, 1]$. The convex hull spanned by a set of points $X = \{x_1, \ldots, x_q\}$ in D is the minimal convex set containing all points in X. We use $\mathrm{Co}(X)$ to denote the convex hull spanned by X. In particular, $\mathrm{Co}(X) = \{\sum_{i=1}^{q} \alpha_i x_i | x_i \in X, \alpha_i \geq 0, \sum_{i=1}^{q} \alpha_i = 1\}$. When $D \subseteq \mathbb{R}$, $\mathrm{Co}(X) = \{x | x \in [\min_i x_i, \max_i x_i]\}$.

5.2 Stability Analysis for Multiple Stationary Leaders

In this section, we study the conditions on, respectively, the directed fixed and switching interaction graphs such that all followers will ultimately converge to the stationary convex hull spanned by the stationary leaders.

Consider the n agents with single-integrator dynamics given by (3.1). Suppose that the leaders are stationary. We let

$$u_i = 0, \quad i \in \mathscr{V}_L,$$

$$u_i = -\sum_{j \in \mathscr{V}_L \bigcup \mathscr{V}_F} a_{ij}(t)[r_i - r_j], \quad i \in \mathscr{V}_F, \tag{5.1}$$

where $a_{ij}(t)$ is the (i,j)th entry of the adjacency matrix $\mathscr{A}(t)$ associated with the directed graph $\mathscr{G}(t) \triangleq [\mathscr{V}, \mathscr{E}(t)]$ characterizing the interaction among the n agents at time t. Note that all r_j, $j \in \mathscr{V}_L$, are constant because the leaders are stationary. Also note that $a_{ij} = 0$, $\forall i \in \mathscr{V}_L$, $\forall j \in \mathscr{V}_L \cup \mathscr{V}_F$, because the leaders have no neighbors.

As mentioned in Chap. 3, all agents share a common inertial coordinate frame. To facilitate later analysis in this section, we let $\mathscr{C}_0$ be the common inertial coordinate frame and rewrite (3.1) by explicitly emphasizing the coordinate representations in $\mathscr{C}_0$ as

$$\dot{r}_i^0 = u_i^0, \quad i = 1, \ldots, n, \tag{5.2}$$

where $r_i^0 \in \mathbb{R}^m$ and $u_i^0 \in \mathbb{R}^m$ are, respectively, the position and the control input of the ith agent represented in $\mathscr{C}_0$, and $\dot{r}_i^0$ is the velocity of the ith agent relative to $\mathscr{C}_0$ represented in $\mathscr{C}_0$. We also rewrite (5.1) as

$$u_i^0 = 0, \quad i \in \mathscr{V}_L,$$

$$u_i^0 = -\sum_{j \in \mathscr{V}_L \bigcup \mathscr{V}_F} a_{ij}(t)[r_i^0 - r_j^0], \quad i \in \mathscr{V}_F. \tag{5.3}$$

5.2.1 Directed Fixed Interaction

In this subsection, we study the case where the directed interaction graph is fixed. We assume that the adjacency matrix $\mathscr{A}$ is constant. Let r^0 denote the column stack vector of all r_i^0. Then the closed-loop system of (5.2) using (5.3) can be written in a vector form as

$$\dot{r}^0 = -(\mathscr{L} \otimes I_m)r^0, \tag{5.4}$$

where $\mathscr{L}$ is the nonsymmetric Laplacian matrix associated with $\mathscr{A}$ and hence $\mathscr{G}$. Without loss of generality, we assume that agents 1 to n_f are followers and agents $n_f + 1$ to n are leaders in the remainder of this chapter. Accordingly, $\mathscr{L}$ can be

partitioned as

$$\begin{bmatrix} \mathscr{L}_1 & \mathscr{L}_2 \\ 0_{n_\ell \times n_f} & 0_{n_\ell \times n_\ell} \end{bmatrix}, \tag{5.5}$$

where $\mathscr{L}_1 \in \mathbb{R}^{n_f \times n_f}$ and $\mathscr{L}_2 \in \mathbb{R}^{n_f \times n_\ell}$. Note that the last n_ℓ rows of $\mathscr{L}$ are all equal to zero because the last n_ℓ agents are the leaders who have no neighbors.

Lemma 5.1. *The matrix $\mathscr{L}_1$ is a nonsingular M-matrix if and only if the directed graph $\mathscr{G}$ has a united directed spanning tree. If $\mathscr{G}$ has a united directed spanning tree, then $-\mathscr{L}_1^{-1}\mathscr{L}_2$ is nonnegative and each row of $-\mathscr{L}_1^{-1}\mathscr{L}_2$ has a sum equal to one.*

Proof: Consider the following nonsymmetric Laplacian matrix given by

$$\widetilde{\mathscr{L}} = \begin{bmatrix} \mathscr{L}_1 & \mathscr{L}_2 \mathbf{1}_{n_\ell} \\ 0_{1 \times n_f} & 0 \end{bmatrix}. \tag{5.6}$$

According to the definition of the directed spanning tree in Sect. 1.2 and the definition of the united directed spanning tree in Definition 5.2, the directed graph associated with $\widetilde{\mathscr{L}}$, denoted as $\widetilde{\mathscr{G}}$, has a directed spanning tree if and only if the directed graph associated with $\mathscr{L}$ (i.e., $\mathscr{G}$) has a united directed spanning tree. From Lemma 1.1, $\widetilde{\mathscr{L}}$ has one simple zero eigenvalue if and only if $\widetilde{\mathscr{G}}$ has a directed spanning tree. Note from (5.6) that $\mathscr{L}_1$ is nonsingular if and only if $\widetilde{\mathscr{L}}$ has one simple zero eigenvalue. Therefore, $\mathscr{L}_1$ is nonsingular if and only if $\mathscr{G}$ has a united directed spanning tree. Because $\mathscr{L}_1$ is diagonally dominant and has nonnegative diagonal entries, it follows from Lemma 1.18 that all eigenvalues of $\mathscr{L}_1$ are either on the open right half plane or at the origin. If $\mathscr{L}_1$ is nonsingular, all eigenvalues of $\mathscr{L}_1$ are on the open right half plane. It thus follows from Definition 1.2 that $\mathscr{L}_1$ is a nonsingular M-matrix if and only if $\mathscr{G}$ has a united directed spanning tree.

We next study the property of $-\mathscr{L}_1^{-1}\mathscr{L}_2$. Because $\mathscr{L}_1$ is a nonsingular M-matrix, it follows from Lemma 1.17 that $\mathscr{L}_1^{-1}$ is nonnegative. Note also that $\mathscr{L}_1 \mathbf{1}_{n_f} + \mathscr{L}_2 \mathbf{1}_{n_\ell} = \mathbf{0}_{n_f}$. That is, $-\mathscr{L}_1^{-1}\mathscr{L}_2 \mathbf{1}_{n_\ell} = \mathbf{1}_{n_f}$. Combining with the fact that both $\mathscr{L}_1^{-1}$ and $-\mathscr{L}_2$ are nonnegative shows that $-\mathscr{L}_1^{-1}\mathscr{L}_2$ is nonnegative and each row of $-\mathscr{L}_1^{-1}\mathscr{L}_2$ has a sum equal to one. ∎

We next state the result in the case of a directed fixed interaction graph. We use r_F^0 and r_L^0 to denote the column stack vectors of, respectively, the followers' positions and the leaders' positions. Note that r_L^0 is constant.

Theorem 5.1. *Suppose that the adjacency matrix $\mathscr{A}$ is constant. Using (5.3) for (5.2), all followers will ultimately converge to the stationary convex hull spanned by the stationary leaders for arbitrary initial conditions if and only if the directed graph $\mathscr{G}$ has a united directed spanning tree. In particular, $r_F^0(t) \to -(\mathscr{L}_1^{-1}\mathscr{L}_2 \otimes I_m)r_L^0$ as $t \to \infty$.*

Proof: (Necessity) When $\mathscr{G}$ does not have a united directed spanning tree, there exists at least one follower, labeled as k, such that all leaders do not have directed

paths to follower k for $t \geq 0$. It follows that the position of follower k is independent of the positions of the leaders for $t \geq 0$. Therefore, follower k cannot always converge to the stationary convex hull spanned by the stationary leaders for arbitrary initial conditions.

(Sufficiency) It follows from (5.4) that

$$\dot{r}_F^0 = -(\mathcal{L}_1 \otimes I_m) r_F^0 - (\mathcal{L}_2 \otimes I_m) r_L^0. \tag{5.7}$$

Taking the Laplace transform on both sides of (5.7) gives

$$s r_F^0(s) - r_F^0(0) = -(\mathcal{L}_1 \otimes I_m) r_F^0(s) - \frac{1}{s}(\mathcal{L}_2 \otimes I_m) r_L^0, \tag{5.8}$$

where $r_F^0(s)$ is the Laplace transform of $r_F^0(t)$. After some simplification, (5.8) can be written as

$$r_F^0(s) = (s I_{mn_f} + \mathcal{L}_1 \otimes I_m)^{-1} \left[r_F^0(0) - \frac{1}{s}(\mathcal{L}_2 \otimes I_m) r_L^0 \right].$$

Because $\mathcal{G}$ has a united directed spanning tree, it follows from Lemma 5.1 that $\mathcal{L}_1$ is a nonsingular M-matrix, which implies that $-(\mathcal{L}_1 \otimes I_m)$ is Hurwitz.[1] Based on the final value theorem, we have

$$\lim_{t \to \infty} r_F^0(t) = \lim_{s \to 0} s r_F^0(s)$$
$$= \lim_{s \to 0} s(s I_{mn_f} + \mathcal{L}_1 \otimes I_m)^{-1} \left[r_F^0(0) - \frac{1}{s}(\mathcal{L}_2 \otimes I_m) r_L^0 \right]$$
$$= -(\mathcal{L}_1 \otimes I_m)^{-1}(\mathcal{L}_2 \otimes I_m) r_L^0 = -(\mathcal{L}_1^{-1} \mathcal{L}_2 \otimes I_m) r_L^0.$$

According to Lemma 5.1 and Definition 5.3, the ultimate positions of the followers, given by $-(\mathcal{L}_1^{-1} \mathcal{L}_2 \otimes I_m) r_L^0$, are in the stationary convex hull spanned by the stationary leaders. ∎

Remark 5.2 Existing consensus algorithms primarily study the case where the nonsymmetric Laplacian matrix has a simple zero eigenvalue. When there exist multiple leaders, the nonsymmetric Laplacian matrix $\mathcal{L}$ in (5.4) has multiple zero eigenvalues. Theorem 5.1 studies this case.

5.2.2 Directed Switching Interaction

In this subsection, we assume that the adjacency matrix $\mathscr{A}(t)$ is constant for $t \in [t_i, t_{i+1})$ and switches at time t_{i+1}, $i = 0, 1, \ldots$. Without loss of generality, let $t_0 = 0$. Let $\mathcal{G}_i$ and $\mathscr{A}_i$ denote, respectively, the directed graph and the adjacency matrix associated with the n agents for $t \in [t_i, t_{i+1})$. We assume that

---

[1] A matrix is Hurwitz if all its eigenvalues are on the open left half plane.

$t_{i+1} - t_i \geq t_L$, where t_L is a positive constant. We also assume that each nonzero and hence positive entry of $\mathscr{A}_i$ has a lower bound $\underline{a}$ and an upper bound $\overline{a}$, where $\underline{a}$ and $\overline{a}$ are positive constants. In the following, given two vectors $x \triangleq [x_1, \ldots, x_p]^T$ and $y \triangleq [y_1, \ldots, y_p]^T$, we use $x \leq y$ to denote that $x_i \leq y_i$, $i = 1, \ldots, p$. Before moving on, we need the following lemmas.

Lemma 5.2 ([147, Comparison Lemma]). *Consider the scalar differential equation*

$$\dot{z} = f(t, z), \quad z(t_0) = \mu_0, \tag{5.9}$$

where $f(t, z)$ is continuous in t and locally Lipschitz in z for all $t \geq t_0$ and all $z \in J \subset \mathbb{R}$. Let $[t_0, T)$ (T could be infinity) be the maximal interval of existence of the solution z, and suppose that $z \in J$ for all $t \in [t_0, T)$. Let ω be a continuous function whose upper right-hand derivative $D^+\omega$ satisfies the differential inequality

$$D^+\omega \leq f(t, \omega), \qquad \omega(t_0) \leq \mu_0, \tag{5.10}$$

where $\omega \in J$ for all $t \in [t_0, T)$. Then $\omega(t) \leq z(t)$ for all $t \in [t_0, T)$.

Lemma 5.3 ([147, Theorem 3.5]). *Let $f(t, x, \lambda)$ be continuous in (t, x, λ) and locally Lipschitz in x (uniformly in t and λ) on $[t_0, t_1] \times D \times \{\|\lambda - \lambda_0\| \leq c\}$, where $D \subset \mathbb{R}^n$ is an open connected set. Let $y(t, \lambda_0)$ be a solution of $\dot{x} = f(t, x, \lambda_0)$ with $y(t_0, \lambda_0) = y_0 \in D$. Suppose that $y(t, \lambda_0)$ is defined and belongs to D for all $t \in [t_0, t_1]$. Then, given $\epsilon > 0$, there is $\delta > 0$ such that if $\|z_0 - y_0\| < \delta$ and $\|\lambda - \lambda_0\| < \delta$, then there is a unique solution $z(t, \lambda)$ of $\dot{x} = f(t, x, \lambda)$ defined on $[t_0, t_1]$, with $z(t_0, \lambda) = z_0$, and $z(t, \lambda)$ satisfies $\|z(t, \lambda) - y(t, \lambda_0)\| < \epsilon$ for all $t \in [t_0, t_1]$.*

Lemma 5.4. *Consider the following vector differential equation*

$$\dot{z} = f(t, z), \qquad z(t_0) = \mu_0, \tag{5.11}$$

where $z \triangleq [z_1, \ldots, z_p]^T \in \mathbb{R}^p$, and $f(t, z) \triangleq [f_1(t, z), \ldots, f_p(t, z)]^T$ is defined such that $f_i(t, z)$, $i = 1, \ldots, p$, is continuous in t and locally Lipschitz in z_i, $i = 1, \ldots, p$, for all $t > t_0$ and all $z \in J \subset \mathbb{R}^p$. Let $[t_0, T)$ (T could be infinity) be the maximal interval of existence of the solution z, and suppose that $z \in J$ for all $t \in [t_0, T)$. Let $\omega \triangleq [\omega_1, \ldots, \omega_p]^T \in \mathbb{R}^p$ be a continuous function whose upper right-hand derivative $D^+\omega$ satisfies the differential inequality

$$D^+\omega \leq f(t, \omega), \qquad \omega(t_0) \leq \mu_0, \tag{5.12}$$

where $\omega \in J$ for all $t \in [t_0, T)$. Then $\omega(t) \leq z(t)$ for all $t \in [t_0, T)$.

Proof: [2] Consider the following vector differential equation

$$\dot{x} = f(t, x) + \lambda, \qquad x(t_0) = z(t_0) \tag{5.13}$$

---

[2] The proof is motivated by that of the Comparison Lemma in [147].

for $i = 1, \ldots, p$, where $x \in \mathbb{R}^p$ and $\lambda \in \mathbb{R}^p$ is a positive constant vector. For $t \in [t_0, t_1]$, where $t_1 > t_0$, it follows from Lemma 5.3 that for any $\epsilon > 0$, there is $\delta > 0$ such that if $\|\lambda\| < \delta$, (5.13) has a unique solution $\xi(t, \lambda)$ defined on $[t_0, t_1]$ and

$$\|\xi(t, \lambda) - z(t)\| < \epsilon, \quad \forall t \in [t_0, t_1].$$

Therefore, we have

$$\|\xi_i(t, \lambda) - z_i(t)\| < \epsilon, \quad \forall t \in [t_0, t_1], \tag{5.14}$$

where $\xi_i(t, \lambda)$ is the ith component of $\xi(t, \lambda)$.

Claim 1: $\omega_i(t) \leq \xi_i(t, \lambda)$ for all $t \in [t_0, t_1]$. We prove this by contradiction. Assume that there exist times $a, b \in (t_0, t_1]$ such that $\omega_i(a) = \xi_i(a, \lambda)$ and $\omega_i(t) > \xi_i(t, \lambda)$ for $a < t \leq b$. Accordingly, we have

$$\omega_i(t) - \omega_i(a) > \xi_i(t, \lambda) - \xi_i(a, \lambda), \quad \forall t \in (a, b],$$

which implies that $D^+\omega_i(a) \geq D^+\xi_i(a, \lambda) = \dot{\xi}_i(a, \xi) = f_i(a, \xi) + \lambda > f_i(a, \xi)$. This contradicts the inequality $D^+\omega \leq f(t, \omega)$.

Claim 2: $\omega_i(t) \leq z_i(t)$ for all $t \in [t_0, t_1]$. Again, we prove this by contradiction. Assume that there exists $a \in (t_0, t_1]$ such that $\omega_i(a) > z_i(a)$. Letting $\epsilon \triangleq \frac{\omega_i(a) - z_i(a)}{2}$ and using (5.14), we obtain that

$$\omega_i(a) - \xi_i(a, \lambda) = \omega_i(a) - z_i(a) + z_i(a) - \xi_i(a, \lambda)$$
$$= 2\epsilon + z_i(a) - \xi_i(a, \lambda) \geq \epsilon,$$

which contradicts the statement of Claim 1. ■

In Lemma 5.4, it is assumed that z is continuously differentiable. We next present a general comparison lemma for vector systems where z is continuous with the upper right-hand derivative of z, D^+z, well defined for all $t \in [0, T)$ while $\dot{z}$ might not be well defined for all $t \in [0, T)$.

Lemma 5.5. *Suppose that $F(t, z) : [t_0, T) \times J \subset \mathbb{R}^p \mapsto \mathbb{R}^p$ is a continuous function satisfying that*

$$D^+F = f(t, z),$$

where $z \in \mathbb{R}^p$, and $f(t, z)$ is piecewise continuous in t and is locally Lipschitz in z when $f(t, z)$ is continuous at t. Let $G(t, \omega) : [t_0, T) \times J \subset \mathbb{R}^p \mapsto \mathbb{R}^p$ be a continuous function whose upper right-hand derivative D^+G satisfies the differential inequality

$$D^+G \leq f(t, \omega), \qquad G[t_0, z(t_0)] \leq F[t_0, \omega(t_0)].$$

Then $G(t) \leq F(t)$ for all $t \in [t_0, T)$.

Proof: Without loss of generality, assume that $f(t, z)$ is continuous in t for $t \in [t_i, t_{i+1})$, $i = 0, \ldots$. For $t \in [t_0, t_1)$, consider a new vector differential equation given by

$$\dot{x} = f(t, x), \qquad x(t_0) = F\big[t_0, z(t_0)\big]. \tag{5.15}$$

Because $D^+ F = f(t, z) \leq f(t, z)$ and $F(t_0) = x(t_0) \leq x(t_0)$ are trivially satisfied, it follows from Lemma 5.4 that $F(t) \leq x(t)$ for all $t \in [t_0, t_1)$. Noting also that $D^+(-F) = -f(t, z) \leq -f(t, z)$ and $-F(t_0) = -x(t_0) \leq -x(t_0)$ are trivially satisfied, it follows from Lemma 5.4 that $-F(t) \leq -x(t)$ for all $t \in [t_0, t_1)$. Combining the two arguments shows that $F(t) = x(t)$ for all $t \in [t_0, t_1)$. Note that $D^+ G \leq f(t, \omega)$ and $G[t_0, z(t_0)] \leq F[t_0, \omega(t_0)] = x(t_0)$. It thus follows from Lemma 5.4 that $G(t) \leq x(t)$ for all $t \in [t_0, t_1)$. Because $F(t) \equiv x(t)$, it follows that $G(t) \leq F(t)$ for all $t \in [t_0, t_1)$. Because $F(t)$ is a continuous function, by employing a similar analysis for $t \in [t_i, t_{i+1})$, $i = 1, \ldots$, it can be shown that $G(t) \leq F(t)$ for all $t \in [t_i, t_{i+1})$, $i = 1, \ldots$. Therefore $G(t) \leq F(t)$ for all $t \in [t_0, T)$. ∎

Lemma 5.6. *Using (5.3) for (5.2), all followers will ultimately converge to the minimal hyperrectangle that contains the stationary leaders and each of whose hyperplanes is normal to one axis of $\mathscr{C}_0$, for arbitrary initial conditions if and only if there exists N_2 such that the union of $\mathscr{G}_i$, $i = N_1, \ldots, N_1 + N_2$, has a united directed spanning tree for any finite N_1.*

Proof: (Necessity) When there does not exist N_2 such that the union of $\mathscr{G}_i$, $i = N_1, \ldots, N_1 + N_2$, has a united directed spanning tree for some N_1, there exists at least one follower, labeled as k, such that all leaders do not have directed paths to follower k for $t \in [t_{N_1}, \infty)$. It follows that the position of follower k is independent of the positions of the leaders for $t \geq t_{N_1}$. Therefore, follower k cannot converge to the minimal hyperrectangle that contains the stationary leaders and each of whose hyperplanes is normal to one axis of $\mathscr{C}_0$ for arbitrary initial conditions.

(Sufficiency) Let $r^0_{i(k)}$ denote the kth, $k = 1, \ldots, m$, component of r^0_i (i.e., the projection of the position of agent i to the kth axis of the inertial coordinate frame $\mathscr{C}_0$). Define $r^+_{L(k)} \triangleq \max_{j \in \mathscr{V}_L} r^0_{j(k)}$ and $r^-_{L(k)} \triangleq \min_{j \in \mathscr{V}_L} r^0_{j(k)}$. Note that $r^+_{L(k)}$ and $r^-_{L(k)}$ are constant because the leaders are stationary. To prove the sufficiency part, it is equivalent to show that $\lim_{t \to \infty} d[r^0_{i(k)}(t), \mathscr{S}_k] = 0$, $\forall i \in \mathscr{V}_F$, $\forall k = 1, \ldots, m$, where $\mathscr{S}_k \triangleq [r^-_{L(k)}, r^+_{L(k)}]$.

Let $\omega_i \triangleq r^0_{i(k)} - r^+_{L(k)}$, $i = 1, \ldots, n$. Consider the function $\omega \triangleq [\omega_1, \ldots, \omega_{n_f}]^T$. Note that

$$D^+ \omega_i = \limsup_{h \to 0^+} \frac{1}{h}\big[\omega_i(t+h) - \omega_i(t)\big] = \limsup_{h \to 0^+} \frac{1}{h}\big[r^0_{i(k)}(t+h) - r^0_{i(k)}(t)\big]$$

$$= \dot{r}^0_{i(k)} = \sum_{j=1}^n a_{ij}(t)(\omega_j - \omega_i), \quad i = 1, \ldots, n_f.$$

Because $\mathscr{A}(t)$ is constant for $t \in [t_0, t_1)$, it follows that for $t \in [t_0, t_1)$

$$D^+ \omega_i = \sum_{j=1}^n a_{ij}(t_0)(\omega_j - \omega_i), \quad i = 1, \ldots, n_f.$$

For $t \in [t_0, t_1)$, consider the closed-loop system given by

$$\dot{z}_i = \sum_{j=1}^{n} a_{ij}(t_0)(z_j - z_i) \triangleq f_i(t, z), \quad i = 1, \ldots, n_f, \qquad (5.16)$$

where $z_i(t_0) = r_{i(k)}^0(t_0) - r_{L(k)}^+$, $i = 1, \ldots, n_f$, $z_j(t) \equiv 0$, $j = n_f + 1, \ldots, n$, for all $t \geq t_0$, and $z \triangleq [z_1, \ldots, z_{n_f}]^T$. Note that $f_i(t, z)$ is continuous in t and locally Lipschitz in z for $t \in [t_0, t_1)$. Because of $r_{j(k)}^0 \leq r_{L(k)}^+$, $\forall j \in \mathcal{V}_L$, by definition, it follows that

$$D^+ \omega \leq f(t, \omega)$$

for $t \in [t_0, t_1)$, where $f \triangleq [f_1, \ldots, f_{n_f}]^T$. Because $\omega(t_0) = z(t_0)$, it then follows from Lemma 5.4 that $\omega(t) \leq z(t)$ for $[t_0, t_1)$. By following a similar analysis, we have that $\omega(t) \leq z(t)$ for $[t_i, t_{i+1})$, $i = 1, 2, \ldots$, which implies that $\omega(t) \leq z(t)$ for all $t \geq t_0$.

Because $z_i(t) = 0$, $i = n_f + 1, \ldots, n$ and $\forall t \geq t_0$, we can view agents $n_f + 1$ to n as a single agent, labeled as agent 0, whose state is 0. For simplicity, we use $\widetilde{\mathcal{G}}_i$, $i = 1, 2, \ldots$, to denote the directed graphs associated with agents 0 to n_f. From Sect. 1.2 and Definition 5.2, if the union of $\mathcal{G}_i$, $i = N_1, \ldots, N_1 + N_2$, has a united directed spanning tree, then the union of $\widetilde{\mathcal{G}}_i$, $i = N_1, \ldots, N_1 + N_2$, has a directed spanning tree (accordingly, agent 0 has directed paths to all followers 1 to n_f). It then follows from Lemma 1.5 that consensus is reached for (5.16) if there exists N_2 such that the union of $\widetilde{\mathcal{G}}_i$, $i = N_1, \ldots, N_1 + N_2$, has a directed spanning tree for any finite N_1. That is, $z_i(t) \to 0$ as $t \to \infty$ under the condition of the lemma. Combining with the fact that $\omega(t) \leq z(t)$ for all $t \geq t_0$ shows that $\limsup_{t\to\infty} \omega(t) \leq \mathbf{0}_{n_f}$, i.e., $\limsup_{t\to\infty} r_{i(k)}^0(t) \leq r_{L(k)}^+$. Similarly, it can be shown that $\liminf_{t\to\infty} r_{i(k)}^0(t) \geq r_{L(k)}^-$.

Combining the previous arguments completes the proof. ∎

Lemma 5.7. *Given n fixed points $r_i \in \mathbb{R}^m$, $i = 1, \ldots, n$, relative to the inertial coordinate frame $\mathcal{C}_0$. The stationary convex hull spanned by the n points is equivalent to the intersection of all minimal hyperrectangles that contains the n points.*

Based on the results in Lemmas 5.6 and 5.7, we are ready to present the following result.

Theorem 5.3. *Using (5.3) for (5.2), all followers will ultimately converge to the stationary convex hull spanned by the stationary leaders for arbitrary initial conditions if and only if there exists N_2 such that the union of $\mathcal{G}_i$, $i = N_1, \ldots, N_1 + N_2$, has a united directed spanning tree for any finite N_1.*

Proof: (Necessity) The necessity part follows the same arguments as in Lemma 5.6.

(Sufficiency) Note that both (5.2) and (5.3) are represented in the inertial coordinate frame $\mathcal{C}_0$. For the purpose of analysis, we intentionally introduce another arbitrary (nonexisting) inertial coordinate frame $\mathcal{C}_1$. Note that there is a unique and reversible map from $\mathcal{C}_1$ to $\mathcal{C}_0$. That is, given any point q, we have that

$$q^0 = R_1^0 q^1 + \nu^0, \tag{5.17}$$

where q^0 and q^1 are, respectively, the coordinates of the point q with respect to $\mathscr{C}_0$ and $\mathscr{C}_1$, R_1^0 is the rotational matrix from $\mathscr{C}_1$ to $\mathscr{C}_0$, and ν^0 is the translational vector from the origin of $\mathscr{C}_0$ to the origin of $\mathscr{C}_1$ represented in $\mathscr{C}_0$. Using (5.3) for (5.2), we have

$$\dot{r}_i^0 = -\sum_{j \in \mathscr{V}_L \bigcup \mathscr{V}_F} a_{ij}(t)\big(r_i^0 - r_j^0\big), \quad i \in \mathscr{V}_F. \tag{5.18}$$

Note that according to (5.17) $r_i^0 = R_1^0 r_i^1 + \nu^0$. It then follows from (5.18) that

$$
\begin{aligned}
R_1^0 \dot{r}_i^1 &= -\sum_{j \in \mathscr{V}_L \bigcup \mathscr{V}_F} a_{ij}(t)\big[\big(R_1^0 r_i^1 + \nu^0\big) - \big(R_1^0 r_j^1 + \nu^0\big)\big] \\
&= -R_1^0 \sum_{j \in \mathscr{V}_L \bigcup \mathscr{V}_F} a_{ij}(t)\big(r_i^1 - r_j^1\big), \quad i \in \mathscr{V}_F,
\end{aligned}
\tag{5.19}
$$

where we have used the fact that R_1^0 and ν^0 are constant to obtain the left hand side of (5.19). It thus follows that

$$\dot{r}_i^1 = -\sum_{j \in \mathscr{V}_L \bigcup \mathscr{V}_F} a_{ij}(t)\big(r_i^1 - r_j^1\big), \quad i \in \mathscr{V}_F. \tag{5.20}$$

From (5.18) and (5.20), it can be noted that the closed-loop system of (5.2) using (5.3) where the positions of all agents are represented with respect to one inertial coordinate frame can be equivalently transformed to the same form when the positions of all agents are represented with respect to any other arbitrarily chosen inertial coordinate frame.

According to Lemma 5.6, if follows that the followers will ultimately converge to the minimal hyperrectangle that contains the stationary leaders and each of whose hyperplanes is normal to one axis of the inertial coordinate frame $\mathscr{C}_1$ under the condition of the theorem.[3] Because the inertial coordinate frame $\mathscr{C}_1$ can be arbitrary, it follows that the followers will ultimately converge to all minimal hyperrectangles that contain the stationary leaders under the condition of the theorem. That is, the followers will ultimately converge to the intersection of all minimal hyperrectangles that contain the stationary leaders under the condition of the theorem. It then follows from Lemma 5.7 that all followers will ultimately converge to the stationary convex hull spanned by the stationary leaders under the condition of the theorem. ∎

Example 5.1. To illustrate the proof of Theorem 5.3, we simply consider an example in the two-dimensional space (see Fig. 5.1). Here all agents share the common inertial coordinate frame $\mathscr{C}_0$. We also arbitrarily choose three other inertial coordinate frames $\mathscr{C}_1$, $\mathscr{C}_2$, and $\mathscr{C}_3$. The four squares denote the four stationary leaders.

---

[3] We emphasize that $\mathscr{C}_1$ does not exist. We introduce $\mathscr{C}_1$ only for analysis. Although the coordinates of a point with respect to $\mathscr{C}_0$ and $\mathscr{C}_1$ are different, the physical location of the point is unique in the space.
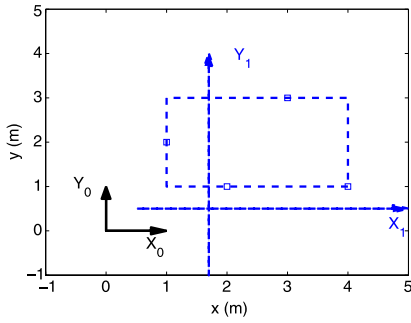
(a) The minimal rectangle containing the four leaders when the closed-loop system is represented in $\mathscr{C}_1$. Each edge of the rectangle is normal to one axis of $\mathscr{C}_1$.
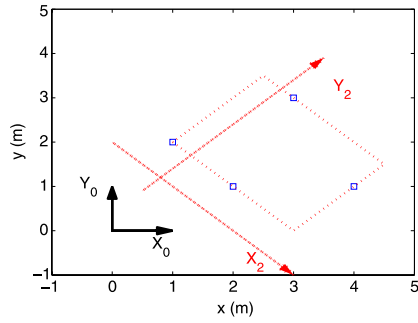
(b) The minimal rectangle containing the four leaders when the closed-loop system is represented in $\mathscr{C}_2$. Each edge of the rectangle is normal to one axis of $\mathscr{C}_2$.
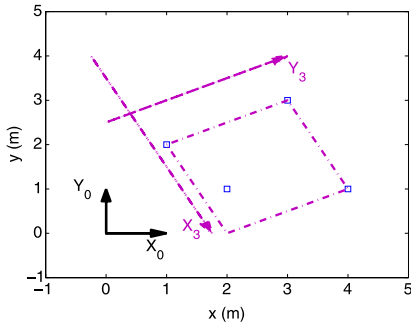
(c) The minimal rectangle containing the four leaders when the closed-loop system is represented in $\mathscr{C}_3$. Each edge of the rectangle is normal to one axis of $\mathscr{C}_3$.
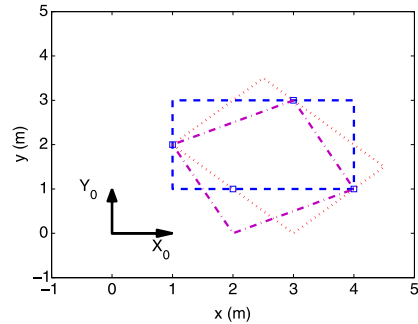
(d) The intersection of the previous three rectangles, which is the convex hull formed by the four leaders.

Fig. 5.1 Illustration of the proof of Theorem 5.3 in a two-dimensional space. The *squares* denote the positions of the four stationary leaders. The physical locations of the leaders are unique in the space. The *blue*, *red*, and *purple rectangles* represent the minimal rectangles that contain the four stationary leaders and each of whose edges is normal to one axis of, respectively, $\mathscr{C}_1$, $\mathscr{C}_2$, and $\mathscr{C}_3$. The intersection of the three minimal rectangles is the stationary convex hull spanned by the four stationary leaders

The blue rectangle (respectively, the red rectangle and the purple rectangle) is the minimal rectangle that contains the stationary leaders and each of whose edges is normal to one axis of $\mathscr{C}_1$ (respectively, $\mathscr{C}_2$ and $\mathscr{C}_3$). Apparently, the intersection of the three minimal rectangles[4] is equivalent to the stationary convex hull spanned by the four stationary leaders.

---

[4] Note that in general we should get the intersection of all minimal rectangles that contain the stationary leaders but here the three minimal rectangles happen to be sufficient.
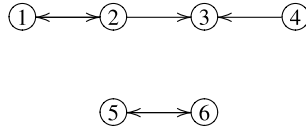
Fig. 5.2 An interaction graph where a subgroup of agents can be viewed as one leader. An *arrow* from i to j denote that agent i is a neighbor of agent j

Remark 5.4 The *coordinate transformation technique* used in the proof of Theorem 5.3 is an effective tool in analyzing the group coordination behavior of a linear system with a linear algorithm in a high-dimensional space when the decoupling technique based on the Kronecker product cannot be applied. Essentially, (5.18) and (5.20) imply that the followers do not need to share a common inertial coordinate frame in the containment control problem in the case of stationary leaders. Each follower can have its own inertial coordinate frame and implement the algorithm according to its own inertial coordinate frame. Similarly, when using the traditional consensus algorithm (2.2) for (2.1), the same coordinate transformation technique as in the proof of Theorem 5.3 can be used without changing the property of the closed-loop system such as whether consensus will be reached. That is, even if each agent has its own inertial coordinate frame, consensus is still reached if the interaction graph has a directed spanning tree jointly.

Remark 5.5 In the previous part of this section, we assume that each leader has no neighbor. However, for some interaction graphs, it is possible to view a subgroup of agents as one leader. For example, in the interaction graph given by Fig. 5.2, agents 1 and 2 (respectively, agents 5 and 6) can reach consensus on a constant value independent of the states of the other agents. The results in this section can also be applied to this case by viewing agents 1 and 2 (respectively, agents 5 and 6) as one leader with the state being the constant consensus equilibrium of agents 1 and 2 (respectively, agents 5 and 6).

Remark 5.6 For the discrete-time consensus algorithm (i.e., the distributed weighted averaging algorithm) (see, e.g., [248, Chap. 2]) with multiple stationary leaders, the convergence result is the same as that in Theorems 5.3 by following a similar analysis.

5.2.3 Simulation

In this section, we present simulation results to validate the theoretical results in Sects. 5.2.1 and 5.2.2. We consider a team consisting of four leaders and six followers in a two-dimensional space.

Under directed fixed interaction, the directed fixed graph $\mathscr{G}$ is shown as in Fig. 5.3. It can be noted that $\mathscr{G}$ has a united directed spanning tree. We choose
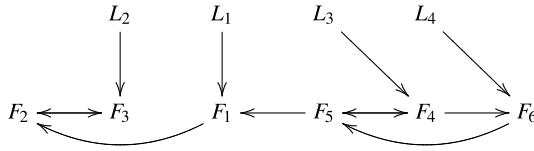
Fig. 5.3 Directed fixed graph $\mathcal{G}$ for a team consisting of four leaders and six followers. Here $L_i, i = 1, \ldots, 4$, denote the leaders while $F_i, i = 1, \ldots, 6$, denote the followers. An *arrow* from L_j or F_j to F_i denote that L_j or F_j is a neighbor of F_i
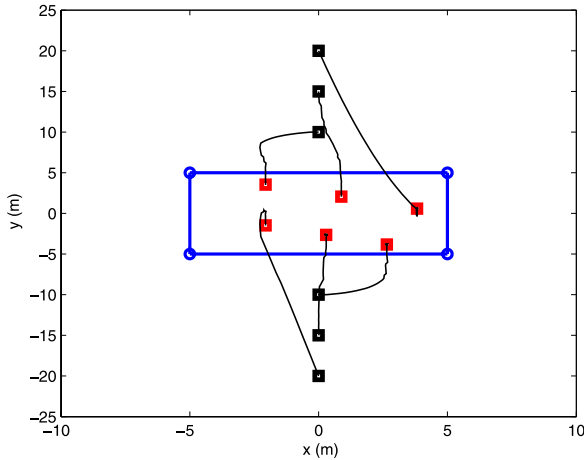
Fig. 5.4 Trajectories of the agents using (5.3) with $\mathcal{G}$ shown in Fig. 5.3. *Circles* denote the positions of the stationary leaders while the *black* and *red squares* denote, respectively, the starting and ending positions of the followers

$a_{ij} = 1$ if $(j, i) \in \mathcal{E}$ and $a_{ij} = 0$ otherwise. The simulation result using (5.3) for (5.2) is shown in Fig. 5.4. It can be seen that all followers ultimately converge to the stationary convex hull spanned by the stationary leaders and the final positions of the followers are constant.

Under directed switching interaction, we let $\mathcal{G}(t)$ switches from $\{\mathcal{G}_{(1)}, \mathcal{G}_{(2)}\}$ as shown in Fig. 5.5. Note that neither $\mathcal{G}_{(1)}$ nor $\mathcal{G}_{(2)}$ has a united directed spanning tree. However, the union of $\mathcal{G}_{(1)}$ and $\mathcal{G}_{(2)}$ is shown in Fig. 5.3, which has a united directed spanning tree. We choose $a_{ij}(t) = 1$ if $(j, i) \in \mathcal{E}(t)$ and $a_{ij}(t) = 0$ otherwise. The simulation result using (5.3) for (5.2) is shown in Fig. 5.5 when $\mathcal{G}$ switches between $\mathcal{G}_{(1)}$ and $\mathcal{G}_{(2)}$ every 1 second. Figures 5.5(a) and 5.5(b) show the trajectories of the agents, respectively, from $t = 0$ s to 20 s and from $t = 5$ s to 20 s. From these two figures, it can be seen that the follows ultimately converge to the stationary convex hull spanned by the stationary leaders despite the fact that the directed interaction graph is switching. In particular, the followers do not have constant final positions because the directed interaction graph is switching.

(a) $\mathscr{G}_{(1)}$

(b) $\mathscr{G}_{(2)}$
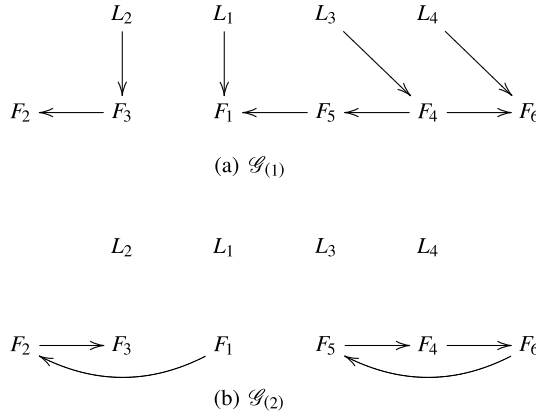
Fig. 5.5 Directed switching graphs $\mathscr{G}_{(1)}$ and $\mathscr{G}_{(2)}$ for a team consisting of four leaders and six followers. Here $L_i, i = 1, 4$, denote the leaders while $F_i, i = 1, \ldots, 6$, denote the followers

(a) $t \in (0, 20)$ s   (b) $t \in (5, 20)$ s
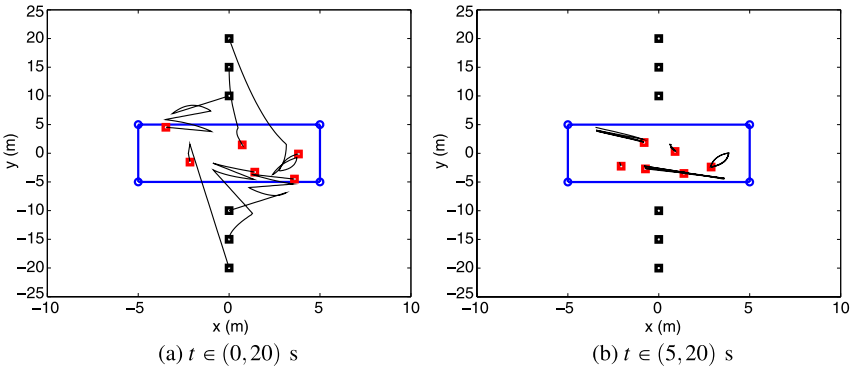
Fig. 5.6 Trajectories of the agents using (5.3) with $\mathscr{G}(t)$ switching from $\{\mathscr{G}_{(1)}, \mathscr{G}_{(2)}\}$ as shown in Fig. 5.5. *Circles* denote the positions of the stationary leaders while the *black* and *red squares* denote, respectively, the starting and ending positions of the followers

5.3 Stability Analysis for Multiple Dynamic Leaders

In this section, we propose a distributed tracking control algorithm without velocity measurements and then analyze the stability condition under both directed fixed and switching interaction graphs. Again all agents share the common inertial coordinate frame $\mathscr{C}_0$. In this section, we omit the superscript 0 in the coordinate representations for the simplicity of notation.

For agents with single-integrator dynamics given by (3.1), we propose the following distributed tracking control algorithm without velocity measurements as

$$u_i = v_i, \quad i \in \mathcal{V}_L,$$

$$u_i = -\alpha \sum_{j \in \mathcal{V}_L \cup \mathcal{V}_F} a_{ij}(t)(r_i - r_j)$$

$$- \beta \operatorname{sgn}\left[\sum_{j \in \mathcal{V}_L \bigcup \mathcal{V}_F} a_{ij}(t)(r_i - r_j) \right], \quad i \in \mathcal{V}_F, \tag{5.21}$$

where $v_i \in \mathbb{R}^m$ denotes the time-varying velocity of leader i, $a_{ij}(t)$ is defined as in (5.1), α is a nonnegative constant scalar, β is a positive constant scalar, and $\operatorname{sgn}(\cdot)$ is defined componentwise. We assume that $\|v_i\| \leq \gamma_\ell, \forall i \in \mathcal{V}_L$, where γ_ℓ is a positive constant.

5.3.1 Directed Fixed Interaction

In this subsection, we consider the case where the directed interaction graph is fixed. We assume that the adjacency matrix $\mathcal{A}$ is constant. Before moving on, we need the following lemma.

Lemma 5.8. *Suppose that a team consists of n followers, labeled as agents 1 to n, and a stationary leader, labeled as agent 0. Let $\overline{\mathcal{G}}(t)$ be the directed graph characterizing the interaction among the leader and the followers at time t. Suppose that in $\overline{\mathcal{G}}(t)$ the leader has directed paths to all followers 1 to n at each time. Let ϵ, ς, ϵ_1, and ϵ_2 be positive constants. Consider the following closed-loop dynamics given by*

$$\dot{r}_i = -\alpha \sum_{j=0}^{n} a_{ij}(t) f_{i,j}(t, r_i, r_j), \quad i = 1, \ldots, n, \tag{5.22}$$

where $r_j \triangleq [r_{j(1)}, \ldots, r_{j(m)}]^T \in \mathbb{R}^m$ is the position of agent j,[5] α is a positive constant, $a_{ij}(t)$ is the (i, j)th entry of the adjacency matrix $\overline{\mathcal{A}}(t)$ associated with $\overline{\mathcal{G}}(t)$, $f_{i,j}(t, r_i, r_j) \triangleq [f_{i,j}[t, r_{i(1)}, r_{j(1)}], \ldots, f_{i,j}[t, r_{i(m)}, r_{j(m)}]]^T$, each component of $f_{ij}(t, r_i, r_j)$ is defined such that for $x, y \in \mathbb{R}$, $f_{i,j}(t, x, y)$ satisfies that

$$f_{i,j}(t, x, y) = \begin{cases} > \epsilon, & x > y \\ < -\epsilon, & x < y \\ 0, & x = y \end{cases} \tag{5.23}$$

or

$$f_{i,j}(t, x, y) = f_{i,j}(x, y) \begin{cases} \geq \varsigma(x - y), & x > y \\ \leq \varsigma(x - y), & x < y \\ = 0, & x = y, \end{cases} \tag{5.24}$$

---

[5] Note that r_0 is constant because the leader is stationary.

$i = 1, \ldots, n, \ \ j = 1, \ldots, n, \ \ f_{i,0}(t, r_i, r_0) \triangleq [f_{i,0}[t, r_{i(1)}, r_{0(1)}], \ldots, \ f_{i,0}[t, r_{i(m)}, r_{0(m)}]]^T$, and each component of $f_{i,0}(t, r_i, r_0)$ is defined such that for $x, y \in \mathbb{R}$, $f_{i,0}(t, x, y)$ satisfies (5.23), (5.24), or

$$
f_{i,0}(t, x, y) \begin{cases} > \epsilon, & x > y, \\ < -\epsilon, & x < y, \\ \in [-\epsilon_1, \epsilon_2], & x = y. \end{cases} \tag{5.25}
$$

Suppose that the Fillipov solution for (5.22) exists. For (5.22), $r_i(t) \rightarrow r_0$ as $t \rightarrow \infty$.

Proof: Define $\tilde{r}_i \triangleq r_i - r_0$, $i = 1, \ldots, n$. Note that r_0 is constant. To show that $\tilde{r}_i(t) \rightarrow \mathbf{0}_m$ as $t \rightarrow \infty$, it is equivalent to show that $\max_i |\tilde{r}_{i(k)}(t)| \rightarrow 0$ as $t \rightarrow \infty$ for all $k = 1, \ldots, m$. Consider the nonnegative function $F[t, \tilde{r}_{(k)}] \triangleq \max_i |\tilde{r}_{i(k)}|$, where $\tilde{r}_{(k)} \triangleq [\tilde{r}_{1(k)}, \ldots, \tilde{r}_{n(k)}]^T$. Suppose that $F[t^\star, \tilde{r}_{(k)}(t^\star)] = 0$. It follows that $\tilde{r}_{i(k)}(t^\star) = 0$, $i = 1, \ldots, n$. It can be shown that $\tilde{r}_{i(k)}(t) = 0$ for all $t \geq t^\star$ if $\tilde{r}_{i(k)}(t^\star) = 0$, $i = 1, \ldots, n$. We next focus on studying the case where $F[t, \tilde{r}_{(k)}] \neq 0$.

When $F[t, \tilde{r}_{(k)}] \neq 0$, the upper right-hand derivative of $F[t, \tilde{r}_{(k)}]$ is given by

$$
D^+ F[t, \tilde{r}_{(k)}] = \limsup_{h \rightarrow 0^+} \frac{1}{h} \left[\max_i |\tilde{r}_{i(k)}(t+h)| - \max_i |\tilde{r}_{i(k)}(t)| \right].
$$

We next study $D^+ F[t, \tilde{r}_{(k)}]$ in the following three cases:

Case 1: $\max_i |\tilde{r}_{i(k)}| = \max_i \tilde{r}_{i(k)}$. That is, there exists at least one follower, labeled as agent j, such that $\tilde{r}_{j(k)} > 0$ and $\max_i |\tilde{r}_{i(k)}| = \tilde{r}_{j(k)}$. In this case, it can be computed that $D^+ F[t, \tilde{r}_{(k)}] = \max_{i \in \arg\max_i \tilde{r}_{i(k)}} D^+ \tilde{r}_{i(k)}$. Note that for any agent j satisfying that $\tilde{r}_{j(k)} = \max_i \tilde{r}_{i(k)}$, $\dot{\tilde{r}}_{j(k)}$ becomes negative if $\tilde{r}_{j(k)}$ increases to be greater than $\max_i \tilde{r}_{i(k)}$. Therefore, $\max_i |\tilde{r}_{i(k)}|$ is a nonincreasing function.

Case 2: $\max_i |\tilde{r}_{i(k)}| = -\min_i \tilde{r}_{i(k)}$. That is, there exists at least one follower, labeled as agent h, such that $\tilde{r}_{h(k)} < 0$ and $\max_i |\tilde{r}_{i(k)}| = -\tilde{r}_{h(k)}$. In this case, it can be computed that $D^+ F[t, \tilde{r}_{(k)}] = \max_{i \in \arg\min_i \tilde{r}_{i(k)}} [-D^+ \tilde{r}_{i(k)}]$. Note that for any agent h satisfying that $\tilde{r}_{h(k)} = \min_i \tilde{r}_{i(k)}$, $\dot{\tilde{r}}_{h(k)}$ becomes positive if $\tilde{r}_{h(k)}$ decreases to be smaller than $\max_i |\tilde{r}_{i(k)}|$. Therefore, $\max_i |\tilde{r}_{i(k)}|$ is a nonincreasing function.

Case 3: $\max_i |\tilde{r}_{i(k)}| = \max_i \tilde{r}_{i(k)} = -\min_i \tilde{r}_{i(k)}$. That is, there exist at least one follower, labeled as agent j, such that $\tilde{r}_{j(k)} > 0$ and $\max_i |\tilde{r}_{i(k)}| = \tilde{r}_{j(k)}$ and at least one follower, labeled as agent h, such that $\tilde{r}_{h(k)} < 0$ and $\max_i |\tilde{r}_{i(k)}| = -\tilde{r}_{h(k)}$. In this case, it can be computed that $D^+ F[t, \tilde{r}_{(k)}] = \max_{i \in \arg\max_i \tilde{r}_{i(k)}, j \in \arg\min_j \tilde{r}_{j(k)}} \{D^+ \tilde{r}_{i(k)}, -D^+ \tilde{r}_{j(k)}\}$. By following the analysis in Cases 1 and 2, it follows that $\max_i |\tilde{r}_{i(k)}|$ is a nonincreasing function.

Define $\eta \triangleq \min\{\varsigma, \frac{\epsilon}{\max_i |\tilde{r}_{i(k)}(0)|}\}$, where ϵ and ς are defined in, respectively, (5.23) and (5.24). Because r_0 is constant, it follows that $D^+ r_{0(k)} = 0$. For Case 1, it can be computed that

$$
\begin{aligned}
D^+ F[t, \tilde{r}_{(k)}] &= \max_{i \in \arg\max_i \tilde{r}_{i(k)}} D^+ \tilde{r}_{i(k)} \\
&\leq \max_{i \in \arg\max_i \tilde{r}_{i(k)}} \left\{ -\alpha \sum_{j=0}^{n} a_{ij}(t) \eta [\tilde{r}_{i(k)} - \tilde{r}_{j(k)}] \right\},
\end{aligned}
\tag{5.26}
$$

where we have used the properties of $f_{i,j}(t, x, y)$ in (5.23) and (5.24) and the fact that $\max_i r_{i(k)}$ is a nonincreasing function, $\max_i |\tilde{r}_{i(k)}|$ is a nonincreasing function, $\max_i \tilde{r}_{i(k)} \geq \tilde{r}_{j(k)}$ for all $j = 1, \ldots, n$, and $\tilde{r}_{0(k)} = 0$. For Case 2, it can also be computed that

$$
\begin{aligned}
D^+ F[t, \tilde{r}_{(k)}] &= \max_{i \in \arg\min_i \tilde{r}_{i(k)}} [-D^+ \tilde{r}_{i(k)}] \\
&\leq \max_{i \in \arg\min_i \tilde{r}_{i(k)}} \left\{ \alpha \sum_{j=0}^{n} a_{ij}(t) \eta [\tilde{r}_{i(k)} - \tilde{r}_{j(k)}] \right\}.
\end{aligned}
\tag{5.27}
$$

For Case 3, it can be computed that $D^+ F[t, \tilde{r}_{(k)}]$ satisfies both (5.26) and (5.27).

Consider the closed-loop dynamics given by

$$
\dot{\tilde{\xi}}_i = -\alpha \sum_{j=0}^{n} a_{ij}(t) \eta (\tilde{\xi}_i - \tilde{\xi}_j), \quad i = 1, \ldots, n,
\tag{5.28}
$$

where $\tilde{\xi}_j \in \mathbb{R}$ and $\tilde{\xi}_0 = 0$. Define $G(t, \tilde{\xi}) \triangleq \max_i |\tilde{\xi}_i|$, where $\tilde{\xi} \triangleq [\tilde{\xi}_1, \ldots, \tilde{\xi}_n]^T$. We also study $D^+ G(t, \tilde{\xi})$ in three cases:

Case 1: $\max_i |\tilde{\xi}_i| = \max_i \tilde{\xi}_i$. That is, there exists at least one follower, labeled as agent j, such that $\tilde{\xi}_j > 0$ and $\max_i |\tilde{\xi}_i| = \tilde{\xi}_j$. In this case, it can be computed that

$$
D^+ G(t, \tilde{\xi}) = \max_{i \in \arg\max_i \tilde{\xi}_i} \left[-\alpha \sum_{j=0}^{n} a_{ij}(t) \eta (\tilde{\xi}_i - \tilde{\xi}_j) \right].
$$

Case 2: $\max_i |\tilde{\xi}_i| = -\min_i \tilde{\xi}_i$. That is, there exists at least one follower, labeled as agent h, such that $\tilde{\xi}_h < 0$ and $\max_i |\tilde{\xi}_i| = -\tilde{\xi}_h$. In this case, it can be computed that

$$
D^+ G(t, \tilde{\xi}) = \max_{i \in \arg\min_i \tilde{\xi}_i} \left[\alpha \sum_{j=0}^{n} a_{ij}(t) \eta (\tilde{\xi}_i - \tilde{\xi}_j) \right].
$$

Case 3: $\max_i |\tilde{\xi}_i| = \max_i \tilde{\xi}_i = -\min_i \tilde{\xi}_i$. That is, there exist at least one follower, labeled as agent j, such that $\tilde{\xi}_j > 0$ and $\max_i |\tilde{\xi}_i| = \tilde{\xi}_j$ and at least one follower, labeled as agent h, such that $\tilde{\xi}_h < 0$ and $\max_i |\tilde{\xi}_i| = -\tilde{\xi}_h$. In this case, it can be computed that

$$D^+ G(t, \tilde{\xi}) = \max_{i \in \arg\max_i \tilde{\xi}_i, j \in \arg\min_i \tilde{\xi}_i} \{D^+ \tilde{\xi}_i, -D^+ \tilde{\xi}_j\}.$$

Note that $\tilde{r}_{0(k)} \equiv 0$ and $\tilde{\xi}_0 \equiv 0$. It follows that $D^+ F[t, \tilde{r}_{(k)}] \leq D^+ G[t, \tilde{r}_{(k)}]$. Because $\tilde{r}_{(k)}(0) = \tilde{\xi}(0)$ (i.e., $F[0, \tilde{r}_{(k)}(0)] = G[0, \tilde{r}_{(k)}(0)]$), it then follows from Lemma 5.5 that $F(t) \leq G(t)$ for all $t \geq 0$. Given (5.28), if in $\overline{\mathscr{G}}(t)$ the leader has directed paths to all followers 1 to n, then it follows from Lemma 1.5 that $\tilde{\xi}_i(t) \to \tilde{\xi}_0 \equiv 0$, $i = 1, \ldots, n$, as $t \to \infty$, which implies that $G(t) \to 0$ as $t \to \infty$. Note from the definition of $F(t)$ that $F(t) \geq 0$ for all $t \geq 0$. It then follows from the fact $F(t) \leq G(t)$ that $F(t) \to 0$ as $t \to \infty$. Therefore, we have that $\tilde{r}_{i(k)}(t) \to 0$ as $t \to \infty$. This completes the proof. ∎

Theorem 5.7. *Suppose that the adjacency matrix $\mathscr{A}$ is constant, $\alpha > 0$, and $\beta > \gamma_l$. Using (5.21) for (3.1), all followers will ultimately converge to the dynamic convex hull spanned by the dynamic leaders for arbitrary initial conditions if and only if the directed graph $\mathscr{G}$ has a united directed spanning tree. In particular, $\left\| r_F(t) + (\mathscr{L}_1^{-1} \mathscr{L}_2 \otimes I_m) r_L(t) \right\| \to 0$ as $t \to \infty$, where r_F and r_L are the column stack vectors of, respectively, the followers' and leaders' positions, and $\mathscr{L}_1$ and $\mathscr{L}_2$ are given in (5.5).*

Proof: (Necessity) The necessity proof is similar to that in Theorem 5.1 and hence omitted here.

(Sufficiency) Define $r \triangleq [r_1^T, \ldots, r_n^T]^T$. Using (5.21), (3.1) can be written in a vector form as

$$\dot{r} = -\alpha(\mathscr{L} \otimes I_m) r - \beta \operatorname{sgn}[(\mathscr{L} \otimes I_m) r] + V, \tag{5.29}$$

where $\mathscr{L}$ is given by (5.5) and $V = [\mathbf{0}_m^T, \ldots, \mathbf{0}_m^T, v_{n_f+1}^T, \ldots, v_n^T]^T$. Let $Z \triangleq [z_1^T, \ldots, z_n^T]^T \triangleq (\mathscr{L} \otimes I_m) r$. It follows that

$$\dot{Z} = (\mathscr{L} \otimes I_m) \dot{r} = -\alpha(\mathscr{L} \otimes I_m) Z - \beta(\mathscr{L} \otimes I_m) \operatorname{sgn}(Z) + (\mathscr{L} \otimes I_m) V. \tag{5.30}$$

Because the last n_ℓ rows of $\mathscr{L}$ are equal to zero, we get $z_i \equiv \mathbf{0}_m$, $i = n_f+1, \ldots, n$. We can thus view agents $n_f + 1$ to n as a single agent, labeled as agent 0, whose state is $\mathbf{0}_m$. When $\mathscr{G}$ has a united directed spanning tree, it follows that agent 0 has directed paths to the n_f followers.

Considering the team consisting of agents 0 to n_f, we know that

$$z_0 \equiv \mathbf{0}_m, \tag{5.31}$$

$$\dot{z}_i = -\sum_{j=1}^{n_f} a_{ij}\big\{\alpha(z_i - z_j) + \beta\big[\operatorname{sgn}(z_i) - \operatorname{sgn}(z_j)\big]\big\}$$

$$\qquad - \sum_{j=n_f+1}^{n} a_{ij}\big[\alpha z_i + \beta \operatorname{sgn}(z_i) - v_j\big], \quad i = 1, \ldots, n_f, \tag{5.32}$$

where we have used (5.30) by noting that $z_i(t) \equiv \mathbf{0}_m$, $i = n_f + 1, \ldots, n$. Denote $z_{i(k)}$ and $v_{i(k)}$, $k = 1, \ldots, m$, as the kth component of, respectively, z_i and v_i. Define $g_{ij} \triangleq \alpha[z_{i(k)} - z_{j(k)}] + \beta\{\operatorname{sgn}[z_{i(k)}] - \operatorname{sgn}[z_{j(k)}]\}$. Because $\alpha > 0$ and $\beta > 0$, when $z_{i(k)} > z_{j(k)}$ (respectively, $z_{i(k)} < z_{j(k)}$), it follows that $g_{ij} \geq \alpha[z_{i(k)} - z_{j(k)}]$ (respectively, $g_{ij} \leq \alpha[z_{i(k)} - z_{j(k)}]$), $i = 1, \ldots, n_f$. In addition, when $z_{i(k)} = z_{j(k)}$, $g_{ij} = 0$. Therefore, g_{ij} satisfies (5.24). Define $h_{ij} \triangleq \alpha z_{i(k)} + \beta \operatorname{sgn}[z_{i(k)}] - v_{j(k)}$. Because $\beta > \gamma_l$, when $z_{i(k)} > z_{0(k)} \equiv 0$ (respectively, $z_{i(k)} < z_{0(k)} \equiv 0$), it follows that $h_{ij} > \beta - \gamma_l > 0$ (respectively, $h_{ij} < -(\beta - \gamma_l) < 0$). In addition, when $z_{i(k)} = z_{0(k)} \equiv 0$, it follows that $h_{ij} = -v_{j(k)} \in [-\beta - \gamma_l, \beta + \gamma_l]$. Therefore, h_{ij} satisfies (5.23). Because agent 0 has directed paths to agents 1 to n_f, it follows from Lemma 5.8 that $z_{i(k)}(t) \to z_{0(k)} \equiv 0$, $i = 1, \ldots, n_f$, as $t \to \infty$. Therefore, it follows that $z_i(t) \to \mathbf{0}_m$ as $t \to \infty$. Note that $Z(t) = (\mathscr{L} \otimes I_m)r(t)$. We have $(\mathscr{L} \otimes I_m)r(t) \to 0_{n \times m}$ as $t \to \infty$. It follows from Lemma 5.5 that $\|r_F(t) + (\mathscr{L}_1^{-1}\mathscr{L}_2 \otimes I_p)r_L(t)\| \to 0$ as $t \to \infty$. That is, all followers will ultimately converge to the dynamic convex hull spanned by the dynamic leaders under the condition of the theorem. ∎

Remark 5.8 Unlike the case of stationary leaders, the case of dynamic leaders requires more stringent conditions on the interaction graphs to guarantee dynamic containment control. This is due to the fact that the leaders move with time-varying velocities rather than remain still.

5.3.2 Directed Switching Interaction

In this subsection, we assume that the adjacency matrix $\mathscr{A}(t)$ is constant for $t \in [t_i, t_{i+1})$ and switches at time t_{i+1} as in Sect. 5.2.2. Before moving on, we need the following lemma.

Lemma 5.9 ([47]). *For a team consisting of n followers with the dynamics given by (3.1) and a leader whose position r_0 satisfies $\|\dot{r}_0\| \leq \gamma_l$. Using (4.1) for (3.1), $\|r_i(t) - r_0(t)\| \to 0$ in finite time if $\alpha \geq 0$, $\beta > \gamma_l$, and the leader has directed paths to all followers 1 to n at each time instant.*

Theorem 5.9. *Suppose that $\beta > \gamma_l$. Using (5.21) for (3.1), all followers will ultimately converge to the dynamic minimal hyperrectangle that contains the dynamic leaders and each of whose hyperplanes is normal to one axis of the initial coordinate frame $\mathscr{C}_0$ for arbitrary initial conditions if the directed graph $\mathscr{G}(t)$ has a united directed spanning tree at each time interval $[t_i, t_{i+1})$, $i = 0, 1, \ldots$.*

Proof: Let $r_{i(k)}$ denote the kth, $k = 1, \ldots, m$, component of r_i (i.e., the projection of the position of agent i to the kth axis of the inertial coordinate frame $\mathscr{C}_0$), and $v_{i(k)}$ denote the kth, $k = 1, \ldots, m$, component of v_i, $i \in \mathscr{V}_L$ (i.e., the projection of the velocity of agent i to the kth axis of $\mathscr{C}_0$). Define $r_{L(k)}^+ \triangleq \max_{j \in \mathscr{V}_L} r_{j(k)}$ and $r_{L(k)}^- \triangleq \min_{j \in \mathscr{V}_L} r_{j(k)}$.[6] To prove the theorem, it is equivalent to show that $\lim_{t \to \infty} d[r_{i(k)}(t), \mathscr{S}_k(t)] = 0$, $\forall i \in \mathscr{V}_F$, $\forall k = 1, \ldots, m$, where $\mathscr{S}_k(t) \triangleq [r_L^-(t), r_L^+(t)]$.

Define $r_{(k)} \triangleq [r_{1(k)}, \ldots, r_{n_f(k)}]^T$. Consider the function $F[t, r_{(k)}] \triangleq \max_{i \in \mathscr{V}_F} r_{i(k)} - r_{L(k)}^+$. It can be computed that

$$D^+ F[t, r_{(k)}] = \limsup_{h \to 0^+} \frac{1}{h} \left[F(t + h) - F(t) \right]$$

$$= \limsup_{h \to 0^+} \frac{1}{h} \left[\max_i r_{i(k)}(t + h) - \max_i r_{i(k)}(t) \right]$$

$$- \limsup_{h \to 0^+} \frac{1}{h} \left[r_{L(k)}^+(t + h) - r_{L(k)}^+(t) \right]$$

$$= \max_{i \in \arg \max_{i \in \mathscr{V}_F} r_{i(k)}} D^+ r_{i(k)} - \max_{i \in \arg \max_{i \in \mathscr{V}_L}} D^+ r_{i(k)}.$$

Because $\mathscr{A}(t)$ is constant for $t \in [t_0, t_1)$, it follows that for $t \in [t_0, t_1)$

$$D^+ F[t, r_{(k)}] = \max_{i \in \arg \max_{i \in \mathscr{V}_F} r_{i(k)}} \left(-\alpha \sum_{j \in \mathscr{V}_L \cup \mathscr{V}_F} a_{ij}(t_0)[r_{i(k)} - r_{j(k)}] \right.$$

$$\left. - \beta \operatorname{sgn} \left\{ \sum_{j \in \mathscr{V}_L \cup \mathscr{V}_F} a_{ij}(t_0)[r_{i(k)} - r_{j(k)}] \right\} \right)$$

$$- \max_{i \in \arg \max_{i \in \mathscr{V}_L}} D^+ r_{i(k)}.$$

Consider the closed-loop system given by

$$\dot{\xi}_i = -\alpha \sum_{j \in \mathscr{V}_L \cup \mathscr{V}_F} a_{ij}(t_0)(\xi_i - \xi_j)$$

$$- \beta \operatorname{sgn} \left[\sum_{j \in \mathscr{V}_L \cup \mathscr{V}_F} a_{ij}(t_0)(\xi_i - \xi_j) \right] - \max_{i \in \arg \max_{i \in \mathscr{V}_L}} D^+ r_{i(k)}, \quad i \in \mathscr{V}_F,$$

$$(5.33)$$

for $t \in [t_0, t_1)$, where $\xi_i(t_0) = r_{i(k)}^0(t_0)$, $\forall i \in \mathscr{V}_F$, and $\xi_j(t) \equiv r_{L(k)}^+(t)$, $\forall j \in \mathscr{V}_L$. Define $\xi \triangleq [\xi_1, \ldots, \xi_{n_f}]^T$. Consider the function $G(t, \xi) \triangleq \max_{i \in \mathscr{V}_F} \xi_i - r_{L(k)}^+$.

---

[6] Different from the proof of Lemma 5.6, where $r_{j(k)}, j \in \mathscr{V}_L$, and hence $r_{L(k)}^+$ and $r_{L(k)}^-$ are constant, $r_{j(k)}, j \in \mathscr{V}_L$, and hence $r_{L(k)}^+$ and $r_{L(k)}^-$ here are varying.

For $t \in [t_0, t_1)$, it can be computed that

$$D^+ G(t, \xi) = \max_{i \in \arg\max_{i \in \mathscr{V}_F} \xi_i} \left\{ -\alpha \sum_{j \in \mathscr{V}_L \bigcup \mathscr{V}_F} a_{ij}(t_0)(\xi_i - \xi_j) \right.$$
$$\left. - \beta \operatorname{sgn}\left[\sum_{j \in \mathscr{V}_L \bigcup \mathscr{V}_F} a_{ij}(t_0)(\xi_i - \xi_j) \right] \right\} - \max_{i \in \arg\max_{i \in \mathscr{V}_L}} D^+ r_{i(k)}.$$

Because $r_{j(k)}(t) \leq r_{L(k)}^+(t)$, $\forall j \in \mathscr{V}_L$, by definition, it follows that

$$D^+ F[t, r_{(k)}] \leq D^+ G[t, r_{(k)}]$$

for $t \in [t_0, t_1)$. Because $F(t_0) = G(t_0)$, it then follows from Lemma 5.5 that $F(t) \leq G(t)$ for $[t_0, t_1)$. By following a similar analysis, we can further show that $F(t) \leq G(t)$ for $[t_i, t_{i+1})$, $i = 1, 2, \ldots$, which implies that $F(t) \leq G(t)$ for all $t \geq t_0$.

Because in (5.33) all agents $n_f + 1$ to n have the same state $r_{L(k)}^+$, those agents can be viewed as a single agent, labeled as agent 0, whose state is $r_{L(k)}^+$. For simplicity, we also use $\widetilde{\mathscr{G}}_i$, $i = 1, \ldots$, to denote the directed graphs associated with agents 0 to n_f. From Sect. 1.2 and Definition 5.2, if $\mathscr{G}(t)$ has a united directed spanning tree, then $\widetilde{\mathscr{G}}_i(t)$ has a directed spanning tree (accordingly, agent 0 has directed paths to all followers 1 to n_f). It then follows from Lemma 5.9 that $|\xi_i(t) - r_{L(k)}^+(t)| \to 0$ as $t \to \infty$ under the condition of the theorem. That is, $G(t) \to 0$ as $t \to \infty$. Combining with the fact that $F(t) \leq G(t)$ shows that $\limsup_{t \to \infty} F(t) \leq 0$, which implies that $\limsup_{t \to \infty} [\max_{i \in \mathscr{V}_F} r_{i(k)}(t) - r_{L(k)}^+(t)] \leq 0$.

Similarly, it can be shown that $\liminf_{t \to \infty} [\min_{i \in \mathscr{V}_F} r_{i(k)}(t) - r_{L(k)}^-(t)] \geq 0$.
Combining the previous arguments completes the proof. ∎

Remark 5.10 In the case of dynamic leaders under a switching interaction graph, all followers might not converge to the dynamic convex hull spanned by the dynamic leaders ultimately except for the one-dimensional case because the closed-loop system depends on the choice of the inertial coordinate frame, which is different from Sect. 5.2.2. To illustrate, we present the following example. Consider a team consisting of four leaders and one follower where the leaders have the same velocity. The interaction graph switches from $\mathscr{G}_{(1)}$ to $\mathscr{G}_{(2)}$ as shown in Fig. 5.7 every 0.4 seconds and the process repeats. The simulation result using (5.21) in the two-dimensional space is given in Fig. 5.8. It can be seen that even if the follower is originally within the dynamic convex hull spanned by the dynamic leaders, it cannot always stay in the dynamic convex hull although the interaction graph has a united directed spanning tree at each time interval. Instead, the follower will ultimately converge to the minimal rectangle that contains the dynamic leaders and each of whose edges is normal to one axis of $\mathscr{C}_0$.
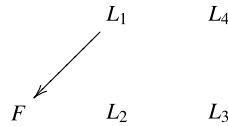
(a) $\mathscr{G}_{(1)}$
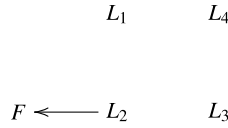
(b) $\mathscr{G}_{(2)}$

Fig. 5.7 Directed switching graphs $\mathscr{G}_{(1)}$ and $\mathscr{G}_{(2)}$ for a team consisting of four leaders and one follower. Here $L_i, i = 1, \ldots, 4$, denote the leaders while F denotes the follower
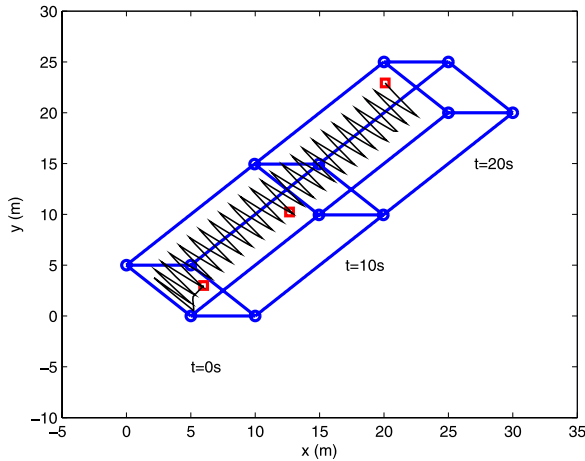
Fig. 5.8 The trajectories of the agents using (5.21) with $\mathscr{G}(t)$ switching from $\{\mathscr{G}_{(1)}, \mathscr{G}_{(2)}\}$ as shown in Fig. 5.7. The *red square* represents the position of the follower and the *blue circles* represent the positions of the four leaders at some snapshots

Remark 5.11 Given $\nu \in \mathbb{R}^m$, $\mathrm{sgn}(\nu)$ in (5.21) is the signum function defined componentwise. The function $\mathrm{sgn}(\nu)$ in (5.21) can also be redefined as[7]

$$\mathrm{sgn}(\nu) = \begin{cases} \mathbf{0}_m, & \nu = \mathbf{0}_m, \\ \frac{\nu}{\|\nu\|}, & \text{otherwise.} \end{cases} \tag{5.34}$$

Under this definition, the closed-loop system of (3.1) using (5.21) is independent of the choice of the inertial coordinate frame. However, all followers might still not

---

[7] In a one-dimensional space, $\mathrm{sgn}(\nu)$ becomes the standard signum function.
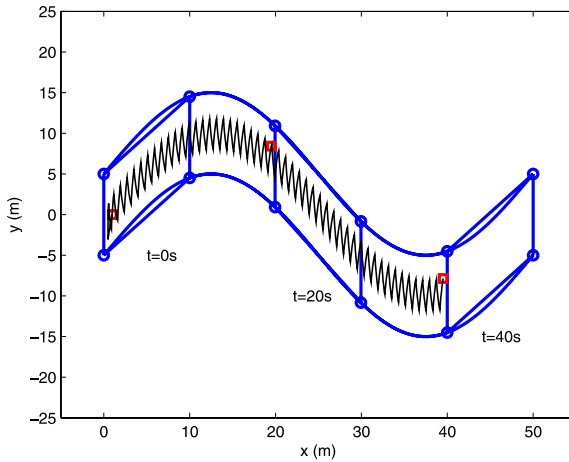
Fig. 5.9 The trajectories of the agents using (5.21) with sgn($\cdot$) defined in (5.34) and $\mathscr{G}(t)$ switching from $\{\mathscr{G}_{(1)}, \mathscr{G}_{(2)}\}$ as shown in Fig. 5.7. The *red square* represents the position of the follower and the *blue circles* represent the positions of the four leaders at some snapshots

converge to the dynamic convex hull spanned by the dynamic leaders ultimately. Similar to the example in Remark 5.10, we consider the team consisting of four leaders and one follower where the leaders have the same velocity and let the interaction graph switch according to the same pattern as in Remark 5.10. The simulation result is given in Fig. 5.9. It can be noted that the follower cannot always stay in the dynamic convex hull spanned by the dynamic leaders even if the follower is initially within the dynamic convex hull.[8]

Remark 5.12 For distributed containment control with multiple dynamic leaders under a switching interaction graph, it might be very difficult to find distributed tracking control algorithms without velocity measurements to guarantee that all followers will ultimately converge to the dynamic convex hull spanned by the dynamic leaders in a high-dimensional space under such a mild connectivity condition that the interaction graph has a united directed spanning tree at each time interval. In a one-dimensional space, the degree of freedom of the dynamic leaders is 1 and only the minimum and maximum states of the dynamic leaders are required to determine the dynamic convex hull spanned by the dynamic leaders. Therefore, the signum function can be used to drive all followers to the dynamic convex hull spanned by the dynamic leaders under the mild connectivity condition. However, in a high-dimensional space, the degree of freedom of the dynamic leaders is larger than 1. The dynamic convex hull spanned by the dynamic leaders might depend on a number of leaders' states in each dimension (instead of only the minimum and maximum states of the dynamic leaders in a one-dimensional space). Therefore,

---

[8] In this case, the followers might not even converge to the minimal hyperrectangle that contains the dynamic leaders and each of whose hyperplanes is normal to one axis of $\mathscr{C}_0$.

the signum function, in general, does not have the capability to drive all followers to the dynamic convex hull spanned by the dynamic leaders in a high-dimensional space under the mild connectivity condition. Similarly, without velocity measurements, the basic linear distributed control algorithms do not have such capability either. Therefore, more information (e.g., velocity measurements, graph switching sequence, etc.) might be needed in order to guarantee distributed containment control in the presence of multiple dynamic leaders under the mild connectivity condition in a high-dimensional space or a stronger connectivity condition might be required.

5.3.3 Simulation

In this section, we present a simulation result to validate the theoretical result in Sect. 5.3.1. We consider a team with four leaders and six followers in the two-dimensional space. The directed fixed graph $\mathscr{G}$ is chosen as Fig. 5.5(a). Figure 5.10 shows the trajectories of the agents using (5.21) for (3.1). It can be noted that all followers ultimately converge to the dynamic convex hull spanned by the dynamic leaders.

5.4 Containment Control with Swarming Behavior

In this section, we study containment control with swarming behavior, namely, cohesion (and hence connectivity maintenance) and dispersion (and hence collision avoidance).
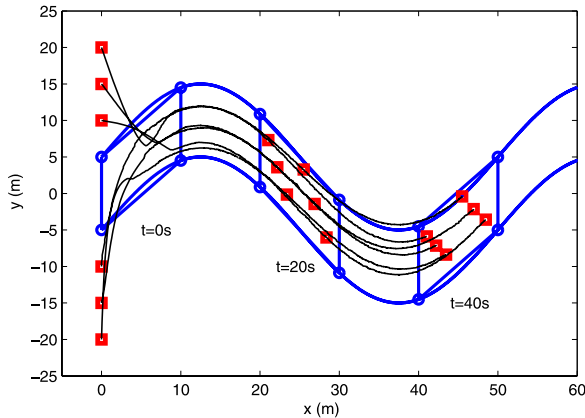
Fig. 5.10 Trajectories of the agents using (5.21) with $\mathscr{G}$ shown in Fig. 5.5(a). *Circles* denote the positions of the dynamic leaders while the *squares* denote the positions of the followers at some snapshots

We assume that all leaders and followers are equipped with transceivers. Let r_L be the transmitting radius of the leaders. Then the transmitting range of leader i is denoted by

$$S_i \triangleq \{y \in \mathbb{R}^m | \|y - r_i\| < r_L\}, \quad i \in \mathcal{V}_L.$$

Let $r_F \leq r_L$ be the transmitting radius of the followers. Then the transmitting range of follower i is denoted by

$$S_i \triangleq \{y \in \mathbb{R}^m | \|y - r_i\| < r_F\}, \quad i \in \mathcal{V}_F.$$

If agent j is in the transmitting range of agent i, it is denoted by $r_j \in S_i$. Then, a directed graph $\mathcal{G} \triangleq (\mathcal{V}_L \cup \mathcal{V}_F, \mathcal{E})$ is used to characterize the interaction among all agents, where $\mathcal{E} \triangleq \{(i, j)|j \neq i, r_j \in S_i\}$. Define the set of neighbors of agent i in the graph $\mathcal{G}$ as $\mathcal{N}_i \triangleq \{j \in \mathcal{V}_L \cup \mathcal{V}_F|(j, i) \in \mathcal{E}\}$. Define $\mathcal{N}_i^L \triangleq \mathcal{N}_i \cap \mathcal{V}_L$, that is, the set of all leaders who are neighbors of agent i, and $\mathcal{N}_i^F \triangleq \mathcal{N}_i \cap \mathcal{V}_F$, that is, the set of all followers who are neighbors of agent i. Analogously, a subgraph $\mathcal{G}_F \triangleq (\mathcal{V}_F, \mathcal{E}_F)$ is used to characterize the interaction among the followers. Note that here $\mathcal{G}_F$ is undirected. Let $0 < d_1 \leq r_F$ be the cohesive distance. Define a subgraph $\mathcal{G}_{FC} \triangleq (\mathcal{V}_F, \mathcal{E}_{FC})$, where $\mathcal{E}_{FC} \triangleq \{(i, j)|j \neq i, \|r_i - r_j\| < d_1, i, j \in \mathcal{V}_F\}$. Note that $\mathcal{G}_{FC} \subseteq \mathcal{G}_F$. Also define $\mathcal{N}_{FC_i} \triangleq \{j \in \mathcal{V}_F|(j, i) \in \mathcal{E}_{FC}\}$.

The main purpose of this section is to design control inputs for the followers such that

- All followers are driven toward the convex hull spanned by the leaders. That is, $\limsup_{t \to \infty} d[r_i(t), \Omega(t)], \forall i \in \mathcal{V}_F$, is bounded, where $\Omega \triangleq \text{Co}(r_j, j \in \mathcal{V}_L)$ is the convex hull spanned by the leaders.
- If initially follower i is within the transmitting range of leader j, then it will be within the transmitting range of the leader for all $t \geq 0$. That is, if $\|r_i(0) - r_j(0)\| < r_L$ for some $i \in \mathcal{V}_F$ and $j \in \mathcal{V}_L$, then $\|r_i(t) - r_j(t)\| < r_L$ for all $t \geq 0$.
- The followers move cohesively like a swarm while preserving connectivity. That is, if $\|r_i(0) - r_j(0)\| < d_1$ for some $i, j \in \mathcal{V}_F$, then $\|r_i(t) - r_j(t)\| < d_1$ for all $t \geq 0$.
- Group dispersion (and hence collision avoidance) is maintained. That is, if $\|r_i(0) - r_j(0)\| > d_2$, where $0 < d_2 < d_1$, for all $i, j \in \mathcal{V}_L \cup \mathcal{V}_F$ and $i \neq j$, then $\|r_i(t) - r_j(t)\| > d_2$ for all $t \geq 0$.

5.4.1 Algorithm Design

To drive all followers towards the convex hull spanned by the leaders, define a potential function

$$V_{i1} \triangleq \frac{1}{2} \left\{ \sum_{k \in \mathcal{N}_i^L(t)} b_{ik} \|r_i - r_k\|^2 + \sum_{k \in [\mathcal{V}_L \setminus \mathcal{N}_i(t)]} b_{ik} r_L^2 \right\}, \quad i \in \mathcal{V}_F,$$

where $b_{ik} > 0$. Note that V_{i1} is not differentiable at $\|r_i - r_k\| = r_L$ for $i \in \mathcal{V}_F$ and $k \in \mathcal{V}_L$, but it is regular. In the remainder of this chapter, the stability analysis is conducted for the Filippov solutions of the closed-loop systems using the proposed algorithms via the nonsmooth analysis in Sect. 1.5. Accordingly, Remarks 4.1 and 4.3 also apply here.

To keep group cohesion and hence connectivity between the followers, define a potential function

$$V_{i2} \triangleq \sum_{j \in \mathcal{N}_{FC_i}(0)} h_{ij} s_{ij}(d_{ij}), \quad i \in \mathcal{V}_F,$$

where $s_{ij}(d_{ij}) \triangleq \frac{1}{\frac{1}{2}d_1^2 - d_{ij}}$, $d_{ij} \triangleq \frac{1}{2}\|r_i - r_j\|^2$, and $h_{ij} = h_{ji} > 0$ for all $i, j \in \mathcal{V}_F$. It is straightforward to verify that $s_{ij} > 0$ when $\|r_i - r_j\| < d_1$ and $s_{ij} = \infty$ when $\|r_i - r_j\| = d_1$. It can be shown that $\frac{\partial s_{ij}}{\partial d_{ij}} = (\frac{1}{2}d_1^2 - d_{ij})^{-2} > 0$ when $\|r_i - r_j\| < d_1$. Therefore, the decrease of d_{ij} will lead to the decrease of s_{ij}. That is, V_{i2} is an attractive function.[9]

In addition, to preserve the connectivity between the leaders and the followers, define a potential function

$$V_{i3} \triangleq \sum_{k \in \mathcal{N}_i^L(0)} h_{ik} q_{ik}(d_{ik}), \quad i \in \mathcal{V}_F,$$

where $q_{ik}(d_{ik}) \triangleq \frac{1}{\frac{1}{2}r_L^2 - d_{ik}}$, $d_{ik} \triangleq \frac{1}{2}\|r_i - r_k\|^2$, and $h_{ik} > 0$ for $i \in \mathcal{V}_F$ and $k \in \mathcal{V}_L$. The function q_{ik} is of a similar form to that of s_{ij} except that d_1 is replaced with r_L.

Remark 5.13 Later, it will be shown that using the proposed algorithms $\mathcal{N}_{FC_i}(0) \subseteq \mathcal{N}_{FC_i}(t)$ and $\mathcal{N}_i^L(0) \subseteq \mathcal{N}_i^L(t)$, for all $t \geq 0$.

To achieve group dispersion and hence collision avoidance, define a potential function

$$V_{i4} \triangleq \sum_{j \neq i} \frac{c_{ij}}{r_{ij}(d_{ij})}, \quad i \in \mathcal{V}_F,$$

where $c_{ij} = c_{ji} > 0$, and

$$r_{ij}(d_{ij}) \triangleq \begin{cases} a_1(d_{ij} - \frac{1}{2}d_2^2) + a_2(d_{ij} - \frac{1}{2}d_2^2)^2, & d_{ij} < \frac{1}{2}r_F^2, \\ a_1(\frac{1}{2}r_F^2 - \frac{1}{2}d_2^2) + a_2(\frac{1}{2}r_F^2 - \frac{1}{2}d_2^2)^2, & d_{ij} \geq \frac{1}{2}r_F^2, \end{cases} \quad (5.35)$$

---

[9] Similar functions have been used in [279].

for all $i, j \in \mathscr{V}_L \cup \mathscr{V}_F$ and $i \neq j$. Here $a_2 < 0$ and $a_1 \triangleq a_2(d_2^2 - r_F^2)$. It is straightforward to verify that $r_{ij}(d_{ij}) > 0$ when $\|r_i - r_j\| > d_2$, $r_{ij}(d_{ij}) = 0$ when $\|r_i - r_j\| = d_2$, and

$$\frac{\partial r_{ij}}{\partial d_{ij}} = \begin{cases} a_1 + 2a_2(d_{ij} - \frac{1}{2}d_2^2), & \|r_i - r_j\| < r_F, \\ 0, & \|r_i - r_j\| \geq r_F. \end{cases}$$

Therefore, V_{i4} is a repulsive potential function and the partial derivative of V_{i4} is spatially distributed. Define

$$V \triangleq V_1 + V_2, \tag{5.36}$$

where $V_1 \triangleq \sum_{i \in \mathscr{V}_F} V_{i1}$ and $V_2 \triangleq \frac{1}{2} \sum_{i \in \mathscr{V}_F} V_{i2} + \sum_{i \in \mathscr{V}_F} V_{i3} + \frac{1}{2} \sum_{i=1}^{n} V_{i4}$.

5.4.2 Analysis for Multiple Stationary Leaders

In this subsection, it is assumed that the leaders are stationary. For the n agents with single-integrator dynamics given by (3.1), we let

$$u_i = 0, \quad i \in \mathscr{V}_L, \tag{5.37a}$$

$$u_i = -\sum_{k \in \mathscr{N}_i^L(t)} b_{ik}(r_i - r_k) - \frac{\partial V_2}{\partial r_i}, \quad i \in \mathscr{V}_F. \tag{5.37b}$$

Then (5.36) and (5.37b) yield

$$u_i = -\sum_{k \in \mathscr{N}_i^L(t)} b_{ik}(r_i - r_k) - \sum_{j \in \mathscr{N}_{FC_i}(0)} h_{ij} \frac{\partial s_{ij}}{\partial d_{ij}}(r_i - r_j)$$

$$- \sum_{k \in \mathscr{N}_i^L(0)} h_{ik} \frac{\partial q_{ik}}{\partial d_{ik}}(r_i - r_k) + \sum_{j \neq i} c_{ij} r_{ij}^{-2} \frac{\partial r_{ij}}{\partial d_{ij}}(r_i - r_j), \quad i \in \mathscr{V}_F.$$

Because $\frac{\partial r_{ij}}{\partial d_{ij}} = 0$, $\forall \|r_i - r_j\| \geq r_F$, it follows that

$$u_i = -\sum_{k \in \mathscr{N}_i^L(t)} b_{ik}(r_i - r_k) - \sum_{j \in \mathscr{N}_{FC_i}(0)} h_{ij} \frac{\partial s_{ij}}{\partial d_{ij}}(r_i - r_j)$$

$$- \sum_{k \in \mathscr{N}_i^L(0)} h_{ik} \frac{\partial q_{ik}}{\partial d_{ik}}(r_i - r_k)$$

$$+ \sum_{j \in \mathscr{N}_i(t)} c_{ij} r_{ij}^{-2} \frac{\partial r_{ij}}{\partial d_{ij}}(r_i - r_j), \quad i \in \mathscr{V}_F. \tag{5.38}$$

Therefore, the algorithm defined by (5.37b) and equivalently (5.38) is spatially distributed.

Theorem 5.14. *Using* (5.37) *for* (3.1)*, suppose that* $\|r_i(0) - r_j(0)\| > d_2$ *for all* $i, j \in \mathscr{V}_L \cup \mathscr{V}_F$ *and* $i \neq j$*. Then*

1. *For all* $t \geq 0$*,* $\|r_i(t) - r_j(t)\| < d_1$ *for all* $i \in \mathscr{V}_F$ *and* $j \in \mathscr{N}_{FC_i}(0)$ *[equivalently,* $\mathscr{N}_{FC_i}(0) \subseteq \mathscr{N}_{FC_i}(t)$ *for all* $i \in \mathscr{V}_F$*],* $\|r_i(t) - r_j(t)\| < r_L$ *for all* $i \in \mathscr{V}_F$ *and* $j \in \mathscr{N}_i^L(0)$ *[equivalently,* $\mathscr{N}_i^L(0) \subseteq \mathscr{N}_i^L(t)$ *for all* $i \in \mathscr{V}_F$*], and* $\|r_i(t) - r_j(t)\| > d_2$ *for all* $i, j \in \mathscr{V}_L \cup \mathscr{V}_F$ *and* $i \neq j$*.*
2. *For all* $i \in \mathscr{V}_F$*, the control input* u_i *is bounded.*
3. *If in the graph* $\mathscr{G}_I(0) \triangleq [\mathscr{V}_L \cup \mathscr{V}_F, \mathscr{E}_I(0)]$*, where* $\mathscr{E}_I(0) \triangleq [\mathscr{E}(0) \backslash \mathscr{E}_F(0)] \cup \mathscr{E}_{FC}(0)$*, for each follower, there exists at least one leader that has a directed path to the follower, then* $\limsup_{t \to \infty} d[r_i(t), \Omega(t)], \forall i \in \mathscr{V}_F$*, is bounded.*

Proof: Consider the Lyapunov function candidate V defined by (5.36). Because $\|r_i(0) - r_j(0)\| > d_2$ for all $i, j \in \mathscr{V}_F \cup \mathscr{V}_L$ and $i \neq j$, it follows from the definition of V in (5.36) that $V(0) < \infty$. Define $r \triangleq [r_1, \ldots, r_n]^T$ and $u \triangleq [u_1, \ldots, u_n]^T$. Using (5.37) for (3.1), it follows that

$$
\begin{aligned}
\widetilde{L}_F V &= \bigcap_{\xi \in \partial V(r)} \xi^T K[u] \\
&= \sum_{i \in \mathscr{V}_L} \bigcap_{\xi_i \in \partial V(r_i)} K[\xi_i^T \dot{r}_i] + \sum_{i \in \mathscr{V}_F} \bigcap_{\xi_i \in \partial V(r_i)} K \Bigg[\xi_i^T \Bigg[- \sum_{k \in \mathscr{N}_i^L(t)} b_{ik}(r_i - r_k) \\
&\quad - \sum_{j \in \mathscr{N}_{FC_i}(0)} h_{ij} \frac{\partial s_{ij}}{\partial d_{ij}}(r_i - r_j) \\
&\quad - \sum_{k \in \mathscr{N}_i^L(0)} h_{ik} \frac{\partial q_{ik}}{\partial d_{ik}}(r_i - r_k) + \sum_{j \in \mathscr{N}_i(t)} c_{ij} r_{ij}^{-2} \frac{\partial r_{ij}}{\partial d_{ij}}(r_i - r_j) \Bigg] \Bigg] \\
&= \sum_{i \in \mathscr{V}_F} \bigcap_{\xi_i \in \partial V(r_i)} K \Bigg[\xi_i^T \Bigg[- \sum_{k \in \mathscr{N}_i^L(t)} b_{ik}(r_i - r_k) \\
&\quad - \sum_{j \in \mathscr{N}_{FC_i}(0)} h_{ij} \frac{\partial s_{ij}}{\partial d_{ij}}(r_i - r_j) \\
&\quad - \sum_{k \in \mathscr{N}_i^L(0)} h_{ik} \frac{\partial q_{ik}}{\partial d_{ik}}(r_i - r_k) + \sum_{j \in \mathscr{N}_i(t)} c_{ij} r_{ij}^{-2} \frac{\partial r_{ij}}{\partial d_{ij}}(r_i - r_j) \Bigg] \Bigg],
\end{aligned}
$$

where $\partial V(r)$ is the generalized gradient of V at r, $\partial V(r_i)$ is the generalized gradient of V at r_i, and we have used the fact that $K[x(t)f(t)] = x(t)K[f(t)]$ for any continuous function $x(t)$ to derive the second equality and the fact that $\dot{r}_i = 0, \forall i \in \mathscr{V}_L$, to derive the last equality. By following a similar analysis to that in the proof of Theorem 4.4, we have $\max \widetilde{L}_F V \leq 0$. It thus follows from Lemma 1.39 that

$$V(t) \leq V(0) < \infty, \quad \forall t \geq 0. \tag{5.39}$$

Suppose that at time t_1, $\|r_i(t_1) - r_j(t_1)\| \leq d_2$ for some $i, j \in \mathscr{V}_L \cup \mathscr{V}_F$ and $i \neq j$. Because the agents move continuously, there must exist a time $t_2 \leq t_1$ such that $\|r_i(t_2) - r_j(t_2)\| = d_2$, which implies that $V_{i4}(t_2) = \infty$. Therefore, it follows that $V(t_2) = \infty$, which contradicts (5.39). Similarly, we can prove the other parts of the first statement.

Note from (5.38) that

$$\|u_i\| \leq \sum_{k \in \mathscr{N}_i^L(t)} b_{ik}\|r_i - r_k\| + \sum_{j \in \mathscr{N}_{FC_i}(0)} h_{ij}\left(\frac{1}{2}d_1^2 - d_{ij}\right)^{-2}\|r_i - r_j\|$$

$$+ \sum_{k \in \mathscr{N}_i^L(0)} h_{ik}\left(\frac{1}{2}r_L^2 - d_{ik}\right)^{-2}\|r_i - r_k\|$$

$$+ \sum_{j \in \mathscr{N}_i(t)} c_{ij}r_{ij}^{-2}\left|a_1 + 2a_2\left(d_{ij} - \frac{1}{2}d_2^2\right)\right|\|r_i - r_j\|.$$

Therefore, the second statement follows from the first statement.

Because $\mathscr{N}_{FC_i}(0) \subseteq \mathscr{N}_{FC_i}(t)$ and $\mathscr{N}_i^L(0) \subseteq \mathscr{N}_i^L(t)$ for all $i \in \mathscr{V}_F$ and $t \geq 0$, and in $\mathscr{G}_I(0)$, for each follower, there exists at least one leader that has a directed path to the follower, it follows that in $\mathscr{G}_I(t)$, for each follower, there exists at least one leader that has a directed path to the follower. The third statement follows directly. ∎

5.4.3 Analysis for Multiple Dynamic Leaders

In this subsection, it is assumed that the leaders are dynamic. For the n agents with single-integrator dynamics given by (3.1), we let

$$u_i = v_i, \quad i \in \mathscr{V}_L, \tag{5.40a}$$

$$u_i = -\sum_{k \in \mathscr{N}_i^L(t)} b_{ik}(r_i - r_k) - \frac{\partial V_2}{\partial r_i}, \quad i \in \mathscr{V}_F, \tag{5.40b}$$

where v_i, $i \in \mathscr{V}_L$, denotes the velocity of leader i. It is assumed that $\|v_i\| \leq \gamma_\ell$, $\forall i \in \mathscr{V}_L$, where γ_ℓ is a positive constant. The first result in this subsection is stated below.

Theorem 5.15. *Using* (5.40) *for* (3.1)*, if the conditions of Theorem* 5.14 *hold and*

$$\|v_k\| \leq \frac{\sum_{i \in \mathscr{N}_k^F(t)} \frac{1}{|\mathscr{N}_i^L(t)|}\|\sum_{k \in \mathscr{N}_i^L(t)} b_{ik}(r_i - r_k) + \frac{\partial V_2}{\partial r_i}\|^2}{\|-\sum_{k \in \mathscr{N}_i^L(t)} b_{ik}(r_i - r_k) + \frac{\partial V_2}{\partial r_k}\|}, \tag{5.41}$$

for all $k \in \mathscr{V}_L$*, then all statements of Theorem* 5.14 *hold.*

Proof: Consider the Lyapunov function candidate V defined by (5.36). Note from (5.41) that

$$\left\| - \sum_{k \in \mathcal{N}_i^L(t)} b_{ik}(r_i - r_k) + \frac{\partial V_2}{\partial r_k} \right\| \|\dot{r}_k\|$$

$$\leq \sum_{i \in \mathcal{N}_k^F(t)} \frac{1}{|\mathcal{N}_i^L(t)|} \left\| \sum_{k \in \mathcal{N}_i^L(t)} b_{ik}(r_i - r_k) + \frac{\partial V_2}{\partial r_i} \right\|^2, \quad k \in \mathcal{V}_L.$$

Define $r \triangleq [r_1, \ldots, r_n]^T$ and $u \triangleq [u_1, \ldots, u_n]^T$. Using (5.40) for (3.1), it follows that

$$\widetilde{L}_F V = \bigcap_{\xi \in \partial V(r)} \xi^T K[u]$$

$$= \sum_{i \in \mathcal{V}_L} \bigcap_{\xi_i \in \partial V(r_i)} K[\xi_i^T \dot{r}_i]$$

$$+ \sum_{i \in \mathcal{V}_F} \bigcap_{\xi_i \in \partial V(r_i)} K\left[\xi_i^T \left[- \sum_{k \in \mathcal{N}_i^L(t)} b_{ik}(r_i - r_k) - \frac{\partial V_2}{\partial r_i} \right] \right],$$

where $\partial V(r)$ is the generalized gradient of V at r, $\partial V(r_i)$ is the generalized gradient of V at r_i, and we have used the fact that $K[x(t)f(t)] = x(t)K[f(t)]$ for any continuous function $x(t)$ to derive the second equality. By following a similar analysis to that in the proof of Theorem 4.4, we have $\max \widetilde{L}_F V \leq 0$. The rest of the proof is similar to that of Theorem 5.14 and is hence omitted here. ∎

Next, it will be shown that Condition (5.41) can be relaxed by using a control law given as

$$u_i = v_i, \quad i \in \mathcal{V}_L, \tag{5.42a}$$

$$u_i = -\left[\sum_{k \in \mathcal{N}_i^L(t)} b_{ik}(r_i - r_k) + \frac{\partial V_2}{\partial r_i} \right]$$

$$- \beta \operatorname{sgn}\left[\sum_{k \in \mathcal{N}_i^L(t)} b_{ik}(r_i - r_k) + \frac{\partial V_2}{\partial r_i} \right], \quad i \in \mathcal{V}_F, \tag{5.42b}$$

where $\operatorname{sgn}(\cdot)$ is the signum function defined componentwise.

Theorem 5.16. *Using (5.42) for (3.1), if the conditions of Theorem 5.14 hold and* $\beta \geq \gamma_\ell$, *then all statements of Theorem 5.14 hold.*

Proof: Consider the Lyapunov function candidate V defined by (5.36). Let V_{ij} be the sum of the coupling terms between r_i and r_j in V_2. Then it follows that

$$\sum_{i \in \mathscr{V}_F} \left[\sum_{k \in \mathscr{N}_i^L(t)} b_{ik}(r_i - r_k) + \frac{\partial V_2}{\partial r_i} \right]$$

$$= \sum_{i \in \mathscr{V}_F} \left[\sum_{k \in \mathscr{N}_i^L(t)} b_{ik}(r_i - r_k) + \sum_{j \in \mathscr{V}_L \cup \mathscr{V}_F} \frac{\partial V_{ij}}{\partial r_i} \right]$$

$$= \sum_{i \in \mathscr{V}_F} \sum_{k \in \mathscr{N}_i^L(t)} b_{ik}(r_i - r_k) + \sum_{i \in \mathscr{V}_F} \sum_{j \in \mathscr{V}_F} \frac{\partial V_{ij}}{\partial r_i} + \sum_{i \in \mathscr{V}_F} \sum_{j \in \mathscr{V}_L} \frac{\partial V_{ij}}{\partial r_i}.$$

It is straightforward to verify that $\sum_{i \in \mathscr{V}_F} \sum_{j \in \mathscr{V}_F} \frac{\partial V_{ij}}{\partial r_i} = 0$, which yields

$$\sum_{i \in \mathscr{V}_F} \left[\sum_{k \in \mathscr{N}_i^L(t)} b_{ik}(r_i - r_k) + \frac{\partial V_2}{\partial r_i} \right]$$

$$= \sum_{i \in \mathscr{V}_F} \sum_{k \in \mathscr{N}_i^L(t)} b_{ik}(r_i - r_k) + \sum_{i \in \mathscr{V}_F} \sum_{j \in \mathscr{V}_L} \frac{\partial V_{ij}}{\partial r_i}$$

$$= \sum_{i \in \mathscr{V}_F} \sum_{k \in \mathscr{N}_i^L(t)} b_{ik}(r_i - r_k) - \sum_{i \in \mathscr{V}_F} \sum_{j \in \mathscr{V}_L} \frac{\partial V_{ij}}{\partial r_j}$$

$$= \sum_{i \in \mathscr{V}_F} \sum_{k \in \mathscr{N}_i^L(t)} b_{ik}(r_i - r_k) - \sum_{j \in \mathscr{V}_L} \frac{\partial V_2}{\partial r_j}. \qquad (5.43)$$

Define $r \triangleq [r_1, \ldots, r_n]^T$ and $u \triangleq [u_1, \ldots, u_n]^T$. Using (5.43), it follows that

$$\widetilde{L}_F V = \bigcap_{\xi \in \partial V(r)} \xi^T K[u]$$

$$= \sum_{i \in \mathscr{V}_L} \bigcap_{\xi_i \in \partial V(r_i)} K\left[\xi_i^T \dot{r}_i \right]$$

$$+ \sum_{i \in \mathscr{V}_F} \bigcap_{\xi_i \in \partial V(r_i)} K\left[\xi_i^T \left\{ -\left[\sum_{k \in \mathscr{N}_i^L(t)} b_{ik}(r_i - r_k) + \frac{\partial V_2}{\partial r_i} \right] \right. \right.$$

$$\left. \left. - \beta \operatorname{sgn}\left[\sum_{k \in \mathscr{N}_i^L(t)} b_{ik}(r_i - r_k) + \frac{\partial V_2}{\partial r_i} \right] \right\} \right],$$

where $\partial V(r)$ and $\partial V(r_i)$ are defined as in the proof of Theorem 5.15 and we have used the fact that $K[x(t)f(t)] = x(t)K[f(t)]$ for any continuous function $x(t)$ to derive the second equality. By following a similar analysis to that in the proof of Theorem 4.4 and using (5.43), we have

(a) $t = 0$ s

(b) $t = 0.025$ s

(c) $t = 0.05$ s

(d) $t = 10$ s
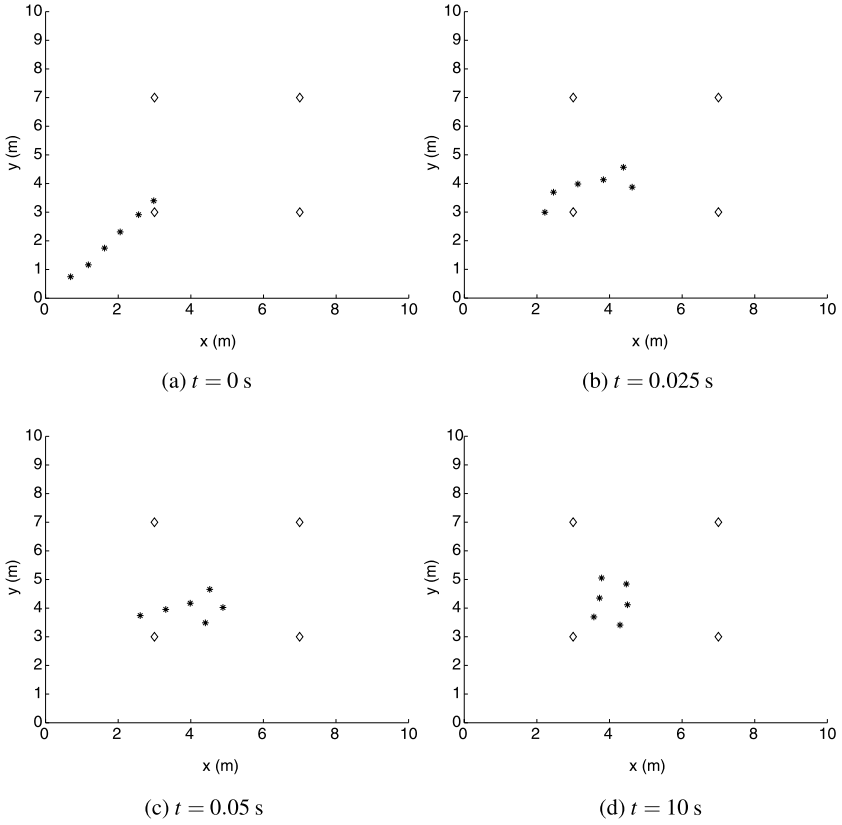
Fig. 5.11 Containment control with swarming behavior in the case of stationary leaders in the two-dimensional space. The leaders are denoted by "$\diamond$", while the followers are represented by "$*$". The parameters are specified as follows: $r_L = 5$, $r_F = 1$, $d_1 = 0.8$, $d_2 = 0.4$, $a_2 = -1$, and $a_1 = a_2(d_2^2 - r_F^2)$

$$
\max \widetilde{L}_F V \leq \max K \left[\gamma_\ell \left\| \sum_{i \in \mathscr{V}_F} \left[\sum_{k \in \mathscr{N}_i^L(t)} b_{ik}(r_i - r_k) + \frac{\partial V_2}{\partial r_i} \right] \right\| \right.
$$

$$
- \sum_{i \in \mathscr{V}_F} \left\| \sum_{k \in \mathscr{N}_i^L(t)} b_{ik}(r_i - r_k) + \frac{\partial V_2}{\partial r_i} \right\|^2
$$

$$
\left. - \beta \left\| \sum_{i \in \mathscr{V}_F} \left[\sum_{k \in \mathscr{N}_i^L(t)} b_{ik}(r_i - r_k) + \frac{\partial V_2}{\partial r_i} \right] \right\| \right].
$$

If $\beta \geq \gamma_\ell$, then $\max \widetilde{L}_F V \leq 0$. The rest of the proof is similar to that of Theorem 5.14 and is hence omitted here.   ∎
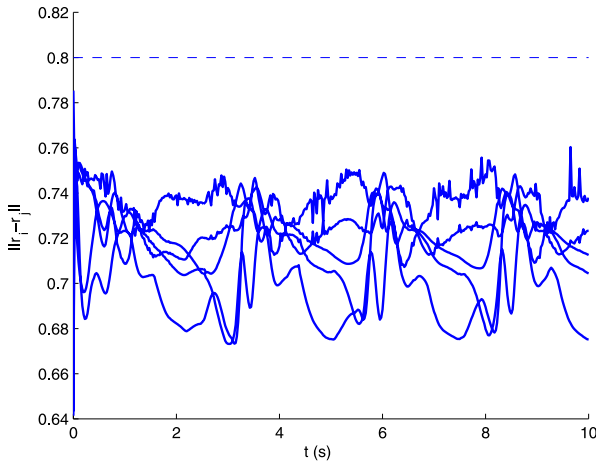
Fig. 5.12 The trajectories of $\|r_i - r_j\|$ for $i \in \mathcal{V}_F$ and $j \in \mathcal{N}_{FC_i}(0)$ and the *dashed line* $\|r_i - r_j\| = d_1$ in the case of stationary leaders
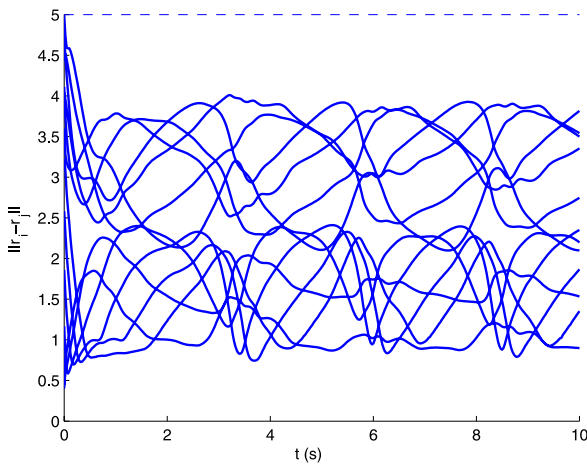
Fig. 5.13 The trajectories of $\|r_i - r_j\|$ for all $i \in \mathcal{V}_F$ and $j \in \mathcal{N}_i^L(0)$ and the *dashed line* $\|r_i - r_j\| = r_L$ in the case of stationary leaders

5.4.4 Simulation

For illustration purposes, a simulation example with stationary leaders in the two-dimensional space is first presented to verify Theorem 5.14. The example includes 4 leaders and 6 followers. Figure 5.11 shows the snapshots of the agents' positions. Initially, the positions of the agents are generated in such a way that $\|r_i(0) - r_j(0)\| < d_1$ for all $i \in \mathcal{V}_F$ and $j \in \mathcal{N}_{FC_i}(0)$, and $\|r_i(0) - r_j(0)\| > d_2$
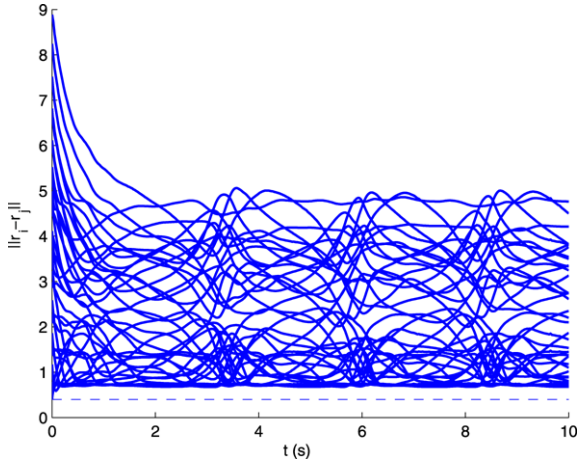
Fig. 5.14 The trajectories of $\|r_i - r_j\|$ for all $i, j \in \mathcal{V}_L \cup \mathcal{V}_F$ and $i \neq j$ and the *dashed line* $\|r_i - r_j\| = d_2$ in the case of stationary leaders

(a) $t = 0$ s

(b) $t = 2.5$ s

(c) $t = 5$ s

(d) $t = 10$ s
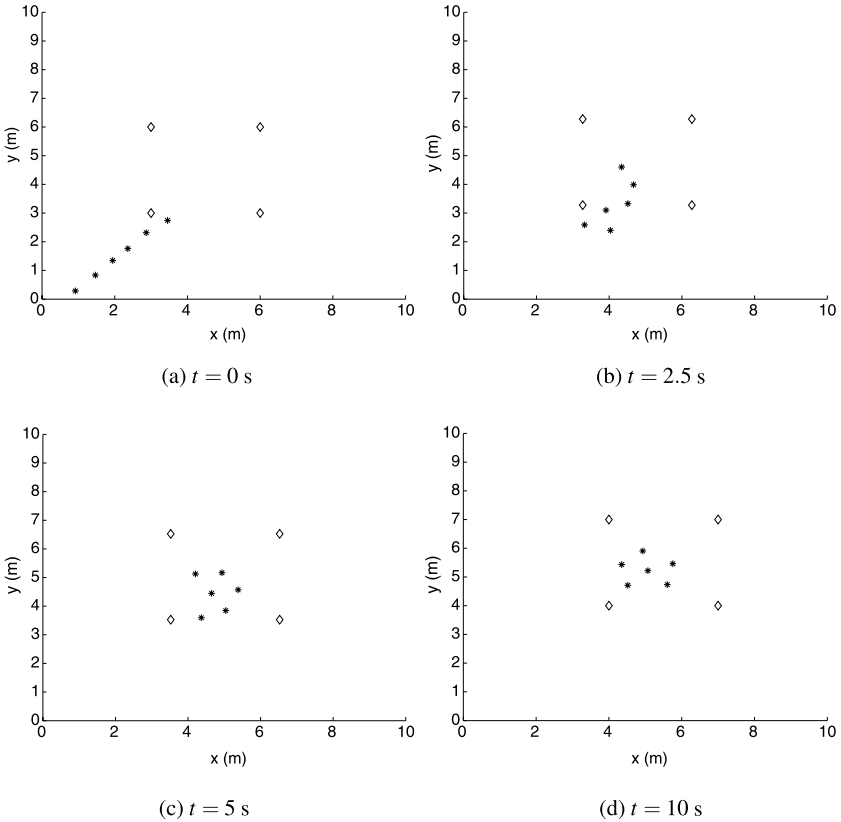
Fig. 5.15 Containment control with swarming behavior in the case of dynamic leaders in the two-dimensional space
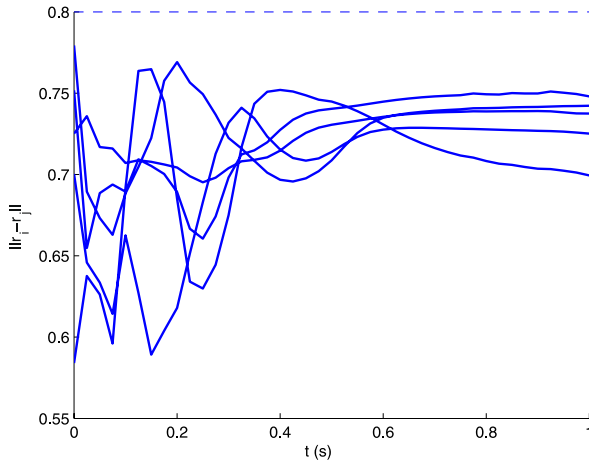
Fig. 5.16 The trajectories of $\|r_i - r_j\|$ for $i \in \mathcal{V}_F$ and $j \in \mathcal{N}_{FC_i}(0)$ and the *dashed line* $\|r_i - r_j\| = d_1$ in the case of dynamic leaders
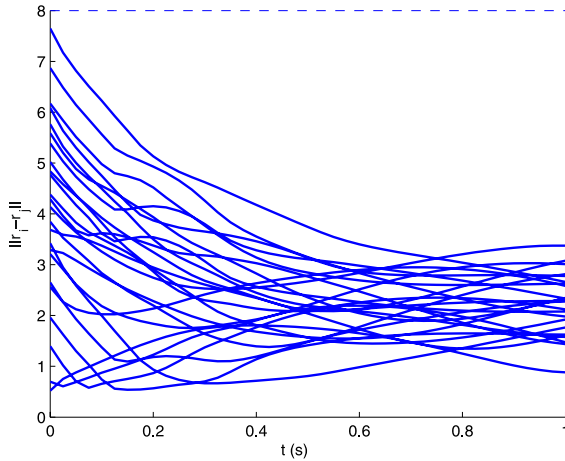
Fig. 5.17 The trajectories of $\|r_i - r_j\|$ for all $i \in \mathcal{V}_F$ and $j \in \mathcal{N}_i^L(0)$ and the *dashed line* $\|r_i - r_j\| = r_L$ in the case of dynamic leaders

for all $i, j \in \mathcal{V}_L \cup \mathcal{V}_F$ and $i \neq j$. The graph $\mathcal{G}_{FC}(0)$ is connected. As can be seen from Fig. 5.11, all followers move toward the convex hull spanned by the leaders while preserving group cohesion and dispersion. Figure 5.12 shows the trajectory of $\|r_i - r_j\|$ for $i \in \mathcal{V}_F$ and $j \in \mathcal{N}_{FC_i}(0)$. It is clear from Fig. 5.12 that for $t \geq 0$ $\|r_i - r_j\| < d_1$ for all $i \in \mathcal{V}_F$ and $j \in \mathcal{N}_{FC_i}(0)$. Figure 5.13 shows the trajectory of $\|r_i - r_j\|$ for $i \in \mathcal{V}_F$ and $j \in \mathcal{N}_i^L(0)$. It is clear from Fig. 5.13 that for $t \geq 0$ $\|r_i - r_j\| < r_L$ for all $i \in \mathcal{V}_F$ and $j \in \mathcal{N}_i^L(0)$. Figure 5.14 shows the trajectory of $\|r_i - r_j\|$ for all $i, j \in \mathcal{V}_L \cup \mathcal{V}_F$ and $i \neq j$. It can be observed that for $t \geq 0$ $\|r_i - r_j\| > d_2$ for all $i, j \in \mathcal{V}_L \cup \mathcal{V}_F$ and $i \neq j$.
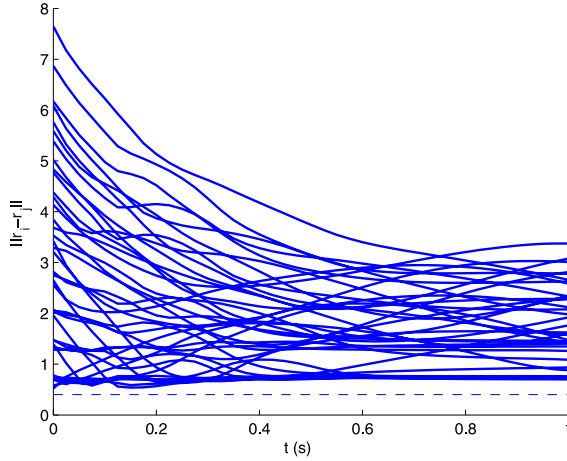
Fig. 5.18 The trajectories of $\|r_i - r_j\|$ for all $i, j \in \mathscr{V}_L \cup \mathscr{V}_F$ and $i \neq j$ and the *dashed line* $\|r_i - r_j\| = d_2$ in the case of dynamic leaders

A simulation example with dynamic leaders in the two dimensional space is then presented to verify Theorem 5.15. The parameters are the same as the ones specified in the case of stationary leaders except that $r_L = 8$. The reason for enlarging r_L is to ensure that every leader has a neighboring follower initially. The leaders move with the same speed. In particular, we let $v_k = [1, 1]^T$, $k \in \mathscr{V}_L$. As can be seen from Figs. 5.15, 5.16, 5.17, and 5.18, the followers move toward the dynamic convex hull spanned by the dynamic leaders while preserving group cohesion and dispersion.

5.5 Notes

The results in this chapter are based mainly on [29, 56]. For other results related to containment control with stationary or dynamic leaders, see [79, 80, 136]. In particular, [136] exploits the theory of partial difference equations and proposes a hybrid control scheme based on stop-and-go rules for the leaders to drive a collection of mobile agents to the convex hull spanned by multiple leaders under an undirected fixed interaction graph. The result is extended in [79] to multiple unicycle agents. A distributed attitude containment control problem is studied in [80] for multiple rigid bodies with multiple stationary leaders under an undirected fixed interaction graph. For other results related to distributed multi-agent coordination using potential functions, see [78, 103, 133, 161, 168, 279], to name a few. In these references, potential functions are constructed to achieve inter-agent collision avoidance, connectivity maintenance, group cohesion, or group dispersion.

Part III
Emergent Models in Distributed Multi-agent Coordination

Chapter 6
Networked Lagrangian Systems

This chapter moves from point models primarily adopted in distributed multi-agent coordination to more realistic Lagrangian models. A class of mechanical systems including autonomous vehicles, robotic manipulators, and walking robots are Lagrangian systems. We focus on fully-actuated Lagrangian systems. We first study distributed leaderless coordination algorithms for networked Lagrangian systems. The objective is to drive a team of agents modeled by Euler–Lagrange equations to achieve desired relative deviations on their vectors of generalized coordinates with local interaction. We then study distributed coordinated regulation and distributed coordinated tracking algorithms in the presence of a leader for networked Lagrangian systems under the constraints that the leader is a neighbor of only a subset of the followers and the followers have only local interaction. In the case of coordinated regulation, the leader has a constant vector of generalized coordinates. In the case of coordinated tracking, the leader has a varying vector of generalized coordinates. In both cases, the objective is to drive the vectors of generalized coordinates of a team of followers modeled by Euler–Lagrange equations to approach that of a leader. Simulation results show the effectiveness of the proposed algorithms.

6.1 Problem Statement

In distributed multi-agent coordination problems, point models are primarily adopted due to their simplicity. However, the point models are often not realistic. Euler–Lagrange equations can be used to model a class of mechanical systems including autonomous vehicles, robotic manipulators, and walking robots. The objective of the current chapter is to study distributed *leaderless* and *leader-following coordination* problems for networked Lagrangian systems. Here we focus on fully-actuated Lagrangian systems. In the leaderless case, there does not exist a leader in the team. The objective is that a team of agents modeled by Euler–Lagrange equations achieves desired relative deviations on their vectors of generalized coordinates with local interaction. In the leader-following case, there exists a leader that specifies the

objective for the whole team. Here the leader can be virtual or physical. In particular, we use the term *coordinated regulation* to refer to the case where the vectors of generalized coordinates of a group of followers modeled by Euler–Lagrange equations approach a constant vector of generalized coordinates of a leader with local interaction. Similar to Chap. 4, we use the term *coordinated tracking* to refer to the case where the vectors of generalized coordinates of a group of followers modeled by Euler–Lagrange equations approach a varying vector of generalized coordinates of a leader with local interaction. A coordinated regulation problem can be viewed as a special case of a coordinated tracking problem. It is worthwhile to mention that the coordinated tracking case becomes much more complex if the leader is a neighbor of only a subset of the followers.

In the leaderless case, we are motivated to derive distributed coordination algorithms when the agents have only local interaction with their neighbors and none of them has the knowledge of the group reference trajectory. The distributed feature of the algorithms makes them scalable to a large number of agents. The leaderless feature of the algorithms makes them suitable for applications where the absolute states of the agents are not what is important but rather all agents achieve relative state deviations. While there are many applications where there exists a group reference trajectory, there are also many applications where leaderless algorithms are important. Examples include rendezvous, flocking, and attitude synchronization. For example, the proposed leaderless algorithms have potential applications in automated rendezvous and docking. In addition, rigid body attitude dynamics can be written in the form of Euler–Lagrange equations. The proposed leaderless algorithms can be used for attitude synchronization of multiple rigid bodies with local interaction. Furthermore, when there is a team of networked mobile vehicles equipped with robotic arms that hold sensors (e.g., iRobot PackBot Explorer), the robotic arms on each mobile vehicle can be modeled by Euler–Lagrange equations. The proposed leaderless algorithms can be used to coordinate the robotic arms and sensors equipped on different mobile vehicles so that a team of mobile vehicles can scan an area cooperatively. We will propose and analyze three algorithms: (i) a fundamental algorithm; (ii) a nonlinear algorithm; and (iii) an algorithm that accounts for unavailability of measurements of generalized coordinate derivatives.

In the leader-following case, we are motivated to derive distributed coordinated regulation and tracking algorithms when the leader is a neighbor of only a subset of the followers and the followers have only local interaction. The presence of a leader can broaden the applications as a group objective can be encapsulated by the leader. We will consider three cases: (i) The leader has a constant vector of generalized coordinates; (ii) The leader has a constant vector of generalized coordinate derivatives; (iii) The leader has a varying vector of generalized coordinate derivatives. In the first case, we propose and analyze distributed algorithms by extending the distributed leaderless coordination algorithms. In the second case, with the aid of a distributed continuous estimator, we propose and analyze, respectively, a distributed model-dependent algorithm and a distributed model-independent algorithm accounting for parametric uncertainties. In the third case, we propose and analyze a distributed model-independent sliding-mode algorithm.

Consider a team of n agents with Euler–Lagrange equations given by

$$M_i(q_i)\ddot{q}_i + C_i(q_i, \dot{q}_i)\dot{q}_i + g_i(q_i) = \tau_i, \quad i = 1, \ldots, n, \tag{6.1}$$

where $q_i \in \mathbb{R}^p$ is the vector of generalized coordinates, $M_i(q_i) \in \mathbb{R}^{p \times p}$ is the symmetric positive-definite inertia matrix, $C_i(q_i, \dot{q}_i)\dot{q}_i \in \mathbb{R}^p$ is the vector of Coriolis and centrifugal torques, $g_i(q_i)$ is the vector of gravitational torques, and $\tau_i \in \mathbb{R}^p$ is the vector of torques produced by the actuators associated with the ith agent.

Throughout the subsequent analysis, we assume that the following assumptions hold [144, 276]:

(A1) (Boundedness) For any i, there exist positive constants $k_{\underline{m}}$, $k_{\bar{m}}$, k_C, k_{C_1}, k_{C_2}, and k_g such that $M_i(q_i) - k_{\underline{m}}I_p$ is positive semidefinite, $M_i(q_i) - k_{\bar{m}}I_p$ is negative semidefinite, $\|g_i(q_i)\| \leq k_g$, $\|C_i(x, y)\| \leq k_C\|y\|$, and $\|C_i(x, z)w - C_i(y, v)w\| \leq k_{C_1}\|z - v\| \|w\| + k_{C_2}\|x - y\| \|w\| \|z\|$ for all vectors $x, y, z, v, w \in \mathbb{R}^p$.

(A2) (Skew-symmetric property) $\dot{M}_i(q_i) - 2C_i(q_i, \dot{q}_i)$ is skew-symmetric (i.e., $y^T[\dot{M}_i(q_i) - 2C_i(q_i, \dot{q}_i)]y = 0$ for all $y \in \mathbb{R}^p$).

(A3) (Linearity in the parameters) $M_i(q_i)\ddot{q}_i + C_i(q_i, \dot{q}_i)\dot{q}_i + g_i(q_i) = Y_i(q_i, \dot{q}_i, \ddot{q}_i)\Theta_i$, where $Y_i(q_i, \dot{q}_i, \ddot{q}_i)$ is the regressor and Θ_i is the constant parameter vector for the ith agent.

Define $q \triangleq [q_1^T, \ldots, q_n^T]^T$ and $\dot{q} \triangleq [\dot{q}_1^T, \ldots, \dot{q}_n^T]^T$. Also define $M(q) \triangleq \mathrm{diag}[M_1(q_1), \ldots, M_n(q_n)]$, $C(q, \dot{q}) \triangleq \mathrm{diag}[C_1(q_1, \dot{q}_1), \ldots, C_n(q_n, \dot{q}_n)]$, and $g(q) \triangleq [g_1^T(q_1), \ldots, g_n^T(q_n)]^T$.

6.2 Distributed Leaderless Coordination for Networked Lagrangian Systems

We consider three distributed leaderless coordination algorithms for networked Lagrangian systems, namely, a fundamental algorithm, a nonlinear algorithm, and an algorithm accounting for unavailability of measurements of generalized coordinate derivatives. Define $\breve{q}_{ij} \triangleq \delta_i - \delta_j$, where $\delta_i \in \mathbb{R}^p$ is constant. Here $\breve{q}_{ij}$ denotes the constant desired relative deviation on vectors of generalized coordinates between agents i and j. The objective here is to design distributed leaderless coordination algorithms for (6.1) such that $q_i(t) - q_j(t) \to \breve{q}_{ij}$ and $\dot{q}_i(t) \to \mathbf{0}_p$ as $t \to \infty$. Before moving on, we need the following lemma:

Lemma 6.1. *Let $\psi : \mathbb{R} \to \mathbb{R}$ be a continuous odd function satisfying that $\psi(x) > 0$ if $x > 0$.[1] Suppose that $\varsigma_i \in \mathbb{R}^p$, $\varphi_i \in \mathbb{R}^p$, $K \in \mathbb{R}^{p \times p}$, and $D \triangleq [d_{ij}] \in \mathbb{R}^{n \times n}$. If D is symmetric, then*

---

[1] For a vector, $\psi(\cdot)$ is defined componentwise.

$$\frac{1}{2}\sum_{i=1}^{n}\sum_{j=1}^{n}d_{ij}(\varsigma_i - \varsigma_j)^T\psi\big[K(\varphi_i - \varphi_j)\big] = \sum_{i=1}^{n}\varsigma_i^T\left\{\sum_{j=1}^{n}d_{ij}\psi\big[K(\varphi_i - \varphi_j)\big]\right\}.$$

Proof: The proof is similar to that of [248, Lemma 4.18] and is hence omitted here.
∎

6.2.1 Fundamental Algorithm

In this section, we consider a fundamental coordination algorithm as

$$\tau_i = g_i(q_i) - \sum_{j=1}^{n}a_{ij}(q_i - q_j - \breve{q}_{ij}) - \sum_{j=1}^{n}b_{ij}(\dot{q}_i - \dot{q}_j) - K_i\dot{q}_i, \qquad (6.2)$$

where $i = 1, \ldots, n$, a_{ij} is the (i,j)th entry of the adjacency matrix $\mathscr{A} \in \mathbb{R}^{n\times n}$ associated with the undirected graph $\mathscr{G}_A \triangleq (\mathscr{V}, \mathscr{E}_A)$ characterizing the interaction among the n agents for q_i, b_{ij} is the (i,j)th entry of the adjacency matrix $\mathscr{B} \in \mathbb{R}^{n\times n}$ associated with the undirected graph $\mathscr{G}_B \triangleq (\mathscr{V}, \mathscr{E}_B)$ characterizing the interaction among the n agents for $\dot{q}_i$, and $K_i \in \mathbb{R}^{p\times p}$ is symmetric positive definite. Note that here $\mathscr{G}_A$ and $\mathscr{G}_B$ are allowed to be different.

Theorem 6.1. *Using* (6.2) *for* (6.1), $q_i(t) - q_j(t) \to \breve{q}_{ij}$ *and* $\dot{q}_i(t) \to \mathbf{0}_p$, $i, j = 1, \ldots, n$, *as* $t \to \infty$ *if the graph* $\mathscr{G}_A$ *is undirected connected and the graph* $\mathscr{G}_B$ *is undirected.*

Proof: Using (6.2), (6.1) can be written as

$$\frac{d}{dt}(q_i - q_j - \breve{q}_{ij}) = \dot{q}_i - \dot{q}_j,$$

$$\frac{d}{dt}\dot{q}_i = -M_i^{-1}(q_i)\Bigg[C_i(q_i, \dot{q}_i)\dot{q}_i + \sum_{j=1}^{n}a_{ij}(q_i - q_j - \breve{q}_{ij}) \quad (6.3)$$

$$+ \sum_{j=1}^{n}b_{ij}(\dot{q}_i - \dot{q}_j) + K_i\dot{q}_i\Bigg].$$

Note that the system (6.3) with states $q_i - q_j - \breve{q}_{ij}$ and $\dot{q}_i$ is nonautonomous due to the dependence of M_i and C_i on q_i. As a result, Lemma 1.31 is no long applicable for (6.3). Instead, we apply Lemma 1.36 to prove the theorem.

Let $\breve{q} \triangleq [\breve{q}_1^T, \ldots, \breve{q}_n^T]^T$ with $\breve{q}_i \triangleq q_i - \delta_i$, and $K \triangleq \mathrm{diag}(K_1, \ldots, K_n)$. Let $\mathscr{L}_A$ and $\mathscr{L}_B$ be, respectively, the Laplacian matrix associated with $\mathscr{A}$ and hence $\mathscr{G}_A$, and $\mathscr{B}$ and hence $\mathscr{G}_B$. Note that both $\mathscr{L}_A$ and $\mathscr{L}_B$ are symmetric positive semidefinite because both $\mathscr{G}_A$ and $\mathscr{G}_B$ are undirected. Let $\tilde{q}$ be a column stack vector of all $q_i - q_j - \breve{q}_{ij}$, where $i < j$ and $a_{ij} > 0$ (i.e., agents i and j are neighbors). Define

$x \triangleq [\tilde{q}^T, \dot{q}^T]^T$. Consider the Lyapunov function candidate for (6.3) as

$$V(t,x) = \frac{1}{2}\breve{q}^T(\mathscr{L}_A \otimes I_p)\breve{q} + \frac{1}{2}\dot{q}^T M(q)\dot{q}.$$

Because the graph $\mathscr{G}_A$ is undirected, it follows from Remark 1.1 and Lemma 1.21 that $\breve{q}^T(\mathscr{L}_A \otimes I_p)\breve{q} = \frac{1}{2}\sum_{i=1}^n \sum_{j=1}^n a_{ij}\|q_i - q_j - \breve{q}_{ij}\|^2$. It thus follows that V is positive definite and decrescent with respect to x. Note that Condition 1 in Lemma 1.36 is satisfied.

The derivative of V is given by

$$\dot{V}(t,x) = \dot{q}^T(\mathscr{L}_A \otimes I_p)\breve{q} + \frac{1}{2}\ddot{q}^T M(q)\dot{q} + \frac{1}{2}\dot{q}^T \dot{M}(q)\dot{q} + \frac{1}{2}\dot{q}^T M(q)\ddot{q}$$

$$= \dot{q}^T(\mathscr{L}_A \otimes I_p)\breve{q} + \dot{q}^T M(q)\ddot{q} + \frac{1}{2}\dot{q}^T \dot{M}(q)\dot{q},$$

where we have used the fact that $M(q)$ is symmetric. Using (6.2), (6.1) can be written in a vector form as

$$M(q)\ddot{q} = -C(q,\dot{q})\dot{q} - (\mathscr{L}_A \otimes I_p)\breve{q} - (\mathscr{L}_B \otimes I_p)\dot{q} - K\dot{q}. \tag{6.4}$$

Note that $\dot{M}(q) - 2C(q,\dot{q})$ is skew symmetric. By applying (6.4), the derivative of V can be written as

$$\dot{V}(t,x) = -\dot{q}^T(\mathscr{L}_B \otimes I_p)\dot{q} - \dot{q}^T K\dot{q} \le 0. \tag{6.5}$$

Therefore, Condition 2 in Lemma 1.36 is satisfied.

Let $W(t,x) \triangleq \dot{q}^T(\mathscr{L}_A \otimes I_p)\breve{q}$. It follows that $|W(t,x)| \le \|\dot{q}\| \|(\mathscr{L}_A \otimes I_p)\breve{q}\|$. Note that (6.5) implies $V[t,x(t)] \le V[0,x(0)]$, $\forall t \ge 0$, which in turn implies that $\|\tilde{q}\|$ and $\|\dot{q}\|$ are bounded. Noting that $(\mathscr{L}_A \otimes I_p)\breve{q}$ is a column stack vector of all $\sum_{j=1}^n a_{ij}(q_i - q_j - \breve{q}_{ij})$, $i = 1, \ldots, n$, it follows that $\|(\mathscr{L}_A \otimes I_p)\breve{q}\|$ is bounded. It thus follows that $|W(t,x)|$ is bounded along the solution trajectory, implying that Condition 3 in Lemma 1.36 is satisfied.

The derivative of W along the solution trajectory of (6.4) is

$$\dot{W}(t,x) = \ddot{q}^T(\mathscr{L}_A \otimes I_p)\breve{q} + \dot{q}^T(\mathscr{L}_A \otimes I_p)\dot{q}$$

$$= -\dot{q}^T C^T(q,\dot{q})M^{-1}(q)(\mathscr{L}_A \otimes I_p)\breve{q}$$

$$- \breve{q}^T(\mathscr{L}_A \otimes I_p)M^{-1}(q)(\mathscr{L}_A \otimes I_p)\breve{q}$$

$$- \dot{q}^T(\mathscr{L}_B \otimes I_p)M^{-1}(q)(\mathscr{L}_A \otimes I_p)\breve{q} - \dot{q}^T K M^{-1}(q)(\mathscr{L}_A \otimes I_p)\breve{q}$$

$$+ \dot{q}^T(\mathscr{L}_A \otimes I_p)\dot{q}.$$

Note that $\|\dot{q}\|$ is bounded. It follows from Assumption (A1) that $\|M^{-1}(q)\|$ and $C(q,\dot{q})\dot{q}$ are bounded. Therefore, $\dot{W}(t,x)$ can be written as $\dot{W}(t,x) = g[\beta(t),x]$,

where g is continuous in both arguments and $\beta(t)$ is continuous and bounded. On the set $\Omega \triangleq \{(\tilde{q}, \dot{q})|\dot{V} = 0\}$, $\dot{q} = \mathbf{0}_{np}$ and $\dot{W}(t, x)$ becomes

$$\dot{W}(t, x) = -\breve{q}^T(\mathscr{L}_A \otimes I_p)M^{-1}(q)(\mathscr{L}_A \otimes I_p)\breve{q}.$$

Note that $M^{-1}(q)$ is symmetric positive definite. It follows from Assumption (A1) that

$$\breve{q}^T(\mathscr{L}_A \otimes I_p)M^{-1}(q)(\mathscr{L}_A \otimes I_p) \geq \frac{1}{k_{\bar{m}}}\left\|(\mathscr{L}_A \otimes I_p)\breve{q}\right\|^2.$$

Also note that $\|(\mathscr{L}_A \otimes I_p)\breve{q}\|^2$ is positive definite with respect to $\tilde{q}$. It follows from Lemma 1.35 that on the set Ω, there exist a class $\mathscr{K}$ function, α, such that $\|(\mathscr{L}_A \otimes I_p)\breve{q}\|^2 \geq \alpha(\|\tilde{q}\|)$. Therefore, for all $x \in \Omega$, $|\dot{W}(t, x)| \geq 1/k_{\bar{m}}\alpha(\|\tilde{q}\|)$. It follows from Lemma 1.37 that Condition 4 in Lemma 1.36 is satisfied. We conclude from Lemma 1.36 that the equilibrium of the system (6.3) (i.e., $\|\tilde{q}\| = 0$ and $\|\dot{q}\| = 0$) is uniformly asymptotically stable, which implies that $q_i(t) - q_j(t) \to \breve{q}_{ij}$ and $\dot{q}_i(t) \to \mathbf{0}_p$ as $t \to \infty$ because $\mathscr{G}_A$ is undirected connected. ∎

6.2.2 Nonlinear Algorithm

In this section, we consider a nonlinear coordination algorithm as

$$\tau_i = g_i(q_i) - \sum_{j=1}^{n} a_{ij}\psi\big[K_q(q_i - q_j - \breve{q}_{ij})\big]$$

$$- \sum_{j=1}^{n} b_{ij}\psi\big[K_{\dot{q}}(\dot{q}_i - \dot{q}_j)\big] - K_i\psi(K_{di}\dot{q}_i), \qquad (6.6)$$

where $i = 1, \ldots, n$, a_{ij} and b_{ij} are defined as in (6.2), K_q, $K_{\dot{q}}$, K_i, and K_{di} are p by p positive-definite diagonal matrices, and $\psi(\cdot)$ is defined in Lemma 6.1 with an additional assumption that $\psi(\cdot)$ is continuously differentiable. In the remainder of the chapter, we use a subscript (j) to denote the jth component of a vector or the jth diagonal entry of a diagonal matrix.

Theorem 6.2. *Using* (6.6) *for* (6.1), $q_i(t) - q_j(t) \to \breve{q}_{ij}$ *and* $\dot{q}_i(t) \to \mathbf{0}_p$, $i, j = 1, \ldots, n$, *as* $t \to \infty$ *if the graph* $\mathscr{G}_A$ *is undirected connected and the graph* $\mathscr{G}_B$ *is undirected.*

Proof: Similar to the proof of Theorem 6.1, using (6.6), (6.1) can be written as a nonautonomous system with states $q_i - q_j - \breve{q}_{ij}$ and $\dot{q}_i$. We apply Lemma 1.36 to prove the theorem. Let $\tilde{q}$ and x be defined as in the proof of Theorem 6.1. Consider the Lyapunov function candidate

$$V(t, x) = \frac{1}{2} \sum_{i=1}^{n} \sum_{j=1}^{n} a_{ij} \sum_{\ell=1}^{p} \int_{0}^{q_{i(\ell)}(t) - q_{j(\ell)}(t) - \check{q}_{ij(\ell)}} \psi[K_{q(\ell)}\tau] \, d\tau$$

$$+ \frac{1}{2} \sum_{i=1}^{n} \dot{q}_i^T M_i(q_i) \dot{q}_i.$$

Note that V is positive definite and decrescent with respect to x. Therefore, Condition 1 in Lemma 1.36 is satisfied.

The derivative of V is given by

$$\dot{V}(t, x) = \frac{1}{2} \sum_{i=1}^{n} \sum_{j=1}^{n} a_{ij} (\dot{q}_i - \dot{q}_j)^T \psi[K_q(q_i - q_j - \check{q}_{ij})]$$

$$+ \frac{1}{2} \sum_{i=1}^{n} [\ddot{q}_i^T M_i(q_i) \dot{q}_i + \dot{q}_i^T \dot{M}_i(q_i) \dot{q}_i + \dot{q}_i^T M_i(q_i) \ddot{q}_i].$$

Using (6.6), (6.1) can be written as

$$M_i(q_i) \ddot{q}_i = - C_i(q_i, \dot{q}_i) \dot{q}_i - \sum_{j=1}^{n} a_{ij} \psi[K_q(q_i - q_j - \check{q}_{ij})]$$

$$- \sum_{j=1}^{n} b_{ij} \psi[K_{\dot{q}}(\dot{q}_i - \dot{q}_j)] - K_i \psi(K_{di} \dot{q}_i). \qquad (6.7)$$

Note that $\mathscr{A}$ is symmetric because the graph $\mathscr{G}_A$ is undirected. It follows from Lemma 6.1 that

$$\frac{1}{2} \sum_{i=1}^{n} \sum_{j=1}^{n} a_{ij} (\dot{q}_i - \dot{q}_j)^T \psi[K_q(q_i - q_j - \check{q}_{ij})]$$

$$= \sum_{i=1}^{n} \dot{q}_i^T \left\{ \sum_{j=1}^{n} a_{ij} \psi[K_q(q_i - q_j - \check{q}_{ij})] \right\}.$$

Also note that $M_i(q_i)$ is symmetric and that $\dot{M}_i(q_i) - 2C_i(q_i, \dot{q}_i)$ is skew symmetric. By applying (6.7), it follows that

$$\dot{V}(t, x) = - \sum_{i=1}^{n} \dot{q}_i^T \left\{ \sum_{j=1}^{n} b_{ij} \psi[K_{\dot{q}}(\dot{q}_i - \dot{q}_j)] + K_i \psi(K_{di} \dot{q}_i) \right\}.$$

Note that $\mathscr{B}$ is symmetric because the graph $\mathscr{G}_B$ is undirected. By applying Lemma 6.1 again, it follows that the derivative of V becomes

$$\dot{V}(t, x) = - \frac{1}{2} \sum_{i=1}^{n} \sum_{j=1}^{n} b_{ij} (\dot{q}_i - \dot{q}_j)^T \psi[K_{\dot{q}}(\dot{q}_i - \dot{q}_j)] - \sum_{i=1}^{n} \dot{q}_i^T K_i \psi(K_{di} \dot{q}_i).$$

Given a vector z and two positive-definite diagonal matrices K_1 and K_2, z and $K_1\psi(K_2 z)$ have the same signs for each component. Therefore, it follows that $\dot{V}(t,x) \leq 0$, which implies that Condition 2 in Lemma 1.36 is satisfied.

Let $W(t,x) \triangleq \sum_{i=1}^{n} \dot{q}_i^T \chi_i$, where

$$\chi_i \triangleq \sum_{j=1}^{n} a_{ij}\psi\big[K_q(q_i - q_j - \check{q}_{ij})\big].$$

Note that $\dot{V}(t,x) \leq 0$ implies $V[t,x(t)] \leq V[0,x(0)]$, $\forall t \geq 0$, which in turn implies that $\tilde{q}$ and $\dot{q}$ are bounded. It thus follows that $\|\chi_i\|$ is also bounded. Similar to the proof of Theorem 6.1, it follows that $|W(t,x)|$ is bounded along the solution trajectory, implying that Condition 3 in Lemma 1.36 is satisfied.

The derivative of $W(t,x)$ along the solution trajectory of (6.7) is

$$\dot{W}(t,x) = -\sum_{i=1}^{n} \dot{q}_i^T C_i^T(q_i, \dot{q}_i) M_i^{-1}(q_i)\chi_i$$

$$-\sum_{i=1}^{n} \left\{\sum_{j=1}^{n} b_{ij}\psi\big[K_{\dot{q}}(\dot{q}_i - \dot{q}_j)\big]\right\}^T M_i^{-1}(q_i)\chi_i$$

$$-\sum_{i=1}^{n} \chi_i^T M_i^{-1}(q_i)\chi_i - \sum_{i=1}^{n} \big[K_i\psi(K_{di}\dot{q}_i)\big]^T M_i^{-1}(q_i)\chi_i + \sum_{i=1}^{n} \dot{q}_i^T \dot{\chi}_i.$$

A similar argument to that in the proof of Theorem 6.1 shows that $\dot{W}(t,x)$ can be written as $\dot{W}(t,x) = g[\beta(t),x]$, where g is continuous in both arguments and $\beta(t)$ is continuous and bounded. On the set $\{(\tilde{q},\dot{q})|\dot{V}=0\}$, $\dot{q} = \mathbf{0}_{np}$ and $\dot{W}(t,x)$ becomes

$$\dot{W}(t,x) = -\sum_{i=1}^{n} \chi_i^T M_i^{-1}(q_i)\chi_i.$$

If $\sum_{i=1}^{n} \chi_i^T \chi_i$ is positive definite with respect to $\tilde{q}$, then a similar argument to that in the proof of Theorem 6.1 implies that Condition 4 in Lemma 1.36 is satisfied. Because $\sum_{i=1}^{n} \chi_i^T \chi_i \geq 0$, equivalently we only need to show that $\sum_{i=1}^{n} \chi_i^T \chi_i = 0$ implies $q_i - q_j - \check{q}_{ij} = \mathbf{0}_p$ for all $a_{ij} > 0$. Suppose that $\sum_{i=1}^{n} \chi_i^T \chi_i = 0$, which implies $\chi_i = \sum_{j=1}^{n} a_{ij}\psi[K_q(q_i - q_j - \check{q}_{ij})] = \mathbf{0}_p$. It thus follows that $\sum_{i=1}^{n} q_i^T \{\sum_{j=1}^{n} a_{ij}\psi[K_q(q_i - q_j - \check{q}_{ij})]\} = 0$, which implies from Lemma 6.1 that $\frac{1}{2}\sum_{i=1}^{n}\sum_{j=1}^{n} a_{ij}(q_i - q_j - \check{q}_{ij})^T \psi[K_q(q_i - q_j - \check{q}_{ij})] = 0$. Note that $\mathscr{G}_A$ is undirected and $q_i - q_j - \check{q}_{ij}$ and $\psi[K_q(q_i - q_j - \check{q}_{ij})]$ have the same signs for each component. It follows that $q_i - q_j - \check{q}_{ij} = \mathbf{0}_p$ for all $a_{ij} > 0$ when $\sum_{i=1}^{n} \chi_i^T \chi_i = 0$. Combining the above arguments, we conclude from Lemma 1.36 that the equilibrium $\|\tilde{q}\| = 0$ and $\|\dot{q}\| = 0$ is uniformly asymptotically stable, which implies that $q_i(t) - q_j(t) \to \check{q}_{ij}$ and $\dot{q}_i(t) \to \mathbf{0}_p$ as $t \to \infty$ because $\mathscr{G}_A$ is undirected connected. $\blacksquare$

6.2.3 Algorithm Accounting for Unavailability of Measurements of Generalized Coordinate Derivatives

Note that (6.2) and (6.6) require measurements of $\dot{q}_i$ and $\dot{q}_i - \dot{q}_j$, where $b_{ij} > 0$. In this section, we consider a coordination algorithm that removes the requirement for the measurements of $\dot{q}_i$ and $\dot{q}_i - \dot{q}_j$ as

$$\dot{\hat{x}}_i = F\hat{x}_i + \sum_{j=1}^{n} b_{ij}(q_i - q_j - \breve{q}_{ij}) + \kappa\breve{q}_i, \tag{6.8a}$$

$$y_i = P\left[F\hat{x}_i + \sum_{j=1}^{n} b_{ij}(q_i - q_j - \breve{q}_{ij}) + \kappa\breve{q}_i\right], \tag{6.8b}$$

$$\tau_i = g_i(q_i) - \sum_{j=1}^{n} a_{ij}\psi\left[K_q(q_i - q_j - \breve{q}_{ij})\right] - y_i, \tag{6.8c}$$

where $i = 1, \ldots, n$, $F \in \mathbb{R}^{p \times p}$ is Hurwitz, κ is a positive scalar, a_{ij} is the (i, j)th entry of the adjacency matrix $\mathscr{A} \in \mathbb{R}^{n \times n}$ associated with the undirected graph $\mathscr{G}_A \triangleq (\mathscr{V}, \mathscr{E}_A)$ characterizing the interaction among the n agents for q_i in (6.8c), b_{ij} is the (i, j)th entry of the adjacency matrix $\mathscr{B} \in \mathbb{R}^{n \times n}$ associated with the undirected graph $\mathscr{G}_B \triangleq (\mathscr{V}, \mathscr{E}_B)$ characterizing the interaction among the n agents for q_i in (6.8a), ψ is defined in (6.6), and $P \in \mathbb{R}^{p \times p}$ is the symmetric positive-definite solution to the Lyapunov equation $F^T P + PF = -Q$ with $Q \in \mathbb{R}^{p \times p}$ being symmetric positive definite.

Theorem 6.3. *Using* (6.8) *for* (6.1), $q_i(t) - q_j(t) \to \breve{q}_{ij}$ *and* $\dot{q}_i(t) \to \mathbf{0}_p$, $i, j = 1, \ldots, n$, *as* $t \to \infty$ *if the graph* $\mathscr{G}_A$ *is undirected connected and the graph* $\mathscr{G}_B$ *is undirected.*

Proof: Similar to the proofs of Theorems 6.1 and 6.2, we apply Lemma 1.36 to prove the theorem. Let $\hat{x} \triangleq [\hat{x}_1^T, \ldots, \hat{x}_n^T]^T$. Let $\tilde{q}$ be defined as in the proof of Theorem 6.2. Let $x \triangleq [\tilde{q}^T, \dot{q}^T, \hat{x}^T]^T$. Consider the Lyapunov function candidate

$$V(t, x) = \frac{1}{2}\sum_{i=1}^{n}\sum_{j=1}^{n} a_{ij}\sum_{\ell=1}^{p}\int_{0}^{q_{i(\ell)}(t) - q_{j(\ell)}(t) - \breve{q}_{ij(\ell)}} \psi[K_{q(\ell)}\tau]\,d\tau$$

$$+ \frac{1}{2}\sum_{i=1}^{n}\dot{q}_i^T M_i(q_i)\dot{q}_i + \frac{1}{2}\dot{\hat{x}}^T (S \otimes I_p)^{-1}(I_n \otimes P)\hat{x},$$

where $S \triangleq \mathscr{L}_B + \kappa I_n$ with $\mathscr{L}_B$ being the Laplacian matrix associated with $\mathscr{B}$ and hence $\mathscr{G}_B$. Note that $\mathscr{L}_B$ is symmetric positive semidefinite because the graph $\mathscr{G}_B$ is undirected. It thus follows that S is symmetric positive definite, so is S^{-1}. From Lemma 1.21, note that $(S \otimes I_p)^{-1} = (S^{-1} \otimes I_p)$. Also note from Lemma 1.21 that $(S^{-1} \otimes I_p)(I_n \otimes P) = S^{-1}I_n \otimes I_pP = I_nS^{-1} \otimes PI_p = (I_n \otimes P)(S^{-1} \otimes I_p)$.

That is, $(S \otimes I_p)^{-1}$ and $I_n \otimes P$ commute. Similarly, it is straightforward to show that $(S \otimes I_p)^{-1}$ and $I_n \otimes F^T$ also commute. Note that $S^{-1}I_n \otimes I_p P$ is symmetric positive definite, so is $(S^{-1} \otimes I_p)(I_n \otimes P)$. It follows that V is positive definite and decrescent with respect to x. Therefore, Condition 1 in Lemma 1.36 is satisfied.

Following the proof of Theorem 6.2, we derive the derivative of V as

$$
\begin{aligned}
\dot{V}(t,x) = & -\sum_{i=1}^{n} \dot{q}_i^T y_i + \frac{1}{2}\dot{\hat{x}}^T \left(I_n \otimes F^T\right)(S \otimes I_p)^{-1}(I_n \otimes P)\dot{\hat{x}} \\
& + \frac{1}{2}\dot{q}^T (S \otimes I_p)^T (S \otimes I_p)^{-1}(I_n \otimes P)\dot{\hat{x}} \\
& + \frac{1}{2}\dot{\hat{x}}^T (S \otimes I_p)^{-1}(I_n \otimes P)(I_n \otimes F)\dot{\hat{x}} \\
& + \frac{1}{2}\dot{\hat{x}}^T (S \otimes I_p)^{-1}(I_n \otimes P)(S \otimes I_p)\dot{q} \\
= & -\sum_{i=1}^{n} \dot{q}_i^T y_i + \frac{1}{2}\dot{\hat{x}}^T (S \otimes I_p)^{-1}\left[I_n \otimes \left(F^T P + PF\right)\right]\dot{\hat{x}} + \dot{q}^T (I_n \otimes P)\dot{\hat{x}} \\
= & -\frac{1}{2}\dot{\hat{x}}^T (S \otimes I_p)^{-1}(I_n \otimes Q)\dot{\hat{x}} \leq 0,
\end{aligned}
$$

where we have used the fact that

$$
\ddot{\hat{x}} = (I_n \otimes F)\dot{\hat{x}} + (S \otimes I_p)\dot{q}, \tag{6.9}
$$

$(S \otimes I_p)^{-1}$ and $I_n \otimes F^T$ commute, $(S \otimes I_p)^{-1}$ and $I_n \otimes P$ commute, $S \otimes I_p = (S \otimes I_p)^T$, $y = (I_n \otimes P)\dot{\hat{x}}$ with $y = [y_1^T, \ldots, y_n^T]^T$, and $(S \otimes I_p)^{-1}(I_n \otimes Q) = S^{-1}I_n \otimes QI_p$ is symmetric positive definite. Therefore, Condition 2 in Lemma 1.36 is satisfied.

Let $W(t,x)$ and χ_i be defined as in the proof of Theorem 6.2. Similar to the proof of Theorem 6.2, it follows that $|W(t,x)|$ is bounded along the solution trajectory, implying that Condition 3 in Lemma 1.36 is satisfied.

The derivative of $W(t,x)$ along the solution trajectory of closed-loop system (6.1) using (6.8) is

$$
\begin{aligned}
\dot{W}(t,x) = & -\sum_{i=1}^{n} \dot{q}_i^T C_i^T(q_i, \dot{q}_i)M_i^{-1}(q_i)\chi_i - \sum_{i=1}^{n} \chi_i^T M_i^{-1}(q_i)\chi_i \\
& -\sum_{i=1}^{n} y_i^T M_i^{-1}(q_i)\chi_i + \sum_{i=1}^{n} \dot{q}_i^T \dot{\chi}_i.
\end{aligned}
$$

Note that $\dot{V} = 0$ implies $\dot{\hat{x}} = \mathbf{0}_{np}$, which in turn implies that $(S \otimes I_p)\dot{q} = \mathbf{0}_{np}$ according to (6.9) and $y_i = \mathbf{0}_p$ by noting that $y_i = P\dot{\hat{x}}_i$ according to (6.8b). Because $S \otimes I_p$ is symmetric positive definite, it follows that $\dot{q} = \mathbf{0}_{np}$. On the set $\{(\tilde{q}, \dot{q}, \dot{\hat{x}})|\dot{V} = 0\}$, $\dot{q} = \mathbf{0}_{np}$, $\dot{\hat{x}} = \mathbf{0}_{np}$, and $\dot{W}(t,x)$ becomes

$$\dot{W}(t,x) = -\sum_{i=1}^{n} \chi_i^T M_i^{-1}(q_i)\chi_i.$$

Therefore, the rest of the proof is similar to that of Theorem 6.2. We conclude that $q_i(t) - q_j(t) \to \check{q}_{ij}$ and $\dot{q}_i(t) \to \mathbf{0}_p$ as $t \to \infty$. ∎

Remark 6.4 Note that without the terms $-\sum_{j=1}^{n} b_{ij}(\dot{q}_i - \dot{q}_j)$ in (6.2), $-\sum_{j=1}^{n} b_{ij}\psi[K_{\dot{q}}(\dot{q}_i - \dot{q}_j)]$ in (6.6), and $\sum_{j=1}^{n} b_{ij}(q_i - q_j - \check{q}_{ij})$ in (6.8a), or equivalently $b_{ij} \equiv 0$, Theorems 6.1, 6.2, and 6.3 are still valid as long as the graph $\mathscr{G}_A$ is undirected connected. However, these terms introduce relative damping between neighboring agents.

6.2.4 Simulation

In this section, we simulate a scenario where six two-link revolute joint arms are coordinated through local interaction using, respectively, the algorithms (6.2), (6.6), and (6.8). For simplicity, we assume that each arm is identical. The Euler–Lagrange equation of each two-link revolute joint arm is given in [276, pp. 259–262]. In particular, the inertia matrix, the vector of Coriolis and centrifugal torques, and the vector of gravitational torques are given as

$$M_i(q_i) = \begin{bmatrix} \Theta_{i(1)} + 2\Theta_{i(2)}\cos[q_{i(2)}] & \Theta_{i(3)} + \Theta_{i(2)}\cos[q_{i(2)}] \\ \Theta_{i(3)} + \Theta_{i(2)}\cos[q_{i(2)}] & \Theta_{i(3)} \end{bmatrix},$$

$$C_i(q_i, \dot{q}_i) = \begin{bmatrix} -\Theta_{i(2)}\sin[q_{i(2)}]\dot{q}_{i(2)} & -\Theta_{i(2)}\sin[q_{i(2)}][\dot{q}_{i(1)} + \dot{q}_{i(2)}] \\ \Theta_{i(2)}\sin[q_{i(2)}]\dot{q}_{i(1)} & 0 \end{bmatrix},$$

$$g_i(q_i) = \begin{bmatrix} \Theta_{i(4)}g\cos[q_{i(1)}] + \Theta_{i(5)}g\cos[q_{i(1)} + q_{i(2)}] \\ \Theta_{i(5)}g\cos[q_{i(1)} + q_{i(2)}] \end{bmatrix},$$

where $q_i \triangleq [q_{i(1)}, q_{i(2)}]^T$, $g = 9.8$ m/s^2 is the acceleration due to gravity, $\Theta_i \triangleq [\Theta_{i(1)}, \Theta_{i(2)}, \Theta_{i(3)}, \Theta_{i(4)}, \Theta_{i(5)}] = [m_1 l_{c1}^2 + m_2(l_1^2 + l_{c2}^2) + J_1 + J_2, m_2 l_1 l_{c2}, m_2 l_{c2}^2 + J_2, m_1 l_{c1} + m_2 l_1, m_2 l_{c2}]$. Here the masses of links 1 and 2 are, respectively, $m_1 = 1$ kg and $m_2 = 0.8$ kg, the lengths of links 1 and 2 are, respectively, $l_1 = 0.8$ m and $l_2 = 0.6$ m, the distances from the previous joint to the center of mass of links 1 and 2 are, respectively, $l_{c1} = 0.4$ m and $l_{c2} = 0.3$ m, and the moments of inertia of links 1 and 2 are, respectively, $J_1 = 0.0533$ kg m^2 and $J_2 = 0.024$ kg m^2.

For simplicity, we assume that the graphs $\mathscr{G}_A$ and $\mathscr{G}_B$ are identical. Figure 6.1 shows $\mathscr{G}_A$ (equivalently, $\mathscr{G}_B$) for the six two-link revolute joint arms. Table 6.1 shows the control parameters for each algorithm. In simulation, we let $q_i(0) = [\frac{\pi}{7}i, \frac{\pi}{8}i]^T$ rad and $\dot{q}(0) = [0.1i - 0.4, -0.1i + 0.5]^T$ rad/s, where $i = 1, \ldots, 6$.
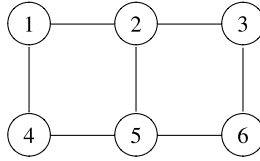
Fig. 6.1 Graph $\mathscr{G}_A$ (equivalently, $\mathscr{G}_B$) for the six two-link revolute joint arms. An *edge* between i and j denotes that agents i and j are neighbors. The *graph* is undirected connected

Table 6.1 Control parameters for each algorithm

Algorithm (6.2):
$K_i = I_2, a_{ij} = b_{ij} = 1$ if $(i, j) \in \mathscr{E}_A$ (or $\mathscr{E}_B$), $\breve{q}_{ij} = \mathbf{0}_2$
Algorithm (6.6):
$K_q = K_{\dot{q}} = K_i = K_{di} = I_2, a_{ij} = b_{ij} = 1$ if $(i, j) \in \mathscr{E}_A$(or $\mathscr{E}_B$), $\breve{q}_{ij} = \mathbf{0}_2$
Algorithm (6.8):
$\Gamma = -4I_2, \kappa = 0.2, P = I_2, K_q = 0.6I_2, a_{ij} = b_{ij} = 2$ if $(i, j) \in \mathscr{E}_A$ (or $\mathscr{E}_B$), $\breve{q}_{ij} = \mathbf{0}_2$
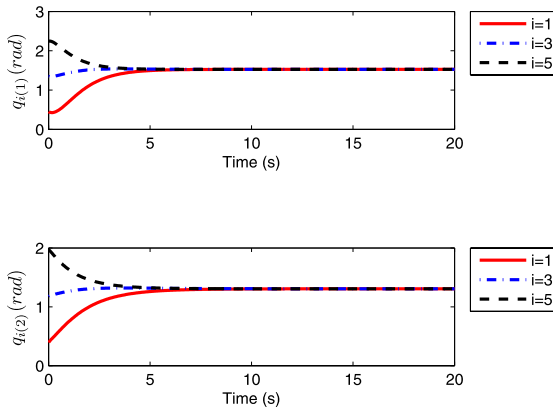
Fig. 6.2 Joint angles of arms 1, 3, and 5 using (6.2)

Figures 6.2, 6.3, and 6.4 show, respectively, the joint angles, their derivatives, and the control torques of arms 1, 3, and 5 using (6.2). Note that the joint angles of all arms achieve coordination while their derivatives converge to zero. Figures 6.5, 6.6, and 6.7 show, respectively, the joint angles, their derivatives, and the control torques of arms 1, 3, and 5 using (6.6), where $\psi(\cdot)$ is chosen as $\tanh(\cdot)$. Note that the joint angles of all arms achieve coordination while their derivatives converge to zero. Figures 6.8, 6.9, and 6.10 show, respectively, the joint angles, their derivatives, and the control torques of arms 1, 3, and 5 using (6.8). The initial conditions $\hat{x}_i(0)$ are chosen randomly. Note that the joint angles of all arms achieve coordination while their derivatives converge to zero even without measurements of absolute and relative joint angle derivatives.
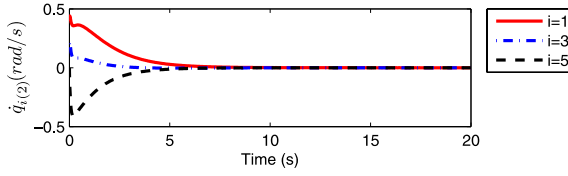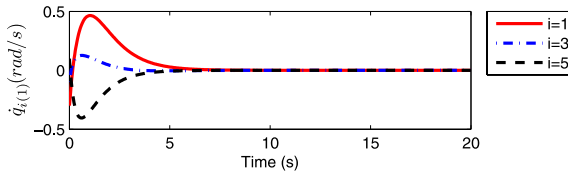
Fig. 6.3 Joint angle derivatives of arms 1, 3, and 5 using (6.2)
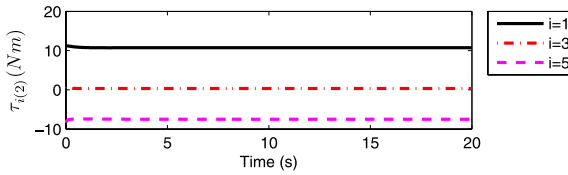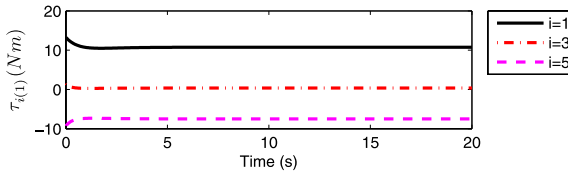
Fig. 6.4 Control torques of arms 1, 3, and 5 using (6.2)
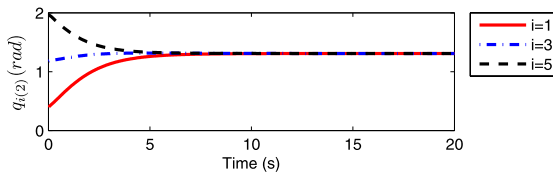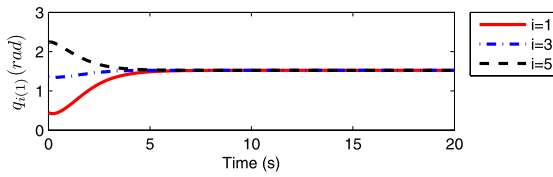
Fig. 6.5 Joint angles of arms 1, 3, and 5 using (6.6)
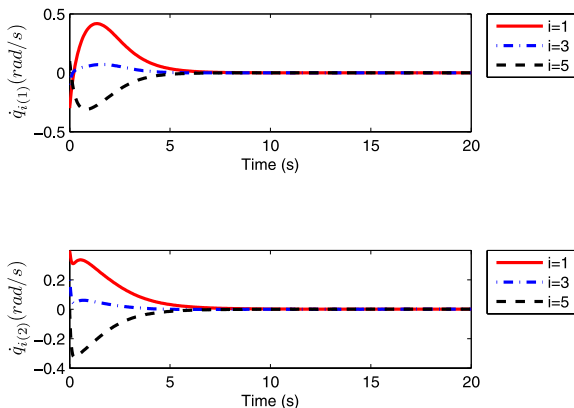
Fig. 6.6 Joint angle derivatives of arms 1, 3, and 5 using (6.6)
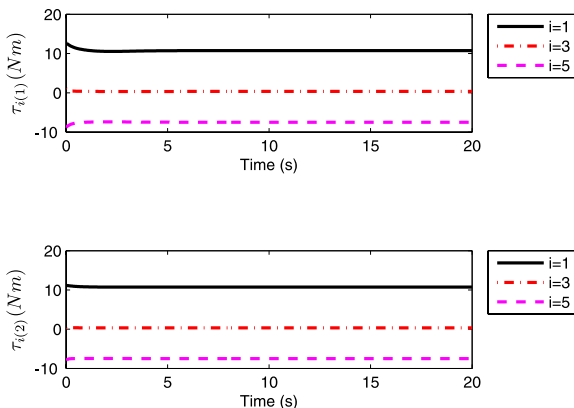
Fig. 6.7 Control torques of arms 1, 3, and 5 using (6.6)
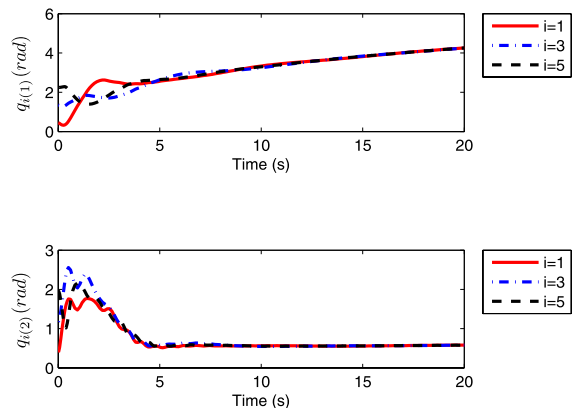
Fig. 6.8 Joint angles of arms 1, 3, and 5 using (6.8)
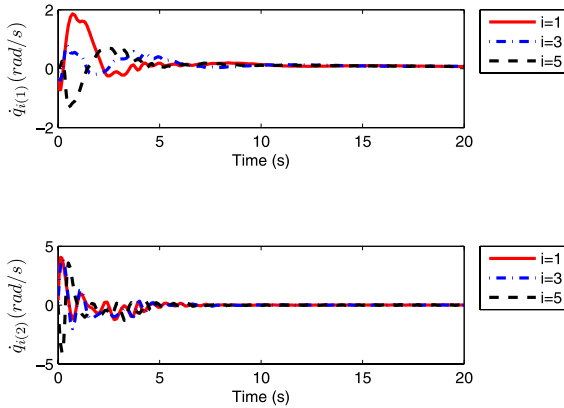
Fig. 6.9 Joint angle derivatives of arms 1, 3, and 5 using (6.8)
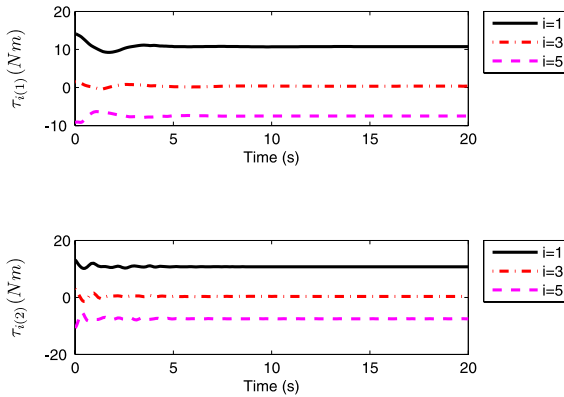
Fig. 6.10 Control torques of arms 1, 3, and 5 using (6.8)

6.3 Distributed Coordinated Regulation and Tracking for Networked Lagrangian Systems

Suppose that there exist n followers, labeled as agents 1 to n, and a leader, labeled as agent 0, in the team. Let $q_0 \in \mathbb{R}^p$ and $\dot{q}_0 \in \mathbb{R}^p$ denote, respectively, the leader's vector of generalized coordinates and vector of generalized coordinate derivatives.

Suppose that in addition to n followers, labeled as agents or followers 1 to n, there exists a leader, labeled as agent 0, in the team. Let $q_0 \in \mathbb{R}^p$ and $\dot{q}_0 \in \mathbb{R}^p$ denote, respectively, the leader's vector of generalized coordinates and vector of generalized coordinate derivatives.

6.3.1 Coordinated Regulation when the Leader's Vector of Generalized Coordinates is Constant

In this subsection, we assume that q_0 is constant (and hence $\dot{q}_0 = \mathbf{0}_p$). The objective here is to design distributed coordinated regulation algorithms for (6.1) such that $q_i(t) \to q_0$ and $\dot{q}_i(t) \to \mathbf{0}_p$ as $t \to \infty$.

We first consider a fundamental coordinated regulation algorithm as

$$\tau_i = g_i(q_i) - \sum_{j=0}^{n} a_{ij}(q_i - q_j) - \sum_{j=0}^{n} b_{ij}(\dot{q}_i - \dot{q}_j), \tag{6.10}$$

where $i = 1, \ldots, n$, $a_{ij}, i, j = 1, \ldots, n$, is the (i, j)th entry of the adjacency matrix $\mathscr{A} \in \mathbb{R}^{n \times n}$ associated with the graph $\mathscr{G}_A \triangleq (\mathscr{V}, \mathscr{E}_A)$ characterizing the interaction among the n followers for q_i, $b_{ij}, i, j = 1, \ldots, n$, is the (i, j)th entry of the adjacency matrix $\mathscr{B} \in \mathbb{R}^{n \times n}$ associated with the graph $\mathscr{G}_B \triangleq (\mathscr{V}, \mathscr{E}_B)$ characterizing the interaction among the n followers for $\dot{q}_i$, $a_{i0} > 0$ (respectively, $b_{i0} > 0$), $i = 1, \ldots, n$, if follower i has access to the vector of generalized coordinates of the leader (respectively, the vector of generalized coordinate derivatives of the leader) and $a_{i0} = 0$ (respectively, $b_{i0} = 0$) otherwise. Note that here $\dot{q}_0 = \mathbf{0}_p$. Also note that $\mathscr{G}_A$ and $\mathscr{G}_B$ are allowed to be different.

Theorem 6.5. *Using (6.10) for (6.1), $q_i(t) \to q_0$ and $\dot{q}_i(t) \to \mathbf{0}_p$, $i = 1, \ldots, n$, as $t \to \infty$ if both $\mathscr{G}_A$ and $\mathscr{G}_B$ are undirected connected, at least one follower has access to q_0 (i.e., at least one $a_{i0} > 0$), and at least one follower has access to $\dot{q}_0$ (i.e., at least one $b_{i0} > 0$).*

Proof: Let $\tilde{q}$ be a column stack vector of $q_i - q_0$, $i = 1, \ldots, n$. Let $\mathscr{L}_A$ and $\mathscr{L}_B$ be, respectively, the Laplacian matrix associated with $\mathscr{A}$ and hence $\mathscr{G}_A$ and $\mathscr{B}$ and hence $\mathscr{G}_B$. Let $H_A \triangleq \mathscr{L}_A + \mathrm{diag}(a_{10}, \ldots, a_{n0})$ and $H_B \triangleq \mathscr{L}_B + \mathrm{diag}(b_{10}, \ldots, b_{n0})$.

Using (6.10), (6.1) can be written as

$$\begin{aligned}
\frac{d}{dt}\tilde{q} &= \dot{q}, \\
\frac{d}{dt}\dot{q} &= -M^{-1}(q)\big[C(q, \dot{q})\dot{q} + (H_A \otimes I_p)\tilde{q} + (H_B \otimes I_p)\dot{q}\big].
\end{aligned} \tag{6.11}$$

Note that the system (6.11) with states $\tilde{q}$ and $\dot{q}$ is autonomous because $q = \tilde{q} + \mathbf{1}_n \otimes q_0$, where q_0 is constant. As a result, Lemma 1.31 can be applied to prove the theorem.

Consider the Lyapunov function candidate

$$V = \frac{1}{2}\tilde{q}^T(H_A \otimes I_p)\tilde{q} + \frac{1}{2}\dot{q}^T M(q)\dot{q}.$$

Because both $\mathscr{G}_A$ and $\mathscr{G}_B$ are undirected connected, at least one $a_{i0} > 0$, and at least one $b_{i0} > 0$, it follows from Lemma 1.6 that both H_A and H_B are symmetric

positive definite. Therefore, V is positive definite and radially bounded with respect to $\tilde{q}$ and $\dot{q}$. The derivative of V is given by

$$\dot{V} = \dot{\tilde{q}}^T (H_A \otimes I_p)\tilde{q} + \frac{1}{2}\ddot{q}^T M(q)\dot{q} + \frac{1}{2}\dot{q}^T \dot{M}(q)\dot{q} + \frac{1}{2}\dot{q}^T M(q)\ddot{q}$$

$$= \dot{q}^T (H_A \otimes I_p)\tilde{q} + \dot{q}^T M(q)\ddot{q} + \frac{1}{2}\dot{q}^T \dot{M}(q)\dot{q},$$

where we have used the fact that $M(q)$ is symmetric and $\dot{\tilde{q}} = \dot{q}$. Using (6.10), (6.1) can be written in a vector form as

$$M(q)\ddot{q} = -C(q, \dot{q})\dot{q} - (H_A \otimes I_p)\tilde{q} - (H_B \otimes I_p)\dot{q}. \tag{6.12}$$

Note that $\dot{M}(q) - 2C(q, \dot{q})$ is skew symmetric. By applying (6.12), the derivative of V can be written as

$$\dot{V} = -\dot{q}^T (H_B \otimes I_p)\dot{q} \leq 0.$$

On the set $\{(\tilde{q}, \dot{q})|\dot{V} = 0\}$, note that $\dot{V} \equiv 0$ implies $\dot{q} \equiv \mathbf{0}_{np}$, which in turn implies $(H_A \otimes I_p)\tilde{q} \equiv \mathbf{0}_{np}$ according to (6.12). Because H_A is symmetric positive definite, it follows that $\tilde{q} \equiv \mathbf{0}_{np}$. By Lemma 1.31, it follows that $\tilde{q}(t) \to \mathbf{0}_{np}$ and $\dot{q}(t) \to \mathbf{0}_{np}$ as $t \to \infty$, which in turn implies that $q_i(t) \to q_0$ and $\dot{q}_i(t) \to \mathbf{0}_p$ as $t \to \infty$. ∎

We next consider a nonlinear coordinated regulation algorithm as

$$\tau_i = g_i(q_i) - \sum_{j=0}^{n} a_{ij}\psi\big[K_q(q_i - q_j)\big] - \sum_{j=0}^{n} b_{ij}\psi\big[K_{\dot{q}}(\dot{q}_i - \dot{q}_j)\big], \tag{6.13}$$

where $i = 1, \ldots, n$, a_{ij} and b_{ij}, $i = 1, \ldots, n$, $j = 0, \ldots, n$, are defined as in (6.10), $K_q \in \mathbb{R}^{p \times p}$ and $K_{\dot{q}} \in \mathbb{R}^{p \times p}$ are positive-definite diagonal matrices, and $\psi(\cdot)$ is defined in Lemma 6.1.

Theorem 6.6. *Using* (6.13) *for* (6.1), $q_i(t) \to q_0$ *and* $\dot{q}_i(t) \to \mathbf{0}_p$, $i = 1, \ldots, n$, *as* $t \to \infty$ *if both* $\mathscr{G}_A$ *and* $\mathscr{G}_B$ *are undirected connected, at least one follower has access to* q_0 *(i.e., at least one* $a_{i0} > 0$*), and at least one follower has access to* $\dot{q}_0$ *(i.e., at least one* $b_{i0} > 0$*).*

Proof: Similar to the proof of Theorem 6.5, using (6.13), (6.1) can be written as an autonomous system with states $q_i - q_0$ and $\dot{q}_i$, $i = 1, \ldots, n$. Consider the Lyapunov function candidate

$$V = \frac{1}{2}\sum_{i=1}^{n} \dot{q}_i^T M_i(q_i)\dot{q}_i + \frac{1}{2}\sum_{i=1}^{n}\sum_{j=1}^{n} a_{ij} \sum_{\ell=1}^{p} \int_0^{q_{i(\ell)}(t) - q_{j(\ell)}(t)} \psi[K_{q(\ell)}\tau]\, d\tau$$

$$+ \sum_{i=1}^{n} a_{i0} \sum_{\ell=1}^{p} \int_0^{q_{i(\ell)}(t) - q_{0(\ell)}} \psi[K_{q(\ell)}\tau]\, d\tau.$$

Note that V is positive definite and radially unbounded with respect to $q_i - q_0$ and $\dot{q}_i$, $i = 1, \ldots, n$, under the condition of the theorem. The rest of the proof is similar to that of Theorem 6.2 by applying Lemma 1.31. ∎

We finally consider a coordinated regulation algorithm that removes the requirement for the measurements of generalized coordinate derivatives as

$$\dot{\hat{x}}_i = \Gamma \hat{x}_i + \sum_{j=0}^{n} b_{ij}(q_i - q_j), \tag{6.14a}$$

$$y_i = P\left[\Gamma \hat{x}_i + \sum_{j=0}^{n} b_{ij}(q_i - q_j) \right], \tag{6.14b}$$

$$\tau_i = g_i(q_i) - \sum_{j=0}^{n} a_{ij}\psi\big[K_q(q_i - q_j)\big] - y_i, \tag{6.14c}$$

where $i = 1, \ldots, n$, $\Gamma \in \mathbb{R}^{p \times p}$ is Hurwitz, a_{ij} and b_{ij}, $i = 1, \ldots, n, j = 0, \ldots, n$, are defined analogously to those in (6.10), and $P \in \mathbb{R}^{p \times p}$ is the symmetric positive-definite solution to the Lyapunov equation $\Gamma^T P + P\Gamma = -Q$ with $Q \in \mathbb{R}^{p \times p}$ being symmetric positive definite.

Theorem 6.7. *Using* (6.14) *for* (6.1), $q_i(t) \to q_0$ *and* $\dot{q}_i(t) \to \mathbf{0}_p$, $i = 1, \ldots, n$, *as* $t \to \infty$ *if both* $\mathscr{G}_A$ *and* $\mathscr{G}_B$ *are undirected connected, at least one follower has access to* q_0 *(i.e., at least one* $a_{i0} > 0$*), and at least one follower has access to* $\dot{q}_0$ *(i.e., at least one* $b_{i0} > 0$*).*

Proof: Similar to the proof of Theorem 6.5, using (6.14), (6.1) can be written as an autonomous system with states $q_i - q_0$, $\dot{q}_i$, and $\dot{\hat{x}}_i$, $i = 1, \ldots, n$. Consider the Lyapunov function candidate

$$V = \frac{1}{2}\sum_{i=1}^{n} \dot{q}_i^T M_i(q_i)\dot{q}_i + \frac{1}{2}\sum_{i=1}^{n}\sum_{j=1}^{n} a_{ij} \sum_{\ell=1}^{p} \int_{0}^{q_{i(\ell)}(t) - q_{j(\ell)}(t)} \psi[K_{q(\ell)}\tau]\,d\tau$$

$$+ \sum_{i=1}^{n} a_{i0} \sum_{\ell=1}^{p} \int_{0}^{q_{i(\ell)}(t) - q_{0(\ell)}} \psi[K_{q(\ell)}\tau]\,d\tau + \frac{1}{2}\dot{\hat{x}}^T (H_B \otimes I_p)^{-1}(I_n \otimes P)\dot{\hat{x}},$$

where $\hat{x} \triangleq [\hat{x}_1^T, \ldots, \hat{x}_n^T]^T$ and $H_B \triangleq \mathscr{L}_B + \text{diag}(b_{10}, \ldots, b_{n0})$. Note that V is positive definite and radially unbounded with respect to $q_i - q_0$, $\dot{q}_i$, $i = 1, \ldots, n$, and $\dot{\hat{x}}$ under the condition of the theorem. The rest of the proof is similar to that of Theorem 6.3 by applying Lemma 1.31. ∎

Remark 6.8 Let $\overline{\mathscr{G}}_A \triangleq (\overline{\mathscr{V}}, \overline{\mathscr{E}}_A)$ and $\overline{\mathscr{G}}_B \triangleq (\overline{\mathscr{V}}, \overline{\mathscr{E}}_B)$ be, respectively, the directed graph characterizing the interaction among the leader and the followers corresponding to, respectively, $\mathscr{G}_A$ and $\mathscr{G}_B$. From the proofs of Theorems 6.5, 6.6, and 6.7, it can be seen that all conclusions of the theorems still hold as long as $\mathscr{G}_A$ and $\mathscr{G}_B$ are undirected and in $\overline{\mathscr{G}}_A$ and $\overline{\mathscr{G}}_B$ the leader has directed paths to all followers or equivalently H_A and H_B are symmetric positive definite (see Lemma 1.6).

6.3.2 Coordinated Tracking when the Leader's Vector of Generalized Coordinate Derivatives is Constant

In this subsection, we assume that $\dot{q}_0$ is constant. The objective here is to design distributed coordinated tracking algorithms for (6.1) such that $q_i(t) - q_0(t) \to \mathbf{0}_p$ and $\dot{q}_i(t) \to \dot{q}_0$ as $t \to \infty$. Before moving on, we need the following lemma.

Lemma 6.2. *For differentiable vectors x, y, and $z \in \mathbb{R}^p$, under Assumption* (A1)*, $\dot{C}_i(x, y)z$ is bounded if all vectors $\dot{x}$, $\dot{y}$, y, and z are bounded.*

Proof: Let $e_j \in \mathbb{R}^p$ denote the vector with 1 as its jth component and 0 elsewhere. Let $C_{i(k,m)}(x, y)$ be the (k, m)th entry of $C_i(x, y)$. For $x \triangleq [x_1, \ldots, x_p]^T \in \mathbb{R}^p$, $y \triangleq [y_1, \ldots, y_p]^T \in \mathbb{R}^p$, and $z \in \mathbb{R}^p$, we have

$$
\begin{aligned}
\dot{C}_{i(k,m)}(x, y) &= \sum_{j=1}^{p} \left[\frac{\partial C_{i(k,m)}(x, y)}{\partial x_j} \dot{x}_j + \frac{\partial C_{i(k,m)}(x, y)}{\partial y_j} \dot{y}_j \right] \\
&= \lim_{\varepsilon \to 0} \sum_{j=1}^{p} \left[\frac{C_{i(k,m)}(x + \varepsilon e_j, y) - C_{i(k,m)}(x, y)}{\varepsilon} \dot{x}_j \right. \\
&\quad \left. + \frac{C_{i(k,m)}(x, y + \varepsilon e_j) - C_{i(k,m)}(x, y)}{\varepsilon} \dot{y}_j \right].
\end{aligned}
$$

It thus follows that

$$
\begin{aligned}
\left\| \dot{C}_i(x, y)z \right\| &= \left\| \begin{bmatrix} \dot{C}_{i(1,1)}(x, y) & \cdots & \dot{C}_{i(1,p)}(x, y) \\ \vdots & \ddots & \vdots \\ \dot{C}_{i(p,1)}(x, y) & \cdots & \dot{C}_{i(p,p)}(x, y) \end{bmatrix} z \right\| \\
&= \left\| \lim_{\varepsilon \to 0} \sum_{j=1}^{p} \left[\frac{C_i(x + \varepsilon e_j, y) - C_i(x, y)}{\varepsilon} \dot{x}_j z \right. \right. \\
&\quad \left. \left. + \frac{C_i(x, y + \varepsilon e_j) - C_i(x, y)}{\varepsilon} \dot{y}_j z \right] \right\| \\
&\leq \lim_{\varepsilon \to 0} \sum_{j=1}^{p} \left[\frac{\| C_i(x + \varepsilon e_j, y)z - C_i(x, y)z \| |\dot{x}_j|}{|\varepsilon|} \right. \\
&\quad \left. + \frac{\| C_i(x, y + \varepsilon e_j)z - C_i(x, y)z \| |\dot{y}_j|}{|\varepsilon|} \right] \\
&\leq \sum_{j=1}^{p} \left(k_{C_2} \|y\| \|z\| |\dot{x}_j| + k_{C_1} \|z\| |\dot{y}_j| \right) \\
&= k_{C_2} \|y\| \|z\| \|\dot{x}\|_1 + k_{C_1} \|z\| \|\dot{y}\|_1, \tag{6.15}
\end{aligned}
$$

where we have used Assumption (A1) to obtain the second inequality. From (6.15), if all vectors $\dot{x}$, $\dot{y}$, y, and z are bounded, it follows that $\dot{C}_i(x, y)z$ is bounded. ∎

6.3.2.1 Model-dependent Coordinated Tracking Algorithm

In this subsection, we propose a distributed model-dependent coordinated tracking algorithm for (6.1) as

$$\tau_i = \tau_{i1} + \tau_{i2} + \tau_{i3}, \tag{6.16a}$$

$$\tau_{i1} = -\sum_{j=0}^{n} a_{ij}(q_i - q_j), \tag{6.16b}$$

$$\tau_{i2} = -\sum_{j=1}^{n} c_{ij}\big[(\dot{q}_i - \hat{v}_i) - (\dot{q}_j - \hat{v}_j)\big] - c_{i0}(\dot{q}_i - \hat{v}_i), \tag{6.16c}$$

$$\tau_{i3} = M_i(q_i)\dot{\hat{v}}_i + C_i(q_i, \dot{q}_i)\hat{v}_i + g_i(q_i), \tag{6.16d}$$

$$\dot{\hat{v}}_i = -\sum_{j=1}^{n} b_{ij}(\hat{v}_i - \hat{v}_j) - b_{i0}(\hat{v}_i - \dot{q}_0), \tag{6.16e}$$

where $i = 1, \ldots, n$, a_{ij} (respectively, b_{ij} and c_{ij}), $i, j = 1, \ldots, n$, is the (i, j)th entry of the adjacency matrix $\mathscr{A} \in \mathbb{R}^{n \times n}$ (respectively, $\mathscr{B} \in \mathbb{R}^{n \times n}$ and $\mathscr{C} \in \mathbb{R}^{n \times n}$) associated with the graph $\mathscr{G}_A \triangleq (\mathscr{V}, \mathscr{E}_A)$ [respectively, $\mathscr{G}_B \triangleq (\mathscr{V}, \mathscr{E}_B)$ and $\mathscr{G}_C \triangleq (\mathscr{V}, \mathscr{E}_C)$] characterizing the interaction among the n followers for q_i (respectively, $\hat{v}_i$ and $\dot{q}_i - \hat{v}_i$), $a_{i0} > 0$ (respectively, $b_{i0} > 0$ and $c_{i0} > 0$) if in $\overline{\mathscr{G}}_A$ (respectively, $\overline{\mathscr{G}}_B$ and $\overline{\mathscr{G}}_C$) the leader is a neighbor of the follower and $a_{i0} = 0$ (respectively, $b_{i0} = 0$ and $c_{i0} = 0$) otherwise, and $\hat{v}_i$ is the ith follower's estimate of the leader's vector of generalized coordinate derivatives. Here $\overline{\mathscr{G}}_A$ (respectively, $\overline{\mathscr{G}}_B$ and $\overline{\mathscr{G}}_C$) is the directed graph characterizing the interaction among the leader and the followers corresponding to $\mathscr{G}_A$ (respectively, $\mathscr{G}_B$ and $\mathscr{G}_C$). Here (6.16b) is used to drive the vector of generalized coordinates of follower i to track those of the followers and the leader who are its neighbors, (6.16c) is used to drive the vector of generalized coordinate derivatives of follower i to track $\hat{v}_i$, (6.16d) is the compute-torque control with compensation, and (6.16e) is used to estimate the leader's vector of generalized coordinate derivatives.

Before presenting our main results, we need the following lemmas.

Lemma 6.3. *If $\mathscr{G}_B$ is undirected connected, and at least one follower has access to the constant $\dot{q}_0$ (i.e., at least one $b_{i0} > 0$), using (6.16e), $\hat{v}_i(t) \to \dot{q}_0$ exponentially as $t \to \infty$.*

Proof: Let $\bar{v}_i \triangleq \hat{v}_i - \dot{q}_0$ and $\bar{v} \triangleq [\bar{v}_1^T, \ldots, \bar{v}_n^T]^T$. Note that $\ddot{q}_0 = 0$ because $\dot{q}_0$ is constant. Then (6.16e) can be written as $\dot{\bar{v}}_i = -\sum_{j=0}^{n} b_{ij}(\bar{v}_i - \bar{v}_j)$, which can be written in a vector form as

$$\dot{\bar{v}} = -(\mathscr{L}_B \otimes I_p)\bar{v} - \big[\text{diag}(b_{10}, \ldots, b_{n0}) \otimes I_p\big]\bar{v} = -(H_B \otimes I_p)\bar{v}, \tag{6.17}$$

where $\mathscr{L}_B$ is the Laplacian matrix associated with $\mathscr{B}$ and hence $\mathscr{G}_B$, $H_B \stackrel{\triangle}{=} \mathscr{L}_B + \mathrm{diag}(b_{10}, \ldots, b_{n0})$, and we have used Lemma 1.21 to obtain the last equality.

Because $\mathscr{G}_B$ is undirected connected and at least one $b_{i0} > 0$, we conclude from Lemma 1.6 that H_B is symmetric positive definite, which means that $\lambda_{\min}(H_B) > 0$. Consider the Lyapunov function candidate $V_0 = \frac{1}{2}\bar{v}^T \bar{v}$. The derivative of V_0 is given by

$$\dot{V}_0 = -\bar{v}^T (H_B \otimes I_p)\bar{v} \le -\lambda_{\min}(H_B)\bar{v}^T \bar{v} = -2\lambda_{\min}(H_B)V_0,$$

After some manipulation, we can get

$$V_0(t) \le V_0(0)e^{-2\lambda_{\min}(H_B)t}. \tag{6.18}$$

Therefore, $\bar{v} = \mathbf{0}_{np}$ is globally exponentially stable, which implies that $\hat{v}_i(t) \to \dot{q}_0$ exponentially as $t \to \infty$. ■

Lemma 6.4 ([225]). *Consider the following cascade system*

$$\dot{x} = f(t, x) + h(x, \xi), \ f(t, 0) = 0, h(x, 0) = 0, \tag{6.19}$$
$$\dot{\xi} = A\xi, \quad (x, \xi) \in \mathbb{R}^n \times \mathbb{R}^m, \tag{6.20}$$

where $f(t, x)$ is continuously differentiable in (t, x), and $h(x, \xi)$ is locally Lipschitz in (x, ξ). When $\xi = 0$, (6.19) can be written as

$$\dot{x} = f(t, x). \tag{6.21}$$

If (6.21) has the origin as a globally asymptotically stable equilibrium, A is Hurwitz, and all solutions of (6.19) and (6.20) are bounded, then the cascade system is globally asymptotically stable at the origin.

We have the following theorem in the case of a constant $\dot{q}_0$.

Theorem 6.9. *Using (6.16) for (6.1), if $\mathscr{G}_A$, $\mathscr{G}_B$, and $\mathscr{G}_C$ are all undirected connected, at least one $a_{i0} > 0$, at least one $b_{i0} > 0$, and at least one $c_{i0} > 0$, $q_i(t) - q_0(t) \to \mathbf{0}_p$, and $\dot{q}_i(t) \to \dot{q}_0$, $i = 1, \ldots, n$, as $t \to \infty$.*

Proof: Let $\tilde{q}$ and $\hat{v}$ be, respectively, a column stack vector of $q_i - q_0$ and $\hat{v}_i$, $i = 1, \ldots, n$. Define $\tilde{v} \stackrel{\triangle}{=} \dot{q} - \hat{v}$. Let $\bar{v}$ be defined in the proof of Lemma 6.3. Note that $\bar{v} = \hat{v} - \mathbf{1}_n \otimes \dot{q}_0$. Using (6.16), (6.1) can be written in a vector form as

$$M(q)\dot{\tilde{v}} = -C(q, \dot{q})\tilde{v} - (H_A \otimes I_p)\tilde{q} - (H_c \otimes I_p)\tilde{v}, \tag{6.22}$$

where $H_A \stackrel{\triangle}{=} \mathscr{L}_A + \mathrm{diag}(a_{10}, \ldots, a_{n0})$ and $H_C \stackrel{\triangle}{=} \mathscr{L}_C + \mathrm{diag}(c_{10}, \ldots, c_{n0})$ with $\mathscr{L}_A$ and $\mathscr{L}_C$ being, respectively, the Laplacian matrix associated with $\mathscr{A}$ and hence $\mathscr{G}_A$ and $\mathscr{C}$ hence $\mathscr{G}_C$. Let $x_1 \stackrel{\triangle}{=} \tilde{q}$, $x_2 \stackrel{\triangle}{=} \tilde{v}$, $x \stackrel{\triangle}{=} [x_1^T, x_2^T]^T$, and $\xi \stackrel{\triangle}{=} \bar{v}$. Equations (6.22) and (6.17) can be written as

$$\dot{x} = \underbrace{\begin{bmatrix} x_2 \\ -M^{-1}(q)[(H_A \otimes I_p)x_1 + Qx_2] \end{bmatrix}}_{f(t,x)} + \underbrace{\begin{bmatrix} \xi \\ \mathbf{0}_{np} \end{bmatrix}}_{h(x,\xi)}, \quad (6.23)$$

$$\dot{\xi} = \underbrace{-(H_B \otimes I_p)}_{A}\xi, \quad (6.24)$$

where $Q \triangleq C(q,\dot{q}) + H_C \otimes I_p$, H_B is defined in (6.17), and we have used the fact that $\dot{x}_1 = \dot{q} - \mathbf{1}_n \otimes \dot{q}_0 = \tilde{v} + \hat{v} - \mathbf{1}_n \otimes \dot{q}_0 = x_2 + \xi$. Note that $q = x_1 + \mathbf{1}_n \otimes q_0$ and that $\dot{q}$ in $C(q,\dot{q})$ and hence in Q is not treated as a state but as a function of t. Hence, (6.23) and (6.24) takes in the form of the cascade system (6.19) and (6.20), and

$$\dot{x} = \underbrace{\begin{bmatrix} x_2 \\ -M^{-1}(q)[(H_A \otimes I_p)x_1 + Qx_2] \end{bmatrix}}_{f(t,x)} \quad (6.25)$$

takes in the form of (6.21).

First, we show that all solutions of (6.23) and (6.24) are bounded. Note that $\mathscr{G}_B$ is undirected connected and at least one $b_{i0} > 0$. From Lemma 6.3, noting that $\xi \equiv \bar{v}$, we get that the solution of (6.24) (i.e., ξ) is bounded. Consider the Lyapunov function candidate as

$$V(t,x) = \frac{1}{2}x_1^T(H_A \otimes I_p)x_1 + \frac{1}{2}x_2^T M(q)x_2. \quad (6.26)$$

Because $\mathscr{G}_A$ is undirected connected and at least one $a_{i0} > 0$, it follows from Lemma 1.6 that H_A is symmetric positive definite. Also note that $M(q)$ in symmetric positive definite. It follows from Assumption (A1) that $V(t,x)$ is positive definite. Therefore, we have

$$V \geq \frac{1}{2}\lambda_{\min}(H_A)\|x_1\|^2 + \frac{1}{2}k_{\underline{m}}\|x_2\|^2$$
$$\geq \frac{1}{2}\min\left[\lambda_{\min}(H_A), k_{\underline{m}}\right]\|x\|^2, \quad (6.27)$$

and

$$\left\|\frac{\partial V}{\partial x}\right\| = \left\|\left\{\left[(H_A \otimes I_p)x_1\right]^T, \left[M(q)x_2\right]^T\right\}^T\right\|$$
$$\leq \max\left[\lambda_{\max}(H_A), k_{\bar{m}}\right]\|\bar{x}\| \leq \gamma\sqrt{V}, \quad (6.28)$$

where $\gamma \triangleq \frac{\sqrt{2}\max[\lambda_{\max}(H_A), k_{\bar{m}}]}{\sqrt{\min[\lambda_{\min}(H_A), k_{\underline{m}}]}}$, and we have used Assumption (A1) to obtain (6.27) and have used (6.27) and Assumption (A1) again to obtain (6.28).

The derivative of V along (6.25) is

$$\dot{V}_{(6.25)} = \frac{\partial V}{\partial t} + \frac{\partial V}{\partial x} f(t, x) = \dot{x}_1^T (H_A \otimes I_p) x_1 + \frac{1}{2} x_2^T \dot{M}(q) x_2 + x_2^T M(q) \dot{x}_2$$

$$= x_2^T (H_A \otimes I_p) x_1 + x_2^T \left[\frac{1}{2} \dot{M}(q) - C(q, \dot{q}) \right] x_2$$

$$- x_2^T \left[(H_A \otimes I_p) x_1 + (H_C \otimes I_p) x_2 \right] = -x_2^T (H_C \otimes I_p) x_2, \quad (6.29)$$

where we have used Assumption (A2) to obtain the last equality. Because $\mathscr{G}_C$ is undirected connected and at least one $c_{i0} > 0$, it follows from Lemma 1.6 that H_C is symmetric positive definite. Therefore, it follows that $\dot{V}_{(6.25)} \leq 0$. Note that

$$\left\| h(x, \xi) \right\| = \left\| \begin{bmatrix} \xi \\ \mathbf{0}_{np} \end{bmatrix} \right\| = \| \xi \|. \quad (6.30)$$

Then, the derivative of V along (6.23) can be written as

$$\dot{V}_{(6.23)} = \frac{\partial V}{\partial t} + \frac{\partial V}{\partial x} f(t, x) + \frac{\partial V}{\partial x} h(x, \xi) = \dot{V}_{(6.25)} + \frac{\partial V}{\partial x} h(x, \xi)$$

$$\leq \left\| \frac{\partial V}{\partial x} \right\| \left\| h(x, \xi) \right\| \leq \gamma \| \xi \| \sqrt{V}, \quad (6.31)$$

where we have used (6.28) and (6.30) to obtain the last inequality. From (6.18), noting that $\xi \equiv \bar{v}$, we can get

$$\int_0^t \left\| \xi(\tau) \right\| d\tau \leq \left\| \xi(0) \right\| \int_0^t e^{-\lambda_{\min}(H_B) \tau} d\tau$$

$$= \frac{\| \xi(0) \|}{\lambda_{\min}(H_B)} \left[1 - e^{-\lambda_{\min}(H_B) t} \right]. \quad (6.32)$$

Note that (6.31) is equivalent to the following inequality

$$\frac{\dot{V}}{\sqrt{V}} \leq \gamma \| \xi \|. \quad (6.33)$$

Integrating both sides of (6.33) from 0 to $t > 0$ and after some manipulation, we obtain

$$\sqrt{V(t, x(t))} \leq \sqrt{V(0, x(0))} + \frac{\gamma}{2} \int_0^t \left\| \xi(\tau) \right\| d\tau$$

$$\leq \sqrt{V(0, x(0))} + \frac{\gamma \| \xi(0) \|}{2 \lambda_{\min}(H_B)}, \quad (6.34)$$

where we have used (6.32) to get the last inequality. From (6.34), we can conclude that $V(t, x)$ is uniformly bounded along the solution of (6.23). It thus follows that the solution of (6.23) (i.e., x_1 and x_2) is bounded.

Second, we show that the system (6.25) is globally asymptotically stable at the origin. Note that from the fact that $V(t, x)$ is positive definite and the fact that

$\dot{V}_{(6.25)} \le 0$ that x_1 and x_2 are bounded in the system (6.25). It thus follows that $\dot{x}_1$ is bounded because $\dot{x}_1 = x_2$ in (6.25). Also note that $\bar{v}$ is bounded from (6.18), $\hat{v}$ is bounded from $\hat{v} = \bar{v} + \mathbf{1}_n \otimes \dot{q}_0$ and the fact that $\dot{q}_0$ is constant, and $\dot{q}$ is bounded from $\dot{q} = x_2 + \hat{v}$. Because $M^{-1}(q)$ is bounded and $C(q, \dot{q})x_2$ is bounded if $\dot{q}$ and x_2 are bounded from Assumption (A1), we can conclude that $\dot{x}_2$ is bounded from (6.25). Thus, we have explicitly shown that all vectors x_1, x_2, $\dot{x}_1$, $\dot{x}_2$, and $\dot{q}$ are bounded. By differentiating $\dot{V}_{(6.25)}$, we can see that $\ddot{V}_{(6.25)}$ is bounded. Therefore, $\dot{V}_{(6.25)}$ is uniformly continuous in time. From Lemma 1.33, we get that $\dot{V}_{(6.25)}(t) \to 0$ as $t \to \infty$. Then from (6.29), we get that $x_2(t) \to \mathbf{0}_{np}$ as $t \to \infty$ because H_C is symmetric positive definite. The second equation in (6.25) can be written as

$$M(q)\dot{x}_2 = -(H_A \otimes I_p)x_1 - Qx_2. \tag{6.35}$$

Differentiating (6.35), we get

$$M(q)\ddot{x}_2 + \dot{M}(q)\dot{x}_2 = -(H_A \otimes I_p)\dot{x}_1 - Q\dot{x}_2 - \dot{C}(q, \dot{q})x_2, \tag{6.36}$$

where we have used the fact that $\dot{Q} = \dot{C}(q, \dot{q})$. From Assumption (A2), we can obtain that $\dot{M}(q) = C(q, \dot{q}) + C^T(q, \dot{q})$. From the proceeding boundedness statements, we can conclude that $\dot{M}(q)\dot{x}_2$ is bounded because $C(q, \dot{q})\dot{x}_2$ is bounded and $\dot{C}(q, \dot{q})x_2$ is bounded from Lemma 6.2. Then from (6.36), it follows that $\ddot{x}_2$ is bounded, which means that $\dot{x}_2$ is uniformly continuous. From Lemma 1.33, we get that $\dot{x}_2(t) \to \mathbf{0}_{np}$ as $t \to \infty$. Because both $x_2(t) \to \mathbf{0}_{np}$ and $\dot{x}_2(t) \to \mathbf{0}_{np}$ as $t \to \infty$, according to (6.35), we can obtain that $(H_A \otimes I_p)x_1(t) \to \mathbf{0}_{np}$ as $t \to \infty$. Note that H_A is symmetric positive definite. It thus follows that $x_1(t) \to \mathbf{0}_{np}$ as $t \to \infty$. Also because V given by (6.26) is radially unbounded with respect to x, it follows that (6.25) is globally asymptotically stable at the origin.

Third, it follows from Lemma 1.6 that A in (6.24) is Hurwitz. We conclude from Lemma 6.4 that the cascade system (6.23) and (6.24) is globally asymptotically stable at the origin, i.e., $x_1(t) \to \mathbf{0}_{np}$, $x_2(t) \to \mathbf{0}_{np}$ and $\xi(t) \to \mathbf{0}_{np}$ as $t \to \infty$. Note that $x_1 = q - \mathbf{1}_n \otimes q_0$. We can get $q_i(t) - q_0(t) \to \mathbf{0}_{np}$, $i = 1, \dots, n$, as $t \to \infty$. Also note that $x_2 = \dot{q} - \mathbf{1}_n \otimes \dot{q}_0 - \xi$. We can conclude that $\dot{q}_i(t) \to \dot{q}_0$, $i = 1, \dots, n$, as $t \to \infty$ because $x_2(t) \to \mathbf{0}_{np}$ and $\xi(t) \to \mathbf{0}_{np}$ as $t \to \infty$. ∎

Remark 6.10 We here show that the conditions in Theorem 6.9 can be relaxed. In fact, the conclusion of Theorem 6.9 holds as long as H_A is symmetric positive definite, $-H_B$ is Hurwitz,[2] and H_C is symmetric positive definite. Lemma 1.6 implies that if $\mathscr{G}_A$ (respectively, $\mathscr{G}_C$) is undirected and in $\overline{\mathscr{G}}_A$ (respectively, $\overline{\mathscr{G}}_C$) the leader has directed paths to all followers, then H_A (respectively, H_C) is symmetric positive definite. Also, in $\overline{\mathscr{G}}_B$, if the leader has directed paths to all followers, then $-H_B$ is Hurwitz. Note that here $\mathscr{G}_B$ can be directed. Therefore, the connectivity conditions in Theorem 6.9 can be relaxed.

---

[2] If $-H_B$ is Hurwitz, so is $-H_B \otimes I_p$. It thus follows that in (6.17) $\bar{v} = \mathbf{0}_{np}$ is globally exponentially stable even if H_B might not be symmetric.

6.3.2.2 Coordinated Tracking Algorithm Accounting for Parametric Uncertainties

In this subsection, we present a distributed coordinated tracking algorithm that accounts for unknown parametric uncertainties of the Euler–Lagrange dynamics. Before moving on, we introduce the following auxiliary variables

$$\dot{q}_{ri} \triangleq \hat{v}_i - \alpha \left[\sum_{j=0}^{n} a_{ij}(q_i - q_j) \right], \tag{6.37}$$

$$s_i \triangleq \dot{q}_i - \dot{q}_{ri} = \dot{q}_i - \hat{v}_i + \alpha \left[\sum_{j=0}^{n} a_{ij}(q_i - q_j) \right], \tag{6.38}$$

where $i = 1, \ldots, n$, α is a positive constant, $\hat{v}_i$ is the ith follower's estimate of the leader's vector of generalized coordination derivatives, $a_{ij}, i, j = 1, \ldots, n$, is the (i, j)th entry of the adjacency matrix $\mathscr{A}$ associated with the graph $\mathscr{G}_A \triangleq (\mathscr{V}, \mathscr{E}_A)$ characterizing the interaction among the n followers for q_i (and $\dot{q}_i$ as shown later on), and $a_{i0} > 0$ if the leader has access to q_0 (and $\dot{q}_0$ as shown later on) and $a_{i0} = 0$ otherwise. From Assumption (A3), we get

$$M_i(q_i)\ddot{q}_{ri} + C_i(q_i, \dot{q}_i)\dot{q}_{ri} + g_i(q_i) = Y_i(q_i, \dot{q}_i, \dot{q}_{ri}, \ddot{q}_{ri})\Theta_i,$$

where $i = 1, \ldots, n$, and Θ_i is the unknown constant parameter vector for the ith follower defined in Assumption (A3).

We propose the following coordinated tracking algorithm for (6.1) in the presence of parametric uncertainties

$$\tau_i = -K_i s_i - \eta(\dot{q}_i - \hat{v}_i) + Y_i \widehat{\Theta}_i, \tag{6.39a}$$

$$\dot{\hat{v}}_i = -\sum_{j=1}^{n} b_{ij}(\hat{v}_i - \hat{v}_j) - b_{i0}(\hat{v}_i - \dot{q}_0), \tag{6.39b}$$

where K_i is a symmetric positive-definite matrix, η is a positive constant, $Y_i \triangleq Y_i(q_i, \dot{q}_i, \dot{q}_{ri}, \ddot{q}_{ri})$, $\widehat{\Theta}_i$ is the estimate of Θ_i, and $b_{ij}, i = 1, \ldots, n, j = 0, \ldots, n$, is defined in (6.16e). Here $\widehat{\Theta}_i$ is updated by the following adaptation law

$$\dot{\widehat{\Theta}}_i = -\Lambda_i Y_i^T s_i, \tag{6.40}$$

where Λ_i is a symmetric positive-definite matrix. Let $\widetilde{\Theta}_i \triangleq \Theta_i - \widehat{\Theta}_i$, and $\widetilde{\Theta}, \Theta, \widehat{\Theta}$, $s, \tilde{q}$, and $\hat{v}$ be, respectively, the column stack vector of $\widetilde{\Theta}_i, \Theta_i, \widehat{\Theta}_i, s_i, \tilde{q}_i \triangleq q_i - q_0$, and $\hat{v}_i, i = 1, \ldots, n$. Note from (6.38) that $\dot{q}_i - \hat{v}_i = s_i - \alpha \sum_{j=0}^{n} a_{ij}(q_i - q_j)$. Hence, the closed-loop system (6.1) using (6.39a) can be written in a vector form as

$$M(q)\dot{s} = -C(q,\dot{q})s - Ks - \eta\big[s - \alpha(H_A \otimes I_p)\tilde{q}\big] - Y\widetilde{\Theta}, \qquad (6.41)$$

where H_A is defined as in (6.22), $Y \triangleq \operatorname{diag}(Y_1, \ldots, Y_n)$, and $K \triangleq \operatorname{diag}(K_1, \ldots, K_n)$.

Theorem 6.11. *Using (6.39) and (6.40) for (6.1), if both $\mathscr{G}_A$ and $\mathscr{G}_B$ are undirected connected, at least one $a_{i0} > 0$, and at least one $b_{i0} > 0$, $q_i(t) - q_0(t) \to \mathbf{0}_p$ and $\dot{q}_i(t) \to \dot{q}_0$, $i = 1, \ldots, n$, as $t \to \infty$ in the presence of parametric uncertainties.*

Proof: Let $x_1 \triangleq \tilde{q}$, $x_2 \triangleq s$, $x \triangleq [x_1^T, x_2^T]^T$, and $\xi \triangleq \hat{v} - \mathbf{1}_n \otimes \dot{q}_0$. Equations (6.41) and (6.39b) can be written as

$$\dot{x} = \underbrace{\begin{bmatrix} x_2 - \alpha(H_A \otimes I_p)x_1 \\ -M^{-1}(q)\big[-\eta\alpha(H_A \otimes I_p)x_1 + Qx_2 + Y\widetilde{\Theta}\big] \end{bmatrix}}_{f(t,x)} + \underbrace{\begin{bmatrix} \xi \\ \mathbf{0}_{np} \end{bmatrix}}_{h(x,\xi)}, \quad (6.42)$$

$$\dot{\xi} = \underbrace{-(H_B \otimes I_p)}_{A}\xi, \qquad (6.43)$$

where $Q \triangleq C(q,\dot{q}) + K + \eta I_n \otimes I_p$ and H_B is defined as in (6.17). Note that $q = x_1 + \mathbf{1}_n \otimes q_0$ and that $\dot{q}$ and $\widetilde{\Theta}$ in (6.42) are not treated as states, but as functions of t. Hence, (6.42) and (6.43) take in the form of the cascade system (6.19) and (6.20), and

$$\dot{x} = \begin{bmatrix} x_2 - \alpha(H_A \otimes I_p)x_1 \\ -M^{-1}(q)\big[-\eta\alpha(H_A \otimes I_p)x_1 + Qx_2 + Y\widetilde{\Theta}\big] \end{bmatrix} \qquad (6.44)$$

takes in the form of (6.21).

First, we will show that all solutions of (6.42) and (6.43) are bounded. Because $\mathscr{G}_A$ (respectively, $\mathscr{G}_B$) is undirected connected and at least one $a_{i0} > 0$ (respectively, $b_{i0} > 0$), it follows from Lemma 1.6 that H_A (respectively, H_B) is symmetric positive definite. We get that the solution of (6.43) (i.e., ξ) is bounded. Consider a nonnegative scalar function as

$$V(t,x) = \frac{\eta\alpha}{2}x_1^T(H_A \otimes I_p)x_1 + \frac{1}{2}x_2^T M(q)x_2 + \frac{1}{2}\widetilde{\Theta}^T \Xi \widetilde{\Theta}, \qquad (6.45)$$

where $\Xi \triangleq \operatorname{diag}(\Lambda_1^{-1}, \ldots, \Lambda_n^{-1})$ is symmetric positive definite. We have

$$V \geq \frac{\eta\alpha}{2}\lambda_{\min}(H_A)\|x_1\|^2 + \frac{1}{2}\underline{k_m}\|x_2\|^2$$
$$\geq \frac{1}{2}\min\big[\eta\alpha\lambda_{\min}(H_A), \underline{k_m}\big]\|x\|^2,$$

and

$$\left\|\frac{\partial V}{\partial x}\right\| = \left\|\left\{\eta\alpha\left[(H_A \otimes I_p)x_1\right]^T, \left[M(q)x_2\right]^T\right\}^T\right\|,$$

$$\leq \max\left[\eta\alpha\lambda_{\max}(H_A), k_{\bar{m}}\right]\|x\| \leq \gamma\sqrt{V},$$

where $\gamma \triangleq \frac{\sqrt{2}\max[\eta\alpha\lambda_{\max}(H_A), k_{\bar{m}}]}{\sqrt{\min[\eta\alpha\lambda_{\min}(H_A), k_{\underline{m}}]}}$.

The derivative of V along (6.44) is

$$\begin{aligned}
\dot{V}_{(6.44)} &= \frac{\partial V}{\partial t} + \frac{\partial V}{\partial x}f(t, x)\\
&= \eta\alpha x_1^T(H_A \otimes I_p)\left[x_2 - \alpha(H_A \otimes I_p)x_1\right]\\
&\quad + \frac{1}{2}x_2^T\dot{M}(q)x_2 + x_2^T M(q)\dot{x}_2 + \widetilde{\Theta}^T\Xi\dot{\widetilde{\Theta}}\\
&= -\eta\left[x_2 - \alpha(H_A \otimes I_p)x_1\right]^T\left[x_2 - \alpha(H_A \otimes I_p)x_1\right]\\
&\quad - x_2^T K x_2,
\end{aligned}\tag{6.46}$$

where we have used Assumption (A2) and the fact that $\dot{\widetilde{\Theta}} = \Xi^{-1}Y^T s$ according to (6.40) and $s \equiv x_2$ to obtain the last equality. Note that $\dot{V}_{(6.44)} \leq 0$ because $\eta > 0$ and K is symmetric positive definite. Then the derivative of V along (6.42) can be written as

$$\begin{aligned}
\dot{V}_{(6.42)} &= \frac{\partial V}{\partial t} + \frac{\partial V}{\partial x}f(t, x) + \frac{\partial V}{\partial x}h(x, \xi) = \dot{V}_{(6.44)} + \frac{\partial V}{\partial x}h(x, \xi)\\
&\leq \left\|\frac{\partial V}{\partial x}\right\|\|h(x, \xi)\| \leq \gamma\|\xi\|\sqrt{V}.
\end{aligned}\tag{6.47}$$

Following the same steps as in the proof of Theorem 6.9, we can easily get that $V(t, x)$ is uniformly bounded along the solution of (6.42), which means that x_1, x_2 and $\widetilde{\Theta}$ are all bounded.

Second, we show that the system (6.44) is globally asymptotically stable at the origin. By following similar boundedness statements in the proof of Theorem 6.9 and applying Lemma 1.33, we conclude that $\dot{V}_{(6.44)}(t) \to 0$ as $t \to \infty$. Then from (6.46) we can get that $x_2(t) - \alpha(H_A \otimes I_p)x_1(t) \to 0$ and $x_2(t) \to 0$ as $t \to \infty$, which means that $(H_A \otimes I_p)x_1(t) \to 0$ as $t \to \infty$. Because H_A is symmetric positive definite, it follows that $x_1(t) \to 0$ as $t \to \infty$. Note that V defined by (6.45) is radially unbounded with respect to x, it follows that the system (6.44) is globally asymptotically stable at the origin.

Third, note that H_B is symmetric positive definite, which implies that A in (6.43) is Hurwitz. We conclude from Lemma 6.4 that the cascade system (6.42) and (6.43) is globally asymptotically stable at the origin, which in turn proves the theorem. ∎

Remark 6.12 In the adaptive case, we need to introduce the auxiliary variables. If we just introduce the adaptation law without the auxiliary variables, and choose the Lyapunov function as (6.26) with an addition of $\frac{1}{2}\widetilde{\Theta}^T\Xi\widetilde{\Theta}$, then $\dot{V}_{(6.44)}$ is negative semidefinite as in (6.29). However, in this case, we cannot get that $x_1(t) \to 0$ from

$x_2(t) \to 0$ as $t \to 0$. By introducing the auxiliary variables defined in (6.37) and (6.38), we need both $\sum_{j=0}^{n} a_{ij}(q_i - q_j)$ and its derivative in the control algorithm (6.39) because they are needed to derive $\dot{q}_{ri}$ and $\ddot{q}_{ri}$ (and hence Y_i). It is therefore required that the interaction graphs associated with the followers for both q_i and $\dot{q}_i$ be the same. In addition, the connectivity condition in Theorem 6.11 can be relaxed similar to that in Remark 6.10.

6.3.3 Coordinated Tracking when the Leader's Vector of Generalized Coordinate Derivatives is Varying

In this subsection, $\dot{q}_0(t)$ is allowed to be varying. The objective here is to design a distributed model-independent sliding-mode algorithm for (6.1) such that $q_i(t) - q_0(t) \to \mathbf{0}_p$ and $\dot{q}_i(t) - \dot{q}_0(t) \to \mathbf{0}_p$ as $t \to \infty$. Define the following auxiliary variables

$$s_i \stackrel{\triangle}{=} \dot{q}_i + \lambda q_i, \quad i = 0, 1, \dots, n, \tag{6.48}$$

where λ is a positive constant. Also define the error variable between s_i and s_0 as

$$\tilde{s}_i \stackrel{\triangle}{=} s_i - s_0 = \dot{q}_i - \dot{q}_0 + \lambda(q_i - q_0), \quad i = 1, \dots, n. \tag{6.49}$$

Then (6.1) can be written as

$$M_i(q_i)\dot{s}_i + C_i(q_i, \dot{q}_i)s_i = \tau_i + \lambda M_i(q_i)\dot{q}_i + \lambda C_i(q_i, \dot{q}_i)q_i - g_i(q_i). \tag{6.50}$$

We propose the distributed coordinated tracking algorithm for (6.50) [and hence (6.1)] as

$$\tau_i = -\alpha \left[\sum_{j=0}^{n} a_{ij}(s_i - s_j) \right] - \beta \left(\sum_{j=1}^{n} a_{ij} \left\{ \mathrm{sgn} \left[\sum_{k=0}^{n} a_{ik}(s_i - s_k) \right] \right. \right.$$

$$\left. \left. - \mathrm{sgn} \left[\sum_{k=0}^{n} a_{jk}(s_j - s_k) \right] \right\} + a_{i0} \mathrm{sgn} \left[\sum_{j=0}^{n} a_{ij}(s_i - s_j) \right] \right), \tag{6.51}$$

where α is a nonnegative constant, β is a positive constant, a_{ij}, $i, j = 1, \dots, n$ is the (i, j)th entry of the adjacency matrix $\mathscr{A}$ associated with the undirected graph $\mathscr{G}_A \stackrel{\triangle}{=} (\mathscr{V}, \mathscr{E}_A)$ characterizing the interaction among the followers, $a_{i0} > 0$ if the leader is a neighbor of follower i and $a_{i0} = 0$ otherwise, and $\mathrm{sgn}(\cdot)$ is defined componentwise. Let s and $\tilde{s}$ be, respectively, the column stack vector of s_i and $\tilde{s}_i$, $i = 1, \dots, n$. We can rewrite the closed-loop system (6.50) [and hence (6.1)] using (6.51) in a vector form as

$$M(q)\dot{\tilde{s}} + C(q,\dot{q})\tilde{s} = -\alpha(H_A \otimes I_p)\tilde{s} - \beta(H_A \otimes I_p)\operatorname{sgn}\big[(H_A \otimes I_p)\tilde{s}\big] + \Delta,$$
(6.52)

where $H_A \overset{\triangle}{=} \mathscr{L}_A + \operatorname{diag}(a_{10}, \ldots, a_{n0})$ with $\mathscr{L}_A$ being the Laplacian matrix associated with $\mathscr{A}$ and hence $\mathscr{G}_A$ and $\Delta \overset{\triangle}{=} -M(q)(\mathbf{1}_n \otimes \dot{s}_0) - C(q,\dot{q})(\mathbf{1}_n \otimes s_0) + \lambda M(q)\dot{q} + \lambda C(q,\dot{q})q - g(q)$. Note that H_A is symmetric positive semidefinite because $\mathscr{G}_A$ is undirected.

Remark 6.13 Note that the algorithm (6.51) is discontinuous. Therefore, the stability analysis of the closed-loop system (6.1) using (6.51) is conducted for the Filippov solutions via the nonsmooth analysis in Sect. 1.5. Accordingly, Remarks 4.1 and 4.3 also apply here.

Before moving on, we need the following assumption on the boundedness of $\dot{q}_0$ and $\ddot{q}_0$:

(A4) Both $\dot{q}_0$ and $\ddot{q}_0$ are bounded, and in particular, $\|\mathbf{1}_n \otimes \dot{q}_0\| \le k_v$ and $\|\mathbf{1}_n \otimes \ddot{q}_0\| \le k_a$.

Remark 6.14 We do not restrict q_0 to be bounded in (A4). Most desired trajectories have the properties of (A4), so (A4) is a reasonable assumption. In the control algorithm (6.51), there is no need to know the value of $\ddot{q}_0$.

Next, we show the boundedness of Δ in (6.52). From Assumption (A1), it follows that $\|g(q)\| \le \sqrt{n}k_g$. Following Assumptions (A1) and (A4), we have

$$\|\Delta\| = \big\| -M(q)(\mathbf{1}_n \otimes \ddot{q}_0) - C(q,\dot{q})(\mathbf{1}_n \otimes \dot{q}_0) + \lambda M(q)\dot{\tilde{q}} + \lambda C(q,\dot{q})\tilde{q} - g(q) \big\|$$
$$\le k_{\bar{m}}k_a + k_C k_v\|\dot{q}\| + \lambda k_{\bar{m}}\|\dot{\tilde{q}}\| + \lambda k_C\|\dot{q}\|\|\tilde{q}\| + \sqrt{n}k_g,$$
(6.53)

where $\tilde{q} \overset{\triangle}{=} q - \mathbf{1}_n \otimes q_0$. Note that (6.49) can be written in a vector form as $\tilde{s} = \dot{\tilde{q}} + \lambda\tilde{q}$. Multiplying $e^{\lambda\tau}$ on both sides and integrating from 0 to t, we have

$$\tilde{q}(t) = e^{-\lambda t}\bigg[\tilde{q}(0) + \int_0^t e^{\lambda\tau}\tilde{s}(\tau)\,d\tau\bigg].$$
(6.54)

Lemma 6.5. *Define a norm-like function* $\|x\|_M \overset{\triangle}{=} \sqrt{x^T M(q)x}$, *where* $x \in \mathbb{R}^{np}$. *Then* $\sqrt{k_{\underline{m}}}\,\|x\| \le \|x\|_M \le \sqrt{k_{\bar{m}}}\,\|x\|$ *for all* $t \ge 0$.

Proof: Note that from Assumption (A1), $k_{\underline{m}}z^T z \le z^T M_i(q_i)z \le k_{\bar{m}}z^T z$ for $z \in \mathbb{R}^p$, $i = 1, \ldots, n$. It thus follows that $k_{\underline{m}}x^T x \le x^T M(q)x \le k_{\bar{m}}x^T x$, which means that $\sqrt{k_{\underline{m}}}\|x\| \le \|x\|_M \le \sqrt{k_{\bar{m}}}\|x\|$. ∎

From (6.54), we have

$$\big\|\tilde{q}(t)\big\| \le e^{-\lambda t}\big\|\tilde{q}(0)\big\| + \frac{\sup_{0 \le \tau \le t}\|\tilde{s}(\tau)\|}{\lambda}\big(1 - e^{-\lambda t}\big).$$
(6.55)

From Lemma 6.5, we can get $\|\tilde{s}(t)\| \le \|\tilde{s}(t)\|_M/\sqrt{k_{\underline{m}}}$ for all $t \ge 0$. It thus follows that $\sup_{0 \le \tau \le t}\|\tilde{s}(\tau)\| \le \sup_{0 \le \tau \le t}\|\tilde{s}(\tau)\|_M/\sqrt{k_{\underline{m}}}$. Define

$$\phi(t) \overset{\triangle}{=} \sup_{0 \le \tau \le t} \|\tilde{s}(\tau)\|_M. \tag{6.56}$$

It follows from (6.55) and (6.56) that

$$\left\|\tilde{q}(t)\right\| \le \left\|\tilde{q}(0)\right\| + \frac{\sup_{0 \le \tau \le t} \|\tilde{s}(\tau)\|}{\lambda} \le \left\|\tilde{q}(0)\right\| + \frac{\phi(t)}{\lambda\sqrt{k_{\underline{m}}}} \overset{\triangle}{=} k_e. \tag{6.57}$$

Note from the definition of $\tilde{s}$ that $\tilde{s} = \dot{\tilde{q}} + \lambda\tilde{q}$. It thus follows that

$$\left\|\dot{\tilde{q}}(t)\right\| = \left\|\tilde{s}(t) - \lambda q_e(t)\right\| \le \frac{\phi(t)}{\sqrt{k_{\underline{m}}}} + \lambda k_e \overset{\triangle}{=} k_{\dot{e}} \tag{6.58}$$

and

$$\left\|\dot{q}(t)\right\| = \left\|\dot{\tilde{q}}(t) + \mathbf{1}_n \otimes \dot{q}_0(t)\right\| \le k_{\dot{e}} + k_v. \tag{6.59}$$

Substituting (6.57)–(6.59) into (6.53), it follows that

$$\begin{aligned}
\|\Delta\| &\le k_{\bar{m}}(k_a + \lambda k_{\dot{e}}) + k_C(k_v + \lambda k_e)(k_{\dot{e}} + k_v) + \sqrt{n}k_g \\
&= a\phi^2(t) + b\phi(t) + c \overset{\triangle}{=} \gamma(t),
\end{aligned} \tag{6.60}$$

where

$$a \overset{\triangle}{=} 2k_C/k_{\underline{m}},$$
$$b \overset{\triangle}{=} \left(3k_Ck_v + 2\lambda k_{\bar{m}} + 3\lambda k_C\|\tilde{q}(0)\|\right)/\sqrt{k_{\underline{m}}},$$
$$c \overset{\triangle}{=} k_{\bar{m}}k_a + \sqrt{n}k_g + k_Ck_v^2 + \left(2\lambda k_Ck_v + \lambda^2 k_{\bar{m}}\right)\|\tilde{q}(0)\| + \lambda^2 k_C\|\tilde{q}(0)\|^2.$$

Noting that a, b, c are positive constants, and $\phi(t) \ge 0$, we get that $\gamma(t)$ is monotonically increasing on $[0, \infty)$ because $\phi(t)$ is monotonically increasing on $[0, \infty)$. If there exists some bounded disturbance in (6.1), with an addition of a constant in c, the following results still hold. Thus, the coordinated tracking algorithm (6.51) is robust to bounded disturbance.

Consider the following Lyapunov function candidate for (6.52) as

$$V = \frac{1}{2}\tilde{s}^T M(q)\tilde{s}. \tag{6.61}$$

It follows that

$$\begin{aligned}
\max \widetilde{L}_F V = \dot{V} &= \tilde{s}^T M(q)\dot{\tilde{s}} + \frac{1}{2}\tilde{s}^T \dot{M}(q)\tilde{s} \\
&= \tilde{s}^T\left\{-\alpha(H_A \otimes I_p)\tilde{s} - \beta(H_A \otimes I_p)\mathrm{sgn}\left[(H_A \otimes I_p)\tilde{s}\right] + \Delta\right\} \\
&= -\alpha\tilde{s}^T(H_A \otimes I_p)\tilde{s} - \beta\left\|(H_A \otimes I_p)\tilde{s}\right\|_1 + \Delta^T\tilde{s}
\end{aligned} \tag{6.62}$$

$$\leq -\alpha \tilde{s}^T (H_A \otimes I_p) \tilde{s} - \beta \| (H_A \otimes I_p) \tilde{s} \| + \| \Delta \| \| \tilde{s} \|$$
$$\leq -\alpha \tilde{s}^T (H_A \otimes I_p) \tilde{s} - \left[\beta \lambda_{\min}(H_A) - \gamma(t) \right] \| \tilde{s} \|, \tag{6.63}$$

where we have used Assumption (A2) to obtain the second equality, the fact that $\|x\| \leq \|x\|_1$ to obtain the first inequality, and the fact that $\|H_A x\| \geq \lambda_{\min}(H_A) x$, $\forall x \in \mathbb{R}^n$, and $\|\Delta\| \leq \gamma(t)$ from (6.60) to obtain the last inequality.

If we can choose β such that $\beta \lambda_{\min}(H_A) - \gamma(t) > 0$,[3] then we can show that $\dot{V}$ is negative definite. However, $\gamma(t)$ is a time-varying function involving $\tilde{s}(t)$, which implies that we need to know all $\tilde{s}_i(t)$, $i = 1, \ldots, n$, at each time to find a proper β. Unfortunately, it is not possible to do so because the leader is the neighbor of only a subset of the followers. So we need the following lemmas.

Lemma 6.6. *If $\beta \lambda_{\min}(H_A) - \gamma(t_1) > 0$ and $\|\tilde{s}(t_1)\| = 0$ at some time $t_1 \geq 0$, then $\|\tilde{s}(t)\| \equiv 0$ for all $t \geq t_1$.*

Proof: Treat t_1 as the initial time. Let $\phi(t)$ be defined as in (6.56) with $0 \leq \tau \leq t$ replaced with $t_1 \leq \tau \leq t$, and let $\gamma(t)$ be defined as in (6.60) with $\tilde{q}(0)$ in the variables b and c replaced with $\tilde{q}(t_1)$. Note that $\|\tilde{s}(t)\|$ is continuous, which implies that $\phi(t)$ and $\gamma(t)$ are also continuous. Because $\beta \lambda_{\min}(H_A) - \gamma(t_1) > 0$, there exists a neighborhood Ω of t_1 such that $\beta \lambda_{\min}(H_A) - \gamma(t) > 0$ when $t \in \Omega_1 \triangleq \Omega \cap \{t > t_1\}$. For $t \in \Omega_1$, from (6.63), we can get that $\dot{V}(t) \leq -[\beta \lambda_{\min}(H_A) - \gamma(t)] \|\tilde{s}\| \leq 0$. Also note that $\|\tilde{s}(t_1)\| = 0$, which means that $V(t_1) = 0$ and $\dot{V}(t_1) = 0$ from (6.62). Because $V(t) \geq 0$ for all $t \geq 0$, we can conclude that $V(t) = 0$, i.e., $\|\tilde{s}(t)\| = 0$, for $t \in \Omega_1$.

We then prove the lemma by contradiction. Suppose that there exists $t_2 > t_1$ such that $\|\tilde{s}(t_2)\| \neq 0$ (and hence $\|\tilde{s}(t_2)\| > 0$). From the continuity of $\|\tilde{s}(t)\|$, there exists $t_3 \in (t_1, t_2)$ and a neighborhood Ω_2 of t_3 such that $\|\tilde{s}(t)\| = 0$ for $t \in [t_1, t_3]$ and $\|\tilde{s}(t)\| > 0$ for $t \in \Omega_3 \triangleq \Omega_2 \cap (t_3, t_2)$. From the definition of $\gamma(t)$, we can get that $\beta \lambda_{\min}(H_A) - \gamma(t_3) = \beta \lambda_{\min}(H_A) - \gamma(t_1) > 0$. From the continuity of $\gamma(t)$, there exists a neighborhood Ω_4 of t_3 such that $\beta \lambda_{\min}(H_A) - \gamma(t) > 0$ for $t \in \Omega_5 \triangleq \Omega_4 \cap (t_3, t_2)$, which means that $\dot{V} \leq -[\beta \lambda_{\min}(H_A) - \gamma(t)] \|\tilde{s}\| \leq 0$ for $t \in \Omega_5$. Also note that $V(t_3) = 0$, $\dot{V}(t_3) = 0$, and $V(t) \geq 0$ for all $t \geq 0$, we can get that $V(t) = 0$, i.e., $\|\tilde{s}(t)\| = 0$, for $t \in \Omega_5$. Note that both Ω_2 and Ω_4 are neighborhoods of t_3. We can get that $\Omega_3 \cap \Omega_5 \neq \varnothing$. Thus, we have that $\|\tilde{s}(t)\| > 0$ for $t \in \Omega_3$ and $\|\tilde{s}(t)\| = 0$ for $t \in \Omega_5$, which results in a contradiction for $t \in \Omega_3 \cap \Omega_5$. ∎

Lemma 6.7. *If β is chosen such that $\beta \lambda_{\min}(H_A) - \gamma(0) > 0$, then $\beta \lambda_{\min}(H_A) - \gamma(t) = \beta \lambda_{\min}(H_A) - \gamma(0) > 0$ for all $t \geq 0$, or there exists $\bar{t} \geq 0$ such that $\|\tilde{s}(t)\| \equiv 0$ for all $t \geq \bar{t}$.*

Proof: From the definition of $\phi(t)$ in (6.56) and $\gamma(t)$ in (6.60), for all $t \geq 0$, we have that $\phi(t) \geq \phi(0)$ and $\gamma(t) \geq \gamma(0)$. Thus, if $\gamma(t) = \gamma(0)$ for all $t \geq 0$, we can

---

[3] Of course, in this case, $\lambda_{\min}(H_A)$ must be positive, implying that H_A must be symmetric positive definite rather than just symmetric positive semidefinite.

conclude our proof. If β is chosen such that $\beta\lambda_{\min}(H_A) - \gamma(0) > 0$, from (6.63), $\dot{V}(0) \leq 0$. If $\dot{V}(0) = 0$, i.e., $\|\tilde{s}(0)\| = 0$, we have that $\|\tilde{s}(t)\| = 0$ for all $t \geq \bar{t} \triangleq 0$ from Lemma 6.6. This conclude our proof.

Because $\tilde{s}(t)$ is continuous, so is V defined in (6.61). If $\dot{V}(0) < 0$, there must exist a neighborhood Ω of 0 such that $V(t) < V(0)$ when $t \in \Omega_1 \triangleq \Omega \cap \{t > 0\}$. If there exits $t_1 > 0$ such that $\gamma(t_1) > \gamma(0)$, from (6.60) and the monotonic property of $\gamma(t)$, we have that $\phi(t_1) > \phi(0)$. From the definition of $\phi(t)$ in (6.56), there must exist $t_2 \in (0, t_1)$ such that $\|\tilde{s}(t_2)\|_M > \|\tilde{s}(0)\|_M$. Without loss of generality, suppose that t_2 is in the interval where $\|\tilde{s}(t)\|_M$ becomes larger than $\|\tilde{s}(0)\|_M$ for the first time. Note that $V(t) = \frac{1}{2}\tilde{s}^T(t)M(q)\tilde{s}(t) = \frac{1}{2}\|\tilde{s}(t)\|_M^2$. Because $V(t) < V(0)$ for all $t \in \Omega_1$, which implies that $\|\tilde{s}(t)\|_M < \|\tilde{s}(0)\|_M$ for all $t \in \Omega_1$. Also note that $\|\tilde{s}(t)\|_M$ is continuous and $\|\tilde{s}(t_2)\|_M > \|\tilde{s}(0)\|_M$. There must exist $t_3 \in (0, t_2)$ such that $\|\tilde{s}(t_3)\|_M = \|\tilde{s}(0)\|_M$ and $\|\tilde{s}(t)\|_M < \|\tilde{s}(0)\|_M$ for all $t \in (0, t_3)$, which means that $V(t_3) = V(0)$ and $V(t) < V(0)$ for all $t \in (0, t_3)$. From the mean value theorem, there is a point $t_4 \in (0, t_3)$ at which $\dot{V}(t_4) = 0$. But on the other hand, $\|\tilde{s}(t_4)\|_M < \|\tilde{s}(0)\|_M$ because $t_4 \in (0, t_3)$. Because for all $t \in (0, t_3), \|\tilde{s}(t)\|_M < \|\tilde{s}(0)\|_M$, it follows that $\phi(t_4) = \phi(0)$, which means that $\gamma(t_4) = \gamma(0)$. We can conclude that $\beta\lambda_{\min}(H_A) - \gamma(t_4) = \beta\lambda_{\min}(H_A) - \gamma(0) > 0$. From (6.63), we have that $\dot{V}(t_4) \leq 0$. On the one hand, if $\dot{V}(t_4) < 0$, there is a contradiction because we have already shown that $\dot{V}(t_4) = 0$, which implies that there does not exist $t_1 > 0$ such that $\gamma(t_1) > \gamma(0)$. Note further that $\gamma(t) \geq \gamma(0)$ for all $t \geq 0$, which means that $\gamma(t) = \gamma(0)$ for all $t \geq 0$, i.e., $\beta\lambda_{\min}(H_A) - \gamma(t) = \beta\lambda_{\min}(H_A) - \gamma(0) > 0$. This conclude our proof. On the other hand, if $\dot{V}(t_4) = 0$, noting that $\dot{V}(t_4) \leq -[\beta\lambda_{\min}(H_A) - \gamma(t_4)]\|\tilde{s}\| \leq 0$ because $\beta\lambda_{\min}(H_A) - \gamma(t_4) > 0$, we can get that $\|\tilde{s}(t_4)\| = 0$. Thus, it follows from Lemma 6.6 that $\|\tilde{s}(t)\| \equiv 0$ for any $t > \bar{t} \triangleq t_4$. This also conclude our proof. ∎

Theorem 6.15. *Suppose that $\mathscr{G}_A$ is undirected connected and the leader is a neighbor of at least one follower (i.e., at least one $a_{i0} > 0$). Using (6.51) for (6.1), $q_i(t) - q_0(t) \to \mathbf{0}_p$ and $\dot{q}_i(t) - \dot{q}_0(t) \to \mathbf{0}_p$, $i = 1, \ldots, n$, exponentially as $t \to \infty$ if β is chosen such that $\beta > \gamma(0)/\lambda_{\min}(H_A)$.*

Proof: Because $\mathscr{G}_A$ is undirected connected and at least one $a_{i0} > 0$, it follows from Lemma 1.6 that H_A is symmetric positive definite. Because $\beta > \gamma(0)/\lambda_{\min}(H_A)$, it follows from Lemma 6.7 that either $\beta\lambda_{\min}(H_A) - \gamma(t) = \beta\lambda_{\min}(H_A) - \gamma(0) > 0$ or there exists $\bar{t} \geq 0$ such that $\|\tilde{s}(t)\| \equiv 0$ for all $t \geq \bar{t}$. In the first case, consider the Lyapunov function candidate given by (6.61). Noting that $V = \frac{1}{2}\|\tilde{s}\|_M^2$, it follows from (6.63) that

$$\dot{V} \leq -\big[\beta\lambda_{\min}(H_A) - \gamma(t)\big]\|\tilde{s}\| \leq -\big[\beta\lambda_{\min}(H_A) - \gamma(0)\big]\frac{\|\tilde{s}\|_M}{\sqrt{k_{\bar{m}}}} = -\eta\sqrt{V},$$

where $\eta \triangleq \sqrt{2/k_{\bar{m}}}[\beta\lambda_{\min}(H_A) - \gamma(0)]$, and we have used the fact that $\|s\| \geq \|s\|_M/\sqrt{k_{\bar{m}}}$ from Lemma 6.5 to obtain the second inequality. After some manipu-

lation, we get

$$2\sqrt{V(t)} \leq 2\sqrt{V(0)} - \eta t.$$

Therefore, we have $V(t) \equiv 0$ and equivalently $\|\tilde{s}(t)\| \equiv 0$ when $t \geq \frac{2\sqrt{V(0)}}{\eta}$. In the second case, there exists $\bar{t} \geq 0$ such that $\tilde{s}(t) \equiv 0$ when $t \geq \bar{t}$. Combining both cases, we can get that $\|\tilde{s}(t)\| \equiv 0$ when $t \geq \bar{t}_1 \triangleq \max\{\frac{2\sqrt{V(0)}}{\eta}, \bar{t}\}$, which implies $\dot{\tilde{q}}(t) + \lambda\tilde{q}(t) \equiv \mathbf{0}_{np}$, $i = 1, \ldots, n$, when $t \geq \bar{t}_1$. Noting that the solution of $\dot{\tilde{q}}(t) + \lambda\tilde{q}(t) \equiv \mathbf{0}_{np}$ is $\tilde{q}(t) = e^{-\lambda(t-\bar{t}_1)}\tilde{q}(\bar{t}_1)$ and $\dot{\tilde{q}}(t) = -\lambda e^{-\lambda(t-\bar{t}_1)}\tilde{q}(\bar{t}_1)$, we can conclude that $q_i(t) - q_0(t) \to \mathbf{0}_p$ and $\dot{q}_i(t) - \dot{q}_0(t) \to \mathbf{0}_p$ exponentially as $t \to \infty$. ∎

Remark 6.16 From Lemma 6.7, β can be chosen according to $\gamma(0)$, which means that the initial values $\|\tilde{q}(0)\|$ and $\|\tilde{s}(0)\|$ should be known by each follower to compute β even if the leader is a neighbor of only a subset of the followers. However, because only the initial value is needed, it is reasonable. Also note that the lower bound of β might be conservative. In reality, a smaller value might be chosen. Moreover, β can be tuned according to the performance of the whole system in practice, so the accurate knowledge of $\|\tilde{q}(0)\|$ and $\|\tilde{s}(0)\|$ might not be needed.

Remark 6.17 Note that the algorithm (6.51) is model-independent. The bound of $\|\Delta\|$ in (6.53) is dependent on the bound of $\|g(q)\|$. In practice, one might know the nominal dynamics of $g_i(q_i)$, denoted as $g_i^0(q_i)$. Assume that $\|g_i(q_i) - g_i^0(q_i)\| \leq k_{\tilde{g}}$, where $k_{\tilde{g}}$ is a known positive constant generally smaller than k_g. If we choose the control algorithm as $\tilde{\tau}_i = \tau_i + g_i^0(q_i)$, then k_g in (6.53) can be replaced with a smaller parameter $k_{\tilde{g}}$. In addition, by doing so, it is no longer required that $\|g_i(q_i)\|$ is bounded. That is, Assumption (A1) can be relaxed.

Remark 6.18 From the proof in Theorem 6.15, the error vector $\tilde{s}$ will first decrease to zero in finite time. Then, $q_i - q_0$ and $\dot{q}_i - \dot{q}_0$ converge zero exponentially fast with an exponential convergence rate λ. In addition, similar to that Remark 6.10, the condition $\mathscr{G}_A$ is undirected connected and at least one $a_{i0} > 0$ in Theorem 6.15 can be relaxed to be the condition that H_A is symmetric positive definite, which in turn implies a weaker connectivity condition.

Remark 6.19 Note that from the algorithm (6.51), only a subset of the followers needs to have access to q_0 and $\dot{q}_0$, and $\ddot{q}_0$ is not needed. It should be noted that (6.51) requires the availability of information (vectors of generalized coordinates and their derivatives) from both the one-hop and two-hop neighbors due to the challenge involved in distributed coordinated tracking of a leader with a varying vector of generalized coordinated derivatives with local interaction. However, only the sign of the information of the two-hop neighbors is required.
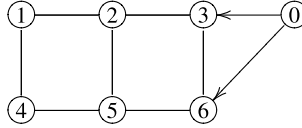
Fig. 6.11 The interaction graph associated with the leader and the six followers. An *edge* between i and j means that followers i and j are neighbors of each other while an *arrow* from 0 to i means that the leader is a neighbor of follower i

6.3.4 Simulation

In this subsection, we simulate a scenario where six two-link revolute joint arms (followers) track a leader with local interaction using, respectively, (6.16), (6.39) and (6.51). The models and the parameters of the followers are given as in Sect. 6.2.4. From the model parameter values in Sect. 6.2.4, we obtain that $k_{\underline{m}} = 0.0256$, $k_{\bar{m}} = 1.2757$, and $k_C = 0.09$. We also assume that the nominal dynamics $g_i^0(q_i)$ is set off from the real dynamics $g_i(q_i)$ by 10%.

We assume that $\mathscr{G}_A$, $\mathscr{G}_B$, and $\mathscr{G}_C$ associated with the followers (also $\mathscr{A}$, $\mathscr{B}$ and $\mathscr{C}$) are identical for simplicity. Figure 6.11 shows the interaction graph associated with the leader and the six followers. In our simulations, we choose $a_{ij} = 1$, $i = 1, \ldots, 6, j = 0, \ldots, 6$, if agent j is a neighbor of agent i, and $a_{ij} = 0$ otherwise. We let $q_i(0) = [\frac{\pi}{7}i, \frac{\pi}{8}i]^T$rad and $\dot{q}_i(0) = [0.05i - 0.2, -0.05i + 0.2]^T$rad/s, where $i = 1, \ldots, 6$. For the algorithms (6.16) and (6.39), the vector of joint angles of the leader are chosen as $q_0(t) = [0.04t, 0.05t]^T$rad, and the vector of joint angle derivatives of the leader is hence $\dot{q}_0 = [0.04, 0.05]^T$rad/s. The control parameters in (6.39) are chosen as $K_i = I_2$, $\alpha = 0.5$, $\eta = 0.5$, and $\Lambda_i = 0.2I_2$. For the algorithm (6.51), the vector of joint angles of the leader is chosen as $q_0(t) = [\cos(\frac{2\pi}{60}t), \sin(\frac{2\pi}{60}t)]^T$rad, the vector of joint angle derivatives of the leader is hence $\dot{q}_0(t) = \frac{2\pi}{60}[-\sin(\frac{2\pi}{60}t), \cos(\frac{2\pi}{60}t)]^T$rad/s, and the control parameters are chosen as $\alpha = 2$, $\lambda = 0.5$, and $\beta = 7.5$.

Figure 6.12 shows the differences between the joint angles of arms 1, 3 and 5 and the leader using (6.16). Figure 6.13 shows the differences between the joint angle derivatives of arms 1, 3 and 5 and the leader using (6.16). Note that all followers' joint angles approach those of the leader and all followers' joint angle derivatives also approach those of the leader.

Figure 6.14 shows the differences between the joint angles of arms 1, 3 and 5 and the leader using (6.39). Figure 6.15 shows the differences between the joint angle derivatives of arms 1, 3 and 5 and the leader using (6.39). Again, note that all followers' joint angles approach those of the leader and all followers' joint angle derivatives also approach those of the leader.

Figure 6.16 shows the differences between the joint angles of arms 1, 3, and 5 and the leader. Figure 6.17 shows the differences between the joint angle derivatives of arms 1, 3, and 5 and the leader using (6.51) by introducing the nominal dynamics $g_i^0(q_i)$ as a compensation term in (6.51). Note that all followers' joint angles ap-
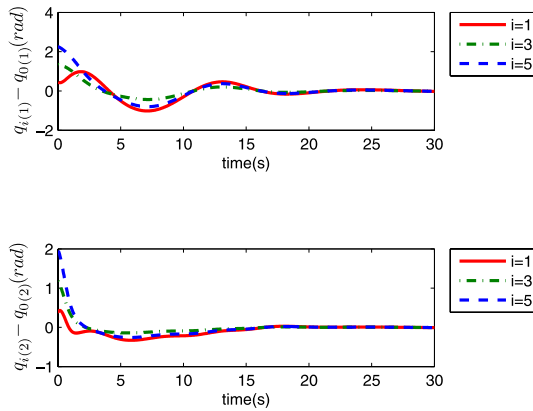
Fig. 6.12 Differences between the joint angles of arms 1, 3, and 5 and the leader using (6.16)
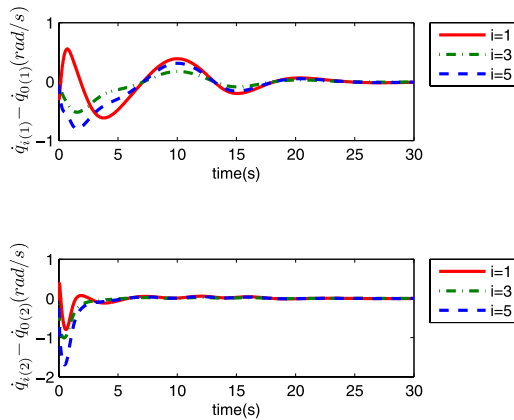
Fig. 6.13 Differences between the joint angle derivatives of arms 1, 3, and 5 and the leader using (6.16)

proach those of the leader and all followers' joint angle derivatives also approach those of the leader.

6.4 Notes

The results in Sect. 6.2 are based mainly on [245]. The results in Sect. 6.3 are mainly based on [189]. For further results on coordination of networked Lagrangian systems, see [52, 59, 62, 64, 119, 254, 275, 284]. In particular, [254] studies position synchronization of robotic manipulators when only position measurements are available under a fully connected interaction graph. In [59], output synchronization is studied for general passive systems under a passivity-based framework, which unifies several existing results on consensus or synchronization in the literature.
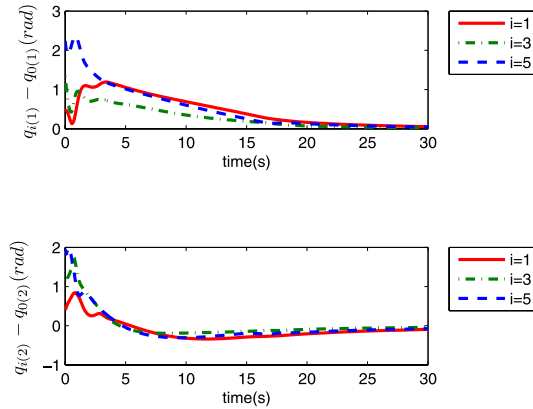
Fig. 6.14 Differences between the joint angles of arms 1, 3, and 5 and the leader using (6.39)
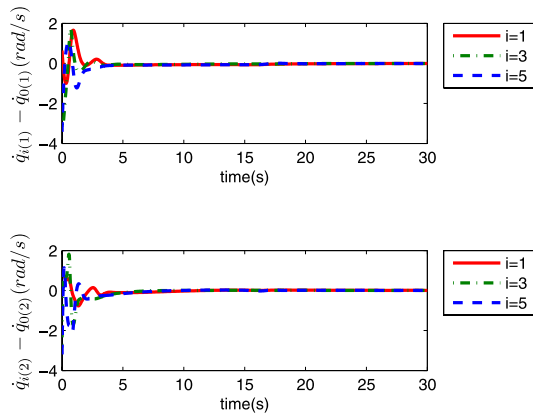
Fig. 6.15 Differences between the joint angle derivatives of arms 1, 3, and 5 and the leader using (6.39)

To use the passivity property, the control law on synchronization of networked Lagrangian systems derived in [59] requires the knowledge of the inertial matrix and the Coriolis and centrifugal torques. In [62], a controller based on potential functions is proposed for networked Lagrangian systems to achieve leaderless flocking (i.e., velocity synchronization and collision avoidance). Communication delays and switching interaction graphs are also considered. In [284], position synchronization of multi-axis motions is addressed via a cross-coupling technique. In [275], output synchronization of networked Lagrangian systems is studied under both fixed and switching interaction graphs in the presence of communication delays. The contraction analysis is used in [64] to study coordinated tracking for multiple robotic manipulators. Utilizing potential functions, [52] designs a control scheme that can force multiple robots modeled by Euler–Lagrange equations to move as a group inside a desired region while maintaining a minimum distance among themselves.
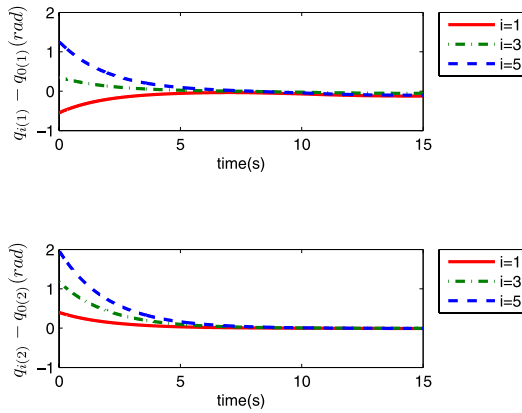
Fig. 6.16 Differences between the joint angles of arms 1, 3, and 5 and the leader using (6.51) with a compensation term $g_i^0(q_i)$
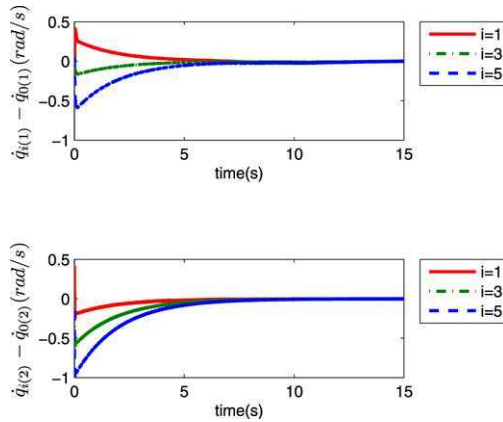
Fig. 6.17 Differences between the joint angle derivatives of arms 1, 3, and 5 and the leader using (6.51) with a compensation term $g_i^0(q_i)$

The robots can achieve velocity synchronization finally. Despite the fact that tracking of a leader or a reference is considered in [52, 64, 275, 284], it is assumed that the leader is a neighbor of all followers or all followers have access to the reference. Unfortunately, this assumption is rather restrictive and not realistic. In [119], the problem of position synchronization of networked Lagrangian systems is studied with communication constraints caused by delays and limited data rates, where the leader modeled by Euler–Lagrange equations is a neighbor of only a subset of the followers and the close-loop system is shown to be input-to-state stable. In the absence of network effects, while the result in [119] can guarantee distributed coordinated regulation where the leader has a constant vector of generalized coordinates, the result is not applicable to ensure distributed coordinated tracking where the leader has a varying vector of generalized coordinates and the leader is a neighbor of only a subset of the followers.

Chapter 7
Networked Fractional-order Systems

This chapter moves from integer-order dynamics to fractional-order dynamics motivated by real-world phenomena. We first study distributed coordination of networked fractional-order systems under a directed fixed interaction graph. We show sufficient conditions on the interaction graph and the fractional order such that coordination is achieved. The coordination equilibrium is also given explicitly. We then study distributed coordination of networked fractional-order systems under a directed switching interaction graph. The convergence conditions on both the interaction graph and the fractional order are presented. We finally propose fractional-order coordination algorithms with absolute/relative damping and study the conditions on the interaction graph and the control gains such that coordination is achieved under a directed fixed interaction graph. Simulation examples are presented as a proof of concept.

7.1 Problem Statement

Many phenomena in nature cannot be explained in the framework of integer-order dynamics, for example, the synchronized motion of agents in fractional circumstances such as macromolecule fluids and porous media. Under these circumstances, the stress–strain relationship demonstrates non-integer-order (i.e., *fractional-order*) dynamics rather than integer-order dynamics as shown in [11–13]. Also, many other phenomena can be explained naturally by coordinated behavior of agents with fractional-order dynamics. Examples include chemotaxis behavior and food seeking of microbes and collective motion of bacteria in lubrications perspired by themselves [65, 156]. Similarly, engineered systems often demonstrate fractional-order dynamics either because the environments in which they are operated are complex or because the system dynamics can be modeled more accurately by fractional-order differential equations than integer-order differential equations. Examples include underwater vehicles operating in lentic lakes composed of microbes and viscoelastic materials, flying vehicles operating in an environment where the influence

of particles in air cannot be ignored (e.g., high-speed flight in duststorm, rain, or snow), and ground vehicles moving on top of carpet, sand, muddy road, or grass. In addition, friction in many real-world applications takes in the form of a fractional-order model instead of an integer-order model. Motivated by the broad application of coordination algorithms in multi-agent systems and the fact that many practical systems demonstrate fractional-order dynamics, we study coordination algorithms for networked fractional-order systems in this chapter.

Fractional calculus can be dated back to the seventeenth century [256]. Fractional calculus studies fractional derivatives, fractional integrals, and their properties. Different from the integer orders of derivatives and integrals in conventional calculus, the orders of derivatives and integrals in fractional calculus are real numbers. The foundations of fractional calculus are laid on [164, 179, 253]. With the development of fractional calculus, its applications are also studied by researchers from different disciplines [217, 229]. Examples include study of formation of particulate aggregates [303] and study of motion of objects in viscoelastic materials [11–13]. In particular, fractional calculus is also introduced into the engineering community to design CRONE controller [219] and synthesize control systems [10], to name a few.

Fractional-order dynamics are also studied from different perspectives. The authors in [108] model the dynamics of self-similar protein in a fractional-order sense because the relaxation processes and the reaction dynamics of the proteins deviate from exponential behavior. In [18], fractional-order dynamics of international commodity prices are demonstrated from the commodity price series. In [229, 231], the authors study fractional-order PID controllers that show better performance than the classical PID controllers when used for control of fractional-order systems. The authors in [194] demonstrate that fractional equations have become a complementary tool in the description of anomalous transport processes in complex systems.

There are mainly two widely used fractional operators: Caputo and Riemann–Liouville (R–L) fractional operators [229]. In physical systems, Caputo fractional operator is more practical than R–L fractional operator because R–L fractional operator has initial value problems. Therefore, in this chapter we will use Caputo fractional operator to model the system dynamics and analyze the stability of the proposed coordination algorithms. Generally, Caputo fractional operator includes Caputo integral and Caputo derivative. Caputo derivative is defined based on the following Caputo integral

$$\,^{C}_{a}D_t^{-p}f(t) = \frac{1}{\Gamma(p)} \int_a^t \frac{f(\tau)}{(t-\tau)^{1-p}} d\tau,$$

where $\,^{C}_{a}D_t^{-p}$ denotes the Caputo integral of order $p \in (0, \ 1]$, $\Gamma(\cdot)$ is the Gamma function, and a is an arbitrary real number. For any real number α, Caputo derivative is defined as

$$\,^{C}_{a}D_t^{\alpha}f(t) = \,^{C}_{a}D_t^{-p}\left[\frac{d^{[\alpha]+1}}{dt^{[\alpha]+1}}f(t)\right], \tag{7.1}$$

where $p \stackrel{\triangle}{=} [\alpha]+1-\alpha \in (0,\,1]$ and $[\alpha]$ is the integer part of α. If α is an integer, then $p = 1$ and (7.1) is equivalent to the integer-order derivative. Because only Caputo fractional operator is used in the following of this chapter, a simple notation $f^{(\alpha)}(t)$ is used to replace ${}_a^C D_t^\alpha f(t)$.

In the following, we will introduce the Laplace transform of Caputo derivative and the Mittag-Leffler function [110] that will be used to analyze the algorithms proposed in this chapter. We first introduce the Laplace transform of Caputo derivative. Let $\mathfrak{L}\{\cdot\}$ denote the Laplace transform of a function. It follows from the formal definition of the Laplace transform $F(s) \stackrel{\triangle}{=} \mathfrak{L}\{f(t)\} = \int_{0^-}^{\infty} e^{-st} f(t)\, dt$ that

$$\mathfrak{L}\{f^{(\alpha)}(t)\} = \begin{cases} s^\alpha F(s) - s^{\alpha-1} f(0^-), & \alpha \in (0, 1] \\ s^\alpha F(s) - s^{\alpha-1} f(0^-) - s^{\alpha-2} \dot{f}(0^-), & \alpha \in (1, 2], \end{cases} \tag{7.2}$$

where $f(0^-) = \lim_{\epsilon \to 0^-} f(\epsilon)$ and $\dot{f}(0^-) = \lim_{\epsilon \to 0^-} \dot{f}(\epsilon)$. We then introduce the Mittag-Leffler function, a function frequently used in the solutions of fractional-order systems. For $\alpha, \beta \in \mathbb{C}$, the Mittag-Leffler function in two parameters is defined as

$$E_{\alpha,\beta}(z) = \sum_{k=0}^{\infty} \frac{z^k}{\Gamma(k\alpha + \beta)}. \tag{7.3}$$

When $\beta = 1$ and $\alpha > 0$, (7.3) can be written in a special case as

$$E_\alpha(z) = \sum_{k=0}^{\infty} \frac{z^k}{\Gamma(k\alpha + 1)}. \tag{7.4}$$

Assume that the agent dynamics are

$$x_i^{(\alpha)}(t) = u_i(t), \quad i = 1, \ldots, n, \tag{7.5}$$

where $x_i(t) \in \mathbb{R}^m$ and $u_i(t) \in \mathbb{R}^m$ represent, respectively, the state and the control input associated with the ith agent, and $x_i^{(\alpha)}(t)$ is the αth derivative of $x_i(t)$ with α being a positive constant. Define $\Delta_{ij} \stackrel{\triangle}{=} \delta_i - \delta_j$, where $\delta_i \in \mathbb{R}^m$ is constant. Here Δ_{ij} denotes the desired relative state deviation between agents i and j. The objective of this chapter is to design distributed coordination algorithms for (7.5) such that coordination is achieved. That is, for all $x_i(0)$ and all $i, j = 1, \ldots, n$, $x_i(t) - x_j(t) \to \Delta_{ij}$ as $t \to \infty$. In the remainder of this chapter, we assume that $m = 1$. However, all results hereafter are still valid for $m > 1$ by the introduction of the Kronecker product.

Remark 7.1 Note that the integer-order dynamics [i.e., α is an integer in (7.5)] is a special case of the fractional-order dynamics.

7.2 Stability Analysis of a Coordination Algorithm for Networked Fractional-order Systems

In this section, we first propose a distributed coordination algorithm for networked fractional-order systems. We then derive the conditions on the interaction graph and the fractional order such that coordination is achieved under, respectively, a directed fixed and switching interaction graph. A coordination algorithm for (7.5) is given by

$$u_i(t) = -\sum_{j=1}^{n} a_{ij}(t)\big[x_i(t) - x_j(t) - \Delta_{ij}\big], \tag{7.6}$$

where $a_{ij}(t)$ is the (i, j)th entry of the adjacency matrix $\mathscr{A}(t)$ associated with the directed graph $\mathscr{G}(t) \stackrel{\triangle}{=} [\mathscr{V}(t), \mathscr{E}(t)]$ characterizing the interaction among the n agents at time t.

7.2.1 Directed Fixed Interaction

In this subsection, we study the case where the directed interaction graph is fixed. We assume that the adjacency matrix $\mathscr{A}$ is constant.

Consider a system

$$\tilde{x}^{(\alpha)}(t) = -A\tilde{x}(t), \tag{7.7}$$

where $\tilde{x}(t) \stackrel{\triangle}{=} [\tilde{x}_1(t), \ldots, \tilde{x}_n(t)]^T \in \mathbb{R}^n$ with $\tilde{x}_i(t) \stackrel{\triangle}{=} x_i(t) - \delta_i$ and $A \in \mathbb{R}^{n \times n}$. Note that A can be written in the Jordan canonical form as

$$A = P \underbrace{\begin{bmatrix} \Lambda_1 & 0 & \cdots & 0 \\ 0 & \Lambda_2 & \cdots & 0 \\ \vdots & \vdots & \ddots & \\ 0 & 0 & \cdots & \Lambda_k \end{bmatrix}}_{\Lambda} P^{-1},$$

where Λ_i, $i = 1, \ldots, k$, are standard Jordan blocks. Without loss of generality, let the initial time $a = 0$ in (7.1). By defining $Y(t) \stackrel{\triangle}{=} P^{-1}\tilde{x}(t)$, (7.7) can be written as

$$Y^{(\alpha)}(t) = -\Lambda Y(t). \tag{7.8}$$

Note that each diagonal entry of Λ is an eigenvalue of A. Let λ_i be the ith eigenvalue of A. Let $y_i(t)$ be the ith component of $Y(t)$. The standard Jordan block Λ_ℓ is

$$
\begin{bmatrix}
\lambda_{j_\ell} & 1 & \cdots & 0 \\
0 & \lambda_{j_\ell+1} & \cdots & 0 \\
\vdots & \vdots & \ddots & \\
0 & 0 & \cdots & \lambda_{j_{\ell+1}-1}
\end{bmatrix},
$$

where $\lambda_{j_\ell} = \cdots = \lambda_{j_{\ell+1}-1}$. It follows that (7.8) can be decoupled into n one-dimensional equations represented by either

$$
y_i^{(\alpha)}(t) = -\lambda_i y_i(t) \tag{7.9}
$$

for the equation corresponding to the Jordan block that has a dimension equal to one or the last equation corresponding to the Jordan block that has a dimension larger than one, or

$$
y_i^{(\alpha)}(t) = -\lambda_i y_i(t) - y_{i+1}(t) \tag{7.10}
$$

otherwise.

Before deriving the main result, we need the following two lemmas regarding the solutions of (7.9) and (7.10).

Lemma 7.1. *The solution of* (7.9) *has the following properties*:

1. *When* $\lambda_i \neq 0$ *and* $\alpha \in (0, \chi_i)$, $\lim_{t \to \infty} y_i(t) = 0$, *where* $\chi_i \triangleq \frac{2[\pi - |\arg(\lambda_i)|]}{\pi}$.[1]
2. *When* $\lambda_i = 0$ *and* $\alpha \in (0, 1]$, $y_i(t) \equiv y_i(0)$, $\forall t \geq 0$.
3. *When* $\lambda_i = 0$ *and* $\alpha \in (1, 2)$, $y_i(t) = y_i(0) + \dot{y}_i(0)t$.
4. *When* $\alpha \in [2, \infty)$, *the system is not stable*.

Proof: (Part 1) By taking the Laplace transform of (7.9), it follows from (7.2) that

$$
Y_i(s) \triangleq \mathcal{L}\{y_i(t)\} = \frac{y_i(0^-)s^{\alpha-1}}{s^\alpha + \lambda_i}, \qquad \alpha \in (0, 1] \tag{7.11}
$$

and

$$
Y_i(s) \triangleq \mathcal{L}\{y_i(t)\} = \frac{y_i(0^-)s^{\alpha-1} + \dot{y}_i(0^-)s^{\alpha-2}}{s^\alpha + \lambda_i}, \qquad \alpha \in (1, 2). \tag{7.12}
$$

From (7.11) and (7.12), it can be seen that the denominator of $Y_i(s)$ is $s^\alpha + \lambda_i$ when $\alpha \in (0, 2)$. It follows from the discussion in [54] that when $\lambda_i \neq 0$ and $\alpha \in (0, \chi_i)$, all poles of $Y_i(s)$ are in the open left half plane. Applying the final value theorem, it follows that $\lim_{t \to \infty} y_i(t) = \lim_{s \to 0} sY_i(s) = 0$.

(Parts 2 and 3) The proofs of Properties 2 and 3 follow from [229].

(Part 4) See [110]. ∎

Lemma 7.2. *Assume that the continuous function* $y_{i+1}(t)$ *in* (7.10) *satisfies* $\lim_{t \to \infty} y_{i+1}(t) = 0$. *When* $\lambda_i \neq 0$ *and* $\alpha \in (0, \chi_i)$, *where* χ_i *is defined in Lemma* 7.1, *the solution of* (7.10) *satisfies that* $\lim_{t \to \infty} y_i(t) = 0$.

---

[1] Here we follow the convention that $\arg(x) \in (-\pi, \pi]$ for $x \in \mathbb{C}$ and $\arg(0) = 0$. Note that $0 \leq \chi_i \leq 2$ by definition. Therefore, $(0, \chi_i) \subseteq (0, 2)$.

Proof: When $\alpha \in (0,1] \cap (0,\chi_i) \neq \varnothing$, by taking the Laplace transform of (7.10), it follows from (7.2) that

$$Y_i(s) = \frac{s^{\alpha-1} y_i(0^-) - Y_{i+1}(s)}{s^\alpha + \lambda_i}. \tag{7.13}$$

It follows from the proof of Property 1 in Lemma 7.1 that the poles of (7.13) are in the open left half plane when $\lambda_i \neq 0$ and $\alpha \in (0,1] \cap (0,\chi_i)$. By applying the final value theorem, it follows that

$$\lim_{t\to\infty} y_i(t) = \lim_{s\to 0} sY_i(s) = \lim_{s\to 0} \frac{s^\alpha y_i(0^-) - sY_{i+1}(s)}{s^\alpha + \lambda_i} = 0,$$

where we have used the fact $\lim_{s\to 0} sY_{i+1}(s) = \lim_{t\to\infty} y_{i+1}(t) = 0$.

When $\alpha \in (1,2) \cap (0,\chi_i) \neq \varnothing$, by taking the Laplace transform of (7.10), it follows from (7.2) that

$$Y_i(s) = \frac{s^{\alpha-1} y_i(0^-) + s^{\alpha-2}\dot{y}_i(0^-) - Y_{i+1}(s)}{s^\alpha + \lambda_i}. \tag{7.14}$$

Following a similar discussion for $\alpha \in (0,1] \cap (0,\chi_i)$ gives that $\lim_{t\to\infty} y_i(t) = 0$.

Combining the above arguments proves the lemma. ∎

For the n-agent system, using (7.6), (7.5) can be written in a vector form as

$$\tilde{x}^{(\alpha)}(t) = -\mathscr{L}\tilde{x}(t), \tag{7.15}$$

where $\tilde{x}(t)$ is defined in (7.7) and $\mathscr{L}$ is the nonsymmetric Laplacian matrix associated with $\mathscr{A}$ and hence $\mathscr{G}$. We next study the conditions on the graph $\mathscr{G}$ and the fractional order α such that coordination is achieved.

Theorem 7.2. *Let λ_i be the ith eigenvalue of $\mathscr{L}$ and $\chi \triangleq \min_{\lambda_i \neq 0} \frac{2[\pi - |\arg(\lambda_i)|]}{\pi}$.[2] Using (7.6) for (7.5), coordination is achieved (i.e., $x_i(t) - x_j(t) \to \Delta_{ij}$ as $t \to \infty$) if the directed fixed graph $\mathscr{G}$ has a directed spanning tree and $\alpha \in (0,\chi)$. In particular, when $\alpha \in (0,1]$, $x_i(t) \to \delta_i + \mathbf{p}^T\tilde{x}(0)$ as $t \to \infty$, where $\mathbf{p} \in \mathbb{R}^n$ is defined in Lemma 1.1 and $\tilde{x}$ is defined in (7.7). When $\alpha \in (1,\chi)$, $|x_i(t) - \delta_i - [\mathbf{p}^T\tilde{x}(0) + \mathbf{p}^T\dot{\tilde{x}}(0)t]| \to 0$ as $t \to \infty$.*

Proof: We let $\mathscr{L}$ play the role of A in (7.7) and write $\mathscr{L}$ in the Jordan canonical form as $\mathscr{L} = P\Lambda P^{-1}$. Also let $Y(t) \triangleq P^{-1}\tilde{x}(t)$ and $y_i(t)$ be the ith component of $Y(t)$. Noting that $\mathscr{G}$ has a directed spanning tree, it follows from Lemma 1.1 that $\mathscr{L}$ has a simple zero eigenvalue and all other eigenvalues have positive real parts. Without loss of generality, let $\lambda_1 = 0$ and $\text{Re}(\lambda_i) > 0$, $i \neq 1$.

We first consider the case where $\alpha \in (0,1]$. Note that $(0,1] \subset (0,\chi)$. Because $\lambda_1 = 0$ is a simple zero eigenvalue, λ_1 satisfies (7.9). It follows from Property 2 in Lemma 7.1 that $y_1(t) \equiv y_1(0)$. When λ_i, $i \neq 1$, satisfies (7.9), it follows

---

[2] Note from the property of nonsymmetric Laplacian matrices, $\text{Re}(\lambda_i) > 0$ when $\lambda_i \neq 0$. It follows that $1 < \chi \leq 2$.

from Property 1 in Lemma 7.1 that $\lim_{t\to\infty} y_i(t) = 0$. When λ_i, $i \neq 1$, satisfies (7.10), suppose that λ_i belongs to the Jordan block Λ_ℓ. Then the last equation corresponding to Λ_ℓ, labeled as $j_{\ell+1} - 1$, satisfies (7.9). It follows from Property 1 in Lemma 7.1 that $\lim_{t\to\infty} y_{j_{\ell+1}-1} = 0$. By applying Lemma 7.2 recursively to $y_{j_{\ell+1}-2}, \ldots, y_{j_\ell}$, it follows that $\lim_{t\to\infty} y_i(t) = 0$. Combining the above arguments gives that $\lim_{t\to\infty} Y(t) = [y_1(0), 0, \ldots, 0]^T$, which implies $\lim_{t\to\infty} \tilde{x}(t) = \lim_{t\to\infty} PY(t) = PSY(0) = PSP^{-1}\tilde{x}(0)$, where $S = [s_{ij}] \in \mathbb{R}^{n\times n}$ has only one nonzero entry $s_{11} = 1$. Note that the first column of P can be chosen as $\mathbf{1}_n$ while the first row of P^{-1} can be chosen as $\mathbf{p}$ by noting that $\mathbf{1}_n$ and $\mathbf{p}$ are, respectively, a right and a left eigenvector of $\mathscr{L}$ associated with $\lambda_1 = 0$ and $\mathbf{p}^T\mathbf{1}_n = 1$. Therefore, $\lim_{t\to\infty} \tilde{x}(t) = PSP^{-1}\tilde{x}(0) = \mathbf{1}_n\mathbf{p}^T\tilde{x}(0)$, that is, $\lim_{t\to\infty} \tilde{x}_i(t) = \mathbf{p}^T\tilde{x}(0)$, which also implies that $x_i(t) - x_j(t) \to \Delta_{ij}$ as $t \to \infty$.

We next study the case where $\alpha \in (1, \chi)$. Note that $(1, \chi) \subseteq (1, 2)$. Similar to the previous discussion for $\alpha \in (0, 1]$, λ_1 satisfies (7.9). It follows from Property 3 in Lemma 7.1 that $y_1(t) = y_1(0) + \dot{y}_1(0)t$. Because $\text{Re}(\lambda_i) > 0$, $i \neq 1$, similar to the previous discussion for $\alpha \in (0, 1]$, it follows from Property 1 in Lemma 7.1 and Lemma 7.2 that $\lim_{t\to\infty} y_i(t) = 0$, $i \neq 1$. Therefore, it follows that $\lim_{t\to\infty} \|Y(t) - [y_1(0) + \dot{y}_1(0)t, 0, \ldots, 0]^T\| = 0$. Similar to the proof for $\alpha \in (0, 1]$, it follows that $\lim_{t\to\infty} |\tilde{x}_i(t) - [\mathbf{p}^T\tilde{x}(0) + \mathbf{p}^T\dot{\tilde{x}}(0)t]| = 0$, which also implies that $x_i(t) - x_j(t) \to \Delta_{ij}$ as $t \to \infty$.

Combining the previous arguments for $\alpha \in (0, 1]$ and $\alpha \in (1, \chi)$ proves the theorem. ∎

As a special case, when the fixed graph $\mathscr{G}$ is undirected, we can obtain the following result.

Corollary 7.1. *Assume that the fixed graph $\mathscr{G}$ is undirected. Using (7.6) for (7.5), coordination is achieved if $\mathscr{G}$ is connected and $\alpha \in (0, 2)$. The coordination equilibria when $\alpha \in (0, 1]$ and $\alpha \in (1, 2)$ are given as in Theorem 7.2.*

Proof: When the fixed undirected graph $\mathscr{G}$ is connected, it follows from Lemma 1.1 that $\mathscr{L}$ has a simple zero eigenvalue and all other eigenvalues are positive, which implies that $\chi = 2$. The statements then follow from the proof of Theorem 7.2. ∎

Remark 7.3 From Theorem 7.2, it can be seen that the final coordination equilibrium of (7.15) for $\alpha \in (0, 1]$ is the same as that of $\dot{\tilde{x}}(t) = -\mathscr{L}\tilde{x}(t)$ under the same $\mathscr{L}$ and $\tilde{x}(0)$.

From Theorem 7.2, it can be seen that the range of the fractional order α is determined by χ. Note that χ is closely related to the eigenvalues of $\mathscr{L}$, which are also related to the number of agents. In the following, we characterize the relationship between α and the number of agents to ensure coordination.

Theorem 7.4. *Assume that there are n agents in the team, where $n \geq 2$. Using (7.6) for (7.5), coordination is achieved if the directed fixed graph $\mathscr{G}$ has a directed spanning tree and $\alpha \in (0, 1 + \frac{2}{n})$.*

Proof: Letting λ_i be the ith eigenvalue of $\mathcal{L}$, it follows from [81] that $\arg(\lambda_i) \in [-\frac{\pi}{2} + \frac{\pi}{n}, \frac{\pi}{2} - \frac{\pi}{n}]$ for all $\lambda_i \neq 0$, which implies that $\chi \geq 1 + \frac{2}{n}$. Therefore, it follows from Theorem 7.2 that the statement holds. ∎

Remark 7.5 Theorem 7.4 implies that in a team consisting of a large number of agents, coordination is ensured when α is small enough. As $n \to \infty$, it follows that $\alpha \in (0, 1]$. This also implies that for fractional-order systems with the order $\alpha \in (0, 1]$, the number of agents in the team, n, does not play a role in determining whether coordination is achieved.

7.2.2 Directed Switching Interaction

In this subsection, we assume that the adjacency matrix $\mathscr{A}(t)$ is constant for $t \in [t_k, t_{k+1})$ and switches at time t_{k+1}, $k = 0, 1, \ldots$. Here we let $t_0 = 0$. Let $\mathscr{G}_k$ and $\mathscr{A}_k$ denote, respectively, the directed graph and the adjacency matrix associated with the n agents for $t \in [t_k, t_{k+1})$. We assume that $t_{k+1} - t_k \geq t_L$, where t_L is a positive constant. We also assume that each nonzero and hence positive entry of $\mathscr{A}_k$ has a lower bound $\underline{a}$ and an upper bound $\overline{a}$, where $\underline{a}$ and $\overline{a}$ are positive constants. Then (7.15) becomes

$$\tilde{x}^{(\alpha)}(t) = -\mathscr{L}_k \tilde{x}(t), \quad t \in [t_k, t_{k+1}), \tag{7.16}$$

where $\mathscr{L}_k \in \mathbb{R}^{n \times n}$ represents the nonsymmetric Laplacian matrix associated with $\mathscr{A}_k$ and hence $\mathscr{G}_k$. Before moving on, we need the following lemma.

Lemma 7.3. *Suppose that $\mathscr{L}$ in (7.15) is constant. When $\alpha \in (1, 2)$, the solution of (7.15) is*

$$\tilde{x}(t) = E_\alpha\big(-\mathscr{L}t^\alpha\big)\tilde{x}(0) + tE_{\alpha,2}\big(-\mathscr{L}t^\alpha\big)\dot{\tilde{x}}(0). \tag{7.17}$$

Proof: Note that $\alpha \in (1, 2)$. By applying the Laplace transform to both sides of (7.15), it follows from (7.2) that

$$s^\alpha \widetilde{X}(s) - s^{\alpha-1}\tilde{x}(0^-) - s^{\alpha-2}\dot{\tilde{x}}(0^-) = -\mathscr{L}\widetilde{X}(s), \tag{7.18}$$

where $\widetilde{X}(s) \stackrel{\triangle}{=} \mathfrak{L}\{\tilde{x}(t)\}$. After some manipulation, (7.18) can be written as

$$\widetilde{X}(s) = \big(s^\alpha I_n + \mathscr{L}\big)^{-1} s^{\alpha-1}\tilde{x}(0^-) + \big(s^\alpha I_n + \mathscr{L}\big)^{-1} s^{\alpha-2}\dot{\tilde{x}}(0^-). \tag{7.19}$$

By applying the inverse Laplace transform to (7.19), it follows from Theorem 3.2 in [171] that (7.17) is a solution of (7.15). Noting also that $\mathscr{L}$ is a constant matrix, it follows from the uniqueness and existence theorem of fractional equations in [229] that (7.17) is the unique solution of (7.15). ∎

Theorem 7.6. *Assume that $\alpha \in (0, 1 + \frac{2}{n})$, where $n \geq 2$. Using (7.6) for (7.5), a necessary condition to guarantee coordination is that there exists a finite constant*

N_2 such that the union of $\mathscr{G}_k$, $k = N_1, \ldots, N_1+N_2$, has a directed spanning tree for any finite N_1. Furthermore, if $\mathscr{G}_k$, $k = 0, 1, \ldots$, has a directed spanning tree, there exists positive $\overline{\Delta}_{k+1}$ such that coordination is achieved when $t_{k+1} - t_k \geq \overline{\Delta}_{k+1}$.[3]

Proof: For the first statement, when there does not exist a finite constant N_2 such that the union of $\mathscr{G}_k, k = N_1, \ldots, N_1 + N_2$, has a directed spanning tree for some N_1, at least one agent, labeled as i, is separated from the other agents for $t \geq t_{N_1}$. It follows that the state of agent i is independent of the states of the other agents for $t \geq t_{N_1}$, which implies that all agents cannot achieve coordination for arbitrary initial conditions.

For the second statement, we first consider the case where $\alpha \in (0, 1]$. It follows from Theorem 3.9 in [171] that for $\alpha \in (0, 1]$ the solution to (7.15) is given by

$$\tilde{x}(t) = E_\alpha\big(-\mathscr{L}t^\alpha\big)\tilde{x}(0).$$

Therefore, the solution to (7.16) is given by

$$\tilde{x}(t_j) = \prod_{i=1}^{j}\big\{E_\alpha\big(-\mathscr{L}_{i-1}t_i^\alpha\big)\big[E_\alpha\big(-\mathscr{L}_{i-1}t_{i-1}^\alpha\big)\big]^{-1}\big\}\tilde{x}(0). \qquad (7.20)$$

Define $V(t) \triangleq \max_i \tilde{x}_i(t) - \min_i \tilde{x}_i(t)$. Note from Theorem 7.2 that for $\alpha \in (0, 1]$, using (7.6) for (7.5), $\tilde{x}_i(t) - \tilde{x}_j(t) \to 0$ as $t \to \infty$ if the fixed interaction graph has a directed spanning tree. That is, if $\mathscr{G}_0$ has a directed spanning tree, then there exists a positive $\overline{\Delta}_1$ such that $V(t_1) < V(0)$ when $t_1 \geq \overline{\Delta}_1$. Similarly, according to (7.20), by considering $[E_\alpha(-\mathscr{L}_0 t_1^\alpha)]^{-1}E_\alpha(-\mathscr{L}_0 t_0^\alpha)\tilde{x}(0)$ as the new initial state, it follows that if $\mathscr{G}_1$ has a directed spanning tree, then there exists a positive $\overline{\Delta}_2$ such that $V(t_2) < V(t_1)$ when $t_2 - t_1 \geq \overline{\Delta}_2$. By following a similar analysis, we know that there exists $\overline{\Delta}_{k+1}$ such that $V(t_{k+1}) < V(t_k)$ when $t_{k+1} - t_k \geq \overline{\Delta}_{k+1}$. It thus follows that $V(t_{k+1}) \to 0$ as $k \to \infty$. Therefore, $\tilde{x}_i(t) - \tilde{x}_j(t) \to 0$, i.e., $x_i(t) - x_j(t) \to \Delta_{ij}$ as $t \to \infty$ under the condition of the theorem.

We then consider the case when $\alpha \in (1, 1 + \frac{2}{n})$. Note that $\alpha \in (1 + \frac{2}{n}) \subseteq (1, 2)$, taking the derivative of (7.17) with respect to t gives that

$$\dot{\tilde{x}}(t) = \frac{1}{t}E_{\alpha,0}\big(-\mathscr{L}t^\alpha\big)\tilde{x}(0) + E_\alpha\big(-\mathscr{L}t^\alpha\big)\dot{\tilde{x}}(0). \qquad (7.21)$$

Combining (7.17) and (7.21) leads to the following vector form

$$\begin{bmatrix} \tilde{x}(t) \\ \dot{\tilde{x}}(t) \end{bmatrix} = \begin{bmatrix} E_\alpha(-\mathscr{L}t^\alpha) & tE_{\alpha,2}(-\mathscr{L}t^\alpha) \\ \frac{1}{t}E_{\alpha,0}(-\mathscr{L}t^\alpha) & E_\alpha(-\mathscr{L}t^\alpha) \end{bmatrix} \begin{bmatrix} \tilde{x}(0) \\ \dot{\tilde{x}}(0) \end{bmatrix}. \qquad (7.22)$$

Therefore, we can get that

---

[3] Here the values of $\overline{\Delta}_{k+1}, k = 0, 1, \ldots$, depend on $\tilde{x}(t_k)$, the fractional-order α, and $\mathscr{G}_k$.

$$
\begin{bmatrix} \tilde{x}(t_1) \\ \dot{\tilde{x}}(t_1) \end{bmatrix} = \begin{bmatrix} E_\alpha(-\mathscr{L}_0 t_1^\alpha) & t_1 E_{\alpha,2}(-\mathscr{L}_0 t_1^\alpha) \\ \frac{1}{t_1} E_{\alpha,0}(-\mathscr{L}_0 t^\alpha) & E_\alpha(-\mathscr{L}_0 t_1^\alpha) \end{bmatrix} \begin{bmatrix} \tilde{x}(0) \\ \dot{\tilde{x}}(0) \end{bmatrix}.
$$

Similarly, we can also get that

$$
\begin{bmatrix} \tilde{x}(t_k) \\ \dot{\tilde{x}}(t_k) \end{bmatrix} = \left(\prod_{i=0}^{k-1} C_i \right) B_{0,0} \begin{bmatrix} \tilde{x}(0) \\ \dot{\tilde{x}}(0) \end{bmatrix}, \tag{7.23}
$$

where $C_0 \triangleq I_{2n}$ and $C_k \triangleq B_{k+1,k+1} B_{k+1,k}^{-1}$, $k = 1, 2, \ldots$, with

$$
B_{m,n} \triangleq \begin{bmatrix} E_\alpha(-\mathscr{L}_m t_{n+1}^\alpha) & t_{n+1} E_{\alpha,2}(-\mathscr{L}_m t_{n+1}^\alpha) \\ \frac{E_{\alpha,0}(-\mathscr{L}_m t_{n+1}^\alpha)}{t_{n+1}} & E_\alpha(-\mathscr{L}_m t_{n+1}^\alpha) \end{bmatrix}.
$$

Note from Theorem 7.2, if $\mathscr{G}_0$ has a directed spanning tree, then it follows that there exists a positive $\overline{\Delta}_1$ such that $V(t_1) < V(0)$ when $t_1 \geq \overline{\Delta}_1$. Similarly, by considering $B_{1,0}^{-1} B_{0,0} \begin{bmatrix} x(0) \\ \dot{x}(0) \end{bmatrix}$ the new initial state, if $\mathscr{G}_1$ has a directed spanning tree, then there exists a positive $\overline{\Delta}_2$ such that $V(t_2) < V(t_1)$ when $t_2 - t_1 \geq \overline{\Delta}_2$. Similarly, if $\mathscr{G}_k, k = 2, 3, \ldots$, has a directed spanning tree, we can also show the existence of $\overline{\Delta}_{k+1}$. Because $V(t_{k+1}) < V(t_k)$, it follows that $V(t_{k+1}) \to 0$ as $k \to \infty$. Therefore, we can get that $\tilde{x}_i(t) - \tilde{x}_j(t) \to 0$, i.e., $x_i(t) - x_j(t) \to \Delta_{ij}$ as $t \to \infty$ under the condition of the theorem. ∎

Remark 7.7 For the system (7.5) with $\alpha = 1$, $x_i(t)$ will decrease if $u_i(t) < 0$ and $x_i(t)$ will increase if $u_i(t) > 0$. However, for the system (7.5) with $\alpha \in (0,1) \cup (1, 1 + \frac{2}{n})$, due to the long memory process of fractional calculus, the aforementioned property does not necessarily hold. Therefore, even if the switching interaction graph has a directed spanning tree at each time interval, coordination might not be achieved ultimately because how fast the graph switches also plays an important role.

Remark 7.8 It can be seen from (7.20) and (7.23) that unlike the integer-order systems, there does not exist a transition matrix for fractional-order systems. Therefore, the analysis for fractional-order systems is more challenging than that for integer-order systems.

7.2.3 Simulation

In this subsection, several simulation results are presented. To illustrate the results in Sect. 7.2.1, we consider a team of twelve agents with a directed fixed graph $\mathscr{G}$ shown by Fig. 7.1. Note that $\mathscr{G}$ has a directed spanning tree with node 1 being the root. We let $a_{ij} = 1$ if $(j, i) \in \mathscr{E}$ and $a_{ij} = 0$ otherwise. Here for simplicity we choose $\delta_i = 0$, which implies that $\Delta_{ij} = 0$. That is, $\tilde{x}(t) = x(t)$, where $x(t) \triangleq$
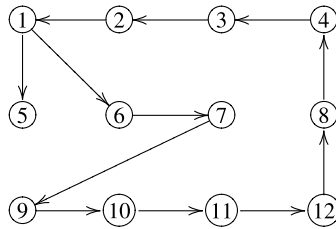
Fig. 7.1 Directed graph $\mathcal{G}$ for twelve agents. An *arrow* from j to i denotes that agent j is a neighbor of agent i

(a) $\alpha = 0.8$

(b) $\alpha = 1$

(c) $\alpha = 1.15$

(d) $\alpha = 1.5$
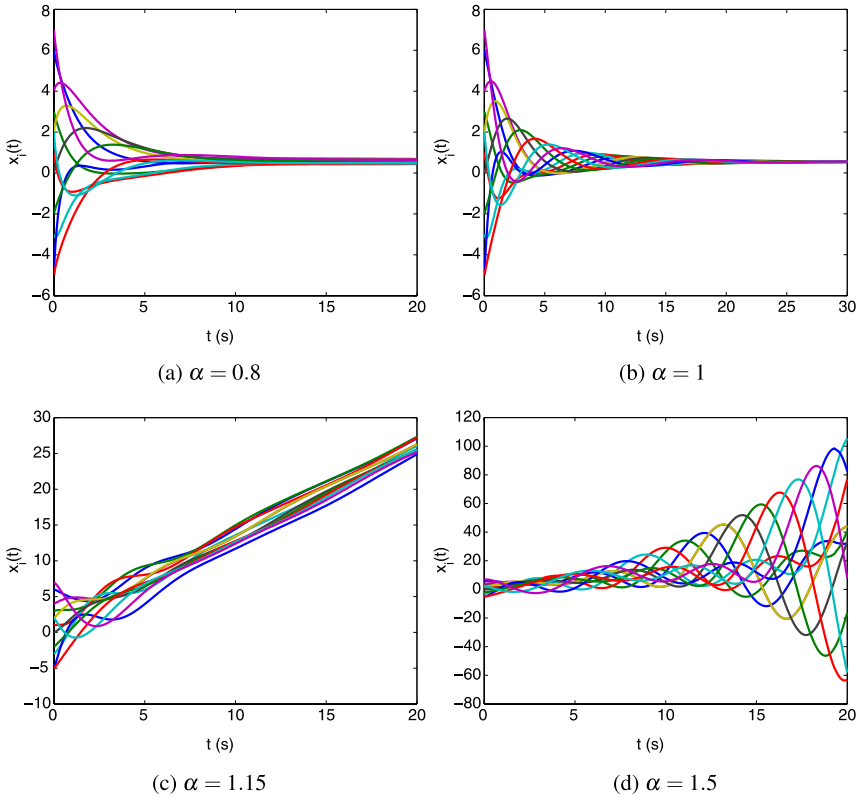
Fig. 7.2 States of the twelve agents using (7.6) with different fractional orders

$[x_1(t), \ldots, x_{12}(t)]^T$ and $\tilde{x}(t) \triangleq [\tilde{x}_1(t), \ldots, \tilde{x}_{12}(t)]^T$ with $\tilde{x}_i(t) \triangleq x_i(t) - \delta_i$. It can be computed that $\mathbf{p} = [\frac{1}{11}, \frac{1}{11}, \frac{1}{11}, \frac{1}{11}, 0, \frac{1}{11}, \frac{1}{11}, \frac{1}{11}, \frac{1}{11}, \frac{1}{11}, \frac{1}{11}, \frac{1}{11}]^T$.

For $\alpha \in (0, 1]$, let the initial states be $x(0) = [6, 3, 1, -3, 4, 2, 0, -5, -2, -5, 2, 7]^T$. When the fractional order is $\alpha = 0.8$, the states of the agents using (7.6) are shown in Fig. 7.2. It can be seen that coordination is achieved with the final coordination equilibrium for $x_i(t)$ being 0.5455, which is equal to $\mathbf{p}^T x(0)$. When $\alpha = 1$ (i.e., the system takes in the form of single-integrator dynamics),

the states of the agents using (7.6) are shown in Fig. 7.2(b). From these two fig-
ures, it can be seen that the coordination equilibria for both cases are the same
given identical initial conditions. For $\alpha \in (1, \chi)$, we let the initial states be $x(0) =$
$[6, 3, 1, -3, 4, 2, 0, -5, -2, -5, 2, 7]^T$ and $\dot{x}(0) = [1, 2, 3, 4, 0, 0, 0, 0, 1, 1, 1, 1]^T$.
It follows from the definition of χ in Theorem 7.2 that $\chi = 1.182$. Figures 7.2(c)
and 7.2(d) show the states using (7.6) when $\alpha = 1.15$ and $\alpha = 1.5$, respectively.
From Fig. 7.2(c), it can be observed that coordination is achieved. From Fig. 7.2(d),
it can be observed that coordination is not achieved due to the fact that $\alpha > \chi$. The
four subfigures in Fig. 7.2 validate Theorem 7.2.

To illustrate the results in Sect. 7.2.2, we consider a team of four agents. We let
$\mathscr{G}(t)$ switch from $\{\mathscr{G}_{(1)}, \mathscr{G}_{(2)}\}$ as shown in Fig. 7.3. Note that both $\mathscr{G}_{(1)}$ and $\mathscr{G}_{(2)}$
have a directed spanning tree. We let $a_{ij}(t) = 1$ if $(j, i) \in \mathscr{E}(t)$ and $a_{ij}(t) = 0$
otherwise. Here for simplicity we choose $\delta_i = 0$, which implies that $\Delta_{ij} = 0$. Fig-
ure 7.4 shows the states of the four agents using (7.6) when $\mathscr{G}(t)$ switches between
$\mathscr{G}_{(1)}$ and $\mathscr{G}_{(2)}$ every 3 seconds with $\alpha = 0.8$. It can be seen that coordination is
achieved in this case.

(a) $\mathscr{G}_{(1)}$ (b) $\mathscr{G}_{(2)}$
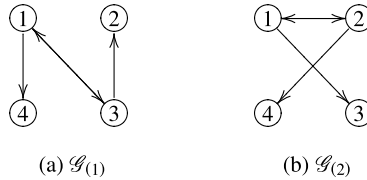
Fig. 7.3 Directed switching graphs $\mathscr{G}_{(1)}$ and $\mathscr{G}_{(2)}$. An *arrow* from j to i denotes that agent j is a
neighbor of agent i
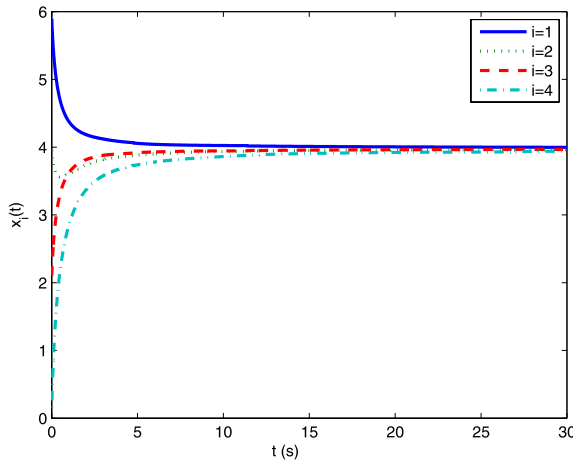
Fig. 7.4 States of the four agents using (7.6) when $\mathscr{G}(t)$ switches between $\mathscr{G}_{(1)}$ and $\mathscr{G}_{(2)}$ as shown
in Fig. 7.3 every 3 seconds with $\alpha = 0.8$

7.3 Stability Analysis of Fractional-order Coordination Algorithms with Absolute/Relative Damping for Networked Fractional-order Systems

In this section, we first propose fractional-order coordination algorithms with, respectively, absolute and relative damping for networked fractional-order systems. We then study the conditions on the interaction graph and the fractional order such that coordination is achieved when using these two algorithms under a directed fixed interaction graph.

7.3.1 Absolute Damping

In this subsection, we propose the following fractional-order coordination algorithm with absolute damping for (7.5) as

$$u_i(t) = -\sum_{j=1}^{n} a_{ij}\left[x_i(t) - x_j(t) - \Delta_{ij}\right] - \beta x_i^{(\alpha/2)}(t), \tag{7.24}$$

where a_{ij} is defined as in (7.6), and β is a positive scalar. Using (7.24), (7.5) can be written in a vector form as

$$\tilde{x}^{(\alpha)}(t) + \beta\tilde{x}^{(\alpha/2)}(t) + \mathscr{L}\tilde{x}(t) = 0, \tag{7.25}$$

where $\tilde{x}(t)$ is defined in (7.7) and $\mathscr{L}$ is defined in (7.15). It then follows that (7.25) can be written as

$$\begin{bmatrix} \tilde{x}(t) \\ \tilde{x}^{(\alpha/2)}(t) \end{bmatrix}^{(\alpha/2)} = \underbrace{\begin{bmatrix} 0_{n\times n} & I_n \\ -\mathscr{L} & -\beta I_n \end{bmatrix}}_{F} \begin{bmatrix} \tilde{x}(t) \\ \tilde{x}^{(\alpha/2)}(t) \end{bmatrix}. \tag{7.26}$$

Note that according to Lemma 3.1, each eigenvalue of $\mathscr{L}$, λ_i, corresponds to two eigenvalues of F, denoted by

$$\mu_{2i-1} = \frac{-\beta + \sqrt{\beta^2 - 4\lambda_i}}{2}, \qquad \mu_{2i} = \frac{-\beta - \sqrt{\beta^2 - 4\lambda_i}}{2}. \tag{7.27}$$

Note that F can be written in the Jordan canonical form as

$$F = P \underbrace{\begin{bmatrix} \Lambda_1 & 0 & \cdots & 0 \\ 0 & \Lambda_2 & \cdots & 0 \\ \vdots & \vdots & \ddots & \\ 0 & 0 & \cdots & \Lambda_k \end{bmatrix}}_{\Lambda} P^{-1},$$

where Λ_i, $i = 1, \ldots, k$, are the standard Jordan blocks. Note that each diagonal entry of Λ is an eigenvalue of F. By defining $Z(t) \triangleq P^{-1}\left[\begin{smallmatrix} \tilde{x}(t) \\ \tilde{x}^{(\alpha/2)}(t) \end{smallmatrix}\right]$, (7.26) can be written as

$$Z^{(\alpha/2)}(t) = \Lambda Z(t). \tag{7.28}$$

Let $z_i(t)$, $i = 1, \ldots, 2n$, be the ith component of $Z(t)$. Similar to the analysis in Sect. 7.2.1, (7.28) can be decoupled into $2n$ one-dimensional equations represented by either

$$z_i^{(\alpha/2)}(t) = \mu_i z_i(t) \tag{7.29}$$

or

$$z_i^{(\alpha/2)}(t) = \mu_i z_i(t) + z_{i+1}(t). \tag{7.30}$$

Theorem 7.9. *Let λ_i be the ith eigenvalue of $\mathcal{L}$, and μ_{2i-1} and μ_{2i} be the two eigenvalues of F corresponding to λ_i. Define $\psi \triangleq \min_{\mu_i \neq 0, i=1,2,\ldots,2n} \frac{4[\pi - |\arg(-\mu_i)|]}{\pi}$. Using (7.24) for (7.5), coordination is achieved (i.e., $x_i(t) - x_j(t) \to \Delta_{ij}$ as $t \to \infty$) if the directed fixed graph $\mathcal{G}$ has a directed spanning tree and $\alpha \in (0, \psi)$. In particular, the following properties hold*:

Case 1. $\beta > \max_{\lambda_i \neq 0} \frac{|\mathrm{Im}(\lambda_i)|}{\sqrt{\mathrm{Re}(\lambda_i)}}$. *When $\alpha \in (0, 2]$, $x_i(t) \to \delta_i + \mathbf{p}^T \tilde{x}(0) + \frac{1}{\beta}\mathbf{p}^T \tilde{x}^{(\alpha/2)}(0)$ as $t \to \infty$, where $\mathbf{p} \in \mathbb{R}^n$ is defined in Lemma 1.1 and $\tilde{x}$ is defined in (7.7). When $\alpha \in (2, \psi)$, $|x_i(t) - \delta_i - \{\mathbf{p}^T \tilde{x}(0) + \frac{1}{\beta}\mathbf{p}^T \tilde{x}^{(\alpha/2)}(0) + [\mathbf{p}^T \dot{\tilde{x}}(0) + \frac{1}{\beta}\mathbf{p}^T \tilde{x}^{(1+\alpha/2)}(0)]t\}| \to 0$ as $t \to \infty$.*

Case 2. $0 < \beta \leq \max_{\lambda_i \neq 0} \frac{|\mathrm{Im}(\lambda_i)|}{\sqrt{\mathrm{Re}(\lambda_i)}}$. *Then we have that $x_i(t) \to \delta_i + \mathbf{p}^T \tilde{x}(0) + \frac{1}{\beta}\mathbf{p}^T \tilde{x}^{(\alpha/2)}(0)$ as $t \to \infty$.*

Proof: (Case 1) When the directed fixed graph $\mathcal{G}$ has a directed spanning tree, if follows from Lemma 1.1 that $\mathcal{L}$ has a simple zero eigenvalue and all other eigenvalues have positive real parts. Without loss of generality, let $\lambda_1 = 0$ and $\mathrm{Re}(\lambda_i) > 0$, $i \neq 1$. For $\lambda_1 = 0$, note from (7.27) that $\mu_1 = 0$ and $\mu_2 = -\beta$. Because the eigenvalue $\lambda_1 = 0$ of $\mathcal{L}$ is simple, it follows from (7.27) that the corresponding eigenvalues $\mu_1 = 0$ and $\mu_2 = -\beta$ of F are also simple. Therefore, both μ_1 and μ_2 satisfy (7.29). Because $\beta > \max_{\lambda_i \neq 0} \frac{|\mathrm{Im}(\lambda_i)|}{\sqrt{\mathrm{Re}(\lambda_i)}}$, it follows from Lemma 3.1 that $\mathrm{Re}(\mu_{2i-1}) < 0$ and $\mathrm{Re}(\mu_{2i}) < 0$, $i \neq 1$. Note that $2 < \psi \leq 4$. We first consider the case where $\alpha \in (0, 2]$. Note from Property 2 in Lemma 7.1 that $z_1(t) \equiv z_1(0)$ and from Property 1 in Lemma 7.1 that $z_2(t) \to 0$ as $t \to \infty$. When μ_{2i-1} and μ_{2i} satisfy (7.29), it then follows from Property 1 of Lemma 7.1 that $z_{2i-1}(t) \to 0$ and $z_{2i}(t) \to 0$ as $t \to \infty$. When μ_{2i-1} and μ_{2i} satisfy (7.30), it then follows from Lemma 7.2 and a similar argument to that in Theorem 7.2 that $z_{2i-1}(t) \to 0$ and $z_{2i}(t) \to 0$ as $t \to \infty$ as well. Combining the above arguments gives that $\lim_{t \to \infty} Z(t) = [z_1(0), 0, \ldots, 0]^T$, which implies $\lim_{t \to \infty}\left[\begin{smallmatrix} \tilde{x}(t) \\ \tilde{x}^{(\alpha/2)}(t) \end{smallmatrix}\right] = \lim_{t \to \infty} PZ(t) = PSZ(0) = PSP^{-1}\left[\begin{smallmatrix} \tilde{x}(0) \\ \tilde{x}^{(\alpha/2)}(0) \end{smallmatrix}\right]$, where $S = [s_{ij}] \in \mathbb{R}^{2n \times 2n}$ has only one nonzero entry $s_{11} = 1$. Note from Lemmas 1.1 and 3.1 that $[\mathbf{1}_n^T, \mathbf{0}_n^T]^T$ and $[\mathbf{p}^T, \frac{1}{\beta}\mathbf{p}^T]^T$ are, respectively, a right and a

left eigenvector of F associated with $\mu_1 = 0$, where $[\mathbf{p}^T, \frac{1}{\beta}\mathbf{p}^T][\mathbf{1}_n^T, \mathbf{0}_n^T]^T = 1$. It thus follows that the first column of P can be chosen as $[\mathbf{1}_n^T, \mathbf{0}_n^T]^T$ while the first row of P^{-1} can be chosen as $[\mathbf{p}^T, \frac{1}{\beta}\mathbf{p}^T]^T$. Therefore, $\lim_{t\to\infty}\begin{bmatrix} \tilde{x}(t) \\ \tilde{x}^{(\alpha/2)}(t) \end{bmatrix} = PSP^{-1}\begin{bmatrix} \tilde{x}(0) \\ \tilde{x}^{(\alpha/2)}(0) \end{bmatrix} = [\mathbf{1}_n^T, \mathbf{0}_n^T][\mathbf{p}^T, \frac{1}{\beta}\mathbf{p}^T]^T\begin{bmatrix} \tilde{x}(0) \\ \tilde{x}^{(\alpha/2)}(0) \end{bmatrix}$, that is, $\lim_{t\to\infty}\tilde{x}_i(t) = \mathbf{p}^T\tilde{x}(0) + \frac{1}{\beta}\mathbf{p}^T\tilde{x}^{(\alpha/2)}(0)$. We next consider the case where $\alpha \in (2, \psi)$. Note from Property 3 of Lemma 7.1 that $z_1(t) = z_1(0) + \dot{z}_1(0)t$. A similar discussion to that for $\alpha \in (0, 2]$ shows that $z_i(t) \to 0$, $i = 2, \ldots, 2n$, as $t \to \infty$. Therefore, it follows that $\lim_{t\to\infty}\|Z(t) - [z_1(0) + \dot{z}_1(0)t, 0, \ldots, 0]^T\| = 0$. Similar to the proof for $\alpha \in (0, 2]$, we can get that $\lim_{t\to\infty}|\tilde{x}_i(t) - \{\mathbf{p}^T\tilde{x}(0) + \frac{1}{\beta}\mathbf{p}^T\tilde{x}^{(\alpha/2)}(0) + [\mathbf{p}^T\dot{\tilde{x}}(0) + \frac{1}{\beta}\mathbf{p}^T\tilde{x}^{(1+\alpha/2)}(0)]t\}| = 0$.

(Case 2) When $0 < \beta \leq \max_{\lambda_i \neq 0} \frac{|\text{Im}(\lambda_i)|}{\sqrt{\text{Re}(\lambda_i)}}$, it follows from Lemma 3.1 that $\text{Re}(\mu_{2i-1}) \geq 0$ for some $\lambda_i \neq 0$, which implies that $\psi \leq 2$. Therefore, we can get that $\alpha \in (0, 2)$. The proof then follows a similar analysis to that of Case 1 when $\alpha \in (0, 2]$. ∎

Remark 7.10 From Theorem 7.9, it can be noted that the control gain β can be chosen as any positive number. Of course, the possible range of α to ensure coordination will be different depending on β. The existing coordination algorithms for double-integrator dynamics with absolute damping studied in [248, Chap. 4] can be viewed as a special case of Theorem 7.9 when $\alpha = 2$. In addition, even when there exists absolute damping, depending on the value of α, the final state derivatives might not be zero as shown in Theorem 7.6, which is different from the results in [248, Chap. 4].

7.3.2 Relative Damping

In this subsection, we propose the following fractional-order coordination algorithm with relative damping for (7.5) as

$$u_i(t) = -\sum_{j=1}^{n} a_{ij}\{[x_i(t) - x_j(t) - \Delta_{ij}] + \gamma[x_i^{(\alpha/2)}(t) - x_j^{(\alpha/2)}(t)]\}, \quad (7.31)$$

where a_{ij} is defined as in (7.6), and γ is a positive scalar. Using (7.31), (7.5) can be written in a vector form as

$$\tilde{x}^{(\alpha)}(t) + \gamma\mathscr{L}\tilde{x}^{(\alpha/2)}(t) + \mathscr{L}\tilde{x}(t) = 0, \quad (7.32)$$

where $\tilde{x}(t)$ is defined in (7.7) and $\mathscr{L}$ is defined in (7.15). It follows that (7.32) can be written as

$$\begin{bmatrix} \tilde{x}(t) \\ \tilde{x}^{(\alpha/2)}(t) \end{bmatrix}^{(\alpha/2)} = \underbrace{\begin{bmatrix} 0_{n \times n} & I_n \\ -\mathscr{L} & -\gamma\mathscr{L} \end{bmatrix}}_{G} \begin{bmatrix} \tilde{x}(t) \\ \tilde{x}^{(\alpha/2)}(t) \end{bmatrix}. \qquad (7.33)$$

Before moving on, we need the following lemma.

Lemma 7.4. *Let ξ_i be the ith eigenvalue of $A \in \mathbb{R}^{n \times n}$ with, respectively, an associated right eigenvector q_i and an associated left eigenvector s_i. Also let $B = \begin{bmatrix} 0_{n \times n} & I_n \\ -A & -\gamma A \end{bmatrix}$, where γ is a positive scalar. Then the eigenvalues of B are given by $\zeta_{2i-1} = \frac{-\gamma\xi_i + \sqrt{\gamma^2\xi_i^2 - 4\xi_i}}{2}$ with the associated right and left eigenvectors given by, respectively, $\begin{bmatrix} q_i \\ \zeta_{2i-1}q_i \end{bmatrix}$ and $\begin{bmatrix} (\zeta_{2i-1} + \gamma\xi_i)s_i \\ s_i \end{bmatrix}$, and $\zeta_{2i} = \frac{-\gamma\xi_i - \sqrt{\gamma^2\xi_i^2 - 4\xi_i}}{2}$, with the associated right and left eigenvectors given by, respectively, $\begin{bmatrix} q_i \\ \zeta_{2i}q_i \end{bmatrix}$ and $\begin{bmatrix} (\zeta_{2i} + \gamma\xi_i)s_i \\ s_i \end{bmatrix}$. When $\mathrm{Re}(\xi_i) > 0$, $\mathrm{Re}(\zeta_{2i-1}) < 0$ and $\mathrm{Re}(\zeta_{2i}) < 0$ if and only if $\gamma > \frac{|\mathrm{Im}(\xi_i)|}{\sqrt{\mathrm{Re}(\xi_i)|\xi_i|}}$.*

Proof: For the first statement, suppose that ζ is an eigenvalue of B with an associated right eigenvector $\begin{bmatrix} f \\ g \end{bmatrix}$, where $f, g \in \mathbb{C}^n$. It follows that $\begin{bmatrix} 0_{n \times n} & I_n \\ -A & -\gamma A \end{bmatrix} \begin{bmatrix} f \\ g \end{bmatrix} = \zeta \begin{bmatrix} f \\ g \end{bmatrix}$, which implies $g = \zeta f$ and $-Af - \gamma Ag = \zeta g$. It thus follows that $-(1 + \gamma\zeta)Af = \zeta^2 f$. Noting that $Aq_i = \xi_i q_i$, we let $f = q_i$. It thus follows that $\zeta^2 = -\xi_i - \gamma\zeta\xi_i$. That is, each eigenvalue of A, ξ_i, corresponds to two eigenvalues of B, denoted by $\zeta_{2i-1,2i} = \frac{-\gamma\xi_i \pm \sqrt{\gamma^2\xi_i^2 - 4\xi_i}}{2}$. Because $g = \zeta f$, it follows that the right eigenvectors associated with ζ_{2i-1} and ζ_{2i} are, respectively, $\begin{bmatrix} q_i \\ \zeta_{2i-1}q_i \end{bmatrix}$ and $\begin{bmatrix} q_i \\ \zeta_{2i}q_i \end{bmatrix}$. A similar analysis can be used to find the left eigenvectors of B associated with ζ_{2i-1} and ζ_{2i}.

For the second statement, note that $\sqrt{\gamma^2\xi_i^2 - 4\xi_i}$ has a nonnegative real part. Because $\zeta_{2i} = \frac{-\gamma\xi_i - \sqrt{\gamma^2\xi_i^2 - 4\xi_i}}{2}$, it follows that $\mathrm{Re}(\zeta_{2i}) < 0$ if $\gamma > 0$. It is left to show the conditions under which $\mathrm{Re}(\zeta_{2i-1}) < 0$. Suppose that γ_i^* is the critical value for γ such that ζ_{2i-1} is on the imaginary axis. Let $\zeta_{2i-1} = \eta_i \iota$, where $\eta_i \in \mathbb{R}$. After some manipulation, it follows that $\gamma_i^* = \frac{|\mathrm{Im}(\xi_i)|}{\sqrt{\mathrm{Re}(\xi_i)|\xi_i|}}$. Note that $\mathrm{Re}(\xi_i) > 0$. It is straightforward to verify that if $\gamma_i > \gamma_i^*$ (respectively, $\gamma_i < \gamma_i^*$), $\mathrm{Re}(\zeta_{2i-1}) < 0$ (respectively, $\mathrm{Re}(\zeta_{2i-1}) > 0$). Therefore, when $\mathrm{Re}(\xi_i) > 0$, $\mathrm{Re}(\zeta_{2i-1}) < 0$ and $\mathrm{Re}(\zeta_{2i}) < 0$ if and only if $\gamma > \frac{|\mathrm{Im}(\xi_i)|}{\sqrt{\mathrm{Re}(\xi_i)|\xi_i|}}$. ∎

According to Lemma 7.4, each eigenvalue of $\mathscr{L}$, λ_i, also corresponds to two eigenvalues of G, denoted by

$$\mu_{2i-1} = \frac{-\gamma\lambda_i + \sqrt{\gamma^2\lambda_i^2 - 4\lambda_i}}{2}, \qquad \mu_{2i} = \frac{-\gamma\lambda_i - \sqrt{\gamma^2\lambda_i^2 - 4\lambda_i}}{2}. \qquad (7.34)$$

Note that G can also be written in the Jordan canonical form as

$$G = Q \begin{bmatrix} \Sigma_1 & 0 & \cdots & 0 \\ 0 & \Sigma_2 & \cdots & 0 \\ \vdots & \vdots & \ddots & \\ 0 & 0 & \cdots & \Sigma_k \end{bmatrix}}_{\Sigma} Q^{-1},$$

where Σ_i, $i = 1, \ldots, k$, are the standard Jordan blocks. Note that each entry of Σ is an eigenvalue of G. By defining $Z(t) \triangleq Q^{-1} \left[\begin{smallmatrix} \tilde{x}(t) \\ \tilde{x}^{(\alpha/2)}(t) \end{smallmatrix} \right]$, (7.33) can be written as

$$Z^{(\alpha/2)}(t) = \Sigma Z(t). \tag{7.35}$$

Let $z_i(t)$, $i = 1, \ldots, 2n$, be the ith component of $Z(t)$. Similar to the analysis of (7.28), (7.35) can be decoupled into $2n$ one-dimensional equations represented by either (7.29) or (7.30).

Theorem 7.11. *Let λ_i be the ith eigenvalue of $\mathscr{L}$, and μ_{2i-1} and μ_{2i} be the two eigenvalues of G corresponding to λ_i. Define $\psi \triangleq \min_{\mu_i \neq 0, i=1,\ldots,2n} \frac{4[\pi - |\arg(-\mu_i)|]}{\pi}$. Using (7.32) for (7.5), coordination is achieved (i.e., $x_i(t) - x_j(t) \to \Delta_{ij}$ as $t \to \infty$) if the directed fixed graph $\mathscr{G}$ has a directed spanning tree and $\alpha \in (0, \psi)$. In addition, the following properties hold*:

Case 1. $\gamma > \max_{\lambda_i \neq 0} \frac{|\mathrm{Im}(\lambda_i)|}{\sqrt{\mathrm{Re}(\lambda_i)|\lambda_i|}}$. *When $\alpha \in (0, 2]$, $|x_i(t) - \delta_i - [\mathbf{p}^T \tilde{x}(0) +$*

$\frac{t^{\alpha/2}}{\Gamma(1+\alpha/2)} \mathbf{p}^T \tilde{x}^{(\alpha/2)}(0)]| \to 0$ *as $t \to \infty$, where $\mathbf{p} \in \mathbb{R}^n$ is defined in Lemma 1.1 and $\tilde{x}$ is defined in (7.7). When $\alpha \in (2, \psi)$, $|x_i(t) - \delta_i - [\mathbf{p}^T \tilde{x}(0) + \frac{t^{\alpha/2}}{\Gamma(1+\alpha/2)} \mathbf{p}^T \tilde{x}^{(\alpha/2)}(0) + \frac{t^{1+\alpha/2}}{\Gamma(2+\alpha/2)} \tilde{x}^{(1+\alpha/2)}(0)]| \to 0$ as $t \to \infty$.*

Case 2. $0 < \gamma \leq \max_{\lambda_i \neq 0} \frac{|\mathrm{Im}(\lambda_i)|}{\sqrt{\mathrm{Re}(\lambda_i)|\lambda_i|}}$. *Then we have that $|x_i(t) - \delta_i - [\mathbf{p}^T \tilde{x}(0) +$*

$\frac{t^{\alpha/2}}{\Gamma(1+\alpha/2)} \mathbf{p}^T \tilde{x}^{(\alpha/2)}(0)]| \to 0$ *as $t \to \infty$.*

Proof: (Case 1) When the directed fixed graph $\mathscr{G}$ has a directed spanning tree, it follows from Lemma 1.1 that $\mathscr{L}$ has a simple zero eigenvalue and all other eigenvalues have positive real parts. Without loss of generality, let $\lambda_1 = 0$ and $\mathrm{Re}(\lambda_i) > 0$, $i \neq 1$. For $\lambda_1 = 0$, note from (7.34) that $\mu_1 = 0$ and $\mu_2 = 0$. It also follows from Lemma 7.4 that the zero eigenvalue of G has algebraic multiplicity equal to two but geometric multiplicity equal to one. Therefore, it follows that $\mu_2 = 0$ satisfies (7.29) and $\mu_1 = 0$ satisfies (7.30). Because $\gamma > \max_{\lambda_i \neq 0} \frac{|\mathrm{Im}(\lambda_i)|}{\sqrt{\mathrm{Re}(\lambda_i)|\lambda_i|}}$, it follows from Lemma 7.4 that $\mathrm{Re}(\mu_{2i-1}) < 0$ and $\mathrm{Re}(\mu_{2i}) < 0$, $i \neq 1$. Note that $2 < \psi \leq 4$. We first consider the case where $\alpha \in (0, 2]$. Note from Property 2 in Lemma 7.1 that $z_2(t) \equiv z_2(0)$. By substituting $z_2(t) = z_2(0)$ into (7.30), it follows that $z_1(t) = z_2(0) \frac{t^{\alpha/2}}{\Gamma(1+\alpha/2)} + z_1(0)$. When μ_{2i-1} and μ_{2i} satisfy (7.29), it then follows from Property 1 of Lemma 7.1 that $z_{2i-1}(t) \to 0$ and $z_{2i}(t) \to 0$ as $t \to \infty$. When μ_{2i-1} and μ_{2i} satisfy (7.30), it then follows from Lemma 7.2 and a similar argument to that in Theorem 7.2 that $z_{2i-1}(t) \to 0$ and $z_{2i}(t) \to 0$

as $t \to \infty$ as well. Similar to the analysis in the proof of Theorem 7.9, note from Lemmas 1.1 and 7.4 that $w_1 = [\mathbf{1}_n^T, \mathbf{0}_n^T]^T$ and $v_1 = [\mathbf{0}_n^T, \mathbf{p}^T]^T$ are, respectively, a right and a left eigenvector associated with $\mu_1 = 0$. Meanwhile, $w_2 = [\mathbf{0}_n^T, \mathbf{1}_n^T]^T$ and $v_2 = [\mathbf{p}^T, \mathbf{0}_n^T]^T$ are, respectively, a generalized right and a generalized left eigenvector associated with $\mu_2 = 0$, where $v_2^T w_1 = 1$ and $v_1^T w_2 = 1$. It thus follows that the first and second columns of Q can be chosen as w_1 and w_2 while the first and second rows of Q^{-1} can be chosen as v_2 and v_1. Because $\left[\begin{smallmatrix} \tilde{x}(t) \\ \tilde{x}^{(\alpha/2)}(t) \end{smallmatrix} \right] = QZ(t)$ and $Z(0) = Q^{-1} \left[\begin{smallmatrix} \tilde{x}(0) \\ \tilde{x}^{(\alpha/2)}(0) \end{smallmatrix} \right]$, after some manipulation, we can get that $\lim_{t\to\infty} \left\| \left[\begin{smallmatrix} \tilde{x}(t) \\ \tilde{x}^{(\alpha/2)}(t) \end{smallmatrix} \right] - \left[\begin{smallmatrix} \mathbf{1}_n \mathbf{p}^T \tilde{x}(0) + \frac{t^{\alpha/2}}{\Gamma(1+\alpha/2)} \mathbf{1}_n \mathbf{p}^T \tilde{x}^{(\alpha/2)}(0) \\ \mathbf{1}_n \mathbf{p}^T \tilde{x}^{(\alpha/2)}(0) \end{smallmatrix} \right] \right\| = 0$, that is, $\lim_{t\to\infty} |\tilde{x}_i(t) - [\mathbf{p}^T \tilde{x}(0) + \frac{t^{\alpha/2}}{\Gamma(1+\alpha/2)} \mathbf{p}^T \tilde{x}^{(\alpha/2)}(0)]| = 0$. We next consider the case where $\alpha \in (2, \psi)$. Note from Property 3 of Lemma 7.1 that $z_2(t) = z_2(0) + \dot{z}_2(0)t$. Because $z_1(t)$ satisfies (7.30), we can get that $z_1(t) = z_1(0) + z_2(0)\frac{t^{\alpha/2}}{\Gamma(1+\alpha/2)} + \dot{z}_2(0)\frac{t^{1+\alpha/2}}{\Gamma(2+\alpha/2)}$. A similar discussion to that for $\alpha \in (0, 2]$ shows that $z_i(t) \to 0$, $i = 3, \ldots, 2n$, as $t \to \infty$. Therefore, it follows that $\lim_{t\to\infty} \|Z(t) - [z_1(0) + z_2(0)\frac{t^{\alpha/2}}{\Gamma(1+\alpha/2)} + \dot{z}_2(0)\frac{t^{1+\alpha/2}}{\Gamma(2+\alpha/2)}, z_2(0) + \dot{z}_2(0)t, 0, \ldots, 0]^T\| = 0$. Similar to the proof for $\alpha \in (0, 2]$, we can get that $\lim_{t\to\infty} |\tilde{x}_i(t) - [\mathbf{p}^T \tilde{x}(0) + \frac{t^{\alpha/2}}{\Gamma(1+\alpha/2)} \mathbf{p}^T \tilde{x}^{(\alpha/2)}(0) + \frac{t^{1+\alpha/2}}{\Gamma(2+\alpha/2)} \tilde{x}^{(1+\alpha/2)}(0)]| = 0$.

(Case 2) When $0 < \gamma \leq \max_{\lambda_i \neq 0} \frac{|\mathrm{Im}(\lambda_i)|}{\sqrt{\mathrm{Re}(\lambda_i)}|\lambda_i|}$, it follows from Lemma 7.4 that $\mathrm{Re}(\mu_{2i-1}) \geq 0$ for some i, which implies that $\psi \leq 2$. Therefore, we can get that $\alpha \in (0, 2)$. The proof then follows a similar analysis to that of Case 1 when $\alpha \in (0, 2]$. ∎

Remark 7.12 From Theorem 7.11, it can be noted that the control gain γ can also be chosen as any positive number. Of course, the range of α to ensure coordination will be different depending on γ. The existing coordination algorithms for double-integrator dynamics with relative damping studied in [248, Chap. 4] can be viewed as a special case of Theorem 7.11 when $\alpha = 2$. In addition, when there exists relative damping, the final state derivatives generally do not approach a constant as shown in Theorem 7.11, which is different from the results in [248, Chap. 4].

7.3.3 Simulation

To illustrate the results in Sects. 7.3.1 and 7.3.2, we consider four agents with a directed fixed graph $\mathscr{G}$ shown by Fig. 7.5. Note that $\mathscr{G}$ has a directed spanning tree. We let $a_{ij} = 1$ if $(j, i) \in \mathscr{E}$ and $a_{ij} = 0$ otherwise. Here for simplicity, we choose $\delta_i = 0$, which implies that $\Delta_{ij} = 0$.

The states of the four agents using (7.24) are shown in Fig. 7.6 with $\alpha = 1.6$ and $\beta = 1$. The states of the four agents using (7.31) are shown in Fig. 7.7 with $\alpha = 1.2$
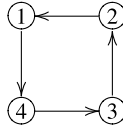
Fig. 7.5 Directed graph $\mathscr{G}$ for four agents. An *arrow* from j to i denotes that agent j is a neighbor of agent i
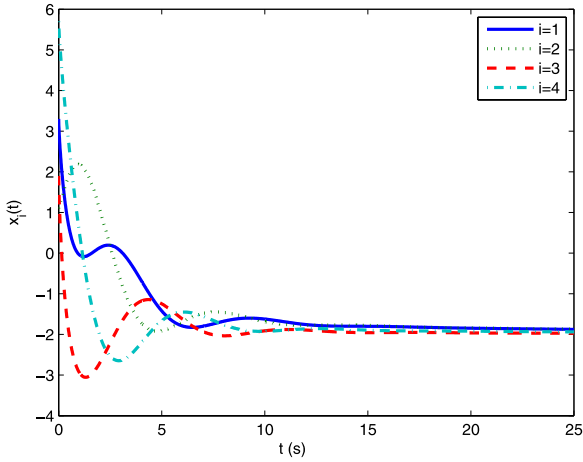
Fig. 7.6 States of the four agents using (7.24) with $\alpha = 1.6$ and $\beta = 1$

(a) $x_i(t)$ (b) $\dot{x}_i(t)$
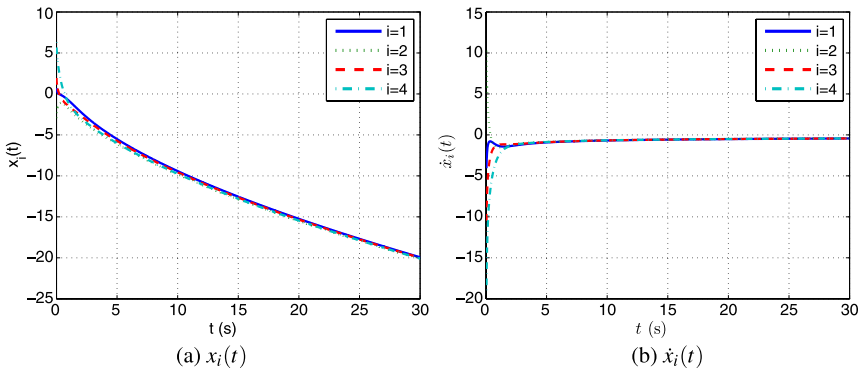
Fig. 7.7 States of the four agents using (7.31) with $\alpha = 1.2$ and $\gamma = 1$

and $\gamma = 1$. It can be noted from Figs. 7.6 and 7.7 that coordination is achieved. In particular, it can be seen from Fig. 7.7(b) that using (7.31) the final state derivatives do not approach a constant when $\alpha = 1.2$ and $\gamma = 1$.

7.4 Notes

The results in this chapter are based mainly on [30, 34, 42, 46]. For results on fractional calculus, see [164, 179, 217, 229, 253, 256]. For results on fractional-order control, see [10, 219, 230, 231].

Part IV
Emergent Issues in Distributed Multi-agent Coordination

Chapter 8
Sampled-data Setting

This chapter considers distributed multi-agent coordination in a sampled-data setting. We first study a distributed sampled-data coordinated tracking algorithm where a group of followers with single-integrator dynamics interacting with their neighbors at discrete-time instants intercepts a dynamic leader who is a neighbor of only a subset of the followers. We propose a PD-like discrete-time algorithm and study the condition on the interaction graph, the sampling period, and the control gain to ensure stability under directed fixed interaction and give the quantitative bound of the tracking errors. We then study convergence of two distributed sampled-data coordination algorithms with respectively, absolute damping and relative damping for double-integrator dynamics under undirected/directed fixed interaction. We show necessary and sufficient conditions on the interaction graph, the sampling period, and the control gain such that coordination is achieved using these two algorithms by using matrix theory, bilinear transformation, and Cauchy theorem. We finally study convergence of the two distributed sampled-data coordination algorithms with respectively, absolute damping and relative damping for double-integrator dynamics under directed switching interaction. We derive sufficient conditions on the interaction graph, the sampling period, and the control gain to guarantee coordination by using the property of infinity products of row-stochastic matrices. Simulation results are presented to show the effectiveness of the theoretical results.

8.1 Sampled-data Coordinated Tracking for Single-integrator Dynamics

In multi-agent coordination, agents might only be able to interact with their neighbors *intermittently* rather than *continuously* due to low bandwidth, unreliable communication channels, limited sensing capabilities, or power and cost constraints. A multi-agent system with intermittent interaction, where agents with continuous-time dynamics are controlled based on information from their neighbors updated at discrete-time instants, can be treated as a sampled-data system consisting of multi-

ple networked subsystems. We are hence motivated to study distributed multi-agent coordination in a sampled-data setting. We explicitly consider the effect of sampled-data control on stability of the agents. In this section, we focus on sampled-data coordinated tracking for single-integrator dynamics.

8.1.1 Algorithm Design

Suppose that in addition to n followers, labeled as agents or followers 1 to n, with single-integrator dynamics given by (3.1), there exists a dynamic leader, labeled as agent 0, whose position is $r_0(t) \in \mathbb{R}^m$. Here the leader can be physical or virtual. Let $\mathscr{G} \triangleq (\mathscr{V}, \mathscr{E})$ be the directed graph characterizing the interaction among the n followers. Let $\overline{\mathscr{G}} \triangleq (\overline{\mathscr{V}}, \overline{\mathscr{E}})$ be the directed graph characterizing the interaction among the leader and the followers corresponding to $\mathscr{G}$.

A proportional-derivative-like (PD-like) continuous-time coordinated tracking algorithm is proposed for (3.1) in [248, Chap. 3] as

$$u_i(t) = \frac{1}{\sum_{j=0}^{n} a_{ij}} \sum_{j=1}^{n} a_{ij} \{ \dot{r}_j(t) - \gamma [r_i(t) - r_j(t)] \}$$
$$+ \frac{a_{i0}}{\sum_{j=0}^{n} a_{ij}} \{ \dot{r}_0(t) - \gamma [r_i(t) - r_0(t)] \}, \tag{8.1}$$

where a_{ij}, $i, j = 1, \ldots, n$, is the (i, j)th entry of the adjacency matrix $\mathscr{A} \in \mathbb{R}^{n \times n}$ associated with the directed graph $\mathscr{G}$, $a_{i0} > 0$, $i = 1, \ldots, n$, if the leader is a neighbor of follower i and $a_{i0} = 0$ otherwise, and γ is a positive gain. The objective of (8.1) is to guarantee that $r_i(t) - r_0(t) \to \mathbf{0}_m, i = 1, \ldots, n$, as $t \to \infty$. Note that (8.1) requires each follower to obtain instantaneous measurements of its neighbors' velocities and the leader's velocity if the leader is a neighbor of the follower. This requirement might not be realistic in real applications. We next propose a PD-like discrete-time coordinated tracking algorithm.

Consider a sampled-data setting where the agents have continuous-time dynamics while the measurements are made at discrete sampling times and the control inputs are based on zero-order hold as

$$u_i(t) = u_i[k], \quad kT \le t < (k+1)T, \tag{8.2}$$

where k denotes the discrete-time index, T denotes the sampling period, and $u_i[k]$ is the control input at $t = kT$. By using direct discretization (see Sect. 1.4), the continuous-time system (3.1) can be discretized as

$$r_i[k+1] = r_i[k] + Tu_i[k], \quad i = 1, \ldots, n, \tag{8.3}$$

where $r_i[k]$ is the position of follower i at $t = kT$. We propose a PD-like discrete-time coordinated tracking algorithm as

$$u_i[k] = \frac{1}{\sum_{j=0}^n a_{ij}} \sum_{j=1}^n a_{ij} \left[\frac{r_j[k] - r_j[k-1]}{T} - \gamma\big(r_i[k] - r_j[k]\big) \right]$$

$$+ \frac{a_{i0}}{\sum_{j=0}^n a_{ij}} \left[\frac{r_0[k] - r_0[k-1]}{T} - \gamma\big(r_i[k] - r_0[k]\big) \right], \qquad (8.4)$$

where $r_0[k]$ denotes the leader's position at $t = kT$, and $\frac{r_j[k]-r_j[k-1]}{T}$ and $\frac{r_0[k]-r_0[k-1]}{T}$ are used to approximate, respectively, $\dot{r}_j(t)$ and $\dot{r}_0(t)$ in (8.1) by noting that $r_j[k+1]$ and $r_0[k+1]$ cannot be accessed at $t = kT$. Note that using (8.4), each follower's position is updated based on its current position and its neighbors' current and previous positions as well as the leader's current and previous positions if the leader is a neighbor of the follower. As a result, (8.4) can be easily implemented in practice. In the following, we assume that all agents are in a one-dimensional space (i.e., $m = 1$) for the simplicity of presentation. However, all results hereafter are still valid for any high-dimensional space by the introduction of the Kronecker product.

8.1.2 Convergence Analysis of the Proportional-derivative-like Discrete-time Coordinated Tracking Algorithm

In this subsection, we analyze the algorithm (8.4). Define the tracking error for follower i as $\varepsilon_i[k] \triangleq r_i[k] - r_0[k]$. It follows that the closed-loop system of (8.3) using (8.4) can be written as

$$\varepsilon_i[k+1] = \varepsilon_i[k] + \frac{T}{\sum_{j=0}^n a_{ij}} \sum_{j=1}^n a_{ij} \left[\frac{\varepsilon_j[k] - \varepsilon_j[k-1]}{T} - \gamma\big(\varepsilon_i[k] - \varepsilon_j[k]\big) \right]$$

$$+ \frac{Ta_{i0}}{\sum_{j=0}^n a_{ij}} \left(\frac{r_0[k] - r_0[k-1]}{T} - \gamma\varepsilon_i[k] \right)$$

$$- \big(r_0[k+1] - r_0[k]\big) + \frac{\sum_{j=1}^n a_{ij}}{\sum_{j=0}^n a_{ij}} \big(r_0[k] - r_0[k-1]\big),$$

which can then be written in a vector form as

$$\varepsilon[k+1] = \big[(1 - T\gamma)I_n + (1 + T\gamma)D^{-1}\mathscr{A}\big]\varepsilon[k] - D^{-1}\mathscr{A}\varepsilon[k-1] + X^r[k], \tag{8.5}$$

where $D \triangleq \mathrm{diag}\{\sum_{j=0}^n a_{1j}, \ldots, \sum_{j=0}^n a_{nj}\}$, $\varepsilon[k] \triangleq [\varepsilon_1[k], \ldots, \varepsilon_n[k]]^T$, $\mathscr{A}$ is the adjacency matrix associated with $\mathscr{G}$, and $X^r[k] \triangleq (2r_0[k] - r_0[k-1] - r_0[k+1])\mathbf{1}_n$. By defining $Y[k+1] \triangleq \left[\begin{smallmatrix} \varepsilon[k+1] \\ \varepsilon[k] \end{smallmatrix}\right]$, it follows from (8.5) that

$$Y[k + 1] = \widetilde{A}Y[k] + \widetilde{B}X^r[k], \tag{8.6}$$

where

$$\widetilde{A} \triangleq \begin{bmatrix} (1 - T\gamma)I_n + (1 + T\gamma)D^{-1}\mathscr{A} & -D^{-1}\mathscr{A} \\ I_n & 0_{n \times n} \end{bmatrix}$$

and $\widetilde{B} \triangleq \begin{bmatrix} I_n \\ 0_{n \times n} \end{bmatrix}$. It follows that the solution of (8.6) is

$$Y[k] = \widetilde{A}^k Y[0] + \sum_{i=1}^{k} \widetilde{A}^{k-i} \widetilde{B} X^r[i - 1]. \tag{8.7}$$

Note that the eigenvalues of $\widetilde{A}$ play an important role in determining the value of $Y[k]$ as $k \to \infty$. In the following, we study the eigenvalues of $\widetilde{A}$. Before moving on, we first study the eigenvalues of $D^{-1}\mathscr{A}$.

Lemma 8.1. *Suppose that in $\overline{\mathscr{G}}$ the leader has directed paths to all followers 1 to n. Then $D^{-1}\mathscr{A}$ satisfies $\|(D^{-1}\mathscr{A})^n\|_\infty < 1$ and $D^{-1}\mathscr{A}$ has all eigenvalues within the unit circle.*[1]

Proof: For the first statement, note that $D^{-1}A$ is nonnegative and each row sum of $D^{-1}A$ is less than or equal to one. Therefore, it follows that $\|D^{-1}A\|_\infty \leq 1$. Denote $\bar{i}_1$ as the set of followers that are the children of the leader, and $\bar{i}_j$, $j = 2, \ldots, \kappa$, as the set of followers that are the children of the followers in $\bar{i}_{j-1}$ but are not in $\bar{i}_r$, $r = 1, \ldots, j - 2$. Because the leader has directed paths to all followers 1 to n, there are at most n edges from the leader to all followers 1 to n, which implies that $\kappa \leq n$. Let p_i and q_i^T denote, respectively, the ith column and row of $D^{-1}\mathscr{A}$. When the leader has directed paths to all followers 1 to n, without loss of generality, assume that the kth follower is a child of the leader, i.e., $a_{k0} > 0$. It follows that $q_k^T \mathbf{1}_n = 1 - \frac{a_{k0}}{\sum_{j=0}^{n} a_{kj}} < 1$. The same property also applies to the other elements in the set $\bar{i}_1$. Similarly, assume that the lth follower (one follower in the set $\bar{i}_2$) is a child of the kth follower (one follower in the set $\bar{i}_1$), which implies that $a_{lk} > 0$. It follows that the sum of the lth row of $(D^{-1}\mathscr{A})^2$ can be written as $q_l^T \sum_{i=1}^{n} p_i \leq q_l^T \mathbf{1}_n = 1 - \frac{a_{lk}}{\sum_{j=0}^{n} a_{lj}} < 1$. Meanwhile, the sum of the kth row of $(D^{-1}\mathscr{A})^2$ is also less than one. A similar analysis shows that each row sum of $(D^{-1}\mathscr{A})^\kappa$ is less than one when the leader has directed paths to all followers 1 to n. That is, $\|(D^{-1}A)^\kappa\|_\infty < 1$. Because $\kappa \leq n$ and $\|D^{-1}\mathscr{A}\|_\infty \leq 1$, $\|(D^{-1}\mathscr{A})^n\|_\infty < 1$ holds.

For the second statement, note from Lemma 1.25 that $\rho[(D^{-1}A)^n] \leq \|(D^{-1}A)^n\|_\infty$. Because $\|(D^{-1}A)^n\|_\infty < 1$, it follows that $\rho[(D^{-1}A)^n] < 1$, which implies that $\rho(D^{-1}A) < 1$. ∎

We next study the conditions under which all eigenvalues of $\widetilde{A}$ are within the unit circle.

---

[1] Note that in $\overline{\mathscr{G}}$ if the leader has directed paths to all followers, then each follower has at least one neighbor, that is, $\sum_{j=0}^{n} a_{ij} > 0$, $i = 1, \ldots, n$. Therefore, D^{-1} exists and (8.4) is well defined.

Lemma 8.2. *Suppose that in $\overline{\mathscr{G}}$ the leader has directed paths to all followers* 1 *to n. Let λ_i be the ith eigenvalue of $D^{-1}\mathscr{A}$. Then $\tau_i > 0$ holds, where $\tau_i \triangleq \frac{2|1-\lambda_i|^2(2[1-\mathrm{Re}(\lambda_i)]-|1-\lambda_i|^2)}{|1-\lambda_i|^4+4[\mathrm{Im}(\lambda_i)]^2}$. If the positive scalars T and γ satisfy*

$$T\gamma < \min\Big\{1, \min_{i=1,\ldots,n} \tau_i\Big\}, \tag{8.8}$$

then $\widetilde{A}$, defined by (8.1.2), has all eigenvalues within the unit circle.

Proof: For the first statement, when the leader has directed paths to all followers 1 to n, it follows from the second statement in Lemma 8.1 that $|\lambda_i| < 1$. It then follows that $|1 - \lambda_i|^2 > 0$ and $|1 - \lambda_i|^2 = 1 - 2\mathrm{Re}(\lambda_i) + [\mathrm{Re}(\lambda_i)]^2 + [\mathrm{Im}(\lambda_i)]^2 < 2[1 - \mathrm{Re}(\lambda_i)]$, which implies that $\tau_i > 0$.

For the second statement, note that the characteristic polynomial of $\widetilde{A}$ is given by

$$\begin{aligned}
&\det(zI_{2n} - \widetilde{A}) \\
&= \det\left(\begin{bmatrix} zI_n - [(1-T\gamma)I_n + (1+T\gamma)D^{-1}\mathscr{A}] & D^{-1}\mathscr{A} \\ -I_n & zI_n \end{bmatrix}\right) \\
&= \det\left([zI_n - (1-T\gamma)I_n - (1+T\gamma)D^{-1}\mathscr{A}]zI_n + D^{-1}\mathscr{A}\right) \\
&= \det\left([z^2 + (T\gamma - 1)z]I_n + [1 - (1+T\gamma)z]D^{-1}\mathscr{A}\right),
\end{aligned}$$

where we have used Lemma 1.22 to obtain the second equality because $zI_n - [(1-T\gamma)I_n + (1+T\gamma)D^{-1}\mathscr{A}]$, $D^{-1}\mathscr{A}$, $-I_n$ and zI_n commute pairwise. Noting that λ_i is the ith eigenvalue of $D^{-1}\mathscr{A}$, we can get that $\det(zI_n + D^{-1}\mathscr{A}) = \prod_{i=1}^n (z + \lambda_i)$. It thus follows that $\det(zI_{2n} - \widetilde{A}) = \prod_{i=1}^n \{z^2 + (T\gamma - 1)z + [1 - (1+T\gamma)z]\lambda_i\}$. Therefore, the roots of $\det(zI_{2n} - \widetilde{A}) = 0$ satisfy that

$$z^2 + [T\gamma - 1 - (1+T\gamma)\lambda_i]z + \lambda_i = 0. \tag{8.9}$$

It can be noted that each eigenvalue of $D^{-1}\mathscr{A}$, λ_i, corresponds to two eigenvalues of $\widetilde{A}$. Instead of computing the roots of (8.9) directly, we apply the bilinear transformation $z = \frac{s+1}{s-1}$ to (8.9) to get

$$T\gamma(1-\lambda_i)s^2 + 2(1-\lambda_i)s + (2+T\gamma)\lambda_i + 2 - T\gamma = 0. \tag{8.10}$$

Because the bilinear transformation is an exact one-to-one mapping from the interior of the unit circle in the complex z-plane to the open left half of the complex s-plane, it follows that (8.9) has all roots within the unit circle if and only if (8.10) has all roots in the open left half plane.

In the following, we study the condition on T and γ under which (8.10) has all roots in the open left half plane. Letting s_1 and s_2 denote the roots of (8.10), it follows from (8.10) that

$$s_1 + s_2 = -\frac{2}{T\gamma}, \tag{8.11}$$

$$s_1 s_2 = \frac{(2 + T\gamma)\lambda_i + 2 - T\gamma}{T\gamma(1 - \lambda_i)}. \tag{8.12}$$

Noting that (8.11) implies that $\text{Im}(s_1) + \text{Im}(s_2) = 0$, we define $s_1 = a_1 + \iota b$ and $s_2 = a_2 - \iota b$. It can be noted that s_1 and s_2 have negative real parts if and only if $a_1 a_2 > 0$ and $a_1 + a_2 < 0$. Note that (8.11) implies $a_1 + a_2 = -\frac{2}{T\gamma} < 0$ because $T\gamma > 0$. We next show a sufficient condition on T and γ such that $a_1 a_2 > 0$ holds. By substituting the definitions of s_1 and s_2 into (8.12), we have $a_1 a_2 + b^2 + \iota(a_2 - a_1)b = \frac{(2+T\gamma)\lambda_i + 2 - T\gamma}{T\gamma(1 - \lambda_i)}$, which implies

$$a_1 a_2 + b^2 = -\frac{2 + T\gamma}{T\gamma} + \frac{4[1 - \text{Re}(\lambda_i)]}{T\gamma|1 - \lambda_i|^2}, \tag{8.13}$$

$$(a_2 - a_1)b = \frac{4\text{Im}(\lambda_i)}{T\gamma|1 - \lambda_i|^2}. \tag{8.14}$$

It follows from (8.14) that $b = \frac{4\text{Im}(\lambda_i)}{T\gamma(a_2 - a_1)|1 - \lambda_i|^2}$. Note that $(a_2 - a_1)^2 = (a_1 + a_2)^2 - 4a_1 a_2 = \frac{4}{T^2\gamma^2} - 4a_1 a_2$. After some manipulation, (8.13) can be written as

$$K_1(a_1 a_2)^2 + K_2 a_1 a_2 + K_3 = 0, \tag{8.15}$$

where $K_1 \triangleq T^2\gamma^2|1 - \lambda_i|^4$, $K_2 \triangleq -|1 - \lambda_i|^4 + (2 + T\gamma)T\gamma|1 - \lambda_i|^4 - 4[1 - \text{Re}(\lambda_i)]T\gamma|1 - \lambda_i|^2$, and $K_3 \triangleq \frac{1}{T\gamma}\{4[1 - \text{Re}(\lambda_i)]|1 - \lambda_i|^2 - (2 + T\gamma)|1 - \lambda_i|^4\} - 4[\text{Im}(\lambda_i)]^2$. It can be computed that $K_2^2 - 4K_1 K_3 = \{|1 - \lambda_i|^4 + (2 + T\gamma)T\gamma|1 - \lambda_i|^4 - 4[1 - \text{Re}(\lambda_i)]T\gamma|1 - \lambda_i|^2\}^2 + 16T^2\gamma^2|1 - \lambda_i|^4[\text{Im}(\lambda_i)]^2 \geq 0$, which implies that (8.15) has two real roots. Because $|\lambda_i| < 1$, it is straightforward to show that $K_1 > 0$. Therefore, a sufficient condition for $a_1 a_2 > 0$ is that $K_2 < 0$ and $K_3 > 0$. When $0 < T\gamma < 1$, because $|1 - \lambda_i|^2 < 2[1 - \text{Re}(\lambda_i)]$ as shown in the proof of the first statement, it follows that $K_2 < -|1 - \lambda_i|^4 + (2 + T\gamma)T\gamma|1 - \lambda_i|^4 - 2T\gamma|1 - \lambda_i|^4 = |1 - \lambda_i|^4[-1 + (T\gamma)^2] \leq 0$. Similarly, when $0 < T\gamma < \tau_i$, it follows that $K_3 > 0$. Therefore, if the positive scalars γ and T satisfy (8.8), all eigenvalues of $\widetilde{A}$ are within the unit circle. ∎

In the following, we apply Lemma 8.2 to derive our main result.

Theorem 8.1. *Suppose that the leader's position $r_0[k]$ satisfies that $|\frac{r_0[k] - r_0[k-1]}{T}| \leq \bar{r}$ (i.e., the changing rate of $r_0[k]$ is bounded), and in $\overline{\mathcal{G}}$ the leader has directed paths to all followers 1 to n. When the positive scalars γ and T satisfy (8.8), using (8.4) for (8.3), the maximum tracking error of the n followers is ultimately bounded by $2T\bar{r}\|(I_{2n} - \widetilde{A})^{-1}\|_\infty$.*

Proof: It follows from (8.7) that

$$\left\|Y[k]\right\|_\infty \leq \left\|\widetilde{A}^k Y[0]\right\|_\infty + \left\|\sum_{i=1}^{k} \widetilde{A}^{k-i} \widetilde{B} X^r[i-1]\right\|_\infty$$

$$\leq \left\|\widetilde{A}^k\right\|_\infty \left\|Y[0]\right\|_\infty + 2T\bar{r} \left\|\sum_{i=0}^{k-1} \widetilde{A}^i\right\|_\infty \left\|\widetilde{B}\right\|_\infty,$$

where we have used the fact that

$$\left\|X^r[i]\right\|_\infty = \left\|\left(2r_0[i] - r_0[i-1] - r_0[i+1]\right)\mathbf{1}_n\right\|_\infty \leq 2T\bar{r}$$

for all i because $\left|\frac{r_0[k]-r_0[k-1]}{T}\right| \leq \bar{r}$. When the leader has directed paths to all followers 1 to n, it follows from Lemma 8.2 that $\widetilde{A}$ has all eigenvalues within the unit circle if the positive scalars T and γ satisfy (8.8). Therefore, $\lim_{k\to\infty} \widetilde{A}^k = 0_{2n\times 2n}$. Also, it follows from Lemma 1.26 that there exists a matrix norm $\|\cdot\|$ such that $\|\widetilde{A}\| < 1$. It then follows from Lemma 1.28 that $(I_{2n} - \widetilde{A})$ is invertible and $(I_{2n} - \widetilde{A})^{-1} = \sum_{i=0}^{\infty} \widetilde{A}^i$, which implies that $\lim_{k\to\infty} \|\sum_{i=0}^{k-1} \widetilde{A}^i\|_\infty = \|(I_{2n} - \widetilde{A})^{-1}\|_\infty$. Also note that $\|\widetilde{B}\|_\infty = 1$. Therefore, we have that $\|Y[k]\|_\infty$ is ultimately bounded by $2T\bar{r}\|(I_{2n} - \widetilde{A})^{-1}\|_\infty$. The theorem then follows directly by noting that $\|Y[k]\|_\infty$ denotes the maximum tracking error of the n followers. ∎

Remark 8.2 From Theorem 8.1, it can be noted that the ultimate bound of the tracking errors using the PD-like discrete-time coordinated tracking algorithm (8.4) is proportional to the sampling period T. As T approaches zero, the tracking errors will go to zero ultimately when the changing rate of the leader's position is bounded and the leader has directed paths to all followers 1 to n.

8.1.3 Comparison Between the Proportional-like and Proportional-derivative-like Discrete-time Coordinated Tracking Algorithms

A proportional-like (P-like) continuous-time coordinated tracking algorithm for (3.1) is given as[2]

$$u_i(t) = -\sum_{j=1}^{n} a_{ij}\left[r_i(t) - r_j(t)\right] - a_{i0}\left[r_i(t) - r_0(t)\right], \qquad (8.16)$$

where a_{ij}, $i = 1, \dots, n$, $j = 0, \dots, n$, are defined as in (8.1). Similar to that in Sect. 8.1.1, the P-like discrete-time coordinated tracking algorithm for (8.3) is given as

---

[2] The algorithm is a natural extension of the consensus algorithm (2.2).

$$u_i[k] = -\sum_{j=1}^{n} a_{ij}\big(r_i[k] - r_j[k]\big) - a_{i0}\big(r_i[k] - r_0[k]\big). \qquad (8.17)$$

Letting ε_i and ε be defined as in Sect. 8.1.2, we rewrite the closed-loop system of (8.3) using (8.17) as

$$\varepsilon_i[k+1] = \varepsilon_i[k] - T\sum_{j=1}^{n} a_{ij}\big(\varepsilon_i[k] - \varepsilon_j[k]\big) - Ta_{i0}\varepsilon_i[k] - \big(r_0[k+1] - r_0[k]\big),$$

which can then be written in a vector form as

$$\varepsilon[k+1] = Q\varepsilon[k] - \big(r_0[k+1] - r_0[k]\big)\mathbf{1}_n, \qquad (8.18)$$

where $Q \triangleq I_n - T\mathscr{L} - T\mathrm{diag}(a_{10}, \ldots, a_{n0})$ with $\mathscr{L}$ being the nonsymmetric Laplacian matrix associated with $\mathscr{A}$ and hence $\mathscr{G}$. Note that Q is nonnegative when $0 < T < \min_{i=1,\ldots,n} \frac{1}{\sum_{j=0}^{n} a_{ij}}$.

Lemma 8.3. *Suppose that in $\overline{\mathscr{G}}$ the leader has directed paths to all followers 1 to n. When $0 < T < \min_{i=1,\ldots,n} \frac{1}{\sum_{j=0}^{n} a_{ij}}$, Q has all eigenvalues within the unit circle.*

Proof: The proof is a direct application of Lemmas 1.18 and 1.6 and is omitted here. ∎

Theorem 8.3. *Suppose that the leader's position $r_0[k]$ satisfies $|\frac{r_0[k]-r_0[k-1]}{T}| \leq \bar{r}$, and in $\overline{\mathscr{G}}$ the leader has directed paths to all followers 1 to n. When $T < \min_{i=1,\ldots,n} \frac{1}{\sum_{j=0}^{n} a_{ij}}$, using (8.17) for (8.3), the maximum tracking error of the n followers is ultimately bounded by $\bar{r}\|[\mathscr{L} + \mathrm{diag}\{a_{10}, \ldots, a_{n0}\}]^{-1}\|_{\infty}$.*

Proof: The solution of (8.18) is

$$\varepsilon[k] = Q^k \varepsilon[0] - \sum_{i=1}^{k} Q^{k-i}\big(r_0[k] - r_0[k-1]\big)\mathbf{1}_n.$$

The proof then follows a similar line to that of Theorem 8.1 by noting that $\|\varepsilon[k]\|_{\infty}$ denotes the maximum tracking error of the n followers. ∎

Remark 8.4 In contrast to the results in Theorem 8.1, the ultimate bound of the tracking errors using the P-like discrete-time coordinated tracking algorithm (8.17) with a dynamic leader is not proportional to the sampling period T. In fact, as shown in [248, Chap. 3], even when T approaches zero, the tracking errors using (8.17) are not guaranteed to go to zero ultimately. The comparison between Theorems 8.1 and 8.3 shows the benefit of the PD-like discrete-time coordinated tracking algorithm over the P-like discrete-time consensus algorithm when there exists a dynamic leader who is a neighbor of only a subset of the followers. As a special case, when the leader's position is constant (i.e., $\bar{r} = 0$), it follows from Theorems 8.1 and 8.3
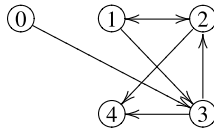
Fig. 8.1 Directed graph $\overline{\mathscr{G}}$ associated with four followers and one leader. An *arrow* from j to i denotes that agent j is a neighbor of agent i

that the tracking errors will go to zero ultimately using both the P-like and PD-like discrete-time coordinated tracking algorithms.[3]

8.1.4 Simulation

In this subsection, a simulation example is presented to illustrate the PD-like discrete-time coordinated tracking algorithm (8.4). To show the benefit of the PD-like discrete-time coordinated tracking algorithm, the related simulation result obtained by applying the P-like discrete-time coordinated tracking algorithm (8.17) is also presented.

We consider a team consisting of four followers and a leader with the directed graph $\overline{\mathscr{G}}$ given by Fig. 8.1. It can be noted that the leader has directed paths to all four followers. We let $a_{ij} = 1$ if agent j is a neighbor of agent i and $a_{ij} = 0$ otherwise. For both (8.4) and (8.17), we let $r_1[0] = 3$, $r_2[0] = 1$, $r_3[0] = -1$, and $r_4[0] = -2$. For (8.4), we also let $r_i[-1] = 0$, $i = 1, \ldots, 4$. The dynamic leader's position is chosen as $r_0[k] = \sin(kT) + kT$.

Figures 8.2(a) and 8.2(b) show, respectively, the positions r_i and the tracking errors $r_i - r_0$ by using (8.4) when $T = 0.3$ s and $\gamma = 1$. From Fig. 8.2(b), it can be seen that the tracking errors are relatively large. Figures 8.2(c) and 8.2(d) show, respectively, r_i and $r_i - r_0$ by using (8.4) when $T = 0.1$ s and $\gamma = 3$. From Fig. 8.2(d), it can be seen that the tracking errors are very small ultimately. We can see that the tracking errors will become smaller if the sampling period becomes smaller. Figures 8.2(e) and 8.2(f) show, respectively, r_i and $r_i - r_0$ by using (8.4) when $T = 0.25$ s and $\gamma = 3$. Note that the product $T\gamma$ is larger than the positive upper bound derived in Theorem 8.1. It can be noted that the tracking errors become unbounded in this case. Figures 8.3(a) and 8.3(b) show, respectively, r_i and $r_i - r_0$ by using (8.17) when $T = 0.1$ s and $\gamma = 3$. By comparing Figs. 8.3(b) and 8.2(d), it can be seen that the tracking errors using (8.17) are much larger than those using (8.4) under the same condition. This shows the benefit of the PD-like discrete-time coordinated tracking algorithm over the P-like discrete-time coordinated tracking algorithm when there exists a dynamic leader who is a neighbor of only a subset of the followers.

---

[3] In this case, the coordinated tracking problem boils down to a coordinated regulation problem because the leader's position is constant.
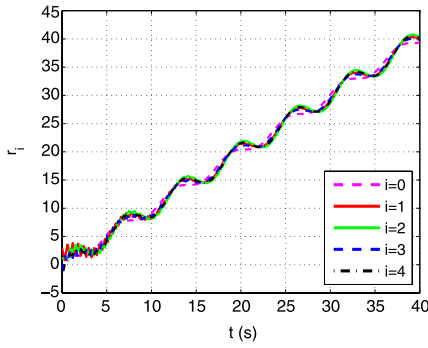
(a) Positions ($T = 0.3$ s and $\gamma = 1$)
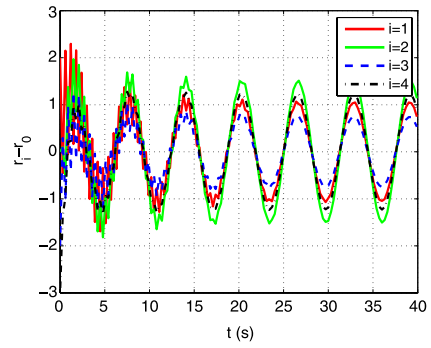
(b) Tracking errors ($T = 0.3$ s and $\gamma = 1$)
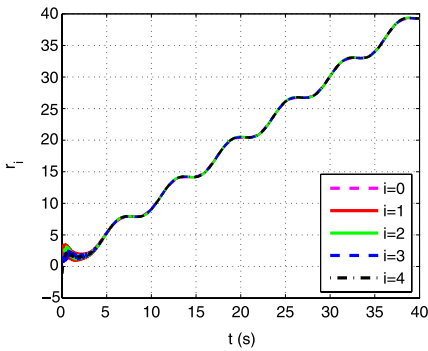
(c) Positions ($T = 0.1$ s and $\gamma = 3$)
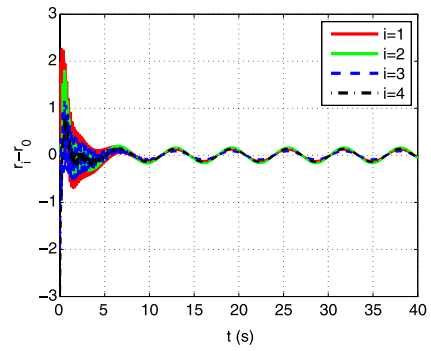
(d) Tracking errors ($T = 0.1$ s and $\gamma = 3$)
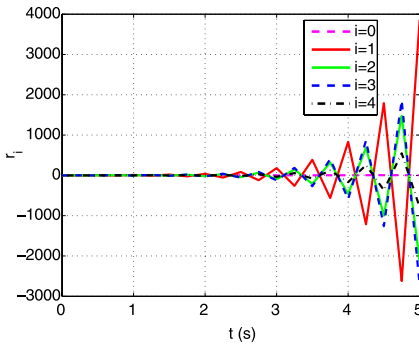
(e) Positions ($T = 0.25$ s and $\gamma = 3$)
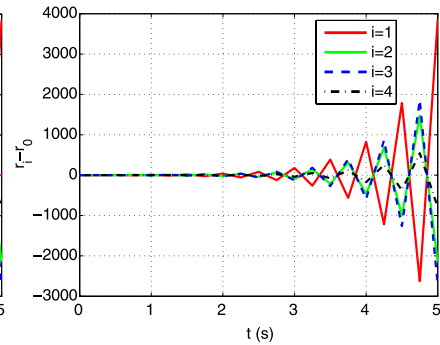
(f) Tracking errors ($T = 0.25$ s and $\gamma = 3$)

Fig. 8.2 Distributed discrete-time coordinated tracking using the PD-like discrete-time coordinated tracking algorithm (8.4) with different T and γ

(a) Positions ($T = 0.1$ s and $\gamma = 3$) (b) Tracking errors ($T = 0.1$ s and $\gamma = 3$)
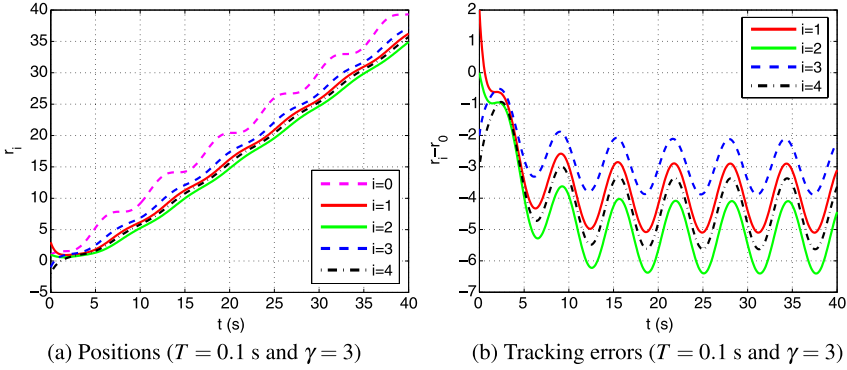
Fig. 8.3 Distributed discrete-time coordinated tracking using the P-like discrete-time coordinated tracking algorithm (8.17)

8.2 Sampled-data Coordination for Double-integrator Dynamics Under Fixed Interaction

In this section, we study sampled-data coordination algorithms for double-integrator dynamics under fixed interaction with, respectively, absolute and relative damping.

8.2.1 Coordination Algorithms with Absolute and Relative Damping

Given n agents with dynamics given by (3.5), consider a sampled-data setting with zero-order hold as (8.2). By using direct discretization (see Sect. 1.4), the continuous-time system (3.5) can be discretized as

$$
\begin{aligned}
r_i[k+1] &= r_i[k] + Tv_i[k] + \frac{T^2}{2}u_i[k], \\
v_i[k+1] &= v_i[k] + Tu_i[k], \quad i = 1, \ldots, n,
\end{aligned}
\tag{8.19}
$$

where $r_i[k] \in \mathbb{R}^m$ and $v_i[k] \in \mathbb{R}^m$ denote, respectively, the position and velocity of the ith agent at $t = kT$. Note that (8.19) is the exact discrete-time dynamics for (3.5) based on zero-order hold in a sampled-data setting.

Define $\Delta_{ij} \triangleq \delta_i - \delta_j$, where $\delta_i \in \mathbb{R}^m$ is constant. Here Δ_{ij} denotes the desired relative position deviation between agent i and agent j. We study the following two coordination algorithms

$$
u_i[k] = -\sum_{j=1}^{n} a_{ij}[k]\big[\big(r_i[k] - r_j[k]\big) - \Delta_{ij}\big] - \alpha v_i[k], \quad i = 1, \ldots, n, \tag{8.20}
$$

and

$$u_i[k] = -\sum_{j=1}^{n} a_{ij}[k]\big[\big(r_i[k] - r_j[k] - \Delta_{ij}\big) + \alpha\big(v_i[k] - v_j[k]\big)\big], \quad i = 1, \dots, n,$$

(8.21)

where $a_{ij}[k]$ is the (i, j)th entry of the adjacency matrix $\mathscr{A}[k]$ associated with the graph $\mathscr{G}[k] \triangleq (\mathscr{V}[k], \mathscr{E}[k])$ characterizing the interaction among the n agents at $t = kT$, and α is a position gain. Coordination is achieved for (8.20) if for all $r_i[0]$ and $v_i[0]$ and all $i, j = 1, \dots, n$, $r_i[k] - r_j[k] \to \Delta_{ij}$ and $v_i[k] \to \mathbf{0}_m$ as $k \to \infty$. Coordination is achieved for (8.21) if for all $r_i[0]$ and $v_i[0]$ and all $i, j = 1, \dots, n$, $r_i[k] - r_j[k] \to \Delta_{ij}$ and $v_i[k] - v_j[k] \to \mathbf{0}_m$ as $k \to \infty$.

In the remainder of the chapter, we assume that all agents are in a one-dimensional space (i.e., $m = 1$) for simplicity. However, all results hereafter still valid for any high-dimensional space by use of the properties of the Kronecker product.

8.2.2 Convergence Analysis of the Sampled-data Coordination Algorithm with Absolute Damping

In this subsection, we analyze the algorithm (8.20) under, respectively, an undirected fixed interaction graph and a directed fixed interaction graph. We assume that $\mathscr{A}$ is constant. In this case, using (8.20), (8.19) can be written in a vector form as

$$\begin{bmatrix} \tilde{r}[k+1] \\ v[k+1] \end{bmatrix} = \underbrace{\begin{bmatrix} I_n - \frac{T^2}{2}\mathscr{L} & (T - \frac{\alpha T^2}{2})I_n \\ -T\mathscr{L} & (1 - \alpha T)I_n \end{bmatrix}}_{F} \begin{bmatrix} \tilde{r}[k] \\ v[k] \end{bmatrix},$$

(8.22)

where $\tilde{r} \triangleq [\tilde{r}_1, \dots, \tilde{r}_n]^T$ with $\tilde{r}_i \triangleq r_i - \delta_i$, $v \triangleq [v_1, \dots, v_n]^T$, and $\mathscr{L}$ is the nonsymmetric Laplacian matrix associated with $\mathscr{A}$ and hence $\mathscr{G}$. To analyze (8.22), we first study the property of F, defined in (8.22). Note that the characteristic polynomial of F is given by

$$\det(zI_{2n} - F)$$

$$= \det\left(\begin{bmatrix} zI_n - (I_n - \frac{T^2}{2}\mathscr{L}) & -(T - \frac{\alpha T^2}{2})I_n \\ T\mathscr{L} & zI_n - (1 - \alpha T)I_n \end{bmatrix}\right)$$

$$= \det\left(\left[zI_n - \left(I_n - \frac{T^2}{2}\mathscr{L}\right)\right][zI_n - (1 - \alpha T)I_n]\right.$$

$$\left. - \left\{T\mathscr{L}\left[-\left(T - \frac{\alpha T^2}{2}\right)I_n\right]\right\}\right)$$

$$= \det\left[(z^2 - 2z + \alpha Tz + 1 - \alpha T)I_n + \frac{T^2}{2}(1 + z)\mathscr{L}\right],$$

where we have used Lemma 1.22 to obtain the second equality.

Let μ_i be the ith eigenvalue of $-\mathcal{L}$, we get that $\det(zI_n + \mathcal{L}) = \prod_{i=1}^{n}(z - \mu_i)$. It thus follows that $\det(zI_{2n} - F) = \prod_{i=1}^{n}(z^2 - 2z + \alpha Tz + 1 - \alpha T - \frac{T^2}{2}(1 + z)\mu_i)$. Therefore, the roots of $\det(zI_{2n} - F) = 0$ (i.e., the eigenvalues of F) satisfy that

$$z^2 + \left(\alpha T - 2 - \frac{T^2}{2}\mu_i\right)z + 1 - \alpha T - \frac{T^2}{2}\mu_i = 0. \tag{8.23}$$

Note that each eigenvalue of $-\mathcal{L}$, μ_i, corresponds to two eigenvalues of F, denoted by λ_{2i-1} and λ_{2i}. Note that $\mathcal{L}$ has at least one zero eigenvalue, without loss of generality, let $\mu_1 = 0$. It follows from (8.23) that $\lambda_1 = 1$ and $\lambda_2 = 1 - \alpha T$. Therefore, F has at least one eigenvalue equal to one. Let $[p^T, q^T]^T$, where $p, q \in \mathbb{R}^n$, be a right eigenvector of F associated with the eigenvalue $\lambda_1 = 1$. It follows that

$$\begin{bmatrix} I_n - \frac{T^2}{2}\mathcal{L} & (T - \frac{\alpha T^2}{2})I_n \\ -T\mathcal{L} & (1 - \alpha T)I_n \end{bmatrix} \begin{bmatrix} p \\ q \end{bmatrix} = \begin{bmatrix} p \\ q \end{bmatrix}.$$

After some manipulation, it follows from Lemma 1.1 that we can choose $p = \mathbf{1}_n$ and $q = \mathbf{0}_n$. Similarly, it can be shown that $[\mathbf{p}^T, (\frac{1}{\alpha} - \frac{T}{2})\mathbf{p}^T]^T$, where $\mathbf{p} \in \mathbb{R}^n$ is defined in Lemma 1.1, is a left eigenvector of F associated with the eigenvalue $\lambda_1 = 1$.

Lemma 8.4. *Using (8.20) for (8.19), $r_i[k] - r_j[k] \to \Delta_{ij}$ and $v_i[k] \to 0$ if and only if one is the unique eigenvalue of F, where F is defined in (8.22), with the maximum modulus. In particular, $r_i[k] \to \delta_i + \mathbf{p}^T \tilde{r}[0] + (\frac{1}{\alpha} - \frac{T}{2})\mathbf{p}^T v[0]$ and $v_i[k] \to 0$ as $k \to \infty$, where $\mathbf{p} \in \mathbb{R}^n$ is defined in Lemma 1.1.*

Proof: (Sufficiency) Note that $p = [\mathbf{1}_n^T, \mathbf{0}_n^T]^T$ and $q = [\mathbf{p}^T, (\frac{1}{\alpha} - \frac{T}{2})\mathbf{p}^T]^T$ are, respectively, a right and left eigenvector of F associated with the eigenvalue one. Also note that $p^T q = 1$. If one is the unique eigenvalue with the maximum modulus, then it follows from Lemma 1.7 that $\lim_{k\to\infty} F^k = \begin{bmatrix} \mathbf{1}_n \\ \mathbf{0}_n \end{bmatrix}[\mathbf{p}^T, (\frac{1}{\alpha} - \frac{T}{2})\mathbf{p}^T]$. Therefore, it follows that $\lim_{k\to\infty}\begin{bmatrix} \tilde{r}[k] \\ v[k] \end{bmatrix} = \lim_{k\to\infty} F^k \begin{bmatrix} \tilde{r}[0] \\ v[0] \end{bmatrix} = \begin{bmatrix} \tilde{r}[0] + (\frac{1}{\alpha} - \frac{T}{2})\mathbf{p}^T v[0] \\ \mathbf{0}_n \end{bmatrix}$.

(Necessity) Note that F can be written in the Jordan canonical form as $F = PJP^{-1}$, where J is the Jordan block matrix. If $\tilde{r}_i[k] \to \mathbf{p}^T \tilde{r}[0] + (\frac{1}{\alpha} - \frac{T}{2})\mathbf{p}^T v[0]$ and $v_i[k] \to 0$ as $k \to \infty$, it follows that $\lim_{k\to\infty} F^k = \begin{bmatrix} \mathbf{1}_n \\ \mathbf{0}_n \end{bmatrix}[\mathbf{p}^T, (\frac{1}{\alpha} - \frac{T}{2})\mathbf{p}^T]$, which has rank one. It thus follows that $\lim_{k\to\infty} J^k$ has rank one, which implies that all but one eigenvalue of F are within the unit circle. Noting that F has at least one eigenvalue equal to one, it follows that one is the unique eigenvalue of F with the maximum modulus. ∎

We first show necessary and sufficient conditions on α and T such that coordination is achieved using (8.20) under an undirected interaction graph. Note that all eigenvalues of $\mathcal{L}$ are real for undirected graphs because $\mathcal{L}$ is symmetric in this case. Before moving on, we need the following lemma.

Lemma 8.5. *The polynomial*

$$z^2 + az + b = 0, \tag{8.24}$$

where $a, b \in \mathbb{C}$, has all roots within the unit circle if and only if all roots of

$$(1 + a + b)s^2 + 2(1 - b)s + b - a + 1 = 0 \qquad (8.25)$$

are in the open left half plane.

Proof: By applying bilinear transformation $z = \frac{s+1}{s-1}$, (8.24) can be rewritten as

$$(s + 1)^2 + a(s + 1)(s - 1) + b(s - 1)^2 = 0,$$

which implies (8.25). Note that the bilinear transformation maps the open left half plane one-to-one onto the interior of the unit circle. The lemma follows directly. ∎

Lemma 8.6. *Suppose that the undirected graph $\mathcal{G}$ is connected. All eigenvalues of F, where F is defined in (8.22), are within the unit circle except one eigenvalue equal to one if and only if the positive α and T are chosen from the set*

$$S_r \triangleq \left\{ (\alpha, T) \,\middle|\, -\frac{T^2}{2} \min_i \mu_i < \alpha T < 2 \right\}.^4 \qquad (8.26)$$

Proof: When the undirected graph $\mathcal{G}$ is connected, it follows from Lemma 1.1 that $\mu_i < 0, i = 2, \ldots, n$, by noting that $\mu_1 = 0$. Also note that $\lambda_1 = 1$ and $\lambda_2 = 1 - \alpha T$. To ensure $|\lambda_2| < 1$, it is required that $0 < \alpha T < 2$. Let $a \triangleq \alpha T - 2 - \frac{T^2}{2}\mu_i$ and $b \triangleq 1 - \alpha T - \frac{T^2}{2}\mu_i$. It follows from Lemma 8.5 that for $\mu_i < 0, i = 2, \ldots, n$, the roots of (8.23) are within the unit circle if and only if all roots of

$$-T^2\mu_i s^2 + \left(T^2\mu_i + 2\alpha T\right)s + 4 - 2\alpha T = 0 \qquad (8.27)$$

are in the open left half plane. Because $-T^2\mu_i > 0, i = 2, \ldots, n$, the roots of (8.27) are always in the open left half plane if and only if $T^2\mu_i + 2\alpha T > 0$ and $4 - 2\alpha T > 0$, which implies that $-\frac{T^2}{2}\mu_i < \alpha T < 2$. Combining the above arguments proves the lemma. ∎

Theorem 8.5. *Suppose that the undirected graph $\mathcal{G}$ is connected. Let $\mathbf{p} \in \mathbb{R}^n$ be defined in Lemma 1.1. Using (8.20) for (8.19), $r_i[k] - r_j[k] \to \Delta_{ij}$ and $v_i[k] \to 0$ if and only if α and T are chosen from S_r, where S_r is defined by (8.26). In particular, $r_i[k] \to \delta_i + \mathbf{p}^T \tilde{r}[0] + (\frac{1}{\alpha} - \frac{T}{2})\mathbf{p}^T v[0]$ and $v_i[k] \to 0$ as $k \to \infty$.*

Proof: The statement follows directly from Lemmas 8.4 and 8.6. ∎

Remark 8.6 From Lemma 8.6, we can get that $T < \frac{2}{\sqrt{-\mu_i}}$. From Lemma 1.18, it follows that $|\mu_i| \leq 2 \max_i \ell_{ii}$, where ℓ_{ii} is the ith diagonal entry of $\mathcal{L}$. Therefore, if $T < \sqrt{\frac{2}{\max_i \ell_{ii}}}$, then we have that $T < \frac{2}{\sqrt{-\mu_i}}$. Note that $\max_i \ell_{ii} = \max_i \sum_{j=1, j \neq i}^n a_{ij}$ represents the maximal in-degree of the nodes in the graph $\mathcal{G}$ under the assumption that $a_{ii} = 0$. Therefore, the sufficient bound of the sampling period is related to the maximal in-degree of the nodes in $\mathcal{G}$.

---

4 Note that S_r is nonempty.

We next show necessary and sufficient conditions on α and T such that coordination is achieved using (8.20) under a directed interaction graph. Because it is not easy to find the explicit bounds for α and T such that the necessary and sufficient conditions are satisfied, we also present sufficient conditions that can be used to compute the explicit bounds for α and T. Note that the eigenvalues of $\mathscr{L}$ might be complex for directed graphs, which makes the analysis more challenging.

Lemma 8.7. *Suppose that the directed graph $\mathscr{G}$ has a directed spanning tree. There exist positive α and T such that the following three conditions are satisfied*:

1. $0 < \alpha T < 2$;
2. *When $\mu_i < 0$, $(\alpha, T) \in S_r$, where S_r is defined by* (8.26);
3. *When $\mathrm{Re}(\mu_i) < 0$ and $\mathrm{Im}(\mu_i) \neq 0$, α and T satisfy that*

   (i) *If $\alpha > \dfrac{|\mu_i|}{\sqrt{-\mathrm{Re}(\mu_i)}}$, then $0 < T < \dfrac{-2\alpha\mathrm{Re}(\mu_i)}{|\mu_i|^2}$.*

   (ii) *If $\dfrac{|\mathrm{Im}(\mu_i)|}{\sqrt{-\mathrm{Re}(\mu_i)}} \leq \alpha \leq \dfrac{|\mu_i|}{\sqrt{-\mathrm{Re}(\mu_i)}}$, then $0 < T < \min\{\overline{T}_{i1}, \dfrac{-2\alpha\mathrm{Re}(\mu_i)}{|\mu_i|^2}\}$, where*

$$\overline{T}_{i1} \triangleq \frac{-2\alpha[\mathrm{Re}(\mu_i)]^2 - 2\,|\mathrm{Im}(\mu_i)|\,\sqrt{[-\mathrm{Re}(\mu_i)][\alpha^2\mathrm{Re}(\mu_i) + |\mu_i|^2]}}{\mathrm{Re}(\mu_i)|\mu_i|^2}.$$

(8.28)

   (iii) *If $0 < \alpha < \dfrac{|\mathrm{Im}(\mu_i)|}{\sqrt{-\mathrm{Re}(\mu_i)}}$, then $0 < T < \min\{\overline{T}_{i2}, \dfrac{-2\alpha\mathrm{Re}(\mu_i)}{|\mu_i|^2}\}$, where*

$$\overline{T}_{i2} \triangleq \frac{-2\alpha[\mathrm{Re}(\mu_i)]^2 + 2\,|\mathrm{Im}(\mu_i)|\,\sqrt{[-\mathrm{Re}(\mu_i)][\alpha^2\mathrm{Re}(\mu_i) + |\mu_i|^2]}}{\mathrm{Re}(\mu_i)|\mu_i|^2}.$$

(8.29)

In addition, all eigenvalues of F, where F is defined in (8.22)*, are within the unit circle except for one eigenvalue equal to one if and only if the previous three conditions are satisfied.*

Proof: For the first statement, when T is sufficiently small, there always exists a positive α such that Conditions 1, 2, and 3 are satisfied.

For the second statement, because $\mu_1 = 0$, it follows that $\lambda_1 = 1$ and $\lambda_2 = 1 - \alpha T$. Therefore, λ_2 is within the unit circle if and only if Condition 1 is satisfied. When $\mu_i < 0$, $i \neq 1$, it follows from a similar line to that in Lemma 8.6 that all roots of F corresponding to μ_i are within the unit circle if and only if Condition 2 is satisfied. We next consider the case when $\mathrm{Re}(\mu_i) < 0$ and $\mathrm{Im}(\mu_i) \neq 0$, $i \neq 1$. Letting s_1 and s_2 be the two roots of (8.27), it follows that $\mathrm{Re}(s_1) + \mathrm{Re}(s_2) = 1 + 2\frac{\alpha}{T}\frac{\mathrm{Re}(\mu_i)}{|\mu_i|^2}$. Therefore, a necessary condition to guarantee that both s_1 and s_2 are in the open left half plane is that $1 + 2\frac{\alpha}{T}\frac{\mathrm{Re}(\mu_i)}{|\mu_i|^2} < 0$, i.e., $\frac{\alpha}{T} > -\frac{|\mu_i|^2}{2\mathrm{Re}(\mu_i)}$. To find the exact bound on T, we assume that one root of (8.27) is on the imaginary axis. Without loss of generality, let $s_1 = \chi\iota$, where $\chi \in \mathbb{R}$. Substituting $s_1 = \chi\iota$ into (8.27) and separating the corresponding real and imaginary parts give that

$$T^2\text{Re}(\mu_i)\chi^2 - T^2\text{Im}(\mu_i)\chi + 4 - 2\alpha T = 0, \tag{8.30}$$

$$T^2\text{Im}(\mu_i)\chi^2 + \big[T^2\text{Re}(\mu_i) + 2\alpha T\big]\chi = 0. \tag{8.31}$$

It follows from (8.31) that

$$\chi = -\frac{T\text{Re}(\mu_i) + 2\alpha}{T\text{Im}(\mu_i)}. \tag{8.32}$$

Substituting (8.32) into (8.30) gives

$$\frac{\text{Re}(\mu_i)[T\text{Re}(\mu_i) + 2\alpha]^2}{[\text{Im}(\mu_i)]^2} + T\big[T\text{Re}(\mu_i) + 2\alpha\big] + 4 - 2\alpha T = 0.$$

After some simplification, we get

$$\text{Re}(\mu_i)|\mu_i|^2 T^2 + 4\alpha\big[\text{Re}(\mu_i)\big]^2 T + 4\alpha^2\text{Re}(\mu_i) + 4\big[\text{Im}(\mu_i)\big]^2 = 0. \tag{8.33}$$

When $\alpha > \frac{|\mu_i|}{\sqrt{-\text{Re}(\mu_i)}}$, it can be computed that

$$\big\{4\alpha\big[\text{Re}(\mu_i)\big]^2\big\}^2 - 4\text{Re}(\mu_i)|\mu_i|^2\big(4\alpha^2\text{Re}(\mu_i) + 4\big[\text{Im}(\mu_i)\big]^2\big)$$

$$= -16\big\{\alpha^2\big[\text{Re}(\mu_i)\big]^2\big[\text{Im}(\mu_i)\big]^2 + \text{Re}(\mu_i)|\mu_i|^2\big[\text{Im}(\mu_i)\big]^2\big\}$$

$$= -16\text{Re}(\mu_i)\big[\text{Im}(\mu_i)\big]^2\big[\alpha^2\text{Re}(\mu_i) + |\mu_i|^2\big] < 0.$$

Therefore, there does not exist a positive T such that one root of (8.27) is on the imaginary axis, which implies that s_1 (respectively, s_2) is always on the open left or right half plane. Because $\text{Re}(s_1) + \text{Re}(s_2) = 1 + 2\frac{\alpha}{T}\frac{\text{Re}(\mu_i)}{|\mu_i|^2}$, when α is sufficiently large, it follows that $\text{Re}(s_1) + \text{Re}(s_2) < 0$. This implies that s_1 (respectively, s_2) is always on the open left half plane when $\alpha > \frac{|\mu_i|}{\sqrt{-\text{Re}(\mu_i)}}$. When $\frac{|\text{Im}(\mu_i)|}{\sqrt{-\text{Re}(\mu_i)}} \leq \alpha \leq \frac{|\mu_i|}{\sqrt{-\text{Re}(\mu_i)}}$, it follows that $4\alpha^2\text{Re}(\mu_i) + 4[\text{Im}(\mu_i)]^2 \geq 0$. Noting that $\text{Re}(\mu_i)|\mu_i|^2 < 0$, it follows that there exists a unique positive $\overline{T}_{i1}$ such that (8.33) holds when $T = \overline{T}_{i1}$, where $\overline{T}_{i1}$ is given by (8.28). Similarly, when $0 < \alpha < \frac{|\text{Im}(\mu_i)|}{\sqrt{-\text{Re}(\mu_i)}}$, it follows that $4\alpha^2\text{Re}(\mu_i) + 4[\text{Im}(\mu_i)]^2 < 0$. Noting also that $\text{Re}(\mu_i)|\mu_i|^2 < 0$, it follows that there are two positive solutions with the smaller one given by $\overline{T}_{i2}$ defined by (8.29).

Combining the previous arguments completes the proof. ∎

Theorem 8.7. *Suppose that the directed graph $\mathscr{G}$ has a directed spanning tree. Let* $\mathbf{p} \in \mathbb{R}^n$ *be defined in Lemma* 1.1. *Using* (8.20) *for* (8.19), $r_i[k] - r_j[k] \to \Delta_{ij}$ *and* $v_i[k] \to 0$ *if and only if α and T are chosen satisfying the conditions in Lemma* 8.7. *In particular,* $r_i[k] \to \delta_i + \mathbf{p}^T\tilde{r}[0] + (\frac{1}{\alpha} - \frac{T}{2})\mathbf{p}^T v[0]$ *and* $v_i[k] \to 0$ *as* $k \to \infty$.

Proof: The statement follows directly from Lemmas 8.4 and 8.7. ∎

From Lemma 8.7, it is not easy to find α and T explicitly such that the conditions in Lemma 8.7 are satisfied. We next present a sufficient condition that can be used to determine the bounds for α and T explicitly. Before moving on, we need the following lemmas and corollary.

Lemma 8.8 ([50, 252]). *All zeros of the complex polynomial*

$$P(z) = z^n + \alpha_1 z^{n-1} + \cdots + \alpha_{n-1} z + \alpha_n$$

satisfy $|z| \leq z_0$, *where* z_0 *is the unique nonnegative solution of the equation*

$$z^n - |\alpha_1| z^{n-1} - \cdots - |\alpha_{n-1}| z - |\alpha_n| = 0.$$

The bound z_0 *is attained if* $\alpha_i = -|\alpha_i|$.

Corollary 8.1. *The roots of* (8.24) *are within the unit circle if* $|a| + |b| < 1$. *Moreover, if* $|a + b| + |a - b| < 1$, *the roots of* (8.24) *are still within the unit circle.*

Proof: According to Lemma 8.8, the roots of (8.24) are within the unit circle if the unique nonnegative solution z_0 of $z^2 - |a|z - |b| = 0$ satisfies $z_0 < 1$. It is straightforward to show that $z_0 = \frac{|a| + \sqrt{|a|^2 + 4|b|}}{2}$. Therefore, the roots of (8.24) are within the unit circle if

$$|a| + \sqrt{|a|^2 + 4|b|} < 2. \tag{8.34}$$

We next discuss the condition under which (8.34) holds. If $b = 0$, then the statements of the corollary hold trivially. If $|b| \neq 0$, we have that

$$\frac{(|a| + \sqrt{|a|^2 + 4|b|})(-|a| + \sqrt{|a|^2 + 4|b|})}{-|a| + \sqrt{|a|^2 + 4|b|}} < 2.$$

After some computation, it follows that (8.34) is equivalent to $|a| + |b| < 1$. Therefore, the first statement of the corollary holds. For the second statement, because $|a| + |b| \leq |a + b| + |a - b|$, if $|a + b| + |a - b| < 1$, then $|a| + |b| < 1$, which implies that the second statement of the corollary also holds. ∎

The following lemma presents a sufficient condition that can be used to find α and T explicitly.

Lemma 8.9. *Suppose that the directed graph* $\mathscr{G}$ *has a directed spanning tree. There exist positive* α *and* T *such that* $S_c \cap S_r$ *is nonempty, where*

$$S_c \triangleq \bigcap_{\forall \mathrm{Re}(\mu_i) < 0 \text{ and } \mathrm{Im}(\mu_i) \neq 0} \left\{ (\alpha, T) \big| |1 + T^2 \mu_i| + |3 - 2\alpha T| < 1 \right\}, \tag{8.35}$$

and

$$S_r \triangleq \bigcap_{\forall \mu_i \leq 0} \left\{ (\alpha, T) | -\frac{T^2}{2} \mu_i < \alpha T < 2 \right\}. \tag{8.36}$$

If α *and* T *are chosen from* $S_c \cap S_r$, *then all eigenvalues of* F *are within the unit circle except one eigenvalue equal to one.*

Proof: For the first statement, we let $\alpha T = \frac{3}{2}$. When $\text{Re}(\mu_i) < 0$ and $\text{Im}(\mu_i) \neq 0$, $|1 + T^2 \mu_i| + |3 - 2\alpha T| < 1$ implies that $|1 + T^2 \mu_i| < 1$ because $\alpha T = \frac{3}{2}$. It thus follows that $0 < T < \frac{\sqrt{-2\text{Re}(\mu_i)}}{|\mu_i|}$ for all $\text{Re}(\mu_i) < 0$ and $\text{Im}(\mu_i) \neq 0$. When $\mu_i \leq 0$, $-\frac{T^2}{2}\mu_i < \alpha T < 2$ can be simplified as $-T^2 \mu_i < \frac{3}{2}$ because $\alpha T = \frac{3}{2}$. It thus follows that $0 < T < \sqrt{\frac{3}{-\mu_i}}$ for all $\mu_i \leq 0$. Let $T_c \triangleq \bigcap_{\forall \text{Re}(\mu_i)<0 \text{ and } \text{Im}(\mu_i)\neq 0} \{T | 0 < T < \frac{\sqrt{-2\text{Re}(\mu_i)}}{|\mu_i|}\}$ and $T_r \triangleq \bigcap_{\forall \mu_i \leq 0} \{T | 0 < T < \sqrt{\frac{3}{-\mu_i}}\}$.[5] It is straightforward to see that $T_c \cap T_r$ is nonempty. Recalling that $\alpha T = \frac{3}{2}$, it follows that $S_c \cap S_r$ is nonempty as well.

For the second statement, note that if the directed graph $\mathscr{G}$ has a directed spanning tree, then it follows from Lemma 1.1 that $\text{Re}(\mu_i) < 0$, $i = 2, \ldots, n$, by noting that $\mu_1 = 0$. Also note that $\lambda_1 = 1$ and $\lambda_2 = 1 - \alpha T$. To ensure that $|\lambda_2| < 1$, it is required that $0 < \alpha T < 2$. When $\text{Re}(\mu_i) < 0$ and $\text{Im}(\mu_i) \neq 0$, it follows from Corollary 8.1 that the roots of (8.23) are within the unit circle if $|1 + T^2 \mu_i| + |3 - 2\alpha T| < 1$, where we have used the second statement of Corollary 8.1 by letting $a = \alpha T - 2 - \frac{T^2}{2}\mu_i$ and $b = 1 - \frac{T^2}{2}\mu_i - \alpha T$. When $\mu_i < 0$, it follows from the proof of Lemma 8.6 that the roots of (8.23) are within the unit circle if $-\frac{T^2}{2}\mu_i < \alpha T < 2$. Combining the above arguments proves the second statement. ∎

Remark 8.8 According to Lemmas 8.4 and 8.9, if α and T are chosen from $S_c \cap S_r$, where S_c is defined by (8.35) and S_r is defined by (8.36), and the directed graph $\mathscr{G}$ has a directed spanning tree, coordination is achieved ultimately. An easy way to choose α and T is to let $\alpha T = \frac{3}{2}$. It then follows that T can be chosen from $T_c \cap T_r$, where T_c and T_r are defined in the proof of Lemma 8.9.

8.2.3 Convergence Analysis of the Sampled-data Coordination Algorithm with Relative Damping

In this subsection, we analyze the algorithm (8.21) under, respectively, an undirected fixed interaction graph and a directed fixed interaction graph. We assume that $\mathscr{A}$ is constant. In this case, using (8.21), (8.19) can be written in a vector form as

$$\begin{bmatrix} \tilde{r}[k+1] \\ v[k+1] \end{bmatrix} = \underbrace{\begin{bmatrix} I_n - \frac{T^2}{2}\mathscr{L} & TI_n - \frac{T^2}{2}\mathscr{L} \\ -T\mathscr{L} & I_n - \alpha T\mathscr{L} \end{bmatrix}}_{G} \begin{bmatrix} \tilde{r}[k] \\ v[k] \end{bmatrix}, \tag{8.37}$$

where $\tilde{r}$, v, and $\mathscr{L}$ are defined as in (8.22). A similar analysis to that for (8.22) shows that the roots of $\det(zI_{2n} - G) = 0$ (i.e., the eigenvalues of G) satisfy

---

[5] When $\mu_i = 0$, $T > 0$ can be chosen arbitrarily.

$$z^2 - \left(2 + \alpha T \mu_i + \frac{1}{2}T^2 \mu_i\right)z + 1 + \alpha T \mu_i - \frac{1}{2}T^2 \mu_i = 0. \tag{8.38}$$

Similarly, each eigenvalue of $-\mathcal{L}$, μ_i, corresponds to two eigenvalues of G, denoted by ρ_{2i-1} and ρ_{2i}. Note that $\mathcal{L}$ has at least one zero eigenvalue. Without loss of generality, let $\mu_1 = 0$, which implies that $\rho_1 = \rho_2 = 1$. Therefore, G has at least two eigenvalues equal to one.

Lemma 8.10. *Using* (8.21) *for* (8.19), $r_i[k] - r_j[k] \to \Delta_{ij}$ *and* $v_i[k] - v_j[k] \to 0$ *as* $k \to \infty$ *if and only if G, where G is defined in* (8.37), *has exactly two eigenvalues equal to one and all other eigenvalues have modulus smaller than one. In particular,* $r_i[k] - \delta_i - (\mathbf{p}^T \tilde{r}[0] + kT\mathbf{p}^T v[0]) \to 0$ *and* $v_i[k] \to \mathbf{p}^T v[0]$ *as* $k \to \infty$, *where* $\mathbf{p} \in \mathbb{R}^n$ *is defined in Lemma 1.1.*

Proof: (Sufficiency) Note from (8.38) that if G has exactly two eigenvalues equal to one (i.e., $\rho_1 = \rho_2 = 1$), then $-\mathcal{L}$ has exactly one eigenvalue equal to zero. Let $[p^T, q^T]^T$, where $p, q \in \mathbb{R}^n$, be a right eigenvector of G associated with the eigenvalue one. It follows that

$$\begin{bmatrix} I_n - \frac{T^2}{2}\mathcal{L} & TI_n - \frac{T^2}{2}\mathcal{L} \\ -T\mathcal{L} & I_n - \alpha T \mathcal{L} \end{bmatrix} \begin{bmatrix} p \\ q \end{bmatrix} = \begin{bmatrix} p \\ q \end{bmatrix}.$$

After some computation, it follows that the eigenvalue one has geometric multiplicity equal to one even if it has algebraic multiplicity equal to two. It also follows from Lemma 1.1 that we can choose $p = \mathbf{1}_n$ and $q = \mathbf{0}_n$. In addition, a generalized right eigenvector associated with the eigenvalue one can be chosen as $[\mathbf{0}_n^T, \frac{1}{T}\mathbf{1}_n^T]^T$. Similarly, it can be shown that $[\mathbf{0}_n^T, T\mathbf{p}_n^T]^T$ and $[\mathbf{p}^T, \mathbf{0}_n^T]^T$ are, respectively, a left eigenvector and generalized left eigenvector associated with the eigenvalue one. Note that G can be written in the Jordan canonical form as $G = PJP^{-1}$, where the columns of P, denoted by p_k, $k = 1, \ldots, 2n$, can be chosen to be the right eigenvectors or generalized right eigenvectors of G, the rows of P^{-1}, denoted by q_k^T, $k = 1, \ldots, 2n$, can be chosen to be the left eigenvectors or generalized left eigenvectors of G such that $p_k^T q_k = 1$ and $p_k^T q_\ell = 0$, $k \neq \ell$, and J is the Jordan block diagonal matrix with the eigenvalues of G being the diagonal entries. Note that $\rho_1 = \rho_2 = 1$ and $|\rho_k| < 1$, $k = 3, \ldots, 2n$. Also note that we can choose $p_1 = [\mathbf{1}_n^T, \mathbf{0}_n^T]^T$, $p_2 = [\mathbf{0}_n^T, \frac{1}{T}\mathbf{1}_n^T]^T$, $q_1 = [\mathbf{p}^T, \mathbf{0}_n^T]^T$, and $q_2 = [\mathbf{0}_n^T, T\mathbf{p}_n^T]^T$. Because $\begin{bmatrix} \tilde{r}[k] \\ v[k] \end{bmatrix} = G^k \begin{bmatrix} \tilde{r}[0] \\ v[0] \end{bmatrix} = PJ^k P^{-1} \begin{bmatrix} \tilde{r}[0] \\ v[0] \end{bmatrix}$ and $\lim_{k \to \infty} \left\| PJ^k P^{-1} - \begin{bmatrix} \mathbf{1}_n & \mathbf{0}_n \\ \mathbf{0}_n & \frac{1}{T}\mathbf{1}_n \end{bmatrix} \begin{bmatrix} 1 & k \\ 0 & 1 \end{bmatrix} \begin{bmatrix} \mathbf{p}^T & \mathbf{0}_n^T \\ \mathbf{0}_n^T & T\mathbf{p}^T \end{bmatrix} \right\| = \lim_{k \to \infty} \left\| PJ^k P^{-1} - \begin{bmatrix} \mathbf{1}_n\mathbf{p}^T & kT\mathbf{1}_n\mathbf{p}^T \\ \mathbf{0}_{n \times n} & \mathbf{1}_n\mathbf{p}^T \end{bmatrix} \right\| = 0$, it follows that $|\tilde{r}_i[k] - \mathbf{p}^T\tilde{r}[0] - kT\mathbf{p}^T v[0]| \to 0$ and $v_i[k] \to \mathbf{p}^T v[0]$ as $k \to \infty$.

(Necessity) Note that G has at least two eigenvalues equal to one. If $\tilde{r}_i[k] - \mathbf{p}^T\tilde{r}[0] - kT\mathbf{p}^T v[0] \to 0$ and $v_i[k] \to \mathbf{p}^T v[0]$ as $k \to \infty$, it follows that F^k has rank two as $k \to \infty$, which in turn implies that J^k has rank two as $k \to \infty$. It follows that G has exactly two eigenvalues equal to one and all other eigenvalues have modulus smaller than one. ∎

We first show necessary and sufficient conditions on α and T such that coordination is achieved using (8.21) under an undirected interaction graph.

Lemma 8.11. *Suppose that the undirected graph $\mathscr{G}$ is connected. All eigenvalues of G, where G is defined in (8.37), are within the unit circle except two eigenvalues equal to one if and only if α and T are chosen from the set*

$$Q_r \triangleq \left\{ (\alpha, T) \middle| \frac{T^2}{2} < \alpha T < -\frac{2}{\min_i \mu_i} \right\}.^{6} \tag{8.39}$$

Proof: Because the undirected graph $\mathscr{G}$ is connected, it follows from Lemma 1.1 that $\mu_i < 0$, $i = 2, \ldots, n$, by noting that $\mu_1 = 0$. Also note that $\rho_1 = \rho_2 = 1$. Let $a = -(2 + \alpha T \mu_i + \frac{1}{2} T^2 \mu_i)$ and $b = 1 + \alpha T \mu_i - \frac{1}{2} T^2 \mu_i$. It follows from Lemma 8.5 that for $\mu_i < 0$, $i = 2, \ldots, n$, the roots of (8.38) are within the unit circle if and only if all roots of

$$-T^2 \mu_i s^2 + \left(T^2 \mu_i - 2\alpha T \mu_i \right) s + 4 + 2\alpha T \mu_i = 0, \tag{8.40}$$

are in the open left half plane. Because $-T^2 \mu_i > 0$, the roots of (8.40) are always in the open left half plane if and only if $4 + 2\alpha T \mu_i > 0$ and $T^2 \mu_i - 2\alpha T \mu_i > 0$, which implies that $\frac{T^2}{2} < \alpha T < -\frac{2}{\mu_i}$, $i = 2, \ldots, n$. Combining the above arguments proves the lemma. ∎

Theorem 8.9. *Suppose that the undirected graph $\mathscr{G}$ is connected. Let $\mathbf{p} \in \mathbb{R}^n$ be defined in Lemma 1.1. Using (8.21), $r_i[k] - r_j[k] \to \Delta_{ij}$ and $v_i[k] - v_j[k] \to 0$ as $k \to \infty$ if and only if α and T are chosen from Q_r, where Q_r is defined by (8.39). In particular, $r_i[k] - \delta_i - (\mathbf{p}^T \tilde{r}[0] + kT\mathbf{p}^T v[0]) \to 0$ and $v_i[k] \to \mathbf{p}^T v[0]$ as $k \to \infty$.*

Proof: The statement follows directly from Lemmas 8.10 and 8.11. ∎

We next show necessary and sufficient conditions on α and T such that coordination is achieved using (8.21) under a directed interaction graph. Note again that the eigenvalues of $\mathscr{L}$ might be complex for directed graphs, which makes the analysis more challenging.

Lemma 8.12. *Suppose that $\mathrm{Re}(\mu_i) < 0$. The roots of (8.38) are within the unit circle if and only if $\frac{\alpha}{T} > \frac{1}{2}$ and $B_i < 0$, where*

$$B_i \triangleq \left(\frac{4\mathrm{Re}(\mu_i)}{|\mu_i|^2 T^2} + \frac{2\alpha}{T} \right) \left(1 - \frac{2\alpha}{T} \right)^2 + \frac{16\mathrm{Im}(\mu_i)^2}{|\mu_i|^4 T^4}. \tag{8.41}$$

Proof: As in the proof of Lemma 8.11, the roots of (8.38) are within the unit circle if and only if the roots of (8.40) are in the open left half plane. Letting s_1 and s_2 denote the roots of (8.40), it follows that

$$s_1 + s_2 = 1 - 2\frac{\alpha}{T} \tag{8.42}$$

---

6 Note that Q_r is nonempty.

and

$$s_1 s_2 = -\frac{4}{\mu_i T^2} - 2\frac{\alpha}{T}. \tag{8.43}$$

Noting that (8.42) implies that $\text{Im}(s_1) + \text{Im}(s_2) = 0$, we define $s_1 = a_1 + \iota b$ and $s_2 = a_2 - \iota b$. Note that s_1 and s_2 have negative real parts if and only if $a_1 + a_2 < 0$ and $a_1 a_2 > 0$. Note from (8.42) that $a_1 + a_2 < 0$ is equivalent to $\frac{\alpha}{T} > \frac{1}{2}$. We next show conditions on α and T such that $a_1 a_2 > 0$ holds. Substituting the definitions of s_1 and s_2 into (8.43) gives $a_1 a_2 + b^2 + \iota(a_2 - a_1)b = -\frac{4}{\mu_i T^2} - 2\frac{\alpha}{T}$, which implies

$$(a_2 - a_1)b = \frac{4\text{Im}(\mu_i)}{|\mu_i|^2 T^2}, \tag{8.44}$$

$$a_1 a_2 + b^2 = \frac{-4\text{Re}(\mu_i)}{|\mu_i|^2 T^2} - 2\frac{\alpha}{T}. \tag{8.45}$$

It follows from (8.44) that $b = \frac{4\text{Im}(\mu_i)}{|\mu_i|^2 T^2(a_2 - a_1)}$. Consider also the fact that $(a_2 - a_1)^2 = (a_2 + a_1)^2 - 4a_1 a_2 = (1 - 2\frac{\alpha}{T})^2 - 4a_1 a_2$. After some manipulation, (8.45) can be written as

$$4(a_1 a_2)^2 + A_i a_1 a_2 - B_i = 0, \tag{8.46}$$

where $A_i \triangleq 4(\frac{4\text{Re}(\mu_i)}{|\mu_i|^2 T^2} + 2\frac{\alpha}{T}) - (1 - 2\frac{\alpha}{T})^2$ and B_i is defined by (8.41). It follows that $A_i^2 + 16B_i = [4(\frac{4\text{Re}(\mu_i)}{|\mu_i|^2 T^2} + 2\frac{\alpha}{T}) + (1 - 2\frac{\alpha}{T})^2]^2 + \frac{16\text{Im}(\mu_i)^2}{|\mu_i|^4 T^4} \geq 0$, which implies that (8.46) has two real roots. Therefore, the necessary and sufficient conditions for $a_1 a_2 > 0$ are $B_i < 0$ and $A_i < 0$. Because $\frac{16\text{Im}(\mu_i)^2}{|\mu_i|^4 T^4} > 0$, if $B_i < 0$ then $4(\frac{4\text{Re}(\mu_i)}{|\mu_i|^2 T^2} + 2\frac{\alpha}{T}) < 0$, which implies $A_i < 0$ as well. Combining the previous arguments proves the lemma. ∎

Lemma 8.13. *Suppose that the directed graph $\mathcal{G}$ has a directed spanning tree. There exist positive α and T such that Q_c is nonempty, where*

$$Q_c \triangleq \bigcap_{\forall \text{Re}(\mu_i) < 0} \left\{ (\alpha, T) \Big| \frac{1}{2} < \frac{\alpha}{T}, B_i < 0 \right\}, \tag{8.47}$$

where B_i is defined by (8.41). All eigenvalues of G, where G is defined in (8.37), are within the unit circle except two eigenvalues equal to one if and only if α and T are chosen from Q_c.

Proof: For the first statement, we let $\alpha > T > 0$, which implies that $\frac{\alpha}{T} > \frac{1}{2}$ holds apparently. Note that $\alpha > T$ implies that $(T - 2\alpha)^2 > \alpha^2$. Therefore, a sufficient condition for $B_i < 0$ is

$$\alpha T < -\frac{8\text{Im}(\mu_i)^2}{|\mu_i|^4 \alpha^2} - \frac{2\text{Re}(\mu_i)}{|\mu_i|^2}. \tag{8.48}$$

To ensure that there are feasible $\alpha > 0$ and $T > 0$ satisfying (8.48), we first need to ensure that the right side of (8.48) is positive, which requires that $\alpha > \frac{2|\text{Im}(\mu_i)|}{|\mu_i|\sqrt{-\text{Re}(\mu_i)}}$ for all $\text{Re}(\mu_i) < 0$. It also follows from (8.48) that $T < -\frac{8\text{Im}(\mu_i)^2}{|\mu_i|^4\alpha^3} - \frac{2\text{Re}(\mu_i)}{|\mu_i|^2\alpha}$ for all $\text{Re}(\mu_i) < 0$. Therefore, (8.47) is ensured to be nonempty if α and T are chosen from, respectively, $\alpha_c \triangleq \bigcap_{\forall \text{Re}(\mu_i) < 0} \{\alpha | \alpha > \frac{2|\text{Im}(\mu_i)|}{|\mu_i|\sqrt{-\text{Re}(\mu_i)}}\}$ and

$$T_c \triangleq \bigcap_{\forall \text{Re}(\mu_i) < 0} \left\{ T \Big| T < -\frac{8\text{Im}(\mu_i)^2}{|\mu_i|^4\alpha^3} - \frac{2\text{Re}(\mu_i)}{|\mu_i|^2\alpha} \text{ and } 0 < T < \alpha \right\}.$$

It is straightforward to see that both α_c and T_c are nonempty. Combining the above arguments shows that Q_c is nonempty.

For the second statement, note that if the directed graph $\mathscr{G}$ has a directed spanning tree, it follows from Lemma 1.1 that $\text{Re}(\mu_i) < 0$, $i = 2, \ldots, n$, by noting that $\mu_1 = 0$. Also note that $\rho_1 = 1$ and $\rho_2 = 1$. When $\text{Re}(\mu_i) < 0$, it follows from Lemma 8.12 that the roots of (8.38) are within the unit circle if and only if $\frac{\alpha}{T} > \frac{1}{2}$ and $B_i < 0$. It thus follows that all eigenvalues of G are within the unit circle except two eigenvalues equal to one if and only if α and T are chosen from Q_c. ∎

Remark 8.10 From the proof of the first statement of Lemma 8.13, an easy way to choose α and T is to let $\alpha > T$. Then α is chosen from α_c and T is chosen from T_c, where α_c and T_c are defined in the proof of Lemma 8.13.

Theorem 8.11. *Suppose that the directed graph $\mathscr{G}$ has a directed spanning tree. Using (8.21) for (8.19), $r_i[k] - r_j[k] \to \Delta_{ij}$ and $v_i[k] - v_j[k] \to 0$ as $k \to \infty$ if and only if α and T are chosen from Q_c, where Q_c is defined by (8.47). In particular, $r_i[k] - \delta_i - (\mathbf{p}^T\tilde{r}[0] + kT\mathbf{p}^Tv[0]) \to 0$ and $v_i[k] \to \mathbf{p}^Tv[0]$ as $k \to \infty$.*

Proof: The proof follows directly from Lemmas 8.11 and 8.13. ∎

8.2.4 Simulation

In this section, we present simulation results to validate the theoretical results derived in Sects. 8.2.2 and 8.2.3. We consider a team of four agents with the directed graph $\mathscr{G}$ shown by Fig. 8.4. Note that $\mathscr{G}$ has a directed spanning tree. The nonsymmetric Laplacian matrix associated with $\mathscr{G}$ is chosen as

$$\mathscr{L} = \begin{bmatrix} 1 & -1 & 0 & 0 \\ 0 & 1.5 & -1.5 & 0 \\ -2 & 0 & 2 & 0 \\ -2.5 & 0 & 0 & 2.5 \end{bmatrix}.$$

It can be computed that for $\mathscr{L}$, $\mathbf{p} = [0.4615, 0.3077, 0.2308, 0]^T$. Here for simplicity, we have chosen $\delta_i = 0$, $i = 1, \ldots, 4$, which implies that $\Delta_{ij} = 0$.
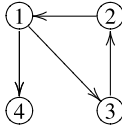
Fig. 8.4 Directed graph $\mathscr{G}$ for four agents. An *arrow* from j to i denotes that agent j is a neighbor of agent i

(a) Positions

(b) Velocities
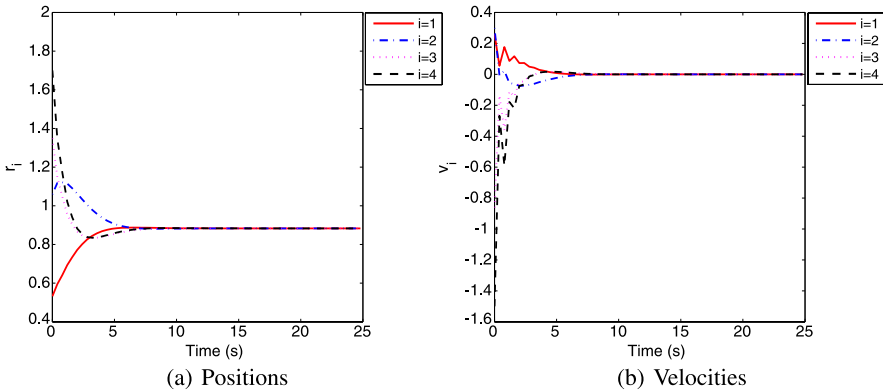
Fig. 8.5 Convergence results using (8.20) with $\alpha = 4$ and $T = 0.4$ s

(a) Positions

(b) Velocities
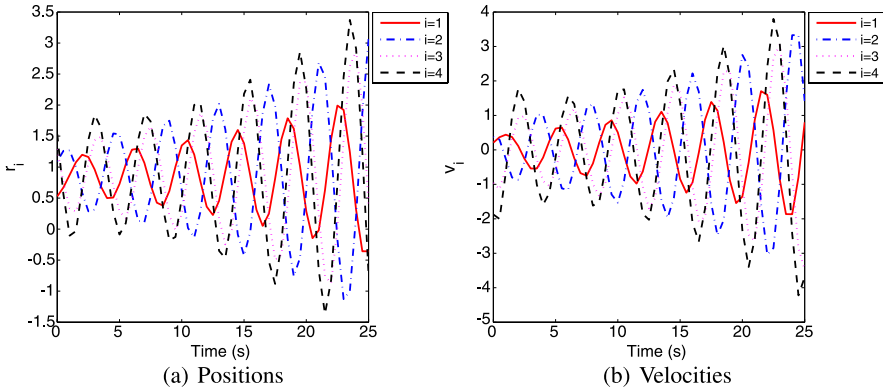
Fig. 8.6 Convergence results using (8.20) with $\alpha = 1.2$ and $T = 0.5$ s

For the coordination algorithm (8.20), let $r_i[0] = 0.5i$, $i = 1, \ldots, 4$, $v_1[0] = -0.1$, $v_2[0] = 0$, $v_3[0] = 0.1$, and $v_4[0] = 0$. Figure 8.5 shows the convergence result using (8.20) with $\alpha = 4$ and $T = 0.4$ s. Note that the conditions in Theorem 8.7 are satisfied. It can be seen that coordination is achieved with the final equilibrium for $r_i[k]$ being 0.8835, which is equal to $\delta_i + \mathbf{p}^T \tilde{r}[0] + (\frac{1}{\alpha} - \frac{T}{2})\mathbf{p}^T v[0]$ as stated in Theorem 8.7. Figure 8.6 shows the convergence result using (8.20) with $\alpha = 1.2$ and $T = 0.5$ s. Note that coordination is not achieved in this case.
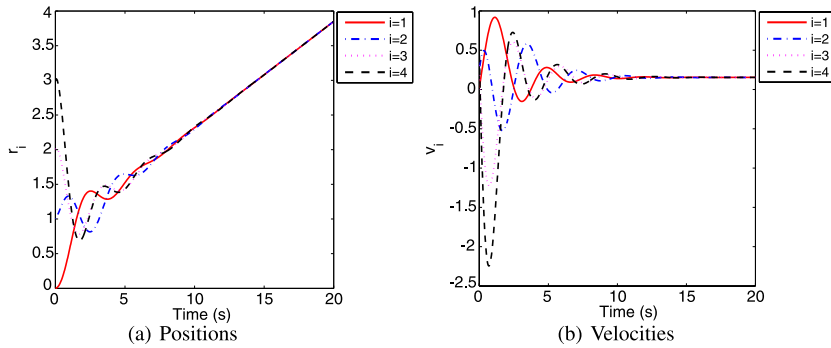
Fig. 8.7 Convergence results using (8.21) with $\alpha = 0.6$ and $T = 0.02$ s
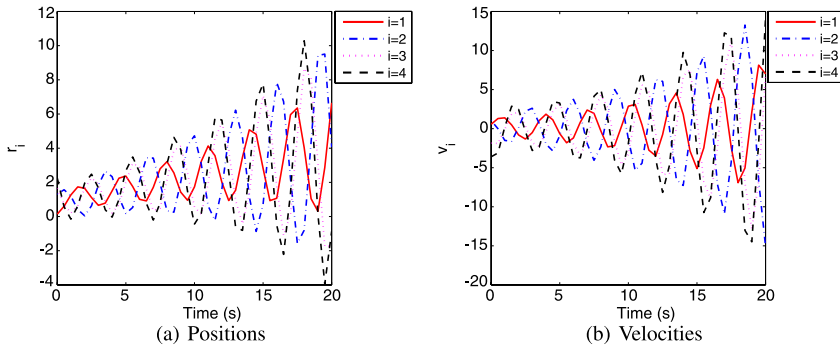
Fig. 8.8 Convergence results using (8.21) with $\alpha = 0.6$ and $T = 0.5$ s

For the coordination algorithm (8.21), let $r_i[0] = i - 1$ and $v_i[0] = 0.2(i - 1)$, $i = 1, \ldots, 4$. Figure 8.7 shows the convergence result using (8.21) with $\alpha = 0.6$ and $T = 0.02$ s. Note that the conditions in Theorem 8.13 are satisfied. It can be seen that coordination is achieved with the final equilibrium for $v_i[k]$ being 0.1538, which is equal to $\mathbf{p}^T v[0]$ as stated in Theorem 8.13. Figure 8.8 shows the convergence result using (8.21) with $\alpha = 0.6$ and $T = 0.5$ s. Note that coordination is not achieved in this case.

8.3 Sampled-data Coordination for Double-integrator Dynamics Under Switching Interaction

In this section, we study (8.20) and (8.21) under directed switching interaction. Note that there are a finite number of possible directed graphs for n agents. We assume that for each possible directed graph, there are a finite number of adjacency matrices associated with the directed graph. Therefore, all nonzero $a_{ij}[k]$ in (8.20) and (8.21) are chosen from a finite set.

8.3.1 Convergence Analysis of the Sampled-data Coordination Algorithm with Absolute Damping

In this subsection, we analyze (8.20) under a directed switching interaction graph. Here $\mathscr{A}[k]$ is switching. In this case, using (8.20), (8.19) can be written in a vector form as

$$\begin{bmatrix} \tilde{r}[k+1] \\ v[k+1] \end{bmatrix} = \underbrace{\begin{bmatrix} I_n - \frac{T^2}{2}\mathscr{L}[k] & (T - \frac{\alpha T^2}{2})I_n \\ -T\mathscr{L}[k] & (1 - \alpha T)I_n \end{bmatrix}}_{F_k} \begin{bmatrix} \tilde{r}[k] \\ v[k] \end{bmatrix}, \tag{8.49}$$

where $\tilde{r}$ and v are defined as in (8.22), and $\mathscr{L}[k]$ is the nonsymmetric Laplacian matrix associated with $\mathscr{A}[k]$ and hence $\mathscr{G}[k]$. Note that the solution of (8.49) can be written as

$$\begin{bmatrix} \tilde{r}[k+1] \\ v[k+1] \end{bmatrix} = \begin{bmatrix} B_k & C_k \\ D_k & E_k \end{bmatrix} \begin{bmatrix} \tilde{r}[0] \\ v[0] \end{bmatrix}, \tag{8.50}$$

where $\begin{bmatrix} B_k & C_k \\ D_k & E_k \end{bmatrix} \triangleq \prod_{i=0}^{k} F_i$. Therefore, B_k, C_k, D_k, and E_k satisfy

$$\begin{bmatrix} B_k \\ D_k \end{bmatrix} = F_k \begin{bmatrix} B_{k-1} \\ D_{k-1} \end{bmatrix} \tag{8.51}$$

and

$$\begin{bmatrix} C_k \\ E_k \end{bmatrix} = F_k \begin{bmatrix} C_{k-1} \\ E_{k-1} \end{bmatrix}. \tag{8.52}$$

Lemma 8.14. *Assume that $\alpha T \neq 2$. Using (8.20) for (8.19), $r_i[k] - r_j[k] \to \Delta_{ij}$ and $v_i[k] \to 0$ as $k \to \infty$ if $\lim_{k\to\infty} B_k$ exists and all rows of $\lim_{k\to\infty} B_k$ are the same for arbitrary initial conditions.*

Proof: When $\lim_{k\to\infty} B_k$ exists and all rows of $\lim_{k\to\infty} B_k$ are the same for arbitrary initial conditions, it follows that $\lim_{k\to\infty} C_k$ exists and all rows of $\lim_{k\to\infty} C_k$ are the same for arbitrary initial conditions as well because (8.51) and (8.52) have the same structure. It then follows from (8.51) that

$$B_k = \left(I_n - \frac{T^2}{2}\mathscr{L}[k] \right) B_{k-1} + \left(T - \frac{\alpha T^2}{2} \right) D_{k-1}. \tag{8.53}$$

Because $\mathscr{L}[k]\mathbf{1}_n = \mathbf{0}_n$ and all rows of $\lim_{k\to\infty} B_{k-1}$ are the same, it follows that $\lim_{k\to\infty} \mathscr{L}[k]B_{k-1} = 0_{n\times n}$. It thus follows that

$$\lim_{k\to\infty} \left(T - \frac{\alpha T^2}{2} \right) D_{k-1} = \lim_{k\to\infty} (B_k - B_{k-1}) = 0_{n\times n}.$$

Because $\alpha T \neq 2$, i.e., $T - \frac{\alpha T^2}{2} \neq 0$, it follows that $\lim_{k\to\infty} D_k = 0_{n\times n}$ for arbitrary initial conditions. Similarly, it follows that $\lim_{k\to\infty} E_k = 0_{n\times n}$ for arbitrary initial conditions because (8.51) and (8.52) have the same structure. Combining the

previous arguments with (8.50) shows that $\tilde{r}_i[k] - \tilde{r}_j[k] \to 0$ and $v_i[k] \to 0$ as $k \to \infty$, which implies that $r_i[k] - r_j[k] \to \Delta_{ij}$ and $v_i[k] \to 0$ as $k \to \infty$. ∎

Note from (8.53) that

$$B_{k-1} = \left(I_n - \frac{T^2}{2}\mathscr{L}[k-1]\right)B_{k-2} + \left(T - \frac{\alpha T^2}{2}\right)D_{k-2}. \qquad (8.54)$$

It follows from (8.51) that

$$D_{k-1} = -T\mathscr{L}[k-1]B_{k-2} + (1 - \alpha T)D_{k-2}. \qquad (8.55)$$

Therefore, it follows from (8.53) and (8.54) that

$$\begin{aligned}
B_k - (1 - \alpha T)B_{k-1} &= \left(I_n - \frac{T^2}{2}\mathscr{L}[k]\right)B_{k-1} \\
&\quad - (1 - \alpha T)\left(I_n - \frac{T^2}{2}\mathscr{L}[k-1]\right)B_{k-2} \\
&\quad + \left(T - \frac{\alpha T^2}{2}\right)\left[D_{k-1} - (1 - \alpha T)D_{k-2}\right]. \qquad (8.56)
\end{aligned}$$

By substituting (8.55) into (8.56), (8.56) can be simplified as

$$B_k = \Phi_{k1}B_{k-1} + \Phi_{k2}B_{k-2}, \qquad (8.57)$$

where

$$\Phi_{k1} \triangleq (2 - \alpha T)I_n - \frac{T^2}{2}\mathscr{L}[k] \qquad (8.58)$$

and

$$\Phi_{k2} \triangleq (\alpha T - 1)I_n - \frac{T^2}{2}\mathscr{L}[k-1]. \qquad (8.59)$$

We next study the conditions on $\mathscr{G}[k]$, T, and α such that $\lim_{k \to \infty} B_k$ exists and all rows of $\lim_{k \to \infty} B_k$ are the same for arbitrary initial conditions. Before moving on, we need the following lemma.

Lemma 8.15. *Suppose that a nonnegative matrix $A \in \mathbb{R}^{n \times n}$ has the same row sum. Let $\overline{A} \triangleq \left[\begin{smallmatrix} 1 & 1 \\ 1 & 1 \end{smallmatrix}\right] \otimes A$. If the directed graph of A has a directed spanning tree, the directed graph of $\overline{A}$ also has a directed spanning tree.*

Proof: Note that the eigenvalues of $\left[\begin{smallmatrix} 1 & 1 \\ 1 & 1 \end{smallmatrix}\right]$ are $\lambda_1 = 0$ and $\lambda_2 = 2$. Let μ_j be the jth eigenvalue of A. Because $\overline{A} = \left[\begin{smallmatrix} 1 & 1 \\ 1 & 1 \end{smallmatrix}\right] \otimes A$, it follows from Lemma 1.21 that the eigenvalues of $\overline{A}$ are $\lambda_i \mu_j, i = 1, 2, j = 1, \ldots, n$. It thus follows that $\rho(\overline{A}) = 2\rho(A)$. If the directed graph of A has a directed spanning tree, it follows from Lemma 1.10 that A has a simple eigenvalue equal to $\rho(A)$, which implies that $\overline{A}$ also has a simple eigenvalue equal to $\rho(\overline{A})$. Therefore, it follows again from Lemma 1.10 that the directed graph of $\overline{A}$ has a directed spanning tree. ∎

Lemma 8.16. *Let Φ_{k1} and Φ_{k2} be defined by, respectively, (8.58) and (8.59). There exist positive α and T such that both Φ_{k1} and Φ_{k2} are nonnegative matrices with positive diagonal entries. If the positive α and T are chosen such that both Φ_{k1} and Φ_{k2} are nonnegative with positive diagonal entries, and there exists a positive integer κ such that for any nonnegative integer k_0, the union of $\mathscr{G}[k]$ across $k \in [k_0, k_0 + \kappa]$ has a directed spanning tree, the iteration (8.57) is stable for arbitrary initial conditions (i.e., $\lim_{k\to\infty} B_k$ exists) and all rows of $\lim_{k\to\infty} B_k$ are the same.*

Proof: For the first statement, consider $\alpha T = \frac{3}{2}$. It follows that if $T^2 < \min_i \frac{1}{\ell_{ii}[k]}$, $k = 0, 1, \ldots$, where $\ell_{ii}[k]$ is the ith diagonal entry of $\mathscr{L}[k]$, then both Φ_{k1} and Φ_{k2} are nonnegative matrices with positive diagonal entries.

For the second statement, rewrite (8.57) as

$$\begin{bmatrix} B_k \\ B_{k-1} \end{bmatrix} = \underbrace{\begin{bmatrix} \Phi_{k1} & \Phi_{k2} \\ I_n & 0_{n\times n} \end{bmatrix}}_{H_k} \begin{bmatrix} B_{k-1} \\ B_{k-2} \end{bmatrix}. \tag{8.60}$$

Note that $\Phi_{k1}\mathbf{1}_n = 2 - \alpha T$, $\Phi_{k2}\mathbf{1}_n = \alpha T - 1$, and $(\Phi_{k1} + \Phi_{k2})\mathbf{1}_n = 1$. When the positive α and T are chosen such that both Φ_{k1} and Φ_{k2} are nonnegative matrices with positive diagonal entries, it follows that H_k is a row-stochastic matrix. It then follows that $H_{k+1}H_k = \begin{bmatrix} \Phi_{(k+1)1}\Phi_{k1} + \Phi_{(k+1)2} & \Phi_{(k+1)1}\Phi_{k2} \\ \Phi_{k1} & \Phi_{k2} \end{bmatrix}$ is also a row-stochastic matrix because the product of row-stochastic matrices is also a row-stochastic matrix. In addition, the diagonal entries of $H_{k+1}H_k$ are positive because both Φ_{k1} and Φ_{k2} are nonnegative matrices with positive diagonal entries. Similarly, for any positive integer m and nonnegative integer ℓ_0, the matrix product $\prod_{i=0}^{m} H_{\ell_0+i}$ is also a row-stochastic matrix with positive diagonal entries. From Lemma 1.8, we have that

$$H_{k+1}H_k \geq \begin{bmatrix} \gamma_1(\Phi_{(k+1)1} + \Phi_{k1}) + \Phi_{(k+1)2} & \gamma_2(\Phi_{(k+1)1} + \Phi_{k2}) \\ \Phi_{k1} & \Phi_{k2} \end{bmatrix}$$

$$\geq \gamma \begin{bmatrix} \Phi_{(k+1)1} + \Phi_{k1} + \Phi_{(k+1)2} & \Phi_{(k+1)1} + \Phi_{k2} \\ \Phi_{k1} & \Phi_{k2} \end{bmatrix}$$

for some positive γ that is determined by $\gamma_1, \gamma_2, \Phi_{k1}, \Phi_{k2}, \Phi_{(k+1)1}$, and $\Phi_{(k+1)2}$, where γ_1 is determined by $\Phi_{(k+1)1}$ and Φ_{k1}, and γ_2 is determined by $\Phi_{(k+1)1}$ and Φ_{k2}. Note also that the directed graph of $\Phi_{(k-1)1}$ is the same as that of Φ_{k2}. We can thus replace Φ_{k2} with $\Phi_{(k-1)1}$ without changing the directed graph of H_k and vice versa. Therefore, it follows from the definitions of Φ_{k1} and Φ_{k2} that $H_{k+1}H_k \geq \hat{\gamma}\begin{bmatrix} \Phi_{(k+1)1} + \Phi_{k1} & \Phi_{(k+1)1} + \Phi_{(k-1)1} \\ \Phi_{k1} & \Phi_{(k-1)1} \end{bmatrix}$ for some positive $\hat{\gamma}$ that is determined by $\Phi_{k1}, \Phi_{k2}, \Phi_{(k+1)1}, \Phi_{(k+1)2}$, and γ. Similarly, $\prod_{i=0}^{m} H_{\ell_0+i}$ satisfies

$$\prod_{i=0}^{m} H_{\ell_0+i} \geq \tilde{\gamma} \begin{bmatrix} \sum_{i=\ell_0}^{\ell_0+m} \Phi_{i1} & \sum_{i=\ell_0+1}^{\ell_0+m} \Phi_{i1} + \Phi_{(\ell_0-1)1} \\ \sum_{i=\ell_0}^{\ell_0+m-1} \Phi_{i1} & \sum_{i=\ell_0+1}^{\ell_0+m-1} \Phi_{i1} + \Phi_{(\ell_0-1)1} \end{bmatrix}$$

$$\geq \tilde{\gamma} \begin{bmatrix} 1 & 1 \\ 1 & 1 \end{bmatrix} \otimes \sum_{i=\ell_0+1}^{\ell_0+m-1} \Phi_{i1} \qquad (8.61)$$

for some positive $\tilde{\gamma}$.

Because there exists a positive integer κ such that for any nonnegative integer k_0, the union of $\mathscr{G}[k]$ across $k \in [k_0, k_0 + \kappa]$ has a directed spanning tree, it follows that the directed graph of $\sum_{i=k_0}^{k_0+\kappa} \Phi_{i1}$ also has a directed spanning tree. Note from (8.61) that $\prod_{i=0}^{\kappa+2} H_{k_0-1+i} \geq \tilde{\gamma} \begin{bmatrix} 1 & 1 \\ 1 & 1 \end{bmatrix} \otimes \sum_{i=k_0}^{k_0+\kappa} \Phi_{i1}$. It follows from Lemma 8.15 that $\begin{bmatrix} 1 & 1 \\ 1 & 1 \end{bmatrix} \otimes \sum_{i=k_0}^{k_0+\kappa} \Phi_{i1}$ has a directed spanning tree, which implies that the directed graph of $\prod_{i=0}^{\kappa+2} H_{k_0-1+i}$ also has a directed spanning tree. Also note that $\prod_{i=0}^{\kappa+2} H_{k_0-1+i}$ is a row-stochastic matrix with positive diagonal entries. It follows from Lemma 1.9 that $\prod_{i=0}^{\kappa+2} H_{k_0-1+i}$ is SIA. It then follows from Lemma 1.12 that $\lim_{k\to\infty} \prod_{i=2}^{k} H_i = \mathbf{1}_{2n} y^T$ for some column vector $y \in \mathbb{R}^{2n}$. Therefore, it follows from (8.60) that $\lim_{k\to\infty} B_k$ exists and all rows of $\lim_{k\to\infty} B_k$ are the same. ∎

Theorem 8.12. *Suppose that there exists a positive integer κ such that for any nonnegative integer k_0, the union of $\mathscr{G}[k]$ across $k \in [k_0, k_0 + \kappa]$ has a directed spanning tree. Let Φ_{k1} and Φ_{k2} be defined by, respectively, (8.58) and (8.59). If the positive α and T are chosen such that both Φ_{k1} and Φ_{k2} are nonnegative with positive diagonal entries, $r_i[k] - r_j[k] \to \Delta_{ij}$ and $v_i[k] \to 0$ as $k \to \infty$.*

Proof: It follows from Lemma 8.16 that $\lim_{k\to\infty} B_k$ exists and all rows of $\lim_{k\to\infty} B_k$ are the same under the condition of the theorem. Because Φ_{k1} is nonnegative with positive diagonal entries, it follows that $\alpha T < 2$ (and hence $\alpha T \neq 2$). It then follows from Lemma 8.14 that $r_i[k] - r_j[k] \to \Delta_{ij}$ and $v_i[k] \to 0$ as $k \to \infty$ under the condition of the theorem. ∎

8.3.2 Convergence Analysis of the Sampled-data Coordination Algorithm with Relative Damping

In this subsection, we analyze (8.21) under a directed switching interaction graph. Here $\mathscr{A}[k]$ is switching. In this case, using (8.21), (8.19) can be written in a vector form as

$$\begin{bmatrix} \tilde{r}[k+1] \\ v[k+1] \end{bmatrix} = \underbrace{\begin{bmatrix} I_n - \frac{T^2}{2}\mathscr{L}[k] & TI_n - \frac{T^2}{2}\mathscr{L}[k] \\ -T\mathscr{L}[k] & I_n - \alpha T\mathscr{L}[k] \end{bmatrix}}_{G_k} \begin{bmatrix} \tilde{r}[k] \\ v[k] \end{bmatrix}, \qquad (8.62)$$

where $\tilde{r}$ and v are defined as in (8.22), and $\mathscr{L}[k]$ is defined as in (8.49). Note that G_k can be written as

$$G_k = \underbrace{\begin{bmatrix} (1-T)I_n - \frac{T^2}{2}\mathscr{L}[k] & TI_n - \frac{T^2}{2}\mathscr{L}[k] \\ \sqrt{T}I_n - T\mathscr{L}[k] & (1-\sqrt{T})I_n - \alpha T\mathscr{L}[k] \end{bmatrix}}_{R_k}$$

$$+ \underbrace{\begin{bmatrix} TI_n & 0_{n\times n} \\ -\sqrt{T}I_n & \sqrt{T}I_n \end{bmatrix}}_{S}. \tag{8.63}$$

In the following, we study the property of the matrix product $\prod_{i=0}^{k} G_i$ defined as

$$\prod_{i=0}^{k} G_i \triangleq \begin{bmatrix} \widetilde{G}_{k1} & \widetilde{G}_{k2} \\ \widetilde{G}_{k3} & \widetilde{G}_{k4} \end{bmatrix}, \tag{8.64}$$

where $\widetilde{G}_{ki} \in \mathbb{R}^{n\times n}$, $i = 1, \ldots, 4$.

Lemma 8.17. *Suppose that the directed graph $\mathscr{G}[k]$, $k = 0, 1, \ldots$, has a directed spanning tree. There exist positive α and T such that the following two conditions are satisfied:*

1. $(1-T)I_n - \frac{T^2}{2}\mathscr{L}[k]$ *and* $(1-\sqrt{T})I_n - \alpha T\mathscr{L}[k]$, $k = 0, 1, \ldots$, *are nonnegative matrices with positive diagonal entries, and* $TI_n - \frac{T^2}{2}\mathscr{L}[k]$ *and* $\sqrt{T}I_n - T\mathscr{L}[k]$, $k = 0, 1, \ldots$, *are nonnegative matrices.*
2. $\|S\|_\infty < 1$, *where S is defined in* (8.63).

In addition, if the positive α and T are chosen such that Conditions 1 and 2 are satisfied, the matrix product $\prod_{i=0}^{k} G_i$ has the property that all rows of each $\widetilde{G}_{ki}$, $i = 1, \ldots, 4$, become the same as $k \to \infty$.

Proof: For the first statement, it can be noted that when T is sufficiently small, Condition 1 is satisfied. Similarly, when $0 < T < \frac{1}{4}$, it follows that $\|S\|_\infty < 1$. Therefore, there exist positive α and T such that Conditions 1 and 2 are satisfied.

For the second statement, it is assumed that α and T are chosen such that Conditions 1 and 2 are satisfied. It can be computed that R_k, $k = 0, 1, \ldots$, are row-stochastic matrices with positive diagonal entries when Condition 1 is satisfied. Note that

$$\prod_{i=0}^{k} G_i = \prod_{i=0}^{k} (R_i + S). \tag{8.65}$$

It follows from the binomial expansion that $\prod_{i=0}^{k} G_i = \sum_{j=1}^{2^{k+1}} \widehat{G}_j$, where $\widehat{G}_j$ is the product of $k + 1$ matrices by choosing either R_i or S in $(R_i + S)$ for $i = 0, \ldots, k$. As $k \to \infty$, $\widehat{G}_j$ takes the following three forms:

Case I. $\widehat{G}_j$ *is constructed from an infinite number of S and a finite number of R_i.*
In this case, it follows that as $k \to \infty$, $\|\widehat{G}_j\|_\infty \leq (\prod_{i=0}^{m} \|R_{\ell_i}\|_\infty)\|S\|_\infty^\infty = \|S\|_\infty^\infty = 0$, where we have used the fact that $\|R_{\ell_i}\|_\infty = 1$ because R_{ℓ_i} is a

row-stochastic matrix and $\|S\|_\infty < 1$ as shown in Condition 2. Therefore, $\widehat{G}_j$ approaches $0_{2n \times 2n}$ as $k \to \infty$.

Case II. $\widehat{G}_j$ *is constructed from an infinite number of S and an infinite number of R_i.* A similar analysis to that in Case I shows that $\widehat{G}_j$ approaches $0_{2n \times 2n}$ as $k \to \infty$.

Case III. $\widehat{G}_j$ *is constructed from a finite number of S and an infinite number of R_i.* In this case, as $k \to \infty$, $\widehat{G}_j$ can be written as

$$\widehat{G}_j = M \underbrace{\prod_j R_{\ell_j}}_{J} N,$$

where J is the product of an infinite number of R_{ℓ_j}, $j = 0, 1, \ldots$, and both M and N are products of a finite number of matrices by choosing either R_i, $i \neq \ell_j$, or S from $(R_i + S)$.[7] It follows from Lemma 8.15 that $\begin{bmatrix} 1 & 1 \\ 1 & 1 \end{bmatrix} \otimes \{(1 - T)I_n - \frac{T^2}{2}\mathscr{L}[k]\}$ has a directed spanning tree if the directed graph of $(1 - T)I_n - \frac{T^2}{2}\mathscr{L}[k]$ has a directed spanning tree. Note that the directed graph of R_k is the same as that of $\begin{bmatrix} 1 & 1 \\ 1 & 1 \end{bmatrix} \otimes (1 - T)I_n - \frac{T^2}{2}\mathscr{L}[k]$ because the directed graphs of all four matrices in Condition 1 of Lemma 8.17 are the same. Because $\mathscr{G}[k]$ has a directed spanning tree, so does $(1 - T)I_n - \frac{T^2}{2}\mathscr{L}[k]$, which further implies that the directed graph of R_k also has a directed spanning tree. Also note that R_k, $k = 0, 1, \ldots$, are row-stochastic matrices with positive diagonal entries. It then follows from Lemma 1.9 that R_{ℓ_j} is SIA. Therefore, it follows from Lemma 1.12 that all rows of J become the same as $k \to \infty$. By writing

$$J = \begin{bmatrix} J_1 & J_2 \\ J_3 & J_4 \end{bmatrix}, \tag{8.66}$$

where $J_i \in \mathbb{R}^{n \times n}$, $i = 1, \ldots, 4$, it follows from the fact that all rows of J become the same as $k \to \infty$ that all rows of J_i, $i = 1, \ldots, 4$, also become the same as $k \to \infty$. It then follows that $R_i J = \begin{bmatrix} (1-T)I_n - \frac{T^2}{2}\mathscr{L}[i] & TI_n - \frac{T^2}{2}\mathscr{L}[i] \\ \sqrt{T}I_n - T\mathscr{L}[i] & (1-\sqrt{T})I_n - \alpha T\mathscr{L}[i] \end{bmatrix} J$ approaches $\begin{bmatrix} (1-T)I_n & TI_n \\ \sqrt{T}I_n & (1-\sqrt{T})I_n \end{bmatrix} J$ as $k \to \infty$, where we have used the fact that $\mathscr{L}[i]J_\ell$ approaches $0_{n \times n}$, $\ell = 1, \ldots, 4$, as $k \to \infty$. By separating $R_i J$ into four $n \times n$ submatrices as that of J in (8.66), all rows of each of the four $n \times n$ submatrices become the same as $k \to \infty$. The same property also applies to the matrix products JR_i, SJ, and JS. A similar analysis shows that the same property also holds for the matrix product formed by pre-multiplying or post-multiplying J by a finite number of R_i and/or S. Therefore, by separating $\widehat{G}_j$ into four $n \times n$ submatrices as those of J in (8.66), it follows that all rows of each of the four $n \times n$ submatrices become the same as $k \to \infty$. Combining the previous arguments shows that as $k \to \infty$, all rows of $\widetilde{G}_{ki}, i = 1, \ldots, 4$, become the same. ∎

---

[7] Here M and N are I_{2n} if neither R_i nor S is chosen.

Theorem 8.13. *Suppose that the directed graph $\mathscr{G}[k]$, $k = 0, 1, \ldots$, has a directed spanning tree. Using (8.21) for (8.19), $r_i[k] - r_j[k] \to \Delta_{ij}[k]$ and $v_i[k] - v_j[k] \to 0$ as $k \to \infty$ when the positive α and T are chosen such that Conditions 1 and 2 in Lemma 8.17 are satisfied.*

Proof: Note that the solution of (8.62) can be written as

$$\begin{bmatrix} \tilde{r}[k+1] \\ v[k+1] \end{bmatrix} = \prod_{i=0}^{k} G_i \begin{bmatrix} \tilde{r}[0] \\ v[0] \end{bmatrix}. \tag{8.67}$$

When the directed graph $\mathscr{G}[k]$, $k = 0, 1, \ldots$, has a directed spanning tree, and Conditions 1 and 2 in Lemma 8.17 are satisfied, it follows that all rows of $\widetilde{G}_{ki}$, $i = 1, \ldots, 4$, become the same as $k \to \infty$. It thus follows from (8.64) and (8.67) that $\tilde{r}_i[k] - \tilde{r}_j[k] \to 0$ and $v_i[k] - v_j[k] \to 0$ as $k \to \infty$, which implies that $r_i[k] - r_j[k] \to \Delta_{ij}$ and $v_i[k] - v_j[k] \to 0$ as $k \to \infty$. ■

Remark 8.14 Note that Theorem 8.12 requires that the interaction graph have a directed spanning tree jointly to guarantee coordination while Theorem 8.13 requires that the interaction graph have a directed spanning tree at each time interval to guarantee coordination. The different connectivity requirement for Theorems 8.12 and 8.13 is caused by different damping terms. For the coordination algorithm with an absolute damping term, when the sampling period and the damping gain are chosen properly, all agents always have a zero final velocity irrespective of the interaction graph. However, for the coordination algorithm with a relative damping term, the agents in general do not have a zero final velocity. From this point of view, it is not surprising to see that the connectivity requirement in Theorem 8.13 corresponding to the relative damping case is more stringent than that in Theorem 8.12 corresponding to the absolute damping case.

Remark 8.15 In Theorem 8.12 (respectively, Theorem 8.13), it is assumed that the sampling period is uniform. When the sampling periods are non-uniform, we can always find corresponding damping gains such that the conditions in Theorem 8.12 (respectively, Theorem 8.13) are satisfied. Therefore, similar results can be obtained in the presence of non-uniform sampling periods if the conditions in Theorem 8.12 (respectively, Theorem 8.13) are satisfied.

8.3.3 Simulation

In this subsection, we present simulation results to illustrate the theoretical results derived in Sects. 8.3.1 and 8.3.2. For both coordination algorithms (8.20) and (8.21), we consider a team of four agents. Here for simplicity, we have chosen $\delta_i = 0$, $i = 1, \ldots, 4$, which implies that $\Delta_{ij} = 0$.

For (8.20), let $r_i[0] = 0.5i$, $i = 1, \ldots, 4$, $v_1[0] = -1$, $v_2[0] = 0$, $v_3[0] = 1$, and $v_4[0] = 0$. The directed graph $\mathscr{G}[k]$ switches from a set $\{\mathscr{G}_{(1)}, \mathscr{G}_{(2)}, \mathscr{G}_{(3)}\}$ as shown

(a) $\mathscr{G}_{(1)}$ (b) $\mathscr{G}_{(2)}$ (c) $\mathscr{G}_{(3)}$ (d) $\mathscr{G}_{(1)}\bigcup\mathscr{G}_{(2)}\bigcup\mathscr{G}_{(3)}$
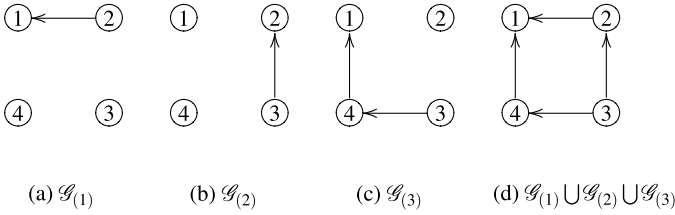
Fig. 8.9 Directed graphs $\mathscr{G}_{(1)}$, $\mathscr{G}_{(2)}$, and $\mathscr{G}_{(3)}$ and their union. An *arrow* from j to i denotes that agent j is a neighbor of agent i

(a) Positions   (b) Velocities
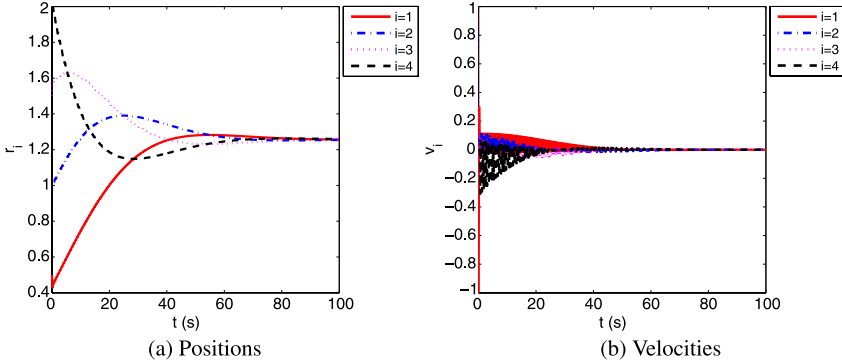
Fig. 8.10 Convergence result using (8.20) when $\mathscr{G}[k]$ switches from a set $\{\mathscr{G}_{(1)},\mathscr{G}_{(2)},\mathscr{G}_{(3)}\}$, $T = 0.2$ s, and $\alpha = 6$

in Fig. 8.9(a)–(c). While $\mathscr{G}_{(i)}$, $i = 1, 2, 3$, does not have a directed spanning tree, their union as shown in Fig. 8.9(d) has a directed spanning tree. We let $a_{ij}[k] = 1$ if $(j, i) \in \mathscr{E}[k]$ and $a_{ij}[k] = 0$ otherwise. We choose $T = 0.2$ s and $\alpha = 6$. It can be computed that the condition in Theorem 8.12 is satisfied. Figures 8.10(a) and 8.10(b) show, respectively, the positions and velocities of the four agents using (8.20) when $\mathscr{G}[k]$ switches from $\mathscr{G}_{(1)}$ to $\mathscr{G}_{(2)}$ and then to $\mathscr{G}_{(3)}$ every sampling period and the same process then repeats. It can be seen that coordination is achieved on positions with a zero final velocity as stated in Theorem 8.12. Note that the velocities of the four agents demonstrate large oscillations as shown in Fig. 8.10(b) because $\mathscr{G}[k]$ does not have a directed spanning tree at each time sampling period and switches very fast.

For (8.21), $r_i[0]$ and $v_i[0]$ are chosen the same as for (8.20). The directed graph $\mathscr{G}[k]$ switches from a set $\{\mathscr{G}_{(4)},\mathscr{G}_{(5)},\mathscr{G}_{(6)}\}$ as shown in Fig. 8.11. Note that each directed graph $\mathscr{G}_{(i)}$, $i = 4, 5, 6$, has a directed spanning tree. Here again we let $a_{ij}[k] = 1$ if $(j, i) \in \mathscr{E}[k]$ and $a_{ij}[k] = 0$ otherwise. We choose $T = 0.1$ s and $\alpha = 1$. It can be computed that the condition in Theorem 8.13 is satisfied. Figures 8.12(a) and 8.12(b) show, respectively, the positions and velocities of the four agents using (8.21) when $\mathscr{G}[k]$ switches from $\mathscr{G}_{(4)}$ to $\mathscr{G}_{(5)}$ and then to $\mathscr{G}_{(6)}$ every sampling period and the same process then repeats. It can be seen that coordination is achieved on positions with a constant final velocity as stated in Theorem 8.13.

(a) $\mathscr{G}_{(4)}$ (b) $\mathscr{G}_{(5)}$ (c) $\mathscr{G}_{(6)}$
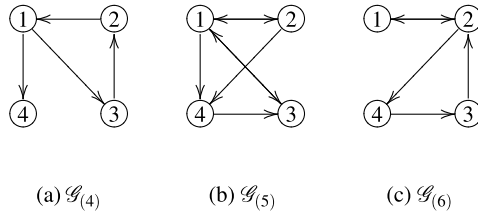
Fig. 8.11 Directed graphs $\mathscr{G}_{(4)}$, $\mathscr{G}_{(5)}$, and $\mathscr{G}_{(6)}$. An *arrow* from j to i denotes that agent j is a neighbor of agent i

(a) Positions   (b) Velocities
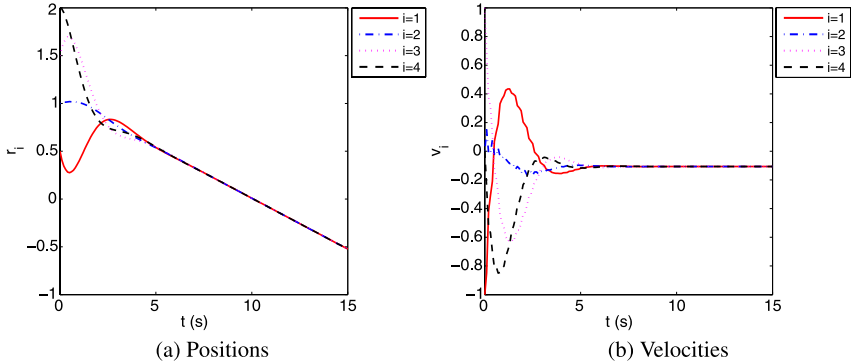
Fig. 8.12 Convergence result using (8.21) when $\mathscr{G}[k]$ switches from a set $\{\mathscr{G}_{(4)}, \mathscr{G}_{(5)}, \mathscr{G}_{(6)}\}$, $T = 0.1$ s, and $\alpha = 1$

(a) Positions   (b) Velocities
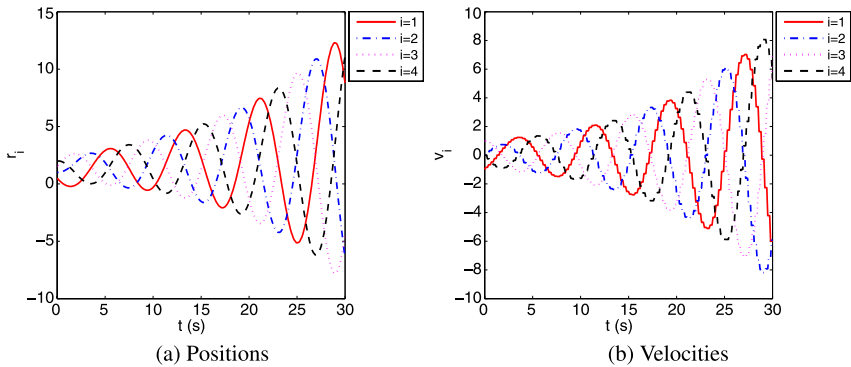
Fig. 8.13 Convergence result using (8.21) when $\mathscr{G}[k]$ switches from a set $\{\mathscr{G}_{(1)}, \mathscr{G}_{(2)}, \mathscr{G}_{(3)}\}$, $T = 0.1$ s, and $\alpha = 1$

We also show an example to illustrate that using (8.21) for (8.19), coordination is not necessarily achieved even if the interaction graph has a directed spanning tree jointly, and α and T satisfy Conditions 1 and 2 in Lemma 8.17. The initial positions and velocities, α, and T are chosen to be the same as those for Figs. 8.12(a) and 8.12(b). Figures 8.13(a) and 8.13(b) show, respectively, the positions and veloc-

ities of the four agents using (8.21) when $\mathscr{G}[k]$ switches from $\mathscr{G}_{(1)}$ to $\mathscr{G}_{(2)}$ then to $\mathscr{G}_{(3)}$ every sampling period and the same process then repeats. It can be seen that coordination is not achieved even when the interaction graph has a directed spanning tree jointly and α and T satisfy Conditions 1 and 2 in Lemma 8.17.

8.4 Notes

The results in this chapter are based mainly on [32, 33, 36, 44, 45, 249]. For further results on distributed multi-agent coordination in a sampled-data setting, see [99, 101, 116, 196, 328]. In particular, [116] shows conditions on sampled-data coordination under an undirected interaction graph through average-energy-like Lyapunov functions. Considering the fact that communication among agents might be unstable, the authors in [196] further study the case of stochastic undirected interaction. However, the stability condition derived in [196] is stringent and difficult to determine. In [99, 101], sampled-data coordination is studied for agents with double-integrator dynamics in both synchronous and asynchronous cases. In particular, the conditions are derived by using linear matrix inequalities. In [328], the mean-square consentability problem is studied for agents with double-integrator dynamics in a sampled-data setting with a stochastically switching interaction graph.

Chapter 9
Optimality Aspect

This chapter considers the optimality aspect in distributed multi-agent coordination. We study optimal linear coordination algorithms for multi-agent systems with single-integrator dynamics in both continuous-time and discrete-time settings from a linear quadratic regulator perspective. We propose two global cost functions, namely, interaction-free and interaction-related cost functions. With the interaction-free cost function, we derive the optimal state feedback gain matrix in both continuous-time and discrete-time settings. It is shown that the optimal gain matrix is a nonsymmetric Laplacian matrix corresponding to a complete directed graph. In addition, we show that any symmetric Laplacian matrix is inverse optimal with respect to a properly chosen cost function. With the interaction-related cost function, we derive the optimal scaling factor for a prespecified symmetric Laplacian matrix associated with an undirected interaction graph in both continuous-time and discrete-time settings. Illustrative examples are given as a proof of concept.

9.1 Problem Statement

Among various studies of distributed linear coordination algorithms, it is natural to ask these questions: Is there an optimal linear coordination algorithm under a given cost function? How to find the optimal linear coordination algorithm? The purpose of this chapter is to study the optimal linear coordination algorithms for agents with single-integrator dynamics from a linear quadratic regulator (LQR) perspective. Instead of studying locally optimal algorithms, we focus on globally optimal algorithms.

The contributions of this chapter are threefold. First, we mathematically prove the conditions under which the square root of a nonsymmetric Laplacian matrix is still a nonsymmetric Laplacian matrix. Second, we explicitly derive the optimal state feedback gain matrix under a given global cost function from an LQR perspective and show that the optimal state feedback gain matrix is a nonsymmetric Laplacian matrix corresponding to a complete directed graph. Third, we derive the

optimal scaling factor for a prespecified symmetric Laplacian matrix associated with an undirected interaction graph. Although it might be intuitively true that a global optimization problem in the context of multi-agent coordination normally requires that each agent have full knowledge of all other agents, it is nontrivial to verify this fact from a theoretical perspective. In particular, for the linear coordination algorithms, it is not clear why the optimal state feedback gain matrix derived from the standard LQR solution is a nonsymmetric Laplacian matrix and why the nonsymmetric Laplacian matrix corresponds to a complete directed graph. In other words, our focus here is not to repeat the standard LQR procedure but to provide a theoretical explanation. We first propose two global cost functions, namely, interaction-free and interaction-related cost functions, in both continuous-time and discrete-time settings. With the interaction-free cost function, we derive the optimal state feedback gain matrix in both continuous-time and discrete-time settings. It is shown that the optimal state feedback gain matrix is a nonsymmetric Laplacian matrix corresponding to a complete directed graph. In addition, we show that any symmetric Laplacian matrix is inverse optimal with respect to a properly chosen cost function. With the interaction-related cost function, we derive the optimal scaling factor for a prespecified symmetric Laplacian matrix associated with an undirected interaction graph in both continuous-time and discrete-time settings.

In the continuous-time setting, consider n agents with single-integrator dynamics given by (3.1). In the discrete-time setting, consider n agents with discretized dynamics of (3.1) given by (8.3). Define $\Delta_{ij} = \delta_i - \delta_j$, where $\delta_i \in \mathbb{R}^m$ is constant. Here Δ_{ij} denotes the desired relative position deviation between agents i and j. In the continuous-time setting, coordination is achieved for the n agents if for all $r_i(0)$ and $i, j = 1, \ldots, n$, $r_i(t) - r_j(t) \to \Delta_{ij}$ as $t \to \infty$. In the discrete-time setting, coordination is achieved for the n agents if for all $r_i[0]$ and $i, j = 1, \ldots, n$, $r_i[k] - r_j[k] \to \Delta_{ij}$ as $k \to \infty$. In the remainder of the chapter, we assume that the agents are in a one-dimensional space for simplicity. However, all results hereafter are still valid for any high-dimensional space by use of the properties of the Kronecker product.

In the continuous-time setting, similar to the cost function used in optimal control problems for systems with linear differential equations, we propose the following two coordination cost functions for (3.1) as

$$J_{fc} = \int_0^\infty \left\{ \sum_{i=1}^n \sum_{j=1}^{i-1} c_{ij} \left[r_i(t) - r_j(t) - \Delta_{ij} \right]^2 + \sum_{i=1}^n \vartheta_i \left[u_i(t) \right]^2 \right\} dt, \quad (9.1)$$

where $c_{ij} \geq 0$ and $\vartheta_i > 0$, and

$$J_{rc} = \int_0^\infty \left\{ \sum_{i=1}^n \sum_{j=1}^{i-1} a_{ij} \left[r_i(t) - r_j(t) - \Delta_{ij} \right]^2 + \sum_{i=1}^n \left[u_i(t) \right]^2 \right\} dt, \quad (9.2)$$

where a_{ij} is the (i, j)th entry of the adjacency matrix $\mathscr{A}$ associated with the graph $\mathscr{G} \triangleq (\mathscr{V}, \mathscr{E})$ characterizing the interaction among the n agents. In (9.1), both

$c_{ij} \geq 0$ and $\vartheta_i > 0$ can be chosen freely. Therefore, J_{fc} is called the *interaction-free cost function*. In contrast, (9.2) depends on the adjacency matrix $\mathscr{A}$ and hence the graph $\mathscr{G}$. Therefore, J_{rc} is called the *interaction-related cost function*. The motivation behind (9.1) and (9.2) is to weigh both the coordination errors $r_i(t) - r_j(t) - \Delta_{ij}$ and the control effort u_i. The corresponding optimization problems can be written as

$$\min_{u_i(t)} J_{fc}, \text{ subject to } (3.1) \tag{9.3}$$

$$\min_{\beta} J_{rc}, \text{ subject to } (3.1) \text{ and } u_i(t) = -\sum_{j=1}^{n} \beta a_{ij} \big[r_i(t) - r_j(t) - \Delta_{ij} \big]. \tag{9.4}$$

In the discrete-time setting, we propose the following interaction-free and interaction-related cost functions for (8.3) as

$$J_{fd} = \sum_{k=0}^{\infty} \sum_{i=1}^{n} \sum_{j=1}^{i-1} c_{ij} \big\{ r_i[k] - r_j[k] - \Delta_{ij} \big\}^2 + \sum_{k=0}^{\infty} \sum_{i=1}^{n} \vartheta_i \big(u_i[k] \big)^2, \tag{9.5}$$

where $c_{ij} \geq 0$ and $\vartheta_i > 0$, and

$$J_{rd} = \sum_{k=0}^{\infty} \sum_{i=1}^{n} \sum_{j=1}^{i-1} a_{ij} \big\{ r_i[k] - r_j[k] - \Delta_{ij} \big\}^2 + \sum_{k=0}^{\infty} \sum_{i=1}^{n} \big(u_i[k] \big)^2, \tag{9.6}$$

where a_{ij} is defined as in (9.4). The corresponding optimization problems can be written as

$$\min_{u_i[k]} J_{fd} \text{ subject to } (8.3) \tag{9.7}$$

$$\min_{\beta} J_{rd} \text{ subject to } (8.3) \text{ and } u_i[k] = -\sum_{j=1}^{n} \beta a_{ij} \big(r_i[k] - r_j[k] - \Delta_{ij} \big). \tag{9.8}$$

9.2 Optimal Linear Coordination Algorithms in a Continuous-time Setting from a Linear Quadratic Regulator Perspective

In this section, we derive the optimal linear coordination algorithms in a continuous-time setting from an LQR perspective. We first derive the optimal state feedback gain matrix using the continuous-time interaction-free cost function (9.1). The optimal gain matrix is later shown to be a nonsymmetric Laplacian matrix corresponding to a complete directed graph. We then find the optimal scaling factor for a prespecified symmetric Laplacian matrix associated with an undirected interaction

graph using the continuous-time interaction-related cost function (9.2). Finally, illustrative examples are provided.

9.2.1 Optimal State Feedback Gain Matrix Using the Interaction-free Cost Function

Note that (9.3) can be written as

$$\min_{u(t)} \underbrace{\int_0^\infty \left[\tilde{r}^T(t)Q\tilde{r}(t) + u^T(t)\Theta u(t) \right] dt}_{J_{fc}} \tag{9.9}$$

$$\text{subject to:} \quad \dot{r}(t) = u(t), \tag{9.10}$$

where $\tilde{r}(t) \triangleq [\tilde{r}_1(t), \ldots, \tilde{r}_n(t)]^T$ with $\tilde{r}_i(t) \triangleq r_i(t) - \delta_i$, $r(t) \triangleq [r_1(t), \ldots, r_n(t)]^T$, $u(t) \triangleq [u_1(t), \ldots, u_n(t)]^T$, $Q \in \mathbb{R}^{n \times n}$ is symmetric with the (i,j)th entry and hence the (j,i)th entry given by $-c_{ij}$ for $i > j$ and the (i,i)th entry given by $\sum_{j=1}^{i-1} c_{ij} + \sum_{j=i+1}^{n} c_{ji}$, and $\Theta \in \mathbb{R}^{n \times n}$ is the positive-definite diagonal matrix with ϑ_i being the ith diagonal entry. It can be noted that Q is a symmetric Laplacian matrix. Therefore, Q is symmetric positive semidefinite. Before moving on, we need the following notations and lemmas.

According to Lemma 1.14, if the characteristic polynomial of an M-matrix $B \in \mathbb{R}^{n \times n}$ has at most a simple zero root, then B has exactly one M-matrix as its square root. In this case, we use $\sqrt{B}$ hereafter to represent the unique M-matrix that is the square root of B.

Lemma 9.1. *Let Q and Θ be defined in* (9.9). *Suppose that Q has a simple zero eigenvalue. Then $\Theta^{-1}Q$ is a nonsymmetric Laplacian matrix* (*and hence an M-matrix*) *with a simple zero eigenvalue and $\sqrt{\Theta^{-1}Q}$ is a nonsymmetric Laplacian matrix with a simple zero eigenvalue.*

Proof: We first note that $\Theta^{-1}Q$ is a nonsymmetric Laplacian matrix because Q is a symmetric Laplacian matrix, Θ is a positive-definite diagonal matrix, and $\Theta^{-1}Q\mathbf{1}_n = \Theta^{-1}\mathbf{0}_n = \mathbf{0}_n$. It thus follows from Lemma 1.15 that $\Theta^{-1}Q$ is also an M-matrix. Because Q is a symmetric Laplacian matrix with a simple zero eigenvalue, it follows from Lemma 1.1 that the undirected graph associated with Q is connected, which implies that the directed graph associated with $\Theta^{-1}Q$ is strongly connected. It thus follows from Lemma 1.1 that the nonsymmetric Laplacian matrix $\Theta^{-1}Q$ also has a simple zero eigenvalue. Therefore, $\sqrt{\Theta^{-1}Q}$ is the unique M-matrix that is the square root of $\Theta^{-1}Q$. We next show that $\sqrt{\Theta^{-1}Q}$ has a simple zero eigenvalue with an associated eigenvector $\mathbf{1}_n$. Let the ith eigenvalue of $\sqrt{\Theta^{-1}Q}$ be λ_i with an associated eigenvector ν_i. It follows that the ith eigenvalue of $\Theta^{-1}Q$ is λ_i^2 with an associated eigenvector ν_i. Because $\Theta^{-1}Q$ has a simple zero

eigenvalue with an associated eigenvector $\mathbf{1}_n$, it follows that $\sqrt{\Theta^{-1}Q}$ has a simple zero eigenvalue with an associated eigenvector $\mathbf{1}_n$. Therefore, it follows from Lemma 1.15 that $\sqrt{\Theta^{-1}Q}$ is a nonsymmetric Laplacian matrix. Combining the above arguments completes the proof. ∎

We next show that the nonsymmetric Laplacian matrix $\sqrt{\Theta^{-1}Q}$ corresponds to a complete directed graph.

Lemma 9.2. *Let Q and Θ be defined in (9.9). Suppose that Q has a simple zero eigenvalue. Then the nonsymmetric Laplacian matrix $\sqrt{\Theta^{-1}Q}$ corresponds to a complete directed graph.*

Proof: Note from Lemma 9.1 that $\sqrt{\Theta^{-1}Q}$ is a nonsymmetric Laplacian matrix with a simple zero eigenvalue. We show that each entry of $\sqrt{\Theta^{-1}Q}$ is nonzero, which implies that $\sqrt{\Theta^{-1}Q}$ corresponds to a complete directed graph. Before moving on, we let q_{ij} denote the (i,j)th entry of Q. We also define $W \triangleq \sqrt{\Theta^{-1}Q}$ and denote w_{ij}, $w_{i,:}$, and $w_{:,i}$ as, respectively, the (i,j)th entry, the ith row, and the ith column of W.

First, we will show that $w_{ij} \neq 0$ if $q_{ij} \neq 0$. We show this statement by contradiction. Assume that $w_{ij} = 0$. Because $\Theta^{-1}Q = W^2$, it follows that $\frac{q_{ij}}{\vartheta_i} = w_{i,:}w_{:,j}$. When $i = j$, it follows from $w_{ii} = 0$ that $w_{i,:} = \mathbf{0}_n^T$ because W is a nonsymmetric Laplacian matrix, which then implies that $\frac{q_{ij}}{\vartheta_i} = w_{i,:}w_{:,j} = 0$. This contradicts the assumption that $q_{ij} \neq 0$. Because W is a nonsymmetric Laplacian matrix, it follows that $w_{ik} \leq 0$, $\forall i \neq k$. When $i \neq j$, because it is assumed that $w_{ij} = 0$, it follows that $\frac{q_{ij}}{\vartheta_i} = w_{i,:}w_{:,j} = \sum_{k=1,k\neq i,k\neq j}^{n} w_{ik}w_{kj} \geq 0$. Because Q is a symmetric Laplacian matrix, it follows that $q_{ij} \leq 0, \forall i \neq j$. Therefore, $\frac{q_{ij}}{\vartheta_i} \geq 0, \forall i \neq j$, implies that $q_{ij} = 0$, which also contradicts the assumption that $q_{ij} \neq 0$.

Second, we will show that $w_{ij} \neq 0$ even if $q_{ij} = 0$. We also show this statement by contradiction. Assume that $w_{ij} = 0$. To ensure that $q_{ij} = 0$, it follows from $\frac{q_{ij}}{\vartheta_i} = w_{i,:}w_{:,j} = \sum_{k=1,k\neq i,k\neq j}^{n} w_{ik}w_{kj}$ that $w_{ik}w_{kj} = 0, \forall k \neq i, \forall k \neq j, k = 1,\ldots,n$. Denote $\hat{k}_1$ as the node set such that $w_{im} \neq 0$ for each $m \in \hat{k}_1$. Then we have $w_{mj} = 0$ for each $m \in \hat{k}_1$ because $w_{ik}w_{kj} = 0$. Similarly, denote $\bar{k}_1$ as the node set such that $w_{mj} \neq 0$ for each $m \in \bar{k}_1$. Then we have $w_{im} = 0$ for each $m \in \bar{k}_1$ because $w_{ik}w_{kj} = 0$. From the discussion in the previous paragraph, when $w_{mj} = 0$, we have $q_{mj} = 0$, which implies that $w_{mp}w_{pj} = 0, \forall p \neq m, \forall p \neq j, p = 1,\ldots,n$. By following a similar analysis, we can consequently define $\hat{k}_i$ and $\bar{k}_i, i = 2,\ldots,\kappa$, where $\hat{k}_i \cap \hat{k}_j = \varnothing, \bar{k}_i \cap \bar{k}_j = \varnothing, \forall j < i$. Because both Q and W have a simple zero eigenvalue, it follows from Lemma 1.1 that the undirected graph associated with Q is connected and the directed graph associated with W has a directed spanning tree. It thus follows that $\kappa \leq n$. Therefore, each entry of $w_{:,j}$ is equal to zero by following the previous analysis for at most n times. This implies that $q_{ij} = 0, \forall i \neq j$, because $\frac{q_{ij}}{\vartheta_i} = w_{i,:}w_{:,j}$. Considering the fact that Q is a symmetric Laplacian matrix, it follows that $q_{ii} = 0$, which also contradicts the fact that the undirected graph associated with Q is connected. ∎

The main result for the optimal control problem (9.9) is given in the following theorem.

Theorem 9.1. *In the optimal control problem* (9.9), *suppose that Q has a simple zero eigenvalue. The optimal coordination algorithm is*

$$u(t) = -\sqrt{\Theta^{-1}Q}\tilde{r}(t). \tag{9.11}$$

The matrix $\sqrt{\Theta^{-1}Q}$ is a nonsymmetric Laplacian matrix with a simple zero eigenvalue corresponding to a complete directed graph. Using (9.11) *for* (9.10), *coordination is achieved.*

Proof: Note that $\dot{r} = u(t)$ is equivalent to $\dot{\tilde{r}} = u(t)$. Consider the following standard LQR problem

$$\min_{u(t)} J_{fc} \quad \text{subject to:} \quad \dot{\tilde{r}}(t) = A\tilde{r}(t) + Bu(t), \tag{9.12}$$

where J_{fc} is given in (9.9), $A = 0_{n\times n}$, and $B = I_n$. It can be noted that (A, B) is controllable, which implies that there exists a unique positive-semidefinite matrix $P \in \mathbb{R}^{n\times n}$ satisfying the continuous-time algebraic Riccati equation

$$A^T P + PA - PB\Theta^{-1}B^T P + Q = 0_{n\times n}. \tag{9.13}$$

It follows from (9.13) that $P\Theta^{-1}P = Q$ by noting that $A = 0_{n\times n}$ and $B = I_n$, which implies that $\Theta^{-1}P\Theta^{-1}P = \Theta^{-1}Q$. It then follows from Lemma 9.1 that $\Theta^{-1}P = \sqrt{\Theta^{-1}Q}$ is also a nonsymmetric Laplacian matrix with a simple zero eigenvalue when Q has a simple zero eigenvalue. Therefore, the optimal control is $u(t) = -\Theta^{-1}B^T P\tilde{r}(t) = -\sqrt{\Theta^{-1}Q}\tilde{r}(t)$. It also follows from Lemma 9.2 that $\sqrt{\Theta^{-1}Q}$ corresponds to a complete directed graph. Note that using (9.11) for (9.10), the closed-loop system becomes $\dot{\tilde{r}}(t) = \dot{r}(t) = -\sqrt{\Theta^{-1}Q}\tilde{r}(t)$. Because $\sqrt{\Theta^{-1}Q}$ is a nonsymmetric Laplacian matrix with a simple zero eigenvalue, it follows from Lemma 1.3 that $\tilde{r}_i(t) - \tilde{r}_j(t) \to 0$ as $t \to \infty$, which implies that $r_i(t) - r_j(t) \to \Delta_{ij}$ as $t \to \infty$.   ∎

Remark 9.2 Note that Q is a symmetric Laplacian matrix. It follows from Lemma 1.1 that the assumption that Q has a simple zero eigenvalue is equivalent to the assumption that the undirected graph corresponding to Q is connected.

Remark 9.3 In fact, the assumption that the symmetric Laplacian matrix Q has a simple zero eigenvalue is also necessary to ensure coordination. If otherwise, the undirected graph corresponding to Q is not connected. It thus follows that $\sum_{i=1}^{n}\sum_{j=1}^{i-1} c_{ij}[r_i(t) - r_j(t) - \Delta_{ij}]^2$ in (9.1) can be written as a sum of at least two independent terms, where each term involves an independent subset of the agents. As a result, the optimal control problem (9.3) and hence (9.9) can be decoupled into at least two independent optimal control problems. By solving the independent optimal control problems, coordination is only guaranteed for each independent subset of the agents but not for all agents.

Remark 9.4 From Theorem 9.1, it can be noted that the graph corresponding to $\sqrt{\Theta^{-1}Q}$ is in general different from that corresponding to Q. Note that $\sqrt{\Theta^{-1}Q}$

is not necessarily symmetric in general. When Θ is a diagonal matrix with identical diagonal entries (i.e., $\Theta = cI_n$, where $c > 0$), $\sqrt{\Theta^{-1}Q}$ is symmetric.

We next show that any symmetric Laplacian matrix $\mathscr{L}$ with a simple zero eigenvalue is inverse optimal with respect to some given cost function.

Theorem 9.5. *Any symmetric Laplacian matrix $\mathscr{L} \in \mathbb{R}^{n \times n}$ with a simple zero eigenvalue is the optimal state feedback gain matrix under the cost function $J = \int_0^\infty [\tilde{r}^T(t)\mathscr{L}^2\tilde{r}(t) + u^T(t)u(t)] \, dt$.*

Proof: By letting $Q = \mathscr{L}^2$ and $\Theta = I_n$, it follows directly from the proof of Theorem 9.1 that $\mathscr{L}$ is the optimal state feedback gain matrix. ∎

9.2.2 Optimal Scaling Factor Using the Interaction-related Cost Function

Suppose that the graph $\mathscr{G}$ is undirected. With the interaction-related cost function (9.2), the optimal control problem (9.4) can be written as

$$\min_\beta \underbrace{\int_0^\infty \left[\tilde{r}^T(t)\mathscr{L}\tilde{r}(t) + u^T(t)u(t)\right] dt}_{J_{rc}} \tag{9.14}$$
$$\text{subject to:} \quad \dot{r}(t) = u(t), \ u(t) = -\beta\mathscr{L}\tilde{r}(t),$$

where $\mathscr{L}$ is the prespecified symmetric Laplacian matrix associated with the adjacency matrix $\mathscr{A}$ and hence the undirected graph $\mathscr{G}$, and β is the scaling factor.

Theorem 9.6. *In the optimal control problem (9.14), suppose that $\mathscr{L}$ has a simple zero eigenvalue. Then the optimal β, denoted by β_{opt}, is $\sqrt{\frac{\tilde{r}^T(0)\tilde{r}(0) - \frac{1}{n}[\mathbf{1}_n^T\tilde{r}(0)]^T[\mathbf{1}_n^T\tilde{r}(0)]}{\tilde{r}^T(0)\mathscr{L}\tilde{r}(0)}}$* [1].

Proof: Note that $u(t) = -\beta\mathscr{L}\tilde{r}(t)$. It follows that $\dot{\tilde{r}}(t) = \dot{r}(t) = -\beta\mathscr{L}\tilde{r}(t)$. It thus follows that $\tilde{r}(t) = e^{-\beta\mathscr{L}t}\tilde{r}(0)$ and hence $u(t) = -\beta\mathscr{L}e^{-\beta\mathscr{L}t}\tilde{r}(0)$. The cost function J_{rc} can then be written as

$$J_{rc} = \int_0^\infty \tilde{r}^T(0)\left[e^{-\beta\mathscr{L}t}\mathscr{L}e^{-\beta\mathscr{L}t} + \beta^2 e^{-\beta\mathscr{L}t}\mathscr{L}^2 e^{-\beta\mathscr{L}t}\right]\tilde{r}(0) \, dt.$$

Taking the derivative of J_{rc} with respect to β gives

$$\frac{dJ_{rc}}{d\beta} = \int_0^\infty \tilde{r}^T(0)\Big[-2\mathscr{L}te^{-\beta\mathscr{L}t}\mathscr{L}e^{-\beta\mathscr{L}t} + 2\beta e^{-\beta\mathscr{L}t}\mathscr{L}^2 e^{-\beta\mathscr{L}t}$$
$$-2\beta^2\mathscr{L}te^{-\beta\mathscr{L}t}\mathscr{L}^2 e^{-\beta\mathscr{L}t}\Big]\tilde{r}(0) \, dt.$$

---

[1] Note that coordination is obviously achieved when $\beta = \beta_{\mathrm{opt}}$.

Setting $\frac{dJ_{rc}}{d\beta} = 0$ gives

$$
\beta^2 \tilde{r}^T(0) \left[\int_0^\infty \mathscr{L} t e^{-\beta \mathscr{L} t} \mathscr{L}^2 e^{-\beta \mathscr{L} t} \, dt \right] \tilde{r}(0)
$$

$$
- \beta \tilde{r}^T(0) \left[\int_0^\infty e^{-\beta \mathscr{L} t} \mathscr{L}^2 e^{-\beta \mathscr{L} t} \, dt \right] \tilde{r}(0)
$$

$$
+ \tilde{r}^T(0) \left[\int_0^\infty \mathscr{L} t e^{-\beta \mathscr{L} t} \mathscr{L} e^{-\beta \mathscr{L} t} \, dt \right] \tilde{r}(0) = 0, \tag{9.15}
$$

where we have used the fact that $\mathscr{L}$ and $e^{-\beta \mathscr{L} t}$ commute. Because $\mathscr{L}$ is symmetric, $\mathscr{L}$ can be diagonalized as

$$
\mathscr{L} = M \underbrace{\begin{bmatrix} \lambda_1 & 0 & \cdots & 0 \\ 0 & \lambda_2 & \cdots & 0 \\ \vdots & \vdots & \ddots & \\ 0 & 0 & \cdots & \lambda_n \end{bmatrix}}_{\Lambda} M^T, \tag{9.16}
$$

where M is an orthogonal matrix, and λ_i is the ith eigenvalue of $\mathscr{L}$. Note that $\mathscr{L}$ has a simple zero eigenvalue. Without loss of generality, we let $\lambda_1 = 0$ and hence $\lambda_i > 0$, $i = 2, \ldots, n$ (see Lemma 1.1). Note that the columns of M can be chosen as the normalized right eigenvectors of $\mathscr{L}$. Also note that $\mathbf{1}_n$ is a right eigenvector of $\mathscr{L}$ associated with the zero eigenvalue. Therefore, we let the first column of M be $\frac{\mathbf{1}_n}{\sqrt{n}}$. Note that

$$
\int_0^\infty \mathscr{L} t e^{-\beta \mathscr{L} t} \mathscr{L}^2 e^{-\beta \mathscr{L} t} \, dt
$$

$$
= \int_0^\infty M \begin{bmatrix} 0 & 0 & \cdots & 0 \\ 0 & e^{-2\beta \lambda_2 t} \lambda_2^3 t & \cdots & 0 \\ \vdots & \vdots & \ddots & \\ 0 & 0 & \cdots & e^{-2\beta \lambda_n t} \lambda_n^3 t \end{bmatrix} M^T \, dt
$$

$$
= \frac{1}{4\beta^2} M \begin{bmatrix} 0 & 0 & \cdots & 0 \\ 0 & \lambda_2 & \cdots & 0 \\ \vdots & \vdots & \ddots & \\ 0 & 0 & \cdots & \lambda_n \end{bmatrix} M^T \tag{9.17}
$$

$$
= \frac{1}{4\beta^2} \mathscr{L}. \tag{9.18}
$$

Similarly, it follows that

$$\int_0^\infty e^{-\beta \mathscr{L} t} \mathscr{L}^2 e^{-\beta \mathscr{L} t} \, dt \tag{9.19}$$

$$= \int_0^\infty M \begin{bmatrix} 0 & 0 & \cdots & 0 \\ 0 & e^{-2\beta\lambda_2 t}\lambda_2^2 & \cdots & 0 \\ \vdots & \vdots & \ddots & \\ 0 & 0 & \cdots & e^{-2\beta\lambda_n t}\lambda_n^2 \end{bmatrix} M^T \, dt \tag{9.20}$$

$$= -\frac{1}{2\beta} M \begin{bmatrix} 0 & 0 & \cdots & 0 \\ 0 & \lambda_2 e^{-2\beta\lambda_2 t}|_0^\infty & \cdots & 0 \\ \vdots & \vdots & \ddots & \\ 0 & 0 & \cdots & \lambda_n e^{-2\beta\lambda_n t}|_0^\infty \end{bmatrix} M^T$$

$$= \frac{1}{2\beta} M \begin{bmatrix} 0 & 0 & \cdots & 0 \\ 0 & \lambda_2 & \cdots & 0 \\ \vdots & \vdots & \ddots & \\ 0 & 0 & \cdots & \lambda_n \end{bmatrix} M^T = \frac{1}{2\beta} \mathscr{L} \tag{9.21}$$

and

$$\int_0^\infty \mathscr{L} t e^{-\beta \mathscr{L} t} \mathscr{L} e^{-\beta \mathscr{L} t} \, dt$$

$$= \int_0^\infty M \begin{bmatrix} 0 & 0 & \cdots & 0 \\ 0 & e^{-2\beta\lambda_2 t}\lambda_2^2 t & \cdots & 0 \\ \vdots & \vdots & \ddots & \\ 0 & 0 & \cdots & e^{-2\beta\lambda_n t}\lambda_n^2 t \end{bmatrix} M^T \, dt$$

$$= -\frac{1}{2\beta} M$$

$$\times \begin{bmatrix} 0 & 0 & \cdots & 0 \\ 0 & \lambda_2 t e^{-2\beta\lambda_2 t}|_0^\infty - \int_0^\infty e^{-2\beta\lambda_2 t}\lambda_2 dt & \cdots & 0 \\ \vdots & \vdots & \ddots & \\ 0 & 0 & \cdots & \lambda_n t e^{-2\beta\lambda_n t}|_0^\infty - \int_0^\infty e^{-2\beta\lambda_n t}\lambda_n dt \end{bmatrix} M^T$$

$$= -\frac{1}{4\beta^2} M \begin{bmatrix} 0 & 0 & \cdots & 0 \\ 0 & e^{-2\beta\lambda_2 t}|_0^\infty & \cdots & 0 \\ \vdots & \vdots & \ddots & \\ 0 & 0 & \cdots & e^{-2\beta\lambda_n t}|_0^\infty \end{bmatrix} M^T$$

$$= -\frac{1}{4\beta^2} M \begin{bmatrix} 0 & 0 & \cdots & 0 \\ 0 & 1 & \cdots & 0 \\ \vdots & \vdots & \ddots & \\ 0 & 0 & \cdots & 1 \end{bmatrix} M^T = \frac{I_n - \frac{1}{n}\mathbf{1}_n\mathbf{1}_n^T}{4\beta^2}, \tag{9.22}$$

where we have used the fact that the first column of M is $\frac{1_n}{\sqrt{n}}$. By substituting (9.18), (9.21), and (9.22) into (9.15), it follows that the optimal β is β_{opt}. ■

Remark 9.7 In Theorem 9.6, we consider a simple case when all agents have the same coupling gain and find the optimal coupling gain explicitly. It is also possible to consider the case when the coupling gains for each agent are different. However, it is, in general, hard to find the optimal coupling gains explicitly. Instead, numerical solutions can be obtained accordingly.

9.2.3 Illustrative Examples

In this subsection, we provide two illustrative examples about the optimal state feedback gain matrix and the optimal scaling factor derived in, respectively, Sect. 9.2.1 and Sect. 9.2.2.

In (9.9), we simply choose

$$
Q = \begin{bmatrix} 2 & -1 & -1 & 0 \\ -1 & 2 & -1 & 0 \\ -1 & -1 & 3 & -1 \\ 0 & 0 & -1 & 1 \end{bmatrix} \quad \text{and} \quad \Theta = \begin{bmatrix} 1 & 0 & 0 & 0 \\ 0 & 2 & 0 & 0 \\ 0 & 0 & 3 & 0 \\ 0 & 0 & 0 & 4 \end{bmatrix}.
$$

It then follows from Theorem 9.1 that the optimal state feedback gain matrix is given by

$$
\sqrt{\Theta^{-1}Q} = \begin{bmatrix} 1.3134 & -0.5459 & -0.5964 & -0.1711 \\ -0.2730 & 0.8491 & -0.4206 & -0.1556 \\ -0.1988 & -0.2804 & 0.8218 & -0.3426 \\ -0.0428 & -0.0778 & -0.2570 & 0.3775 \end{bmatrix}.
$$

Note that the optimal gain matrix is a nonsymmetric Laplacian matrix corresponding to a complete directed graph. Also note that the graph associated with Q is different from that associated with $\sqrt{\Theta^{-1}Q}$.

In (9.14), we simply choose

$$
\mathscr{L} = \begin{bmatrix} 2 & -1 & -1 & 0 \\ -1 & 2 & 1 & 0 \\ -1 & -1 & 3 & -1 \\ 0 & 0 & -1 & 1 \end{bmatrix}
$$

and the initial state $\tilde{r}(0) = [1, 2, 3, 4]^T$. Figure 9.1 shows how the cost function J_{rc} evolves as the scaling factor β increases. From Theorem 9.6, it can be computed that the optimal scaling factor is $\beta_{\mathrm{opt}} = 0.845$, which is consistent with the result shown in Fig. 9.1.
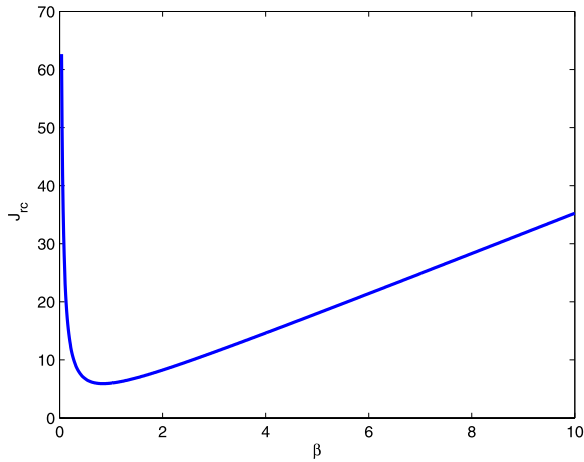
Fig. 9.1 Evolution of the cost function J_{rc} as a function of β

9.3 Optimal Linear Coordination Algorithms in a Discrete-time Setting from a Linear Quadratic Regulator Perspective

In this section, we study the optimal linear coordination algorithms in a discrete-time setting from an LQR perspective. As shown later, the analysis in the discrete-time case is more challenging than that in the continuous-time case. We will first derive the optimal state feedback gain matrix using the discrete-time interaction-free cost function (9.5). The optimal gain matrix is later shown to be a nonsymmetric Laplacian matrix corresponding to a completed directed graph. We then find the optimal scaling factor for a prespecified symmetric Laplacian matrix associated with an undirected interaction graph using the discrete-time interaction-related cost function (9.6). Finally, illustrative examples are provided.

9.3.1 Optimal State Feedback Gain Matrix Using the Interaction-free Cost Function

Note that (9.7) can be written as

$$\min_{u[k]} \underbrace{\sum_{k=0}^{\infty} \big(\tilde{r}^T[k] Q \tilde{r}[k] + u^T[k] \Theta u[k] \big)}_{J_{fd}} \tag{9.23}$$

$$\text{subject to:} \quad r[k+1] = r[k] + Tu[k], \tag{9.24}$$

where $\tilde{r}[k] \overset{\triangle}{=} [\tilde{r}_1[k], \ldots, \tilde{r}_n[k]]^T$ with $\tilde{r}_i[k] \overset{\triangle}{=} r_i[k] - \delta_i$, $r[k] \overset{\triangle}{=} [r_1[k], \ldots, r_n[k]]^T$, $u[k] \overset{\triangle}{=} [u_1[k], \ldots, u_n[k]]^T$, and Q and Θ are defined as in (9.9). Before moving on, we need the following lemmas.

Lemma 9.3. *Let $P_1 \in \mathbb{R}^{n \times n}$ be a row-stochastic matrix with positive diagonal entries satisfying that P_1 has a simple eigenvalue equal to one and all other eigenvalues are within the unit circle. Let $P_2 \in \mathbb{R}^{n \times n}$ be a nonnegative matrix satisfying that $\rho(P_2) < 1$. Denote*

$$X_{i+1,j} = \frac{1}{2}\big[P_j + (X_{i,j})^2\big], \qquad X_{0,j} = 0_{n \times n}, \tag{9.25}$$

for $j = 1, 2$. Then $\lim_{i \to \infty} X_{i,j}$, $j = 1, 2$, exists. Denote $X_j^\star \overset{\triangle}{=} \lim_{i \to \infty} X_{i,j}$, $j = 1, 2$. If P_1 and P_2 commute, the following statements hold:

1. *$X_j^\star$ and P_k commute for $j, k = 1, 2$;*
2. *$X_1^\star$ and $X_2^\star$ commute.*

Proof: It follows from Lemma 1.7 and Definition 1.1 that P_1 is semiconvergent. Also it follows from Lemma 1.27 and Definition 1.1 that P_2 is also semiconvergent. It then follows from Property (c) in Lemma 1.13 that (9.25) is convergent. That is, $\lim_{i \to \infty} X_{i,j}$, $j = 1, 2$, exists. We next show that Statements 1 and 2 hold by induction. It can be computed from (9.25) that $X_{1,1} = \frac{1}{2}P_1$ and $X_{1,2} = \frac{1}{2}P_2$. Therefore, it is easy to verify that P_k and $X_{1,j}$ commute for $j, k = 1, 2$. Similarly, $X_{1,1}$ and $X_{1,2}$ also commute. Assume that P_k and $X_{\ell,j}$ commute for $j, k = 1, 2$ and $X_{\ell,1}$ and $X_{\ell,2}$ commute. It can be computed from (9.25) that $X_{\ell+1,j} = \frac{1}{2}[P_j + (X_{\ell,j})^2]$ for $j = 1, 2$. It can also be easily verified that $X_{\ell+1,j}$ and P_k commute for $j, k = 1, 2$. In addition, we also have that

$$\begin{aligned} X_{\ell+1,1}X_{\ell+1,2} &= \frac{1}{4}\big[P_1 + (X_{\ell,1})^2\big]\big[P_2 + (X_{\ell,2})^2\big] \\ &= \frac{1}{4}\big[P_1 P_2 + (X_{\ell,1})^2 P_2 + P_1(X_{\ell,2})^2 + (X_{\ell,1})^2(X_{\ell,2})^2\big] \\ &= \frac{1}{4}\big[P_2 P_1 + P_2(X_{\ell,1})^2 + (X_{\ell,2})^2 P_1 + (X_{\ell,2})^2(X_{\ell,1})^2\big] \\ &= X_{\ell+1,2}X_{\ell+1,1}, \end{aligned}$$

where we have used the assumption that P_k and $X_{\ell,j}$ commute for $j, k = 1, 2$ and $X_{\ell,1}$ and $X_{\ell,2}$ commute to derive the final result. Therefore, $X_{\ell+1,1}$ and $X_{\ell+1,2}$ also commute. By induction, P_k and $\lim_{i \to \infty} X_{i,j}$ commute for $j, k = 1, 2$ and $\lim_{i \to \infty} X_{i,1}$ and $\lim_{i \to \infty} X_{i,2}$ commute. Because $X_j^\star = \lim_{i \to \infty} X_{i,j}$, $j = 1, 2$, the lemma holds clearly. ∎

Lemma 9.4 ([152]). *Let $A \in \mathbb{R}^{n \times n}$ and $B \in \mathbb{R}^{n \times n}$. If $AB = BA$, then $\rho(A+B) \leq \rho(A) + \rho(B)$.*

Lemma 9.5. *Let $G \in \mathbb{R}^{n \times n}$ be a nonsymmetric Laplacian matrix with a simple zero eigenvalue. Suppose that $\gamma \geq 0$. Then $\sqrt{G + \gamma I_n}\sqrt{G}$ is a nonsymmetric Laplacian matrix with a simple zero eigenvalue.*[2]

Proof: When $\gamma = 0$, the proof is trivial. When $\gamma > 0$, the proof follows tow steps:

Step 1. *The off-diagonal entries of $\sqrt{G + \gamma I_n}\sqrt{G}$ are nonpositive.* Because $G = [g_{ij}]$ is a nonsymmetric Laplacian matrix, G can be written as $G = s(I_n - P)$, where $s > 2 \max_i g_{ii}$, and P is a row-stochastic matrix with positive diagonal entries. Because G has a simple zero eigenvalue, it follows that P has a simple eigenvalue equal to one and all other eigenvalues are within the unit circle. Therefore, it follows from Lemma 1.7 and Definition 1.1 that P is semiconvergent. It follows from Property (c) in Lemma 1.13 that the iteration (1.3) is convergent. According to part (a) in Lemma 1.13, $\sqrt{G} = \sqrt{s}(I_n - X^\star)$, where $X^\star = \lim_{i \to \infty} X_i$ with $\alpha = 1$ in (1.3). Similarly, $G + \gamma I_n$ can be written as $G + \gamma I_n = (s + \gamma)(I_n - \frac{s}{s+\gamma}P)$, where $s > 2 \max_i g_{ii}$. By following a similar analysis to that of G, it follows that $\sqrt{G + \gamma I_n} = \sqrt{s + \gamma}(I_n - \widehat{X}^\star)$, where $\widehat{X}^\star = \lim_{i \to \infty} X_i$ with P replaced with $\frac{s}{s+\gamma}P$ and $\alpha = 1$ in (1.3). With P and $\frac{s}{s+\gamma}P$ playing the role of, respectively, P_1 and P_2 in Lemma 9.3, it follows from parts (a) and (c) in Lemma 1.13 and Lemma 9.3 that $X^\star$ and $\widehat{X}^\star$ commute because P and $\frac{s}{s+\gamma}P$ commute. Then we have

$$\frac{1}{\sqrt{s(s + \gamma)}}\sqrt{G + \gamma I_n}\sqrt{G}$$

$$= (I_n - X^\star - \widehat{X}^\star + X^\star \widehat{X}^\star)$$

$$= I_n - \frac{1}{2}\left[P + (X^\star)^2\right] - \frac{1}{2}\left[\frac{s}{s+\gamma}P + (\widehat{X}^\star)^2\right] + X^\star \widehat{X}^\star \qquad (9.26)$$

$$= I_n - \frac{1}{2}\left[P + \frac{s}{s+\gamma}P + (X^\star - \widehat{X}^\star)^2\right], \qquad (9.27)$$

where we have used the fact that $X^\star = \frac{1}{2}[P + (X^\star)^2]$ and $\widehat{X}^\star = \frac{1}{2}[\frac{s}{s+\gamma}P + (\widehat{X}^\star)^2]$ as shown in part (c) of Lemma 1.13 to derive (9.26) and the fact that $X^\star$ and $\widehat{X}^\star$ commute to derive (9.27).

From (9.27), a sufficient condition to show that the off-diagonal entries of $\sqrt{G + \gamma I_n}\sqrt{G}$ are nonpositive is to show that $X^\star - \widehat{X}^\star$ is nonnegative because P is a row-stochastic matrix. We next show that this condition can be satisfied. It follows from part (a) of Lemma 1.13 that $I - P = (I_n - X^\star)^2$ and $I - \frac{s}{s+\gamma}P = (I_n - \widehat{X}^\star)^2$ when $\alpha = 1$. Therefore, we have

---

[2] Note that $G + \gamma I_n$, $\gamma \geq 0$, is an M-matrix with at most one zero eigenvalue. Note also that G is an M-matrix with a simple zero eigenvalue. Therefore, $\sqrt{G + \gamma I_n}$ and $\sqrt{G}$ are well defined.

$$\frac{\gamma}{s+\gamma}P = (I_n - \widehat{X}^\star)^2 - (I_n - X^\star)^2$$

$$= 2(X^\star - \widehat{X}^\star) - (X^\star - \widehat{X}^\star)(X^\star + \widehat{X}^\star)$$

$$= (X^\star - \widehat{X}^\star)(2I_n - X^\star - \widehat{X}^\star). \tag{9.28}$$

We next show that $2I_n - X^\star - \widehat{X}^\star$ is a nonsingular M-matrix and then use Lemma 1.17 to show that $X^\star - \widehat{X}^\star$ is nonnegative. Because $G + \gamma I_n$ is a nonsingular M-matrix from Definition 1.2, it follows from Lemma 1.16 that $\sqrt{G + \gamma I_n}$ is also a nonsingular M-matrix. Because $\sqrt{G + \gamma I_n} = \sqrt{s + \gamma}(I_n - \widehat{X}^\star)$, it follows that $\rho(\widehat{X}^\star) < 1$ according to Definition 1.2. Similarly, it follows from Lemma 1.14 that $\sqrt{G}$ is an M-matrix. Because $\sqrt{G} = \sqrt{s}(I_n - X^\star)$, it follows that $\rho(X^\star) \leq 1$ according to Definition 1.2. Because $\widehat{X}^\star$ and $X^\star$ commute, it then follows from Lemma 9.4 that $\rho(\widehat{X}^\star + X^\star) \leq \rho(\widehat{X}^\star) + \rho(X^\star) < 2$. Therefore, $2I_n - X^\star - \widehat{X}^\star$ is a nonsingular M-matrix according to Definition 1.2. Because $2I_n - X^\star - \widehat{X}^\star$ is a nonsingular M-matrix, it follows from Lemma 1.17 that $(2I_n - X^\star - \widehat{X}^\star)^{-1}$ is nonnegative, which implies that $X^\star - \widehat{X}^\star$ is nonnegative because $X^\star - \widehat{X}^\star = \frac{\gamma}{s+\gamma}P(2I_n - X^\star - \widehat{X}^\star)^{-1}$ and P is a row-stochastic matrix. Therefore, it follows from (9.27) that the off-diagonal entries of $\sqrt{G + \gamma I_n}\sqrt{G}$ are nonpositive.

Step 2. $\sqrt{G + \gamma I_n}\sqrt{G}$ *is a nonsymmetric Laplacian matrix with a simple zero eigenvalue.* Similar to the analysis in Lemma 9.1, it follows that $\sqrt{G}$ has a simple zero eigenvalue with a corresponding eigenvector $\mathbf{1}_n$. Then $\sqrt{G + \gamma I_n}\sqrt{G}$ also has a simple zero eigenvalue with a corresponding eigenvector $\mathbf{1}_n$ because $\sqrt{G + \gamma I_n}$ is a nonsingular M-matrix as shown in Step 1. Combining with Step 1 indicates that $\sqrt{G + \gamma I_n}\sqrt{G}$ is a nonsymmetric Laplacian matrix with a simple zero eigenvalue.   ∎

Lemma 9.6. *Let $G \in \mathbb{R}^{n \times n}$ be a nonsymmetric Laplacian matrix with a simple zero eigenvalue. Suppose that $\gamma > 0$. Then $\sqrt{G + \gamma I_n}\sqrt{G} - G$ is also a nonsymmetric Laplacian matrix with a simple zero eigenvalue.*

Proof: It follows from Step 1 in the proof of Lemma 9.5 that $\sqrt{G} = \sqrt{s}(I_n - X^\star)$, $\sqrt{G + \gamma I_n} = \sqrt{s + \gamma}(I_n - \widehat{X}^\star)$, and $X^\star$ and $\widehat{X}^\star$ commute. It follows that $\sqrt{G}$ and $\sqrt{G + \gamma I_n}$ also commute. It can be computed that $\overline{P} \triangleq \sqrt{G + \gamma I_n}\sqrt{G} + G$ is the solution of the following matrix equation

$$P^2 - 2PG - \gamma G = 0_{n \times n}, \tag{9.29}$$

where we have used the fact that $\sqrt{G + \gamma I_n}\sqrt{G}$ and G commute because $\sqrt{G + \gamma I_n}$ and $\sqrt{G}$ commute and $G = \sqrt{G}\sqrt{G}$. From Lemma 9.5, we know that $\sqrt{G + \gamma I_n}\sqrt{G}$ is a nonsymmetric Laplacian matrix, which implies that $\overline{P}$ is also a nonsymmetric Laplacian matrix. Therefore, $\gamma I_n + 2\overline{P}$ is a nonsingular M-matrix according to Definition 1.2. From (9.29), we can get that

$$G = (\gamma I_n + 2\overline{P})^{-1}\overline{P}^2 = \frac{1}{2}(\gamma I_n + 2\overline{P})^{-1}(\gamma I_n + 2\overline{P} - \gamma I_n)\overline{P}$$
$$= \frac{1}{2}\big[I_n - \gamma(\gamma I_n + 2\overline{P})^{-1}\big]\overline{P},$$

which implies that

$$\frac{1}{2}\gamma(\gamma I_n + 2\overline{P})^{-1}\overline{P} = \frac{1}{2}\overline{P} - G = \frac{1}{2}\big(\sqrt{G + \gamma I_n}\sqrt{G} - G\big). \tag{9.30}$$

Note also that

$$\gamma(\gamma I_n + 2\overline{P})^{-1}\overline{P} = \frac{1}{2}\gamma\big[I_n - \gamma(\gamma I_n + 2\overline{P})^{-1}\big]. \tag{9.31}$$

Combining (9.30) and (9.31) gives that

$$\sqrt{G + \gamma I_n}\sqrt{G} - G = \gamma\big[I_n - \gamma(\gamma I_n + 2\overline{P})^{-1}\big]. \tag{9.32}$$

Because $\gamma I_n + 2\overline{P}$ is a nonsingular M-matrix, it follows from Lemma 1.17 that $(\gamma I_n + 2\overline{P})^{-1}$ is nonnegative. It then follows from (9.32) that the off-diagonal entries of $\sqrt{G + \gamma I_n}\sqrt{G} - G$ are nonpositive.

Because the off-diagonal entries of $\sqrt{G + \gamma I_n}\sqrt{G} - G$ are nonpositive, to show that $\sqrt{G + \gamma I_n}\sqrt{G} - G$ is a nonsymmetric Laplacian matrix with a simple zero eigenvalue, it is sufficient to show that $\sqrt{G + \gamma I_n}\sqrt{G} - G$ has a simple zero eigenvalue with an associated eigenvector $\mathbf{1}_n$. Letting μ be an eigenvalue of G with an associated eigenvector ν, it can be computed that $(G + \gamma I_n)\nu = (\mu + \gamma)\nu$, which implies that the corresponding eigenvalue of $\sqrt{G + \gamma I_n}$ is given by $\sqrt{\mu + \gamma}$ with an associated eigenvector ν. Therefore, the corresponding eigenvalue of $\sqrt{G + \gamma I_n}\sqrt{G} - G$ is given by $\sqrt{\mu + \gamma}\sqrt{\mu} - \mu$ with an associated eigenvector ν. Noting that the nonsymmetric Laplacian matrix G has a simple zero eigenvalue, it follows that $\sqrt{G + \gamma I_n}\sqrt{G} - G$ also has a simple zero eigenvalue because $\sqrt{\mu + \gamma}\sqrt{\mu} - \mu \neq 0$ if $\mu \neq 0$. Note also that $(\sqrt{G + \gamma I_n}\sqrt{G} - G)\mathbf{1}_n = \mathbf{0}_n$ because $\sqrt{G}\mathbf{1}_n = \mathbf{0}_n$ and $G\mathbf{1}_n = \mathbf{0}_n$. Therefore, $\sqrt{G + \gamma I_n}\sqrt{G} - G$ is a nonsymmetric Laplacian matrix with a simple zero eigenvalue. ∎

Lemma 9.7. *Let $B = [b_{ij}] \in \mathbb{R}^{n \times n}$ be a nonsingular M-matrix. If each off-diagonal entry of B is not equal to zero (and hence negative), B^{-1} is positive.*

Proof: From Definition 1.2, $B = \alpha I_n - C$. By choosing $\alpha > \max_i b_{ii}$, it follows that C is positive. Because B is a nonsingular M-matrix, it follows from Definition 1.2 that $\rho(C) < \alpha$ and hence $\rho(\frac{C}{\alpha}) < 1$. Note that $B^{-1} = \alpha^{-1}(I_n - \frac{C}{\alpha})^{-1}$. It follows from Lemmas 1.28 and 1.26 that $(I_n - \frac{C}{\alpha})^{-1} = \sum_{i=0}^{\infty}(\frac{C}{\alpha})^i$. Because C is positive, it follows directly that B^{-1} is positive. ∎

Lemma 9.8. *Let Q and Θ be defined in (9.23). Suppose that Q has a simple zero eigenvalue. Suppose that $\gamma > 0$. Then $W \triangleq \sqrt{\Theta^{-1}Q + \gamma I_n}\sqrt{\Theta^{-1}Q} - \Theta^{-1}Q$ is a nonsymmetric Laplacian matrix with a simple zero eigenvalue corresponding to a complete directed graph.*

Proof: Note that Q has a simple zero eigenvalue. It follows from Lemmas 9.1 and 9.6 that W is a nonsymmetric Laplacian matrix with a simple zero eigenvalue. We study how W evolves when γ increases. Taking the derivative of $\Theta^{-1}Q + \gamma I_n$ with respect to γ gives

$$\frac{d(\Theta^{-1}Q + \gamma I_n)}{d\gamma} = I_n. \tag{9.33}$$

Note that $\Theta^{-1}Q + \gamma I_n$, where $\gamma > 0$, is a nonsingular M-matrix. It follows from Lemma 1.16 that $\sqrt{\Theta^{-1}Q + \gamma I_n}$ is also a nonsingular M-matrix. We also have

$$\frac{d(\sqrt{\Theta^{-1}Q + \gamma I_n})^2}{d\gamma} = 2\sqrt{\Theta^{-1}Q + \gamma I_n}\frac{d\sqrt{\Theta^{-1}Q + \gamma I_n}}{d\gamma}. \tag{9.34}$$

Therefore, it follows from (9.33) and (9.34) that $\frac{d\sqrt{\Theta^{-1}Q + \gamma I_n}}{d\gamma} = \frac{1}{2} \times (\sqrt{\Theta^{-1}Q + \gamma I_n})^{-1}$. It then follows that

$$\frac{d\sqrt{\Theta^{-1}Q + \gamma I_n}\sqrt{\Theta^{-1}Q}}{d\gamma}$$
$$= \frac{d\sqrt{\Theta^{-1}Q + \gamma I_n}}{d\gamma}\sqrt{\Theta^{-1}Q}$$
$$= \frac{1}{2}\big(\sqrt{\Theta^{-1}Q + \gamma I_n}\big)^{-1}\sqrt{\Theta^{-1}Q}$$
$$= \frac{1}{2}I_n - \frac{1}{2}\big(\sqrt{\Theta^{-1}Q + \gamma I_n}\big)^{-1}\big(\sqrt{\Theta^{-1}Q + \gamma I_n} - \sqrt{\Theta^{-1}Q}\big)$$
$$= \frac{1}{2}I_n - \frac{\gamma}{2}\big(\sqrt{\Theta^{-1}Q + \gamma I_n}\big)^{-1}\big(\sqrt{\Theta^{-1}Q + \gamma I_n} + \sqrt{\Theta^{-1}Q}\big)^{-1}. \tag{9.35}$$

By following a similar analysis to that of Lemma 9.2, we can show that each entry of $\sqrt{\Theta^{-1}Q + \gamma I_n}$ is not equal to zero. It follows from Lemma 9.7 that each entry of $(\sqrt{\Theta^{-1}Q + \gamma I_n})^{-1}$ is positive. Similarly, each entry of $(\sqrt{\Theta^{-1}Q + \gamma I_n} + \sqrt{\Theta^{-1}Q})^{-1}$ is also positive. It then follows from (9.35) that each off-diagonal entry of $\frac{d\sqrt{\Theta^{-1}Q + \gamma I_n}\sqrt{\Theta^{-1}Q}}{d\gamma}$ is negative, which implies that the off-diagonal entries of W will decrease when γ increases. Noting that $W = 0_{n \times n}$ when $\gamma = 0$, it follows that all off-diagonal entries of W are less than zero for all $\gamma > 0$. W corresponds to a complete directed graph. ∎

The main result for the optimal control problem (9.23) is given in the following theorem.

Theorem 9.8. *In the optimal control problem* (9.23)*, suppose that Q has a simple zero eigenvalue. The optimal coordination algorithm is*

$$u[k] = -K\tilde{r}[k], \tag{9.36}$$

where $K \triangleq \frac{T[\sqrt{\Theta^{-1}Q+4I_n/T^2}\sqrt{\Theta^{-1}Q}-\Theta^{-1}Q]}{2}$. *The matrix* K *is a nonsymmetric Laplacian matrix with a simple zero eigenvalue corresponding to a complete directed graph. Using* (9.36) *for* (9.24)*, coordination is achieved.*

Proof: Note that $r[k+1] = r[k] + Tu[k]$ is equivalent to $\tilde{r}[k+1] = \tilde{r}[k] + Tu[k]$. Consider the following LQR problem

$$\min_{u[k]} J_{fd} \quad \text{subject to:} \quad \tilde{r}[k+1] = A\tilde{r}[k] + Bu[k],$$

where J_{fd} is defined in (9.23), $A = I_n$, and $B = TI_n$. It can be noted that (A, B) is controllable, which implies that there exists a unique positive-semidefinite matrix $P \in \mathbb{R}^{n \times n}$ satisfying the discrete-time algebraic Riccati equation

$$P = Q + A^T \left[P - PB(\Theta + B^T PB)^{-1} B^T P \right] A. \tag{9.37}$$

Noting that $A = I_n$ and $B = TI_n$, we can simplify (9.37) as

$$Q = T^2 P (\Theta + T^2 P)^{-1} P. \tag{9.38}$$

By multiplying Θ^{-1} on both sides of (9.38), after some manipulation, we can get that

$$\Theta^{-1}Q = T^2 \Theta^{-1} P (I_n + T^2 \Theta^{-1} P)^{-1} \Theta^{-1} P. \tag{9.39}$$

Note that

$$(I_n + T^2 \Theta^{-1} P)^{-1} T^2 \Theta^{-1} P = I_n - (I_n + T^2 \Theta^{-1} P)^{-1}. \tag{9.40}$$

By substituting (9.40) into (9.39), after some manipulation, we can get that

$$\Theta^{-1}Q = \Theta^{-1} P \left[I_n - (I_n + T^2 \Theta^{-1} P)^{-1} \right], \tag{9.41}$$

which can be simplified as

$$(\Theta^{-1}P)^2 - \Theta^{-1}Q(\Theta^{-1}P) - \frac{1}{T^2}\Theta^{-1}Q = 0_{n \times n}. \tag{9.42}$$

It can be computed that (9.42) holds when $\Theta^{-1}P = \frac{\Theta^{-1}Q + \sqrt{\Theta^{-1}Q + 4I_n/T^2}\sqrt{\Theta^{-1}Q}}{2}$. The optimal control strategy is given by $u[k] = -F\tilde{r}[k]$, where

$$F = (I_n + T^2 \Theta^{-1} P)^{-1} T \Theta^{-1} P = T (\Theta^{-1}P - \Theta^{-1}Q) = K,$$

where we have used (9.41) to derive the third equality. It follows from Lemma 9.8 that K is a nonsymmetric Laplacian matrix that corresponds to a complete directed graph.

We next show that coordination is achieved using (9.36) for (9.24) (i.e., $r_i[k] - r_j[k] \to \Delta_{ij}$ or equivalently $\tilde{r}_i[k] - \tilde{r}_j[k] \to 0$ as $k \to \infty$). Note that K is a nonsymmetric Laplacian matrix with a simple zero eigenvalue and $I_n - TK$ has

nonnegative off-diagonal entries and all row sums equal to one. According to Lemmas 1.1 and 1.11, coordination is achieved if $I_n - TK$ has positive diagonal entries. With $\frac{T^2}{4}\Theta^{-1}Q$ playing the role of G and $\gamma = 1$, it follows from a similar argument to that in the beginning of the proof of Lemma 9.6 that $\sqrt{\frac{T^2}{4}\Theta^{-1}Q + I_n}$ and $\sqrt{\frac{T^2}{4}\Theta^{-1}Q}$ commute. After some manipulation, we have

$$I_n - TK = \left(\sqrt{\frac{T^2}{4}\Theta^{-1}Q + I_n} - \sqrt{\frac{T^2}{4}\Theta^{-1}Q} \right)^2.$$

By following a similar proof to that of Lemma 9.8, we have that $\sqrt{\frac{T^2}{4}\Theta^{-1}Q + I_n} - \sqrt{\frac{T^2}{4}\Theta^{-1}Q}$ is an M-matrix with each entry not equal to zero. Combining with Definition 1.2 shows that all diagonal entries of $I_n - TK$ are positive. Therefore, coordination is achieved when using (9.36) for (9.24). ∎

Remark 9.9 From Theorem 9.8, it is easy to verify that when T approaches zero, the optimal state feedback gain matrix is the same as that in the continuous-time case in Theorem 9.1. In addition, the matrix K is not necessarily symmetric. When Θ is a diagonal matrix with identical diagonal entries (i.e., $\Theta = cI_n$, where $c > 0$), K is symmetric.

Remark 9.10 In Theorem 9.1 (correspondingly, Theorem 9.8), a standard LQR problem is solved. The solution can be solved using the standard Matlab command. However, it is not clear why the optimal state feedback gain matrix derived from the standard LQR perspective is a nonsymmetric Laplacian matrix corresponding to a complete directed graph. The contribution of Sect. 9.2.1 (correspondingly, Sect. 9.3.1) is that we mathematically prove the conditions under which the square root of a nonsymmetric Laplacian matrix is still a nonsymmetric Laplacian matrix, explicitly derive the optimal state feedback gain matrix under a given global cost function, and show that the gain matrix is a nonsymmetric Laplacian matrix corresponding to a complete directed graph. Although it might be intuitively true that a global optimization problem in the context of multi-agent coordination normally requires that each agent have full knowledge of all other agents, it is nontrivial to theoretically prove this fact. We have provided a theoretical explanation.

Similar to the discussion in Sect. 9.2, we next show that any symmetric Laplacian matrix $\mathscr{L}$ with a simple zero eigenvalue is inverse optimal with respect to some given cost function.

Theorem 9.11. *Any symmetric Laplacian matrix $\mathscr{L} = [\ell_{ij}] \in \mathbb{R}^{n \times n}$ with a simple zero eigenvalue is the optimal state feedback gain matrix under the cost function $J = \sum_{k=0}^{\infty} (\tilde{r}[k]Q\tilde{r}[k] + u[k]u[k])$, where $Q \triangleq (I_n - T\mathscr{L})^{-1}\mathscr{L}^2$ and $0 < T < \frac{1}{2}\min_i \frac{1}{\ell_{ii}}$.*

Proof: When $0 < T < \frac{1}{2}\min_i \frac{1}{\ell_{ii}}$, it follows from Lemma 1.18 that $\rho(T\mathscr{L}) < 1$. It then follows from Lemmas 1.26 and 1.28 that $I_n - T\mathscr{L}$ is invertible and $(I_n - $

$T\mathscr{L})^{-1} = \sum_{i=0}^{\infty}(T\mathscr{L})^i$. Because $\mathscr{L}$ is symmetric positive semidefinite with a simple zero eigenvalue, it then follows that Q is symmetric positive semidefinite with a simple zero eigenvalue by noting that $Q = (I_n - T\mathscr{L})^{-1}\mathscr{L}^2$. Also note that $(I_n - T\mathscr{L})Q = \mathscr{L}^2$, i.e., $Q = T\mathscr{L}Q + \mathscr{L}^2$, which implies that

$$\begin{aligned}(2\mathscr{L} + TQ)^2 &= 4\mathscr{L}^2 + 4T\mathscr{L}Q + (TQ)^2 = 4\big(\mathscr{L}^2 + T\mathscr{L}Q\big) + (TQ)^2 \\ &= 4Q + (TQ)^2.\end{aligned} \tag{9.43}$$

By taking the square root of both sides of (9.43) and some simplification, we can get $\frac{T(\sqrt{Q + 4I_n/T^2}\sqrt{Q} - Q)}{2} = \mathscr{L}$. Applying Theorem 9.8 finishes the proof. ∎

9.3.2 Optimal Scaling Factor Using the Interaction-related Cost Function

Suppose that the graph $\mathscr{G}$ is undirected. With the interaction-related cost function (9.6), the optimal control problem (9.8) can be written as:

$$\min_{\beta} \underbrace{\sum_{k=0}^{\infty}\big(\tilde{r}^T[k]\mathscr{L}\tilde{r}[k] + u^T[k]u[k]\big)}_{J_{rd}} \tag{9.44}$$

$$\text{subject to:} \quad r[k+1] = r[k] + Tu[k], \ u[k] = -\beta\mathscr{L}\tilde{r}[k],$$

where $\mathscr{L}$ is the prespecified symmetric Laplacian matrix associated with the adjacency matrix $\mathscr{A}$ and hence the undirected graph $\mathscr{G}$, and β is the scaling factor.

Theorem 9.12. *Let $0 = \lambda_1 \leq \lambda_2 \leq \cdots \leq \lambda_n$ be the eigenvalues of $\mathscr{L}$. In the optimal control problem (9.44), suppose that $\mathscr{L}$ has a simple zero eigenvalue. Then the optimal β, denoted by β_{opt}, satisfies $\frac{-T+\sqrt{T^2 + \frac{4}{\lambda_n}}}{2} \leq \beta_{\text{opt}} \leq \frac{-T+\sqrt{T^2 + \frac{4}{\lambda_2}}}{2}$.* [3]

Proof: Note that $u[k] = \beta\mathscr{L}\tilde{r}[k]$. It follows that $\tilde{r}[k+1] = \tilde{r}[k] - \beta T\mathscr{L}\tilde{r}[k]$. It follows that $\tilde{r}[k] = (I_n - \beta T\mathscr{L})^k\tilde{r}[0]$ and hence $u[k] = -\beta\mathscr{L}(I_n - \beta T\mathscr{L})^k\tilde{r}[0]$. Therefore, J_{fd} can be written as $J_{fd} = \sum_{k=0}^{\infty}\tilde{r}^T[0][(I_n - \beta T\mathscr{L})^k\mathscr{L}(I_n - \beta T\mathscr{L})^k + \beta^2(I_n - \beta T\mathscr{L})^k\mathscr{L}^2(I_n - \beta T\mathscr{L})^k]\tilde{r}[0]$. By rewriting $\mathscr{L}$ in a diagonal form as shown in (9.16), J_{rd} can be further written as

$$\begin{aligned}J_{rd} = \sum_{k=0}^{\infty}\tilde{r}^T[0]M\big[(I_n - \beta T\Lambda)^k\Lambda(I_n - \beta T\Lambda)^k \\ + \beta^2(I_n - \beta T\Lambda)^k\Lambda^2(I_n - \beta T\Lambda)^k\big]M^T\tilde{r}[0].\end{aligned}$$

---

[3] Note that there always exists a positive β such that coordination is achieved. In this case, J_r is finite. Therefore, when $\beta = \beta_{\text{opt}}$ coordination is always guaranteed because otherwise J_r will go to infinity, which will then result in a contradiction.

Because $\mathscr{L}$ has a simple zero eigenvalue, it follows that $\lambda_i > 0$, $i = 2, \ldots, n$. After some manipulation, we have that

$$
J_{rd} = \tilde{r}^T[0]M
\begin{bmatrix}
0 & 0 & \cdots & 0 \\
0 & \frac{\frac{1}{T}}{\frac{2\beta+T}{1+\beta^2\lambda_2}-T} & \cdots & 0 \\
\vdots & \vdots & \ddots & \vdots \\
0 & 0 & \cdots & \frac{\frac{1}{T}}{\frac{2\beta+T}{1+\beta^2\lambda_n}-T}
\end{bmatrix}
M^T\tilde{r}[0]
$$

$$
= \sum_{i=2}^{n} \frac{\frac{1}{T}}{\frac{2\beta+T}{1+\beta^2\lambda_i}-T} y_i^2,
$$

where y_i is the ith component of $M^T\tilde{r}[0]$. For $i = 2, \ldots, n$, taking the derivative of $\frac{2\beta+T}{1+\beta^2\lambda_i} - T$ with respect to β and setting the derivative to zero gives

$$
\frac{2(1+\beta^2\lambda_i) - 2\beta\lambda_i(2\beta+T)}{(1+\beta^2\lambda_i)^2} = 0.
$$

It can be computed that $\beta = \frac{-T+\sqrt{T^2+\frac{4}{\lambda_i}}}{2}$. Note that for $\beta < \frac{-T+\sqrt{T^2+\frac{4}{\lambda_n}}}{2}$, J_{rd} will decrease when β increases because $\frac{\frac{1}{T}}{\frac{2\beta+T}{1+\beta^2\lambda_i}-T}$ increases when β increases, $i = 2, \ldots, n$. Similarly, for $\beta > \frac{-T+\sqrt{T^2+\frac{4}{\lambda_2}}}{2}$, J_{rd} will increase when β increases because $\frac{\frac{1}{T}}{\frac{2\beta+T}{1+\beta^2\lambda_i}-T}$ decreases when β increases, $i = 2, \ldots, n$. Combining the previous arguments shows that $\frac{-T+\sqrt{T^2+\frac{4}{\lambda_n}}}{2} \le \beta_{\text{opt}} \le \frac{-T+\sqrt{T^2+\frac{4}{\lambda_2}}}{2}$. ∎

Remark 9.13 The problem stated in Theorem 9.12 is essentially a polynomial optimization problem. Numerical optimization methods [162] can be used to solve this problem.

9.3.3 Illustrative Examples

In this subsection, we provide two illustrative examples about the optimal state feedback gain matrix and the optimal scaling factor derived in, respectively, Sect. 9.3.1 and Sect. 9.3.2.

In (9.23), let Q and Θ be chosen as in Sect. 9.2.3 and the sampling period $T = 0.1$ s. It then follows from Theorem 9.8 that the optimal state feedback gain matrix is

$$
\begin{bmatrix}
1.2173 & -0.498 & -0.5484 & -0.1709 \\
-0.249 & 0.8007 & -0.3963 & -0.1554 \\
-0.1828 & -0.2642 & 0.7734 & -0.3264 \\
-0.0427 & -0.0777 & -0.2448 & 0.3653
\end{bmatrix}.
$$
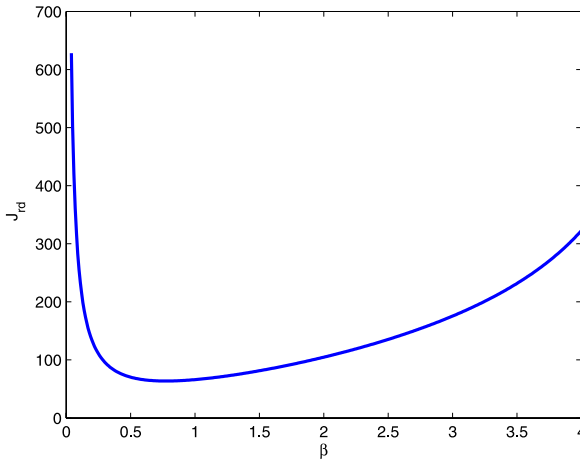
Fig. 9.2 Evolution of the cost function J_{rd} as a function of β

Note that the optimal gain matrix is a nonsymmetric Laplacian matrix corresponding to a complete directed graph.

In (9.44), let $\mathscr{L}$ and the initial state $\tilde{r}[0]$ be chosen as in Sect. 9.2.3. Figure 9.2 shows how the cost function J_{rd} evolves as the scaling factor β increases. From Theorem 9.12, it can be computed that the optimal scaling factor satisfies $0.45 \leq \beta_{\mathrm{opt}} \leq 0.95$, which is consistent with the result shown in Fig. 9.2.

9.4 Notes

The results in this chapter are based mainly on [31, 35]. For further results on the optimality aspect in distributed multi-agent coordination, see [19, 72, 148, 259, 308]. In particular, in [19], a locally optimal nonlinear consensus algorithm is proposed by imposing individual objectives. In [72], an optimal interaction graph, a de Bruijn's graph, is proposed in the average consensus problem. In [259], a semi-decentralized optimal control strategy is designed by minimizing the individual cost functions. In addition, cooperative game theory is employed to ensure cooperation in the presence of a team cost function. In [148], an iterative algorithm is proposed to maximize the second smallest eigenvalue of a symmetric Laplacian matrix to optimize the control system performance. In [308], the fastest converging linear iteration is studied by using semidefinite programming.

Chapter 10
Time Delay

This chapter considers time delays in distributed multi-agent coordination. The time delays are inevitable in networked systems. Time-domain and frequency-domain approaches are used to study leaderless and leader-following coordination algorithms with communication and input delays under a directed interaction graph. We consider both the single-integrator and double-integrator dynamics and present stability or boundedness conditions. Several interesting phenomena are analyzed and explained. Simulation results are presented to support the theoretical results.

10.1 Problem Statement

Time delays are inevitable in networked systems due to the finite speed of information transmission and processing. The time delays are usually classified as input delays and communication delays. The input delays can be caused by information processing while the communication delays can be caused by information propagation from one agent to another. In multi-agent coordination, it is meaningful to study leaderless and leader-following coordination problems where there exist time delays. In the leaderless case, the objective is that a team of agents achieves desired relative positions with local interaction. Similar to Chap. 6, we use the term *coordinated regulation* to refer to the case where a group of followers intercepts a stationary leader with a constant position with local interaction. Similar to Chap. 4, we use the term *coordinated tracking* to refer to the case where a group of followers intercepts a dynamic leader with a varying position. Note that coordinated regulation can be viewed as a special case of coordinated tracking. In both coordinated regulation and coordinated tracking, the leader can be physical or virtual.

This chapter studies both leaderless and leader-following coordination algorithms with communication and input delays for, respectively, single-integrator dynamics and double-integrator dynamics under a directed interaction graph. We analyze stability or boundedness conditions by using time-domain and frequency-domain approaches. The contributions of the current chapter are fourfold. First, we

assume that the interaction graph is directed and has a directed spanning tree, which is more general than the assumption that the interaction graph is undirected and connected or the interaction graph is directed and is strongly connected and balanced. Second, both communication and input delays are considered in the cases of leaderless coordination, coordinated regulation when the leader's position is constant, and coordinated tracking with full access to the leader's velocity for single-integrator dynamics while in the cases of leaderless coordination, coordinated tracking when the leader's velocity is constant, and coordinated tracking with full access to the leader's acceleration for double-integrator dynamics, which guarantees the completeness of the algorithms. Third, we show that for single-integrator dynamics the communication delay will not influence the stability of the system in the case of coordinated tracking with partial access to the leader's velocity. Fourth, as a byproduct, we find that when there exists the communication delay, the final group velocity is always dampened to zero using the leaderless coordination algorithm for double-integrator dynamics rather than a possibly nonzero constant as in the standard leaderless coordination algorithm for double-integrator dynamics in the absence of delays.

10.2 Coordination for Single-integrator Dynamics with Communication and Input Delays Under Directed Fixed Interaction

In this section, we consider the case where the agents are modeled by single-integrator dynamics given by (3.1). We assume that the agents are in a one-dimensional space for simplicity. However, all results hereafter all still valid for any high-dimensional space by use of the properties of the Kronecker product.

10.2.1 Leaderless Coordination

Define $\Delta_{ij} \triangleq \delta_i - \delta_j$, where δ_i is constant. Here Δ_{ij} denotes the desired relative position deviation between agents i and j. Consider the following leaderless coordination algorithm with both communication and input delays for (3.1) as

$$u_i(t) = -\frac{1}{\sum_{j=1}^{n} a_{ij}} \sum_{j=1}^{n} a_{ij} \big[r_i(t - \tau_1) - r_j(t - \tau_1 - \tau_2) - \Delta_{ij} \big], \quad i = 1, \ldots, n,$$

(10.1)

where τ_1 and τ_2 are, respectively, the input and communication delays, and a_{ij}, $i, j = 1, \ldots, n$, is the (i, j)th entry of the adjacency matrix $\mathscr{A}$ associated with the directed graph $\mathscr{G} \triangleq (\mathscr{V}, \mathscr{E})$ characterizing the interaction among the n agents. Let $\mathscr{L}$ be the nonsymmetric Laplacian matrix associated with $\mathscr{A}$ and hence $\mathscr{G}$. Here

we assume that every agent has a neighbor, which implies that $\sum_{j=1}^{n} a_{ij} > 0$, $i = 1, \ldots, n$. The objective of (10.1) is to achieve coordination, that is, $r_i(t) - r_j(t) \to \Delta_{ij}$ as $t \to \infty$ when there exist both communication and input delays.

Using (10.1), (3.1) can be written in a vector form as

$$\dot{\breve{r}}(t) = -\breve{r}(t - \tau_1) + A\breve{r}(t - \tau_1 - \tau_2), \tag{10.2}$$

where $\breve{r} \triangleq [\breve{r}_1, \ldots, \breve{r}_n]^T$ with $\breve{r}_i \triangleq r_i - \delta_i$ and $A \triangleq [\hat{a}_{ij}] \in \mathbb{R}^{n \times n}$ is defined as $\hat{a}_{ij} \triangleq a_{ij} / \sum_{j=1}^{n} a_{ij}$, $i, j = 1, \ldots, n$. Let $L \triangleq [\hat{\ell}_{ij}] \in \mathbb{R}^{n \times n}$ be defined as $L \triangleq I_n - A$. Compared with $\mathscr{A}$ (respectively, $\mathscr{L}$), A (respectively, L) can be viewed as another adjacency matrix (respectively, nonsymmetric Laplacian matrix) associated with $\mathscr{G}$ by choosing a different weight for each edge $(j, i) \in \mathscr{E}$. That is, the original weight a_{ij} for the edge (j, i) is replaced with a new weight $\frac{a_{ij}}{\sum_{j=1}^{n} a_{ij}}$. When $\mathscr{G}$ has a directed spanning tree and each agent has a neighbor, it follows from Lemma 1.1 that L has a simple zero eigenvalue and all other eigenvalues have positive real parts. We have the following singular vector decomposition given as

$$W^{-1}LW = \begin{bmatrix} \widetilde{L} & \mathbf{0}_{n-1} \\ \mathbf{0}_{n-1}^T & 0 \end{bmatrix}. \tag{10.3}$$

Here without loss of generality, we choose the last column of W to be $\mathbf{1}_n$ by noting that $\mathbf{1}_n$ is a right eigenvector of L associated with the zero eigenvalue. Therefore, the last row of W^{-1} is $\mathbf{p}^T$, where $\mathbf{p} \in \mathbb{R}^n$ is defined in Lemma 1.1 with L playing the role of $\mathscr{L}$. It follows that when $\mathscr{G}$ has a directed spanning tree and each agent has a neighbor, all eigenvalues of $\widetilde{L}$ have positive real parts.

Define $\tilde{r} \triangleq W^{-1}\breve{r}$. Denote $\tilde{r}_{1:n-1,:}$ as the first $n - 1$ rows of $\tilde{r}$ and $\tilde{r}_{n,:}$ as the last row of $\tilde{r}$. Note that $A = I_n - L$. It follows from (10.3) that $W^{-1}AW = \begin{bmatrix} I_{n-1} - \widetilde{L} & \mathbf{0}_{n-1} \\ \mathbf{0}_{n-1}^T & 1 \end{bmatrix}$. Define

$$\widetilde{A} \triangleq I_{n-1} - \widetilde{L}. \tag{10.4}$$

By multiplying W^{-1} on both sides of (10.2), it follows that (10.2) can be rewritten as

$$\begin{bmatrix} \dot{\tilde{r}}_{1:n-1,:}(t) \\ \dot{\tilde{r}}_{n,:}(t) \end{bmatrix} = -\begin{bmatrix} \tilde{r}_{1:n-1,:}(t - \tau_1) \\ \tilde{r}_{n,:}(t - \tau_1) \end{bmatrix}$$
$$+ \begin{bmatrix} \widetilde{A} & \mathbf{0}_{n-1} \\ \mathbf{0}_{n-1}^T & 1 \end{bmatrix} \begin{bmatrix} \tilde{r}_{1:n-1,:}(t - \tau_1 - \tau_2) \\ \tilde{r}_{n,:}(t - \tau_1 - \tau_2) \end{bmatrix}. \tag{10.5}$$

Equation (10.5) can be decoupled into the following two equations:

$$\dot{\tilde{r}}_{1:n-1,:}(t) = -\tilde{r}_{1:n-1,:}(t - \tau_1) + \widetilde{A}\tilde{r}_{1:n-1,:}(t - \tau_1 - \tau_2), \tag{10.6a}$$
$$\dot{\tilde{r}}_{n,:}(t) = -\tilde{r}_{n,:}(t - \tau_1) + \tilde{r}_{n,:}(t - \tau_1 - \tau_2). \tag{10.6b}$$

Theorem 10.1. *Suppose that the directed fixed graph $\mathscr{G}$ has a directed spanning tree and every agent has a neighbor. There exist positive $\overline{\tau_1}$ and $\overline{\tau_2}$ such that for $\tau_1 \in [0, \overline{\tau_1}]$ and $\tau_2 \in [0, \overline{\tau_2}]$, the following three conditions[1] are satisfied:*

(i) $2\tau_1 + \tau_2 < 1$.
(ii) $1 - \frac{1-e^{-s\tau_1}}{s} + \lambda_i(\widetilde{A})\frac{1-e^{-s(\tau_1+\tau_2)}}{s} \neq 0$, *for all $s \in \mathbb{C}^+$.*
(iii) *The matrix*

$$Q_{fc} \triangleq -\widetilde{L}^T P_{fc} - P_{fc}\widetilde{L} + \tau_1 S_{fc} + (\tau_1 + \tau_2)H_{fc} + \tau_1 \widetilde{L}^T P_{fc} S_{fc}^{-1} P_{fc}\widetilde{L}$$
$$+ (\tau_1 + \tau_2)\widetilde{L}^T P_{fc}\widetilde{A}H_{fc}^{-1}\widetilde{A}^T P_{fc}\widetilde{L} \tag{10.7}$$

is symmetric negative definite, where $P_{fc} \in \mathbb{R}^{(n-1)\times(n-1)}$ is a symmetric positive-definite matrix chosen properly such that $-\widetilde{L}^T P_{fc} - P_{fc}\widetilde{L}$ is symmetric negative definite, and $S_{fc} \in \mathbb{R}^{(n-1)\times(n-1)}$ and $H_{fc} \in \mathbb{R}^{(n-1)\times(n-1)}$ are arbitrary symmetric positive-definite matrices.

In addition, if $\tau_1 \in [0, \overline{\tau_1}]$ and $\tau_2 \in [0, \overline{\tau_2}]$, using (10.1) for (3.1), for all $r_i(0)$ and all $i, j = 1, \ldots, n$, $r_i(t) - r_j(t) \to \Delta_{ij}$ as $t \to \infty$. In particular, $r_i(t) \to \frac{\mathbf{p}^T \check{r}(0)}{1+\tau_2} + \delta_i$, $i = 1, \ldots, n$, as $t \to \infty$, where $\mathbf{p} \in \mathbb{R}^n$ is defined after (10.3).

Proof: For the first statement, it is straightforward to see that there exist positive $\overline{\tau_1}$ and $\overline{\tau_2}$ such that for $\tau_1 \in [0, \overline{\tau_1}]$ and $\tau_2 \in [0, \overline{\tau_2}]$ Conditions (i) and (ii) are satisfied. For Condition (iii), because $\mathscr{G}$ has a directed spanning tree and each agent has a neighbor, all eigenvalues of $\widetilde{L}$ have positive real parts. Therefore, there always exists a symmetric positive-definite matrix $P_{fc} \in \mathbb{R}^{(n-1)\times(n-1)}$ such that $-\widetilde{L}^T P_{fc} - P_{fc}\widetilde{L}$ is symmetric negative definite. It follows from (10.7) that when $\tau_1 = \tau_2 = 0$, $Q_{fc} = -\widetilde{L}^T P_{fc} - P_{fc}\widetilde{L}$. Due to the continuity of Q_{fc} with respect to τ_1 and τ_2, there must exist positive $\overline{\tau_1}$ and $\overline{\tau_2}$ such that for $\tau_1 \in [0, \overline{\tau_1}]$ and $\tau_2 \in [0, \overline{\tau_2}]$, Q_{fc} is symmetric negative definite.

For the second statement, we show that if $\tau_1 \in [0, \overline{\tau_1}]$ and $\tau_2 \in [0, \overline{\tau_2}]$, (10.6a) is asymptotically stable at the origin while (10.6b) is stable. It follows from Lemma 1.44 that the stability of the following system

$$\frac{d}{dt}\left[\tilde{r}_{1:n-1,:}(t) - \int_{-\tau_1}^0 \tilde{r}_{1:n-1,:}(t+\theta)\,d\theta + \widetilde{A}\int_{-\tau_1-\tau_2}^0 \tilde{r}_{1:n-1,:}(t+\theta)\,d\theta\right]$$
$$= -\widetilde{L}\tilde{r}_{1:n-1,:}(t) \tag{10.8}$$

implies the stability of (10.6a) under Condition (ii) of the theorem. Consider the Lyapunov function candidate

---

[1] Note that here the three conditions are used to obtain the upper bounds $\overline{\tau_1}$ and $\overline{\tau_2}$ for allowable delays.

$$V\big[(\tilde{r}_{1:n-1,:})_t\big] = \chi^T P_{fc}\chi + \int_{-\tau_1}^{0}\int_{t+\theta}^{t} \tilde{r}_{1:n-1,:}^T(\xi)S_{fc}\tilde{r}_{1:n-1,:}(\xi)\,d\xi\,d\theta$$

$$+ \int_{-\tau_1-\tau_2}^{0}\int_{t+\theta}^{t} \tilde{r}_{1:n-1,:}^T(\xi)H_{fc}\tilde{r}_{1:n-1,:}(\xi)\,d\xi\,d\theta,$$

where $\chi \triangleq \tilde{r}_{1:n-1,:}(t) - \int_{-\tau_1}^{0}\tilde{r}_{1:n-1,:}(t+\theta)\,d\theta + \widetilde{A}\int_{-\tau_1-\tau_2}^{0}\tilde{r}_{1:n-1,:}(t+\theta)\,d\theta$.
Taking the derivative of V along (10.8) gives

$$\dot{V}\big[(\tilde{r}_{1:n-1,:})_t\big] \leq \tilde{r}_{1:n-1,:}^T(t)Q_{fc}\tilde{r}_{1:n-1,:}(t),$$

where we have used Lemma 1.23 to derive the inequality. Note that $\alpha_1\|\mathscr{D}[(\tilde{r}_{1:n-1,:})_t]\| \leq V[(\tilde{r}_{1:n-1,:})_t] \leq \alpha_2\|(\tilde{r}_{1:n-1,:})_t\|_c$, where

$$\mathscr{D}\big[(\tilde{r}_{1:n-1,:})_t\big] \triangleq \tilde{r}_{1:n-1,:}(t) - \int_{-\tau_1}^{0}\tilde{r}_{1:n-1,:}(t+\theta)\,d\theta + \widetilde{A}\int_{-\tau_1-\tau_2}^{0}\tilde{r}_{1:n-1,:}(t+\theta)\,d\theta,$$

$\|(\tilde{r}_{1:n-1,:})_t\|_c \triangleq \sup_{\theta\in[-\tau_1-\tau_2,0]}\|\tilde{r}_{1:n-1,:}(t+\theta)\|$, $\alpha_1 = \lambda_{\min}(P_{fc})$, and $\alpha_2 = \lambda_{\max}(P_{fc}) + \tau_1\lambda_{\max}(S_{fc}) + (\tau_1+\tau_2)\lambda_{\max}(H_{fc})$. Also note that Q_{fc} is symmetric negative definite under Condition (iii) of the theorem. It follows from Lemma 1.41 that (10.8) is asymptotically stable at the origin. Therefore, if Conditions (ii) and (iii) of the theorem are satisfied, (10.6a) is asymptotically stable at the origin.

For (10.6b), we apply the Nyquist stability criterion to find its stability condition. After Laplace transformation, (10.6b) can be written as

$$s\tilde{r}_{n,:}(s) - \tilde{r}_{n,:}(0) = -e^{-\tau_1 s}\tilde{r}_{n,:}(s) + e^{-(\tau_1+\tau_2)s}\tilde{r}_{n,:}(s),$$

which implies that $\tilde{r}_{n,:}(s) = \frac{\tilde{r}_{n,:}(0)}{s+e^{-\tau_1 s}-e^{-(\tau_1+\tau_2)s}}$. Therefore, the stability of (10.3b) is determined by the distribution of the roots of

$$s = -e^{-\tau_1 s} + e^{-(\tau_1+\tau_2)s}. \tag{10.9}$$

Note that $s = 0$ is a root of (10.9). To study the other roots, define $f(s) \triangleq [e^{-\tau_1 s} - e^{-(\tau_1+\tau_2)s}]/s$. According to the Nyquist stability criterion, if the trajectory of $f(\iota\omega), \forall\omega \in (-\infty,\infty)$, does not enclose the point $(-1,0)$, then the other roots of (10.9) are stable. One sufficient condition is that $\mathrm{Re}[f(\iota\omega)] > -1, \forall\omega \in (-\infty,\infty)$. Note that $\mathrm{Re}[f(\iota\omega)] = \frac{\sin[(\tau_1+\tau_2)\omega]}{\omega} - \frac{\sin(\tau_1\omega)}{\omega} \geq -(\tau_1+\tau_2) - \tau_1 = -(2\tau_1+\tau_2)$. Therefore, it follows that (10.6b) is marginally stable at the origin under Condition (i) of the theorem.

Note that $\lim_{t\to\infty}\tilde{r}_{1:n-1,:}(t) = \mathbf{0}_{n-1}$. Also note that

$$\lim_{t\to\infty}\tilde{r}_{n,:}(t) = \lim_{s\to 0}s\tilde{r}_{n,:}(s) = \frac{s\tilde{r}_{n,:}(0)}{s+e^{-\tau_1 s}-e^{-(\tau_1+\tau_2)s}} = \frac{\tilde{r}_{n,:}(0)}{1+\tau_2}.$$

Because $\breve{r} = W\tilde{r}$ and the last column of W is $\mathbf{1}_n$, it follows that $\lim_{t\to\infty} \breve{r}(t) = \lim_{t\to\infty} W\tilde{r}(t) = \lim_{t\to\infty} \mathbf{1}_n \tilde{r}_{n,:}(t) = \frac{\mathbf{1}_n \tilde{r}_{n,:}(0)}{1+\tau_2}$, which implies that $\breve{r}_i(t) - \breve{r}_j(t) \to 0$ as $t \to \infty$, that is, $r_i(t) - r_j(t) \to \Delta_{ij}$ as $t \to \infty$. Because the last row of W^{-1} is $\mathbf{p}$, it follows that $\tilde{r}_{n,:}(0) = \mathbf{p}^T \breve{r}(0)$. Therefore, it follows that $r_i(t) \to \frac{\mathbf{p}^T \breve{r}(0)}{1+\tau_2} + \delta_i$ as $t \to \infty$. ∎

Remark 10.2 Note that the additional dynamics caused by the model transformation from (10.6a) to (10.8) can be characterized by the solutions of the following complex equation [210]

$$\det\left[I_{n-1} - I_{n-1}\frac{1 - e^{-s\tau_1}}{s} + \widetilde{A}\frac{1 - e^{-s(\tau_1+\tau_2)}}{s}\right] = 0, \quad s \in \mathbb{C}.$$

Thus, if $\tau_1 + (\tau_1 + \tau_2)\|\widetilde{A}\| < 1$, there are no additional eigenvalues induced by the model transformation from (10.6a) to (10.8), which implies that the condition $\tau_1 + (\tau_1 + \tau_2)\|\widetilde{A}\| < 1$ can be used to replace Condition (ii) in Theorem 10.1.

Remark 10.3 If we let $S_{fc} = H_{fc} = I_{n-1}$ in (10.7), Condition (iii) in Theorem 10.1 can be written as

$$\overline{\tau_1} + \overline{\tau_2} < \frac{\lambda_{\min}(\widetilde{L}^T P_{fc} + P_{fc}\widetilde{L})}{2 + \|\widetilde{L}^T P_{fc}\|^2 + \|\widetilde{L}^T P_{fc}\widetilde{A}\|^2}.$$

10.2.2 Coordinated Regulation when the Leader's Position is Constant

In this subsection, we assume that in addition to n followers, labeled as agents or followers 1 to n, there exists a leader, labeled as agent 0, with position r_0. We assume that r_0 is constant. Let $\mathcal{G} \triangleq (\mathcal{V}, \mathcal{E})$ be the directed graph characterizing the interaction among the n followers. Let $\overline{\mathcal{G}} \triangleq (\overline{\mathcal{V}}, \overline{\mathcal{E}})$ be the directed graph characterizing the interaction among the leader and the followers corresponding to $\mathcal{G}$.

Consider the following coordinated regulation algorithm with both communication and input delays for the n followers with single-integrator dynamics given by (3.1) as

$$u_i(t) = -\frac{1}{\sum_{j=0}^n a_{ij}} \sum_{j=0}^n a_{ij}\big[r_i(t - \tau_1) - r_j(t - \tau_1 - \tau_2)\big], \quad i = 1, \ldots, n,$$

$$(10.10)$$

where τ_1 and τ_2 are, respectively, the input and communication delays, a_{ij}, $i, j = 1, \ldots, n$, is the (i, j)th entry of the adjacency matrix $\mathcal{A}$ associated with $\mathcal{G}$, and $a_{i0} > 0$ if the leader is a neighbor of agent i and $a_{i0} = 0$ otherwise. Note that in $\overline{\mathcal{G}}$ if the leader has directed paths to all followers 1 to n, it follows that $\sum_{j=0}^n a_{ij} > 0$,

$i = 1, \ldots, n$. The objective of (10.10) is to guarantee coordinated regulation, i.e., $r_i(t) \to r_0$ as $t \to \infty$.

Define $\bar{r}_i \triangleq r_i - r_0$ and $\bar{r} \triangleq [\bar{r}_1, \ldots, \bar{r}_n]^T$. Define $\overline{A} \triangleq [\bar{a}_{ij}] \in \mathbb{R}^{n \times n}$ as $\bar{a}_{ij} \triangleq a_{ij}/\sum_{j=0}^{n} a_{ij}$. Using (10.10), (3.1) can be written in a vector form as

$$\dot{\bar{r}}(t) = -\bar{r}(t - \tau_1) + \overline{A}\bar{r}(t - \tau_1 - \tau_2), \tag{10.11}$$

where we have used the fact that r_0 is constant. Before moving on, we need the following lemma regarding $(I_n - \overline{A})$.

Lemma 10.1. *All eigenvalues of $I_n - \overline{A}$ have positive real parts if in $\overline{\mathscr{G}}$ the leader has directed paths to all followers 1 to n.*

Proof: The lemma follows from Lemma 8.1 by noting that all eigenvalues of $\overline{A}$ are within the unit circle if the leader has directed paths to all followers. ∎

Theorem 10.4. *Suppose that in $\overline{\mathscr{G}}$ the leader has directed paths to all followers 1 to n. There exist positive $\overline{\tau_1}$ and $\overline{\tau_2}$ such that for $\tau_1 \in [0, \overline{\tau_1}]$ and $\tau_2 \in [0, \overline{\tau_2}]$, the following two conditions are satisfied*:

(i) $1 - \frac{1 - e^{-s\tau_1}}{s} + \lambda_i(\overline{A})\frac{1 - e^{-s(\tau_1 + \tau_2)}}{s} \neq 0, \forall s \in \mathbb{C}^+.$
(ii) *The matrix*

$$\begin{aligned} Q_{fr} \triangleq &(\overline{A} - I_n)^T P_{fr} + P_{fr}(\overline{A} - I_n) + \tau_1 S_{fr} + (\tau_1 + \tau_2)H_{fr} \\ &+ \tau_1\big[(\overline{A} - I_n)^T P_{fr} S_{fr}^{-1} P_{fr}(\overline{A} - I_n)\big] \\ &+ (\tau_1 + \tau_2)\big[(\overline{A} - I_n)^T P_{fr}\overline{A}H_{fr}^{-1}\overline{A}^T P_{fr}(\overline{A} - I_n)\big] \end{aligned}$$

is symmetric negative definite, where $P_{fr} \in \mathbb{R}^{n \times n}$ is a symmetric positive-definite matrix chosen properly such that $(\overline{A} - I_n)^T P_{fr} + P_{fr}(\overline{A} - I_n)$ is symmetric negative definite, and $S_{fr} \in \mathbb{R}^{n \times n}$ and $H_{fr} \in \mathbb{R}^{n \times n}$ are arbitrary symmetric positive-definite matrices.

In addition, if $\tau_1 \in [0, \overline{\tau_1}]$ and $\tau_2 \in [0, \overline{\tau_2}]$, using (10.10) for (3.1), for all $r_i(0)$, $i = 1, \ldots, n$, $r_i(t) \to r_0$ as $t \to \infty$.

Proof: For the first statement, it is straightforward to see that there exist positive $\overline{\tau_1}$ and $\overline{\tau_2}$ such that for $\tau_1 \in [0, \overline{\tau_1}]$ and $\tau_2 \in [0, \overline{\tau_2}]$, Condition (i) is satisfied. Because in $\overline{\mathscr{G}}$ the leader has directed paths to all followers, it follows from Lemma 10.1 that all eigenvalues of $I_n - \overline{A}$ have positive real parts. A similar analysis to that in Theorem 10.1 shows that there exist positive $\overline{\tau_1}$ and $\overline{\tau_2}$ such that for $\tau_1 \in [0, \overline{\tau_1}]$ and $\tau_2 \in [0, \overline{\tau_2}]$, Condition (ii) is satisfied.

For the second statement, it follows from Lemma 1.44 that the stability of the following system

$$\frac{d}{dt}\left[\bar{r}(t) - \int_{-\tau_1}^{0} \bar{r}(t + \theta)\, d\theta + \overline{A}\int_{-\tau_1 - \tau_2}^{0} \bar{r}(t + \theta)\, d\theta\right] = (\overline{A} - I_n)\bar{r}(t) \tag{10.12}$$

implies the stability of (10.11) under Condition (i) of the theorem. Consider the Lyapunov function candidate

$$V(\bar{r}_t) = \chi^T P_{fr} \chi + \int_{-\tau_1}^{0} \int_{t+\theta}^{t} \bar{r}^T(\xi) S_{fr} \bar{r}(\xi) \, d\xi \, d\theta$$

$$+ \int_{-\tau_1-\tau_2}^{0} \int_{t+\theta}^{t} \bar{r}^T(\xi) H_{fr} \bar{r}(\xi) \, d\xi \, d\theta,$$

where $\chi \triangleq \bar{r}(t) - \int_{-\tau_1}^{0} \bar{r}(t+\theta) \, d\theta + \overline{A} \int_{-\tau_1-\tau_2}^{0} \bar{r}(t+\theta) \, d\theta$. Taking the derivative of V along (10.12) gives

$$\dot{V}(\bar{r}_t) \leq \bar{r}^T(t) Q_{fr} \bar{r}(t),$$

where we have used Lemma 1.23 to derive the inequality. Thus, a similar analysis to that in the proof of Theorem 10.1 shows that if the two conditions of the theorem are satisfied, (10.11) is asymptotically stable at the origin. ∎

Remark 10.5 Although the approaches used in the leaderless coordination case and the coordinated regulation case are similar, the control objectives are different. In the leaderless coordination case, the final positions of each agent are determined by the interaction graph and the time delays rather than being prespecified. However, in the coordinated regulation case, there exists a leader that prespecifies the final position, and the control objective is to guarantee that the final positions of all followers approach the position of the leader. Also the result in the case of coordinated regulation can be generalized to general weights while in the case of leaderless coordination special weights are required (i.e., $\sum_{j=1}^{n} \hat{a}_{ij} = 1$). In addition, note that Remarks 10.2 and 10.3 are still valid in the coordinated regulation case.

10.2.3 Coordinated Tracking with Full Access to the Leader's Velocity

In this subsection, we consider the case where the leader's position r_0 is varying. We assume that $|\dot{r}_0| < \delta_v$ and $|\ddot{r}_0| < \delta_a$, where δ_v and δ_a are positive constants. We also assume that all followers have access to $\dot{r}_0$.

Consider the coordinated tracking algorithm with both communication and input delays for the n followers with single-integrator dynamics given by (3.1) as

$$u_i(t) = \dot{r}_0(t - \tau_1 - \tau_2)$$

$$- \frac{1}{\sum_{j=0}^{n} a_{ij}} \sum_{j=0}^{n} a_{ij} \big[r_i(t - \tau_1) - r_j(t - \tau_1 - \tau_2) \big], \quad i = 1, \ldots, n,$$

$$(10.13)$$

where τ_1 and τ_2 are, respectively, the input and communication delays, and a_{ij}, $i = 1, \ldots, n$, $j = 0, \ldots, n$, is defined as in (10.10). Using (10.13), (3.1) can be

written in a vector form as

$$\dot{\bar{r}} = -\bar{r}(t - \tau_1) + \overline{A}\bar{r}(t - \tau_1 - \tau_2) + R_{ft}, \tag{10.14}$$

where $\bar{r}$ and $\overline{A}$ are defined as in Sect. 10.2.2, and $R_{ft} \triangleq \mathbf{1}_n[\dot{r}_0(t - \tau_1 - \tau_2) - \dot{r}_0(t) + r_0(t - \tau_1 - \tau_2) - r_0(t - \tau_1)]$. By using (1.10), it follows that $R_{ft} = -\mathbf{1}_n \int_{-\tau_1-\tau_2}^{0} \ddot{r}_0(t + \theta)\, d\theta - \mathbf{1}_n \int_{-\tau_1-\tau_2}^{-\tau_1} \dot{r}_0(t + \theta)\, d\theta$.

Theorem 10.6. *Suppose that in $\mathscr{G}$ the leader has directed paths to all followers* 1 *to n. There exist positive $\overline{\tau_1}$ and $\overline{\tau_2}$ such that for $\tau_1 \in [0, \overline{\tau_1}]$ and $\tau_2 \in [0, \overline{\tau_2}]$,*

$$Q_{ft} \triangleq (\overline{A} - I_n)^T P_{fr} + P_{fr}(\overline{A} - I_n) + \tau_1 \big(P_{fr} + P_{fr}\overline{A}P_{fr}^{-1}\overline{A}^T P_{fr} + 2q_f P_{fr} \big)$$
$$+ (\tau_1 + \tau_2)\big(P_{fr}\overline{A}P_{fr}^{-1}\overline{A}^T P_{fr} + P_{fr}\overline{A}^2 P_{fr}^{-1}(\overline{A}^T)^2 P_{fr} + 2q_f P_{fr} \big)$$

is symmetric negative definite, where P_{fr} is defined in Theorem 10.4 and q_f is an arbitrary real number satisfying $q_f > 1$. In addition, if $\tau_1 \in [0, \overline{\tau_1}]$ and $\tau_2 \in [0, \overline{\tau_2}]$, using (10.13) for (3.1), for all $r_i(0)$ and all $i = 1, \dots, n$, $|r_i(t) - r_0(t)|$ is uniformly ultimately bounded. In particular, the ultimate bound for $\|\bar{r}(t)\|$ is given by $\frac{\lambda_{\max}(P_{fr})a_f}{\lambda_{\min}(P_{fr})\kappa_f \lambda_{\min}(-Q_{ft})}$, where $a_f \triangleq 2[(\tau_1 + \tau_2)\delta_a + \tau_2\delta_v][\|P_{fr}\| + \tau_1\|P_{fr}\| + (\tau_1 + \tau_2)\|P_{fr}\overline{A}\|]$, and κ_f is an arbitrary real number satisfying $0 < \kappa_f < 1$.

Proof: The proof of the first statement is similar to that in Theorem 10.4 and is hence omitted here. For the second statement, using (1.10), we transform (10.14) to the following system

$$\frac{d}{dt}\bar{r}(t) = (\overline{A} - I_n)\bar{r}(t) + \int_{-\tau_1}^{0} \dot{\bar{r}}(t + \theta)\, d\theta - \overline{A}\int_{-\tau_1-\tau_2}^{0} \dot{\bar{r}}(t + \theta)\, d\theta + R_{ft}$$

$$= (\overline{A} - I_n)\bar{r}(t) + \int_{-\tau_1}^{0} \big[\overline{A}\bar{r}(t - \tau_1 - \tau_2 + \theta) - \bar{r}(t - \tau_1 + \theta) \big]\, d\theta$$
$$+ \int_{-\tau_1}^{0} R_{ft}(t + \theta)\, d\theta$$
$$+ \overline{A}\int_{-\tau_1-\tau_2}^{0} \big[\bar{r}(t - \tau_1 + \theta) - \overline{A}\bar{r}(t - \tau_1 - \tau_2 + \theta) \big]\, d\theta$$
$$- \overline{A}\int_{-\tau_1-\tau_2}^{0} R_{ft}(t + \theta)\, d\theta + R_{ft}$$

$$= (\overline{A} - I_n)\bar{r}(t) - \int_{-2\tau_1}^{-\tau_1} \bar{r}(t + \theta)\, d\theta + \overline{A}\int_{-2\tau_1-\tau_2}^{-\tau_1-\tau_2} \bar{r}(t + \theta)\, d\theta$$
$$+ \int_{-\tau_1}^{0} R_{ft}(t + \theta)\, d\theta + \overline{A}\int_{-2\tau_1-\tau_2}^{-\tau_1} \bar{r}(t + \theta)\, d\theta$$
$$- \overline{A}^2 \int_{-2\tau_1-2\tau_2}^{-\tau_1-\tau_2} \bar{r}(t + \theta)\, d\theta - \overline{A}\int_{-\tau_1-\tau_2}^{0} R_{ft}(t + \theta)\, d\theta + R_{ft}. \tag{10.15}$$

Consider the Lyapunov function candidate $V(\bar{r}) = \bar{r}^T(t)P_{fr}\bar{r}(t)$. Taking the derivative of $V(\bar{r})$ along (10.15) gives

$$
\begin{aligned}
\dot{V}(\bar{r}) \leq{}& \bar{r}^T(t)\big[(\overline{A} - I_n)^T P_{fr} + P_{fr}(\overline{A} - I_n)\big]\bar{r}(t) + \tau_1\bar{r}^T(t)P_{fr}P_{fr}^{-1}P_{fr}\bar{r}(t) \\
&+ \int_{-2\tau_1}^{-\tau_1} \bar{r}^T(t+\theta)P_{fr}\bar{r}(t+\theta)\,d\theta + \tau_1\bar{r}^T(t)P_{fr}\overline{A}P_{fr}^{-1}\overline{A}^T P_{fr}\bar{r}(t) \\
&+ \int_{-2\tau_1-\tau_2}^{-\tau_1-\tau_2} \bar{r}^T(t+\theta)P_{fr}\bar{r}(t+\theta)\,d\theta \\
&+ 2\|\bar{r}\|\,\|P_{fr}\|\big[\tau_1(\tau_1+\tau_2)\delta_a + \tau_1\tau_2\delta_v\big] \\
&+ (\tau_1+\tau_2)\bar{r}^T P_{fr}\overline{A}P_{fr}^{-1}\overline{A}^T P_{fr}\bar{r} + \int_{-2\tau_1-\tau_2}^{-\tau_1} \bar{r}^T(t+\theta)P_{fr}\bar{r}(t+\theta)\,d\theta \\
&+ (\tau_1+\tau_2)\bar{r}^T P_{fr}(\overline{A})^2 P_{fr}^{-1}\big(\overline{A}^T\big)^2 P_{fr}\bar{r} \\
&+ \int_{-2\tau_1-2\tau_2}^{-\tau_1-\tau_2} \bar{r}^T(t+\theta)P_{fr}\bar{r}(t+\theta)\,d\theta \\
&+ 2\|\bar{r}\|\|P_{fr}\overline{A}\|\big[(\tau_1+\tau_2)(\tau_1+\tau_2)\delta_a + (\tau_1+\tau_2)\tau_2\delta_v\big] \\
&+ 2\|\bar{r}\|\|P_{fr}\|\big[(\tau_1+\tau_2)\delta_a + \tau_2\delta_v\big],
\end{aligned}
$$

where we have used Lemma 1.23 and the facts that $|\dot{r}_0| < \delta_v$ and $|\ddot{r}_0| < \delta_a$ to derive the inequality. Take $p(s) = q_f s$. If $V[\bar{r}(t+\theta)] < p\{V[\bar{r}(t)]\} = q_f V[\bar{r}(t)]$ for $-2\tau_1 - 2\tau_2 \leq \theta \leq 0$, we have

$$
\begin{aligned}
\dot{V}(\bar{r}) \leq{}& \bar{r}^T(t)\big[(\overline{A} - I_n)^T P_{fr} + P_{fr}(\overline{A} - I_n)\big]\bar{r}(t) + \tau_1\bar{r}^T(t)(P_{fr} + q_f P_{fr})\bar{r}(t) \\
&+ \tau_1\bar{r}^T(t)\big(P_{fr}\overline{A}P_{fr}^{-1}\overline{A}^T P_{fr} + q_f P_{fr}\big)\bar{r}(t) \\
&+ (\tau_1+\tau_2)\bar{r}^T(t)\big(P_{fr}\overline{A}P_{fr}^{-1}\overline{A}^T P_{fr} + q_f P_{fr}\big)\bar{r}(t) \\
&+ (\tau_1+\tau_2)\bar{r}^T(t)\big(P_{fr}\overline{A}^2 P_{fr}^{-1}\big(\overline{A}^T\big)^2 P_{fr} + q_f P_{fr}\big)\bar{r}(t) \\
&+ 2\|\bar{r}(t)\|\|P_{fr}\|\big[\tau_1(\tau_1+\tau_2)\delta_a + \tau_1\tau_2\delta_v\big] \\
&+ 2\|\bar{r}(t)\|\|P_{fr}\overline{A}\|\big[(\tau_1+\tau_2)(\tau_1+\tau_2)\delta_a + (\tau_1+\tau_2)\tau_2\delta_v\big] \\
&+ 2\|\bar{r}(t)\|\|P_{fr}\|\big[(\tau_1+\tau_2)\delta_a + \tau_2\delta_v\big] \\
\leq{}& \bar{r}(t)^T(t)Q_{ft}\bar{r}(t)(t) + a_f\|\bar{r}(t)\|.
\end{aligned}
$$

If $\tau_1 \in [0, \overline{\tau_1}]$ and $\tau_2 \in [0, \overline{\tau_2}]$, we have that $\lambda_{\min}(-Q_{ft}) > 0$. Given $0 < \kappa_f < 1$, if $\|\bar{r}(t)\| \geq \frac{a_f}{\kappa_f\lambda_{\min}(-Q_{ft})}$, we can obtain that

$$
\begin{aligned}
\dot{V}(\bar{r}) &\leq -(1-\kappa_f)\lambda_{\min}(-Q_{ft})\|\bar{r}(t)\|^2 - \kappa_f\lambda_{\min}(-Q_{ft})\|\bar{r}(t)\|^2 + a_f\|\bar{r}(t)\| \\
&\leq -(1-\kappa_f)\lambda_{\min}(-Q_{ft})\|\bar{r}(t)\|^2.
\end{aligned}
$$

Therefore, it follows from Lemma 1.42 that $\|\bar{r}(t)\|$ is uniformly ultimately bounded, which implies that $|r_i(t) - r_0(t)|$ is uniformly ultimately bounded. Moreover, it can

be computed that the ultimate bound for $\|\bar{r}(t)\|$ is given by $\frac{\lambda_{\max}(P_{fr})a_f}{\lambda_{\min}(P_{fr})\kappa_f\lambda_{\min}(-Q_{ft})}$ by following a similar analysis to that in [145, pp. 172–174]. ∎

Remark 10.7 Note that if $\tau_1 = \tau_2 = 0$, then $\lim_{t\to\infty}\|\bar{r}(t)\| = 0$. Also note when τ_1 and τ_2 are larger, the ultimate bound will also be larger. □

10.2.4 Coordinated Tracking with Partial Access to the Leader's Velocity

In this subsection, we assume that the leader's varying position r_0 and velocity $\dot{r}_0$ are available to only a subset of all followers. We assume that $|r_0|$ and $|\dot{r}_0|$ are bounded. We also assume that there exists only the communication delay.

Consider the following coordinated tracking algorithm with the communication delay for the n followers with single-integrator dynamics given by (3.1) as

$$u_i(t) = \frac{1}{\sum_{j=0}^{n} a_{ij}} \sum_{j=0}^{n} a_{ij}\big\{\dot{r}_j(t - \tau_2) - \big[r_i(t) - r_j(t - \tau_2)\big]\big\}, \quad i = 1, \ldots, n,$$

$$(10.16)$$

where τ_2 is the communication delay and a_{ij}, $i = 1, \ldots, n$, $j = 0, \ldots, n$, is defined as in (10.10). Using (10.16), (3.1) can be written in a vector form as

$$\dot{\bar{r}}(t) = \overline{A}\dot{\bar{r}}(t - \tau_2) - \bar{r}(t) + \overline{A}\bar{r}(t - \tau_2) + R_{fft}, \qquad (10.17)$$

where $\bar{r}$ and $\overline{A}$ are defined as in Sect. 10.2.2, and $R_{fft} \triangleq [\dot{r}_0(t - \tau_2) - \dot{r}_0(t)]\mathbf{1}_n - [r_0(t) - r_0(t - \tau_2)]\mathbf{1}_n$.

Theorem 10.8. *Suppose that in $\overline{\mathcal{G}}$ the leader has directed paths to all followers 1 to n. Using (10.16) for (3.1), for all $r_i(0)$ and all $i = 1, \ldots, n$, $|r_i(t) - r_0(t)|$ is uniformly ultimately bounded no matter how large the communication delay is.*

Proof: First, it follows from Lemma 8.1 that $\rho(\overline{A}) < 1$, which means that the neutral operator $\mathscr{D}\bar{r}_t = \bar{r}(t) - \overline{A}\bar{r}(t - \tau_2)$ is stable. Consider a Lyapunov function candidate $V(\bar{r}) = \bar{r}^T(t)\bar{r}(t)$. Taking the derivative of $V(\bar{r})$ along (10.17) gives

$$\dot{V}(\mathscr{D}\bar{r}_t) = (\mathscr{D}\bar{r}_t)^T\big[-\bar{r}(t) + \overline{A}\bar{r}(t - \tau_2) + R_{fft}\big]$$
$$= -(\mathscr{D}\bar{r}_t)^T(\mathscr{D}\bar{r}_t) + (\mathscr{D}\bar{r}_t)R_{fft}.$$

In then follows that

$$\dot{V}(\mathscr{D}\bar{r}_t) \leq -\|\mathscr{D}\bar{r}_t\|\big(\|\mathscr{D}\bar{r}_t\| - \|R_{fft}\|\big).$$

If $\|\mathscr{D}\bar{r}_t\| > \|R_{fft}\|$, we have $\dot{V}(\mathscr{D}\bar{r}_t) < 0$. Therefore, it follows from Lemma 1.43 that $\|\bar{r}(t)\|$ is uniformly ultimately bounded, which implies that $|r_i(t) - r_0(t)|$ is ultimately bounded. ∎

Remark 10.9 From Theorem 10.8, it can be noted that the communication delay does not jeopardize the stability of the closed-loop tracking error system (10.17) in the case of coordinated tracking with partial access to the leader's velocity for single-integrator dynamics. However, with the increase of the communication delay, the tracking errors will increase as well.

Remark 10.10 In real applications, the derivatives of the neighbors' positions $\dot{r}_j(t - \tau_2)$ can be calculated by using numerical differentiation. For example, $\dot{r}_j(t - \tau_2)$ can be approximated by $[r_j(kT - \tau_2) - r_j(kT - T - \tau_2)]/T$, where k is the discrete-time index and T is the sampling period.

10.3 Coordination for Double-integrator Dynamics with Communication and Input Delays Under Directed Fixed Interaction

In this section, we consider the case where the agents are modeled by double-integrator dynamics given by (3.5). We again assume that the agents are in a one-dimensional space for simplicity. However, all results hereafter are still valid for any high-dimensional space by use of the properties of the Kronecker product.

10.3.1 Leaderless Coordination

Consider the following leaderless coordination algorithm with both communication and input delays for (3.5) as

$$u_i(t) = -\frac{1}{\sum_{j=1}^n a_{ij}} \sum_{j=1}^n a_{ij} \left[r_i(t - \tau_1) - r_j(t - \tau_1 - \tau_2) - \Delta_{ij} \right]$$

$$- \frac{\gamma_c}{\sum_{j=1}^n a_{ij}} \sum_{j=1}^n a_{ij} \left[v_i(t - \tau_1) - v_j(t - \tau_1 - \tau_2) \right], \quad i = 1, \ldots, n,$$

$$(10.18)$$

where τ_1 and τ_2 are, respectively, the input and communication delays, a_{ij}, $i, j = 1, \ldots, n$, is defined as in (10.1), Δ_{ij} is defined as in Sect. 10.2.1, and γ_c is a positive gain. Here we also assume that every agent has a neighbor, which implies that $\sum_{j=1}^n a_{ij} > 0$, $i = 1, \ldots, n$. The objective of (10.18) is to achieve coordination, that is, $r_i(t) - r_j(t) \to \Delta_{ij}$ and $v_i(t) - v_j(t) \to 0$ as $t \to \infty$ when there exist both communication and input delays.

Using (10.18), (3.5) can be written in a vector form as

$$\dot{\breve{r}}(t) = v(t), \tag{10.19a}$$

$$\dot{v}(t) = -\breve{r}(t - \tau_1) + A\breve{r}(t - \tau_1 - \tau_2) - \gamma_c v(t - \tau_1)$$
$$+ \gamma_c A v(t - \tau_1 - \tau_2), \tag{10.19b}$$

where $\breve{r} \triangleq [\breve{r}_1, \ldots, \breve{r}_n]^T$ with $\breve{r}_i \triangleq r_i - \delta_i$, $v \triangleq [v_1, \ldots, v_n]^T$, and A is defined as in (10.2). Define $\tilde{r} \triangleq W^{-1}\breve{r}$ and $\tilde{v} \triangleq W^{-1}v$, where W is defined as in (10.3). Denote $\tilde{r}_{1:n-1,:}$ and $\tilde{v}_{1:n-1,:}$ as the first $n-1$ rows of, respectively, $\tilde{r}$ and $\tilde{v}$. Denote $\tilde{r}_{n,:}$ and $\tilde{v}_{n,:}$ as the last row of, respectively, $\tilde{r}$ and $\tilde{v}$. By multiplying W^{-1} on both sides of (10.19) and after some manipulation, we obtain the following three equations

$$\dot{\tilde{z}}(t) = A_0 \tilde{z}(t) + A_1 \tilde{z}(t - \tau_1) + A_2 \tilde{z}(t - \tau_1 - \tau_2), \tag{10.20a}$$

$$\dot{\tilde{r}}_{n,:}(t) = \tilde{v}_{n,:}(t), \tag{10.20b}$$

$$\dot{\tilde{v}}_{n,:}(t) = -\tilde{r}_{n,:}(t - \tau_1) + \tilde{r}_{n,:}(t - \tau_1 - \tau_2) - \gamma_c \tilde{v}_{n,:}(t - \tau_1)$$
$$+ \gamma_c \tilde{v}_{n,:}(t - \tau_1 - \tau_2), \tag{10.20c}$$

where

$$\tilde{z} \triangleq \left[\tilde{r}_{1:n-1,:}^T, \tilde{v}_{1:n-1,:}^T \right]^T, \qquad A_0 \triangleq \begin{bmatrix} 0_{(n-1)\times(n-1)} & I_{n-1} \\ 0_{(n-1)\times(n-1)} & 0_{(n-1)\times(n-1)} \end{bmatrix},$$

$$A_1 \triangleq \begin{bmatrix} 0_{(n-1)\times(n-1)} & 0_{(n-1)\times(n-1)} \\ -I_{n-1} & -\gamma_c I_{n-1} \end{bmatrix},$$

$$A_2 \triangleq \begin{bmatrix} 0_{(n-1)\times(n-1)} & 0_{(n-1)\times(n-1)} \\ \widetilde{A} & \gamma_c \widetilde{A} \end{bmatrix},$$

and $\widetilde{A}$ is defined as in (10.4).

Theorem 10.11. *Suppose that the directed fixed graph $\mathscr{G}$ has a directed spanning tree, every agent has a neighbor, and $\gamma_c > \overline{\gamma}_c \triangleq \max_{\mu_i \neq 0} \frac{|\mathrm{Im}(\mu_i)|}{\sqrt{\mathrm{Re}(\mu_i)|\mu_i|}}$, where μ_i is the ith eigenvalue of L defined after (10.2). There exist positive $\overline{\tau_1}$ and $\overline{\tau_2}$ such that for $\tau_1 \in [0, \overline{\tau_1}]$ and $\tau_2 \in [0, \overline{\tau_2}]$, the following three conditions are satisfied:*

(i) $\gamma_c(2\tau_1 + \tau_2) + \frac{(2\tau_1 + \tau_2)\tau_2}{2} < 1$.

(ii) $1 + \lambda_i(A_1)\frac{1 - e^{-s\tau_1}}{s} + \lambda_i(A_2)\frac{1 - e^{-s(\tau_1 + \tau_2)}}{s} \neq 0$, *for all $s \in \mathbb{C}^+$.*

(iii) *The matrix*

$$Q_{\mathrm{sc}} \triangleq (A_0 + A_1 + A_2)^T P_{\mathrm{sc}} + P_{\mathrm{sc}}(A_0 + A_1 + A_2) + \overline{\tau_1} S_{\mathrm{sc}} + (\overline{\tau_1} + \overline{\tau_2})H_{\mathrm{sc}}$$
$$+ \overline{\tau_1}\left[(A_0 + A_1 + A_2)^T P_{\mathrm{sc}} A_1 S_{\mathrm{sc}}^{-1} A_1^T P_{\mathrm{sc}}(A_0 + A_1 + A_2) \right]$$
$$+ (\overline{\tau_1} + \overline{\tau_2})\left[(A_0 + A_1 + A_2)^T P_{\mathrm{sc}} A_2 H_{\mathrm{sc}}^{-1} A_2^T P_{\mathrm{sc}}(A_0 + A_1 + A_2) \right]$$

is symmetric negative definite, where $P_{\mathrm{sc}} \in \mathbb{R}^{(2n-2)\times(2n-2)}$ is a symmetric positive-definite matrix chosen properly such that $(A_0 + A_1 + A_2)^T P_{\mathrm{sc}} +$

$P_{sc}(A_0 + A_1 + A_2)$ *is symmetric negative definite, and* $S_{sc} \in \mathbb{R}^{(2n-2)\times(2n-2)}$ *and* $H_{sc} \in \mathbb{R}^{(2n-2)\times(2n-2)}$ *are arbitrary symmetric positive-definite matrices.*

In addition, if $\tau_1 \in [0, \overline{\tau_1}]$ *and* $\tau_2 \in [0, \overline{\tau_2}]$, *using* (10.18) *for* (3.5), *for all* $r_i(0)$ *and* $v_i(0)$ *and all* $i, j = 1, \ldots, n$, $r_i(t) - r_j(t) \to \Delta_{ij}$ *and* $v_i(t) - v_j(t) \to 0$ *as* $t \to \infty$. *In particular,* $r_i(t) \to \frac{\mathbf{p}^T v(0)}{\tau_2} + \delta_i$ *and* $v_i(t) \to 0$, $i = 1, \ldots, n$, *as* $t \to \infty$, *where* $\mathbf{p} \in \mathbb{R}^n$ *is defined after* (10.3).

Proof: For the first statement, it is straightforward to see that there exist positive $\overline{\tau_1}$ and $\overline{\tau_2}$ such that for $\tau_1 \in [0, \overline{\tau_1}]$ and $\tau_2 \in [0, \overline{\tau_2}]$, Conditions (i) and (ii) are satisfied. For Condition (iii), because $\mathscr{G}$ has a directed spanning tree and each agent has a neighbor, all eigenvalues of $\widetilde{L}$ have positive real parts. Also note that $\widetilde{L} = I_{n-1} - \widetilde{A}$. It follows that

$$A_0 + A_1 + A_2 = \begin{bmatrix} 0_{(n-1)\times(n-1)} & I_{n-1} \\ -\widetilde{L} & -\gamma_c \widetilde{L} \end{bmatrix}.$$

Because all eigenvalues of $\widetilde{L}$ are also the $n - 1$ nonzero eigenvalues of L and $\gamma_c > \overline{\gamma}_c$, it follows from Lemma 7.4 that all eigenvalues of $A_0 + A_1 + A_2$ have negative real parts. Thus there always exists a symmetric positive-definite matrix P_{sc} to guarantee that $(A_0 + A_1 + A_2)^T P_{sc} + P_{sc}(A_0 + A_1 + A_2)$ is symmetric negative definite. A similar analysis to that in Theorem 10.1 shows that there exist positive $\overline{\tau_1}$ and $\overline{\tau_2}$ such that for $\tau_1 \in [0, \overline{\tau_1}]$ and $\tau_2 \in [0, \overline{\tau_2}]$, Condition (iii) is satisfied.

For the second statement, we show that if $\tau_1 \in [0, \overline{\tau_1}]$ and $\tau_2 \in [0, \overline{\tau_2}]$, (10.20a) is asymptotically stable while (10.20b) is stable. It follows from Lemma 1.44 that the stability of the following system

$$\frac{d}{dt}\left[\tilde{z}(t) + A_1 \int_{-\tau_1}^0 \tilde{z}(t+\theta)\,d\theta + A_2 \int_{-\tau_1-\tau_2}^0 \tilde{z}(t+\theta)\,d\theta\right]$$
$$= (A_0 + A_1 + A_2)\tilde{z}(t) \tag{10.21}$$

implies the stability of (10.20a) if Condition (ii) in the theorem is satisfied. Then, consider the Lyapunov function candidate

$$V(\tilde{z}_t) = \chi^T P_{sc} \chi$$
$$+ \int_{-\tau_1}^0 \int_{t+\theta}^t \tilde{z}(\xi)^T S_{sc} \tilde{z}(\xi)\,d\xi\,d\theta + \int_{-\tau_1-\tau_2}^0 \int_{t+\theta}^t \tilde{z}(\xi)^T H_{sc} \tilde{z}(\xi)\,d\xi\,d\theta,$$

where $\chi \triangleq \tilde{z}(t) + A_1 \int_{-\tau_1}^0 \tilde{z}(t+\theta)\,d\theta + A_2 \int_{-\tau_1-\tau_2}^0 \tilde{z}(t+\theta)\,d\theta$. Taking the derivative of $V(\tilde{z}_t)$ along (10.21) gives

$$\dot{V}(\tilde{z}_t) \le \tilde{z}(t)^T Q_{sc} \tilde{z}(t).$$

A similar analysis to that in the proof of Theorem 10.1 shows that if Conditions (ii) and (iii) are satisfied, (10.20a) is asymptotically stable at the origin. For

(10.20b) and (10.20c), we apply the Nyquist stability criterion to find the stability condition. Applying Laplace transform to (10.20b) and (10.20c), we obtain that $\tilde{r}_{n,:}(s) = \frac{s\tilde{r}_{n,:}(0)+\tilde{v}_{n,:}(0)}{s^2+(\gamma_c s+1)[e^{-\tau_1 s}-e^{-(\tau_1+\tau_2)s}]}$. Therefore, the stability of (10.20b) and (10.20c) is determined by the distribution of the roots

$$s^2 + (\gamma_c s + 1)\big[e^{-\tau_1 s - e^{-(\tau_1+\tau_2)s}}\big] = 0. \tag{10.22}$$

Note that (10.22) has two zero roots. To study the other roots, define $g(s) \triangleq (\gamma_c s + 1) \times [e^{-\tau_1 s} - e^{-(\tau_1+\tau_2)s}]/s^2$. By using the Nyquist stability criterion, it follows that the roots of (10.22) are stable if $\mathrm{Re}[g(\iota\omega)] > -1, \forall\omega \in (-\infty, \infty)$. Because

$$
\begin{aligned}
\mathrm{Re}\big[g(\iota\omega)\big] &= \frac{-\gamma_c \sin(\tau_1\omega) + \gamma_c \sin[(\tau_1 + \tau_2)\omega]}{\omega} + \frac{-\cos(\tau_1\omega) + \cos[(\tau_1 + \tau_2)\omega]}{\omega^2} \\
&= \frac{-\gamma_c \sin(\tau_1\omega) + \gamma_c \sin[(\tau_1 + \tau_2)\omega]}{\omega} - \frac{2\sin[\frac{(2\tau_1+\tau_2)}{2}\omega]\sin(\frac{\tau_2}{2}\omega)}{\omega^2} \\
&\geq -\gamma_c\tau_1 - \gamma_c(\tau_1 + \tau_2) - \frac{(2\tau_1 + \tau_2)\tau_2}{2},
\end{aligned}
$$

it follows that (10.20b) and (10.20c) are marginally stable under Condition (i) of the theorem. Note that the asymptotical stability of (10.20a) implies that $\lim_{t\to\infty} \tilde{z}(t) = \mathbf{0}_{2n-2}$. Also by using the final value theorem, it follows that $\lim_{t\to\infty} \tilde{r}_{n,:}(t) = \frac{\tilde{v}_{n,:}(0)}{\tau_2}$. After similar manipulation to that in Theorem 10.1, it follows that $r_i(t) \to \frac{\mathbf{p}^T v(0)}{\tau_2} + \delta_i$ and $v_i(t) \to 0$ (and hence $r_i(t) - r_j(t) \to \Delta_{ij}$ and $v_i(t) - v_j(t) \to 0$) as $t \to \infty$. ∎

Remark 10.12 Due to the existence of the communication delay, using (10.18) for (3.5), the final velocity is dampened to zero instead of a possible nonzero constant as compared with the standard consensus algorithm for double-integrator dynamics [248, Chap. 4]. Also note that if there exists only the input delay, the final velocity is a possibly nonzero constant, which is consistent with the results using the standard consensus algorithm for double-integrator dynamics in [248, Chap. 4].

Remark 10.13 Note that compared with the case for single-integrator dynamics in Sect. 10.2.1, the case for double-integrator dynamics requires more stringent conditions to guarantee coordination.

10.3.2 Coordinated Tracking when the Leader's Velocity is Constant

In this subsection, we assume that in addition to n followers, labeled as agents or followers 1 to n, there exists a leader, labeled as agent 0, with position r_0 and ve-

locity v_0. Here we assume that v_0 is constant. Let $\mathscr{G} \triangleq (\mathscr{V}, \mathscr{E})$ and $\overline{\mathscr{G}} \triangleq (\overline{\mathscr{V}}, \overline{\mathscr{E}})$ be defined as in Sect. 10.2.2.

Consider the following coordinated tracking algorithm with both communication and input delays for the n followers with double-integrator dynamics given by (3.5) as

$$
u_i(t) = -\frac{1}{\sum_{j=0}^n a_{ij}} \sum_{j=0}^n a_{ij} \big[r_i(t-\tau_1) - r_j(t-\tau_1-\tau_2) \big]
$$
$$
- \frac{\gamma_r}{\sum_{j=0}^n a_{ij}} \sum_{j=0}^n a_{ij} \big[v_i(t-\tau_1) - v_j(t-\tau_1-\tau_2) \big], \quad i = 1, \dots, n,
$$
(10.23)

where τ_1 and τ_2 are, respectively, the input and communication delays, a_{ij}, $i = 1, \dots, n$, $j = 0, \dots, n$, is defined as in (10.10), and γ_r is a positive gain. Note that in $\overline{\mathscr{G}}$ if the leader has directed paths to all followers 1 to n, it follows that $\sum_{j=0}^n a_{ij} > 0$, $i = 1, \dots, n$.

Using (10.23), (3.5) can be written in a vector form as

$$
\dot{\overline{\chi}}(t) = \overline{A}_0 \overline{\chi}(t) + \overline{A}_1 \overline{\chi}(t-\tau_1) + \overline{A}_2 \overline{\chi}(t-\tau_1-\tau_2) + R_{\mathrm{sr}},
$$
(10.24)

where $\bar{r} \triangleq [r_1 - r_0, \dots, r_n - r_0]^T$, $\bar{v} \triangleq [v_1 - v_0, \dots, v_n - v_0]^T$, $\overline{\chi} \triangleq [\bar{r}^T, \bar{v}^T]^T$, $\overline{A}_0 \triangleq \begin{bmatrix} 0_{n \times n} & I_n \\ 0_{n \times n} & 0_{n \times n} \end{bmatrix}$, $\overline{A}_1 \triangleq \begin{bmatrix} 0_{n \times n} & 0_{n \times n} \\ -I_n & -\gamma_r I_n \end{bmatrix}$, $\overline{A}_2 \triangleq \begin{bmatrix} 0_{n \times n} & 0_{n \times n} \\ \overline{A} & \gamma_r \overline{A} \end{bmatrix}$, and $R_{\mathrm{sr}} \triangleq \begin{bmatrix} \mathbf{0}_n \\ -\tau_2 v_0 \mathbf{1}_n \end{bmatrix}$. Note that here $\overline{A}$ is defined before (10.11) and we have used the fact that v_0 is constant. By letting $\zeta \triangleq (\overline{A}_0 + \overline{A}_1 + \overline{A}_2)^{-1} R_{\mathrm{sr}}$ and $\widehat{\chi} \triangleq \overline{\chi} - \zeta$, we can transform (10.24) as

$$
\dot{\widehat{\chi}} = \overline{A}_0 \widehat{\chi}(t) + \overline{A}_1 \widehat{\chi}(t-\tau_1) + \overline{A}_2 \widehat{\chi}(t-\tau_1-\tau_2).
$$
(10.25)

Theorem 10.14. *Suppose that in $\overline{\mathscr{G}}$ the leader has directed paths to all followers 1 to n and $\gamma_r > \overline{\gamma}_r \triangleq \max_i \frac{|\mathrm{Im}(\mu_i)|}{\sqrt{\mathrm{Re}(\mu_i)}|\mu_i|}$, where μ_i is the ith eigenvalue of $I_n - \overline{A}$. There exist positive $\overline{\tau_1}$ and $\overline{\tau_2}$ such that for $\tau_1 \in [0, \overline{\tau_1}]$ and $\tau_2 \in [0, \overline{\tau_2}]$, the following two conditions are satisfied:*

(i) $1 + \lambda_i(\overline{A}_1) \frac{1 - e^{-s\tau_1}}{s} + \lambda_i(\overline{A}_2) \frac{1 - e^{-s(\tau_1 + \tau_2)}}{s} \neq 0$, *for all $s \in \mathbb{C}^+$.*
(ii) *The matrix*

$$
Q_{\mathrm{sr}} \triangleq (\overline{A}_0 + \overline{A}_1 + \overline{A}_2)^T P_{\mathrm{sr}} + P_{\mathrm{sr}}(\overline{A}_0 + \overline{A}_1 + \overline{A}_2) + \tau_1 S_{\mathrm{sr}} + (\tau_1 + \tau_2) H_{\mathrm{sr}}
$$
$$
+ \tau_1 \big[(\overline{A}_0 + \overline{A}_1 + \overline{A}_2)^T P_{\mathrm{sr}} \overline{A}_1 S_{\mathrm{sr}}^{-1} \overline{A}_1^T P_{\mathrm{sr}}(\overline{A}_0 + \overline{A}_1 + \overline{A}_2) \big]
$$
$$
+ (\tau_1 + \tau_2) \big[(\overline{A}_0 + \overline{A}_1 + \overline{A}_2)^T P_{\mathrm{sr}} \overline{A}_2 H_{\mathrm{sr}}^{-1} \overline{A}_2^T P_{\mathrm{sr}}(\overline{A}_0 + \overline{A}_1 + \overline{A}_2) \big]
$$

is symmetric negative definite, where $P_{\mathrm{sr}} \in \mathbb{R}^{2n \times 2n}$ is a symmetric positive-definite matrix chosen properly such that $(\overline{A}_0 + \overline{A}_1 + \overline{A}_2)^T P_{\mathrm{sr}} + P_{\mathrm{sr}}(\overline{A}_0 + $

$\overline{A}_1 + \overline{A}_2)$ is symmetric negative definite, and $S_{\mathrm{sr}} \in \mathbb{R}^{2n \times 2n}$ and $H_{\mathrm{sr}} \in \mathbb{R}^{2n \times 2n}$ are arbitrary symmetric positive-definite matrices.

In addition, if $\tau_1 \in [0, \overline{\tau_1}]$ and $\tau_2 \in [0, \overline{\tau_2}]$, using (10.23) for (3.5), $\bar{r}(t) \rightarrow \tau_2 v_0 (I_n - \overline{A})^{-1} \mathbf{1}_n$ and $\bar{v}(t) \rightarrow \mathbf{0}_n$ as $t \rightarrow \infty$.

Proof: For the first statement, it is straightforward to show that Condition (i) is satisfied. For Condition (ii), note that $\overline{A}_0 + \overline{A}_1 + \overline{A}_2 = \begin{bmatrix} \mathbf{0}_{n \times n} & I_n \\ -(I_n - \overline{A}) & -\gamma_r (I_n - \overline{A}) \end{bmatrix}$. Because in $\mathscr{G}$ the leader has directed paths to all followers, it follows from Lemma 10.1 that all eigenvalues of $I_n - \overline{A}$ have positive real parts. Because $\gamma_r > \overline{\gamma}_r$, it thus follows from Lemma 7.4 that all eigenvalues of $\overline{A}_0 + \overline{A}_1 + \overline{A}_2$ have negative real parts. The rest of the proof is similar to that in Theorem 10.1.

For the second statement, it follows from Lemma 1.44 that the stability of the following system

$$\frac{d}{dt}\left[\widehat{\chi}(t) + \overline{A}_1 \int_{-\tau_1}^{0} \widehat{\chi}(t + \theta)\,d\theta + \overline{A}_2 \int_{-\tau_1 - \tau_2}^{0} \widehat{\chi}(t + \theta)\,d\theta \right]$$
$$= (\overline{A}_0 + \overline{A}_1 + \overline{A}_2)\widehat{\chi}(t) \tag{10.26}$$

implies the stability of (10.25) under Condition (i) of the theorem. Then, consider a Lyapunov function candidate

$$V(\widehat{\chi}_t) = \varphi^T P_{\mathrm{sr}} \varphi + \int_{-\tau_1}^{0} \int_{t+\theta}^{t} \widehat{\chi}^T(\xi) S_{\mathrm{sr}} \widehat{\chi}(\xi)\,d\xi\,d\theta$$
$$+ \int_{-\tau_1 - \tau_2}^{0} \int_{t+\theta}^{t} \widehat{\chi}^T(\xi) H_{\mathrm{sr}} \widehat{\chi}(\xi)\,d\xi\,d\theta,$$

where $\varphi \triangleq \widehat{\chi}(t) + \overline{A}_1 \int_{-\tau_1}^{0} \widehat{\chi}(t+\theta)\,d\theta + \overline{A}_2 \int_{-\tau_1 - \tau_2}^{0} \widehat{\chi}(t+\theta)\,d\theta$. Taking the derivative of $V(\widehat{\chi}_t)$ along (10.26) gives

$$\dot{V}(\widehat{\chi}_t) \leq \widehat{\chi}^T(t) Q_{\mathrm{sr}} \widehat{\chi}(t),$$

where we have used Lemma 1.23 to derive the inequality. A similar analysis to that in the proof of Theorem 10.1 shows that (10.25) is asymptotically stable at the origin, which implies that $\widehat{\chi}(t) \rightarrow \mathbf{0}_{2n}$ as $t \rightarrow \infty$. Note that $\zeta = [\tau_2 v_0 [(I_n - \overline{A})^{-1} \mathbf{1}_n]^T, \mathbf{0}_n^T]^T$ by computation and $\overline{\chi} = \widehat{\chi} + \zeta$. It follows that $\bar{r}(t) \rightarrow \tau_2 v_0 (I_n - \overline{A})^{-1} \mathbf{1}_n$ and $\bar{v}(t) \rightarrow \mathbf{0}_n$ as $t \rightarrow \infty$. ∎

Corollary 10.1. *Suppose that the conditions in Theorem 10.14 hold. If $v_0 = 0$, then $r_i(t) \rightarrow r_0$ and $v_i(t) \rightarrow 0$ as $t \rightarrow \infty$.*

Remark 10.15 Note that different from the results in the case for single-integrator dynamics in Sect. 10.2.2, the tracking errors of the followers $r_i(t) - r_0(t)$ might not approach zero but approach possibly different constants in the case of double-integrator dynamics.

10.3.3 Coordinated Tracking with Full Access to the Leader's Acceleration

In this subsection, we consider the case where the leader's position r_0 and velocity v_0 are varying. We assume that all followers have access to $\dot{v}_0$. We also assume that $|v_0| < \delta_v$, $|\dot{v}_0| < \delta_a$, and $|\ddot{v}_0| < \delta_{\dot{a}}$, where δ_v, δ_a and $\delta_{\dot{a}}$ are positive constants.

Consider the following coordinated tracking algorithm with both communication and input delays for the n followers with double-integrator dynamics given by (3.5) as

$$u_i(t) = \dot{v}_0(t - \tau_1 - \tau_2) - \frac{1}{\sum_{j=0}^n a_{ij}} \sum_{j=0}^n a_{ij}\big\{\big[r_i(t-\tau_1) - r_j(t - \tau_1 - \tau_2)\big]$$
$$+ \gamma_t\big[v_i(t - \tau_1) - v_j(t - \tau_1 - \tau_2)\big]\big\}, \quad i = 1, \dots, n, \tag{10.27}$$

where τ_1 and τ_2 are, respectively, the input and communication delays, a_{ij}, $i = 1, \dots, n$, $j = 0, \dots, n$, is defined as in (10.10), and γ_t is a positive gain. Using (10.27), (3.5) can be written in a vector form as

$$\dot{\overline{\chi}}(t) = \overline{A}_0\overline{\chi}(t) + \overline{A}_1\overline{\chi}(t - \tau_1) + \overline{A}_2\overline{\chi}(t - \tau_1 - \tau_2) + R_{\mathrm{st}}, \tag{10.28}$$

where $\overline{\chi}$ is defined as in (10.24), $\overline{A}_0$, $\overline{A}_1$, and $\overline{A}_2$ are defined as in (10.24) with γ_r replaced with γ_t, $R_{\mathrm{st}} \triangleq \big[\begin{smallmatrix} \mathbf{0}_n \\ R_1 \end{smallmatrix}\big]$, and $R_1 \triangleq \mathbf{1}_n[\dot{v}_0(t - \tau_1 - \tau_2) - \dot{v}_0(t) + r_0(t - \tau_1 - \tau_2) - r_0(t - \tau_1) + \gamma_t v_0(t - \tau_1 - \tau_2) - v_0(t - \tau_1)]$. By using (1.10), it follows that $R_1 = -\mathbf{1}_n\int_{-\tau_1-\tau_2}^0 \ddot{v}_0(t+\theta)\,d\theta - \mathbf{1}_n\int_{-\tau_1-\tau_2}^{-\tau_1} v_0(t+\theta)\,d\theta - \gamma_t\mathbf{1}_n\int_{-\tau_1-\tau_2}^{-\tau_1} \dot{v}_0(t+\theta)\,d\theta$.

Theorem 10.16. *Suppose that in $\overline{\mathscr{G}}$ the leader has directed paths to all followers* 1 *to n and $\gamma_t > \overline{\gamma}_r$, where $\overline{\gamma}_r$ is defined in Theorem* 10.14. *There exist positive $\overline{\tau_1}$ and $\overline{\tau_2}$ such that for $\tau_1 \in [0, \overline{\tau_1}]$ and $\tau_2 \in [0, \overline{\tau_2}]$,*

$$Q_{\mathrm{st}} \triangleq (\overline{A}_0 + \overline{A}_1 + \overline{A}_2)^T P_{\mathrm{sr}} + P_{\mathrm{sr}}(\overline{A}_0 + \overline{A}_1 + \overline{A}_2)$$
$$+ \tau_1\big(P_{\mathrm{sr}}\overline{A}_1\overline{A}_0 P_{\mathrm{sr}}^{-1}\overline{A}_0^T\overline{A}_1^T P_{\mathrm{sr}} + P_{\mathrm{sr}}(\overline{A}_1)^2 P_{\mathrm{sr}}^{-1}\big(\overline{A}_1^T\big)^2 P_{\mathrm{sr}}$$
$$+ P_{\mathrm{sr}}\overline{A}_1\overline{A}_2 P_{\mathrm{sr}}^{-1}\overline{A}_2^T\overline{A}_1^T P_{\mathrm{sr}} + 3q_s P_{\mathrm{sr}}\big)$$
$$+ (\tau_1 + \tau_2)\big(P_{\mathrm{sr}}\overline{A}_2\overline{A}_0 P_{\mathrm{sr}}^{-1}\overline{A}_0^T\overline{A}_2^T P_{\mathrm{sr}} + P_{\mathrm{sr}}\overline{A}_2\overline{A}_1 P_{\mathrm{sr}}^{-1}\overline{A}_1^T\overline{A}_2^T P_{\mathrm{sr}}$$
$$+ P_{\mathrm{sr}}(\overline{A}_2)^2 P_{\mathrm{sr}}^{-1}\big(\overline{A}_2^T\big)^2 P_{\mathrm{sr}} + 3q_s P_{\mathrm{sr}}\big)$$

is symmetric negative definite, where P_{sr} is defined in Theorem 10.14 *and q_s is an arbitrary real number satisfying $q_s > 1$. In addition, if $\tau_1 \in [0, \overline{\tau_1}]$ and $\tau_2 \in [0, \overline{\tau_2}]$, using (10.27) for (3.5), for all $r_i(0)$ and $v_i(0)$ and all $i = 1, \dots, n$, $|r_i(t) - r_0(t)|$ and $|v_i(t) - v_0(t)|$ are uniformly ultimately bounded. In particular, the ultimate bound for $\|\overline{\chi}(t)\|$ is given by $\frac{\lambda_{\max}(P_{\mathrm{sr}})a_s}{\lambda_{\min}(P_{\mathrm{sr}})\kappa_s\lambda_{\min}(-Q_{\mathrm{st}})}$, where $a_s \triangleq 2[\|P_{\mathrm{sr}}\| + \|P_{\mathrm{sr}}\overline{A}_1\|\tau_1 + \|P_{\mathrm{sr}}\overline{A}_2\|(\tau_1 + \tau_2)][(\tau_1 + \tau_2)\delta_{\dot{a}} + \tau_2\delta_v + \gamma_t\tau_2\delta_a]$, and κ_s is an arbitrary real number satisfying $0 < \kappa_s < 1$.*

Proof: The proof for the first statement is similar to that in Theorem 10.14 and is hence omitted here. For the second statement, using (1.10), we transform (10.28) to the following system

$$
\frac{d}{dt}\overline{\chi}(t) = (\overline{A}_0 + \overline{A}_1 + \overline{A}_2)\overline{\chi}(t) - \overline{A}_1 \int_{-\tau_1}^0 \dot{\overline{\chi}}(t+\theta)\, d\theta
$$

$$
- \overline{A}_2 \int_{-\tau_1-\tau_2}^0 \dot{\overline{\chi}}(t+\theta)\, d\theta + R_{\mathrm{st}}
$$

$$
= (\overline{A}_0 + \overline{A}_1 + \overline{A}_2)\overline{\chi}(t)
$$

$$
- \overline{A}_1 \int_{-\tau_1}^0 \big[\overline{A}_0\overline{\chi}(t+\theta)
$$

$$
+ \overline{A}_1\overline{\chi}(t-\tau_1+\theta) + \overline{A}_2\overline{\chi}(t-\tau_1-\tau_2+\theta)\big]\, d\theta
$$

$$
- \overline{A}_2 \int_{-\tau_1-\tau_2}^0 \big[\overline{A}_0\overline{\chi}(t+\theta) + \overline{A}_1\overline{\chi}(t-\tau_1+\theta)
$$

$$
+ \overline{A}_2\overline{\chi}(t-\tau_1-\tau_2+\theta)\big]\, d\theta
$$

$$
- \overline{A}_1 \int_{-\tau_1}^0 R_{\mathrm{st}}(t+\theta)\, d\theta - \overline{A}_2 \int_{-\tau_1-\tau_2}^0 R_{\mathrm{st}}(t+\theta)\, d\theta + R_{\mathrm{st}}
$$

$$
= (\overline{A}_0 + \overline{A}_1 + \overline{A}_2)\overline{\chi}(t) - \overline{A}_1\overline{A}_0 \int_{-\tau_1}^0 \overline{\chi}(t+\theta)\, d\theta - \overline{A}_1^2 \int_{-2\tau_1}^{-\tau_1} \overline{\chi}(t+\theta)\, d\theta
$$

$$
- \overline{A}_1\overline{A}_2 \int_{-2\tau_1-\tau_2}^{-\tau_1-\tau_2} \overline{\chi}(t+\theta)\, d\theta - \overline{A}_2\overline{A}_0 \int_{-\tau_1-\tau_2}^0 \overline{\chi}(t+\theta)\, d\theta
$$

$$
- \overline{A}_2\overline{A}_1 \int_{-2\tau_1-\tau_2}^{-\tau_1} \overline{\chi}(t+\theta)\, d\theta - \overline{A}_2^2 \int_{-2\tau_1-2\tau_2}^{-\tau_1-\tau_2} \overline{\chi}(t+\theta)\, d\theta
$$

$$
- \overline{A}_1 \int_{-\tau_1}^0 R_{\mathrm{st}}(t+\theta)\, d\theta - \overline{A}_2 \int_{-\tau_1-\tau_2}^0 R_{\mathrm{st}}(t+\theta)\, d\theta + R_{\mathrm{st}}.
$$

Consider the Lyapunov function candidate $V(\overline{\chi}) = \overline{\chi}^T(t)P_{\mathrm{sr}}\overline{\chi}(t)$. Taking the derivative of $V(\overline{\chi})$ along (10.28) gives

$$
\dot{V}(\overline{\chi}) \le \overline{\chi}^T \big[(\overline{A}_0 + \overline{A}_1 + \overline{A}_2)^T P_{\mathrm{sr}} + P_{\mathrm{sr}}(\overline{A}_0 + \overline{A}_1 + \overline{A}_2)\big]\overline{\chi}
$$

$$
+ \tau_1 \overline{\chi}^T P_{\mathrm{sr}}\overline{A}_1\overline{A}_0 P_{\mathrm{sr}}^{-1}\overline{A}_0^T \overline{A}_1^T P_{\mathrm{sr}}\overline{\chi}
$$

$$
+ \int_{-\tau_1}^0 \overline{\chi}^T(t+\theta)P_{\mathrm{sr}}\overline{\chi}(t+\theta)\, d\theta + \tau_1 \overline{\chi}^T P_{\mathrm{sr}}(\overline{A}_1)^2 P_{\mathrm{sr}}^{-1}\big(\overline{A}_1^T\big)^2 P_{\mathrm{sr}}\overline{\chi}
$$

$$
+ \int_{-2\tau_1}^{-\tau_1} \overline{\chi}^T(t+\theta)P_{\mathrm{sr}}\overline{\chi}(t+\theta)\, d\theta + \tau_1 \overline{\chi}^T P_{\mathrm{sr}}\overline{A}_1\overline{A}_2 P_{\mathrm{sr}}^{-1}\overline{A}_2^T \overline{A}_1^T P_{\mathrm{sr}}\overline{\chi}
$$

$$
+ \int_{-2\tau_1-\tau_2}^{-\tau_1-\tau_2} \overline{\chi}^T(t+\theta)P_{\mathrm{sr}}\overline{\chi}(t+\theta)\, d\theta
$$

$$
+ (\tau_1+\tau_2)\overline{\chi}^T P_{\mathrm{sr}}\overline{A}_2\overline{A}_0 P_{\mathrm{sr}}^{-1}\overline{A}_0^T \overline{A}_2^T P_{\mathrm{sr}}\overline{\chi}
$$

$$+ \int_{-\tau_1 - \tau_2}^{0} \overline{\chi}^T(t + \theta) P_{\text{sr}} \overline{\chi}(t + \theta) \, d\theta$$

$$+ (\tau_1 + \tau_2) \overline{\chi}^T P_{\text{sr}} \overline{A}_2 \overline{A}_1 P_{\text{sr}}^{-1} \overline{A}_1^T \overline{A}_2^T P_{\text{sr}} \overline{\chi}$$

$$+ \int_{-2\tau_1 - \tau_2}^{-\tau_1} \overline{\chi}^T(t + \theta) P_{\text{sr}} \overline{\chi}(t + \theta) \, d\theta$$

$$+ (\tau_1 + \tau_2) \overline{\chi}^T P (\overline{A}_2)^2 P_{\text{sr}}^{-1} \left(\overline{A}_2^T \right)^2 P_{\text{sr}} \overline{\chi}$$

$$+ \int_{-2\tau_1 - 2\tau_2}^{-\tau_1 - \tau_2} \overline{\chi}^T(t + \theta) P_{\text{sr}} \overline{\chi}(t + \theta) \, d\theta$$

$$+ 2 \|\overline{\chi}\| \|P_{\text{sr}}\| \left[(\tau_1 + \tau_2) \delta_{\dot{a}} + \tau_2 \delta_v + \gamma_t \tau_2 \delta_a \right]$$

$$+ 2 \|\overline{\chi}\| \|P_{\text{sr}} \overline{A}_1\| \tau_1 \left[(\tau_1 + \tau_2) \delta_{\dot{a}} + \tau_2 \delta_v + \gamma_t \tau_2 \delta_a \right]$$

$$+ 2 \|\overline{\chi}\| \|P_{\text{sr}} \overline{A}_2\| (\tau_1 + \tau_2) \left[(\tau_1 + \tau_2) \delta_{\dot{a}} + \tau_2 \delta_v + \gamma_t \tau_2 \delta_a \right],$$

where we have used Lemma 1.23 and the facts that $|v_0| < \delta_v$, $|\dot{v}_0| < \delta_a$, and $|\ddot{v}_0| < \delta_{\dot{a}}$ to derive the inequality. Take $p(s) = q_s s$. If $V[\overline{\chi}(t + \theta)] < p\{V[\overline{\chi}(t)]\} = q_s V[\overline{\chi}(t)]$ for $-2\tau_1 - 2\tau_2 \leq \theta \leq 0$, by following a similar analysis to that in the proof of Theorem 10.6, we have

$$\dot{V}(\overline{\chi}) \leq \overline{\chi}^T(t) Q_{\text{st}} \overline{\chi}(t) + a_s \|\overline{\chi}(t)\|.$$

If $\tau_1 \in [0, \overline{\tau_1}]$ and $\tau_2 \in [0, \overline{\tau_2}]$, we have that $\lambda_{\min}(-Q_{\text{st}}) > 0$. Given $0 < \kappa_s < 1$, if $\|\overline{\chi}(t)\| \geq \frac{a_s}{\kappa_s \lambda_{\min}(-Q_{\text{st}})}$, we can obtain

$$\dot{V}(\overline{\chi}) \leq -(1 - \kappa_s) \lambda_{\min}(-Q_{\text{st}}) \|\overline{\chi}(t)\|^2 - \kappa_s \lambda_{\min}(-Q_{\text{st}}) \|\overline{\chi}(t)\|^2 + a_s \|\overline{\chi}(t)\|$$
$$\leq -(1 - \kappa_s) \lambda_{\min}(-Q_{\text{st}}) \|\overline{\chi}(t)\|^2.$$

Therefore, it follows from Lemma 1.42 that $\|\overline{\chi}(t)\|$ is uniformly ultimately bounded, which implies that $|r_i(t) - r_0(t)|$ and $|v_i(t) - v_0(t)|$ are uniformly ultimately bounded. Moreover, it can be computed that the ultimate bound for $\|\overline{\chi}(t)\|$ is given by $\frac{\lambda_{\max}(P_{\text{sr}}) a_s}{\lambda_{\min}(P_{\text{sr}}) \kappa_s \lambda_{\min}(-Q_{\text{st}})}$ by following a similar analysis to that in [145, pp. 172–174]. ∎

10.3.4 Coordinated Tracking with Partial Access to the Leader's Acceleration

In this subsection, we assume the leader's varying position r_0, velocity v_0, and acceleration $\dot{v}_0$ are available to only a subset of all followers. We assume that $|r_0|$, $|v_0|$, and $|\dot{v}_0|$ are bounded. We also assume that there exists only the communication delay.

Consider the following coordinated tracking algorithm for the n followers with double-integrator dynamics given by (3.5) as

$$u_i(t) = \frac{1}{\sum_{j=0}^{n} a_{ij}} \sum_{j=0}^{n} a_{ij} \big\{ \dot{v}_j(t - \tau_2) - \big[r_i(t) - r_j(t - \tau_2) \big]$$

$$- \gamma_{ft} \big[v_i(t) - v_j(t - \tau_2) \big] \big\}, \quad i = 1, \ldots, n, \tag{10.29}$$

where τ_2 is the communication delay, a_{ij}, $i = 1, \ldots, n$, $j = 0, \ldots, n$, is defined as in (10.10), and γ_{ft} is a positive gain. Using (10.29), (3.5) can be written in a vector form as

$$\dot{\overline{\chi}}(t) = D_f \dot{\overline{\chi}}(t - \tau_2) + \overline{A}_{f0} \overline{\chi} + \overline{A}_{f1} \overline{\chi}(t - \tau_2) + R_{\text{sft}}, \tag{10.30}$$

where $\overline{\chi}$ is defined as in (10.24), $D_f \triangleq \begin{bmatrix} 0_{n \times n} & 0_{n \times n} \\ 0_{n \times n} & \overline{A} \end{bmatrix}$, $\overline{A}_{f0} \triangleq \begin{bmatrix} 0_{n \times n} & I_n \\ -I_n & -\gamma_{ft} I_n \end{bmatrix}$, $\overline{A}_{f1} \triangleq \begin{bmatrix} 0_{n \times n} & 0_{n \times n} \\ \overline{A} & \gamma_{ft} \overline{A} \end{bmatrix}$, $R_{\text{sft}} \triangleq \begin{bmatrix} 0_n \\ R_2 \end{bmatrix}$, and $R_2 \triangleq [\dot{v}_0(t - \tau_2) - \dot{v}_0(t)]\mathbf{1}_n - [r_0(t) - r_0(t - \tau_2)]\mathbf{1}_n - \gamma_{ft}[v_0(t) - v_0(t - \tau_2)]\mathbf{1}_n$. Note that here $\overline{A}$ is defined before (10.11).

Theorem 10.17. *Suppose that in $\overline{\mathscr{G}}$ the leader has directed paths to all followers* 1 *to* n*, and $\gamma_{ft} > \overline{\gamma}_r$, where $\overline{\gamma}_r$ is defined in Theorem* 10.14*. Using* (10.29) *for* (3.5)*, for all $r_i(0)$ and $v_i(0)$ and all $i = 1, \ldots, n$, $|r_i(t) - r_0(t)|$ and $|v_i(t) - v_0(t)|$ are uniformly ultimately bounded if*

$$\lambda > 2 q_{\text{sf}} \sqrt{\frac{\lambda_{\max}(P_{\text{sr}})}{\lambda_{\min}(P_{\text{sr}})}} \| P_{\text{sr}} (\overline{A}_{f0} D_f + \overline{A}_{f1}) \| + 2 \| P_{\text{sr}} \overline{A}_{f1} \|, \tag{10.31}$$

where $\lambda \triangleq \lambda_{\min}[-(\overline{A}_{f0} + \overline{A}_{f1})^T P_{\text{sr}} - P_{\text{sr}}(\overline{A}_{f0} + \overline{A}_{f1})]$,[2] $P_{\text{sr}} \in \mathbb{R}^{2n \times 2n}$ is a symmetric positive-definite matrix chosen properly such that $(\overline{A}_{f0} + \overline{A}_{f1})^T P_{\text{sr}} + P_{\text{sr}}(\overline{A}_{f0} + \overline{A}_{f1})$ is symmetric negative definite, and q_{sf} is an arbitrary real number satisfying $q_{\text{sf}} > 1$.

Proof: First, it follows from Lemma 8.1 that $\rho(\overline{A}) < 1$, which implies that $\rho(D_f) < 1$. Therefore, the neutral operator $\mathscr{D}\overline{\chi}_t = \overline{\chi} - D_f \overline{\chi}(t - \tau_2)$ is stable. Consider a Lyapunov function candidate $V(\overline{\chi}) = \overline{\chi}^T(t) P_{\text{sr}} \overline{\chi}(t)$. Taking the derivative of $V(\overline{\chi})$ along (10.30) gives

$$\dot{V}(\mathscr{D}\overline{\chi}_t) = 2(\mathscr{D}\overline{\chi}_t)^T P_{\text{sr}} \big[\overline{A}_{f0} \overline{\chi} + \overline{A}_{f1} \overline{\chi}(t - \tau_2) + R_{\text{sft}} \big]$$

$$= 2(\mathscr{D}\overline{\chi}_t)^T P_{\text{sr}} \big[\overline{A}_{f0}(\mathscr{D}\overline{\chi}_t) + \overline{A}_{f0} D_f \overline{\chi}(t - \tau_2) + \overline{A}_{f1} \overline{\chi}(t - \tau_2) + R_{\text{sft}} \big]$$

---

[2] Note that $\overline{A}_{f0} + \overline{A}_{f1} = \begin{bmatrix} 0_{n \times n} & I_n \\ -(I_n - \overline{A}) & -\gamma_{ft}(I_n - \overline{A}) \end{bmatrix}$. Similar to the proof of the first statement in Theorem 10.14, it follows that all eigenvalues of $\overline{A}_{f0} + \overline{A}_{f1}$ have negative real parts under the condition of the theorem.

$$= (\mathscr{D}\overline{\chi}_t)^T \left[(\overline{A}_{f0} + \overline{A}_{f1})^T P_{\mathrm{sr}} + P_{\mathrm{sr}}(\overline{A}_{f0} + \overline{A}_{f1}) \right] (\mathscr{D}\overline{\chi}_t)$$
$$+ 2(\mathscr{D}\overline{\chi}_t)^T P_{\mathrm{sr}} (\overline{A}_{f0} D_f + \overline{A}_{f1}) \overline{\chi}(t - \tau_2)$$
$$- 2(\mathscr{D}\overline{\chi}_t)^T P_{\mathrm{sr}} \overline{A}_{f1} (\mathscr{D}\overline{\chi}_t) + 2(\mathscr{D}\overline{\chi}_t)^T P_{\mathrm{sr}} R_{\mathrm{sft}}.$$

Let $p(s) = q_{\mathrm{sf}}^2 s$. If $V[\overline{\chi}(\theta)] < p[V(\mathscr{D}\overline{\chi}_t)]$ for $t - \tau_2 \leq \xi \leq t$, it is equivalent that $\overline{\chi}^T(\theta) P_{\mathrm{sr}} \overline{\chi}(\theta) < q_{\mathrm{sf}}^2 (\mathscr{D}\overline{\chi}_t)^T P_{\mathrm{sr}} (\mathscr{D}\overline{\chi}_t)$ for $t - \tau_2 \leq \theta \leq t$. Therefore, we have $\|\overline{\chi}(t - \tau_2)\| < q_{\mathrm{sf}} \sqrt{\frac{\lambda_{\max}(P_{\mathrm{sr}})}{\lambda_{\min}(P_{\mathrm{sr}})}} \|\mathscr{D}\overline{\chi}_t\|$. Thus, it follows that

$$\dot{V}(\mathscr{D}\overline{\chi}_t) \leq - \lambda \|\mathscr{D}\overline{\chi}_t\|^2 + 2q_{\mathrm{sf}} \sqrt{\frac{\lambda_{\max}(P_{\mathrm{sr}})}{\lambda_{\min}(P_{\mathrm{sr}})}} \|P_{\mathrm{sr}}(\overline{A}_{f0} D_f + \overline{A}_{f1})\| \|\mathscr{D}\overline{\chi}_t\|^2$$
$$+ 2\|P_{\mathrm{sr}} \overline{A}_{f1}\| \|\mathscr{D}\overline{\chi}_t\|^2 + 2\|P_{\mathrm{sr}} R_{\mathrm{sft}}\| \|\mathscr{D}\overline{\chi}_t\|.$$

Therefore, if (10.31) holds, it follows from Lemma 1.43 that $\|\overline{\chi}(t)\|$ is uniformly ultimately bounded, which implies that $|r_i(t) - r_0(t)|$ and $|v_i(t) - v_0(t)|$ are uniformly ultimately bounded. ∎

Remark 10.18 Note that different from the case for single-integrator dynamics where the tracking errors are bounded no matter how large the communication delay is, a certain delay independent condition (10.31) has to be satisfied beforehand to ensure the tracking errors are uniformly ultimate bounded in the case of double-integrator dynamics.

10.4 Simulation

In this section, we present simulation results to validate the theoretical results in Sects. 10.2 and 10.3. For the leaderless coordination problem, we consider a team of six agents with the adjacency matrix $\mathscr{A}$ chosen as

$$\mathscr{A} = \begin{bmatrix} 0 & 5 & 0 & 2.5 & 0 & 2.5 \\ 8 & 0 & 1 & 0 & 1 & 0 \\ 0 & 2 & 0 & 2 & 3 & 3 \\ 1 & 0 & 1 & 0 & 8 & 0 \\ 0 & 1.2 & 0 & 1.8 & 0 & 7 \\ 5 & 1 & 0 & 2 & 2 & 0 \end{bmatrix}.$$

For the leader-following coordination problem, we consider a team consisting of six followers and one leader. The adjacency matrix $\mathscr{A}$ associated with the six followers is defined as
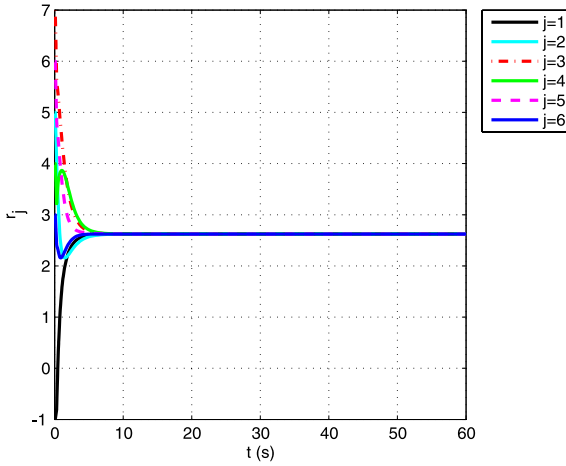
Fig. 10.1 Agents' positions using (10.1)

$$\mathscr{A} = \begin{bmatrix} 0 & 1 & 0 & 1 & 0 & 0 \\ 8 & 0 & 1 & 0 & 1 & 0 \\ 0 & 3 & 0 & 0 & 0 & 3 \\ 1 & 0 & 0 & 0 & 1 & 0 \\ 0 & 1.2 & 0 & 1.8 & 0 & 7 \\ 5 & 1 & 0 & 0 & 4 & 0 \end{bmatrix}.$$

We also let $a_{10} = 1$, $a_{30} = 4$, $a_{40} = 8$, and $a_{i0} = 0$ otherwise.

For single-integrator dynamics, we choose $r(0) = [-1, 5, 7, 4, 6, 3]^T$, where r is a column stack vector of all r_i, $i = 1, \ldots, 6$. For (10.1), we let $\Delta_{ij} = 0$ for simplicity. For (10.10), we let $r_0 = 3.5$. For (10.13), we let $r_0(t) = 3.5 - 4\cos(\frac{t}{4})$. For all (10.1), (10.10), and (10.13), the input delay and the communication delay are chosen as, respectively, $\tau_1 = 0.1$ s and $\tau_2 = 0.2$ s. For (10.16), we let $r_0(t) = 3.5 - 4\cos(\frac{t}{4})$ and the communication delay be $\tau_2 = 0.2$ s.

Figures 10.1, 10.2, 10.3, and 10.4 show the positions of the agents using, respectively, (10.1), (10.10), (10.13), and (10.16). It can be seen from Figs. 10.1 and 10.2 that the agents achieve, respectively, leaderless coordination and coordinated regulation. In the case of coordinated tracking, Figs. 10.3 and 10.4 show that the tracking errors are uniformly ultimately bounded due to the existence of the delays and the fact that the leader is dynamic.

For double-integrator dynamics, we choose $r(0) = [-0.4, 0.5, 0.7, 0.4, 1.2, 0.3]^T$ and $v(0) = [-0.1, 0.2, 0.7, 0.4, -0.1, 0.3]^T$. For (10.18), we let $\Delta_{ij} = 0$ for simplicity. For (10.23), we consider two subcases. In one subcase, we let $r_0 = -0.2$ and $v_0 = 0$. In the other subcase, we let $r_0(t) = -0.2 + 0.1t$ and $v_0 = 0.1$. For (10.27), we let $r_0(t) = -0.2 + 0.3t - 1.6\sin(\frac{t}{4})$ and $v_0(t) = 0.3 - 0.4\cos(\frac{t}{4})$. For all (10.18), (10.23), and (10.27), we choose $\tau_1 = 0.3$ s and $\tau_2 = 0.1$ s. For (10.29), we let $r_0(t) = -0.2 + 0.3t - 1.6\sin(\frac{t}{4})$, $v_0(t) = 0.3 - 0.4\cos(\frac{t}{4})$, and $\tau_2 = 0.1$ s.
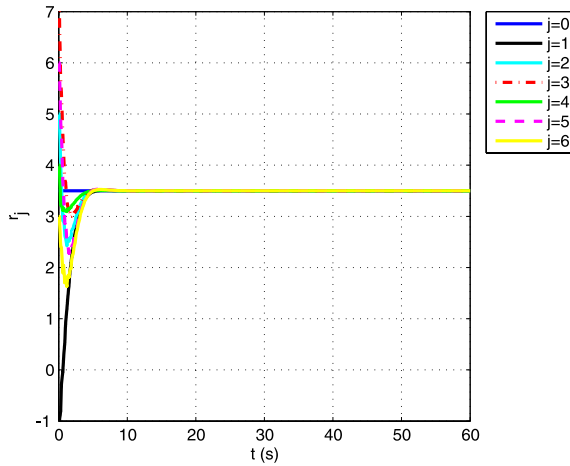
Fig. 10.2 Agents' positions using (10.10)
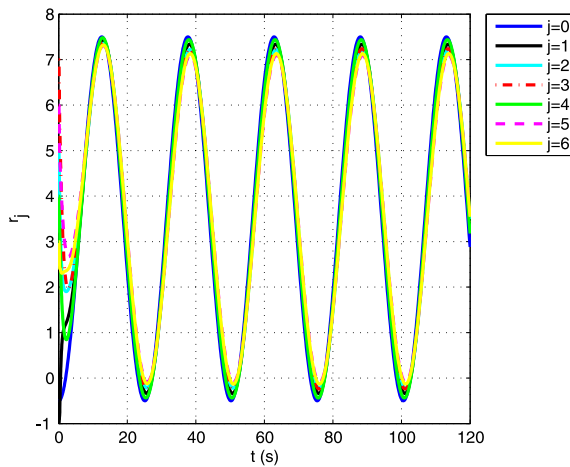
Fig. 10.3 Agents' positions using (10.13)

Figure 10.5 the positions and velocities of the agents using (10.18). It is interesting to notice that unlike the result using the standard consensus algorithm with relative damping for double-integrator dynamics [248, Chap. 4], the final velocities of the agents are always dampened to zero rather than a possibly nonzero constant. Figures 10.6 and 10.7 show the positions and velocities using (10.23) with, respectively, $v_0 = 0$ and $v_0 = 0.1$. It is worth noticing that when v_0 is a nonzero constant (respectively, zero), the tracking errors $r_i(t) - r_0(t)$ approach constant values (respectively, zero). Figures 10.8 and 10.9 show the positions and velocities using, respectively, (10.27) and (10.29). The tracking errors are uniformly ultimately bounded due to the existence of the delays and the fact that the leader is dynamic.
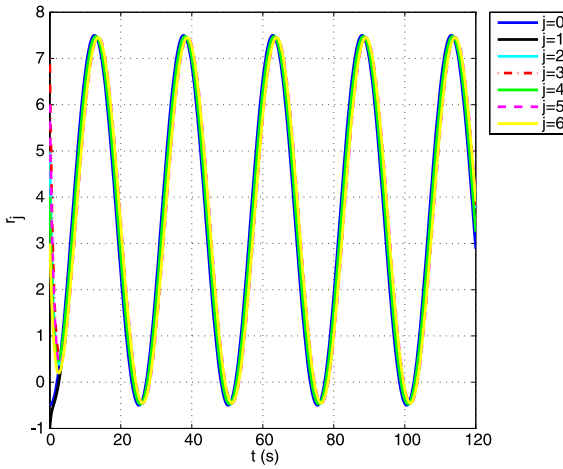
Fig. 10.4 Agents' positions using (10.16)
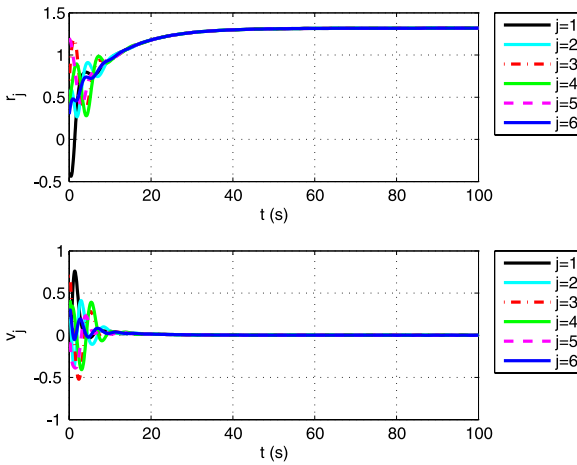
Fig. 10.5 Agents' positions using (10.18)

10.5 Notes

The results in this chapter are based mainly on [190, 191]. For further results on distributed multi-agent coordination with time delays, see [126, 174, 192, 199, 206, 214, 228, 264, 283, 285, 290, 291, 316, 322, 323]. A frequency-domain approach is used in [214] to find the stability conditions for a leaderless coordination algorithm with input delays. A time-domain approach based on Lyapunov–Krasovaskii theorem is adopted in [174] to obtain the stability conditions for a similar leaderless coordination algorithm with uniform input delays under a strongly connected and balanced interaction graph. Besides leaderless coordination algorithms, leader-
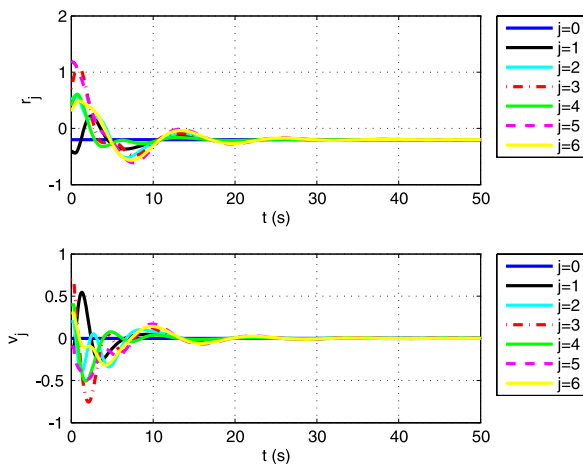
Fig. 10.6 Agents' positions using (10.23) with $v_0 = 0$
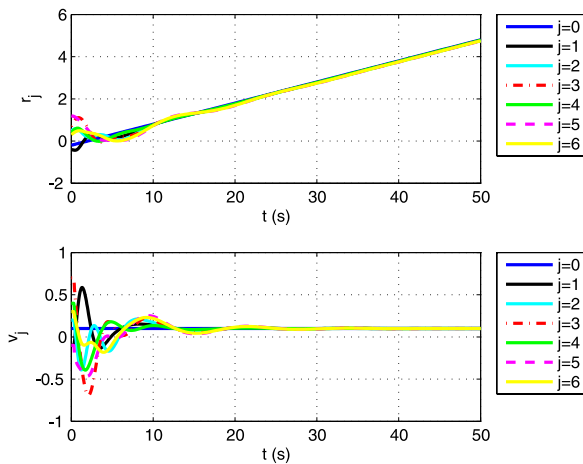
Fig. 10.7 Agents' positions using (10.23) with $v_0 = 0.1$

following coordination algorithms with input delays are also studied. By combining the results in [174] and [120], the authors in [228] propose a first-order coordinated tracking algorithm with input delays, where an estimator is used to estimate the leader's velocity. In [174, 214, 228], the interaction graph is assumed to be either undirected or strongly connected and balanced. The extension to the case where the interaction graph has a directed spanning tree and the input delays are non-uniform is provided in [291], where a frequency-domain approach is adopted to find conditions to achieve leaderless coordination. Except for input delays, the influence of communication delays on coordination algorithms is also studied. It is shown in [199] shows that communication delays will not jeopardize the stability
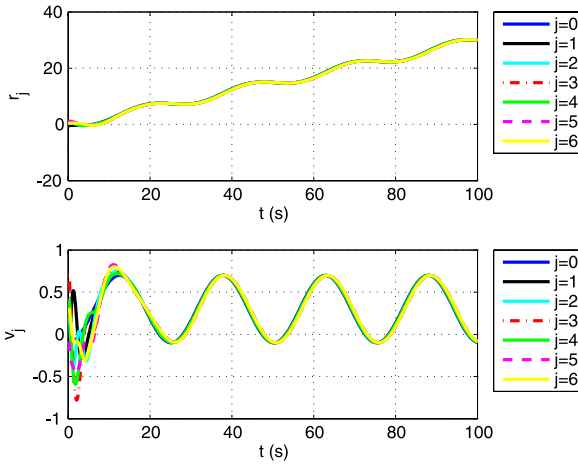
Fig. 10.8 Agents' positions using (10.27)
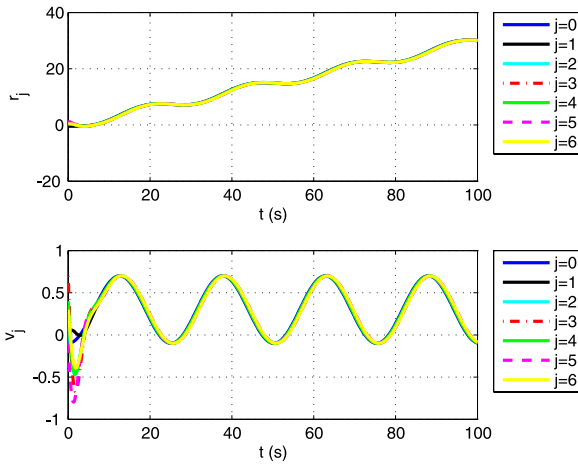
Fig. 10.9 Agents' positions using (10.29)

of a first-order leaderless coordination algorithm under a directed interaction graph. A similar algorithm is discussed in [264], where the effect of the initial conditions is highlighted. A second-order coordinated regulation algorithm with non-uniform communication delays is studied in [206], where a damping term is used to regulate the velocities of all agents to zero and the interaction graph is assumed to be undirected. The case with both communication and input delays is studied in [290], where a first-order leaderless coordination algorithm is studied in a discrete-time setting by a frequency-domain approach.

References

1. Agaev, R., Chebotarev, P.: The matrix of maximum out forests of a digraph and its applications. Autom. Remote Control **61**(9), 1424–1450 (2000)
2. Agaev, R., Chebotarev, P.: On the spectra of nonsymmetric Laplacian matrices. Linear Algebra Appl. **399**, 157–178 (2005)
3. Akar, M., Shorten, R.: Distributed probabilistic synchronization algorithms for communication networks. IEEE Trans. Autom. Control **53**(1), 389–393 (2008)
4. Alefeld, G., Schneider, N.: On square roots of M-matrices. Linear Algebra Appl. **42**, 119–132 (1982)
5. Angeli, D., Bliman, P.-A.: Tight estimates for convergence of some non-stationary consensus algorithms. Syst. Control Lett. **57**(12), 996–1004 (2008)
6. Angeli, D., Bliman, P.-A.: Convergence speed of unsteady distributed consensus: Decay estimate along the settling spanning–trees. SIAM J. Control Optim. **48**(1), 1–32 (2009)
7. Antonelli, G., Chiaverini, S.: Kinematic control of platoons of autonomous vehicles. IEEE Trans. Robot. **22**(6), 1285–1292 (2006)
8. Arcak, M.: Passivity as a design tool for group coordination. IEEE Trans. Autom. Control **52**(8), 1380–1390 (2007)
9. Arsie, A., Frazzoli, E.: Efficient routing of multiple vehicles with no explicit communications. Int. J. Robust Nonlinear Control **18**(2), 154–164 (2008)
10. Axtell, M., Bise, M.E.: Fractional calculus applications in control systems. In: Proceedings of the IEEE National Aerospace and Electronics Conference, pp. 563–566, Dayton, OH, May 1990
11. Bagley, R.L., Torvik, P.J.: Fractional calculus—A different approach to the analysis of viscoelastically damped structures. AIAA J. **21**(5), 741–748 (1983)
12. Bagley, R.L., Torvik, P.J.: A theoretical basis for the application of fractional calculus to viscoelasticity. J. Theol. **27**(3), 201–210 (1983)
13. Bagley, R.L., Torvik, P.J.: On the fractional calculus model of viscoelastic behavior. J. Theol. **30**(1), 133–155 (1986)
14. Bai, H., Arcak, M., Wen, J.T.: Adaptive design for reference velocity recovery in motion coordination. Syst. Control Lett. **57**(8), 602–610 (2008)
15. Bai, H., Arcak, M., Wen, J.T.: Adaptive motion coordination: Using relative velocity feedback to track a reference velocity. Automatica **45**(4), 1020–1025 (2009)
16. Baldassarre, G., Trianni, V., Bonani, M., Mondada, F., Dorigo, M., Nolfi, S.: Self-organized coordinated motion in groups of physically connected robots. IEEE Trans. Syst. Man Cybern., Part B **37**(1), 224–239 (2007)
17. Barbarossa, S., Scutari, G.: Bio-inspired sensor network design. IEEE Signal Process. Mag. **24**(3), 26–35 (2007)
18. Barkoulas, J., Labys, W.C., Onochie, J.: Fractional dynamics in international commodity prices. J. Futures Mark. **17**(2), 161–189 (1997)

19. Bauso, D., Giarre, L., Pesenti, R.: Non-linear protocols for optimal distributed consensus in networks of dynamic agents. Syst. Control Lett. **55**(11), 918–928 (2006)
20. Bauso, D., Giarre, L., Pesenti, R.: Consensus in noncooperative dynamic games: A multiretailer inventory application. IEEE Trans. Autom. Control **53**(4), 998–1003 (2008)
21. Bauso, D., Giarre, L., Pesenti, R.: Consensus for networks with unknown but bounded disturbances. SIAM J. Control Optim. **48**(3), 1756–1770 (2009)
22. Ben-Asher, Y., Feldman, S., Gurfil, P., Feldman, M.: Distributed decision and control for cooperative UAVs using ad hoc communication. IEEE Trans. Control Syst. Technol. **16**(3), 268–278 (2008)
23. Bliman, P.-A., Ferrari-Trecate, G.: Average consensus problems in networks of agents with delayed communications. Automatica **44**(8), 1985–1995 (2008)
24. Bopardikar, S.D., Bullo, F., Hespanha, J.P.: On discrete-time pursuit-evasion games with sensing limitations. IEEE Trans. Robot. **24**(6), 1429–1439 (2008)
25. Bopardikar, S.D., Bullo, F., Hespanha, J.P.: A cooperative homicidal chauffeur game. Automatica **45**(7), 1771–1777 (2009)
26. Borrelli, F., Keviczky, T.: Distributed LQR design for identical dynamically decoupled systems. IEEE Trans. Autom. Control **53**(8), 1901–1912 (2008)
27. Bullo, F., Cortés, J., Martínez, S.: Distributed Control of Robotic Networks. Applied Mathematics Series. Princeton University Press, Princeton (2009)
28. Calafiore, G.C., Abrate, F.: Distributed linear estimation over sensor networks. Int. J. Control **82**(5), 868–882 (2009)
29. Cao, Y., Ren, W.: Containment control with multiple stationary or dynamic leaders under a directed interaction graph. In: Proceedings of the IEEE Conference on Decision and Control, pp. 3014–3019, Shanghai, China, December 2009
30. Cao, Y., Ren, W.: Distributed coordination of fractional-order systems with extensions to directed dynamic networks and absolute/relative damping. In: Proceedings of the IEEE Conference on Decision and Control, pp. 7125–7130, Shanghai, China, December 2009
31. Cao, Y., Ren, W.: LQR-based optimal linear consensus algorithms. In: Proceedings of the American Control Conference, pp. 5204–5209, St. Louis, MO, June 2009
32. Cao, Y., Ren, W.: Sampled-data formation control under dynamic directed interaction. In: Proceedings of the American Control Conference, pp. 5186–5191, St. Louis, MO, June 2009
33. Cao, Y., Ren, W.: Multi-vehicle coordination for double-integrator dynamics in a sampled-data setting. Int. J. Robust Nonlinear Control **20**(9), 987–1000 (2010)
34. Cao, Y., Ren, W.: Distributed formation control for fractional-order systems: Dynamic interaction and absolute/relative damping. Syst. Control Lett. **59**(3–4), 362–370 (2010)
35. Cao, Y., Ren, W.: Optimal linear consensus algorithms: An LQR perspective. IEEE Trans. Syst. Man Cybern., Part B **40**(3), 819–830 (2010)
36. Cao, Y., Ren, W.: Sampled-data discrete-time coordination algorithms for double-integrator dynamics under dynamic directed interaction. Int. J. Control **83**(3), 506–515 (2010)
37. Cao, Y., Ren, W.: Distributed coordinated tracking via a variable structure approach—Part I: Consensus tracking. In: Proceedings of the American Control Conference, pp. 4744–4749, Baltimore, MD, June 2010
38. Cao, Y., Ren, W.: Distributed coordinated tracking via a variable structure approach—Part II: Swarm tracking. In: Proceedings of the American Control Conference, pp. 4750–4755, Baltimore, MD, June 2010
39. Cao, Y., Ren, W.: Distributed coordinated tracking with reduced interaction via a variable structure approach. IEEE Trans. Autom. Control (2010). doi:10.1109/TAC.2010.2049517
40. Cao, Z., Tan, M., Li, L., Gu, N., Wang, S.: Cooperative hunting by distributed mobile robots based on local interaction. IEEE Trans. Robot. **22**(2), 403–407 (2006)
41. Cao, J., Chen, G., Li, P.: Global synchronization in an array of delayed neural networks with hybrid coupling. IEEE Trans. Syst. Man Cybern., Part B **38**(2), 488–498 (2008)
42. Cao, Y., Li, Y., Ren, W., Chen, Y.: Distributed coordination algorithms for multiple fractional-order systems. In: Proceedings of the IEEE Conference on Decision and Control, pp. 2920–2925, Cancun, Mexico, December 2008

43. Cao, M., Morse, A.S., Anderson, B.D.O.: Agreeing asynchronously. IEEE Trans. Autom. Control **53**(8), 1826–1838 (2008)

44. Cao, Y., Ren, W., Li, Y.: Distributed discrete-time consensus with a time-varying reference state. In: Proceedings of the AIAA Guidance, Navigation, and Control Conference, Honolulu, HI, August 2008. Paper No. AIAA 2008-7174

45. Cao, Y., Ren, W., Li, Y.: Distributed discrete-time coordinated tracking with a time-varying reference state and limited communication. Automatica **45**(5), 1299–1305 (2009)

46. Cao, Y., Li, Y., Ren, W., Chen, Y.: Distributed coordination of networked fractional-order systems. IEEE Trans. Syst. Man Cybern., Part B **40**(2), 362–370 (2010)

47. Cao, Y., Ren, W., Meng, Z.: Decentralized finite-time sliding mode estimators and their applications in decentralized finite-time formation tracking. Syst. Control Lett. **59**(9), 522–529 (2010)

48. Carli, R., Bullo, F.: Quantized coordination algorithms for rendezvous and deployment. SIAM J. Control Optim. **48**(3), 1251–1274 (2009)

49. Cassandras, C.G., Li, W.: Sensor networks and cooperative control. Eur. J. Control **11**(4–5), 436–463 (2005)

50. Cauchy, A.-L.: Exercices de mathematiques, iv annee. de Bure Freres, Paris (1829)

51. Ceccarelli, N., Marco, M.D., Garulli, A., Giannitrapani, A.: Collective circular motion of multi-vehicle systems. Automatica **44**(12), 3025–3035 (2008)

52. Cheah, C.C., Hou, S.P., Slotine, J.J.E.: Region-based shape control for a swarm of robots. Automatica **45**(10), 2406–2411 (2009)

53. Chebotarev, P.Y., Agaev, R.P.: Coordination in multiagent systems and Laplacian spectra of digraphs. Autom. Remote Control **70**(3), 128–142 (2009)

54. Chen, Y., Ahn, H.-S., Podlubny, I.: Robust stability check of fractional order linear time invariant systems with interval uncertainties. Signal Process. **86**(10), 2611–2618 (2006)

55. Chen, F., Chen, Z., Xiang, L., Liu, Z., Yuan, Z.: Reaching a consensus via pinning control. Automatica **45**(5), 1215–1220 (2009)

56. Chen, F., Ren, W., Lin, Z.: Multi-agent coordination with cohesion, dispersion, and containment control. In: Proceedings of the American Control Conference, pp. 4756–4761, Baltimore, MD, June 2010

57. Cheong, J., Niculescu, S.-I., Kim, C.: Motion synchronization control of distributed multisubsystems with invariant local natural dynamics. IEEE Trans. Robot. **25**(2), 382–398 (2009)

58. Chopra, N.: Output synchronization of networked passive systems. PhD thesis, University of Illinois at Urbana-Champaign, Urbana, IL (2006)

59. Chopra, N., Spong, M.W.: Passivity-based control of multi-agent systems. In: Kawamura, S., Svinin, M. (eds.) Advances in Robot Control: From Everyday Physics to Human-Like Movements, pp. 107–134. Springer, Berlin (2006)

60. Chopra, N., Spong, M.W.: On exponential synchronization of Kuramoto oscillators. IEEE Trans. Autom. Control **54**(2), 353–357 (2009)

61. Chopra, N., Spong, M.W., Lozano, R.: Synchronization of bilateral teleoperators with time delay. Automatica **44**(8), 2142–2148 (2008)

62. Chopra, N., Stipanovic, D.M., Spong, M.W.: On synchronization and collision avoidance for mechanical systems. In: Proceedings of the American Control Conference, pp. 3713–3718, Seattle, WA, June 2008

63. Chung, S.-J.: Nonlinear control and synchronization of multiple Lagrangian systems with application to tethered formation flight spacecraft. PhD thesis, Massachusetts Institute of Technology, Cambridge, MA (2007)

64. Chung, S.-J., Slotine, J.-J.E.: Cooperative robot control and concurrent synchronization of Lagrangian systems. IEEE Trans. Robot. **25**(3), 686–700 (2009)

65. Cohen, I., Golding, I., Ron, I.G., Ben-Jacob, E.: Biofluiddynamics of lubricating bacteria. Math. Methods Appl. Sci. **24**(17–18), 1429–1468 (2001)

66. Cortés, J.: Discontinuous dynamical systems: A tutorial on solutions, nonsmooth analysis, and stability. IEEE Control Syst. Mag. **28**(3), 36–73 (2008)

67. Cortés, J.: Distributed algorithms for reaching consensus on general functions. Automatica **44**(3), 726–737 (2008)
68. Cortés, J., Martínez, S., Karatas, T., Bullo, F.: Coverage control for mobile sensing networks. IEEE Trans. Robot. Autom. **20**(2), 243–255 (2004)
69. Cucker, F., Smale, S.: Emergent behavior in flocks. IEEE Trans. Autom. Control **52**(5), 852–862 (2007)
70. DeGroot, M.H.: Reaching a consensus. J. Am. Stat. Assoc. **69**(345), 118–121 (1974)
71. DeLellis, P., diBernardo, M., Garofalo, F.: Novel decentralized adaptive strategies for the synchronization of complex networks. Automatica **45**(5), 1312–1318 (2009)
72. Delvenne, J.-C., Carli, R., Zampieri, S.: Optimal strategies in the average consensus problem. Syst. Control Lett. **58**(10–11), 759–765 (2009)
73. Demetriou, M.A., Hussein, I.I.: Estimation of spatially distributed processes using mobile spatially distributed sensor network. SIAM J. Control Optim. **48**(1), 266–291 (2009)
74. Derenick, J.C., Spletzer, J.R.: Convex optimization strategies for coordinating large-scale robot formations. IEEE Trans. Robot. **23**(6), 1252–1259 (2007)
75. Dierks, T., Jagannathan, S.: Neural network control of mobile robot formations using rise feedback. IEEE Trans. Syst. Man Cybern., Part B **39**(2), 332–347 (2009)
76. Dimarogonas, D.V., Kyriakopoulos, K.J.: On the rendezvous problem for multiple nonholonomic agents. IEEE Trans. Autom. Control **52**(5), 916–922 (2007)
77. Dimarogonas, D.V., Kyriakopoulos, K.J.: A connection between formation infeasibility and velocity alignment in kinematic multi-agent systems. Automatica **44**(10), 2648–2654 (2008)
78. Dimarogonas, D.V., Kyriakopoulos, K.J.: Inverse agreement protocols with application to distributed multi-agent dispersion. IEEE Trans. Autom. Control **54**(3), 657–663 (2009)
79. Dimarogonas, D.V., Egerstedt, M., Kyriakopoulos, K.J.: A leader-based containment control strategy for multiple unicycles. In: Proceedings of the IEEE Conference on Decision and Control, pp. 5968–5973, San Diego, CA, December 2006
80. Dimarogonas, D.V., Tsiotras, P., Kyriakopoulos, K.J.: Leader-follower cooperative attitude control of multiple rigid bodies. Syst. Control Lett. **58**(6), 429–435 (2009)
81. Dmitriev, N., Dynkin, E.: On the characteristic numbers of a stochastic matrix. C. R. (Dokl.) Acad. Sci. URSS **49**(3), 159–162 (1946)
82. Do, K.D.: Bounded controllers for formation stabilization of mobile agents with limited sensing ranges. IEEE Trans. Autom. Control **52**(3), 569–576 (2007)
83. Do, K.D.: Formation tracking control of unicycle-type mobile robots with limited sensing ranges. IEEE Trans. Control Syst. Technol. **16**(3), 527–538 (2008)
84. Dong, W., Farrell, J.A.: Cooperative control of multiple nonholonomic mobile agents. IEEE Trans. Autom. Control **53**(6), 1434–1448 (2008)
85. Dong, W., Farrell, J.A.: Decentralized cooperative control of multiple nonholonomic dynamic systems with uncertainty. Automatica **45**(3), 706–710 (2009)
86. Dunbar, W.B.: Distributed receding horizon control of dynamically coupled nonlinear systems. IEEE Trans. Autom. Control **52**(7), 1249–1263 (2007)
87. Dunbar, W.B., Murray, R.M.: Distributed receding horizon control for multi-vehicle formation stabilization. Automatica **42**(4), 549–558 (2006)
88. Eguchi, T., Hirasawa, K., Hu, J., Ota, N.: A study of evolutionary multiagent models based on symbiosis. IEEE Trans. Syst. Man Cybern., Part B **36**(1), 179–193 (2006)
89. Fang, L., Antsaklis, P.J.: Asynchronous consensus protocols using nonlinear paracontractions theory. IEEE Trans. Autom. Control **53**(10), 2351–2355 (2008)
90. Fax, J.A., Murray, R.M.: Information flow and cooperative control of vehicle formations. IEEE Trans. Autom. Control **49**(9), 1465–1476 (2004)
91. Ferrari-Trecate, G., Buffa, A., Gati, M.: Analysis of coordination in multi-agent systems through partial difference equations. IEEE Trans. Autom. Control **51**(6), 1058–1063 (2006)
92. Filippov, A.F.: Differential Equations with Discontinuous Righthand Sides. Kluwer Academic, Dordrecht (1988)
93. Finke, J., Passino, K.M.: Stable cooperative vehicle distributions for surveillance. ASME J. Dyn. Syst. Meas. Control **129**(5), 597–608 (2007)

94. Finke, J., Passino, K.M., Sparks, A.G.: Stable task load balancing strategies for cooperative control of networked autonomous air vehicles. IEEE Trans. Control Syst. Technol. **14**(5), 789–803 (2006)

95. Franco, E., Parisini, T., Polycarpou, M.M.: Design and stability analysis of cooperative receding-horizon control of linear discrete-time agents. Int. J. Robust Nonlinear Control **17**(11), 982–1001 (2007)

96. Franco, E., Magni, L., Parisini, T., Polycarpou, M.M., Raimondo, D.M.: Cooperative constrained control of distributed agents with nonlinear dynamics and delayed information exchange: A stabilizing receding-horizon approach. IEEE Trans. Autom. Control **53**(1), 324–338 (2008)

97. Fua, C.-H., Ge, S.S., Do, K.D., Lim, K.-W.: Multirobot formations based on the queue-formation scheme with limited communication. IEEE Trans. Robot. **23**(6), 1160–1169 (2007)

98. Ganguli, A., Cortés, J., Bullo, F.: Multirobot rendezvous with visibility sensors in nonconvex environments. IEEE Trans. Robot. **25**(2), 340–352 (2009)

99. Gao, Y., Wang, L.: Consensus of multiple double-integrator agents with intermittent measurement. Int. J. Robust Nonlinear Control **20**(10), 1140–1155 (2009)

100. Gao, C., Cortés, J., Bullo, F.: Notes on averaging over acyclic digraphs and discrete coverage control. Automatica **44**(8), 2120–2127 (2008)

101. Gao, Y., Wang, L., Xie, G., Wu, B.: Consensus of multi-agent systems based on sampled-data control. Int. J. Control **82**(12), 2193–2205 (2009)

102. Gazi, V., Fidan, B.: Control and coordination of multi-agent dynamic systems: Models and approaches. In: Sahin, E., Spears, W.M., Winfield, A.F.T. (eds.) Swarm Robotics. Lecture Notes in Computer Science, pp. 71–102, vol. 4433. Springer, Berlin (2005)

103. Gazi, V., Passino, K.M.: Stability analysis of swarms. IEEE Trans. Autom. Control **48**(4), 692–697 (2003)

104. Ghabcheloo, R., Aguiar, A.P., Pascoal, A., Silvestre, C., Kaminer, I., Hespanha, J.: Coordinated path-following in the presence of communication losses and time delays. SIAM J. Control Optim. **48**(1), 234–265 (2009)

105. Ghrist, R., Lavalle, S.M.: Nonpositive curvature and Pareto optimal coordination of robots. SIAM J. Control Optim. **45**(5), 1697–1713 (2006)

106. Gil, A.E., Passino, K.M., Cruz, J.B.: Stable cooperative surveillance with information flow constraints. IEEE Trans. Control Syst. Technol. **16**(5), 856–868 (2008)

107. Giovanini, L., Balderud, J., Katebi, R.: Autonomous and decentralized mission planning for clusters of UUVs. Int. J. Control **80**(7), 1169–1179 (2007)

108. Glöckle, W.G., Nonnenmacher, T.F.: A fractional calculus approach to self-similar protein dynamics. Biophys. J. **68**(1), 46–53 (1995)

109. Godsil, C., Royle, G.: Algebraic Graph Theory. Graduate Texts in Mathematics, vol. 207. Springer, New York (2001)

110. Gorenflo, R., Mainardi, F.: Fractional oscillations and Mittag-Leffler functions (1996). Available online: citeseer.ist.psu.edu/gorenflo96fractional.html

111. Graham, A.: Kronecker Products and Matrix Calculus With Applications. Halsted, New York (1981)

112. Gu, D.: A differential game approach to formation control. IEEE Trans. Control Syst. Technol. **16**(1), 85–93 (2008)

113. Gustavi, T., Hu, X.: Observer-based leader-following formation control using onboard sensor information. IEEE Trans. Robot. **24**(6), 1457–1462 (2008)

114. Hale, J.K., Lunel, S.M.V.: Introduction to Functional Differential Equations. Springer, New York (1993)

115. Hatano, Y., Mesbahi, M.: Agreement over random networks. IEEE Trans. Autom. Control **50**(11), 1867–1872 (2005)

116. Hayakawa, T., Matsuzawa, T., Hara, S.: Formation control of multi-agent systems with sampled information. In: Proceedings of the IEEE Conference on Decision and Control, pp. 4333–4338, San Diego, CA, December 2006

117. Hendrickx, J.M., Anderson, B.D.O., Delvenne, J.-C., Blondel, V.D.: Directed graphs for the analysis of rigidity and persistence in autonomous agent systems. Int. J. Robust Nonlinear Control **17**(11), 960–981 (2007)

118. Hirai, H., Miyazaki, F.: Dynamic coordination between robots: Self-organized timing selection in a juggling-like ball-passing task. IEEE Trans. Syst. Man Cybern., Part B **36**(4), 738–754 (2006)

119. Hokayem, P.F., Stipanovic, D.M., Spong, M.W.: Semiautonomous control of multiple networked Lagrangian systems. Int. J. Robust Nonlinear Control **19**(18), 2040–2055 (2009)

120. Hong, Y., Hu, J., Gao, L.: Tracking control for multi-agent consensus with an active leader and variable topology. Automatica **42**(7), 1177–1182 (2006)

121. Hong, Y., Chen, G., Bushnell, L.: Distributed observers design for leader-following control of multi-agent networks. Automatica **44**(3), 846–850 (2008)

122. Horn, R.A., Johnson, C.R.: Matrix Analysis. Cambridge University Press, Cambridge (1985)

123. Hou, Z.-G., Cheng, L., Tan, M.: Decentralized robust adaptive control for the multiagent system consensus problem using neural networks. IEEE Trans. Syst. Man Cybern., Part B **39**(3), 636–647 (2009)

124. Hristu-Varsakelis, D., Shao, C.: A bio-inspired pursuit strategy for optimal control with partially constrained final state. Automatica **43**(7), 1265–1273 (2007)

125. http://www.mathpages.com/home/kmath593/kmath593.htm

126. Hu, J., Hong, Y.: Leader-following coordination of multiagent systems with coupling time delays. IET Control Theory Appl. **374**(2), 853–863 (2007)

127. Hu, J., Prandini, M., Tomlin, C.: Conjugate points in formation constrained optimal multi-agent coordination: A case study. SIAM J. Control Optim. **45**(6), 2119–2137 (2006)

128. Huang, M., Caines, P.E., Malhame, R.P.: Large-population cost-coupled LQG problems with nonuniform agents: Individual-mass behavior and decentralized ϵ-Nash equilibria. IEEE Trans. Autom. Control **52**(9), 1560–1571 (2007)

129. Hui, Q., Haddad, W.M.: Distributed nonlinear control algorithms for network consensus. Automatica **44**(9), 2375–2381 (2008)

130. Hui, Q., Haddad, W.M., Bhat, S.P.: Finite-time semistability and consensus for nonlinear dynamical networks. IEEE Trans. Autom. Control **53**(8), 1887–1890 (2008)

131. Hussein, I.I., Stipanovic, D.M.: Effective coverage control for mobile sensor networks with guaranteed collision avoidance. IEEE Trans. Control Syst. Technol. **15**(4), 642–657 (2007)

132. Jadbabaie, A., Lin, J., Morse, A.S.: Coordination of groups of mobile autonomous agents using nearest neighbor rules. IEEE Trans. Autom. Control **48**(6), 988–1001 (2003)

133. Ji, M., Egerstedt, M.: Distributed coordination control of multiagent systems while preserving connectedness. IEEE Trans. Robot. **23**(4), 693–703 (2007)

134. Ji, M., Egerstedt, M.: A graph-theoretic characterization of controllability for multi-agent systems. In: Proceedings of the American Control Conference, pp. 4588–4593, New York City, NY, July 2007

135. Ji, M., Muhammad, A., Egerstedt, M.: Leader-based multi-agent coordination: Controllability and optimal control. In: Proceedings of the American Control Conference, pp. 1358–1363, Minneapolis, MN, June 2006

136. Ji, M., Ferrari-Trecate, G., Egerstedt, M., Buffa, A.: Containment control in mobile networks. IEEE Trans. Autom. Control **53**(8), 1972–1975 (2008)

137. Ji, Z., Wang, Z., Lin, H., Wang, Z.: Controllability of multi-agent systems with time-delay in state and switching topology. Int. J. Control **83**(2), 371–386 (2010)

138. Jiang, F., Wang, L.: Finite-time information consensus for multi-agent systems with fixed and switching topologies. Physica D **238**(16), 1550–1560 (2009)

139. Jin, Z., Shima, T., Schumacher, C.J.: Optimal scheduling for refueling multiple autonomous aerial vehicles. IEEE Trans. Robot. **22**(4), 682–693 (2006)

140. Johansson, B., Speranzon, A., Johansson, M., Johansson, K.H.: On decentralized negotiation of optimal consensus. Automatica **44**(4), 1175–1179 (2008)

141. Justh, E.W., Krishnaprasad, P.S.: Equilibria and steering laws for planar formations. Syst. Control Lett. **52**(1), 25–38 (2004)

142. Kaminka, G.A., Schechter-Glick, R., Sadov, V.: Using sensor morphology for multirobot formations. IEEE Trans. Robot. **24**(2), 271–282 (2008)
143. Kashyap, A., Basar, T., Srikant, R.: Quantized consensus. Automatica **43**(7), 1192–1203 (2007)
144. Kelly, R., Santibanez, V., Loria, A.: Control of Robot Manipulators in Joint Space. Springer, London (2005)
145. Khalil, H.K.: Nonlinear Systems. Macmillan Co., New York (1992)
146. Khalil, H.K.: Nonlinear Systems, 2nd edn. Prentice Hall, Upper Saddle River (1996)
147. Khalil, H.K.: Nonlinear Systems, 3rd edn. Prentice Hall, Upper Saddle River (2002)
148. Kim, Y., Mesbahi, M.: On maximizing the second smallest eigenvalue of a state-dependent graph Laplacian. IEEE Trans. Autom. Control **51**(1), 116–120 (2006)
149. Kim, T.-H., Sugie, T.: Cooperative control for target-capturing task based on a cyclic pursuit strategy. Automatica **43**(8), 1426–1431 (2007)
150. Kim, Y., Gu, D.-W., Postlethwaite, I.: Spectral radius minimization for optimal average consensus and output feedback stabilization. Automatica **45**(6), 1379–1386 (2009)
151. Kingston, D., Beard, R.W., Holt, R.S.: Decentralized perimeter surveillance using a team of UAVs. IEEE Trans. Robot. **24**(6), 1394–1404 (2008)
152. Kittaneh, F.: Spectral radius inequalities for Hilbert space operators. Proc. Am. Math. Soc. **134**(2), 385–390 (2005)
153. Kloder, S., Hutchinson, S.: Path planning for permutation-invariant multirobot formations. IEEE Trans. Robot. **22**(4), 650–665 (2006)
154. Kolmanovskii, V., Myshkis, A.: Applied Theory of Functional Differential Equations. Kluwer Academic, Dordrecht (1992)
155. Kovacs, I., Silver, D.S., Williams, S.G.: Determinants of block matrices and Schur's formula (1999)
156. Kozlovsky, Y., Cohen, I., Golding, I., Ben-Jacob, E.: Lubricating bacteria model for branching growth of bacterial colonies. Phys. Rev. E **59**(6), 7025–7035 (1999)
157. Krick, L., Broucke, M.E., Francis, B.A.: Stabilisation of infinitesimally rigid formations of multi-robot networks. Int. J. Control **82**(3), 423–439 (2009)
158. Krogstad, T.R., Gravdahl, J.T.: 6-DOF mutual synchronization of formation flying spacecraft. In: Proceedings of the IEEE Conference on Decision and Control, pp. 5706–5711, San Diego, CA, December 2006
159. Kunwar, F., Benhabib, B.: Rendezvous-guidance trajectory planning for robotic dynamic obstacle avoidance and interception. IEEE Trans. Syst. Man Cybern., Part B **36**(6), 1432–1441 (2006)
160. Lafferriere, G., Williams, A., Caughman, J., Veerman, J.J.P.: Decentralized control of vehicle formations. Syst. Control Lett. **54**(9), 899–910 (2005)
161. Lalish, E., Morgansen, K.A., Tsukamaki, T.: Decentralized reactive collision avoidance for multiple unicycle-type vehicles. In: Proceedings of the American Control Conference, pp. 5055–5061, Seattle, WA, June 2008
162. Lasserre, J.B.: Global optimization with polynomials and the problem of moments. SIAM J. Optim. **11**(3), 796–817 (2001)
163. Laub, A.J.: Matrix Analysis for Scientists and Engineers. SIAM, Philadelphia (2005)
164. Laurent, H.: Sur le calcul des dérivées à indices quelconques. Nouv. Ann. Math. **3**(3), 240–252 (1884)
165. Lavaei, J., Murray, R.M.: On quantized consensus by means of gossip algorithm—Part I: Convergence proof. In: Proceedings of the American Control Conference, pp. 394–401, St. Louis, MO, June 2009
166. Lavaei, J., Murray, R.M.: On quantized consensus by means of gossip algorithm—Part II: Convergence time. In: Proceedings of the American Control Conference, pp. 2958–2965, St. Louis, MO, June 2009
167. Laventalla, K., Cortés, J.: Coverage control by multi-robot networks with limited-range anisotropic sensory. Int. J. Control **82**(6), 1113–1121 (2009)

168. Leonard, N.E., Fiorelli, E.: Virtual leaders, artificial potentials and coordinated control of groups. In: Proceedings of the IEEE Conference on Decision and Control, pp. 2968–2973, Orlando, Florida, December 2001

169. Leonard, N.E., Paley, D.A., Lekien, F., Sepulchre, R., Fratantoni, D.M., Davis, R.E.: Collective motion, sensor networks, and ocean sampling. Proc. IEEE **95**(1), 48–74 (2007)

170. Li, W.: Stability analysis of swarms with general topology. IEEE Trans. Syst. Man Cybern., Part B **38**(4), 1084–1097 (2008)

171. Li, Y., Chen, Y.: Fractional order linear quadratic regulator. In: Proceedings of the IEEE/ASME International Conference on Mechtronic and Embedded Systems and Applications, pp. 363–368. Beijing, China, October 2008

172. Li, Z., Duan, Z., Chen, G., Huang, L.: Consensus of multi-agent systems and synchronization of complex networks: A unified viewpoint. IEEE Trans. Circuits. Syst. I **57**(1), 213–224 (2010)

173. Liang, J., Wang, Z., Liu, Y., Liu, X.: Global synchronization control of general delayed discrete-time networks with stochastic coupling and disturbances. IEEE Trans. Syst. Man Cybern., Part B **38**(4), 1073–1083 (2008)

174. Lin, P., Jia, Y.: Average consensus in networks of multi-agents with both switching topology and coupling time-delay. Physica A **387**(1), 303–313 (2008)

175. Lin, P., Jia, Y.: Distributed rotating formation control of multi-agent systems. Syst. Control Lett. **59**(10), 587–595 (2010)

176. Lin, Z., Broucke, M., Francis, B.: Local control strategies for groups of mobile autonomous agents. IEEE Trans. Autom. Control **49**(4), 622–629 (2004)

177. Lin, Z., Francis, B., Maggiore, M.: State agreement for continuous-time coupled nonlinear systems. SIAM J. Control Optim. **46**(1), 288–307 (2007)

178. Lin, P., Jia, Y., Li, L.: Distributed robust H_∞ consensus control in directed networks of agents with time-delay. Syst. Control Lett. **57**(8), 643–653 (2008)

179. Liouville, J.: Mémoire sur le calcul des différentielles à indices quelconques. J. Éc. Polytech. **13**(21), 71–162 (1832)

180. Liu, H.-T., Shan, J., Sun, J.C.D.: Adaptive synchronization control of multiple spacecraft formation flying. ASME J. Dyn. Syst. Meas. Control **129**(3), 337–342 (2007)

181. Liu, B., Chu, T., Wang, L., Xie, G.: Controllability of a leader–follower dynamic network with switching topology. IEEE Trans. Autom. Control **53**(4), 1009–1013 (2008)

182. Lopes, O.: Forced oscillations in nonlinear neutral differential equations. SIAM J. Appl. Math. **29**(1), 196–207 (1975)

183. Lynch, N.A.: Distributed Algorithms. Morgan Kaufmann, San Francisco (1996)

184. Lynch, K.M., Schwartz, I.B., Yang, P., Freeman, R.A.: Decentralized environmental modeling by mobile sensor networks. IEEE Trans. Robot. **24**(3), 710–724 (2008)

185. Ma, H.-B.: Decentralized adaptive synchronization of a stochastic discrete-time multiagent dynamic model. SIAM J. Control Optim. **48**(2), 859–880 (2009)

186. Ma, C.-Q., Zhang, J.-F.: Necessary and sufficient conditions for consensusability of linear multi-agent systems. IEEE Trans. Autom. Control **55**(5), 1263–1268 (2010)

187. Marshall, J.A., Broucke, M.E., Francis, B.A.: Pursuit formations of unicycles. Automatica **42**(1), 3–12 (2006)

188. Martínez, S., Bullo, F.: Optimal sensor placement and motion coordination for target tracking. Automatica **42**(4), 661–668 (2006)

189. Mei, J., Ren, W., Ma, G.: Distributed coordinated tracking for multiple Euler–Lagrange systems. In: Proceedings of the IEEE Conference on Decision and Control, Atlanta, GA, December 2010

190. Meng, Z., Ren, W., Cao, Y., You, Z.: Leaderless and leader-following consensus with communication and input delays under a directed network topology. IEEE Trans. Syst. Man Cybern., Part B (2010). doi:10.1109/TSMCB.2010.2045891

191. Meng, Z., Ren, W., Cao, Y., You, Z.: Some stability and boundedness conditions for second-order leaderless and leader-following consensus with communication and input delays. In: Proceedings of the American Control Conference, pp. 574–579, Baltimore, MD, June 2010

192. Meng, Z., Yu, W., Ren, W.: Discussion on: "Consensus of second-order delayed multi-agent systems with leader-following". Eur. J. Control **16**(2), 200–205 (2010)
193. Mesbahi, M., Egerstedt, M.: Graph Theoretic Methods in Multiagent Networks. Princeton University Press, Princeton (2010)
194. Metzler, R., Klafter, J.: The random walk's guide to anomalous diffusion: A fractional dynamics approach. Phys. Rep. **339**(1), 1–77 (2000)
195. Michiels, W., Morarescu, C.-I., Niculescu, S.-I.: Consensus problems with distributed delays, with application to traffic flow models. SIAM J. Control Optim. **48**(1), 77–101 (2009)
196. Mohanarajah, G., Hayakawa, T.: Influence of stochastic communication loss on the stability of a formation of multiple agents. In: Proceedings of the American Control Conference, pp. 341–346, New York City, NY, December 2007
197. Moore, K., Lucarelli, D.: Decentralized adaptive scheduling using consensus variables. Int. J. Robust Nonlinear Control **17**(10–11), 921–940 (2007)
198. Moore, B.J., Passino, K.M.: Decentralized redistribution for cooperative patrol. Int. J. Robust Nonlinear Control **18**(2), 165–195 (2008)
199. Moreau, L.: Stability of continuous-time distributed consensus algorithms. In: Proceedings of the IEEE Conference on Decision and Control, pp. 3998–4003, Paradise Island, Bahamas, December 2004
200. Moreau, L.: Stability of multi-agent systems with time-dependent communication links. IEEE Trans. Autom. Control **50**(2), 169–182 (2005)
201. Morse, A.S.: Supervisory control of families of linear set-point controllers-Part 1: Exact matching. IEEE Trans. Autom. Control **41**(10), 1413–1431 (1996)
202. Moshtagh, N., Jadbabaie, A.: Distributed geodesic control laws for flocking of nonholonomic agents. IEEE Trans. Autom. Control **52**(4), 681–686 (2007)
203. Motee, N., Jadbabaie, A.: Optimal control of spatially distributed systems. IEEE Trans. Autom. Control **53**(7), 1616–1629 (2008)
204. Mourikis, A.I., Roumeliotis, S.I.: Optimal sensor scheduling for resource-constrained localization of mobile robot formations. IEEE Trans. Robot. **22**(5), 917–931 (2006)
205. Mourikis, A.I., Roumeliotis, S.I.: Performance analysis of multirobot cooperative localization. IEEE Trans. Robot. **22**(4), 666–681 (2006)
206. Munz, U., Papachristodoulou, A., Allgower, F.: Delay-dependent rendezvous and flocking of large scale multi-agent systems with communication delays. In: Proceedings of the IEEE Conference on Decision and Control, pp. 2038–2043, Cancun, Mexico, December 2008
207. Murray, R.M.: Recent research in cooperative control of multivehicle systems. ASME J. Dyn. Syst. Meas. Control **129**(5), 571–583 (2007)
208. Nair, S., Leonard, N.E.: Stable synchronization of mechanical system networks. SIAM J. Control Optim. **47**(2), 661–683 (2008)
209. Niculescu, S.-I.: Delay Effects on Stability: A Robust Control Approach. Springer, London (2003)
210. Niculescu, S.-I., Chen, J.: Frequency sweeping tests for asymptotic stability: A model transformation for multiple delays. In: Proceedings of the IEEE Conference on Decision and Control, pp. 4678–4683, Phoenix, AZ, December 1999
211. O'Grady, R., Christensen, A.L., Dorigo, M.: Swarmorph: Multirobot morphogenesis using directional self-assembly. IEEE Trans. Robot. **25**(3), 738–743 (2009)
212. Olfati-Saber, R.: Flocking for multi-agent dynamic systems: Algorithms and theory. IEEE Trans. Autom. Control **51**(3), 401–420 (2006)
213. Olfati-Saber, R., Murray, R.M.: Distributed cooperative control of multiple vehicle formations using structural potential functions. In: Proceedings of the IFAC World Congress, pp. 495–500, Barcelona, Spain, July 2002
214. Olfati-Saber, R., Murray, R.M.: Consensus problems in networks of agents with switching topology and time-delays. IEEE Trans. Autom. Control **49**(9), 1520–1533 (2004)
215. Olfati-Saber, R., Fax, J.A., Murray, R.M.: Consensus and cooperation in networked multi-agent systems. Proc. IEEE **95**(1), 215–233 (2007)
216. Olshevsky, A., Tsitsiklis, J.N.: Convergence speed in distributed consensus and averaging. SIAM J. Control Optim. **48**(1), 33–55 (2009)

217. Orbach, R.: Fractal phenomena in disordered systems. Annu. Rev. Mater. Sci. **19**, 497–525 (1989)
218. Orqueda, O.A.A., Zhang, X.T., Fierro, R.: An output feedback nonlinear decentralized controller for unmanned vehicle co-ordination. Int. J. Robust Nonlinear Control **17**(12), 1106–1128 (2007)
219. Oustaloup, A., Sabatier, J., Lanusse, P.: From fractal robustness to CRONE control. Fract. Calc. Appl. Anal. **2**(1), 1–30 (1999)
220. Paden, B., Panja, R.: Globally asymptotically stable 'PD+' controller for robot manipulators. Int. J. Control **47**(6), 1697–1712 (1988)
221. Paden, B., Sastry, S.: A calculus for computing Filippov's differential inclusion with application to the variable structure control of robot manipulators. IEEE Trans. Circuits Syst. **CAS-34**(1), 73–82 (1987)
222. Paley, D.A.: Cooperative control of collective motion for ocean sampling with autonomous vehicles. PhD thesis, Princeton University, Princeton, NJ (2007)
223. Paley, D.A.: Stabilization of collective motion on a sphere. Automatica **45**(1), 212–216 (2009)
224. Paley, D.A., Leonard, N.E., Sepulchre, R.: Stabilization of symmetric formations to motion around convex loops. Syst. Control Lett. **57**(3), 209–215 (2008)
225. Panteley, E., Loria, A.: Growth rate conditions for uniform asymptotic stability of cascaded time-varying systems. Automatica **37**(3), 453–460 (2001)
226. Pavone, M., Frazzoli, E.: Decentralized policies for geometric pattern formation and path coverage. ASME J. Dyn. Syst. Meas. Control **129**(5), 633–643 (2007)
227. Peasgood, M., Clark, C.M., McPhee, J.: A complete and scalable strategy for coordinating multiple robots within roadmaps. IEEE Trans. Robot. **24**(2), 283–292 (2008)
228. Peng, K., Yang, Y.: Leader-following consensus problem with a varying-velocity leader and time-varying delays. Physica A **388**(2–3), 193–208 (2009)
229. Podlubny, I.: Fractional Differential Equations. Academic Press, San Diego (1999)
230. Podlubny, I.: Fractional-order systems and PI$^\lambda$D$^\mu$-controllers. IEEE Trans. Autom. Control **44**(1), 208–213 (1999)
231. Podlubny, I., Dorcak, L., Kostial, I.: On fractional derivatives, fractional-order dynamic systems and PI$^\lambda$D$^\mu$-controllers. In: Proceedings of the IEEE Conference on Decision and Control, pp. 4985–4990, San Diego, CA, 1997
232. Porfiri, M., Stilwell, D.J.: Consensus seeking over random weighted directed graphs. IEEE Trans. Autom. Control **52**(9), 1767–1773 (2007)
233. Porfiri, M., Roberson, D.G., Stilwell, D.J.: Tracking and formation control of multiple autonomous agents: A two-level consensus approach. Automatica **43**(8), 1318–1328 (2007)
234. Purvis, K.B., Astrom, K.J., Khammash, M.: Estimation and optimal configurations for localization using cooperative UAVs. IEEE Trans. Control Syst. Technol. **16**(5), 947–958 (2008)
235. Qu, Z.: Cooperative Control of Dynamical Systems. Springer, London (2009)
236. Qu, Z., Wang, J., Hull, R.A.: Cooperative control of dynamical systems with application to autonomous vehicles. IEEE Trans. Autom. Control **53**(4), 894–911 (2008)
237. Rahmani, A., Ji, M., Mesbahi, M., Egerstedt, M.: Controllability of multi-agent systems from a graph-theoretic perspective. SIAM J. Control Optim. **48**(1), 162–186 (2009)
238. Ramirez-Riberos, J.L., Pavone, M., Frazzoli, E., Miller, D.W.: Distributed control of spacecraft formations via cyclic pursuit: Theory and experiments. J. Guid. Control Dyn. **33**(5), 1655–1669 (2010)
239. Ren, W.: Distributed attitude alignment in spacecraft formation flying. Int. J. Adapt. Control Signal Process. **21**(2–3), 95–113 (2007)
240. Ren, W.: Multi-vehicle consensus with a time-varying reference state. Syst. Control Lett. **56**(7–8), 474–483 (2007)
241. Ren, W.: Collective motion from consensus with Cartesian coordinate coupling—Part i: Single-integrator kinematics. In: Proceedings of the IEEE Conference on Decision and Control, pp. 1006–1011, Cancun, Mexico, December 2008

242. Ren, W.: Collective motion from consensus with Cartesian coordinate coupling—Part ii: Double-integrator dynamics. In: Proceedings of the IEEE Conference on Decision and Control, pp. 1012–1017, Cancun, Mexico, December 2008

243. Ren, W.: Synchronization of coupled harmonic oscillators with local interaction. Automatica **44**(12), 3195–3200 (2008)

244. Ren, W.: Collective motion from consensus with Cartesian coordinate coupling. IEEE Trans. Autom. Control **54**(6), 1330–1335 (2009)

245. Ren, W.: Distributed leaderless consensus algorithms for networked Euler–Lagrange systems. Int. J. Control **82**(11), 2137–2149 (2009)

246. Ren, W.: Consensus tracking under directed interaction topologies: Algorithms and experiments. IEEE Trans. Control Syst. Technol. **18**(1), 230–237 (2010)

247. Ren, W., Beard, R.W.: Consensus seeking in multiagent systems under dynamically changing interaction topologies. IEEE Trans. Autom. Control **50**(5), 655–661 (2005)

248. Ren, W., Beard, R.W.: Distributed Consensus in Multi-vehicle Cooperative Control. Communications and Control Engineering. Springer, London (2008)

249. Ren, W., Cao, Y.: Convergence of sampled-data consensus algorithms for double-integrator dynamics. In: Proceedings of the IEEE Conference on Decision and Control, pp. 3965–3970, Cancun, Mexico, December 2008

250. Ren, W., Beard, R.W., Atkins, E.M.: Information consensus in multivehicle cooperative control. IEEE Control Syst. Mag. **27**(2), 71–82 (2007)

251. Ren, W., Chao, H., Bourgeous, W., Sorensen, N., Chen, Y.: Experimental validation of consensus algorithms for multivehicle cooperative control. IEEE Trans. Control Syst. Technol. **16**(4), 745–752 (2008)

252. Riddell, R.C.: Upper bounds on the moduli of the zeros of a polynomial. Math. Mag. **47**(5), 267–273 (1974)

253. Riemann, B.: Versuch einer allgemeinen auffasung der integration und differentiation. The Collected Works of Bernhard Riemann, pp. 353–366 (1953)

254. Rodriguez-Angeles, A., Nijmeijer, H.: Mutual synchronization of robots via estimated state feedback: A cooperative approach. IEEE Trans. Control Syst. Technol. **9**(4), 380–386 (2004)

255. Rogge, J.A., Aeyels, D.: Vehicle platoons through ring coupling. IEEE Trans. Autom. Control **53**(6), 1370–1377 (2008)

256. Ross, B.: Fractional calculus. Math. Mag. **50**(3), 115–122 (1977)

257. Sarlette, A., Sepulchre, R.: Consensus optimization on manifolds. SIAM J. Control Optim. **48**(1), 56–76 (2009)

258. Sarlette, A., Sepulchre, R., Leonard, N.E.: Autonomous rigid body attitude synchronization. Automatica **45**(2), 572–577 (2009)

259. Semsar, E., Khorasani, K.: Optimal control and game theoretic approaches to cooperative control of a team of multi-vehicle unmanned systems. In: Proceedings of the IEEE Conference on Networking, Sensing, and Control, pp. 628–633, London, UK, April 2007

260. Semsar-Kazerooni, E., Khorasani, K.: Optimal consensus algorithms for cooperative team of agents subject to partial information. Automatica **44**(11), 2766–2777 (2008)

261. Semsar-Kazerooni, E., Khorasani, K.: An optimal cooperation in a team of agents subject to partial information. Int. J. Control **82**(3), 571–583 (2009)

262. Sepulchre, R., Paley, D.A., Leonard, N.E.: Stabilization of planar collective motion: All-to-all communication. IEEE Trans. Autom. Control **52**(5), 811–824 (2007)

263. Sepulchre, R., Paley, D.A., Leonard, N.E.: Stabilization of planar collective motion with limited communication. IEEE Trans. Autom. Control **53**(3), 706–719 (2008)

264. Seuret, A., Dimarogonas, D.V., Johansson, K.H.: Consensus under communication delay. In: Proceedings of the IEEE Conference on Decision and Control, pp. 4922–4927, Cancun, Mexico, December 2008

265. Shamma, J. (ed.): Cooperative Control of Distributed Multi-agent Systems. Wiley–Interscience, Hoboken (2008)

266. Shevitz, D., Paden, B.: Lyapunov stability theory of nonsmooth systems. IEEE Trans. Autom. Control **39**(9), 1910–1914 (1994)

267. Shi, G., Hong, Y.: Global target aggregation and state agreement of nonlinear multi-agent systems with switching topologies. Automatica **45**(5), 1165–1175 (2009)
268. Shi, H., Wang, L., Chu, T.: Flocking of multi-agent systems with a dynamic virtual leader. Int. J. Control **82**(1), 43–58 (2009)
269. Shucker, B., Murphey, T.D., Bennett, J.K.: Convergence-preserving switching for topology-dependent decentralized systems. IEEE Trans. Robot. **24**(6), 1405–1415 (2008)
270. Simeone, O., Spagnolini, U., Bar-Ness, Y., Strogatz, S.H.: Distributed synchronization in wireless networks. IEEE Signal Process. Mag. **25**(5), 81–97 (2008)
271. Sinha, A., Ghose, D.: Generalization of linear cyclic pursuit with application to rendezvous of multiple autonomous agents. IEEE Trans. Autom. Control **51**(11), 1819–1824 (2006)
272. Slotine, J.-J.E., Li, W.: Applied Nonlinear Control. Prentice Hall, Englewood Cliffs (1991)
273. Smith, R.S., Hadaegh, F.Y.: Closed-loop dynamics of cooperative vehicle formations with parallel estimators and communication. IEEE Trans. Autom. Control **52**(8), 1404–1414 (2007)
274. Speranzon, A.: Coordination, consensus and communication in multi-robot control systems. PhD thesis, Royal Institute of Technology, Stockholm, Sweden (2006)
275. Spong, M.W., Chopra, N.: Synchronization of networked Lagrangian systems. In: Bullo, F., Fujimoto, K. (eds.) Lagrangian and Hamiltonian Methods for Nonlinear Control. Lecture Notes in Control and Information Sciences, pp. 47–59. Springer, New York (2007)
276. Spong, M.W., Hutchinson, S., Vidyasagar, M.: Robot Modeling and Control. Wiley, New York (2006)
277. Stan, G.-B., Sepulchre, R.: Analysis of interconnected oscillators by dissipativity theory. IEEE Trans. Autom. Control **52**(2), 256–270 (2007)
278. Stankovic, S.S., Stankovic, M.S., Stipanovic, D.M.: Consensus based overlapping decentralized estimator. IEEE Trans. Autom. Control **54**(2), 410–415 (2009)
279. Su, H., Wang, X., Chen, G.: A connectivity-preserving flocking algorithm for multi-agent systems based only on position measurements. Int. J. Control **82**(7), 1334–1343 (2009)
280. Su, H., Wang, X., Lin, Z.: Flocking of multi-agents with a virtual leader. IEEE Trans. Autom. Control **54**(2), 293–307 (2009)
281. Su, H., Wang, X., Lin, Z.: Synchronization of coupled harmonic oscillators in a dynamic proximity network. Automatica **45**(10), 2286–2291 (2009)
282. Su, H., Wang, X., Chen, G.: Rendezvous of multiple mobile agents with preserved network connectivity. Syst. Control Lett. **59**(5), 313–322 (2010)
283. Sun, Y., Wang, L.: Consensus of multi-agent systems in directed networks with nonuniform time-varying delays. IET Control Theory Appl. **54**(7), 1607–1613 (2009)
284. Sun, D., Shao, X., Feng, G.: A model-free cross-coupled control for position synchronization of multi-axis motions: Theory and experiments. IEEE Trans. Control Syst. Technol. **15**(2), 306–314 (2007)
285. Sun, Y., Wang, L., Xie, G.: Average consensus in networks of dynamic agents with switching topologies and multiple time-varying delays. Syst. Control Lett. **57**(2), 175–183 (2008)
286. Tahbaz-Salehi, A., Jadbabaie, A.: A necessary and sufficient condition for consensus over random networks. IEEE Trans. Autom. Control **53**(3), 791–795 (2008)
287. Tang, Z., Ozguner, U.: Cooperative sensor deployment for multi-target monitoring. Int. J. Robust Nonlinear Control **18**(2), 196–217 (2008)
288. Tanner, H.G.: On the controllability of nearest neighbor interconnections. In: Proceedings of the IEEE Conference on Decision and Control, pp. 2467–2472, Atlantis, Bahamas, December 2004
289. Tanner, H.G., Jadbabaie, A., Pappas, G.J.: Flocking in fixed and switching networks. IEEE Trans. Autom. Control **52**(5), 863–868 (2007)
290. Tian, Y.-P., Liu, C.-L.: Consensus of multi-agent systems with diverse input and communication delays. IEEE Trans. Autom. Control **53**(9), 2122–2128 (2008)
291. Tian, Y.-P., Liu, C.-L.: Robust consensus of multi-agent systems with diverse input delays and asymmetric interconnection perturbations. Automatica **45**(5), 1347–1353 (2009)
292. Tsitsiklis, J.N.: Problems in decentralized decision making and computation. PhD thesis, Massachusetts Institute of Technology, Massachusetts, MA (1984)

293. Tsitsiklis, J.N., Bertsekas, D.P., Athans, M.: Distributed asynchronous deterministic and stochastic gradient optimization algorithms. IEEE Trans. Autom. Control **31**(9), 803–812 (1986)

294. Tuna, S.E.: Synchronizing linear systems via partial-state coupling. Automatica **44**(8), 2179–2184 (2008)

295. Vicsek, T., Czirok, A., Jacob, E.B., Cohen, I., Schochet, O.: Novel type of phase transitions in a system of self-driven particles. Phys. Rev. Lett. **75**(6), 1226–1229 (1995)

296. Vrancx, P., Verbeeck, K., Nowe, A.: Decentralized learning in Markov games. IEEE Trans. Syst. Man Cybern., Part B **38**(4), 976–981 (2008)

297. Wang, X., Hong, Y.: Finite-time consensus for multi-agent networks with second-order agent dynamics. In: Proceedings of the IFAC World Congress, pp. 15185–15190, Seoul, Korea, July 2008

298. Wang, W., Slotine, J.-J.E.: Contraction analysis of time-delayed communications and group cooperation. IEEE Trans. Autom. Control **51**(4), 712–717 (2006)

299. Wang, W., Slotine, J.-J.E.: A theoretical study of different leader roles in networks. IEEE Trans. Autom. Control **51**(7), 1156–1161 (2006)

300. Wang, L., Dai, H., Kong, X., Sun, Y.: Synchronization of uncertain complex dynamical networks via adaptive control. Int. J. Robust Nonlinear Control **19**(5), 495–511 (2009)

301. Wei, M., Cruz, J.B.: Role of cooperation in coupling game theory. Int. J. Control **80**(4), 611–623 (2007)

302. Winkler, R.L.: The consensus of subjective probability distributions. Manag. Sci. **15**(2), B61–B75 (1968)

303. Witten, T.A., Sander, L.M.: Diffusion-limited aggregation, a kinetic critical phenomenon. Phys. Rev. Lett. **47**(19), 1400–1403 (1981)

304. Wolfowitz, J.: Products of indecomposable, aperiodic, stochastic matrices. Proc. Am. Math. Soc. **15**(5), 733–736 (1963)

305. Wu, C.W.: Synchronization and convergence of linear dynamics in random directed networks. IEEE Trans. Autom. Control **51**(7), 1207–1210 (2006)

306. Wu, C.W.: Synchronization in Complex Networks of Nonlinear Dynamical Systems. Singapore, World Scientific (2007)

307. Xiang, J., Wei, W., Li, Y.: Synchronized output regulation of linear networked systems. IEEE Trans. Autom. Control **54**(6), 1336–1341 (2009)

308. Xiao, L., Boyd, S.: Fast linear iterations for distributed averaging. Syst. Control Lett. **53**(1), 65–78 (2004)

309. Xiao, F., Wang, L.: State consensus for multi-agent systems with switching topologies and time-varying delays. Int. J. Control **79**(10), 1277–1284 (2006)

310. Xiao, F., Wang, L.: Asynchronous consensus in continuous-time multi-agent systems with switching topology and time-varying delays. IEEE Trans. Autom. Control **53**(8), 1804–1816 (2008)

311. Xiao, F., Wang, L., Chen, J., Gao, Y.: Finite-time formation control for multi-agent systems. Automatica **45**(11), 2605–2611 (2009)

312. Xie, G., Liu, H., Wang, L., Jia, Y.: Consensus in networked multi-agent systems via sampled control: Fixed topology case. In: Proceedings of the American Control Conference, pp. 3902–3907, St. Louis, MO, July 2009

313. Xie, G., Liu, H., Wang, L., Jia, Y.: Consensus in networked multi-agent systems via sampled control: Switching topology case. In: Proceedings of the American Control Conference, pp. 4525–4530, St. Louis, MO, July 2009

314. Yang, Y., Polycarpou, M.M., Minai, A.A.: Multi-UAV cooperative search using an opportunistic learning method. ASME J. Dyn. Syst. Meas. Control **129**(5), 716–728 (2007)

315. Yang, P., Freeman, R.A., Lynch, K.M.: Multi-agent coordination by decentralized estimation and control. IEEE Trans. Autom. Control **53**(11), 2480–2496 (2008)

316. Yang, H., Zhu, X., Zhang, S.: Consensus of second-order delayed multi-agent systems with leader-following. Eur. J. Control **16**(2), 188–199 (2010)

317. Yao, J., Ordonez, R., Gazi, V.: Swarm tracking using artificial potentials and sliding mode control. ASME J. Dyn. Syst. Meas. Control **129**(5), 749–754 (2007)

318. Yao, J., Wang, H.O., Guan, Z.-H., Xu, W.: Passive stability and synchronization of complex spatio-temporal switching networks with time delays. Automatica **45**(7), 1721–1728 (2009)

319. Yu, C., Anderson, B.D.O., Dasgupta, S., Fidan, B.: Control of minimally persistent formations in the plane. SIAM J. Control Optim. **48**(1), 206–233 (2009)

320. Yu, W., Cao, J., Chen, G., Lu, J., Han, J., Wei, W.: Local synchronization of a complex network model. IEEE Trans. Syst. Man Cybern., Part B **39**(1), 230–241 (2009)

321. Yu, W., Chen, G., Lü, J.: On pinning synchronization of complex dynamical networks. Automatica **45**(2), 429–435 (2009)

322. Yu, W., Chen, G., Cao, M.: Some necessary and sufficient conditions for second-order consensus in multi-agent dynamical systems. Automatica **46**(6), 1089–1095 (2010)

323. Yu, W., Chen, G., Cao, M., Kurths, J.: Second-order consensus for multi-agent systems with directed topologies and nonlinear dynamics. IEEE Trans. Syst. Man Cybern., Part B **40**(3), 881–891 (2010)

324. Zavlanos, M.M., Pappas, G.J.: Potential fields for maintaining connectivity of mobile networks. IEEE Trans. Robot. **23**(4), 812–816 (2007)

325. Zavlanos, M.M., Pappas, G.J.: Distributed connectivity control of mobile networks. IEEE Trans. Robot. **24**(6), 1416–1428 (2008)

326. Zavlanos, M.M., Jadbabaie, A., Pappas, G.J.: Flocking while preserving network connectivity. In: Proceedings of the IEEE Conference on Decision and Control, pp. 2919–2924, New Orleans, LA, December 2007

327. Zhang, F., Leonard, N.E.: Coordinated patterns of unit speed particles on a closed curve. Syst. Control Lett. **56**(6), 397–407 (2007)

328. Zhang, Y., Tian, Y.-P.: Consentability and protocol design of multi-agent systems with stochastic switching topology. Automatica **45**(5), 1195–1201 (2009)

329. Zhou, J., Lu, J. an, Lu, J.: Adaptive synchronization of an uncertain complex dynamical network. IEEE Trans. Autom. Control **51**(4), 652–656 (2006)

330. Zhou, J., Lu, J. an, Lu, J.: Pinning adaptive synchronization of a general complex dynamical network. Automatica **44**(4), 996–1003 (2008)

331. Zhou, J., Wang, Q.: Convergence speed in distributed consensus over dynamically switching random networks. Automatica **45**(6), 1455–1461 (2009)

332. Zhu, X., Kim, Y., Merrell, R., Minor, M.A.: Cooperative motion control and sensing architecture in compliant framed modular mobile robots. IEEE Trans. Robot. **23**(5), 1095–1102 (2007)

333. Zhu, Y., Qi, H., Cheng, D.: Synchronisation of a class of networked passive systems with switching topology. Int. J. Control **82**(7), 1326–1333 (2009)

Index